2014 July 28; submitted to AJ

The Multiplicity of Massive Stars: A High Angular Resolution Survey with the HST Fine Guidance Sensor[1]

E. J. Aldoretta[2,3], S. M. Caballero-Nieves[4], D. R. Gies[2], E. P. Nelan[5], D. J. Wallace[6,7], W. I. Hartkopf[8], T. J. Henry[2], W.-C. Jao[2], J. Maíz Apellániz[9], B. D. Mason[8], A. F. J. Moffat[3], R. P. Norris[2], N. D. Richardson[3], and S. J. Williams[10]

emily@astro.umontreal.ca, s.caballero@sheffield.ac.uk, gies@chara.gsu.edu, nelan@stsci.edu, debra.j.wallace@nasa.gov, william.hartkopf@usno.navy.mil, thenry@chara.gsu.edu, jao@chara.gsu.edu, jmaiz@iaa.es, brian.mason@usno.navy.mil, moffat@astro.umontreal.ca, norris@chara.gsu.edu, richardson@astro.umontreal.ca, williams@astro.noa.gr

ABSTRACT

We present the results of an all-sky survey made with the Fine Guidance Sensor on *Hubble Space Telescope* to search for angularly resolved binary systems among the massive stars. The sample of 224 stars is comprised mainly of Galactic

[2]Center for High Angular Resolution Astronomy, Department of Physics and Astronomy, Georgia State University, P. O. Box 5060, Atlanta, GA 30302-5060, USA

[3]Département de physique and Centre de Recherche en Astrophysique du Québec (CRAQ), Université de Montreal, CP 6128 Succ. A., Centre-Ville, Montréal, Québec H3C 3J7, Canada

[4]Department of Physics and Astronomy, University of Sheffield, Hicks Building, Hounsfield Road, Sheffield, S3 7RH, United Kingdom

[5]Space Telescope Science Institute, 3700 San Martin Drive, Baltimore, MD 21218, USA

[6]Department of Natural Science, University of South Carolina – Beaufort, 801 Carteret Street, Beaufort, SC 29902, USA

[7]Current address: NASA, Astrophysics Division, 300 E Street, SW, Washington, DC 20546-0001, USA

[8]US Naval Observatory, Astrometry Department, 3450 Massachusetts Avenue NW, Washington, DC 20392-5420, USA

[9]Instituto de Astrofísica de Andalucía – CSIC, Glorieta de la Astronomía, s/n. E-18008, Granada, Spain

[10]Institute for Astronomy, Astrophysics, Space Applications & Remote Sensing, National Observatory of Athens, Lofos Nymfon, Thiseio, P. O. Box 20048, GR-11810 Athens, Greece

O- and B-type stars and Luminous Blue Variables, plus a few luminous stars in the Large Magellanic Cloud. The FGS TRANS mode observations are sensitive to detection of companions with an angular separation between $0''.01$ and $1''.0$ and brighter than $\triangle m = 5$. The FGS observations resolved 52 binary and 6 triple star systems and detected partially resolved binaries in 7 additional targets (43 of these are new detections). These numbers yield a companion detection frequency of 29% for the FGS survey. We also gathered literature results on the numbers of close spectroscopic binaries and wider astrometric binaries among the sample, and we present estimates of the frequency of multiple systems and the companion frequency for subsets of stars residing in clusters and associations, field stars, and runaway stars. These results confirm the high multiplicity fraction, especially among massive stars in clusters and associations. We show that the period distribution is approximately flat in increments of $\log P$. We identify a number of systems of potential interest for long term orbital determinations, and we note the importance of some of these companions for the interpretation of the radial velocities and light curves of close binaries that have third companions.

Subject headings: binaries: general — stars: early-type — stars: massive — techniques: high angular resolution

1. Introduction

The formation of a star from a huge natal cloud presents a formidable problem of angular momentum redistribution (Larson 2010). Low mass stars may accomplish the removal of angular momentum through mass loss coupled with the stellar magnetic field (Matt & Pudritz 2008). However, the situation appears to be different for the formation of massive stars that lack pervasive magnetic fields (Zinnecker & Yorke 2007). These stars may form through disk accretion processes (Krumholz et al. 2009; Kuiper & Yorke 2013) and/or competitive accretion of smaller protostars (Bonnell & Bate 2005; Bonnell & Smith 2011); in both cases the angular momentum may be deposited into the orbital motion of nearby companion stars (Kratter et al. 2008; Bate 2012). Once formed, the massive binary systems may stand the

[1]Based on observations made with the NASA/ESA Hubble Space Telescope, obtained at the Space Telescope Science Institute, which is operated by the Association of Universities for Research in Astronomy, Inc., under NASA contract NAS 5-26555. These observations are associated with programs 11212, 11901, 11943, and 11944.

best chance to survive the many dynamical encounters that probably occur in dense cluster environments (Kaczmarek et al. 2011).

There is ample evidence that the binary and multiple star frequency is remarkably high among massive stars (Duchêne & Kraus 2013). Spectroscopic surveys of Galactic OB stars by Chini et al. (2012), Kobulnicky et al. (2012), Sana et al. (2012), and Sota et al. (2014), and of the LMC Tarantula Nebula region by Sana et al. (2013b) demonstrate that the binary frequency may be $\approx 70\%$ for binaries with periods smaller than 3000 d. The incidence of longer period binaries has been explored through speckle interferometry by Mason et al. (1998, 2009), adaptive optics by Turner et al. (2008) and Close et al. (2012), and Lucky Imaging by Maíz Apellániz (2010) and Peter et al. (2012). These studies also demonstrate the high incidence of binaries and multiples among longer period systems. However, because of the great distances of most massive stars, there still exists a significant observational gap in our knowledge of binaries with periods of years to centuries that have radial velocity variations that are too small to measure or angular separations that are only resolvable with optical long baseline interferometry (Kraus et al. 2009; ten Brummelaar et al. 2011; Sana et al. 2011, 2014). It is critical to fill in this gap with new observations in order to determine the nature of the period distribution and to estimate the total binary frequency (Sana et al. 2013b).

The Fine Guidance Sensor (FGS) on the *Hubble Space Telescope* offers us a particularly attractive means to resolve such close visual binaries for even relatively faint targets (Nelan et al. 2014). The prime FGS1r instrument is capable of resolving binaries as close as 10 milliarcsec (mas) for stars as faint as $V = 16$ mag. The FGS instrument was used to explore the binary frequency of massive stars in two Galactic environments of special interest, the Carina Association by Nelan et al. (2004, 2010) and the Cyg OB2 association by Caballero-Nieves et al. (2014). In both cases the binary frequency over the angular range of $0\farcs01$ to $1\farcs0$ was found to be $\approx 22\%$.

Here we describe a new all-sky FGS survey of the massive stars that we have made with a number of broad goals in mind. Our primary task is to explore how binary properties vary with environment, in particular to search for evidence of different binary frequencies among massive stars in clusters and associations and those in the field (especially runaway stars). A second goal is to compare the binary statistics in this angular range with those for close spectroscopic and wider separated systems in order to place constraints on the overall period distribution of massive binaries. Thirdly, we identify individual systems of particular interest where the distant companion may influence our interpretation of the spectra or light curve of the primary target and may serve for future mass determination through measured orbital motion. We describe the observations and sample in §2, and then discuss the binary

detection methods and results in §3. The issues surrounding the companion frequency and period distribution are outlined in §4 and §5, respectively, and we summarize our conclusions in §6.

2. FGS Observations

The Fine Guidance Sensor aboard the *Hubble Space Telescope* acts as a single aperture, shearing interferometer that forms interference fringes through a Koesters prism due to tilt differences in the incoming wavefront (Nelan et al. 2014). There are three FGS instruments on *HST* that are used for precise pointing of the telescope, and one of these, FGS1r, is designated for science applications. In the TRANS mode of operation the FGS1r scans across the target in two orthogonal directions, and it produces an x and y coordinate, fringe visibility curve (or "S-curve"). FGS observations of binary stars produce an S-curve that is the sum of fringe patterns for each component at a position that corresponds to the projection of the binary separation along the x and y vectors (§3).

The observations began as a SNAP program in Cycle 16 (GO-11212), and we selected targets all around the sky so that they could be easily scheduled into one orbit slots between other programs. It was subsequently expanded into a Director's Discretionary program (GO-11901, 11943, 11944) around the time of the last servicing mission in order to optimize telescope usage when options with other instruments were very limited. Consequently, the observations were made over the period 2007 to 2009 in a large number of single orbit pointings. All the observations were made with the ND5 filter (brighter targets) or F583W filter (fainter targets) that record a broad range of the optical spectrum[11] ($\approx 4600 - 7000$ Å). Multiple scans were recorded of each target with an angular step size of 1 mas, and the scans usually extended $\pm 1\farcs0$ from the main target (or longer in some cases where a wider companion was known). Note that the FGS detectors record all the flux from sources within the field of view (FOV $\approx 5 \times 5$ arcsec^2), and although the detector response is uniform close to the target, the photometric response varies significantly for sources near the edge of the FOV. Special calibration is necessary to obtain reliable magnitude differences for companions near the periphery.

All the observations were processed with the FGS pipeline software (Nelan et al. 2014). First, the archived observations were extracted into individual scans using CALFGSA, which was also used to assess the data quality and to create a number of associated files that document the properties of the scans and observations. Then we used the routine PTRANS

[11]http://www.stsci.edu/hst/fgs/design/filters

to gather the individual scans, coalign them, and spatially smooth the combined results. Finally, we applied a simple spline fit to rectify the distant parts of each summed scan to a zero average.

We selected our targets primarily from the Galactic O-Star Catalog[12] (Maíz-Apellániz et al. 2004; Maíz Apellániz et al. 2013), which we supplemented with other fainter targets from the catalog of Cruz-González et al. (1974) and with a selection of Luminous Blue Variable (LBV) stars (van Genderen 2001). Two interlopers were accidentally included in the sample, the hot subdwarf CD-45°5058 = KS 292 (Rauch et al. 1991) and the K-giant BD-3°2178 (Pickles & Depagne 2010), which has been confused in the literature with the nearby hot subdwarf BD-3°2179. Both of these (apparently single) stars are excluded from the discussion in §4 and §5. The targets are listed in order of increasing right ascension in Table 1 , which provides the celestial coordinates, star name, the Johnson V magnitude, and $B-V$ color (Mermilliod & Mermilliod 1994). Column 5 gives the spectral classification of the brightest component from (in most cases) Sota et al. (2011, 2014); LBV classifications are from contemporaneous spectra described by Richardson et al. (2012). Columns 6 to 10 give information about the star's environment, runaway status, distance, spectroscopic binary status, and a recent spectroscopic reference, all gathered from a literature search for each object (see §4). Column 12 summarizes the number of companions detected in the FGS observations (§3), and the number of additional companions detected through spectroscopy or as wide visual binaries are given in columns 11 and 13, respectively (see §4). Column 14 lists other commonly used names for the targets and a code to identify the LBV (or candidate LBV) stars.

3. Companion Star Detection

The detection of the signal of a stellar companion in the FGS scans depends primarily on the angular projected separation and magnitude difference. Each star in the FGS FOV produces a fringe pattern, and the observed scan will take the form

$$S(x)_{obs} = \sum_{i=1}^{n} f_i \; S(x - x_i) \tag{1}$$

where each of n stars contributes a flux fraction $f_i = \frac{F_i}{\sum F_j}$ and has a relative projected offset position x_i. The function $S(\triangle x)$ represents the apparent fringe pattern produced by a single unresolved star. We show in Figure Set 1 the full collection of 251 merged scans

[12]http://ssg.iaa.es/en/content/galactic-o-star-catalog/

of our targets (available in full in the electronic version of the paper), and the central two panels of these figures show the final scans along the orthogonal x and y axes. A single star (cf. HD108, Fig. 1.1) shows a simple fringe oscillation pattern, while a fully resolved binary star (cf. HD73882, Fig. 1.135) shows two clearly separated fringe patterns. In general, the relatively bright and widely separated companions are immediately detected upon inspection, but detection is more challenging with fainter companions or those cases of close companions where the fringe patterns largely overlap. Our detection scheme relies upon a comparison of the observed scans with those for a set of single stars that act as calibrator scans. We first apply a set of detection tests developed by Caballero-Nieves et al. (2014), and if a resolved component is found, then we make a detailed fit of the observed scan with a selection of calibrator scans. Below we review the testing criteria and fitting procedure, and our results are summarized in Table 2 for resolved systems, Table 3 for partially resolved systems, and Table 4 for apparently single, unresolved systems.

The detailed form of the fringe pattern $S(\triangle x)$ depends upon the color of the star and filter used (Horch et al. 2006) as well as the time of observation relative to that of a servicing mission or other adjustments of the instrument. We selected the calibrators from a set of scans that appeared to be those of single stars from our program (see Table 4 below) and of red, low mass stars observed in programs GO-11943 and 11944. These scans were subsequently checked for binary interlopers with the tests described below before establishing final lists of calibrator scans. The scans were arranged into four categories based on filter (FND5 or F583W) and time of observation (before or after the final servicing mission on BY 2009.06), and they were ordered according to $B - V$ color. In most cases we relied upon all the available calibrators with colors within ± 0.5 mag of the target's $B - V$ color (usually numbering between 6 and 50 cases).

The first clues about the presence of a companion come from a visual inspection of the scans for multiple fringe patterns and from a measurement of the fringe amplitude dilution caused by the flux of the other star(s) (see eq. 1). The latter is measured by the S-curve peak-to-peak amplitude ratio (given as "sppr" in the central panels of Figure Set 1), which is the mean of the ratio of observed to calibrator full amplitude among the set of selected calibrators. A value of sppr < 0.92 is often an indication of the presence of another flux source in the FGS FOV (Caballero-Nieves et al. 2014).

We tested for the presence of resolved companions using a cross-correlation function (CCF) method developed by Caballero-Nieves et al. (2014). This is an iterative scheme that compares the CCF of a target with a calibrator scan to the CCF of the calibrator with itself. The first step is to align and rescale the calibrator CCF with the main peak in the target CCF, and then this rescaled calibrator CCF is subtracted to search for residual peaks in the

target CCF from companions. The results of this first step (denoted RCCF for "Residuals from the CCF subtraction") are shown in the top two panels of Figure Set 1. A vertical dashed line at the origin shows the position where the primary signal was removed. Then, we sequentially identify any remaining CCF peaks that attain a strength $> 4\sigma$(CCF), where σ(CCF) is the standard deviation at that scan position among the collection of calibrator scan CCFs (shown as the light gray line in the upper panels of Figure Set 1). These peaks are also indicated by vertical dashed lines in Figure Set 1. Then, we use the scaling and offset parameters for each identified component to make a model composite scan, which is shown as a dashed line in the central panels (often hidden within the line thickness of the observed scan plot). Finally, the difference between the observed and model scans is shown on an expanded amplitude scale in the lower panels of Figure Set 1, where the $\pm\sigma$(CCF) region is indicated by light gray shading.

Note that all the CCF results shown in Figure Set 1 refer to a mean CCF derived from the CCFs of the target with each of the selected calibrator scans. Most of our targets are relatively bright and the merged scans have good S/N properties, so the main source of uncertainty in binary detection is related to how well the calibrator scans match the target scan. Consequently, the detection criterion for a CCF peak is based on its strength relative to the scatter we find among the calibrator scans. Simulation tests made by Caballero-Nieves (2012) indicate that our $> 4\sigma$(CCF) criterion will result in no more than a single accidental detection in a sample as large as ours. Indeed, there are potentially other plausible detection cases that can be made by inspection of the CCF plots in Figure Set 1, but for the purposes of this paper, we generally include only those that meet this stringent requirement in order to avoid false detections.

The CCF method yields ambiguous results for very close companions (with projected separations generally less than 20 mas) because in the first iteration the calibrator CCF will be matched to a position between the components where the composite CCF peaks. In such a situation the residual CCF will show two comparable peaks around the origin. Hence we require a second test to deal with close binaries that create blended fringe patterns. Caballero-Nieves et al. (2014) showed that in such blended cases the difference between the observed and calibrator scans will have a functional shape proportional to the second derivative of the calibrator scan,

$$\begin{aligned} S(x)_{\rm bin} - S(x)_{\rm cal} &= \frac{1}{1+r} S(-(\frac{r}{1+r})\Delta x) + \frac{r}{1+r} S(+(\frac{1}{1+r})\Delta x) - S(x) \\ &= \frac{1}{2}\frac{r}{(1+r)^2}(\Delta x)^2 S''(x) \equiv a S''(x) \end{aligned} \tag{2}$$

where Δx is the projected separation and $r = F_2/F_1$ is the flux ratio. This relation shows that the single parameter a that can be derived from the blend is a function of both r and

$|\Delta x|$, so that these parameters cannot be determined independently. However, the relation also demonstrates that close binaries can be detected by searching for those cases where the amplitude of the second derivative coefficient a is large and positively valued. We applied this second derivative test for detection by requiring $a > 4\sigma(a)$, where a and $\sigma(a)$ are the mean and standard deviation of fits of eq. 2 from the set of selected calibrator scans. Those cases that met this criterion are shown with a thick gray line portraying the fit in the lower panels of Figure Set 1 (cf. HD65087, Fig. 1.117).

Once we had identified those resolved components with the CCF method, we then made a non-linear, least squares fit of the scans using the Levenberg-Marquardt algorithm with the IDL function *mpfitfun* (Markwardt 2009). We did not make fits for the close blended scans because of the inherent ambiguity in the parameters in such cases (see eq. 2). The binary or triple star fit was made of the positions and amplitudes of the fringe patterns for each component using a model of the form of eq. 1 but with independent parameters for the amplitude of each component. Starting values for each parameter were taken from the CCF results. The fits were made with each selected calibrator, and the final adopted values and uncertainties were estimated from the mean and standard deviation of the fitting parameters from the calibrator set.

We found that it was preferable to have independent amplitude scaling parameters for each component (rather than coefficients referenced to the flux of the primary as in eq. 1) in order to deal effectively with the general scaling mismatch between the target and calibrator scans. The magnitude differences were then obtained as $-2.5 \log F_i/F_1$ for each component. In order to check our results, we compare in Figure 2 the derived magnitude differences (mean of x and y-axis fits) with those obtained by *Hipparcos* (Perryman & ESA 1997) for some of the mutually detected wide binaries. The excellent agreement indicates that our magnitude estimates and their uncertainties are apparently reliable and free of systematic problems.

There are generally four possible outcomes for binary detection along each axis: (1) the fringe appearance is consistent with that of a single star, (2) the second derivative test indicates a blended component, (3) the fringes of a companion are resolved by the CCF test, or (4) a companion exists beyond the scan range but within the FGS FOV and causes a dilution of the fringe amplitude of the target (see eq. 1). If a system is triple, then the same set of outcomes is possible for the third component (all dependent upon the orientation of the component in the sky relative to the scan axes). We attempted to decide upon these outcomes based upon an inter-comparison of the test results between axes and the parameters of those known binary systems. The Appendix provides notes about those cases where the outcomes were ambiguous or problematical.

The results for systems that were resolved along at least one axis are collected in Table 2. The entries are listed in order of increasing right ascension and by date of observation where multiple observations were made. Columns 1 and 2 give the coordinates and name (same as in Table 1), and column 3 gives the discovery designation from the Washington Double Star (WDS) Catalog (Mason et al. 2001)[13]. If the FGS observation is the first detection, then "FGS" is listed along with a component designation made following the nomenclature used in the WDS (Hartkopf & Mason 2004). Columns 4 and 5 give the date and filter for the observation. Columns 6, 7, and 8 give the position angle θ, separation ρ, and magnitude difference $\triangle m$ determined by our non-linear, least squares fits of the scans. In most cases the component is resolved in both axes. Then the position angle is determined from the projected axial separations and the telescope orientation on the sky (from the PA_APER keyword in the observation header file), the separation is the square root of the sum of the squares of the projected axial separations, and the magnitude difference is the error weighted average of the x and y values. In other cases, the component is resolved on only one axis, but has a significant second derivative coefficient a for the other axis. Then the absolute value of the close separation $|\Delta x|$ is derived using the flux ratio r from the resolved axis result and the relation between a, r, and $|\Delta x|$ from eq. 2. This yields a reliable value for ρ, but there are two possible θ angles that correspond to the choice of $\pm|\Delta x|$. We list in Table 2 the θ estimate for $+|\Delta x|$ and the Appendix notes give the other possible θ value. There are several cases where the companion is probably beyond the scan range along one axis, and for these there is no θ estimate and only a lower limit for ρ. Column 9 gives the number of the Figure Set 1 plot that corresponds to the observation, and column 10 provides codes for notes about the specific system.

Table 3 lists those cases where the second derivative test indicated the presence of a blended component along at least one axis (and the target is not included in Table 2). Table 3 has the same format as Table 2, except for columns 6, 7, and 8 that are used differently. The second derivative coefficient a depends on both flux ratio and separation (see eq. 2), and we can set a minimum separation for a flux ratio $r = 1$,

$$\rho_{\rm min} = \sqrt{8}\sqrt{a_x + a_y} \tag{3}$$

where a_x and a_y are the positively valued, second derivative coefficients measured for the x and y scans, respectively. This lower limit is given in column 8 of Table 3. If the flux ratio r eventually becomes known, then the actual separation will be given by

$$\rho = \rho_{\rm min}\frac{1+r}{2\sqrt{r}}. \tag{4}$$

[13]http://ad.usno.navy.mil/wds/

There is a four-fold ambiguity in the derived position angle θ depending on the signs of $|\Delta x|$ and $|\Delta y|$. Columns 6 and 7 give ${}^a\theta_1$ which is the ambiguous position angle for $(+|\Delta x|, +|\Delta y|)$ and ${}^a\theta_2$ which is the ambiguous position angle for $(+|\Delta x|, -|\Delta y|)$; add 180° to each of these to arrive at the remaining two possibilities. We can check on the validity of these estimates for the second derivative detection of a close companion of HD37022C = θ^1 Ori C that is a binary with an orbit derived from long baseline interferometry (Kraus et al. 2009). Kraus et al. (2009) report a VLTI measurement at about the same time as the *HST* FGS observation with $\rho = 19.1$ mas and $\theta = 241°$. If we adopt their optical flux ratio $r = 0.30$, then eq. 4 and $\rho_{\rm min}$ yield estimates of $\rho = (17.9 \pm 3.0)$ mas and $\theta = (247 \pm 19)°$, in agreement with the contemporaneous VLTI measurement.

Table 4 lists the remaining systems for which we find no evidence of a companion. The format of Table 4 consists of the same first four and last two columns of Table 2. Altogether, of our sample of 226 stars, we resolved 52 binary and 6 triple systems (Table 2), partially resolved 7 binaries (Table 3), leaving 161 stars unresolved (Table 4). Only 29 of the systems were known prior to this FGS survey.

We show in Figure 3 the total separations and magnitude differences for all the components that we detected. The partially resolved systems are plotted assuming that the components have the same flux ($r = 1$). The solid line connecting diamond shaped symbols shows the expected faint limit for companion detection by the CCF method, and the dotted line illustrates the expected limit for detection of close companions by the second derivative test (all for similar FGS scans from Caballero-Nieves et al. 2014). Our detections fall within the expected range for the most part, reaching as faint as $\triangle m = 5$ for widely separated binaries (but less for closer binaries). The smallest separations we can detect are about 10 mas (Table 3). For example, while we did detect the close binary HD37022C = θ^1 Ori C ($\rho = 19.1$ mas; Fig. 1.34), we failed to resolve the relatively bright companion of HD150136 (Fig. 1.196) with a separation of 7 mas (Sana et al. 2013a; Sanchez-Bermudez et al. 2013).

4. Companion Frequency

We found that 65 of 224 targets (omitting the subdwarf CD-45°5058 = KS 292 and the K-giant star BD-3°2178) or 29% of the sample have a visual companion in the angular range from 0.″01 to 1.″0. This detection rate compares well with earlier surveys of massive stars in the Carina Association (22%; Nelan et al. 2004, 2010) and in Cyg OB2 (22%; Caballero-Nieves et al. 2014). We find 6 of the 13 LBV or candidate LBV stars to have companions, but four of these are located in the LMC where source crowding is an issue, so we do not consider this high binary fraction to be unusual. However, in order to study

the total multiplicity fraction, we must also consider what is known about closer binaries (detected as spectroscopic binaries) and wider binaries (detected by speckle interferometry, adaptive optics, and other astrometric methods). We have collected information on the binary companions of our sample through a literature review of the spectroscopic properties and a search through the WDS catalog for wider pairs. Furthermore, we have supplemented our sample of 224 stars with 81 others from the prior FGS surveys: 23 stars in the Carina association (Nelan et al. 2004, 2010) (omitting HDE303308 which is already part of our main survey) and 58 stars from the Cyg OB2 association (Caballero-Nieves et al. 2014). The information on these additional 81 stars is gathered at the bottom of Table 1 for the convenience of readers. Table 1, column 9 lists a code describing the spectroscopic status and column 10 gives a reference for the literature source. Spectroscopic binaries are identified with the code "SB" that is usually followed by the number of spectral components observed (1 for a single-lined binary, 2 for a double-lined binary, and higher if additional components are known). The code may include a suffix of "O" for systems with orbital determinations, "E" for eclipsing or ellipsoidal systems, and "?" for suspected systems (for example, for systems with a large radial velocity range but no orbit or those where double lines are reported). A code of "C" indicates a star with apparent constant radial velocity. Many of the targets are assigned a code of "U" for unknown status in cases where there are only a few or no radial velocity measurements. The total number of probable spectroscopic companions (not including those detected in the FGS survey) is listed in column 11 of Table 1. Columns 12 and 13 give the numbers of visual companions found in our survey and from inspection of the WDS, respectively.

We are also interested in the binary properties as a function of environment because stars ejected from their natal clusters may preferentially be single stars. Table 1, column 6 lists the name of the cluster or association of membership or the entry "Field" if no membership is known. Most of these assignments come from earlier work by Humphreys (1978), Moffat et al. (1979), Garmany et al. (1982), and the cluster database WEBDA[14]. We note that several of these "clusters" are in fact groups of only several luminous stars, but nevertheless, their existence shows that the target still resides among the stars where it was born. de Wit et al. (2005) have shown that some so-called field stars are the brightest members of clusters with a host of fainter stars (e.g., HD52533, HD195592), and we suspect that many of the targets assigned to the field category in Table 1 may turn out to be members of unrecognized clusters. The runaway stars in the sample (Mason et al. 2009) are indicated by an entry of "yes" in column 7 of Table 1.

[14]http://www.univie.ac.at/webda/webda.html

We caution that some of the wider, resolved companions may be field stars along the line of sight. Furthermore, some of the targets reside in rich star clusters, and their companions may be cluster members that are not necessarily orbiting the primary target. The probability of such a chance alignment may be estimated from the nearby surface density of stars with a magnitude less than that of the companion, $\Sigma(V < V_c)$. Correia et al. (2006) show that the probability of finding a field star at a separation ρ from the target is given by

$$p(\Sigma, \rho) = 1 - e^{-\pi\Sigma\rho^2}. \quad (5)$$

We estimated Σ in practice by collecting stellar F-magnitudes (covering the 579–642 nm range) in the region within a radius of $15'$ from the target that we extracted from the UCAC4 catalog (Zacharias et al. 2013). We then formed cumulative distribution functions with magnitude for each set and made a linear fit of the logarithm of cumulative star counts with magnitude (Lafrenière et al. 2014). We used this fit to estimate Σ for the magnitude of a given companion star, and then we estimated the probability of chance alignment for the companion's projected separation ρ. Companions with a probability $p < 0.01$ are good candidates for physically related objects.

The companions detected in the FGS survey have small projected separations and are generally bright, so the probability of a chance alignment is much smaller than the $p = 0.01$ criterion. However, the situation is different for some of the more widely separated companions in the WDS sample. For example, there are seven companions listed in the WDS for HD190918, but only four of these meet the probability criterion. This star is a member of the open cluster NGC6871, so it is possible that the remaining three companions are cluster members. Long term proper motion investigations will be required to determine which of these companions are actually gravitationally bound to HD190918.

Additional factors should be considered in assessing the status of the companions listed in the WDS. For example, the runaway star HD34078 = AE Aur is listed with three companions in the WDS. This is a surprising result because this star was probably ejected from the Ori OB1 association through an encounter between binary stars (Gualandris et al. 2004), and the star is expected to be single at present. A closer examination of the notes in the WDS indicates that the Aa,Ab companion is an artifact of adaptive optics imaging and that the AB companion is "very doubtful". Furthermore, according to UCAC4, the AC companion is probably 3.5 mag fainter than the magnitude listed in the WDS, so that its probability of chance alignment is above the adopted criterion. The tentative conclusion is that HD34078 has no physically related companions, consistent with expectations. However, for the purposes of this work, we decided to retain all the companions listed in the WDS, pending the further research that will be required to settle their true nature. Thus, we caution that the companion numbers presented here from the WDS sample must be regarded as probable

overestimates of the actual numbers of bound companions.

Table 5 summarizes the numbers of companions according to their environmental parameter: cluster/association, field, or runaway groups. We removed the four targets in the LMC from the total sample ($n = 224 + 81 - 4 = 301$) because of crowding issues related to the large distance of the LMC. The companion numbers are first presented in section A for the resolved binaries in the FGS sample. The number n(FGS) gives the number of targets with one or more detected companions in each environmental group. The next row gives the corresponding frequency of multiple systems (MF = number with any companion divided by the total number). The uncertainty estimates are based upon the binomial statistical approach of Cameron (2011) for a confidence interval of $c = 0.683$ (equivalent to 1σ), and they represent the average of the almost equal lower and upper confidence limits. The third row reports the companion frequency (CF = number of companions divided by the number of targets). The uncertainties in this case were estimated by a bootstrap method of random sampling of the data in the subsets (cf. Raghavan et al. 2010). The three rows in section B of Table 5 give the same values for the WDS sample. The estimates of MF are similar for the two samples and the cluster/association and field stars, but the MF estimate for the runaway stars and the CF estimates are all larger for the WDS sample. We suggest that this is due to overestimates of companion numbers in the WDS.

Section C of Table 5 lists the same n, MF, and CF values for the spectroscopic binaries in this sample. The number n(SBO+E) counts the number of targets with known orbital periods, i.e., those with spectroscopic orbits and/or eclipsing light curves. The next three rows list the corresponding numbers for possible spectroscopic binaries (with a status listing of "SB1?" or "SB2?" in Table 1), constant velocity stars, and stars with unknown spectroscopic binary properties, respectively. Stars in the latter group were omitted in the calculation of MF and CF for the spectroscopic binaries. The next four rows give the MF and CF estimates based upon two samples of the spectroscopic binaries, those with known period (SBO+E) and those known and suspected binaries (SBO+E+?).

Section D of Table 5 gives the combined MF and CF estimates for two counting schemes. The first combines the numbers of spectroscopic binaries with known period plus the numbers of FGS binaries. In this case we ignore any suspected spectroscopic binaries and all the WDS companions, so these statistics are noted as MF(min) and CF(min) because they represent reliable minimum fractions. The second counting scheme sums all the known and suspected spectroscopic binaries, FGS companions, and WDS companions. These are representative of the observed maximum fractions, because they include some spectroscopic targets that may be velocity variable for reasons other than a binary companion and they include some unrelated companions from the WDS catalog.

The high frequency of multiple systems among the SB category is similar to that found in recent spectroscopic surveys (Chini et al. 2012; Sana et al. 2012, 2013b; Sota et al. 2014), and our results confirm the trend that the ejected stars (runaway and some field stars) have a lower frequency of multiple systems than stars still in their natal clusters. This trend is also seen among the FGS visual binaries, but it is probably absent for the WDS sample because the bound companion numbers are overestimated for our WDS sample (recall the case of the runaway star AE Aur discussed previously). The relatively high frequency of multiple systems among the resolved binaries is also striking, and this verifies the importance of the more distant companions to the total numbers of companions (Mason et al. 1998, 2009; Peter et al. 2012). The companion frequency is also very high among the cluster/association stars, reaching a value between 0.7 and 1.7 companions per target after combining the SB, FGS, and WDS samples.

The numbers presented in Table 5 represent the properties of observed companions, and transforming these into the total numbers of multiple systems requires a careful consideration of observational selection effects and assumptions about the period and mass ratio distributions (Kiminki & Kobulnicky 2012; Sana et al. 2013b). For example, the FGS survey is limited to companions brighter than $\triangle m = 5$, which corresponds approximately to $M_2/M_1 > 0.1$, so we miss companions with a mass below a few solar masses. Such faint companions may be detected with adaptive optics (AO) imaging over a limited angular separation range (Turner et al. 2008), but such AO observations are incomplete for our sample. Single high resolution measurements may also miss those systems that are close to a small separation conjunction phase at the time of observation. The spectroscopic binary numbers are based on observations with very diverse spectral resolution, wavelength coverage, and temporal cadence properties, and we suspect that many more binaries will be detected and/or verified in ongoing radial velocity investigations. Furthermore, the diversity of mass, age, and orbital periods in our sample may mix populations with differing binary properties (Kaczmarek et al. 2011). The binary statistics in Table 5 should therefore be regarded as the result of a convolution of the actual distributions with the observational selection effects that limit detections.

5. Orbital Period Distribution

We collected from the literature orbital periods for 83 of the SBO or SBE binary systems listed in Table 1. The visual binaries have much longer periods that are only beginning to be sampled, and there are published periods for only five visual binaries in our sample (HD37022, Kraus et al. 2009; HD25639, Gorda et al. 2007; HD37468, Turner et al. 2008;

HD47839, Cvetković et al. 2010; HD193322, ten Brummelaar et al. 2011). However, we may obtain an approximate orbital period for the visual binaries by considering their angular separation, distance, and probable mass. The angular separation in the sky depends on orbital orientation and phase, and for circular orbits, we expect that the projected separation generally underestimates the actual semimajor axis. On the other hand, many long period binaries have orbits with a large eccentricity, so that we observe them most of the time with a separation $(1 + e)\times$ larger than the semimajor axis. Brandeker et al. (2006) made Monte-Carlo simulations of the ratio of projected separation to semimajor axis for an ensemble of binaries with a commonly adopted eccentricity distribution $f(e) = 2e$, and they found that this ratio has a value of 1.0 ± 0.7, where the uncertainty represents the HWHM of the distribution (see their Fig. 9). Consequently, we estimated the semimajor axis a for the visual binaries by $a \approx \rho d$, where a is measured in AU, ρ in arcsec, and d in parsecs. Table 1, column 8 lists the adopted distances for the targets, which were taken from WEBDA for cluster members and from Mel'Nik & Dambis (2009) for association stars. Distances for the field stars were generally collected from spectroscopic parallaxes given by Garmany et al. (1980) or Gudennavar et al. (2012). If no distance estimate was found, then we calculated the spectroscopic parallax ourselves using the magnitude, colors, and spectral classifications in Table 1 with intrinsic colors from Wegner (1994), a ratio of total-to-selective extinction of $R = 3.1$, and absolute magnitudes from Balona & Crampton (1974) and Martins et al. (2005). We then estimated the orbital period P using Kepler's Third Law and mass estimates for the primary from the spectral classification – mass calibration of Martins et al. (2005) (their Tables 4, 5, and 6). Note that we have ignored the need to adjust the period upwards because the spectroscopic parallaxes probably underestimate the true distance (binaries are brighter than the primary alone), and likewise ignored a downwards period adjustment because the mass estimate is low (binaries are more massive than the single primary). However, these changes are minor compared to the uncertainties inherent in our assumed equivalence of a and ρ. Our final tally of orbital periods for visual binaries in our sample amounts to 89 estimates for companions from the FGS detections plus 207 others for companions from the WDS catalog.

Our goal in this section is to determine the frequency of multiple systems MF as function of the binary orbital period. This requires a determination of the number of targets in the sample for which our methods would probably find a binary over a given period range. Consequently, we need to consider the period range sensitivity for each method of binary detection. A fortunate spectroscopic observer may discover a binary in a single measurement of a double-lined system, but the determination of an orbital period for a spectroscopic binary generally requires a significant effort of repeated observations. Thus, the exploration space to determine a binary period grows with the number of observations and the duration between

the first and last spectroscopic observations. We extracted this observational duration from the papers cited in Table 1 for each of the targets with a spectroscopic status different from "U" (unknown), and then we estimated the period detection range for each target as 1 day (smallest contact binary) to the full duration of observations. We then constructed a logarithmic period grid using time in years and a bin size of 1 dex, and we determined the number of targets in each period bin where the spectroscopic duration is sufficient to measure at least one binary orbital period. This summation included cases where only a fraction of the $\log P$ bin range was covered by adding the ratio of the covered range to the full 1 dex bin size. Then the multiplicity fraction was calculated as the ratio of number of measured periods to the summed number of targets for which detection was possible within each $\log P$ bin. Note that our simple characterization of the period detection range fails to represent the true complexity of the time series associated with the spectroscopic observations. For example, a series of nightly observations made over one week plus a single observation made one month later would be taken at face value as suitable to detect periods up to one month, when, in fact, such a series is most sensitive to periods of a week or less. Thus, by using only the full duration of the observing sequence, we probably overestimate the detection efficiency at longer periods, and this may lead to a modest underestimate of $MF(\log P)$ at the longer orbital periods associated with the spectroscopic observations.

We used a similar approach to find $MF(\log P)$ for the visual binaries detected in the FGS survey and listed in the WDS catalog. The period range of detectability for these cases depends on the projected separation, distance, and stellar masses, and we used the distances from Table 1 and masses from calibrations based upon spectral classification to determine P from projected angular separation (in the same way as we did for the detected binaries). The FGS scans are sensitive to binaries in the $0\farcs01$ to $1\farcs0$ range, while the WDS appears to list systems over a broader range of $\approx 0\farcs1$ to $\approx 100''$. We adopted these angular ranges in setting the period range for binary detection for each target in our sample, and then we estimated the summed target number and multiplicity fraction in each $\log P$ bin in the same way as for the spectroscopic sample. Note that we took care not to double count those systems detected in the FGS survey that also appear in the WDS catalog.

We show our resulting $MF(\log P)$ relation as a set of histograms in Figure 4. The detected multiplicity fractions are shown individually for the SB, FGS, and WDS sets, and then the sum of these is shown as the final histogram (representing the total found from all methods). This summed distribution appears to be approximately flat, but we need to bear in mind a number of selection effects that may influence the appearance of the distribution. The low $\log P$ part of the distribution that is estimated from spectroscopic data is probably systematically low, because inclusion in the plot requires a significant observational effort, and we expect that a large fraction of the systems with a spectroscopic status of "SB1?"

and "SB2?" in Table 1 will indeed turn out to be real short-period binaries. Furthermore, it is likely that observers may tend to favor short-period over long-period binaries, because of the extended labor required to determine periods for the long-period systems. On the other hand, it is relatively simple to estimate an approximate period for a visual binary from a single high angular resolution observation, and such observations are sensitive to relatively faint and lower mass companions, so we might expect that the visual binary MF would tend to be relatively higher than the spectroscopic MF. We caution that the large number of companions found in the WDS may result partially from the inclusion of field stars or cluster members that may or may not be gravitationally bound to the target star. This problem increases at the long end of the $\log P$ distribution (largest separation systems) where the estimated orbital periods become a significant fraction of the stellar lifetime. If, for example, we replace the last two highly populated bins in Figure 4 with the average in the shorter period bins, then the total multiplicity fraction integrated over all period bins is 1.14, consistent will the idea that most massive stars have at least one companion.

A number of investigators have explored the binary star period distribution, with a particular emphasis on the shorter period systems ($P < 10$ d). Kiminki & Kobulnicky (2012) developed a Monte-Carlo approach to sample the intrinsic distributions of binary parameters in a way comparable to their extensive spectroscopic observations of the massive stars in the Cyg OB2 association. They used a power law distribution for orbital period of the form $f(\log P) \propto (\log P)^{\beta}$, and their experiments suggest $\beta = +0.2 \pm 0.4$, consistent with a flat distribution with $\beta = 0$ (Öpik's Law). On the other hand, Sana et al. (2013b) used a similar Monte-Carlo method to fit spectroscopic results for a large sample of O-type stars in the Tarantula Nebula region of the LMC, and they find a best fit power law distribution with $\beta = -0.45 \pm 0.30$. Their result is consistent with that from an analysis of Milky Way eclipsing binaries by Moe & Di Stefano (2013), who find $\beta = -0.4 \pm 0.3$. However, we caution that the distribution of shorter period systems may be more complicated and include a local maximum in numbers for periods in the range of 4 to 10 days (Barbá et al. 2010; Kiminki & Kobulnicky 2012; Sana et al. 2013b), so that a multi-component model is more appropriate than a single power law (Sana & Evans 2011). Our results (Fig. 4) suggest that the distribution in $\log P$ is approximately flat when we consider the full range in orbital periods.

6. Conclusions

Our FGS survey has provided us with a new and uniform sample of high angular resolution observations to explore the multiple star properties of massive stars in the projected

separation range from 0.″01 to 1.″0 for companions brighter than $\triangle m = 5$ mag. We used detection techniques developed by Caballero-Nieves et al. (2014) to identify both faint companions and those close to the angular resolution limit. In total, we detected 59 binary systems and 6 triple systems among our sample of 224 stars, yielding a frequency of multiple systems of 29%. Six of the 13 LBV or LBV candidates observed are found to have companions. Many of the resolved binaries also have one component that is a spectroscopic binary, so our results will help in the interpretation of their composite spectra. For example, all three of the bright stars BD+00°1617 A,B,C that line up in the center of the cluster Bochum 2 are resolved binaries, and two of these (B and C) are also short period spectroscopic binaries (Munari & Tomasella 1999), forming hierarchies like those observed in the Orion Trapezium cluster (Close et al. 2012). Although most of the resolved binaries are distant and the projected separations imply a large semimajor axis, we do find a number of relatively nearby systems with close companions with probable orbital periods less than one century (including HD155913, HD158186, HDE229232, HDE303308, HD160529, HD164794 and HD195592). These will be important targets for long term observation for orbital and mass determinations.

We considered the binary star census of the complete sample (301 stars = 224 stars from this work less 4 LMC stars plus an additional 81 stars from earlier FGS studies) by collecting information from the literature on the numbers of close spectroscopic binaries and by searching the Washington Double Star Catalog for additional companions with angular separations mostly greater than one arcsec. The number of companions was compared between the spectroscopic (SB) and resolved (FGS, WDS) samples to determine the frequency of multiple systems and the companion frequency among stars residing in clusters and associations and in the field, and among runaway stars. These statistics for the SB and FGS samples confirm the trend that stars close to their place of birth have relatively more companions, consistent with the idea that stars ejected from clusters are preferentially single objects. The number of wide companions in the WDS sample may be overestimated because of the inclusion of cluster members and chance alignment cases rather than bound companions. The total number of companions per target among cluster and association stars falls in the range from 0.7 to 1.7 depending upon the inclusion of suspected spectroscopic binaries and the WDS companions.

We investigated the period distribution of the known binaries in this sample by collecting measured orbital periods for spectroscopic binaries and by estimating the periods for resolved binaries from their projected separation, distance, and probable mass. We constructed a histogram of the multiplicity frequency as a function of $\log P$ by accounting for the probable range in detectable period for each target that was set by the duration of the observations for spectroscopic binaries and by the angular separation range associated with the FGS

and WDS measurements for the visual binaries. The resulting distribution is approximately flat over nine decades in $\log P$, consistent with Öpik's Law. However, there remain some significant observational selection effects that may eventually alter this conclusion. Detailed spectroscopic and high angular resolution studies of massive stars in specific clusters with known distances will be particularly helpful in assessing the importance of such selection effects and determining the complete binary properties of a young massive star population (cf. Kiminki & Kobulnicky 2012; Sana et al. 2013b).

We are grateful to Denise Taylor of STScI for her remarkably effective efforts that made these *HST* observations possible. We also thank John Subasavage, Sergio Dieterich, and Adric Riedel for their support of the FGS work at Georgia State University. Support for *HST* proposal numbers GO-11212, 11901, 11943, and 11944 was provided by NASA through a grant from the Space Telescope Science Institute, which is operated by the Association of Universities for Research in Astronomy, Incorporated, under NASA contract NAS5-26555. Institutional support has been provided from the GSU College of Arts and Sciences and from the Research Program Enhancement fund of the Board of Regents of the University System of Georgia, administered through the GSU Office of the Vice President for Research and Economic Development. JMA acknowledges support from [a] the Spanish Government Ministerio de Economía y Competitividad (MINECO) through grants AYA2010-15 081 and AYA2010-17 631 and [b] the Consejería de Educación of the Junta de Andalucía through grant P08-TIC-4075. AFJM is grateful to NSERC (Canada) and FQRNT (Quebec) for financial assistance. NDR gratefully acknowledges his CRAQ (Quebec) fellowship. This research has made use of the Washington Double Star Catalog maintained at the U. S. Naval Observatory and the WEBDA database, operated at the Institute for Astronomy of the University of Vienna.

Facilities: HST

A. Notes on Individual Stars

024044.94+611656.1 = HD16429. McSwain (2003) found that the spectrum is a composite of an SB1 system and constant velocity component. We assumed that one of these is the angularly resolved companion for counting purposes.

025107.97+602503.9 = HD17505. The companion is resolved on the y-axis only and is far off-axis along the x-direction. The results are consistent with the separation $2\farcs15$ and position angle $92\fdg7$ found by Maíz Apellániz (2010), although our estimated magnitude difference is slightly larger. Sota et al. (2011) obtained resolved spectra of both components and

found that both are O-type stars. Note that component A of this pair is itself a spectroscopic triple star system (Hillwig et al. 2006).

040751.39+621948.4 = HD25639 = SZ Cam. Resolved on both axes for the first observation (at a position consistent with that found by Balega et al. 2007), but only resolved along the y-axis in the second observation. We adopted the magnitude difference from the first observation and the second derivative amplitude a_x to estimate $|\triangle x|$ for the second observation. Gorda et al. (2007) show that the system consists of a short period eclipsing binary with a distant companion that is probably also a binary (making the system a hierarchical quadruple). We assumed that the resolved component CHR 209 Ea,Eb is this second system for counting purposes.

051618.15+341844.3 = HD34078. We did not detect the close ($\rho = 0\farcs35$) companion of AE Aur discovered by Turner et al. (2008) (TRN 17 Aa,Ab), which may have been an artifact of their adaptive optics observations (see §4).

051756.06-691603.9 = HDE269321. This close pair is resolved along the y-axis only in both of our closely spaced observations.

051814.36-691501.1 = HD35343 = S Dor. The companion is beyond the x-axis scan range in the second (short scan) observation.

053051.48-690258.6 = HDE269662. The companion is close, faint, and detected along the y-axis only in two closely spaced observations.

053522.90-052457.8 = HD37041A = θ^2 Ori A. The CHR 249 Aa,Ab pair is clearly resolved in the first observation, but in the second short scan observation the companion is beyond the scan range in x and is only partially resolved in the y direction.

062715.78+145321.2 = HD45314. Mason et al. (1998) used speckle interferometry to resolve this target as a binary with a separation of $0\farcs054$ (named CHR 251 AB), but it was not resolved again in subsequent speckle observations (Mason et al. 2009). It appears single in the FGS scans.

064548.70-071839.0 = ALS85. This is a triple system where components B and C are comparable in brightness. Consequently, the correspondence between the components observed in both axes is ambiguous. Table 2 lists the result where the closer component is assumed to be B in both cases. If B has the larger projected separation in the y-axis scan, then the result for A,B is $\theta = 219\fdg87 \pm 0\fdg18$ and $\rho = 0\farcs3378 \pm 0\farcs0013$ and the result for A,C is $\theta = 233\fdg29 \pm 0\fdg20$ and $\rho = 0\farcs3117 \pm 0\farcs0011$.

071842.49-245715.8 = HD57061. τ CMa is a multiple system with two components

revealed by the FGS observations. The wider component was detected along both axes in the first observation, but only along the x-axis in the second observation. There is a low amplitude peak in the cross correlation function for the second observation near the expected projected separation ($\triangle y \approx +0.19$) but it is below the adopted detection threshold. The system consists of a long period SB1 and a short period eclipsing system (van Leeuwen & van Genderen 1997; Stickland et al. 1998), and we assumed that these two correspond to the bright resolved pair FIN 313 Aa,Ab. The WDS currently identifies Ab as the brighter of the two central objects, so we subtracted 180° in position angle and changed the sign of $\triangle m$ to make our results consistent with the others in the WDS for the Aa,Ab pair. The wider component Ab,E appears in the WDS with a 180° difference in position angle, but a reassessment of AstraLux Lucky Imaging observations by Maíz Apellániz (2010) indicates a placement consistent with the FGS results.

075220.28-262546.7 = HD64315. This system was resolved as a binary by Mason et al. (2009) and named WSI 54 AB. Recent observations by Hartkopf et al. (2012) agree with the position angle and separation estimated from the FGS observations (Table 2). However, speckle observations by Tokovinin et al. (2010) suggest that the system may consist of a triple in a linear configuration, and hence our binary measurements may correspond to the center of light of the two companions. The fit of the x-axis scan with two components is marginal, but experiments with three component fits made little or no improvement, so we present the binary results in Table 2 for simplicity. Lorenzo et al. (2010) present a spectroscopic study and argue that the system consists of one SB2 system with a period of $P = 2.71$ d plus one SBE system with a period of 1.018 d. We assumed that each of these correspond to components of the resolved binary for counting purposes.

081517.15-354414.6 = CD-35 4384. This is a triple system with an inner companion Ab detected by FGS. It was difficult to rectify the low frequency trends in these long scans (particularly for the x-axis) and the magnitude difference for the wide pair Aa,B is taken from the y-axis result. Note that the actual uncertainty in magnitude difference may be larger than quoted in Table 2, because we do not account for spatial photometric sensitivity variations that become significant for widely separated systems.

081903.90-360844.9 = CD-35 4471. The companion was resolved along the y-axis only, but the second derivative test was nearly met for the x-axis result. Thus, we estimated $|\triangle x|$ from the y-axis magnitude difference and second derivative amplitude a_x. The result given in Table 2 corresponds to an assumed position at $+\triangle x$; for a projected position of $-\triangle x$, the position angle is $\theta = 146\overset{\circ}{.}4 \pm 6\overset{\circ}{.}1$.

084351.09-460346.5 = CD-45 4462. The FGS scans reveal this as a triple system. All three components appear in the y-axis scan, but the central pair is blended together in the

x-axis scan. However, the second derivative amplitude is quite large for the central blend, so we estimated $|\triangle x|$ from the y-axis magnitude difference and second derivative amplitude a_x. Table 2 lists the position angle of A,B for $+\triangle x$, and the position angle for $-\triangle x$ is $\theta = 20\overset{\circ}{.}0 \pm 3\overset{\circ}{.}3$. All the magnitude differences are from the y-scan results.

085322.01-460208.8 = CD-45 4676. The B companion is resolved along the y-axis and blended with the central fringe along the x-axis. The second derivative test criterion is met in the latter case, so we estimated $|\triangle x|$ from the y-axis magnitude difference and second derivative amplitude a_x. The position angle for $+\triangle x$ is given in Table 2, and that for $-\triangle x$ is $\theta = 342\overset{\circ}{.}31 \pm 0\overset{\circ}{.}09$.

090221.56-484154.4 = CD-48 4352. This target appears as a triple in the y-axis scan and appears single in the x-axis scan. However, the central fringe in the x-axis scan passes the second derivative test, and we assume that the implied fringe broadening is due only to the closer and brighter B component (i.e., that the wider and fainter C component falls beyond the recorded x-axis scan). Then we estimated $|\triangle x|$ from the y-axis magnitude difference and second derivative amplitude a_x. The $+|\triangle x|$ solution is used for the position angle in Table 2, and the result for $-|\triangle x|$ is $\theta = 18\overset{\circ}{.}6 \pm 2\overset{\circ}{.}9$.

100639.88-572533.1 = CPD-56 2853. The faint companion is resolved along the y-axis only. In this case the projected separation ($\triangle y = 0\overset{''}{.}2$) is wide enough that we cannot say whether or not the the companion is blended or off-scan along the x-axis, and consequently we simply present a lower limit for the separation in Table 2.

104505.85-594006.4 = HDE303308. This target was detected as a close binary in earlier FGS observations by Nelan et al. (2004, 2010) with $\theta = 122^\circ \pm 32^\circ$ and $\rho = 0\overset{''}{.}015 \pm 0\overset{''}{.}002$ (resolved on the y-axis only). We obtained two additional observations that do not resolve the system. However, the second derivative test was suggestive of a companion (reaching a S/N ratio of 3.3 for the y-axis scan of the second observation, but still below our detection criterion of S/N > 4). Taking the second derivative amplitudes at their face values yields the minimum separations and position angles given in Table 3. Note that solution ${}^a\theta_2$ in the first observation is consistent with ${}^a\theta_1$ in the second observation. The fact that three independent observations all yield similar binary parameters indicates that this system is probably a long period, wide binary. The spectroscopic status is controversial. Chini et al. (2012) found the star to be radial velocity constant in ten observations. On the other hand, Levato et al. (1991) measured one very low radial velocity over an eight night run, consistent with a short period eccentric binary orbit. Consequently, we label the spectroscopic status as "SB1?" in Table 1.

164120.41-484546.6 = HD150136. The companion resolved in x only is consistent in

position and magnitude difference with the known A,B pair. A companion with $\rho = 0\farcs0073$ detected in VLTI Amber observations by Sanchez-Bermudez et al. (2013) is too close to be resolved in the FGS data. Sana et al. (2013a) discuss the orbits of the close binary and third star, and we include their period estimates in the spectroscopic category for Figure 4.

172912.93-313203.4 = HD158186. A companion is detected along the y-axis only. We adopt $\triangle x = 0$ in Table 2.

181512.97-202316.7 = HD167263. The close pair of 16 Sgr (CHR255 Aa,Ab) was observed in three previous speckle measurements with a position angle difference of 180° from the FGS results, but this is not unexpected for stars of similar brightness.

181805.90-121433.3 = HD167971. De Becker et al. (2012) resolved this system with the VLTI and argued that it has an orbital period $P > 20$ yr. However, the separation was about 9 mas in 2008, which was too close for resolution with the somewhat noisier FGS scans we obtained. It is a hierarchical triple system with a close central binary.

182119.55-162226.1 = HD168625. This target appears triple in the x-scans but double in the y-scan. It is not clear which of the two components in the x-scan corresponds to the single component in the y-scan, but we assumed that the component B with the smaller projected separation along the x-axis corresponds to the resolved component along the y-axis (and that component C falls beyond the range recorded for the y-scan). The magnitude differences are taken from the x-axis data. The central fringe appeared somewhat asymmetrical in both x and y compared to those for the calibrator stars. Note that in the long scans made after 2009.1 (like this case) we often observe a weak feature at $\triangle x = -1\farcs2$ that has a systematic origin and should not be confused with a faint companion. Only companion B is recorded along the x-axis in the second, short scan observation. Component B is probably the companion detected in VLT-NACO observations by Martayan et al. (2012).

200329.40+360130.5 = HD190429. Long scans were made to detect the signal of the wide B component. There are a few reports of a closer and fainter companion MCA 59 Aa,Ab at a separation of $\approx 0\farcs1$ (most recently by Mason et al. 1998). However, this close companion is not detected in the FGS scans.

201806.99+404355.5 = HD193322A. This is a remarkable multiple system that is the subject of a detailed study with the CHARA Array long baseline interferometer by ten Brummelaar et al. (2011). The FGS observations resolve the Aa,Ab pair along the y-axis, but the pair is blended in the x-axis scan. A blend is indicated by the second derivative test and we used the y-scan magnitude difference and second derivative amplitude to find $|\triangle x|$. The solution using $-|\triangle x|$ is listed in Table 2, and the separation and position angle estimates agree well with contemporaneous CHARA Array measurements (ten Brummelaar

et al. 2011).

201851.71+381646.5 = HD193443A. This system appears in the WDS with the brighter component identified as B, so we added 180° to the position angle and changed the sign of $\triangle m$ for consistency with the results in the WDS.

213857.62+572920.5 = HD206267. This pair is resolved along the y-axis only, but the projected separation and magnitude difference are consistent with those for the known MIU 2 Aa,Ab system if the projected separation is small along the x-axis. The results in Table 2 assume $\triangle x = 0$. The system is an hierarchical triple (Stickland 1995; Burkholder et al. 1997), and we assumed that the resolved companion is the third star identified in the spectrum.

REFERENCES

Albacete Colombo, J. F., Morrell, N. I., Niemela, V. S., & Corcoran, M. F. 2001, MNRAS, 326, 78

Alduseva, V. I., Aslanov, A. A., Kolotilov, E. A., & Cherepashchuk, A. M. 1982, Soviet Astronomy Letters, 8, 386

Bagnuolo, Jr., W. G., & Barry, D. J. 1996, ApJ, 469, 347

Bagnuolo, Jr., W. G., Gies, D. R., Riddle, R., & Penny, L. R. 1999, ApJ, 527, 353

Balega, I. I., Balega, Y. Y., Maksimov, A. F., et al. 2007, Astrophysical Bulletin, 62, 339

Balona, L., & Crampton, D. 1974, MNRAS, 166, 203

Barbá, R. H., Gamen, R., Arias, J. I., et al. 2010, in Revista Mexicana de Astronomia y Astrofisica, vol. 27, Vol. 38, Revista Mexicana de Astronomia y Astrofisica Conference Series, 30–32

Bassino, L. P. 1985, AJ, 90, 2249

Bate, M. R. 2012, MNRAS, 419, 3115

Blomme, R., De Becker, M., Runacres, M. C., van Loo, S., & Setia Gunawan, D. Y. A. 2007, A&A, 464, 701

Bonnell, I. A., & Bate, M. R. 2005, MNRAS, 362, 915

Bonnell, I. A., & Smith, R. J. 2011, in IAU Symposium, Vol. 270, Computational Star Formation, ed. J. Alves, B. G. Elmegreen, J. M. Girart, & V. Trimble (Cambridge, UK: Cambridge University Press), 57–64

Boyajian, T. S., Gies, D. R., Baines, E. K., et al. 2007a, PASP, 119, 742

Boyajian, T. S., Gies, D. R., Dunn, J. P., et al. 2007b, ApJ, 664, 1121

Brandeker, A., Jayawardhana, R., Khavari, P., Haisch, Jr., K. E., & Mardones, D. 2006, ApJ, 652, 1572

Burkholder, V., Massey, P., & Morrell, N. 1997, ApJ, 490, 328

Buscombe, W., & Kennedy, P. M. 1965, MNRAS, 130, 281

Caballero-Nieves, S. M. 2012, PhD thesis, Georgia State University

Caballero-Nieves, S. M., Nelan, E. P., Gies, D. R., et al. 2014, AJ, 147, 40

Cameron, E. 2011, PASA, 28, 128

Cappa de Nicolau, C. E., Niemela, V. S., & Arnal, E. M. 1986, AJ, 92, 1414

Chentsov, E. L., & Gorda, E. S. 2004, Astronomy Letters, 30, 461

Chentsov, E. L., Klochkova, V. G., Panchuk, V. E., Yushkin, M. V., & Nasonov, D. S. 2013, Astronomy Reports, 57, 527

Chini, R., Hoffmeister, V. H., Nasseri, A., Stahl, O., & Zinnecker, H. 2012, MNRAS, 424, 1925

Chochol, D., & Grygar, J. 1974, Bulletin of the Astronomical Institutes of Czechoslovakia, 25, 231

Christy, J. W. 1977, ApJ, 217, 127

Clark, J. S., Najarro, F., Negueruela, I., et al. 2012, A&A, 541, A145

Close, L. M., Puglisi, A., Males, J. R., et al. 2012, ApJ, 749, 180

Conti, P. S., Ebbets, D., Massey, P., & Niemela, V. S. 1980, ApJ, 238, 184

Conti, P. S., Leep, E. M., & Lorre, J. J. 1977, ApJ, 214, 759

Correia, S., Zinnecker, H., Ratzka, T., & Sterzik, M. F. 2006, A&A, 459, 909

Corti, M., Niemela, V., & Morrell, N. 2003, A&A, 405, 571

Crampton, D. 1972, MNRAS, 158, 85

Crampton, D., & Fisher, W. A. 1974, Publications of the Dominion Astrophysical Observatory Victoria, 14, 283

Cruz-González, C., Recillas-Cruz, E., Costero, R., Peimbert, M., & Torres-Peimbert, S. 1974, Rev. Mexicana Astron. Astrofis., 1, 211

Cvetković, Z., Vince, I., & Ninković, S. 2010, New A, 15, 302

De Becker, M., Linder, N., & Rauw, G. 2010, New A, 15, 76

De Becker, M., & Rauw, G. 2004, A&A, 427, 995

De Becker, M., Rauw, G., & Linder, N. 2009, ApJ, 704, 964

De Becker, M., Rauw, G., & Manfroid, J. 2004, A&A, 424, L39

De Becker, M., Sana, H., Absil, O., Le Bouquin, J.-B., & Blomme, R. 2012, MNRAS, 423, 2711

de Wit, W. J., Testi, L., Palla, F., & Zinnecker, H. 2005, A&A, 437, 247

Denoyelle, J. 1987, A&AS, 70, 373

Duchêne, G., & Kraus, A. 2013, ARA&A, 51, 269

Duflot, M., Figon, P., & Meyssonnier, N. 1995, A&AS, 114, 269

Feast, M. W., Thackeray, A. D., & Wesselink, A. J. 1955, MmRAS, 67, 51

—. 1957, MmRAS, 68, 1

Fullerton, A. W., Gies, D. R., & Bolton, C. T. 1996, ApJS, 103, 475

García, B., Malaroda, S., Levato, H., Morrell, N., & Grosso, M. 1998, PASP, 110, 53

Garcia-Lario, P., Riera, A., & Manchado, A. 1998, A&A, 334, 1007

Garmany, C. D., Conti, P. S., & Chiosi, C. 1982, ApJ, 263, 777

Garmany, C. D., Conti, P. S., & Massey, P. 1980, ApJ, 242, 1063

Gies, D. R., & Bolton, C. T. 1986, ApJS, 61, 419

Gies, D. R., Fullerton, A. W., Bolton, C. T., et al. 1994, ApJ, 422, 823

Gies, D. R., Mason, B. D., Hartkopf, W. I., et al. 1993, AJ, 106, 2072

Gorda, S. Y., Balega, Y. Y., Pluzhnik, E. A., & Shkhagosheva, Z. U. 2007, Astrophysical Bulletin, 62, 352

Götz, D., Falanga, M., Senziani, F., et al. 2007, ApJ, 655, L101

Groh, J. H., Hillier, D. J., & Damineli, A. 2011, ApJ, 736, 46

Grundstrom, E. D., Boyajian, T. S., Finch, C., et al. 2007, ApJ, 660, 1398

Gualandris, A., Portegies Zwart, S., & Eggleton, P. P. 2004, MNRAS, 350, 615

Gudennavar, S. B., Bubbly, S. G., Preethi, K., & Murthy, J. 2012, ApJS, 199, 8

Harmanec, P. 1987, Bulletin of the Astronomical Institutes of Czechoslovakia, 38, 283

Hartkopf, W. I., & Mason, B. D. 2004, in Revista Mexicana de Astronomia y Astrofisica Conference Series, ed. C. Allen & C. Scarfe, Vol. 21, 83–90

Hartkopf, W. I., Tokovinin, A., & Mason, B. D. 2012, AJ, 143, 42

Hill, G., Hilditch, R. W., Aikman, G. C. L., & Khalesseh, B. 1994, A&A, 282, 455

Hill, G., & Holmgren, D. E. 1995, A&A, 297, 127

Hill, P. W. 1971, MmRAS, 75, 1

Hillwig, T. C., Gies, D. R., Bagnuolo, Jr., W. G., et al. 2006, ApJ, 639, 1069

Horch, E. P., Franz, O. G., Wasserman, L. H., & Heasley, J. N. 2006, AJ, 132, 836

Huang, W., & Gies, D. R. 2006, ApJ, 648, 580

Humphreys, R. M. 1978, ApJS, 38, 309

Israelian, G., Herrero, A., Musaev, F., et al. 2000, MNRAS, 316, 407

Kaczmarek, T., Olczak, C., & Pfalzner, S. 2011, A&A, 528, A144

Kiminki, D. C., & Kobulnicky, H. A. 2012, ApJ, 751, 4

Kiminki, D. C., Kobulnicky, H. A., Kinemuchi, K., et al. 2007, ApJ, 664, 1102

Kobulnicky, H. A., Smullen, R. A., Kiminki, D. C., et al. 2012, ApJ, 756, 50

Kobulnicky, H. A., Kiminki, D. C., Lundquist, M. J., et al. 2014, ApJS, in press

Kratter, K. M., Matzner, C. D., & Krumholz, M. R. 2008, ApJ, 681, 375

Kraus, S., Weigelt, G., Balega, Y. Y., et al. 2009, A&A, 497, 195

Krumholz, M. R., Klein, R. I., McKee, C. F., Offner, S. S. R., & Cunningham, A. J. 2009, Science, 323, 754

Kuiper, R., & Yorke, H. W. 2013, ApJ, 772, 61

Lafrenière, D., Jayawardhana, R., van Kerkwijk, M. H., Brandeker, A., & Janson, M. 2014, ApJ, 785, 47

Larson, R. B. 2010, Reports on Progress in Physics, 73, 014901

Levato, H., Malaroda, S., Morrell, N., Garcia, B., & Hernandez, C. 1991, ApJS, 75, 869

Levato, H., Morrell, N., Garcia, B., & Malaroda, S. 1988, ApJS, 68, 319

Lorenzo, J., Simón-Díaz, S., Negueruela, I., & Vilardell, F. 2010, in Astronomical Society of the Pacific Conference Series, Vol. 435, Binaries - Key to Comprehension of the Universe, ed. A. Prša & M. Zejda (San Francisco: ASP), 409

Machado, M. A. D., de Araújo, F. X., Pereira, C. B., & Fernandes, M. B. 2002, A&A, 387, 151

Mahy, L., Martins, F., Machado, C., Donati, J.-F., & Bouret, J.-C. 2011, A&A, 533, A9

Mahy, L., Rauw, G., De Becker, M., Eenens, P., & Flores, C. A. 2013, A&A, 550, A27

Maíz Apellániz, J. 2010, A&A, 518, A1

Maíz-Apellániz, J., Walborn, N. R., Galué, H. Á., & Wei, L. H. 2004, ApJS, 151, 103

Maíz Apellániz, J., Sota, A., Morrell, N. I., et al. 2013, in Massive Stars: From alpha to Omega, arXiv/1306.6417

Markova, N., Puls, J., Scuderi, S., Simón-Díaz, S., & Herrero, A. 2011, A&A, 530, A11

Markwardt, C. B. 2009, in Astronomical Society of the Pacific Conference Series, Vol. 411, Astronomical Data Analysis Software and Systems XVIII, ed. D. A. Bohlender, D. Durand, & P. Dowler (San Francisco: ASP), 251

Martayan, C., Lobel, A., Baade, D., et al. 2012, in Astronomical Society of the Pacific Conference Series, Vol. 464, Circumstellar Dynamics at High Resolution, ed. A. C. Carciofi & T. Rivinius (San Francisco: ASP), 293

Martins, F., Schaerer, D., & Hillier, D. J. 2005, A&A, 436, 1049

Mason, B. D., Gies, D. R., Hartkopf, W. I., et al. 1998, AJ, 115, 821

Mason, B. D., Hartkopf, W. I., Gies, D. R., Henry, T. J., & Helsel, J. W. 2009, AJ, 137, 3358

Mason, B. D., Wycoff, G. L., Hartkopf, W. I., Douglass, G. G., & Worley, C. E. 2001, AJ, 122, 3466

Massey, P. 2000, PASP, 112, 144

Matt, S., & Pudritz, R. E. 2008, ApJ, 681, 391

Mayer, P., Lorenz, R., & Drechsel, H. 1997, A&A, 320, 109

Mayer, P., Lorenz, R., Drechsel, H., & Abseim, A. 2001, A&A, 366, 558

McSwain, M. V. 2003, ApJ, 595, 1124

McSwain, M. V., Boyajian, T. S., Grundstrom, E. D., & Gies, D. R. 2007, ApJ, 655, 473

Mel'Nik, A. M., & Dambis, A. K. 2009, MNRAS, 400, 518

Mermilliod, J.-C., & Mermilliod, M. 1994, Catalogue of Mean UBV Data on Stars (Berlin, Heidelberg, New York: Springer-Verlag)

Michalska, G., Niemczura, E., Pigulski, A., Steślicki, M., & Williams, A. 2013, MNRAS, 429, 1354

Moe, M., & Di Stefano, R. 2013, ApJ, 778, 95

Moffat, A. F. J., Jackson, P. D., & Fitzgerald, M. P. 1979, A&AS, 38, 197

Munari, U., & Tomasella, L. 1999, A&A, 343, 806

Muntean, V., Moffat, A. F. J., Chené, A. N., & de La Chevrotière, A. 2009, MNRAS, 399, 1977

Nazé, Y., Antokhin, I. I., Sana, H., Gosset, E., & Rauw, G. 2005, MNRAS, 359, 688

Nazé, Y., Mahy, L., Damerdji, Y., et al. 2012, A&A, 546, A37

Nazé, Y., Vreux, J.-M., & Rauw, G. 2001, A&A, 372, 195

Nelan, E., Younger, J., Makidon, R. B., et al. 2014, Fine Guidance Sensor Instrument Handbook for Cycle 22 v.21.0 (Baltimore: Space Telescope Science Institute)

Nelan, E. P., Walborn, N. R., Wallace, D. J., et al. 2004, AJ, 128, 323

—. 2010, AJ, 139, 2714

Neubauer, F. J. 1943, ApJ, 97, 300

Otero, S. A. 2005, Information Bulletin on Variable Stars, 5631, 1

Otero, S. A., & Wils, P. 2005, Information Bulletin on Variable Stars, 5644, 1

Penny, L. R. 1996, ApJ, 463, 737

Penny, L. R., Gies, D. R., Wise, J. H., Stickland, D. J., & Lloyd, C. 2002, ApJ, 575, 1050

Perryman, M. A. C., & ESA, eds. 1997, ESA Special Publication, Vol. 1200, The HIPPARCOS and TYCHO catalogues. Astrometric and photometric star catalogues derived from the ESA HIPPARCOS Space Astrometry Mission

Peter, D., Feldt, M., Henning, T., & Hormuth, F. 2012, A&A, 538, A74

Peton-Jonas, D. 1981, A&AS, 45, 193

Petrie, R. M., & Pearce, J. A. 1961, Publications of the Dominion Astrophysical Observatory Victoria, 12, 1

Pickles, A., & Depagne, É. 2010, PASP, 122, 1437

Popper, D. M. 1944, ApJ, 100, 94

—. 1950, ApJ, 111, 495

Raboud, D. 1996, A&A, 315, 384

Raghavan, D., McAlister, H. A., Henry, T. J., et al. 2010, ApJS, 190, 1

Rauch, T., Heber, U., Hunger, K., Werner, K., & Neckel, T. 1991, A&A, 241, 457

Rauw, G., Crowther, P. A., Eenens, P. R. J., Manfroid, J., & Vreux, J.-M. 2002, A&A, 392, 563

Rauw, G., Sana, H., Gosset, E., et al. 2000, A&A, 360, 1003

Rauw, G., Sana, H., Spano, M., et al. 2012, A&A, 542, A95

Richardson, N. D., Gies, D. R., Morrison, N. D., et al. 2012, in Astronomical Society of the Pacific Conference Series, Vol. 465, Proceedings of a Scientific Meeting in Honor of Anthony F. J. Moffat, ed. L. Drissen, C. Rubert, N. St-Louis, & A. F. J. Moffat (San Francisco: ASP), 160

Richardson, N. D., Gies, D. R., & Williams, S. J. 2011a, AJ, 142, 201

Richardson, N. D., Morrison, N. D., Gies, D. R., et al. 2011b, AJ, 141, 120

Rzaev, A. K., & Panchuk, V. E. 2008, Astronomy Reports, 52, 237

Sana, H., & Evans, C. J. 2011, in IAU Symposium, Vol. 272, IAU Symposium, ed. C. Neiner, G. Wade, G. Meynet, & G. Peters (Cambridge, UK: Cambridge Univ. Press), 474–485

Sana, H., Gosset, E., & Evans, C. J. 2009, MNRAS, 400, 1479

Sana, H., Le Bouquin, J.-B., De Becker, M., et al. 2011, ApJ, 740, L43

Sana, H., Le Bouquin, J.-B., Mahy, L., et al. 2013a, A&A, 553, A131

Sana, H., de Mink, S. E., de Koter, A., et al. 2012, Science, 337, 444

Sana, H., de Koter, A., de Mink, S. E., et al. 2013b, A&A, 550, A107

Sana, H., Le Bouquin, J.-B., Lacour, S., et al. 2014, ApJ, submitted

Sanchez-Bermudez, J., Schödel, R., Alberdi, A., et al. 2013, A&A, 554, L4

Simón-Díaz, S., Caballero, J. A., & Lorenzo, J. 2011, ApJ, 742, 55

Sota, A., Maíz Apellániz, J., Morrell, N. I., et al. 2014, ApJS, 211, 10

Sota, A., Maíz Apellániz, J., Walborn, N. R., et al. 2011, ApJS, 193, 24

Stahl, O., Wade, G., Petit, V., Stober, B., & Schanne, L. 2008, A&A, 487, 323

Stickland, D. J. 1995, The Observatory, 115, 180

—. 1996, The Observatory, 116, 294

—. 1997, The Observatory, 117, 37

Stickland, D. J., Koch, R. H., Pachoulakis, I., & Pfeiffer, R. J. 1994, The Observatory, 114, 107

Stickland, D. J., & Lloyd, C. 2001, The Observatory, 121, 1

Stickland, D. J., Lloyd, C., & Koch, R. H. 1997, The Observatory, 117, 143

Stickland, D. J., Lloyd, C., & Sweet, I. 1998, The Observatory, 118, 7

Stone, R. C. 1982, ApJ, 261, 208

ten Brummelaar, T. A., O'Brien, D. P., Mason, B. D., et al. 2011, AJ, 142, 21

Thackeray, A. D. 1966, MNRAS, 134, 97

Thackeray, A. D., Tritton, S. B., & Walker, E. N. 1973, MmRAS, 77, 199

Tokovinin, A., Mason, B. D., & Hartkopf, W. I. 2010, AJ, 139, 743

Tubbesing, S., Kaufer, A., Stahl, O., et al. 2002, A&A, 389, 931

Turner, N. H., ten Brummelaar, T. A., Roberts, L. C., et al. 2008, AJ, 136, 554

Underhill, A. B., & Hill, G. M. 1994, ApJ, 432, 770

van Genderen, A. M. 2001, A&A, 366, 508

van Leeuwen, F., & van Genderen, A. M. 1997, A&A, 327, 1070

Wegner, W. 1994, MNRAS, 270, 229

Williams, A. M., Gies, D. R., Bagnuolo, Jr., W. G., et al. 2001, ApJ, 548, 425

Williams, S. J. 2011, PhD thesis, Georgia State University

Williams, S. J., Gies, D. R., Hillwig, T. C., McSwain, M. V., & Huang, W. 2011, AJ, 142, 146

—. 2013, AJ, 145, 29

Wilson, R. E. 1953, Carnegie Institute Washington D.C. Publication, 601, 1

Zacharias, N., Finch, C. T., Girard, T. M., et al. 2013, AJ, 145, 44

Zinnecker, H., & Yorke, H. W. 2007, ARA&A, 45, 481

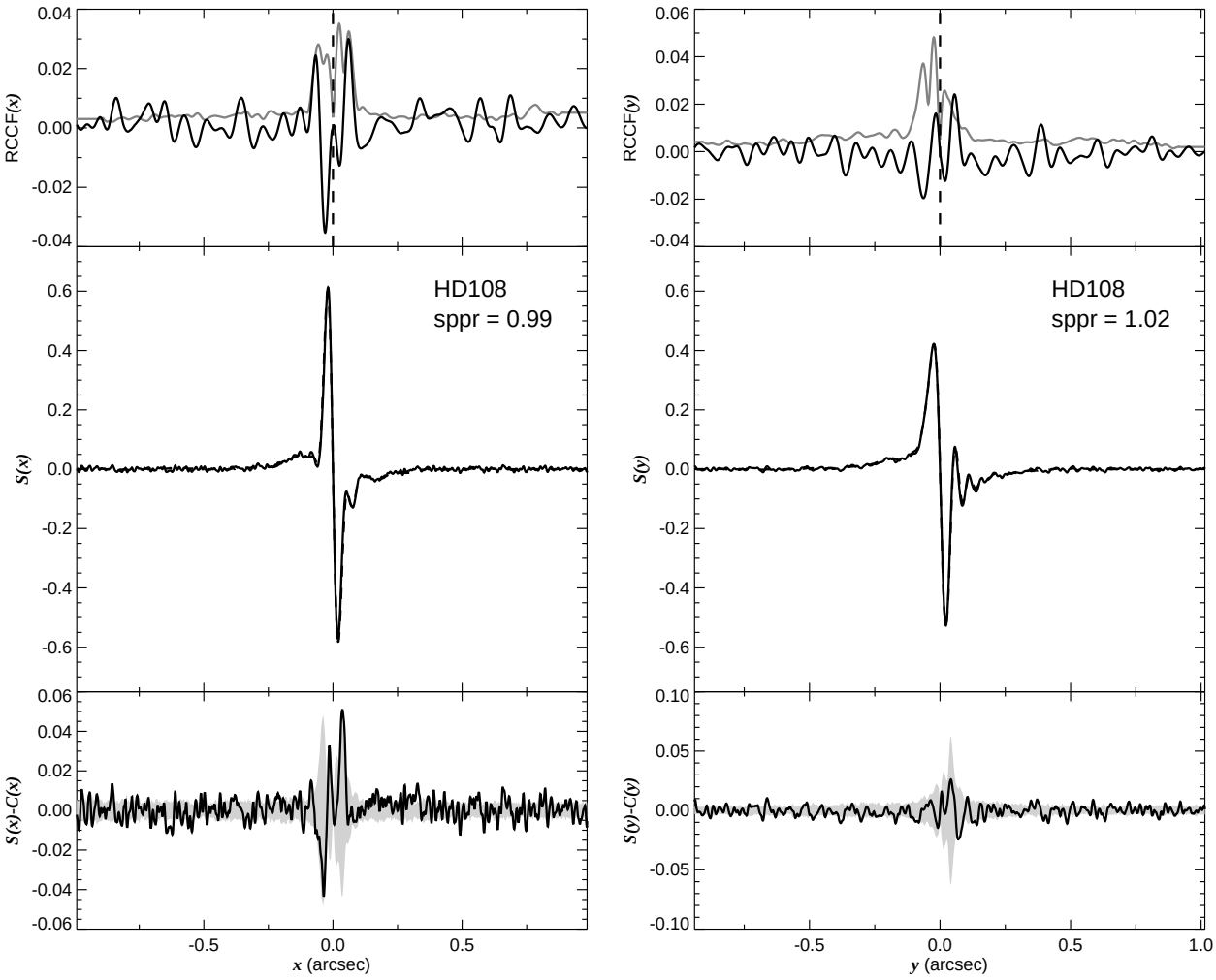

Fig. 1.1.— The FGS scans and binary detection tests for target 000603.39+634046.8 = HD108 obtained on BY 2008.5566. Figures 1.1 – 1.251 are available in the online version of the Journal.

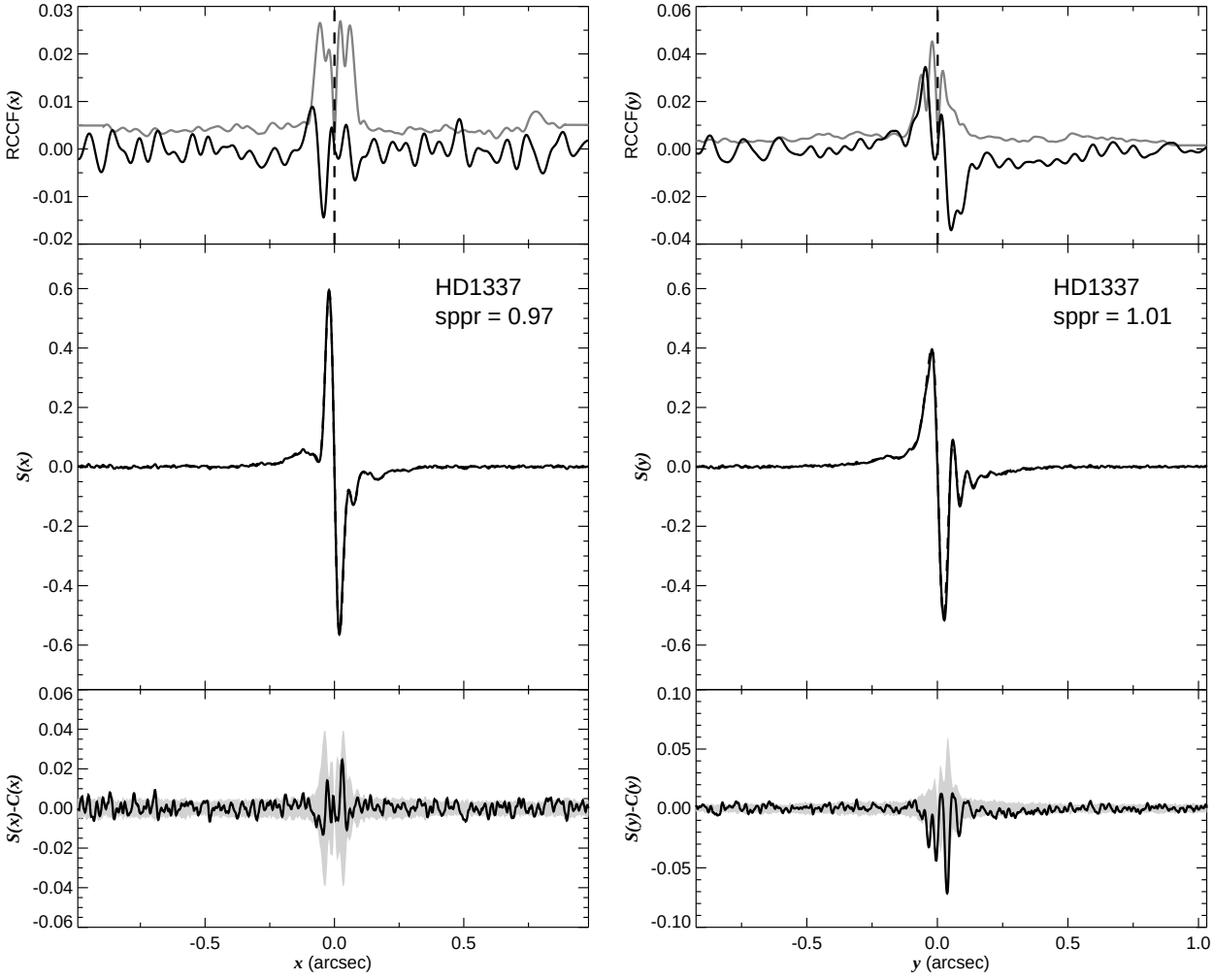

Fig. 1.2.— The FGS scans and binary detection tests for target 001743.06+512559.1 = HD1337 obtained on BY 2008.7090.

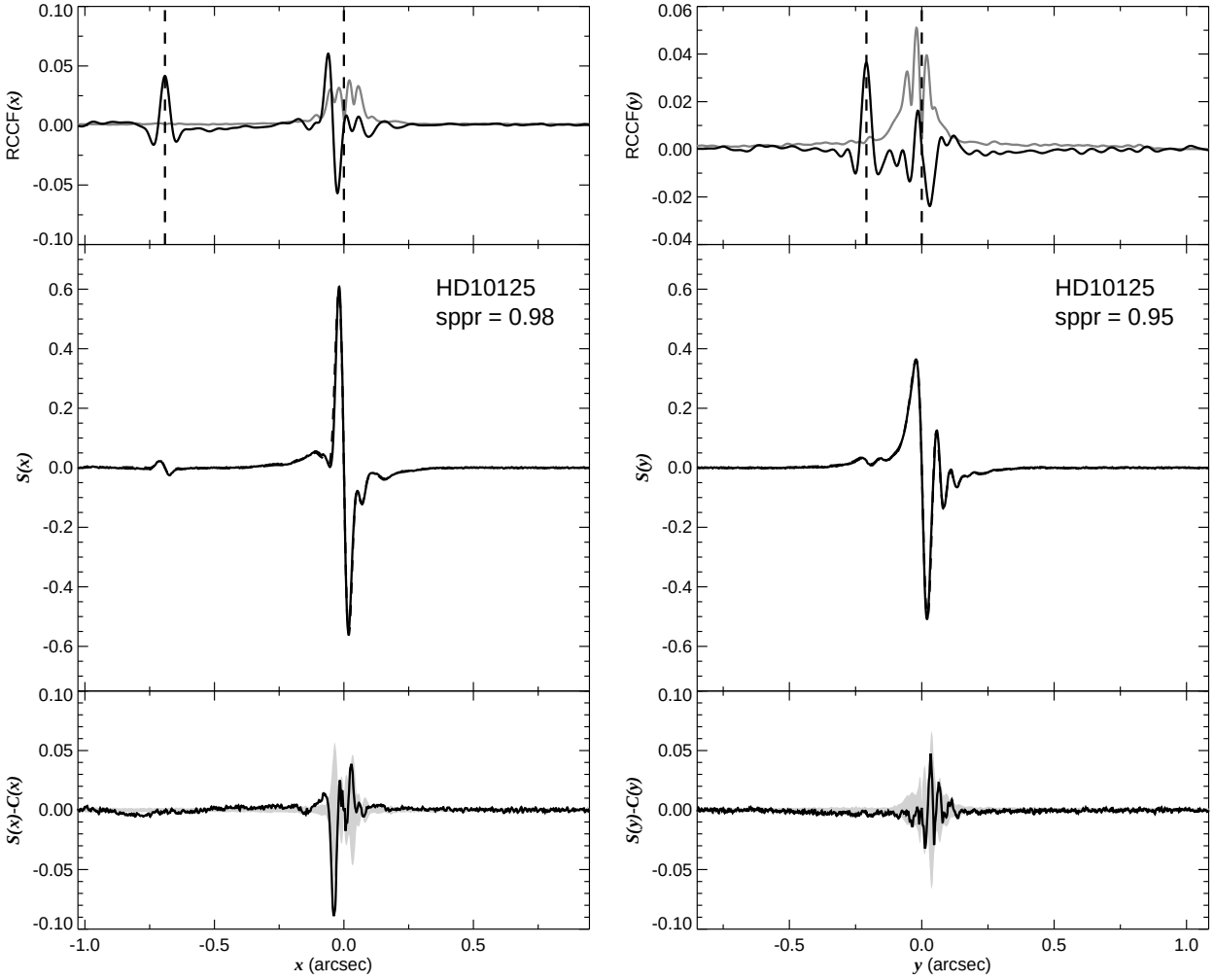

Fig. 1.3.— The FGS scans and binary detection tests for target 014052.76+641023.1 = HD10125 obtained on BY 2008.0775.

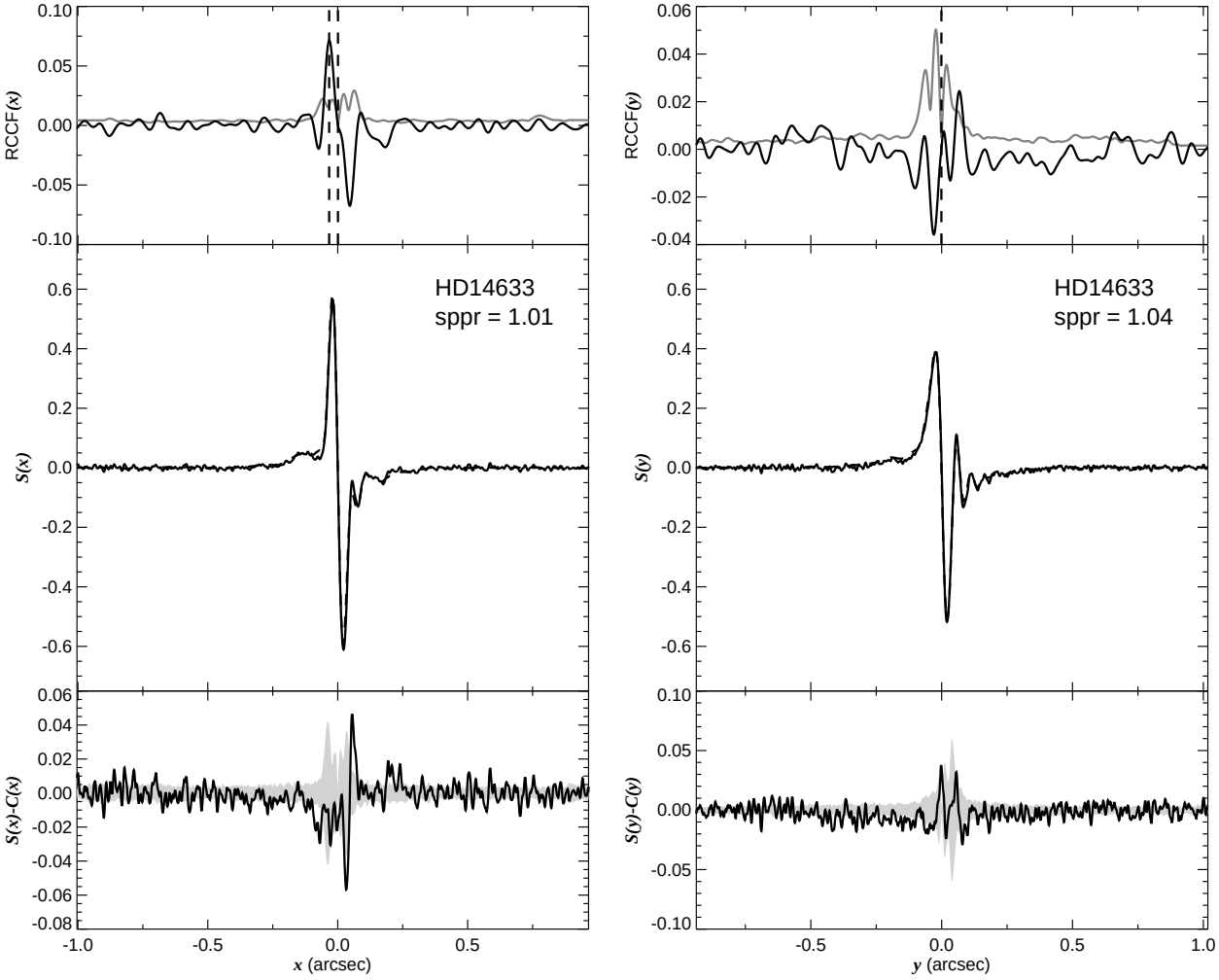

Fig. 1.4.— The FGS scans and binary detection tests for target 022254.29+412847.7 = HD14633 obtained on BY 2007.8425.

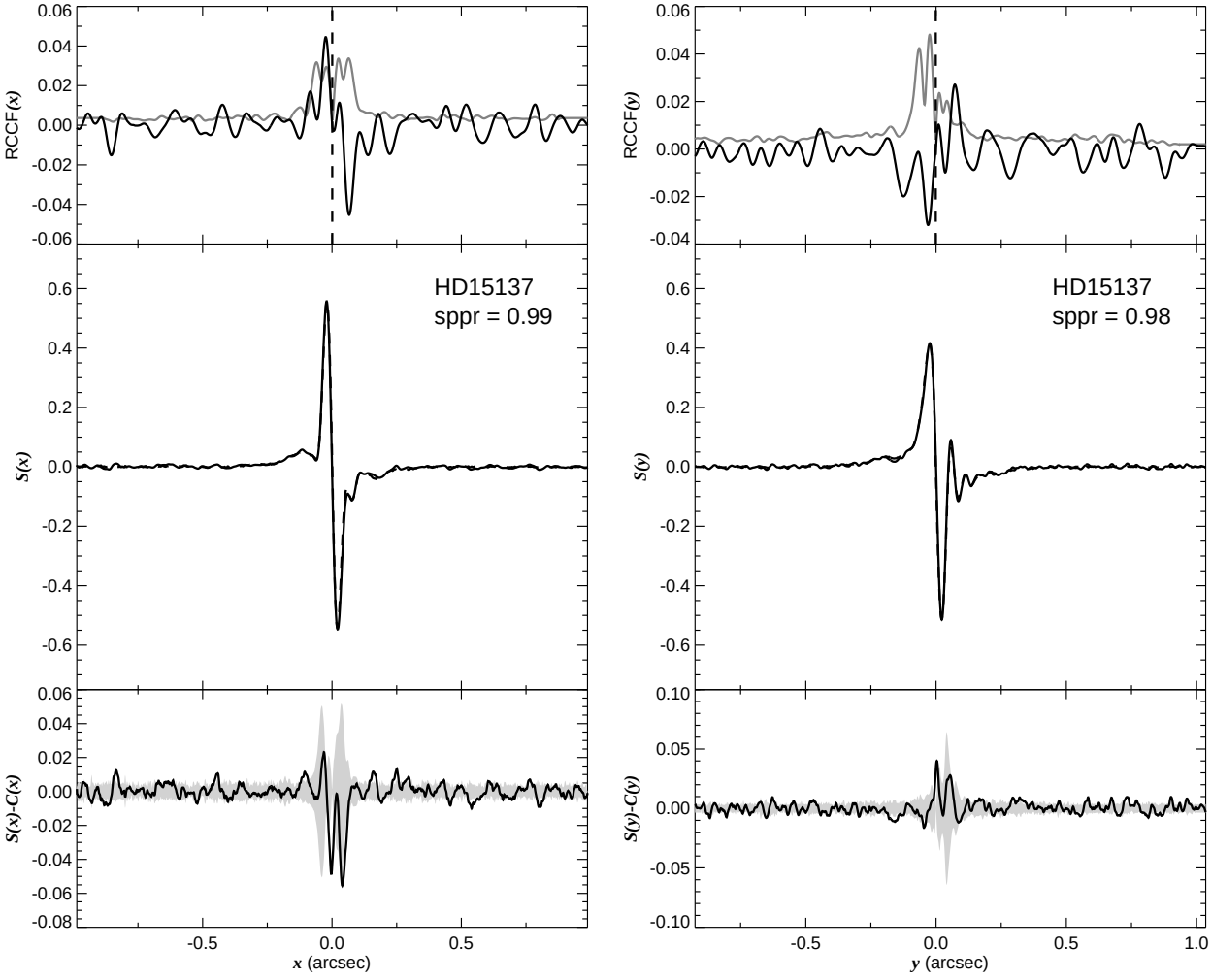

Fig. 1.5.— The FGS scans and binary detection tests for target 022759.81+523257.6 = HD15137 obtained on BY 2007.6777.

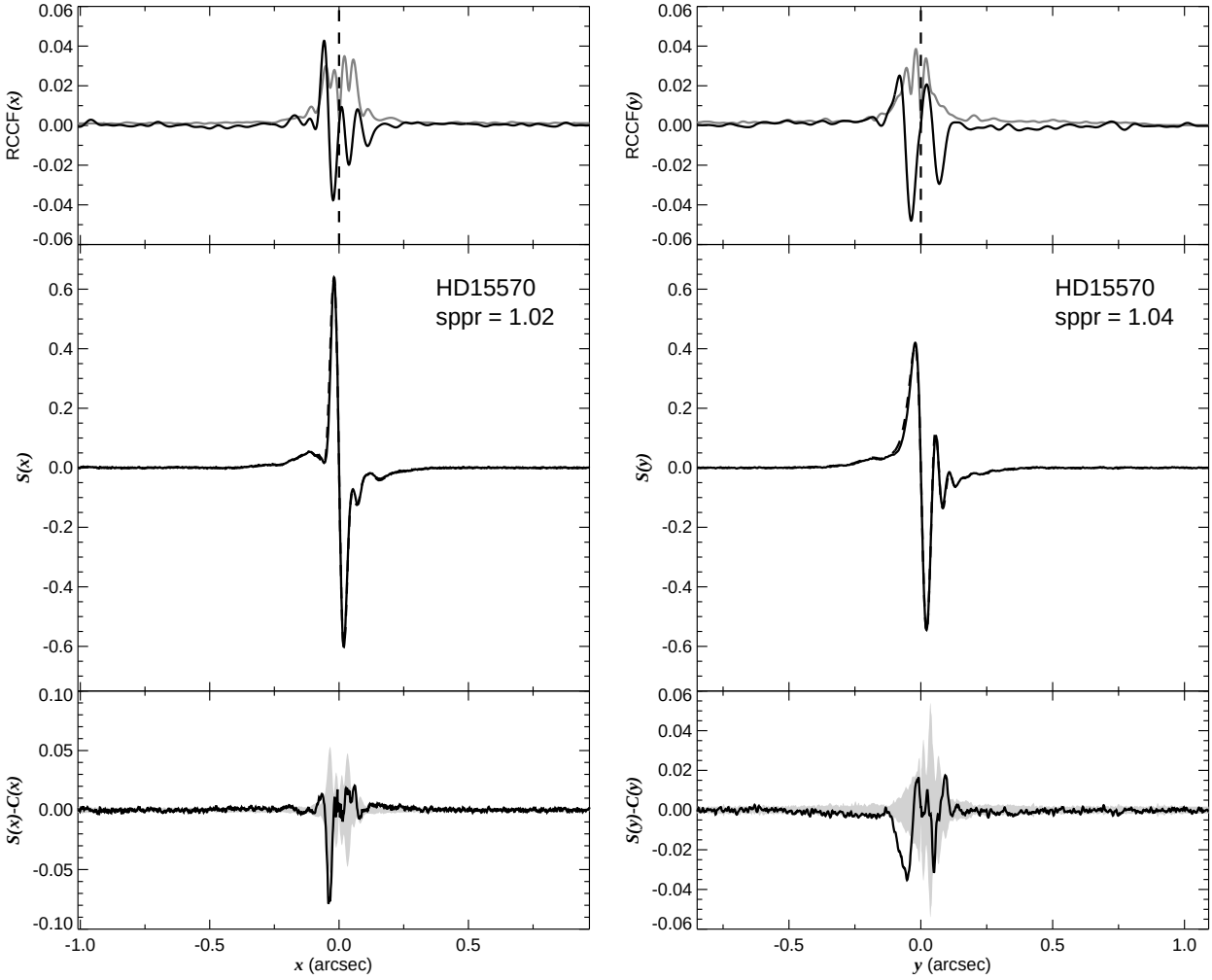

Fig. 1.6.— The FGS scans and binary detection tests for target 023249.42+612242.1 = HD15570 obtained on BY 2007.6478.

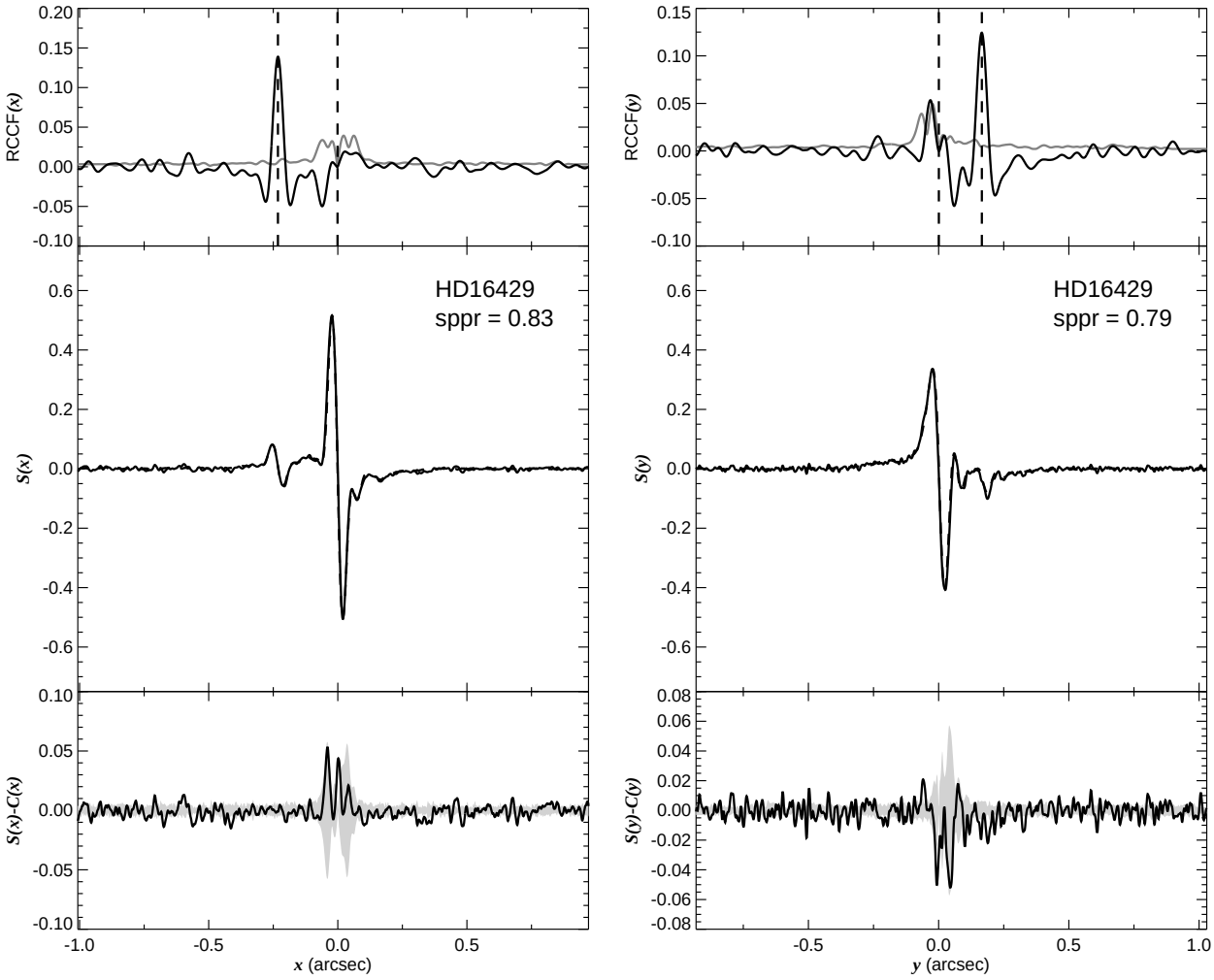

Fig. 1.7.— The FGS scans and binary detection tests for target 024044.94+611656.1 = HD16429 obtained on BY 2007.6831.

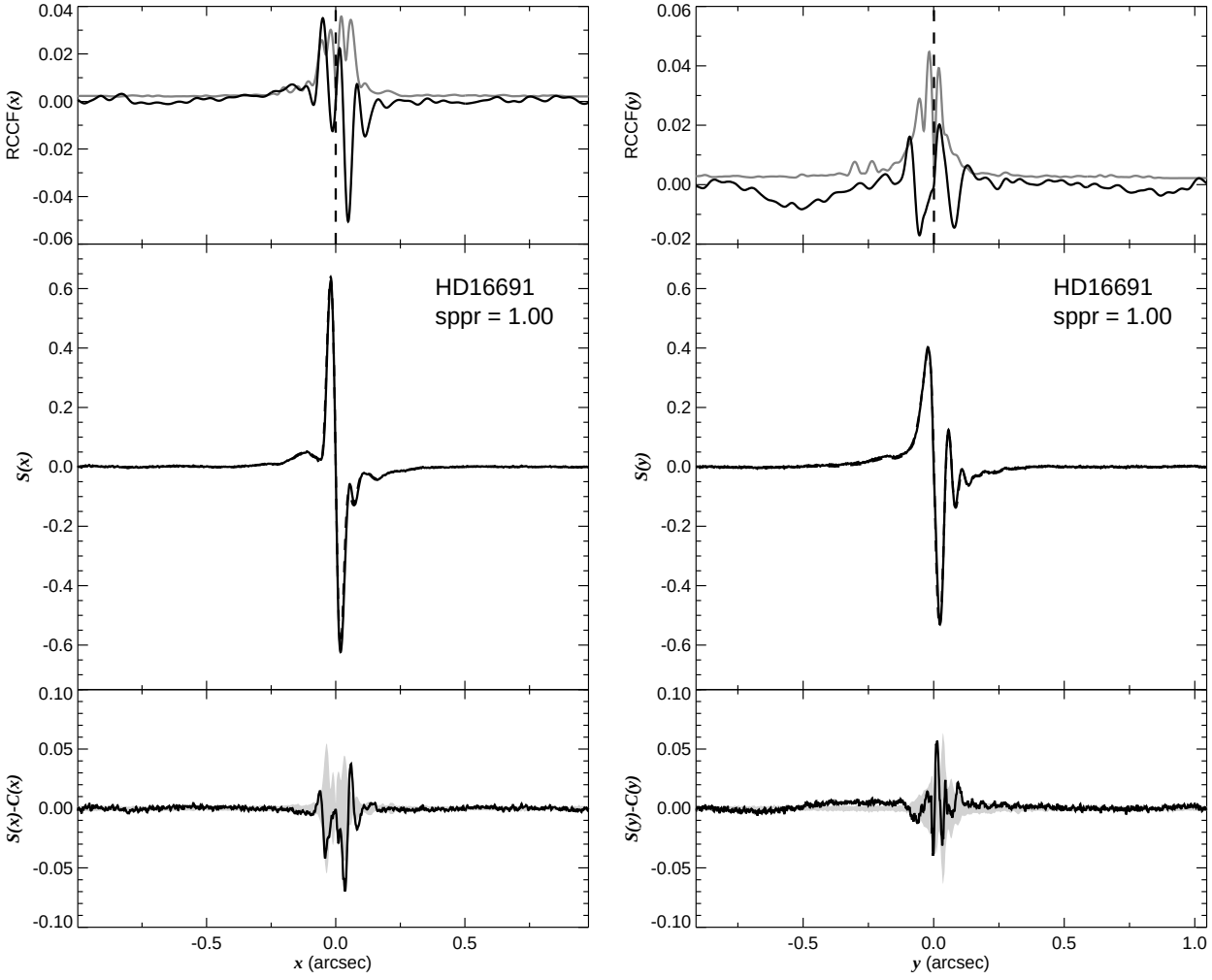

Fig. 1.8.— The FGS scans and binary detection tests for target 024252.03+565416.5 = HD16691 obtained on BY 2007.5274.

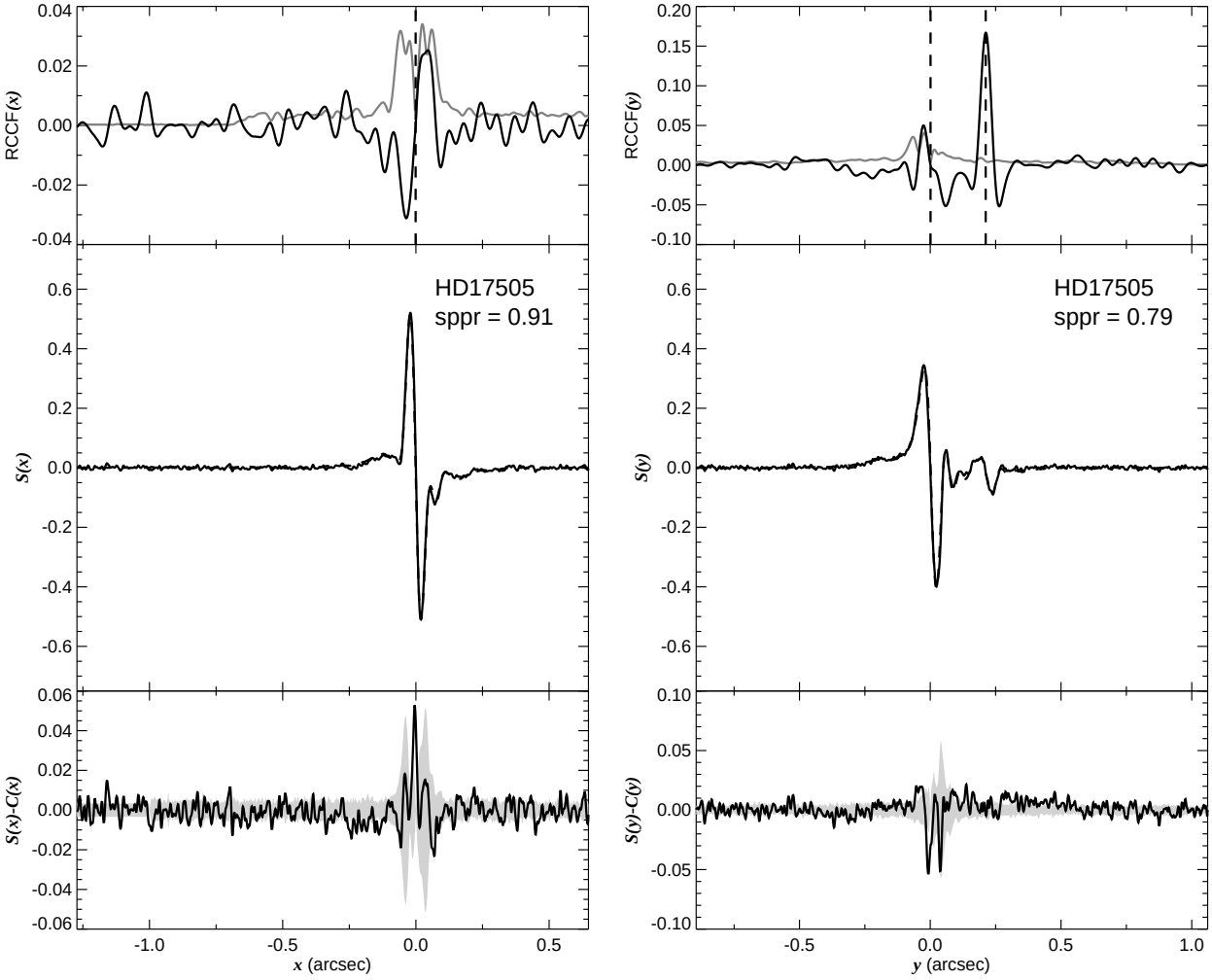

Fig. 1.9.— The FGS scans and binary detection tests for target 025107.97+602503.9 = HD17505 obtained on BY 2008.5621.

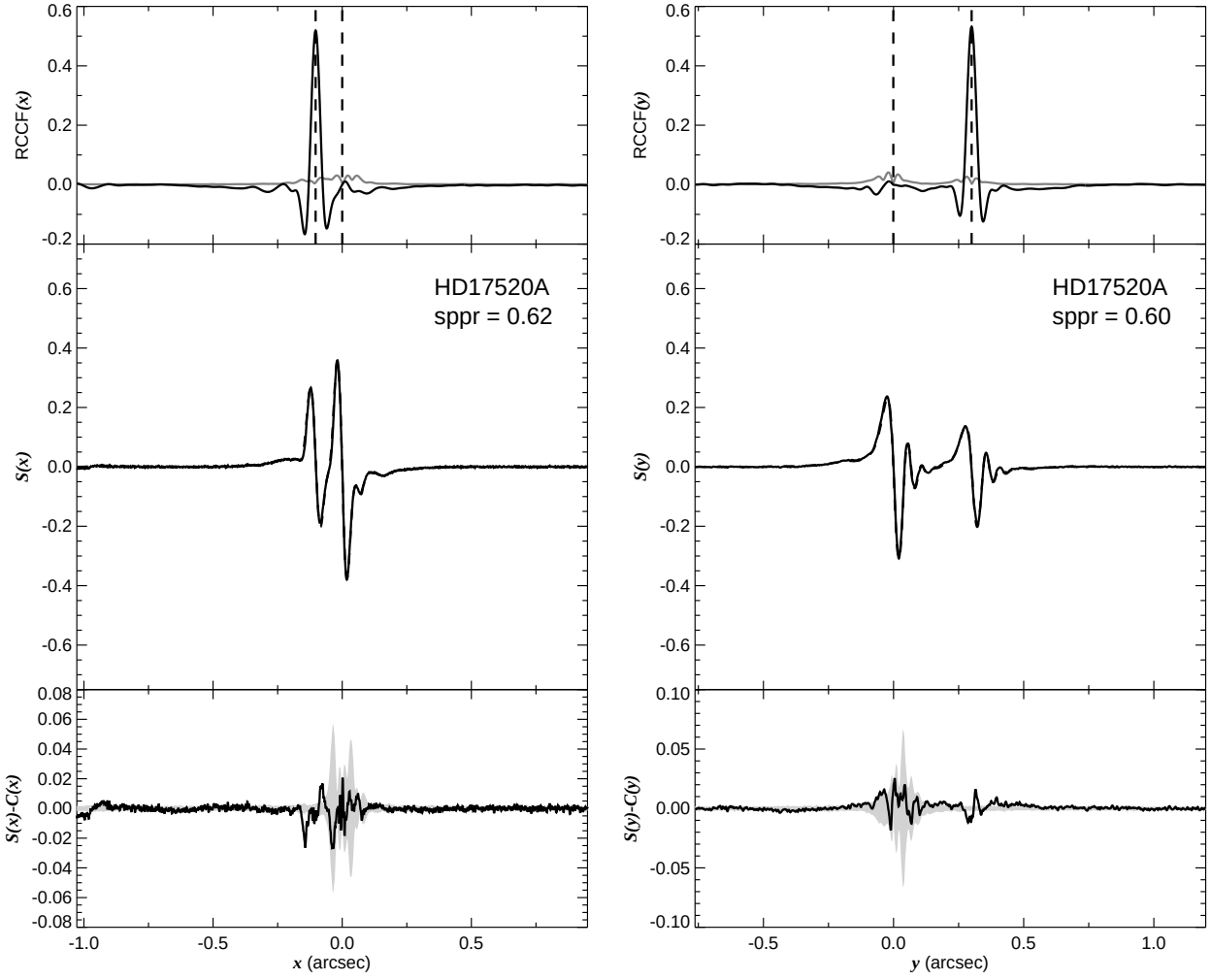

Fig. 1.10.— The FGS scans and binary detection tests for target 025114.46+602309.8 = HD17520 obtained on BY 2008.2139.

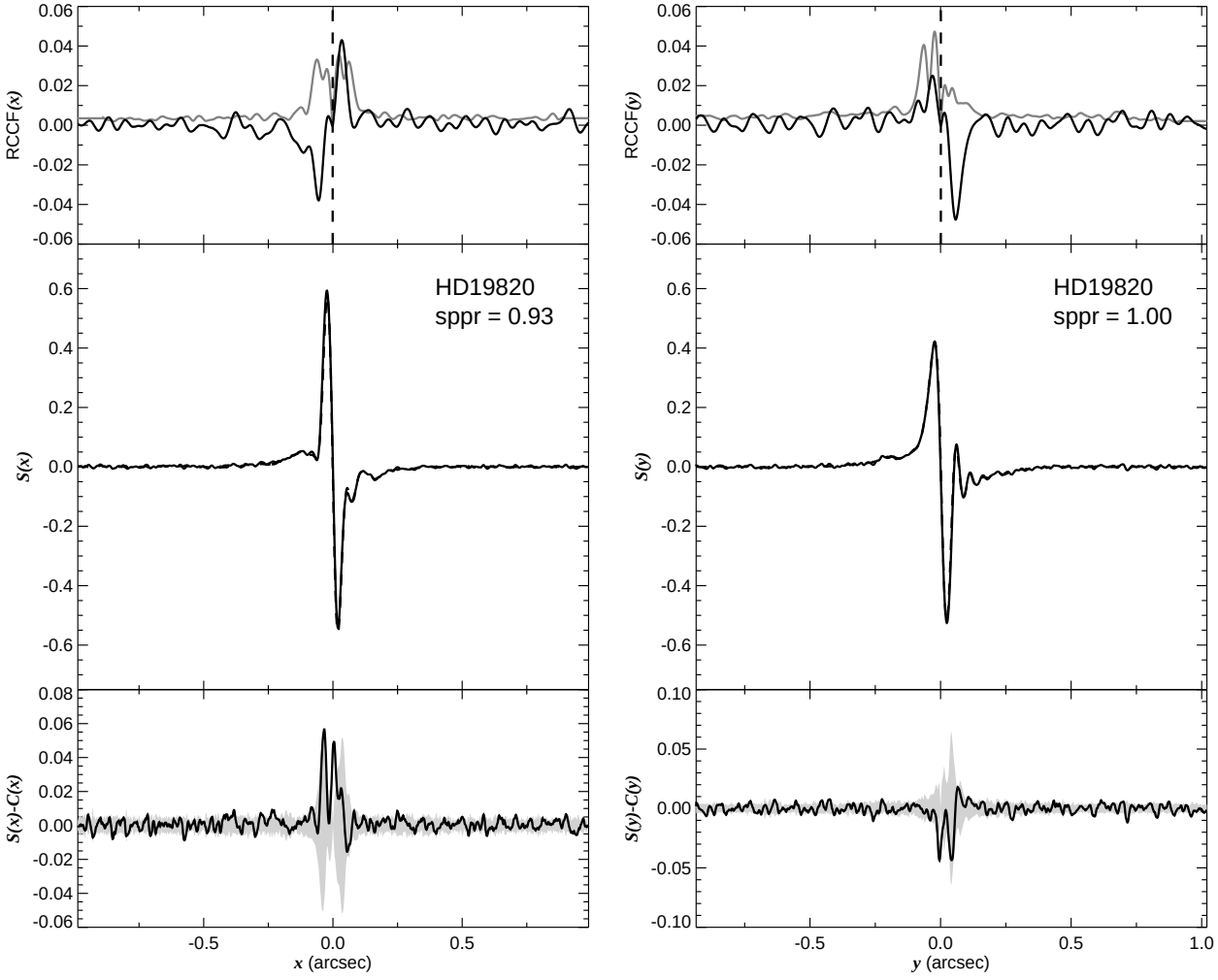

Fig. 1.11.— The FGS scans and binary detection tests for target 031405.34+593348.5 = HD19820 obtained on BY 2008.5757.

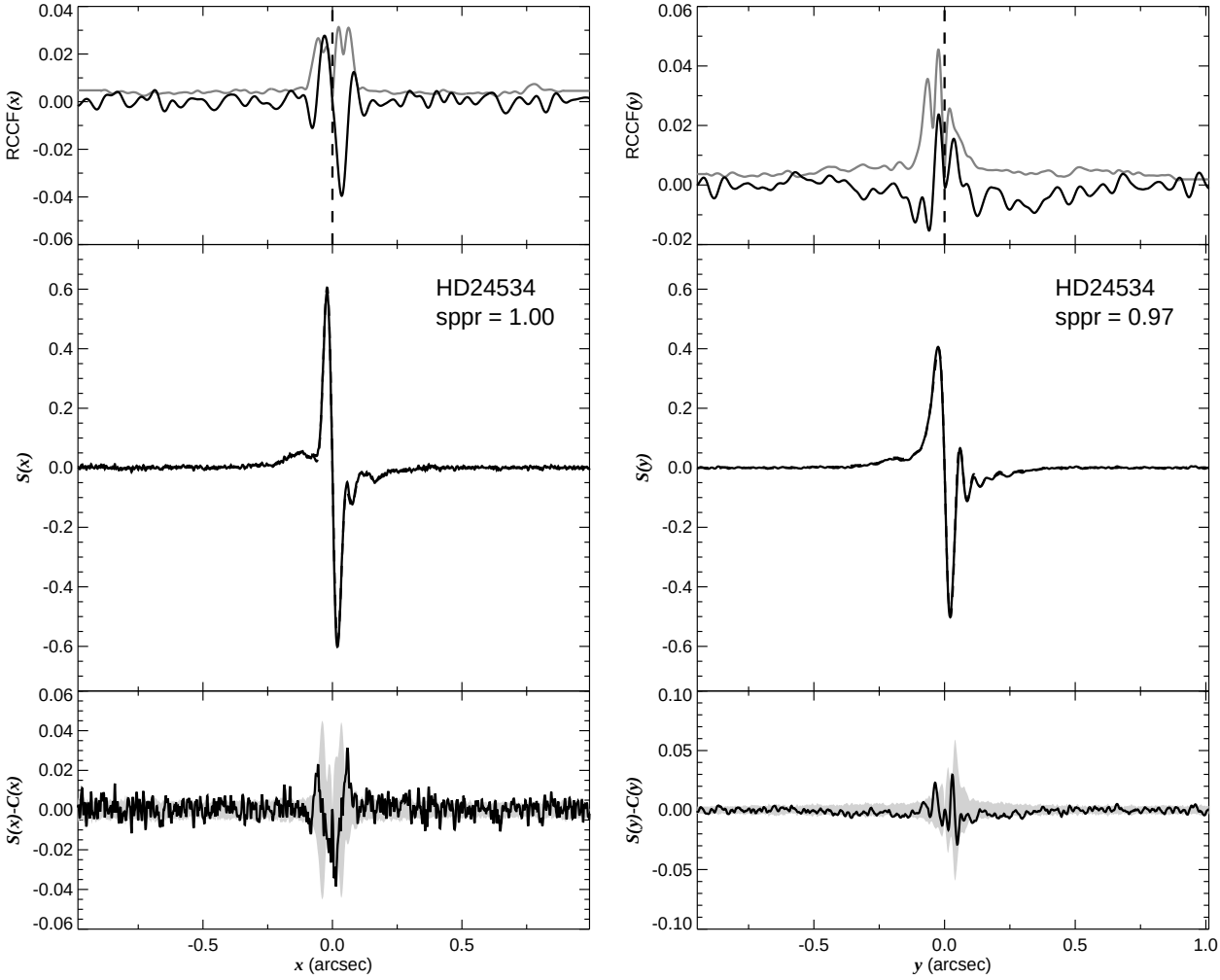

Fig. 1.12.— The FGS scans and binary detection tests for target 035523.08+310245.0 = HD24534 obtained on BY 2007.8372.

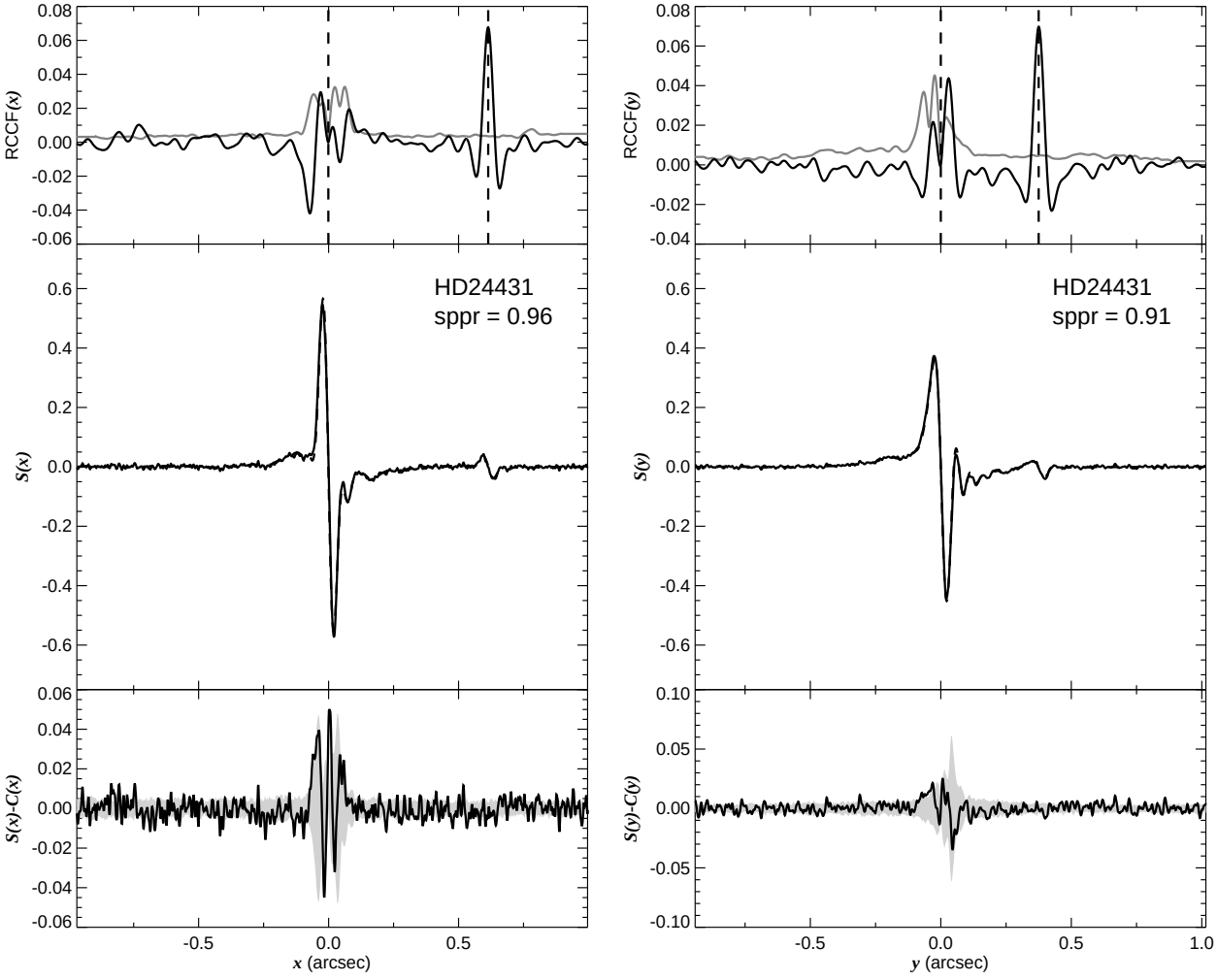

Fig. 1.13.— The FGS scans and binary detection tests for target 035538.42+523828.8 = HD24431 obtained on BY 2007.8465.

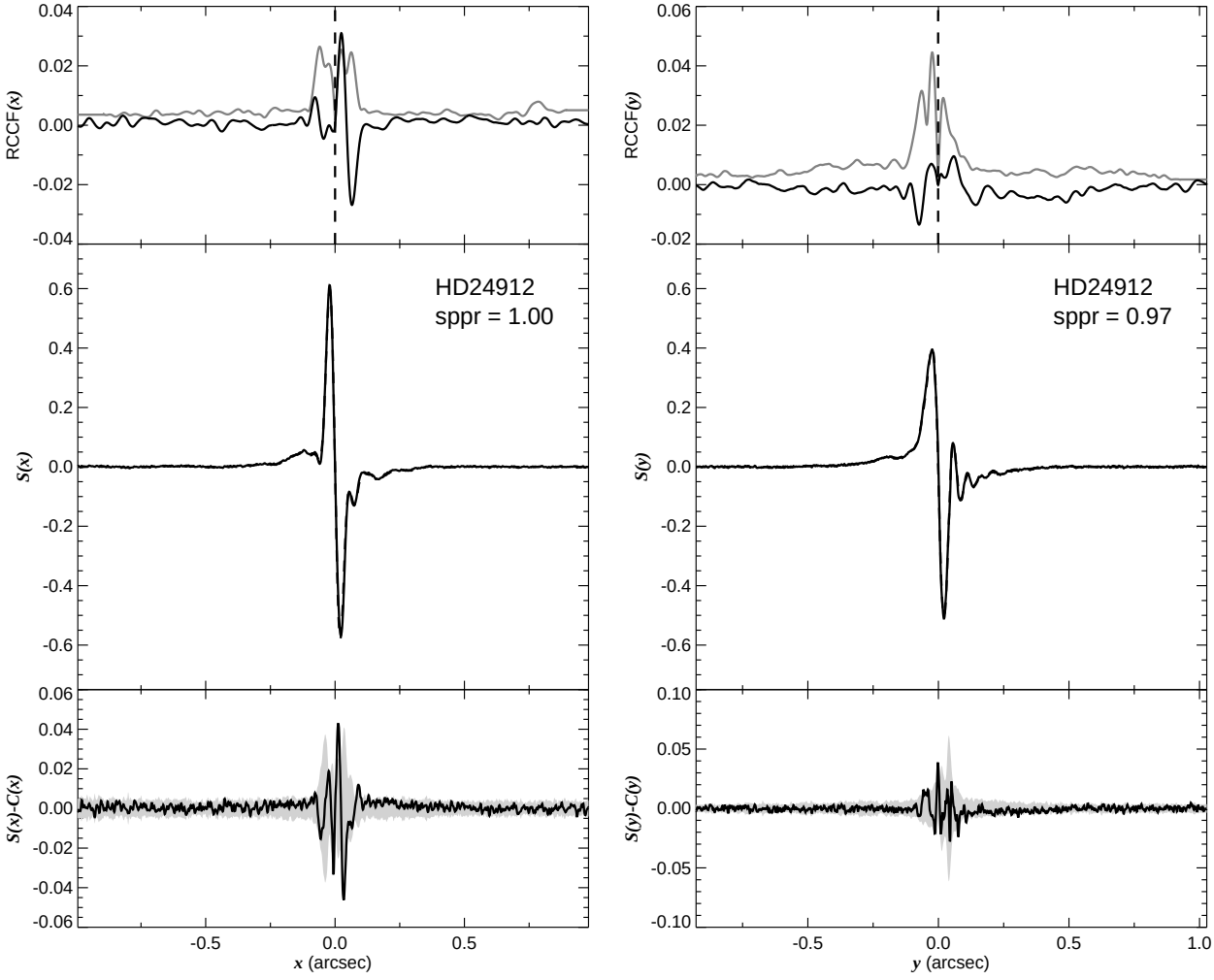

Fig. 1.14.— The FGS scans and binary detection tests for target 035857.90+354727.7 = HD24912 obtained on BY 2008.7092.

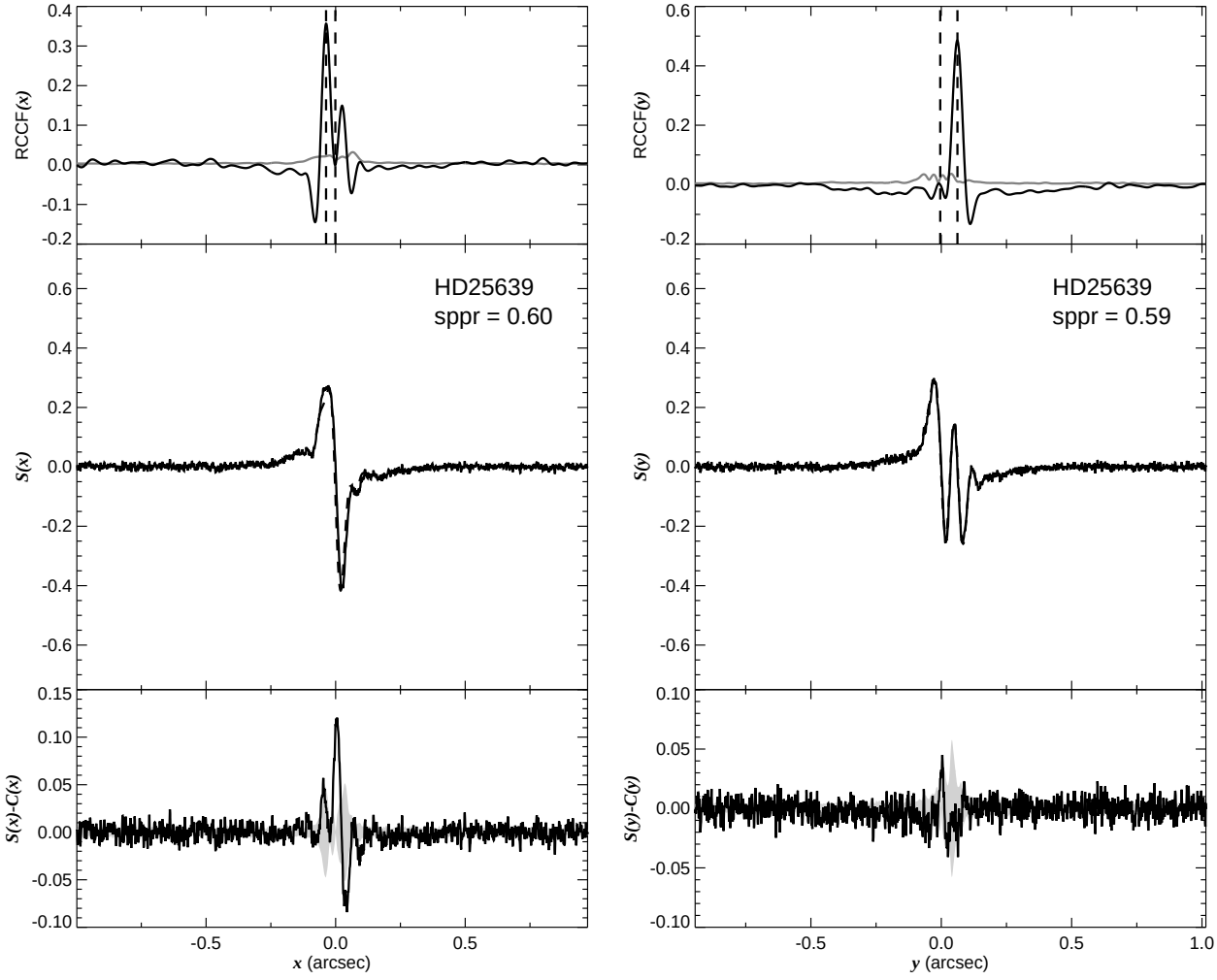

Fig. 1.15.— The FGS scans and binary detection tests for target 040751.39+621948.4 = HD25639 obtained on BY 2007.7682.

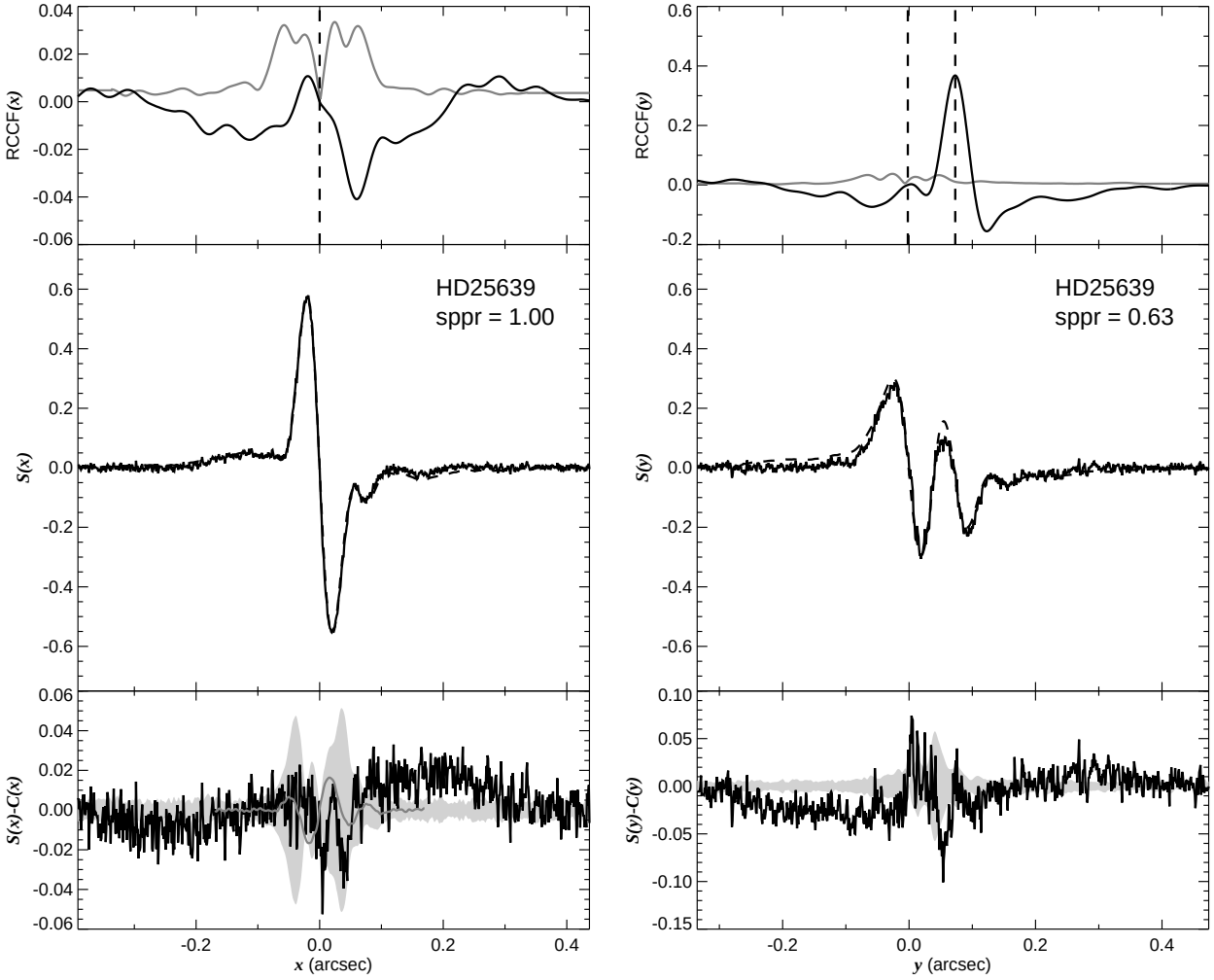

Fig. 1.16.— The FGS scans and binary detection tests for target 040751.39+621948.4 = HD25639 obtained on BY 2008.8682.

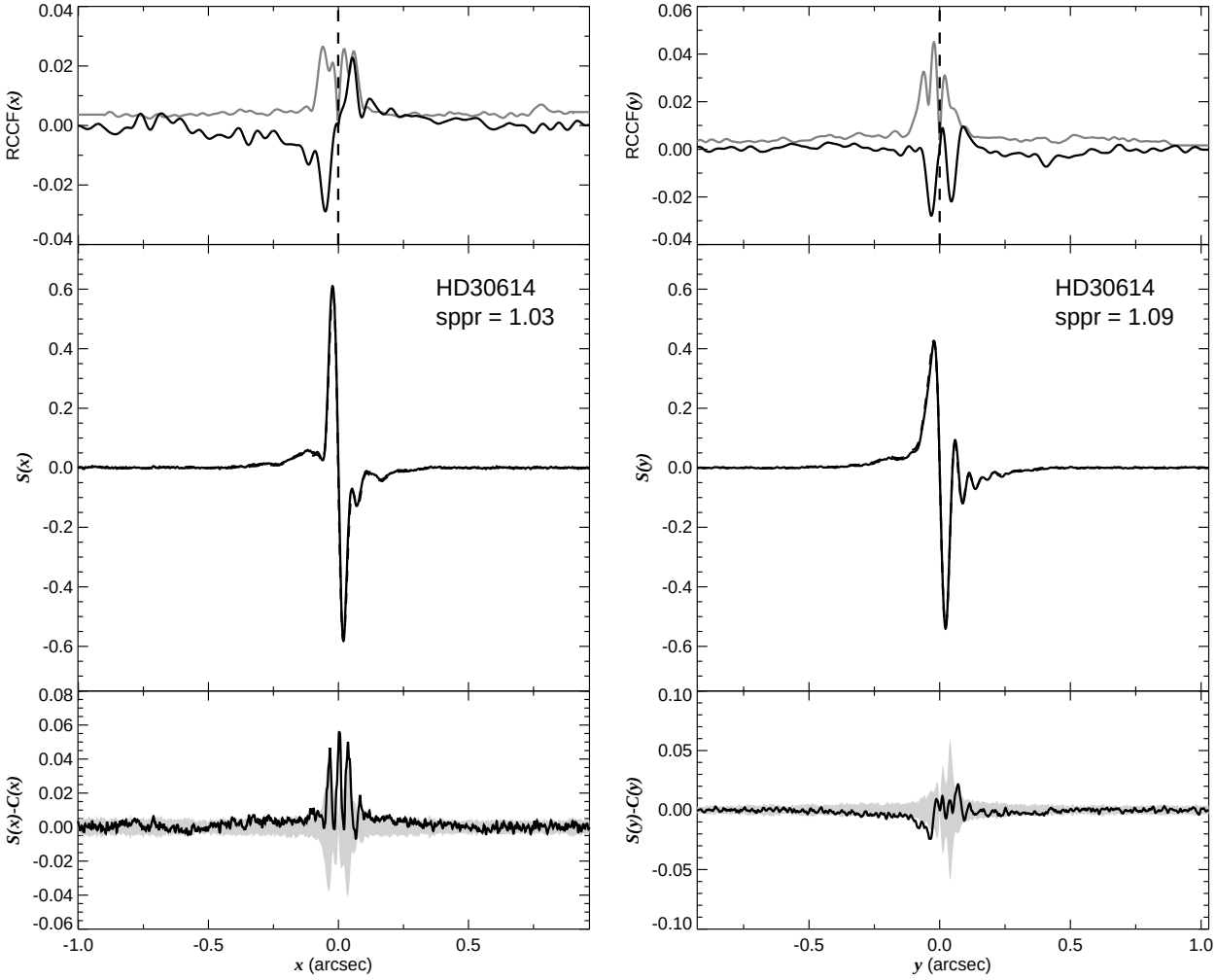

Fig. 1.17.— The FGS scans and binary detection tests for target 045403.01+662033.6 = HD30614 obtained on BY 2007.6615.

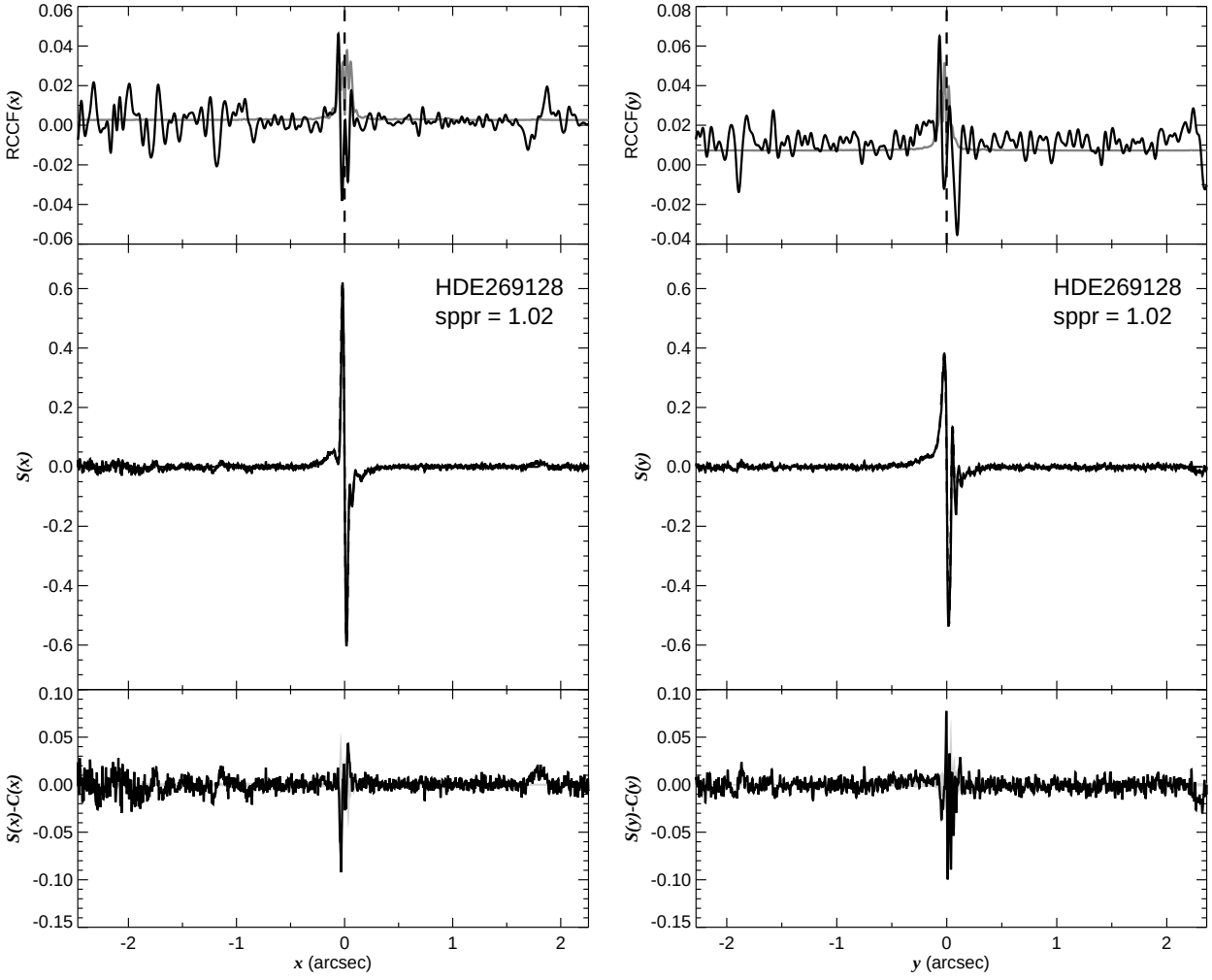

Fig. 1.18.— The FGS scans and binary detection tests for target 051022.79−684623.8 = HDE269128 obtained on BY 2008.9280.

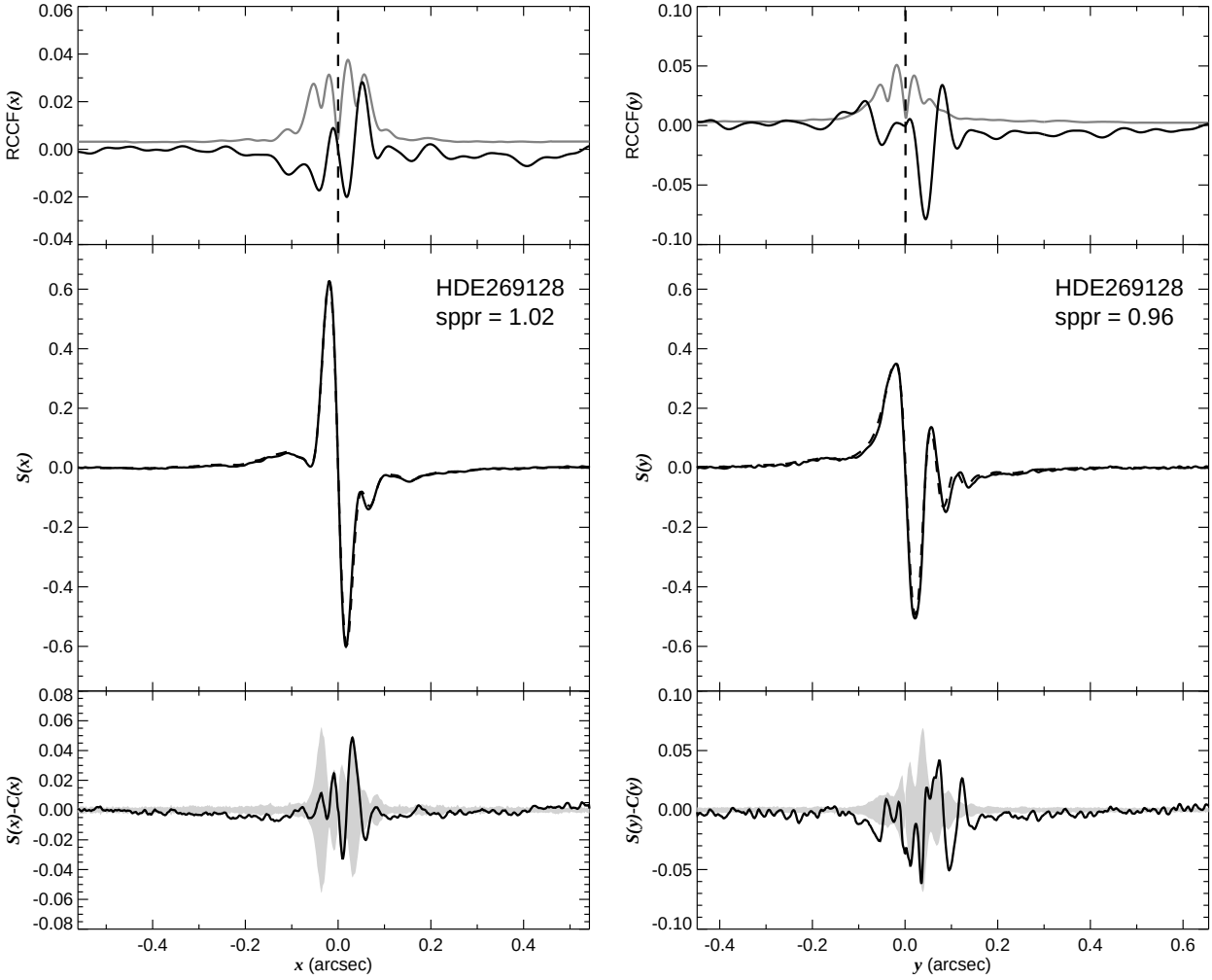

Fig. 1.19.— The FGS scans and binary detection tests for target 051022.79−684623.8 = HDE269128 obtained on BY 2008.9280.

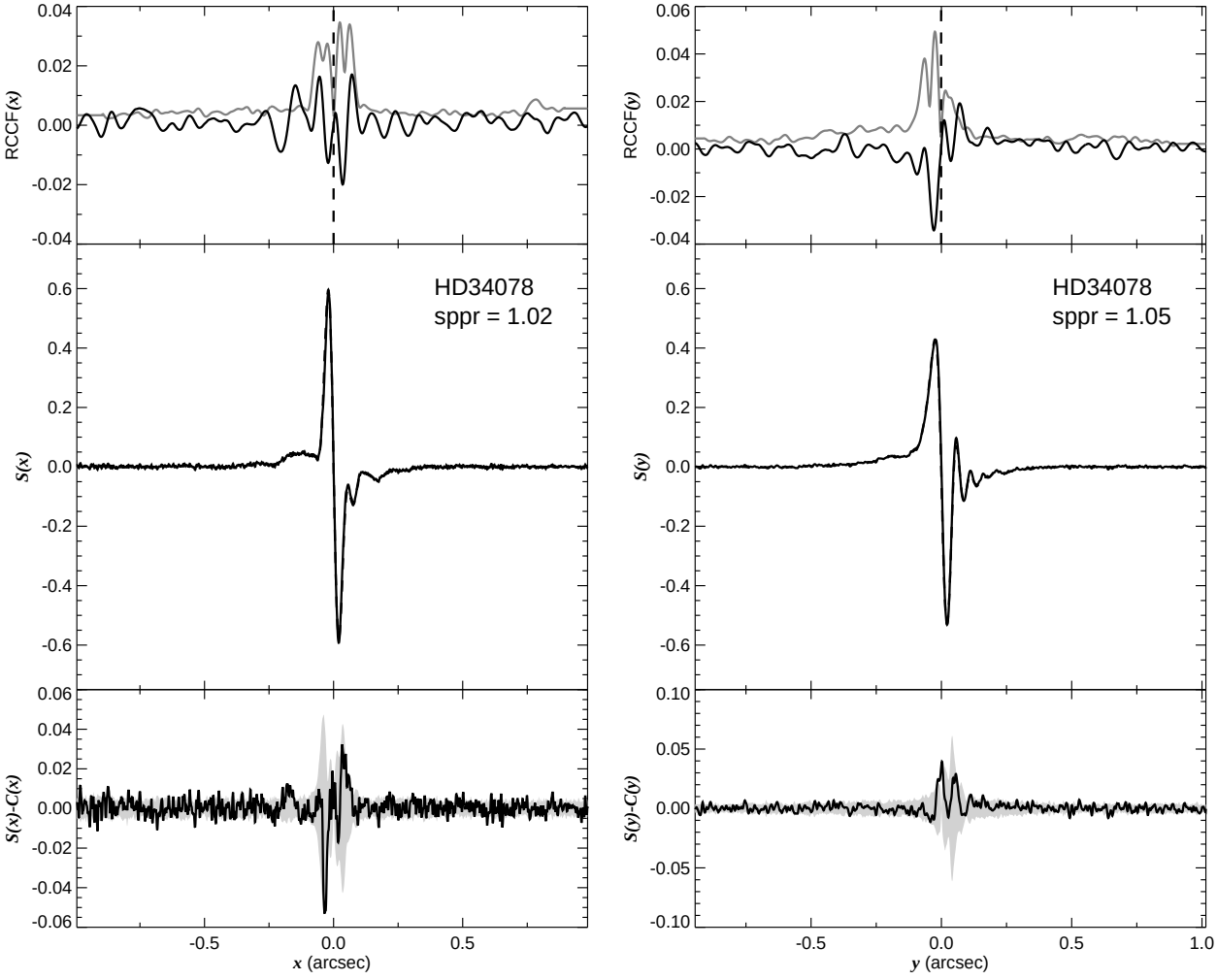

Fig. 1.20.— The FGS scans and binary detection tests for target 051618.15+341844.3 = HD34078 obtained on BY 2008.7276.

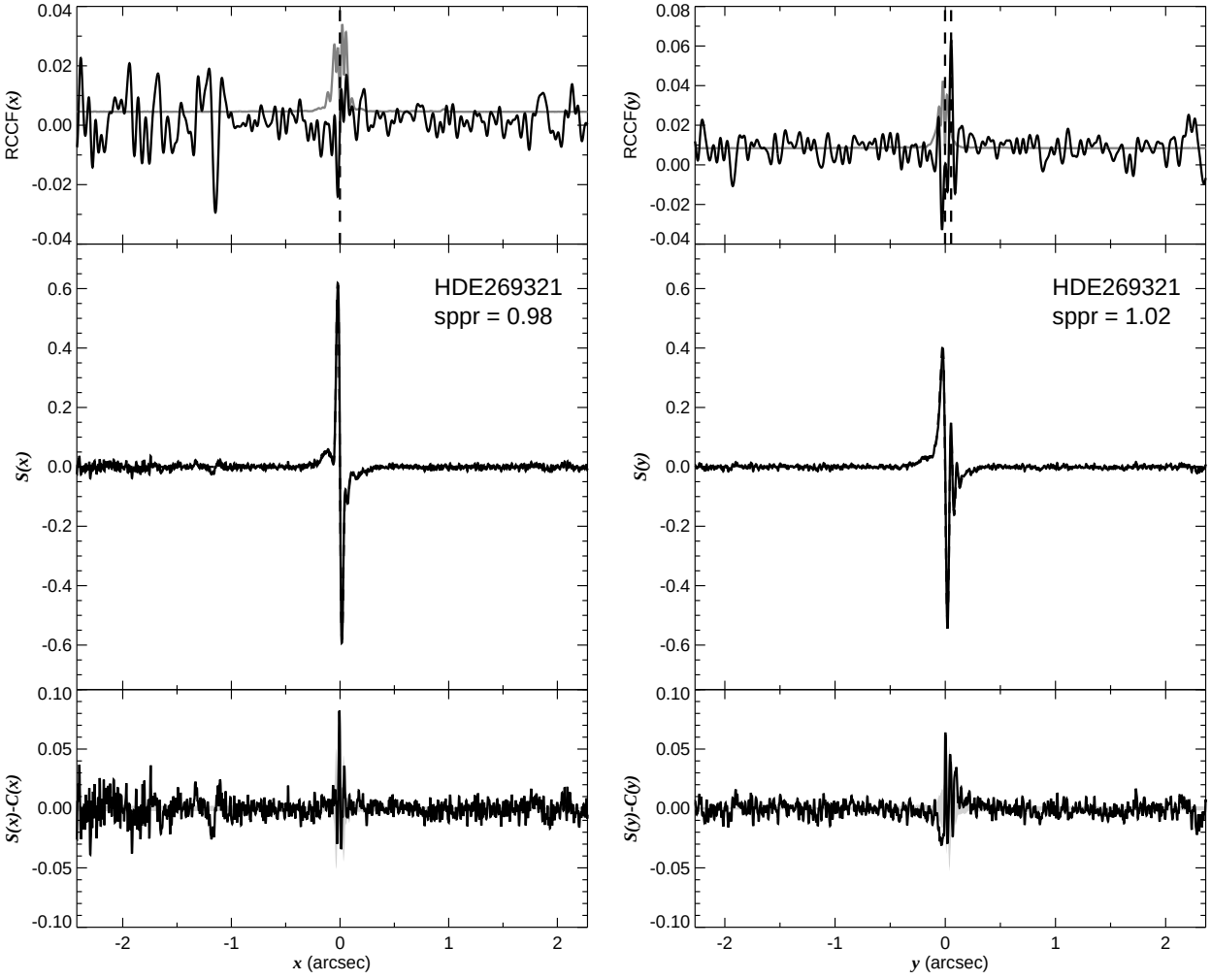

Fig. 1.21.— The FGS scans and binary detection tests for target 051756.06−691603.9 = HDE269321 obtained on BY 2008.9247.

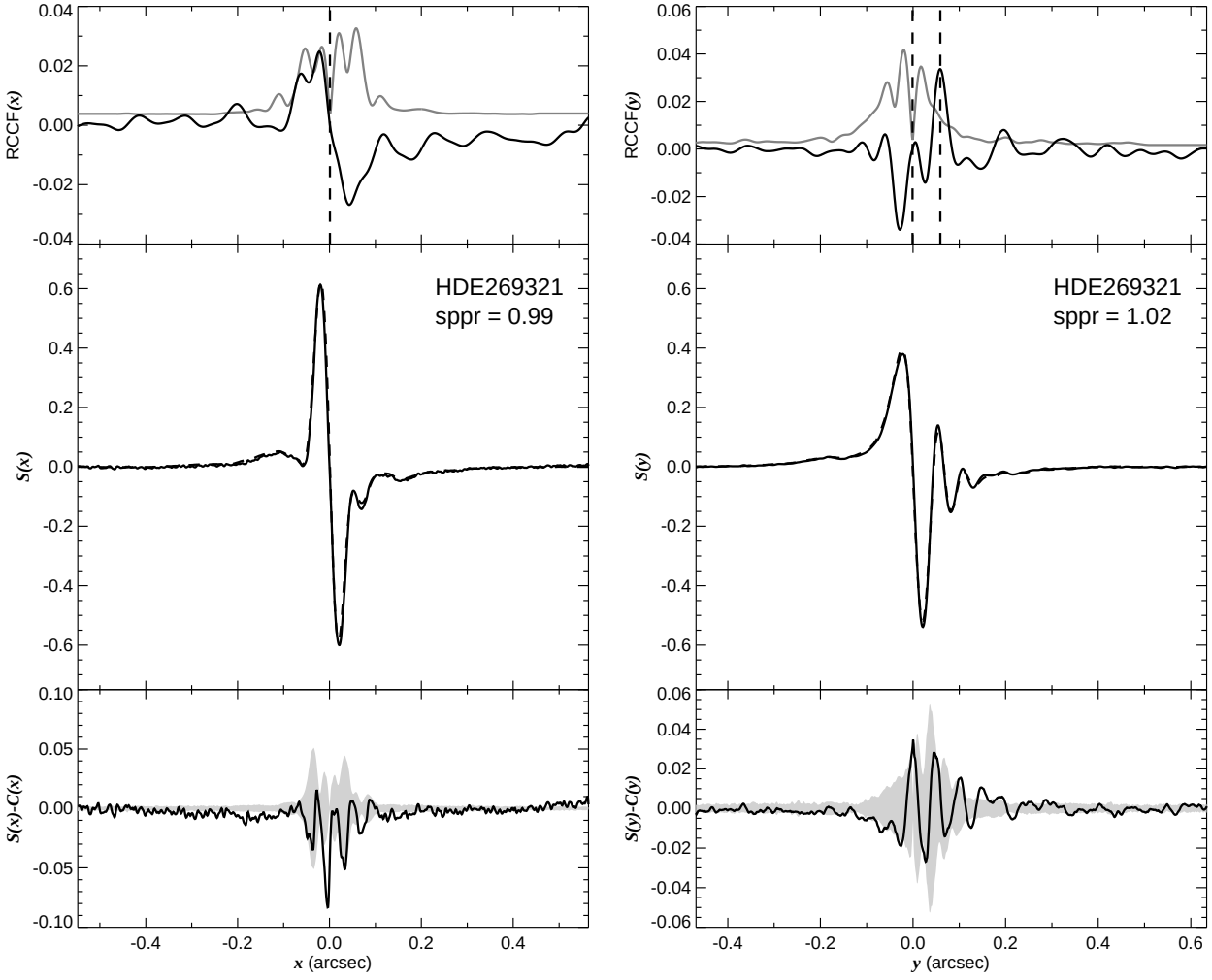

Fig. 1.22.— The FGS scans and binary detection tests for target 051756.06−691603.9 = HDE269321 obtained on BY 2008.9248.

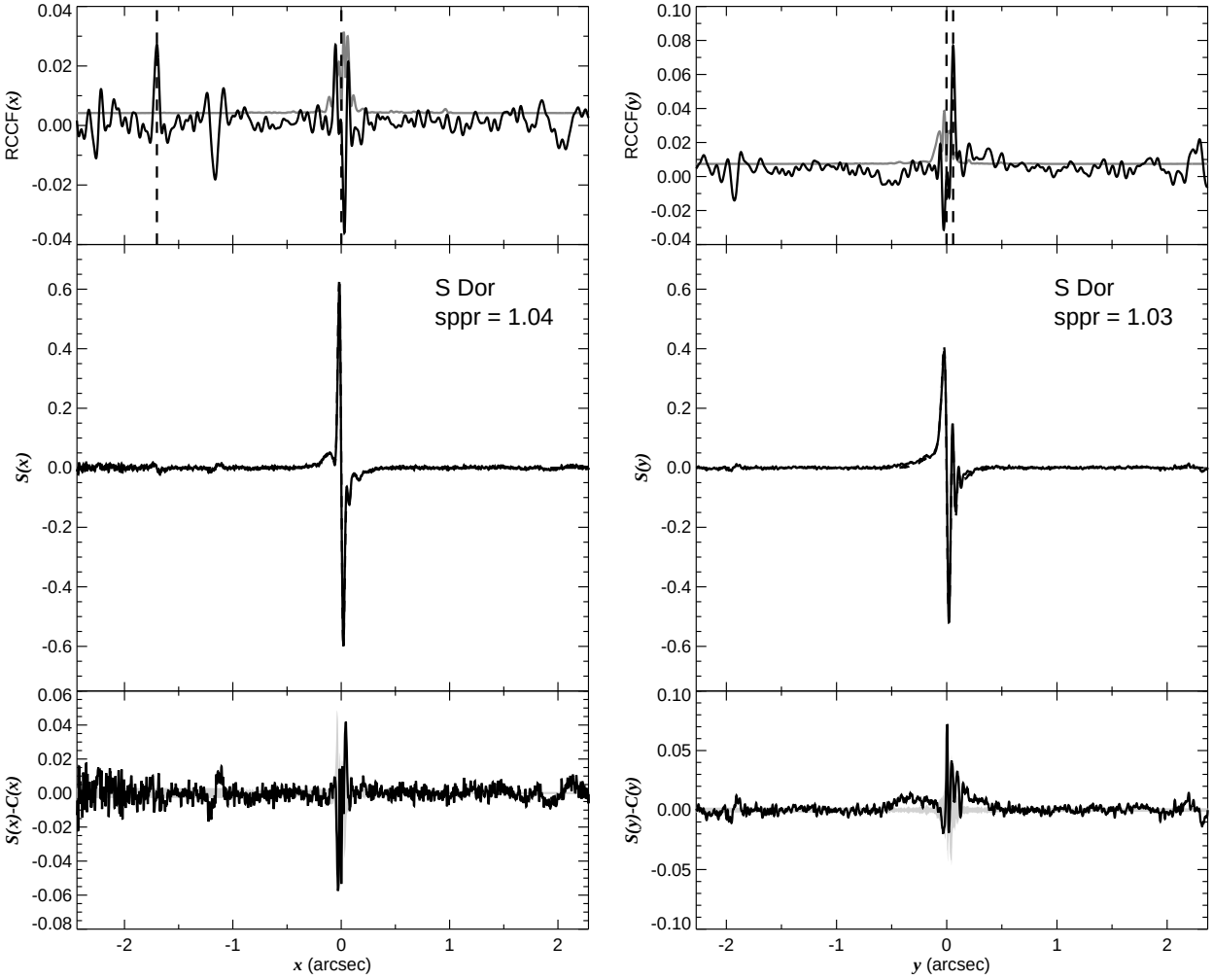

Fig. 1.23.— The FGS scans and binary detection tests for target 051814.36−691501.1 = HD35343 obtained on BY 2008.9246.

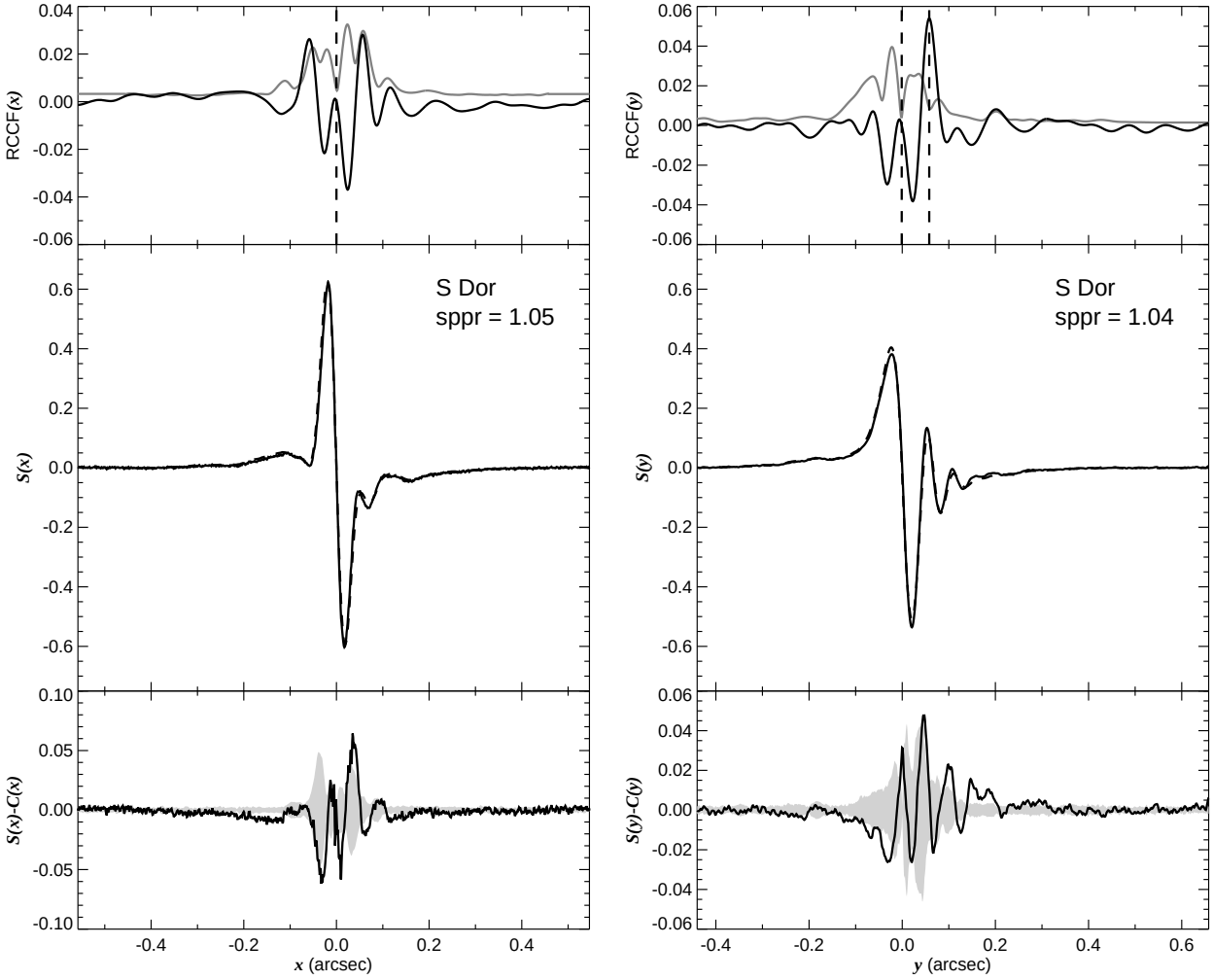

Fig. 1.24.— The FGS scans and binary detection tests for target 051814.36−691501.1 = HD35343 obtained on BY 2008.9246.

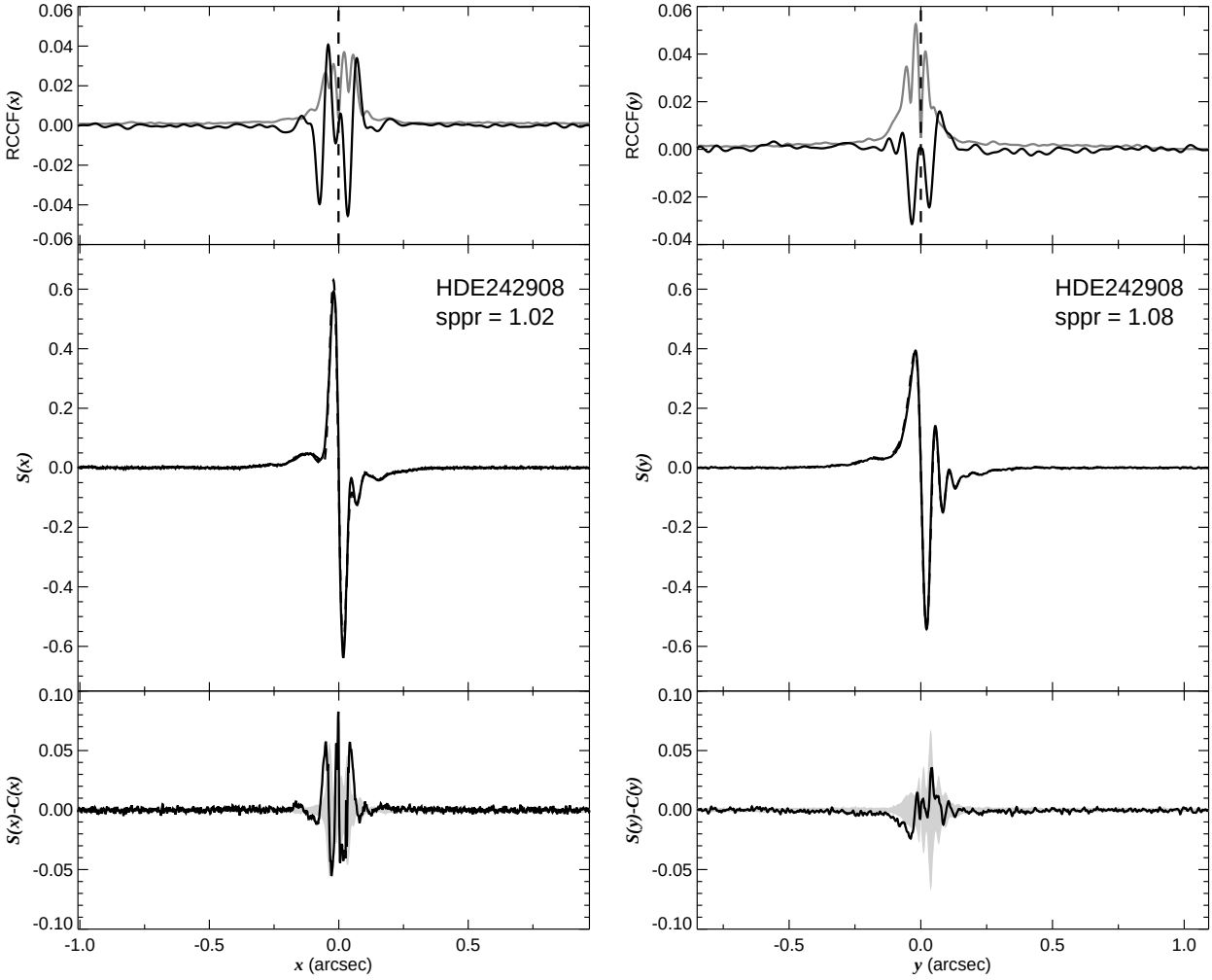

Fig. 1.25.— The FGS scans and binary detection tests for target 052229.30+333050.5 = HDE242908 obtained on BY 2007.6279.

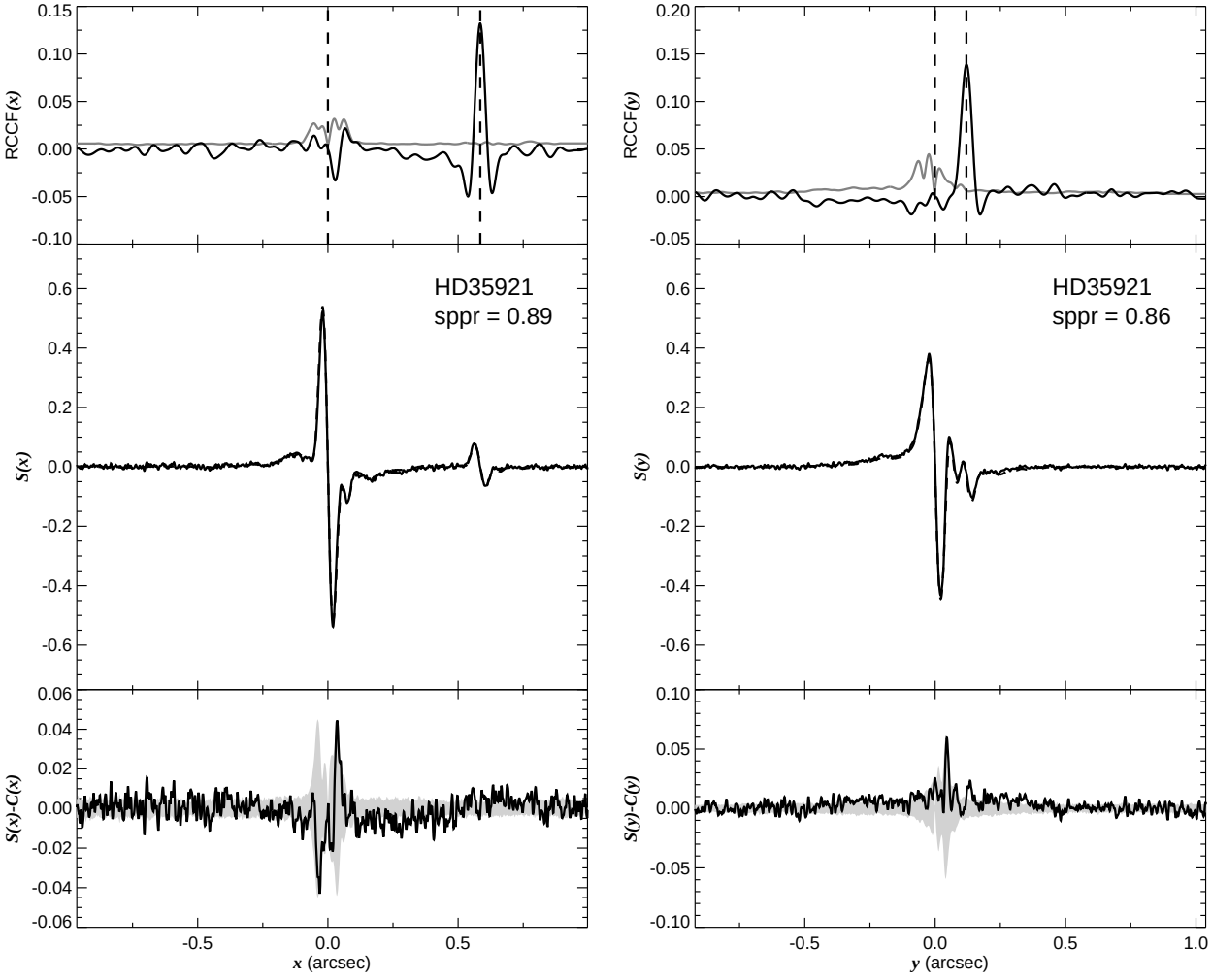

Fig. 1.26.— The FGS scans and binary detection tests for target 052942.65+352230.1 = HD35921 obtained on BY 2008.7278.

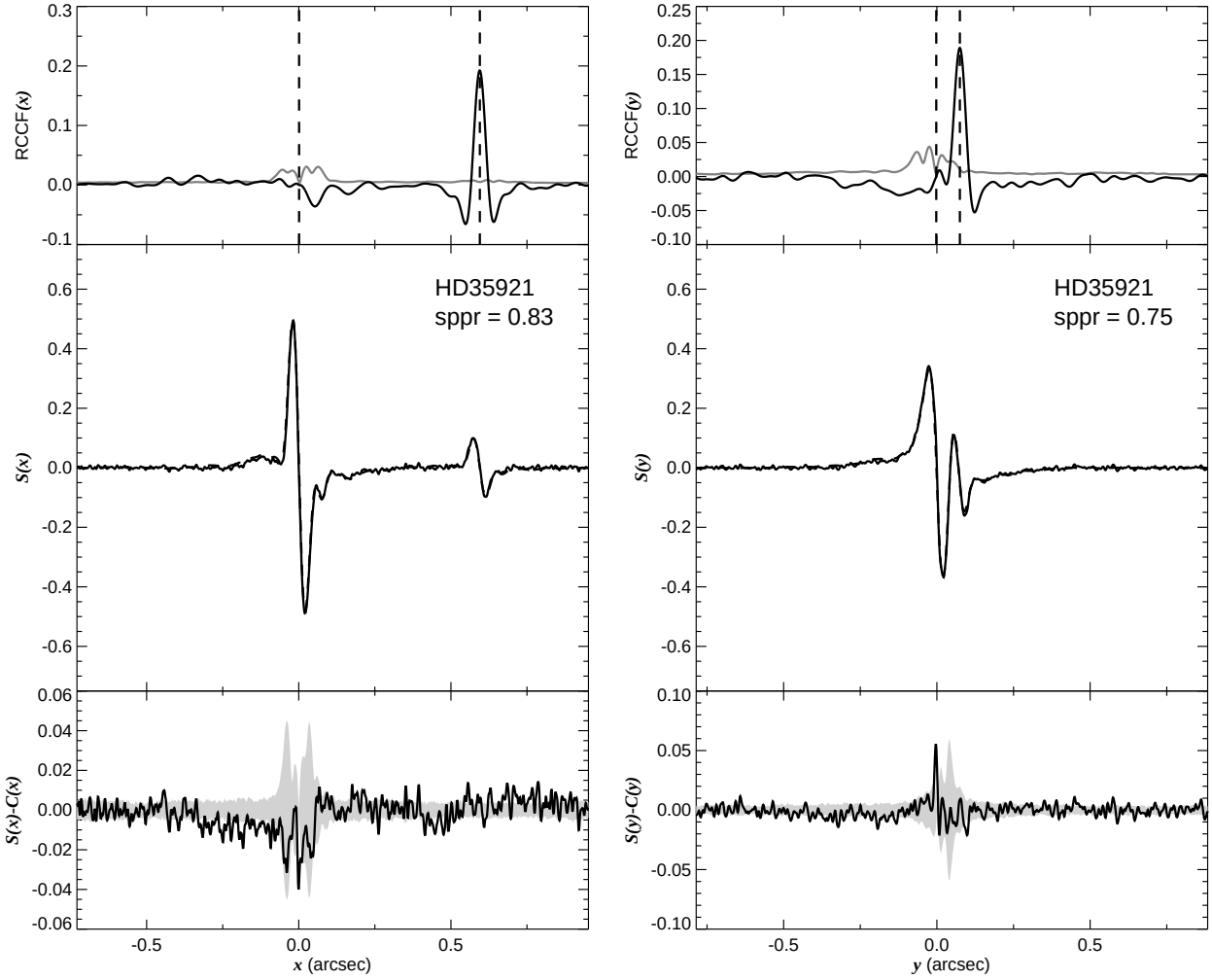

Fig. 1.27.— The FGS scans and binary detection tests for target 052942.65+352230.1 = HD35921 obtained on BY 2008.7847.

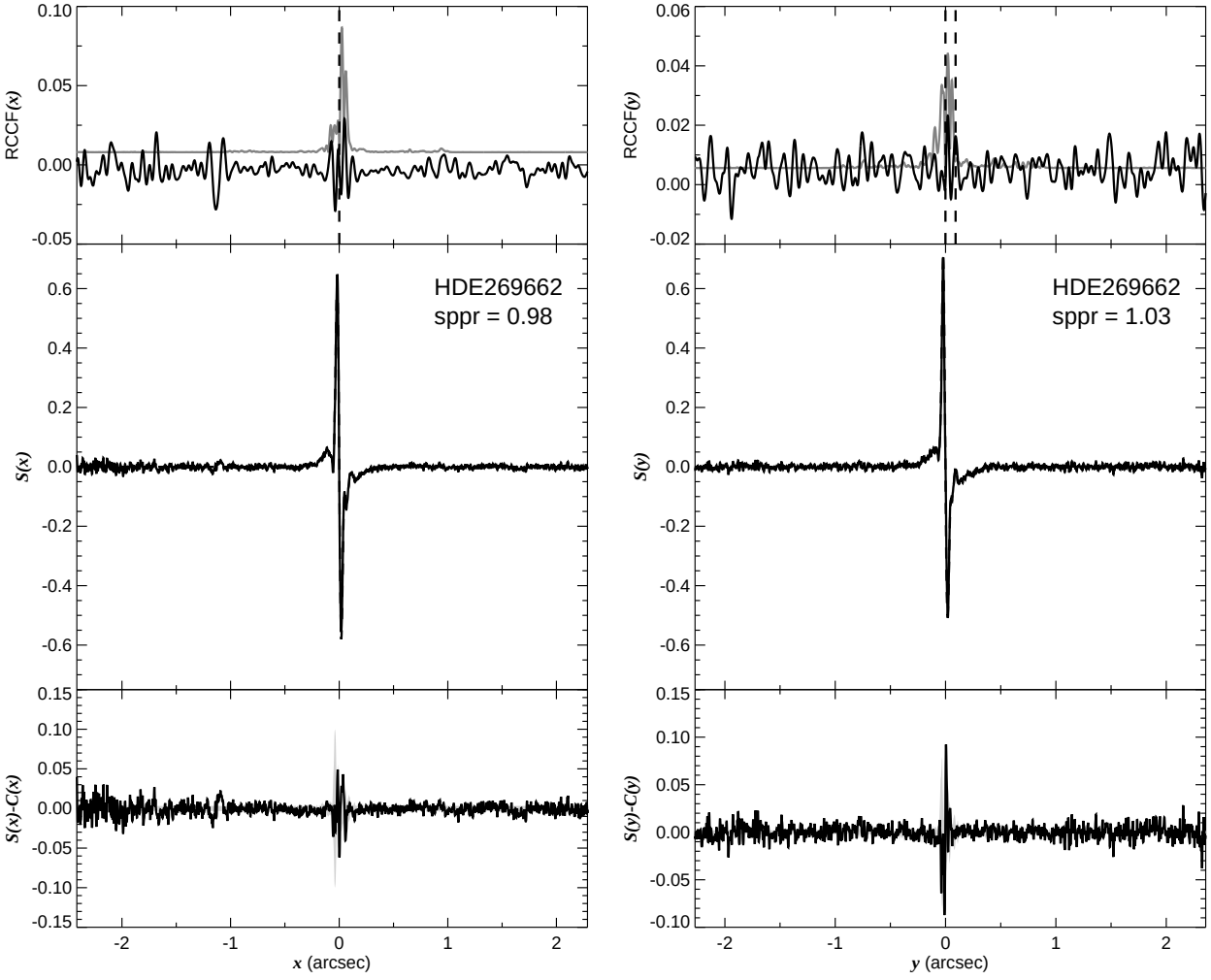

Fig. 1.28.— The FGS scans and binary detection tests for target 053051.48−690258.6 = HDE269662 obtained on BY 2009.3530.

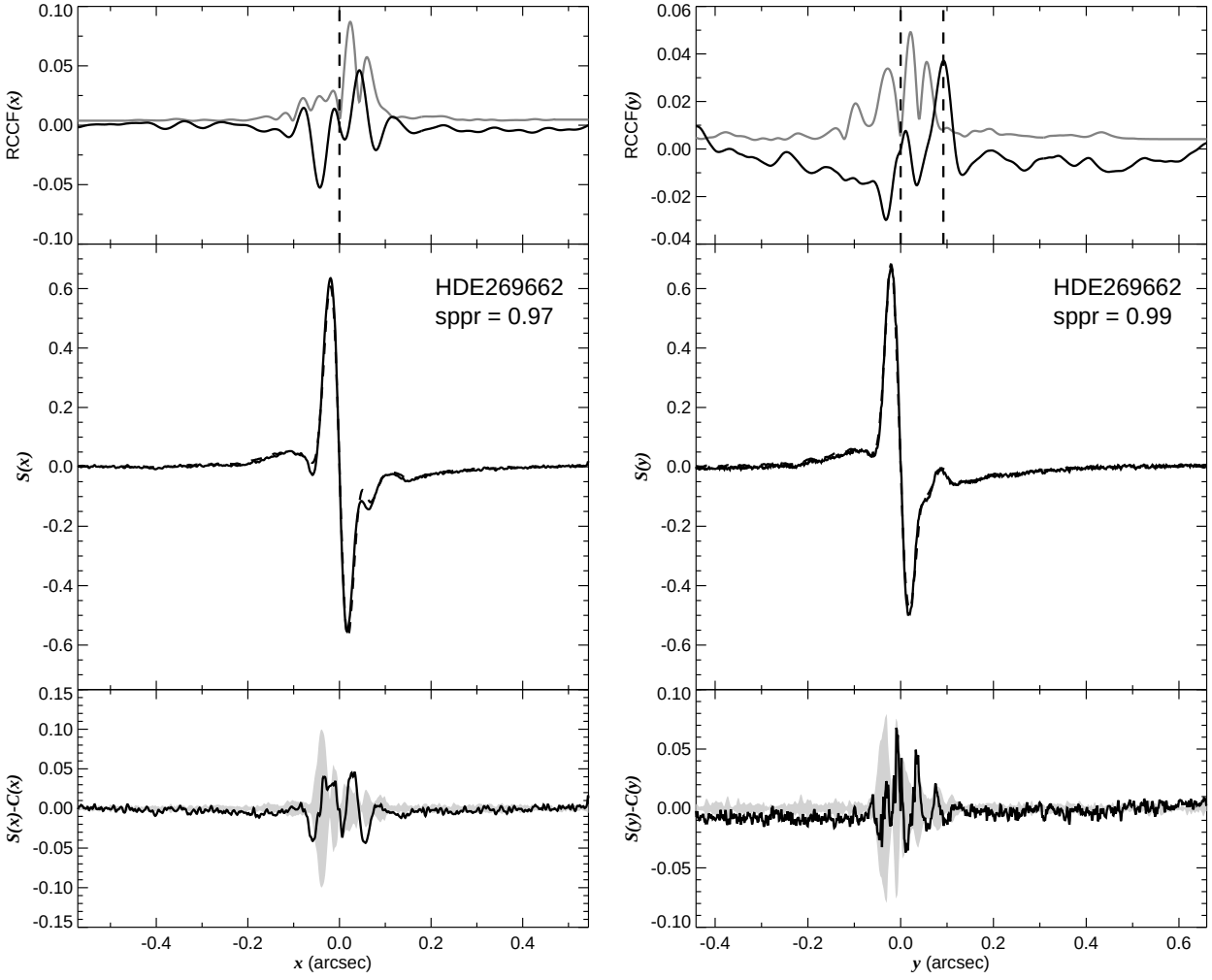

Fig. 1.29.— The FGS scans and binary detection tests for target 053051.48−690258.6 = HDE269662 obtained on BY 2009.3530.

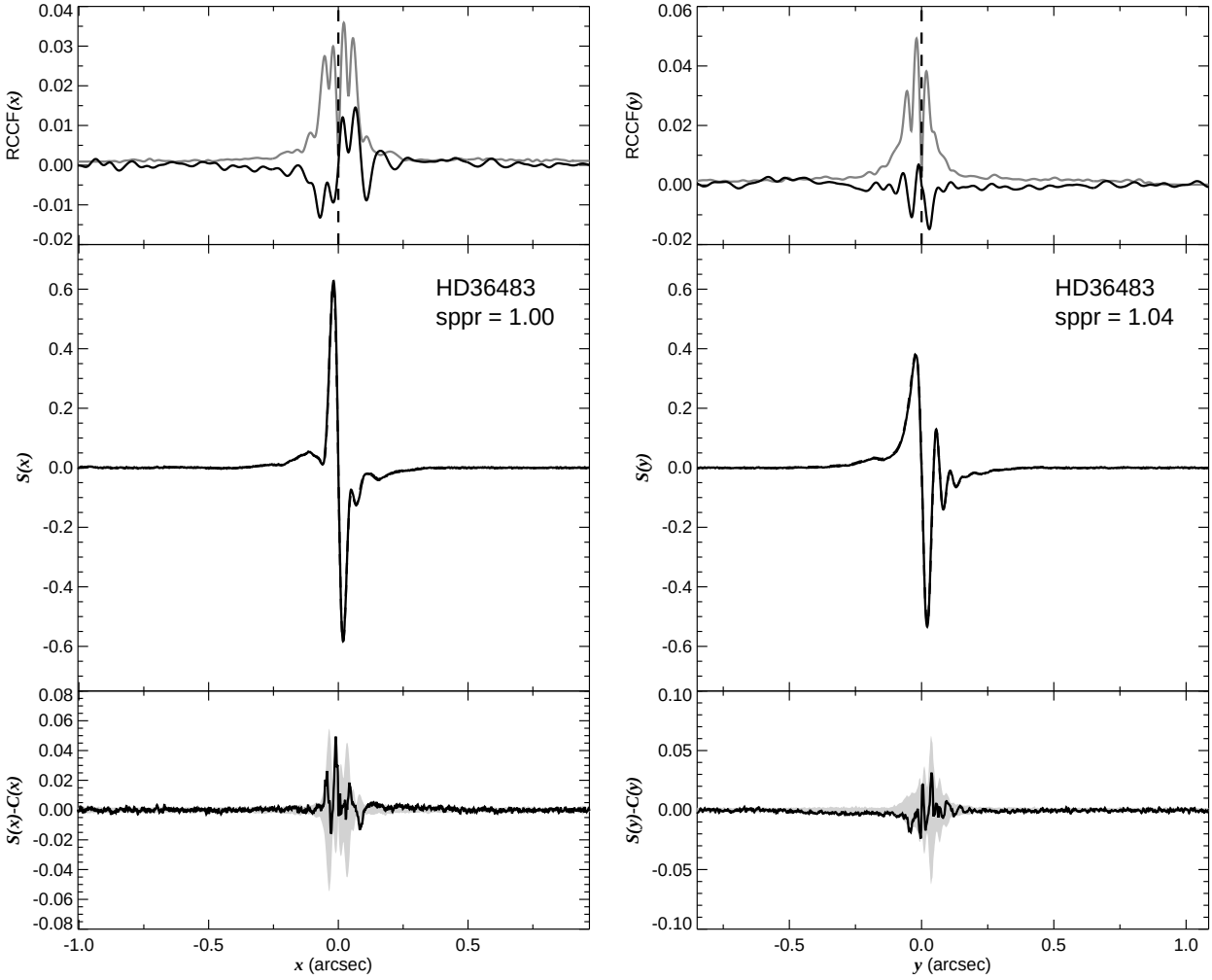

Fig. 1.30.— The FGS scans and binary detection tests for target 053341.15+362735.0 = HD36483 obtained on BY 2007.6529.

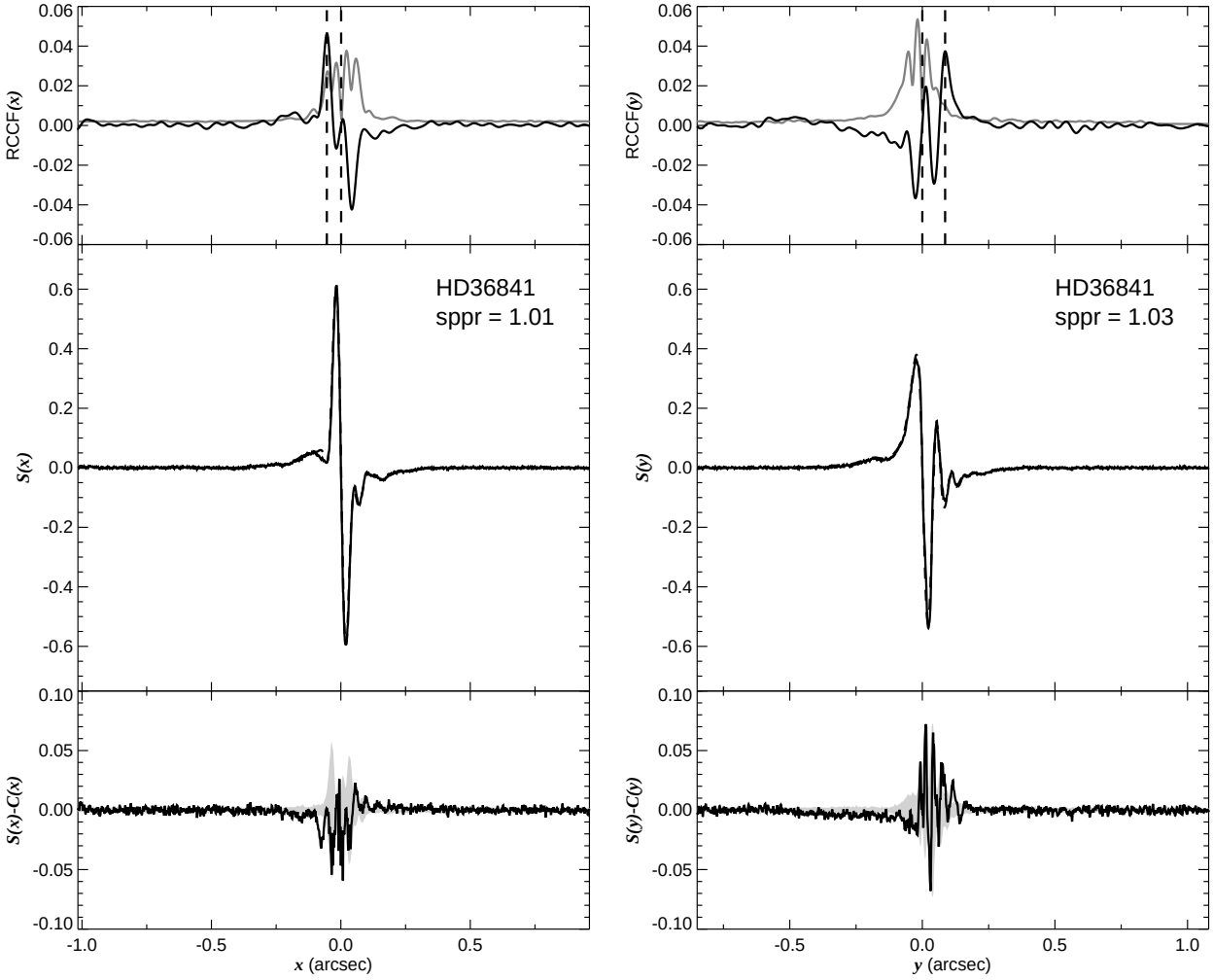

Fig. 1.31.— The FGS scans and binary detection tests for target 053433.72−002311.5 = HD36841 obtained on BY 2008.8472.

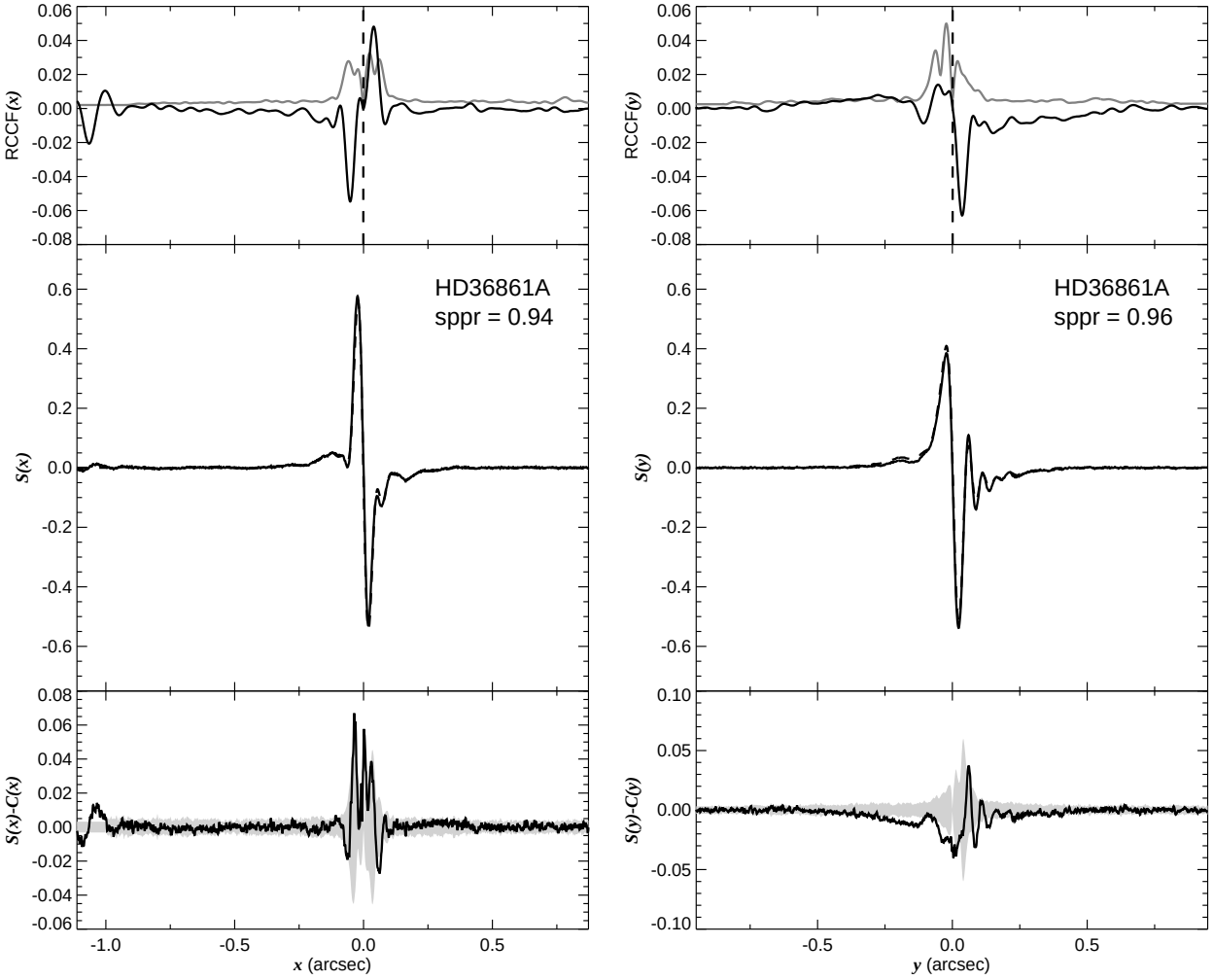

Fig. 1.32.— The FGS scans and binary detection tests for target 053508.28+095603.0 = HD36861 obtained on BY 2008.7110.

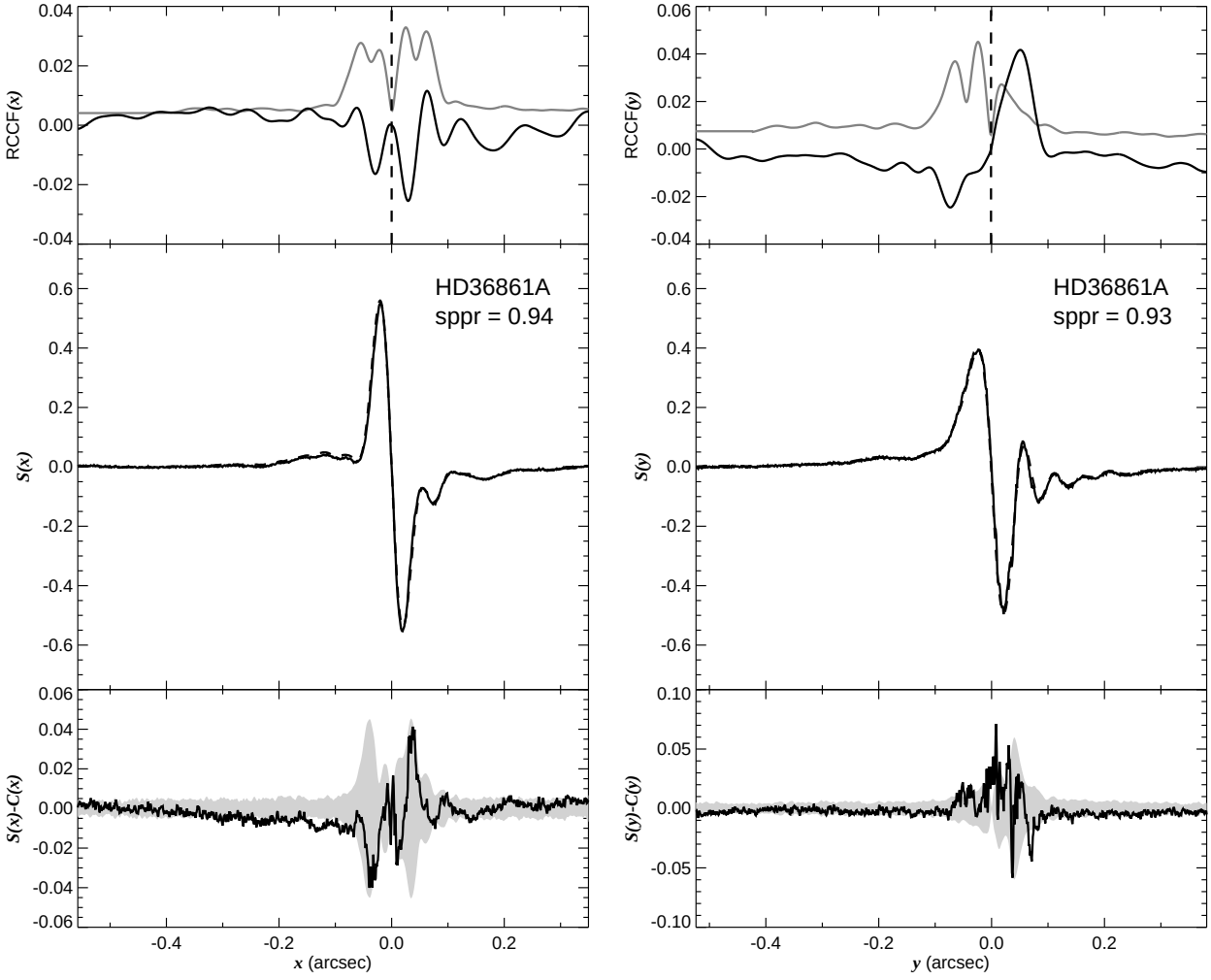

Fig. 1.33.— The FGS scans and binary detection tests for target 053508.28+095603.0 = HD36861 obtained on BY 2008.8065.

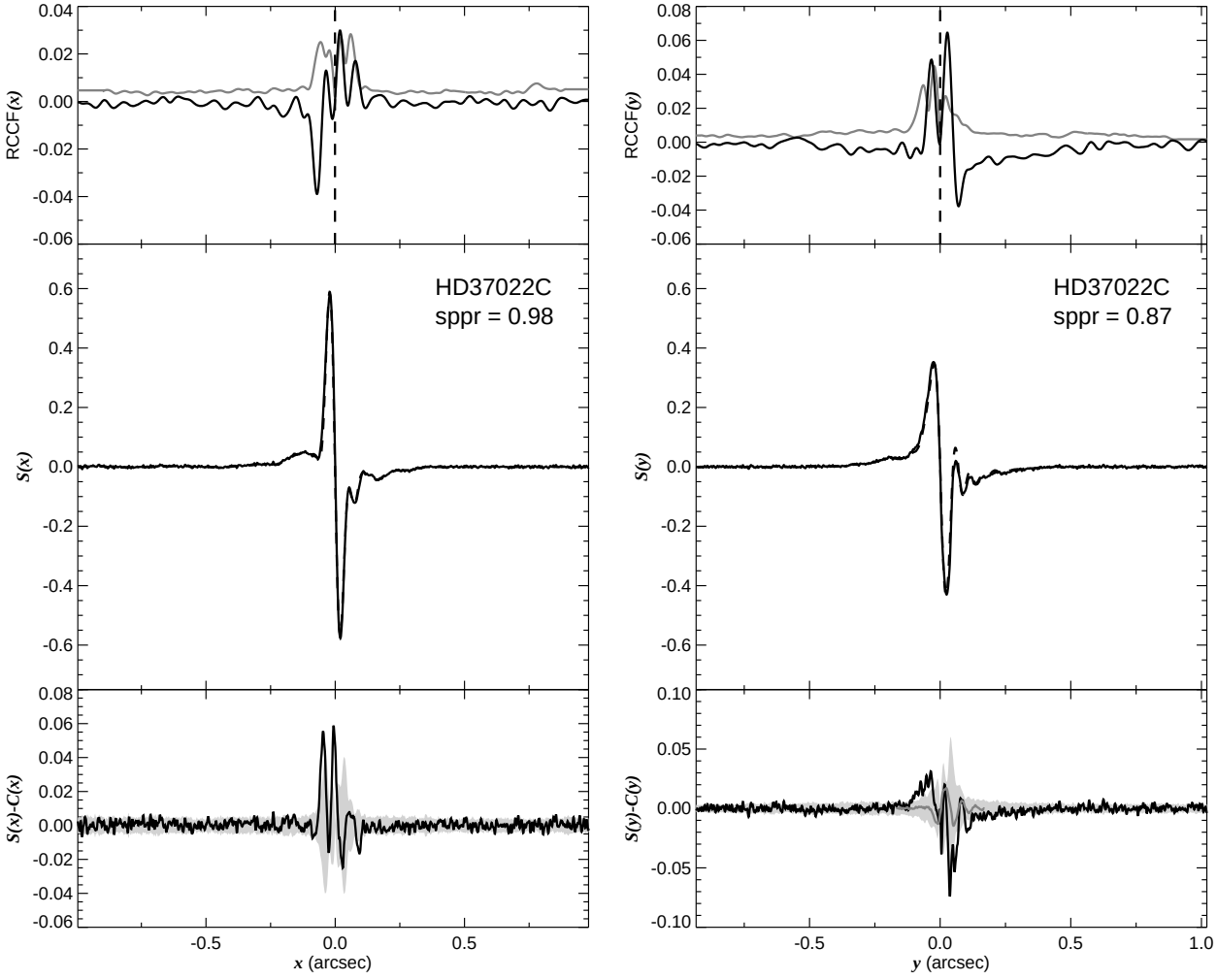

Fig. 1.34.— The FGS scans and binary detection tests for target 053516.47−052322.9 = HD37022 obtained on BY 2007.9029.

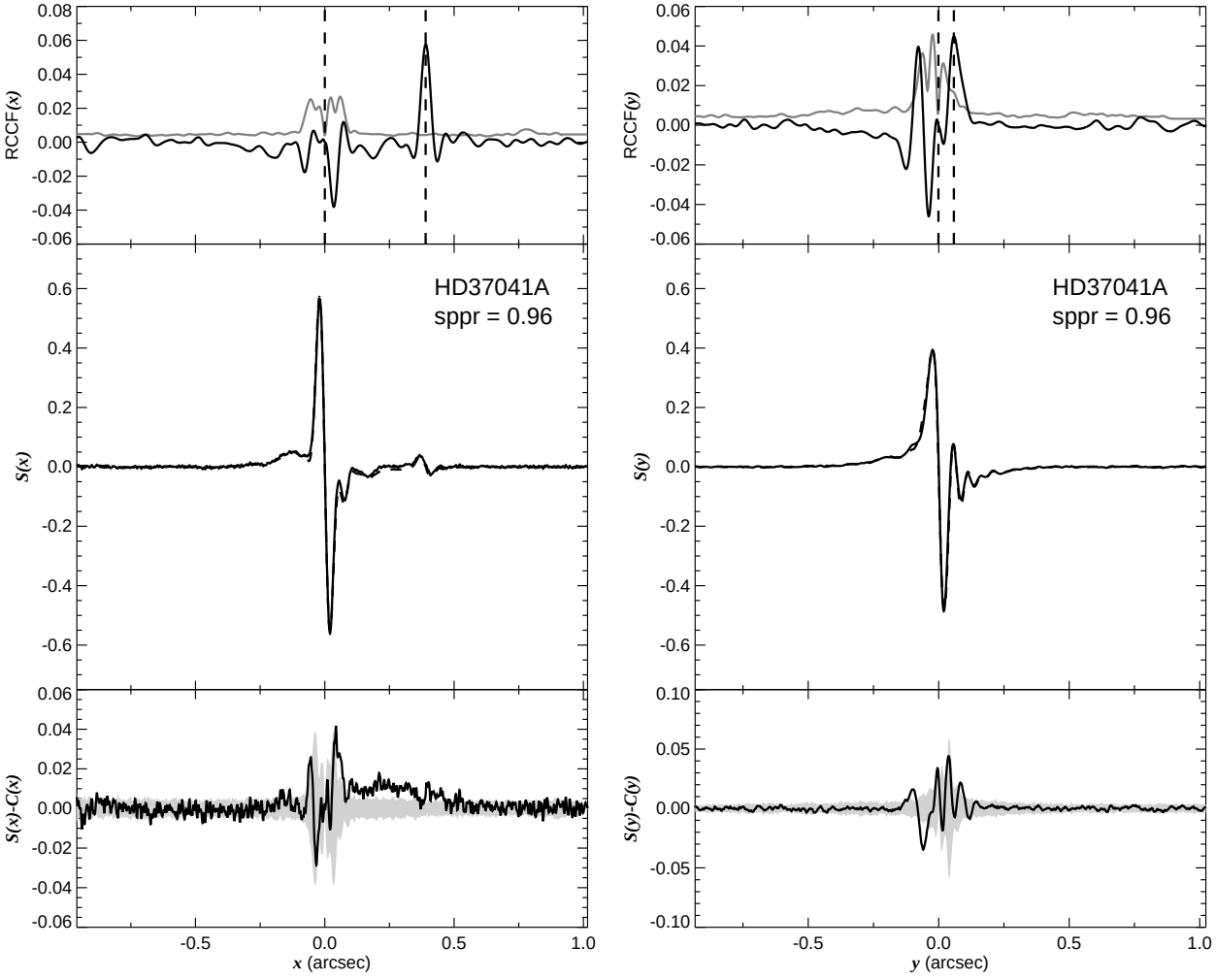

Fig. 1.35.— The FGS scans and binary detection tests for target 053522.90−052457.8 = HD37041 obtained on BY 2008.7283.

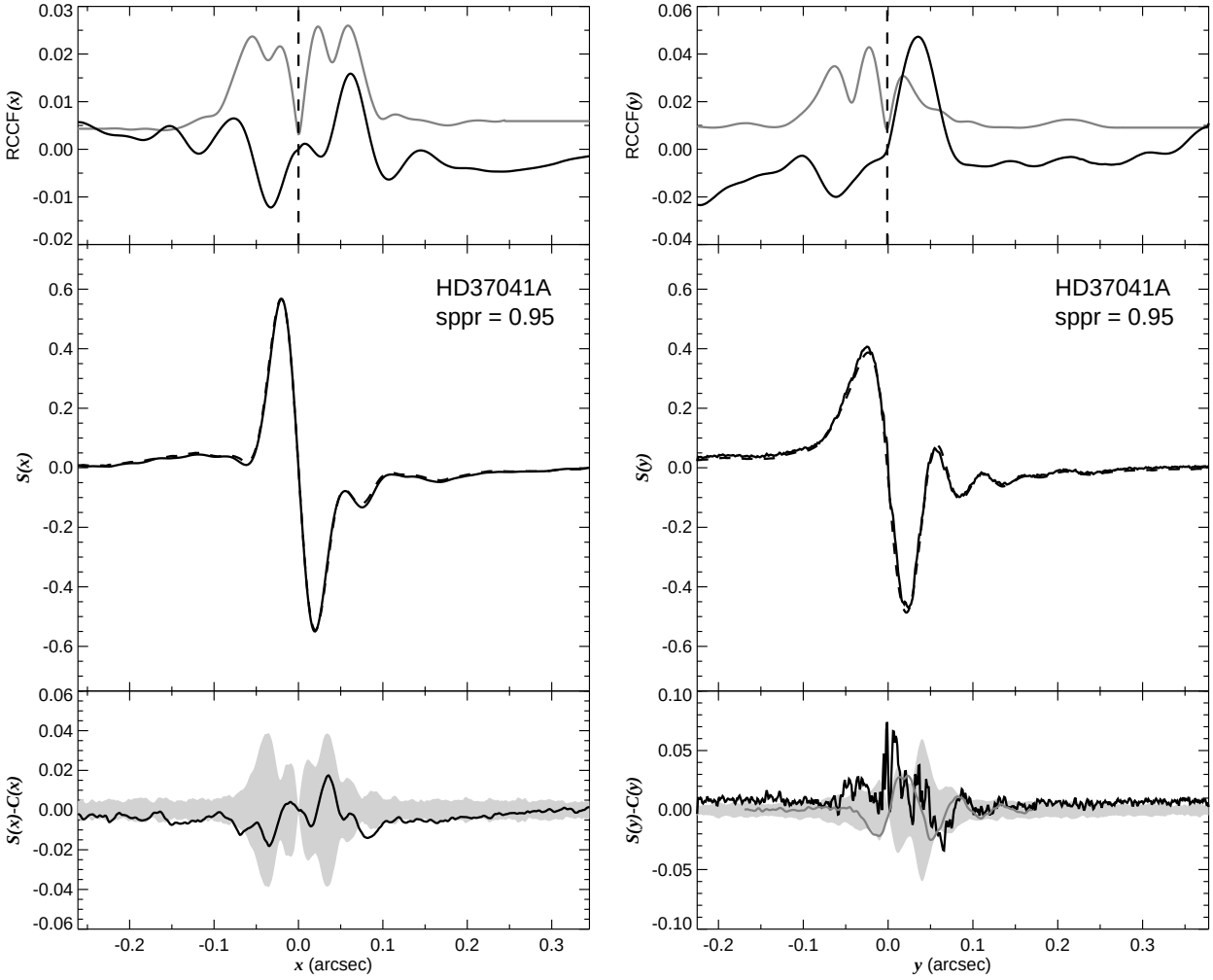

Fig. 1.36.— The FGS scans and binary detection tests for target 053522.90−052457.8 = HD37041 obtained on BY 2008.8452.

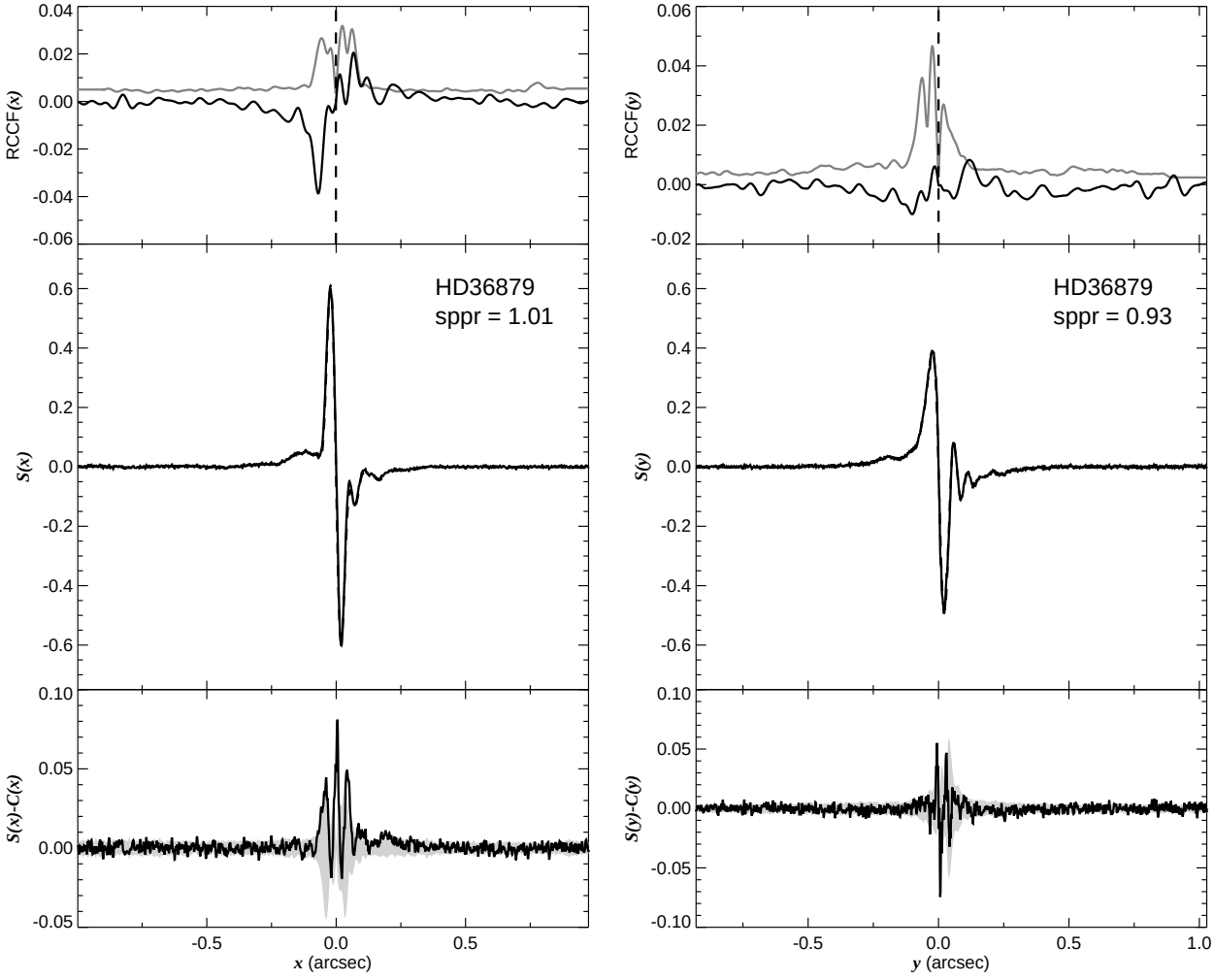

Fig. 1.37.— The FGS scans and binary detection tests for target 053540.53+212411.7 = HD36879 obtained on BY 2008.7587.

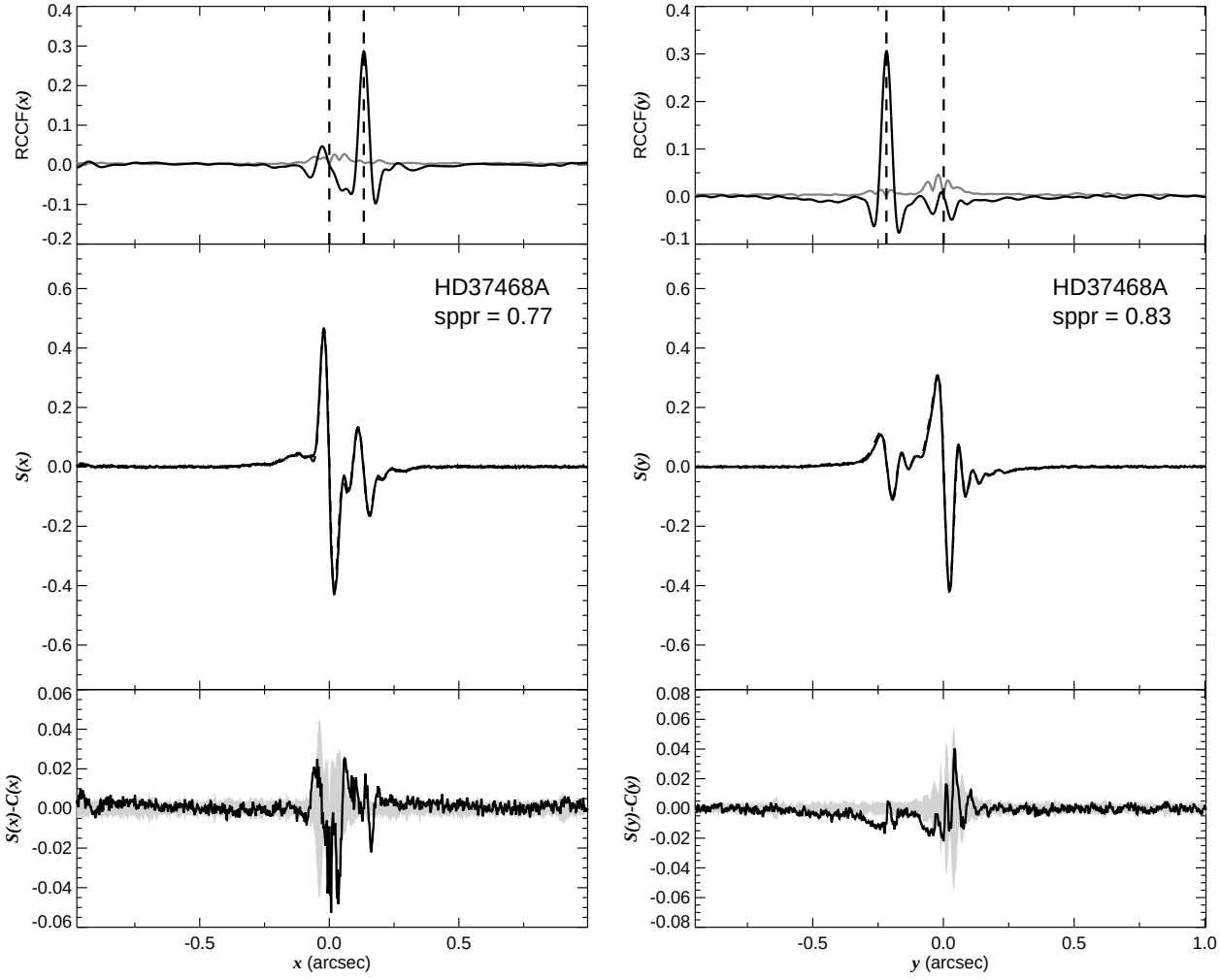

Fig. 1.38.— The FGS scans and binary detection tests for target 053844.77−023600.2 = HD37468 obtained on BY 2008.0092.

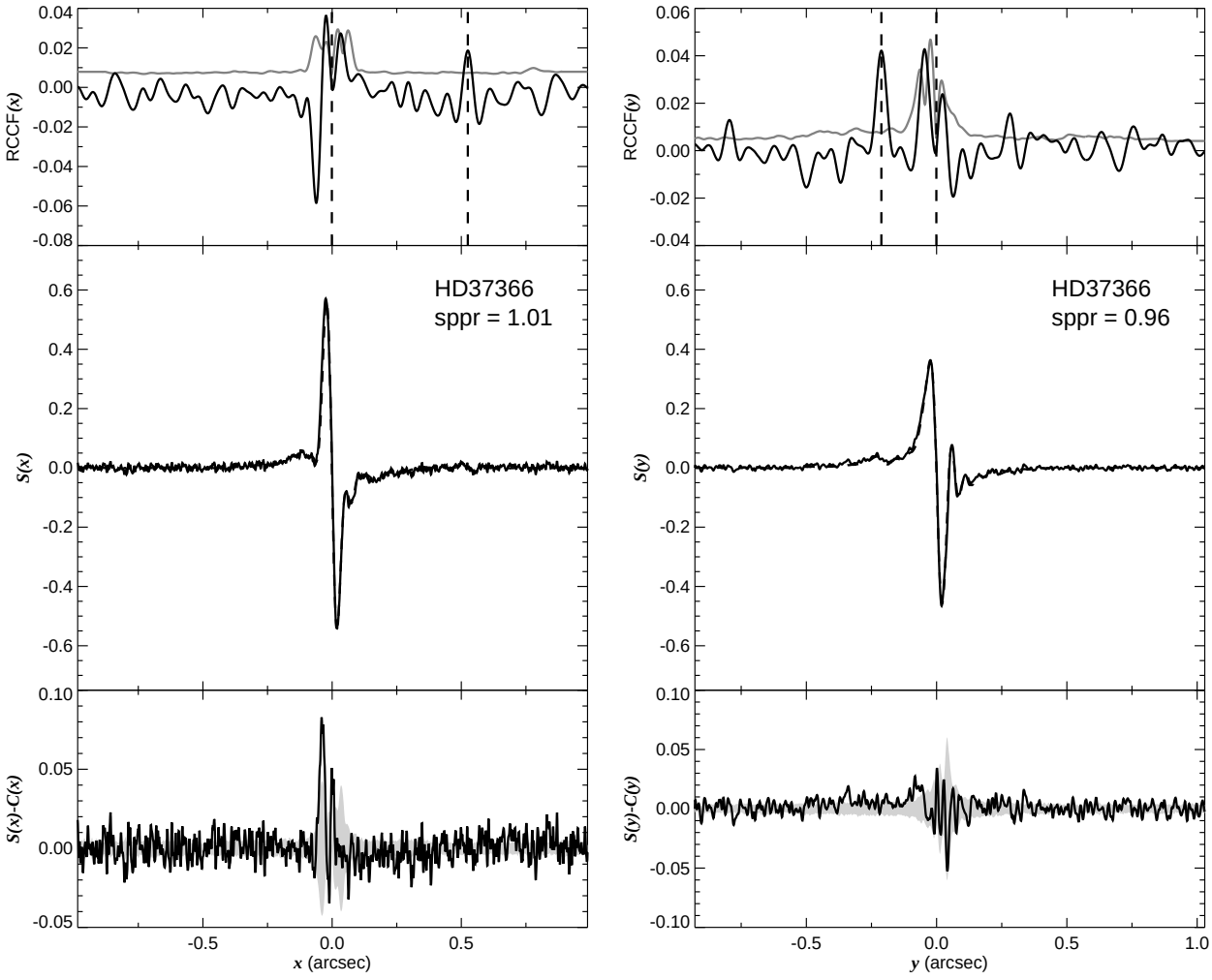

Fig. 1.39.— The FGS scans and binary detection tests for target 053924.80+305326.8 = HD37366 obtained on BY 2008.7449.

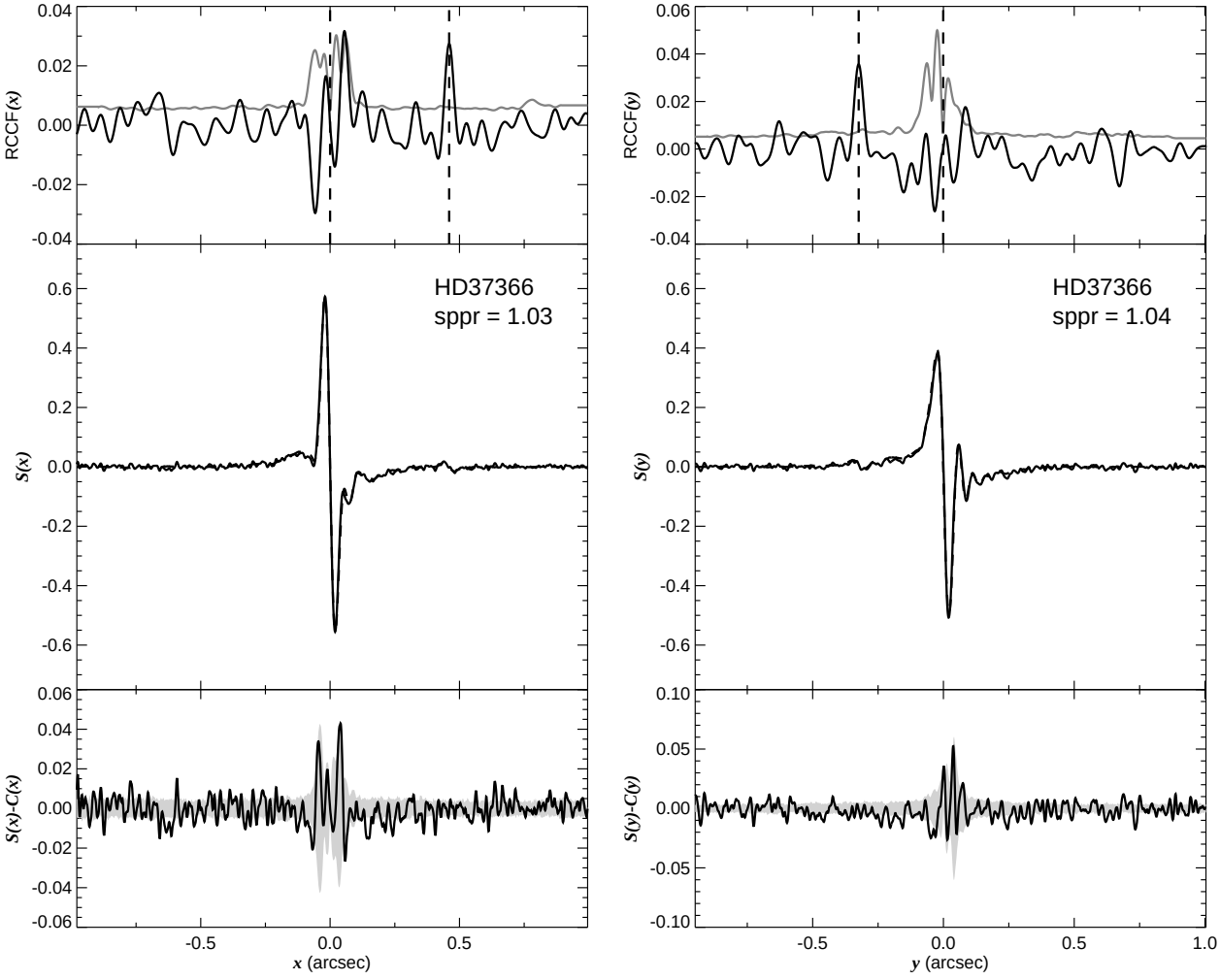

Fig. 1.40.— The FGS scans and binary detection tests for target 053924.80+305326.8 = HD37366 obtained on BY 2008.8647.

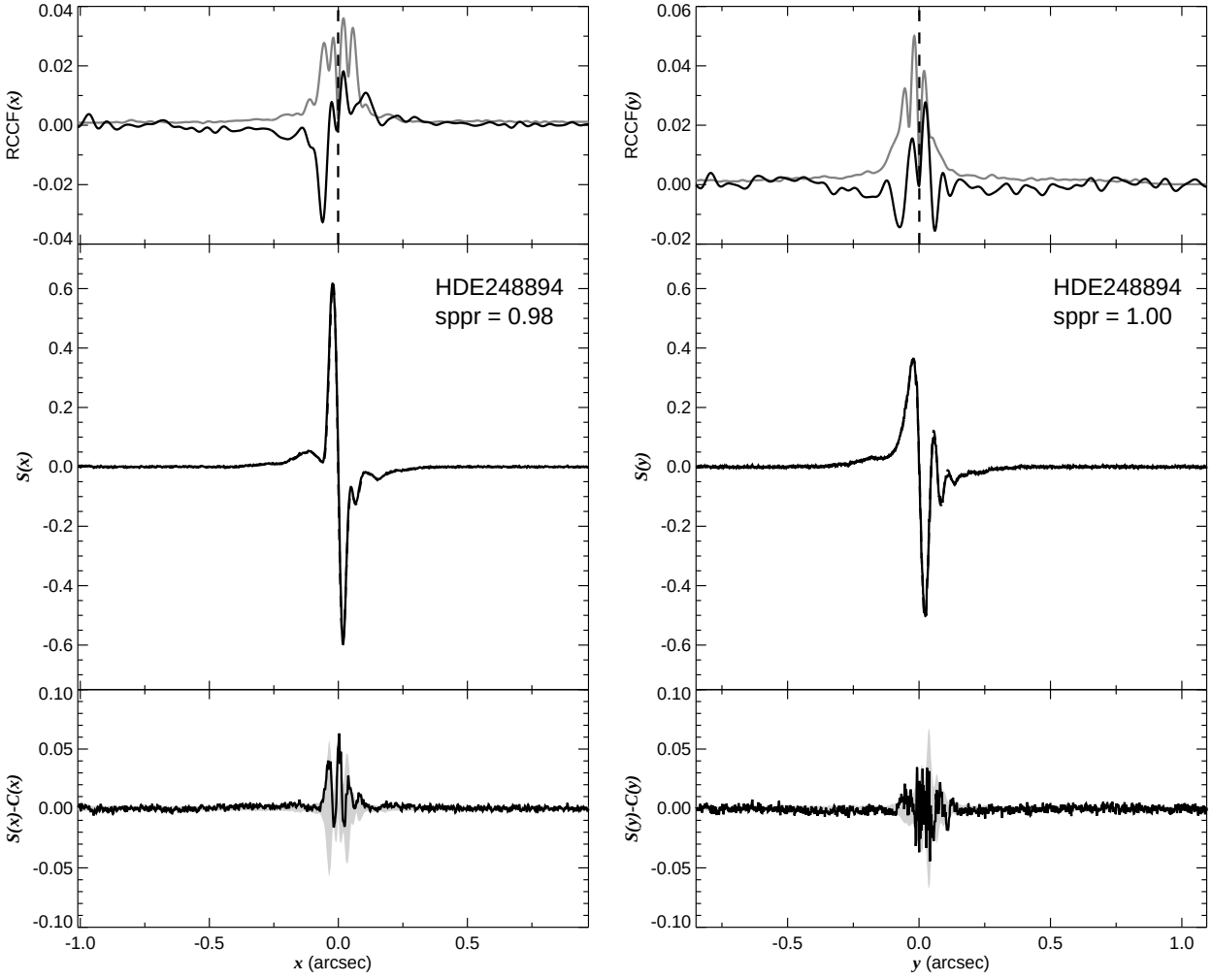

Fig. 1.41.— The FGS scans and binary detection tests for target 055358.21+205234.7 = HDE248894 obtained on BY 2008.7642.

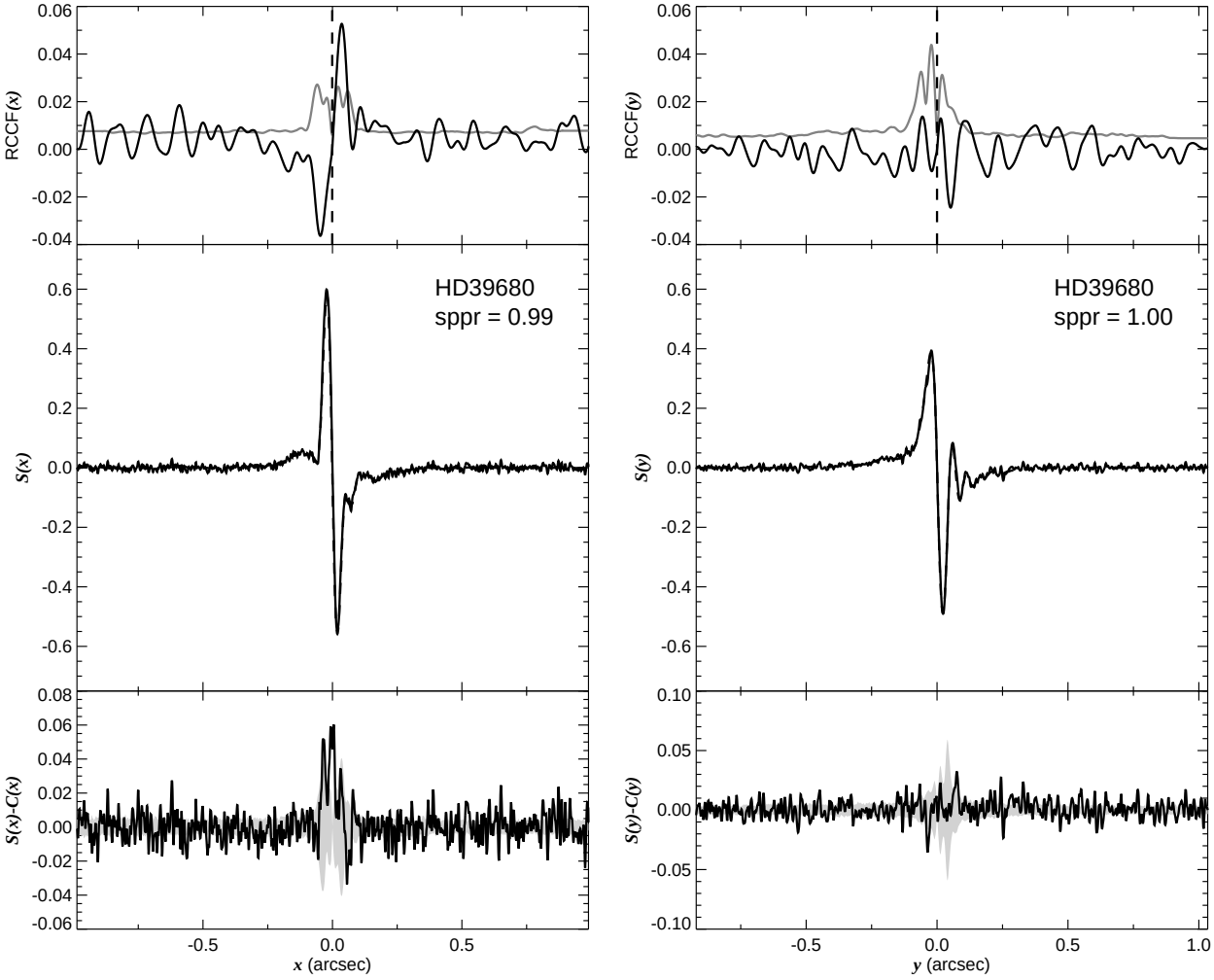

Fig. 1.42.— The FGS scans and binary detection tests for target 055444.73+135117.1 = HD39680 obtained on BY 2008.7094.

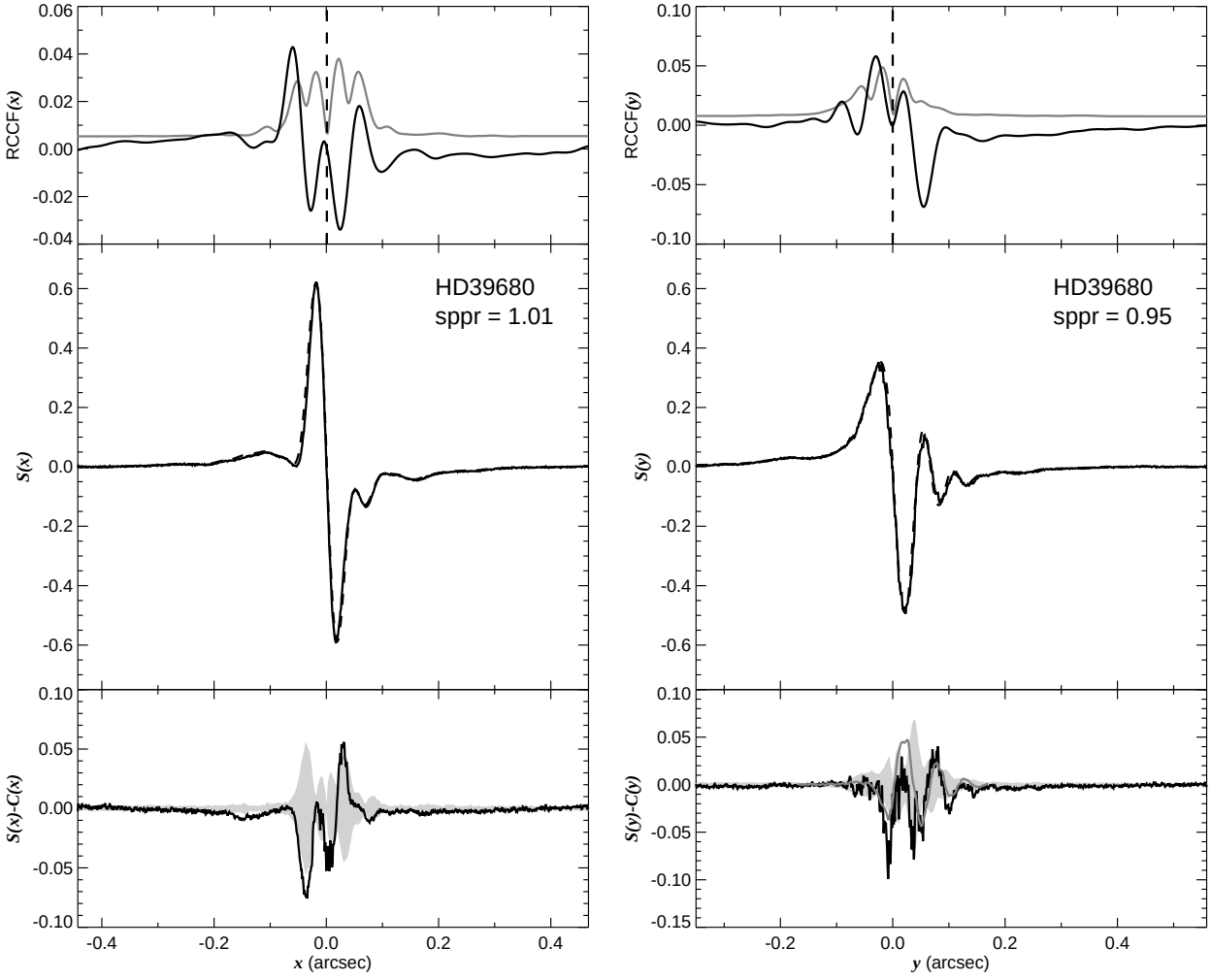

Fig. 1.43.— The FGS scans and binary detection tests for target 055444.73+135117.1 = HD39680 obtained on BY 2008.8514.

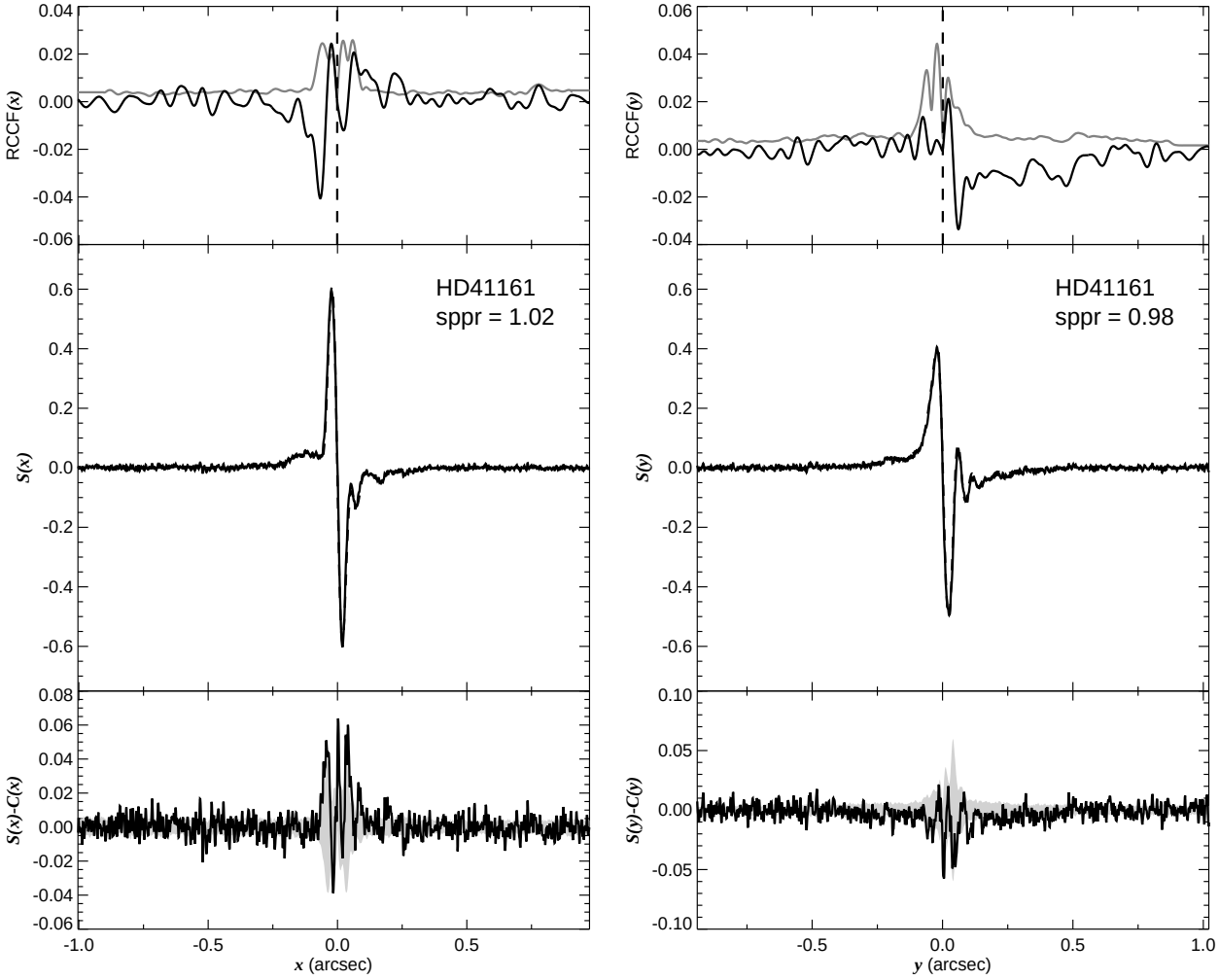

Fig. 1.44.— The FGS scans and binary detection tests for target 060552.46+481457.4 = HD41161 obtained on BY 2007.8598.

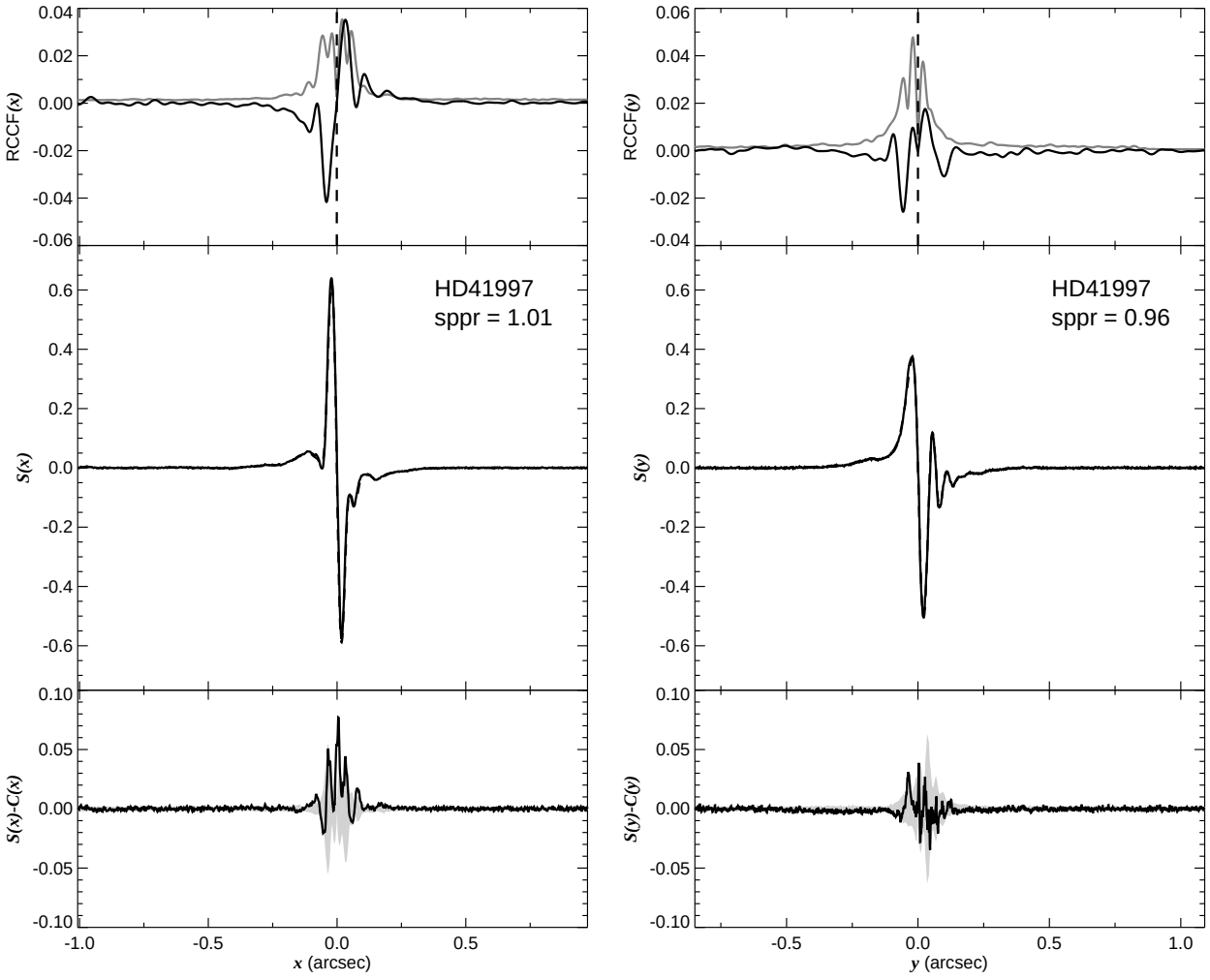

Fig. 1.45.— The FGS scans and binary detection tests for target 060855.82+154218.2 = HD41997 obtained on BY 2008.7096.

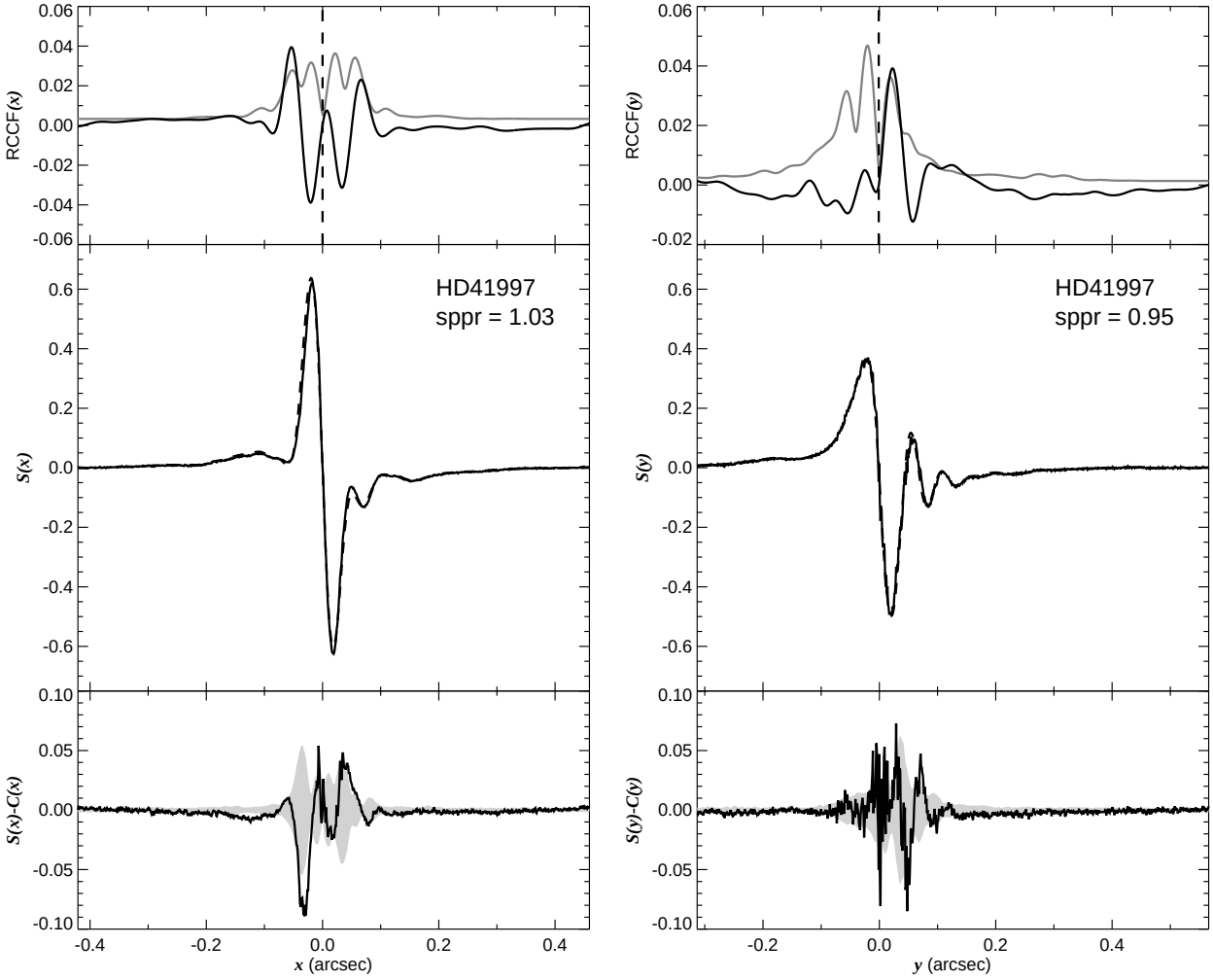

Fig. 1.46.— The FGS scans and binary detection tests for target 060855.82+154218.2 = HD41997 obtained on BY 2008.8678.

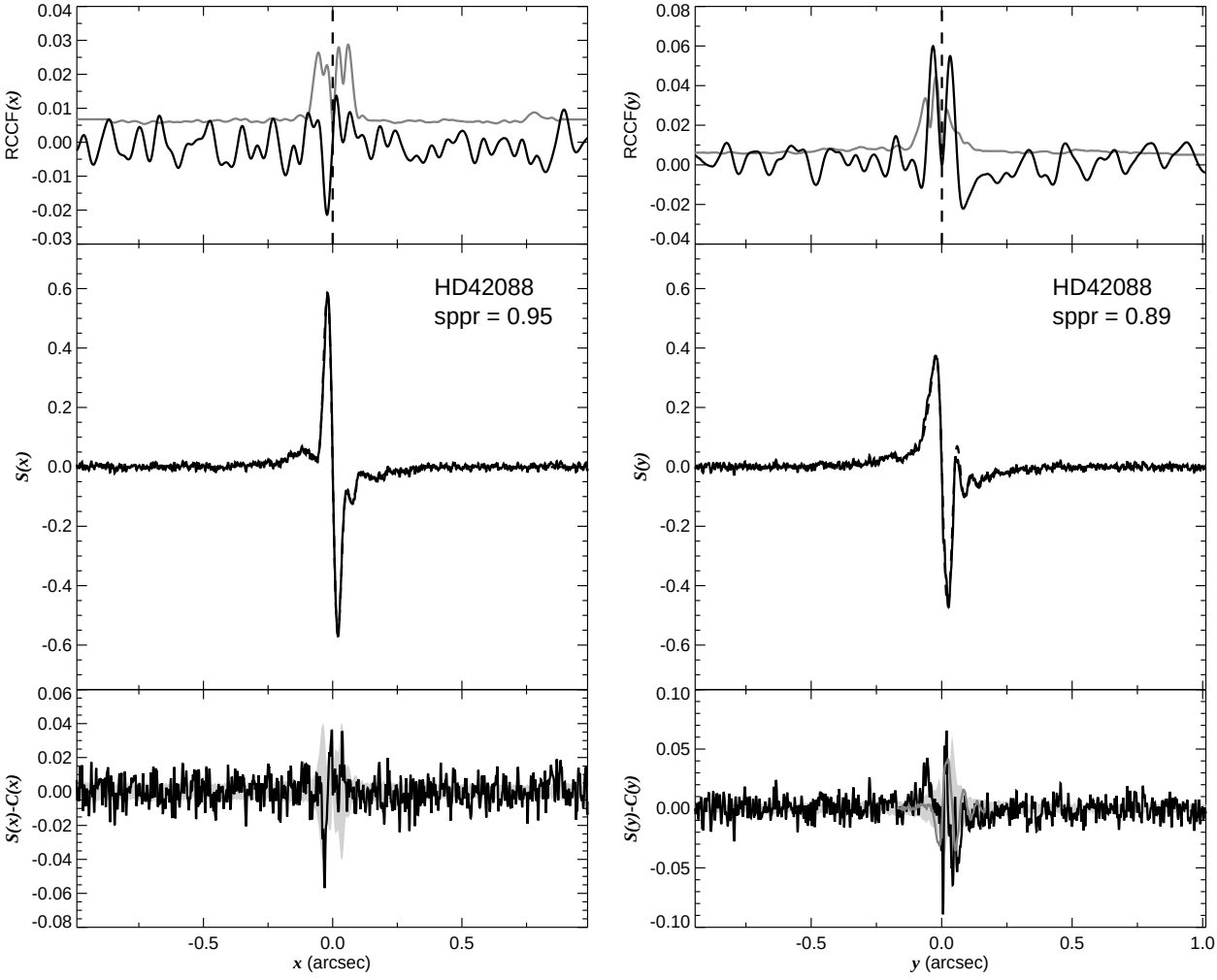

Fig. 1.47.— The FGS scans and binary detection tests for target 060939.57+202915.5 = HD42088 obtained on BY 2008.7644.

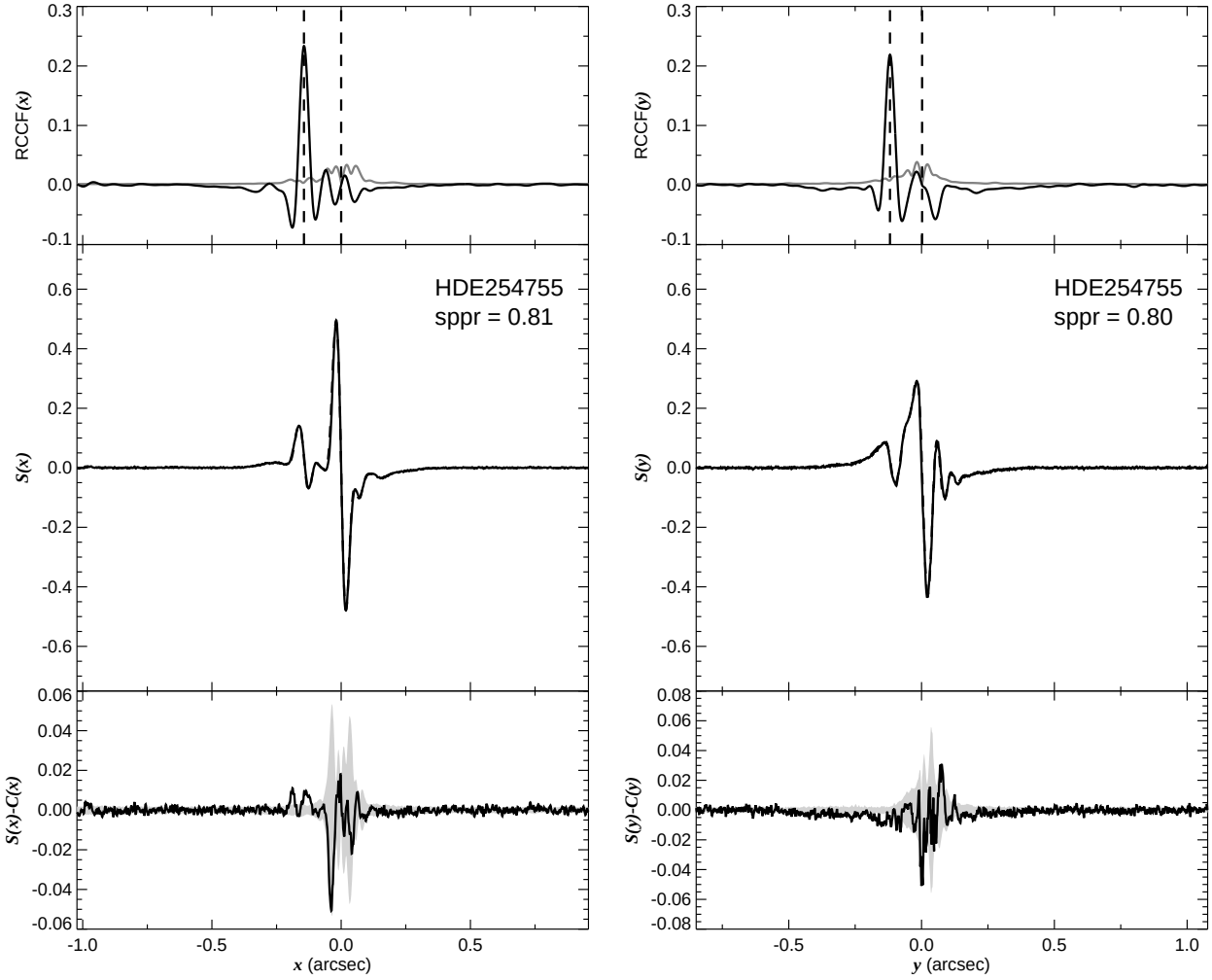

Fig. 1.48.— The FGS scans and binary detection tests for target 061831.77+224045.1 = HDE254755 obtained on BY 2008.7781.

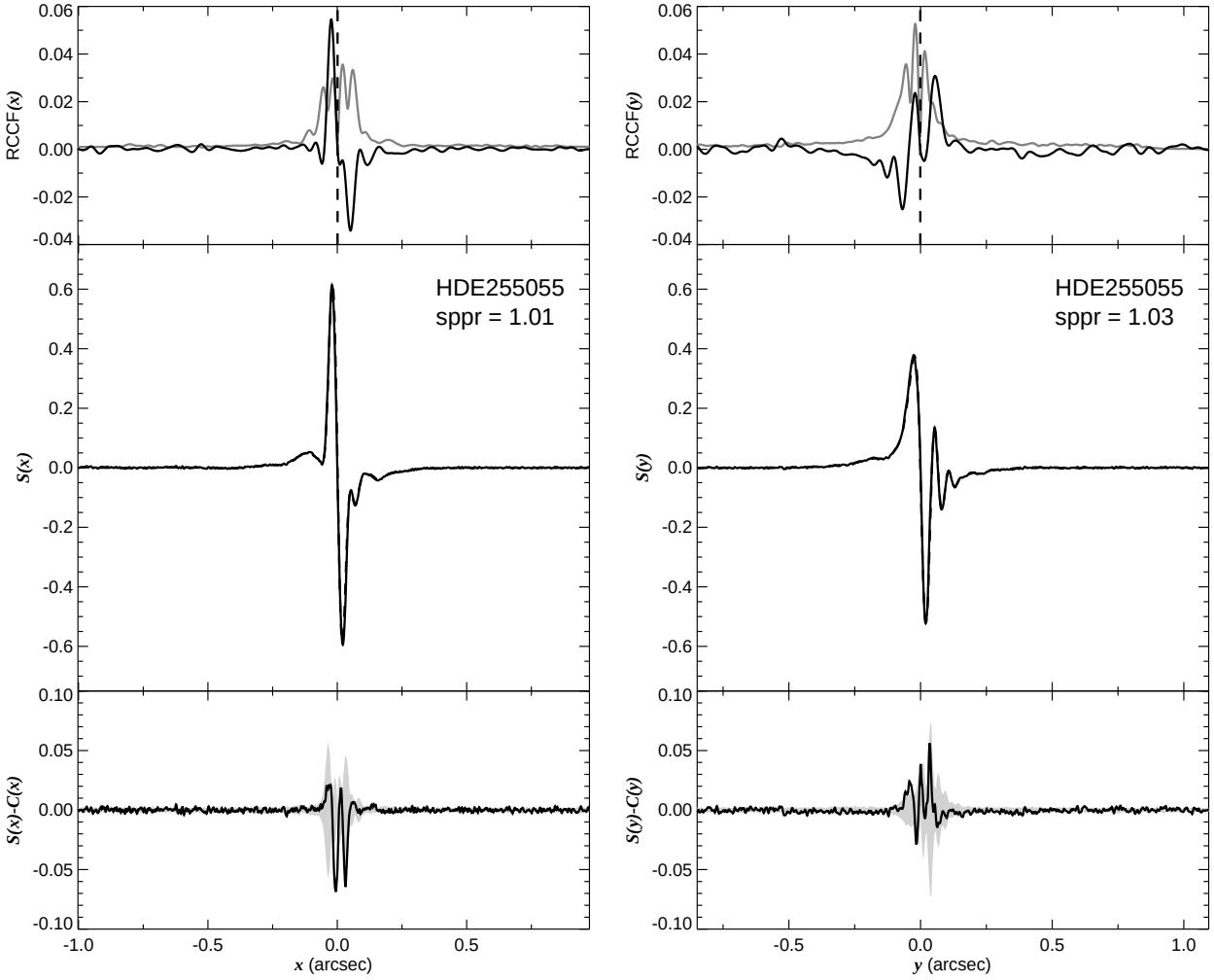

Fig. 1.49.— The FGS scans and binary detection tests for target 061941.65+231720.2 = HDE255055 obtained on BY 2008.7655.

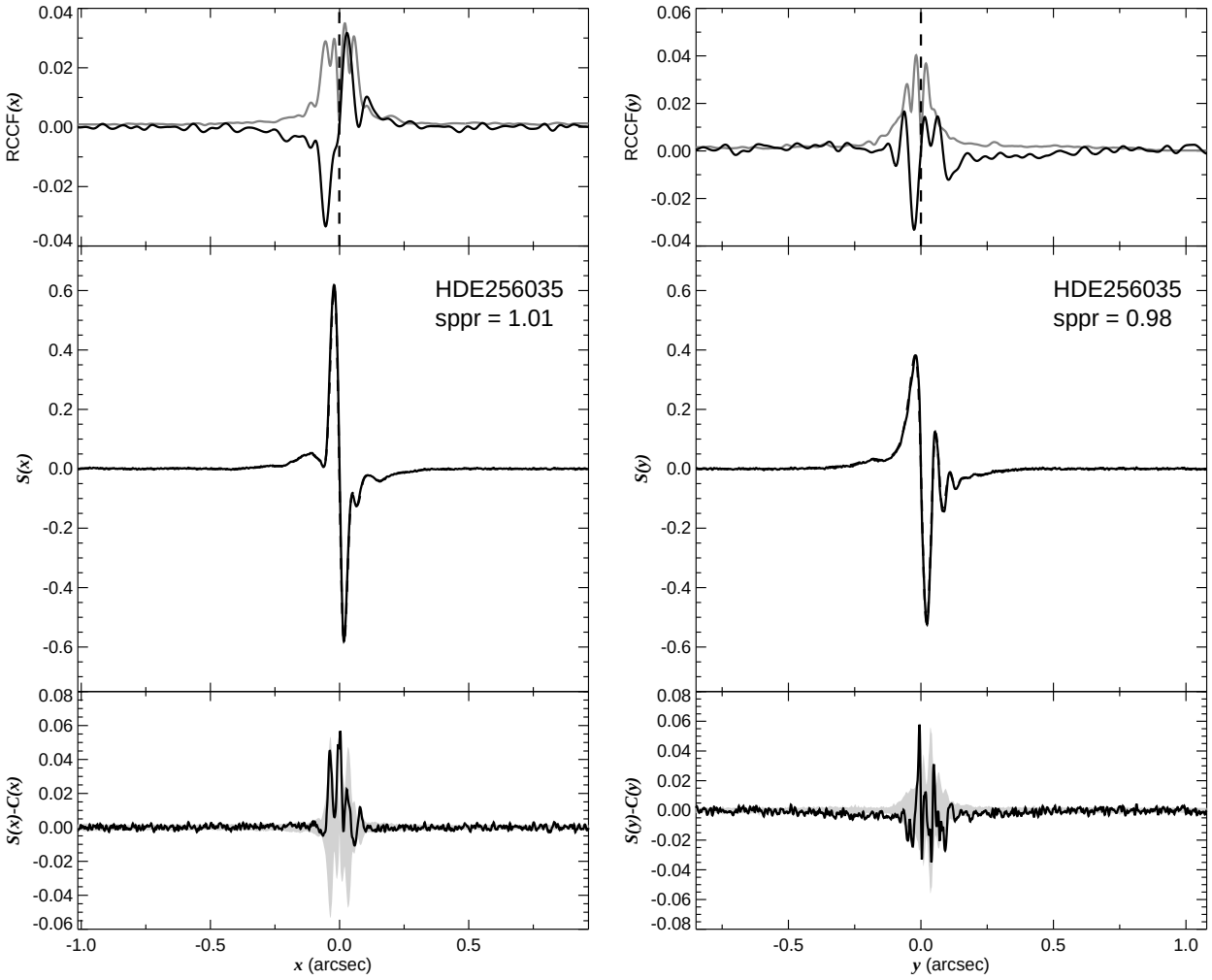

Fig. 1.50.— The FGS scans and binary detection tests for target 062258.24+225146.2 = HDE256035 obtained on BY 2008.7648.

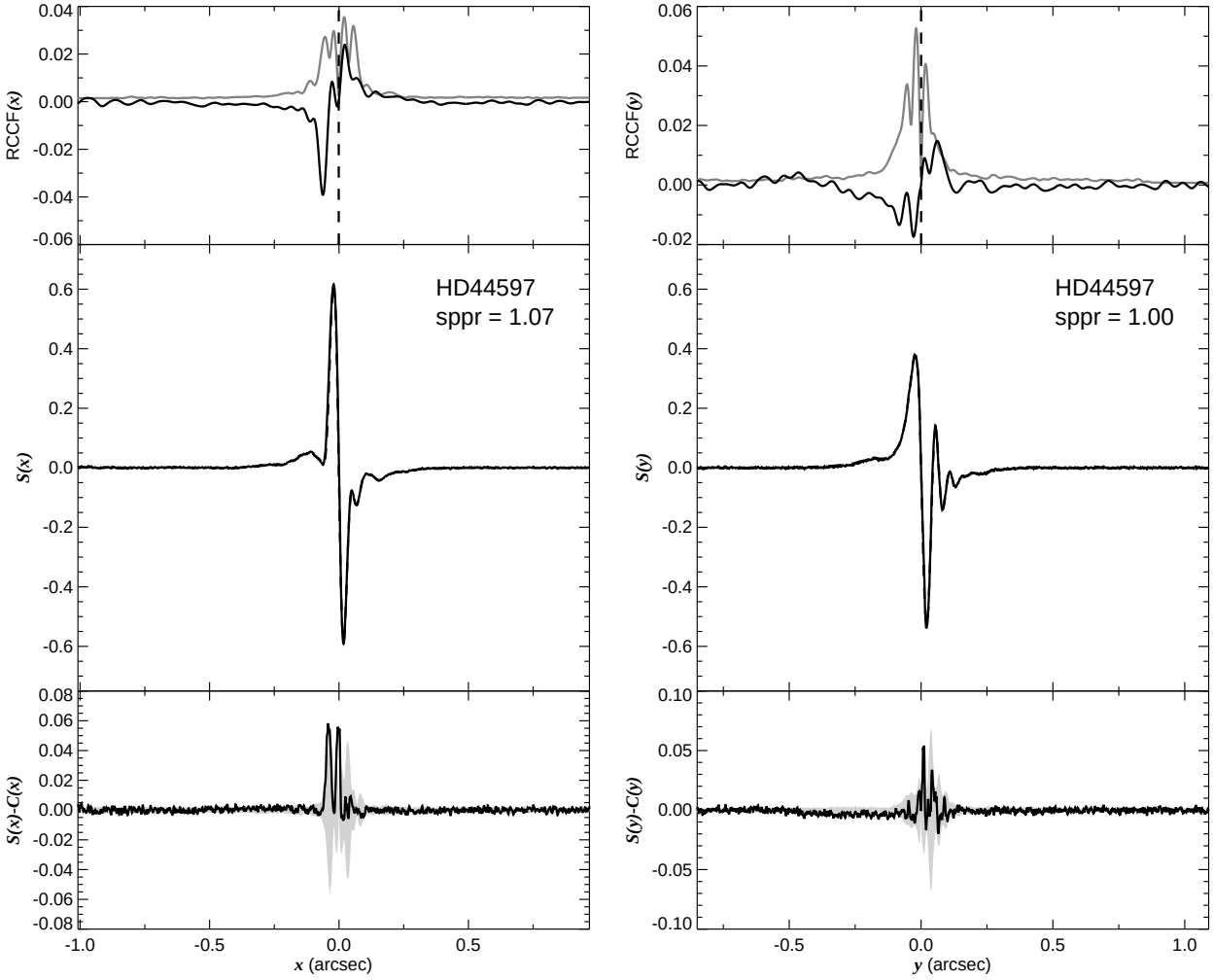

Fig. 1.51.— The FGS scans and binary detection tests for target 062328.54+202331.7 = HD44597 obtained on BY 2008.7650.

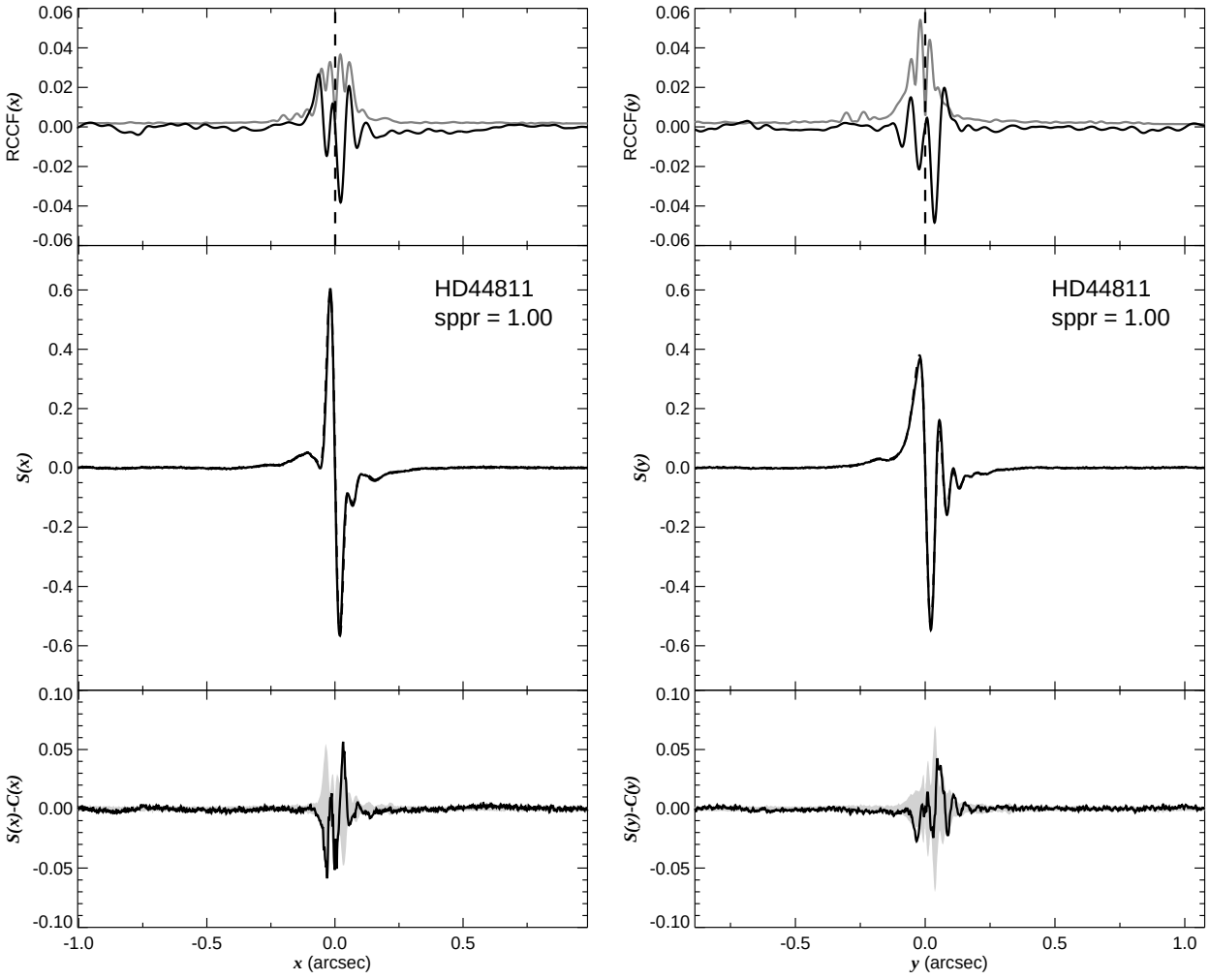

Fig. 1.52.— The FGS scans and binary detection tests for target 062438.36+194215.8 = HD44811 obtained on BY 2008.7085.

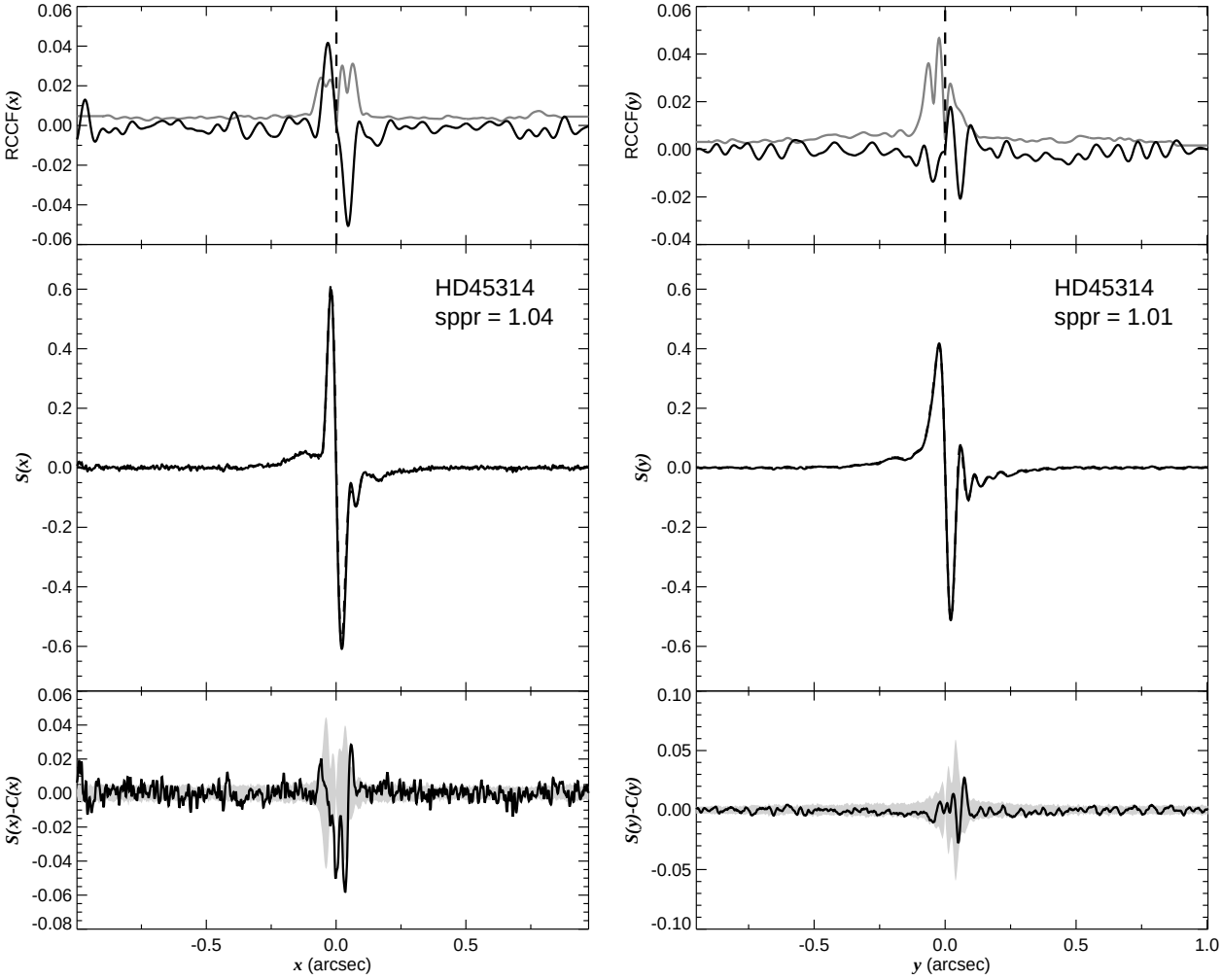

Fig. 1.53.— The FGS scans and binary detection tests for target 062715.78+145321.2 = HD45314 obtained on BY 2008.0037.

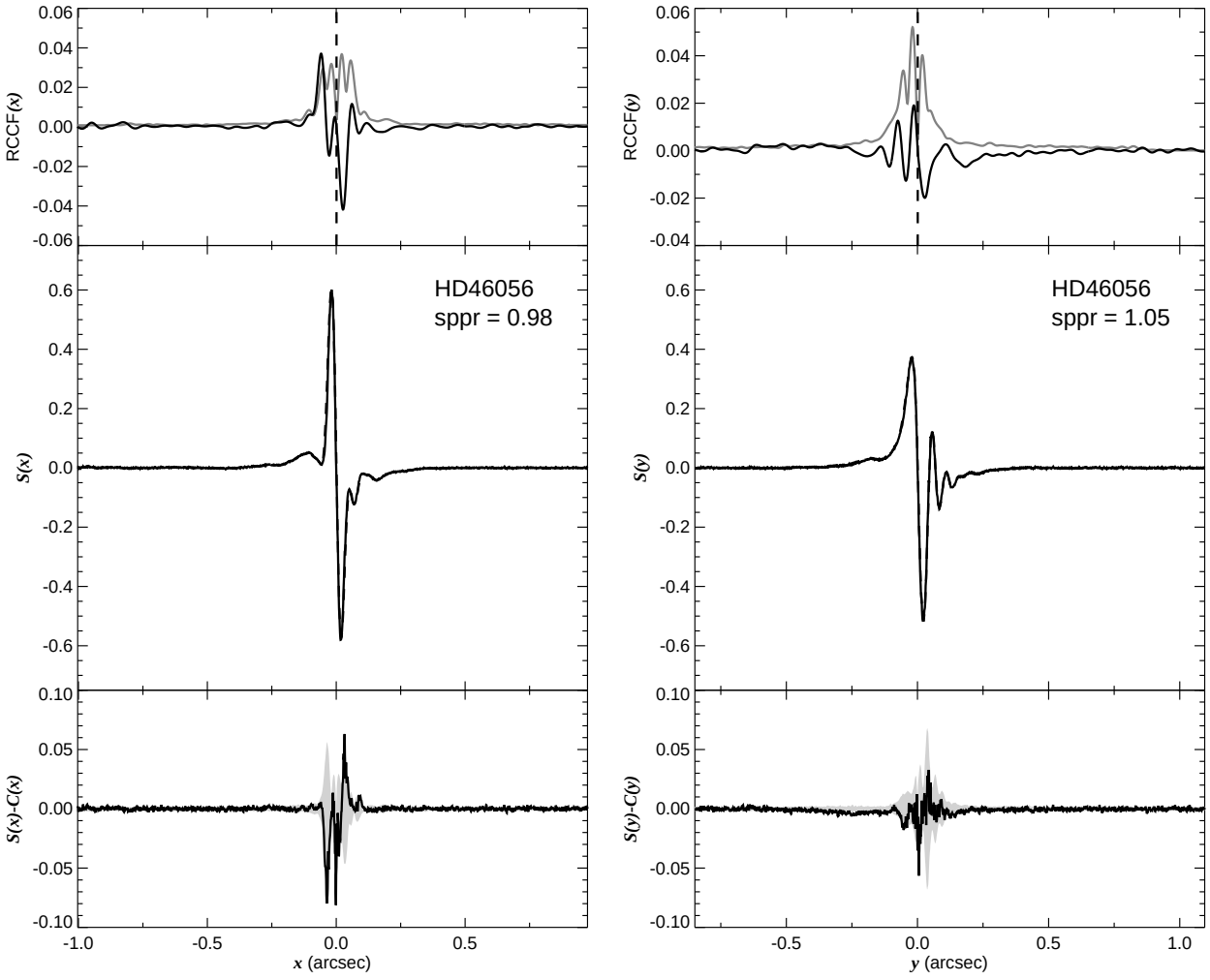

Fig. 1.54.— The FGS scans and binary detection tests for target 063120.87+045003.3 = HD46056 obtained on BY 2008.7653.

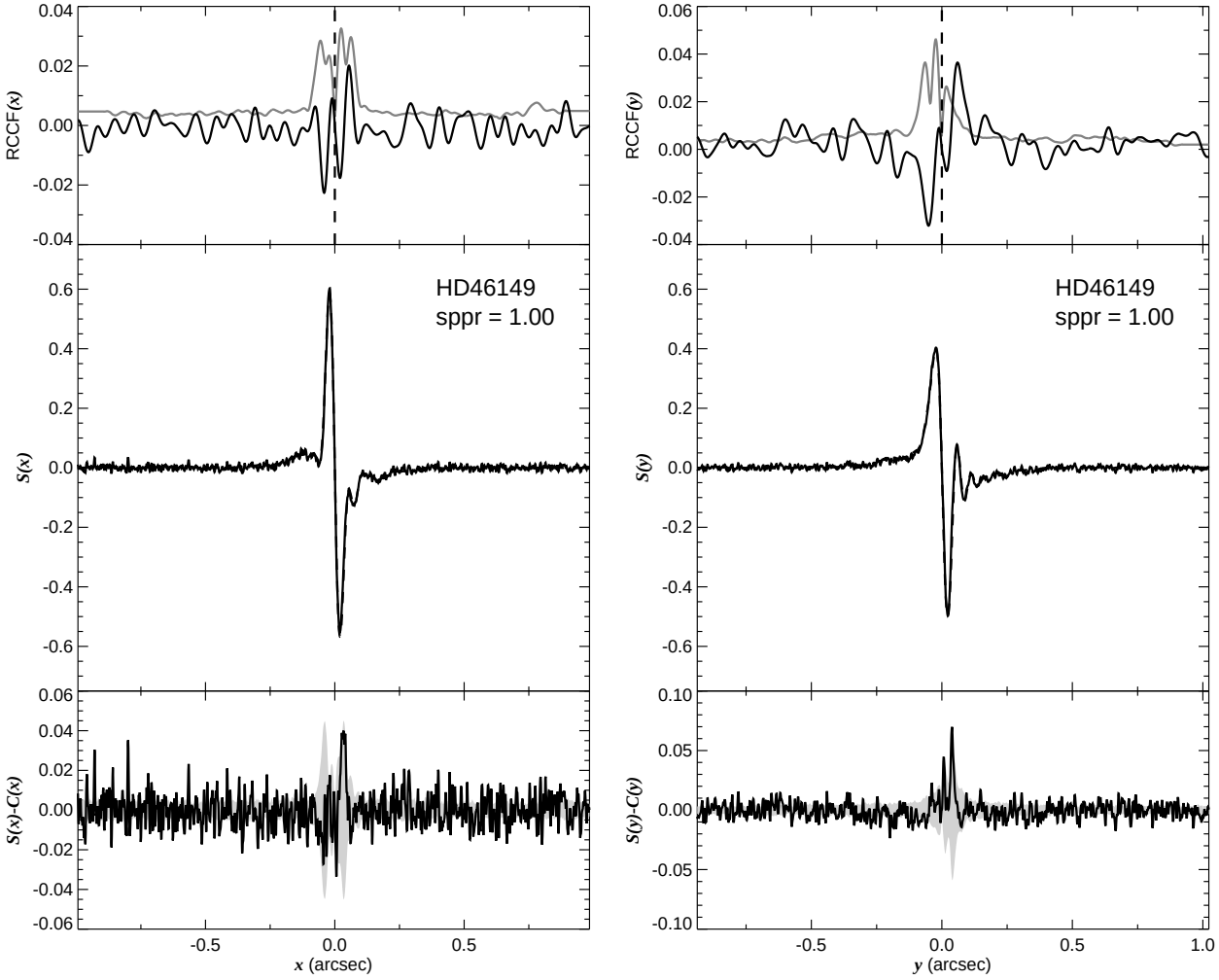

Fig. 1.55.— The FGS scans and binary detection tests for target 063152.53+050159.2 = HD46149 obtained on BY 2007.6908.

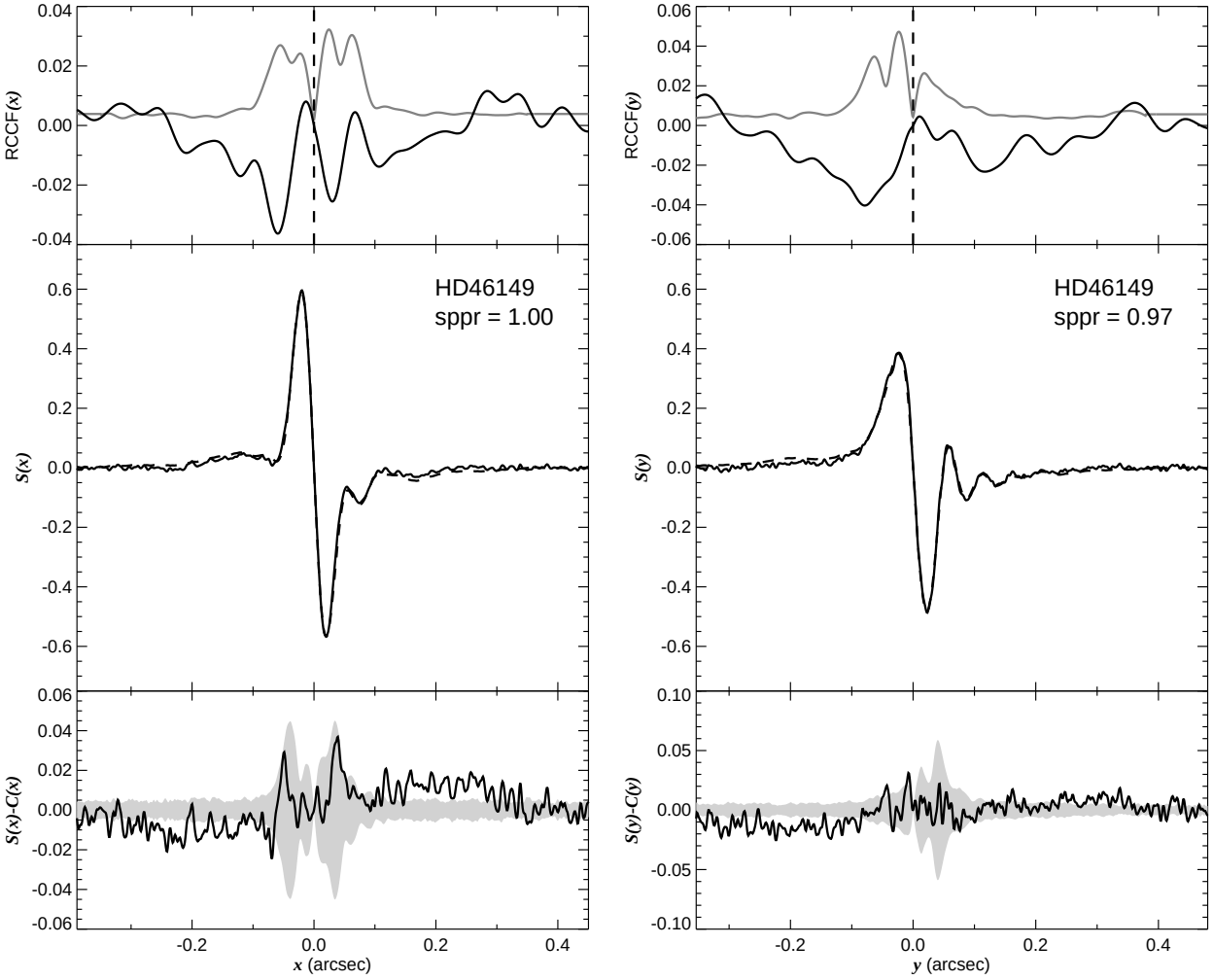

Fig. 1.56.— The FGS scans and binary detection tests for target 063152.53+050159.2 = HD46149 obtained on BY 2008.8454.

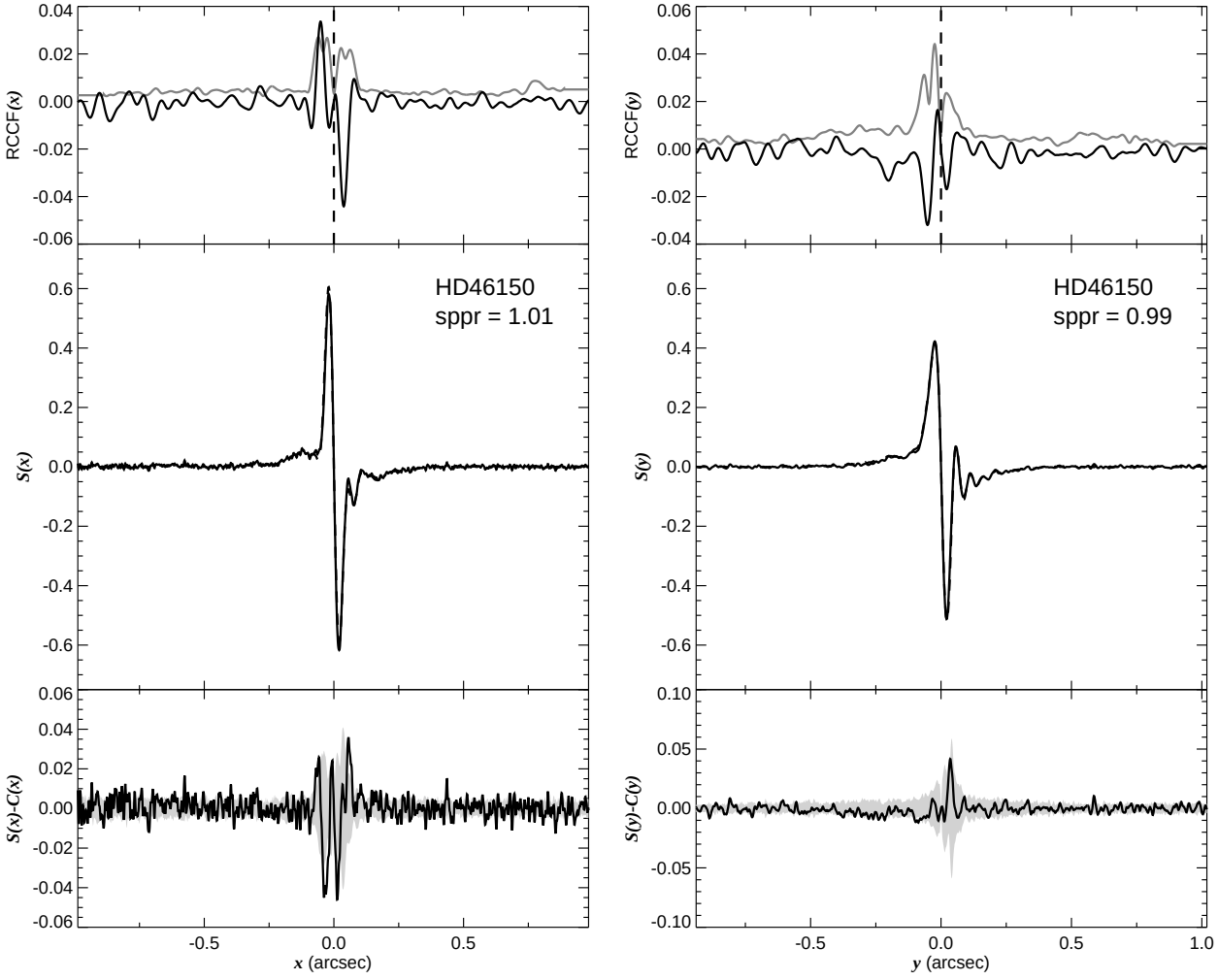

Fig. 1.57.— The FGS scans and binary detection tests for target 063155.52+045634.3 = HD46150 obtained on BY 2008.0311.

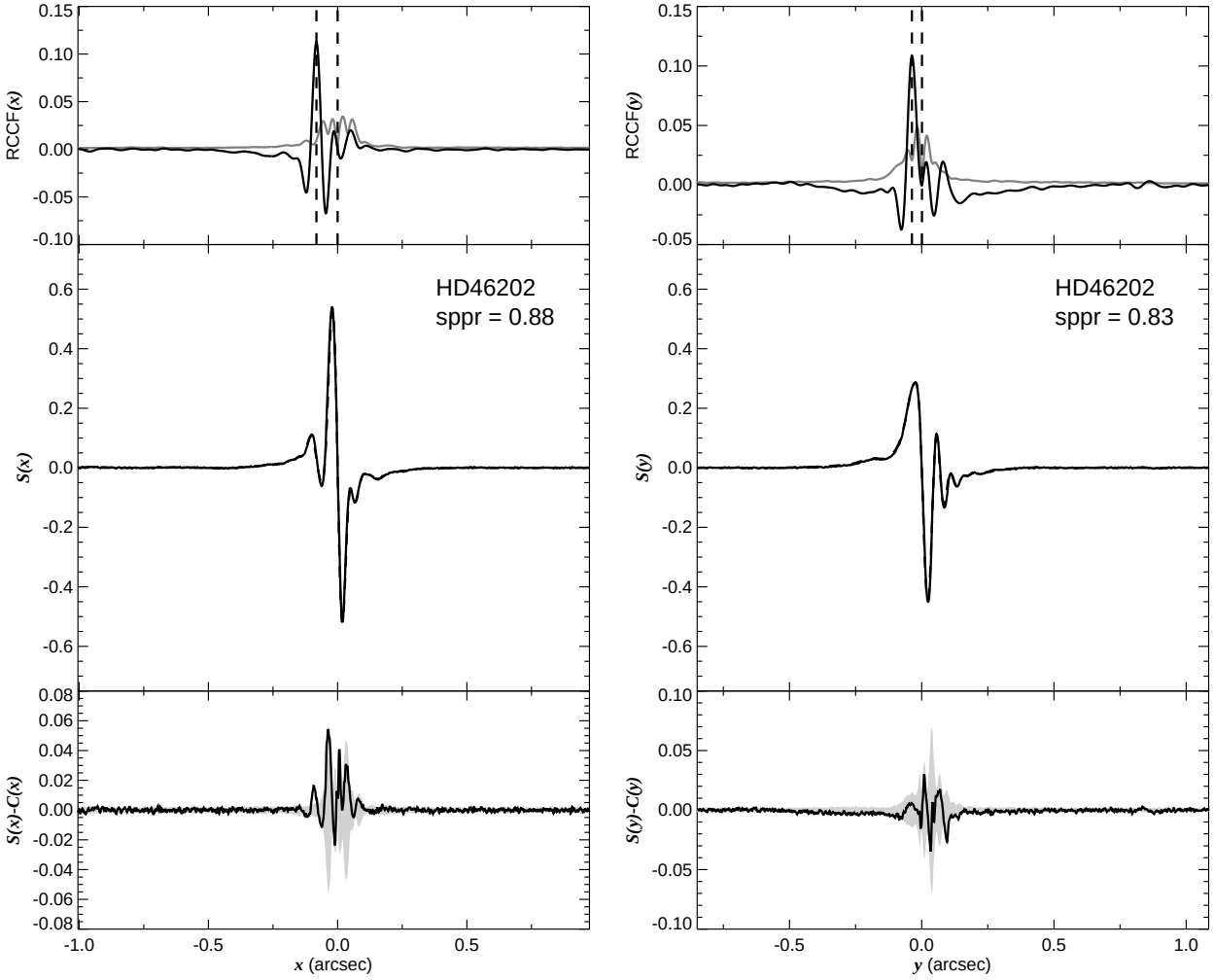

Fig. 1.58.— The FGS scans and binary detection tests for target 063210.47+045759.8 = HD46202 obtained on BY 2008.7417.

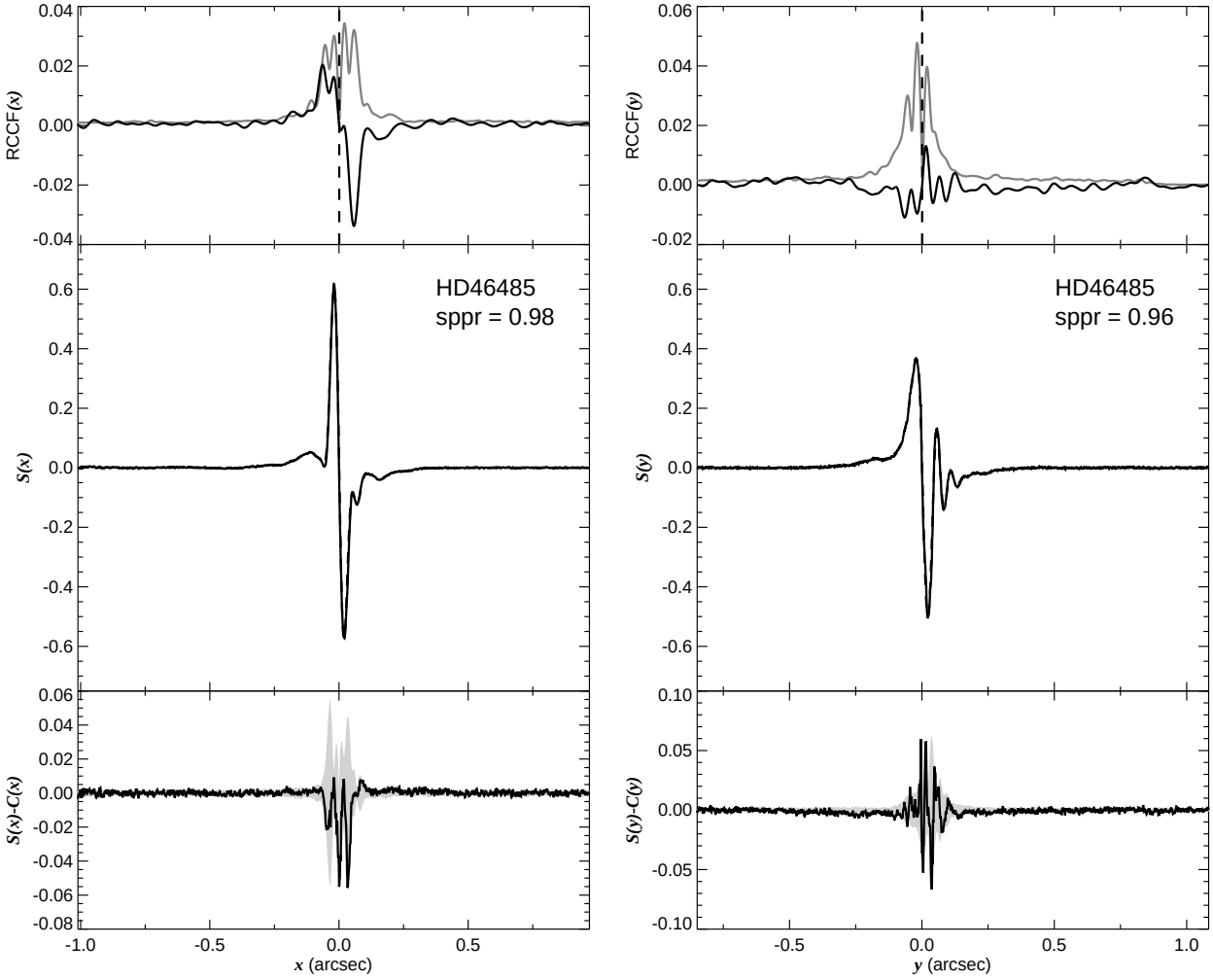

Fig. 1.59.— The FGS scans and binary detection tests for target 063350.96+043131.6 = HD46485 obtained on BY 2008.7730.

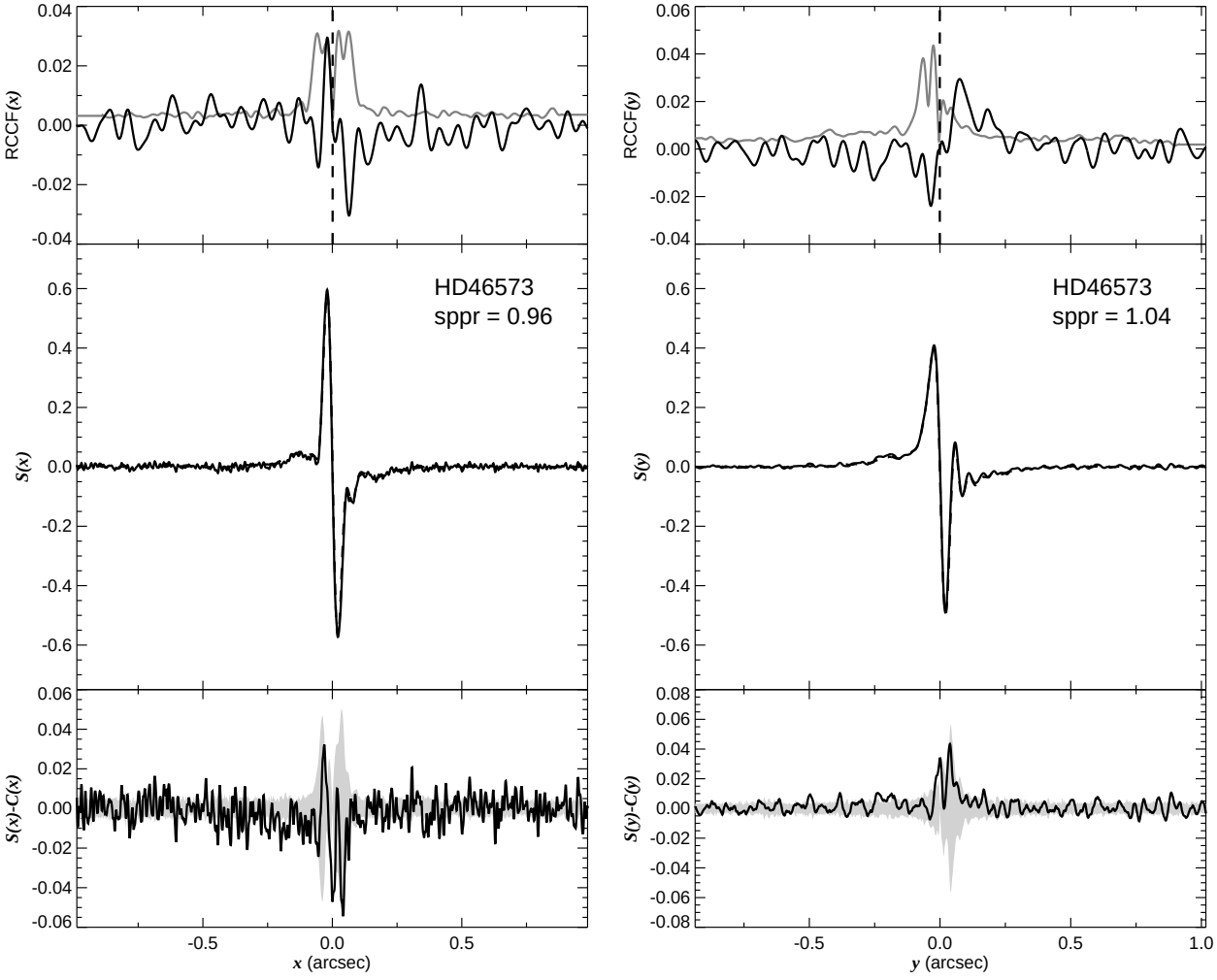

Fig. 1.60.— The FGS scans and binary detection tests for target 063423.57+023202.9 = HD46573 obtained on BY 2008.7684.

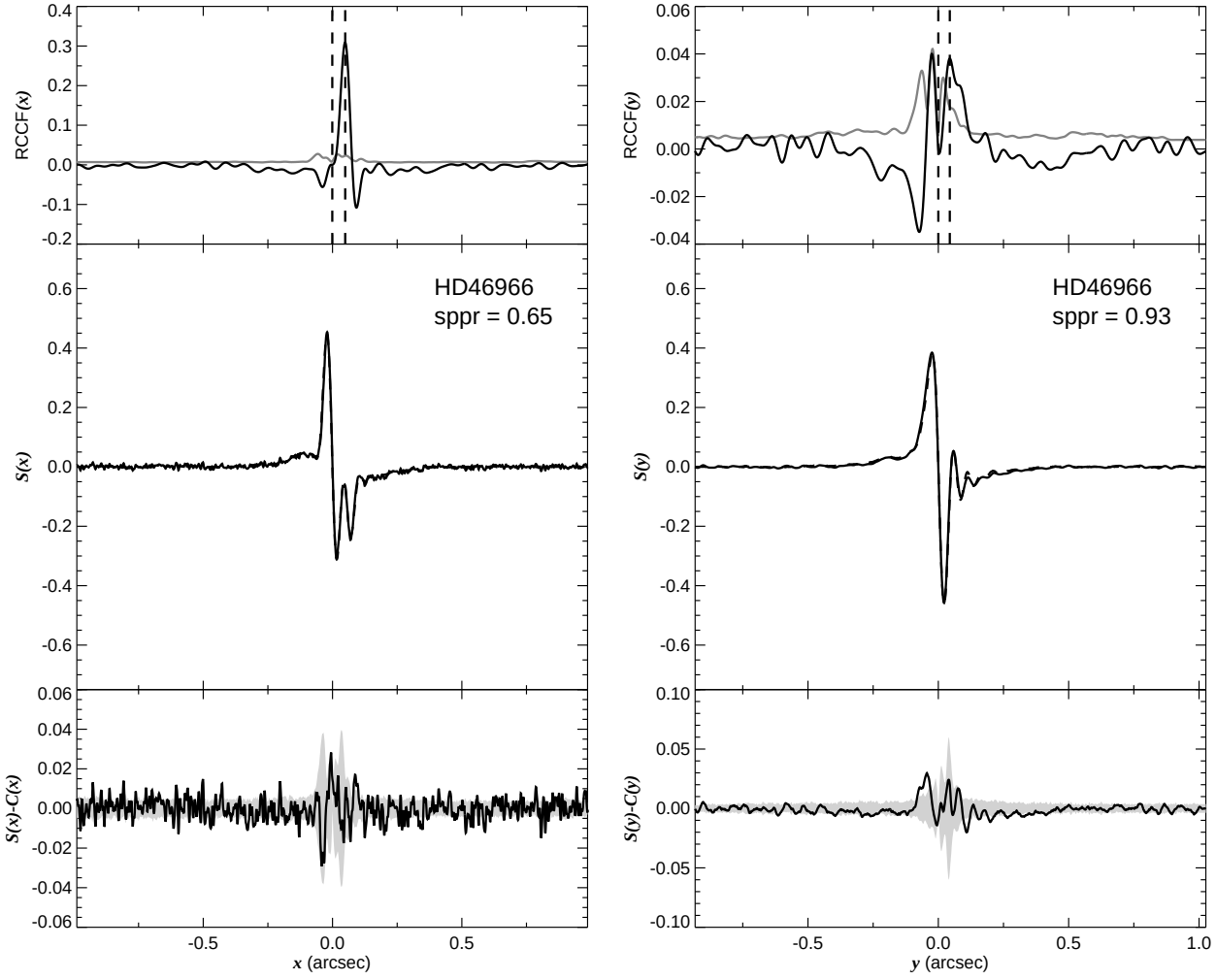

Fig. 1.61.— The FGS scans and binary detection tests for target 063625.89+060459.5 = HD46966 obtained on BY 2008.7282.

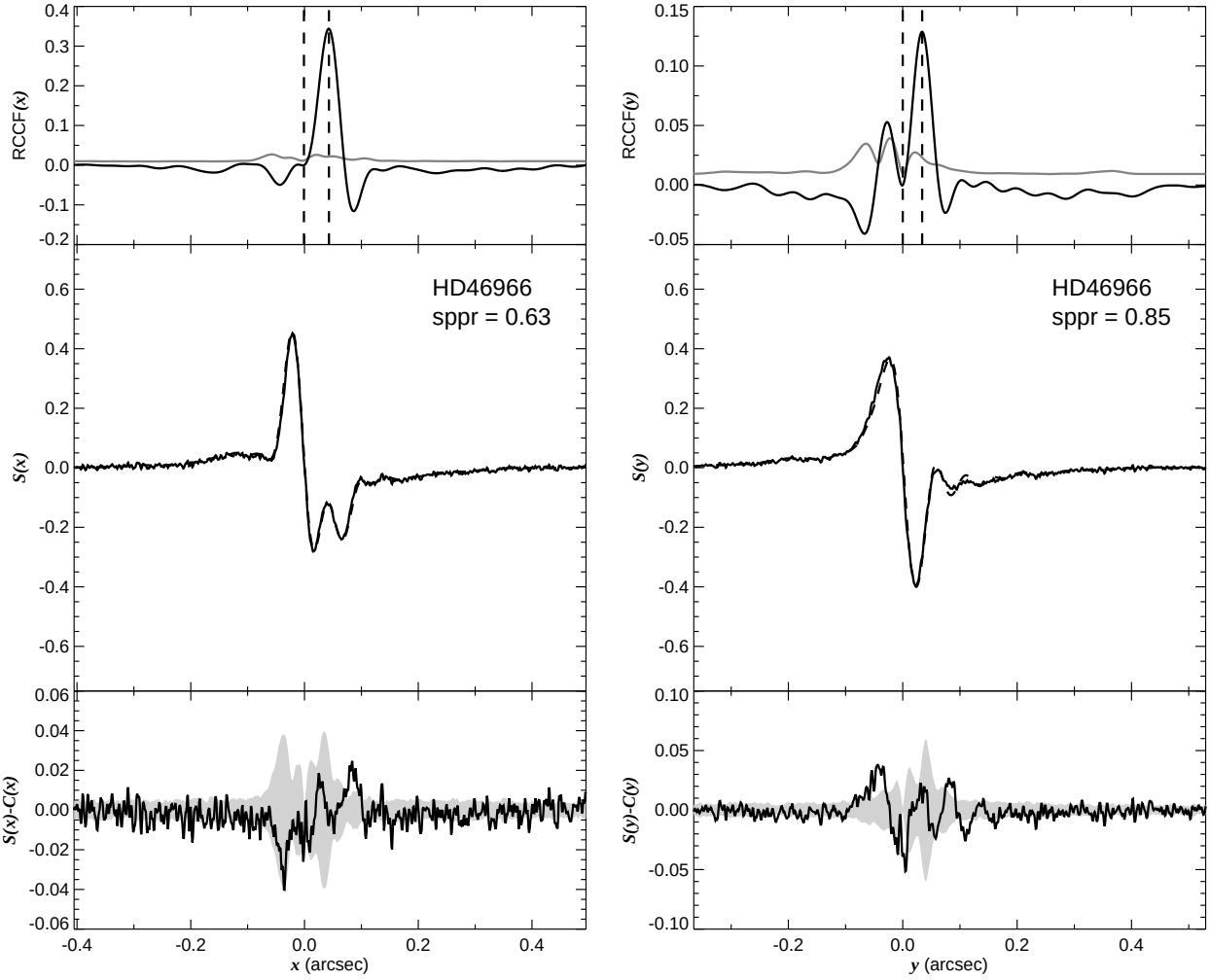

Fig. 1.62.— The FGS scans and binary detection tests for target 063625.89+060459.5 = HD46966 obtained on BY 2008.8651.

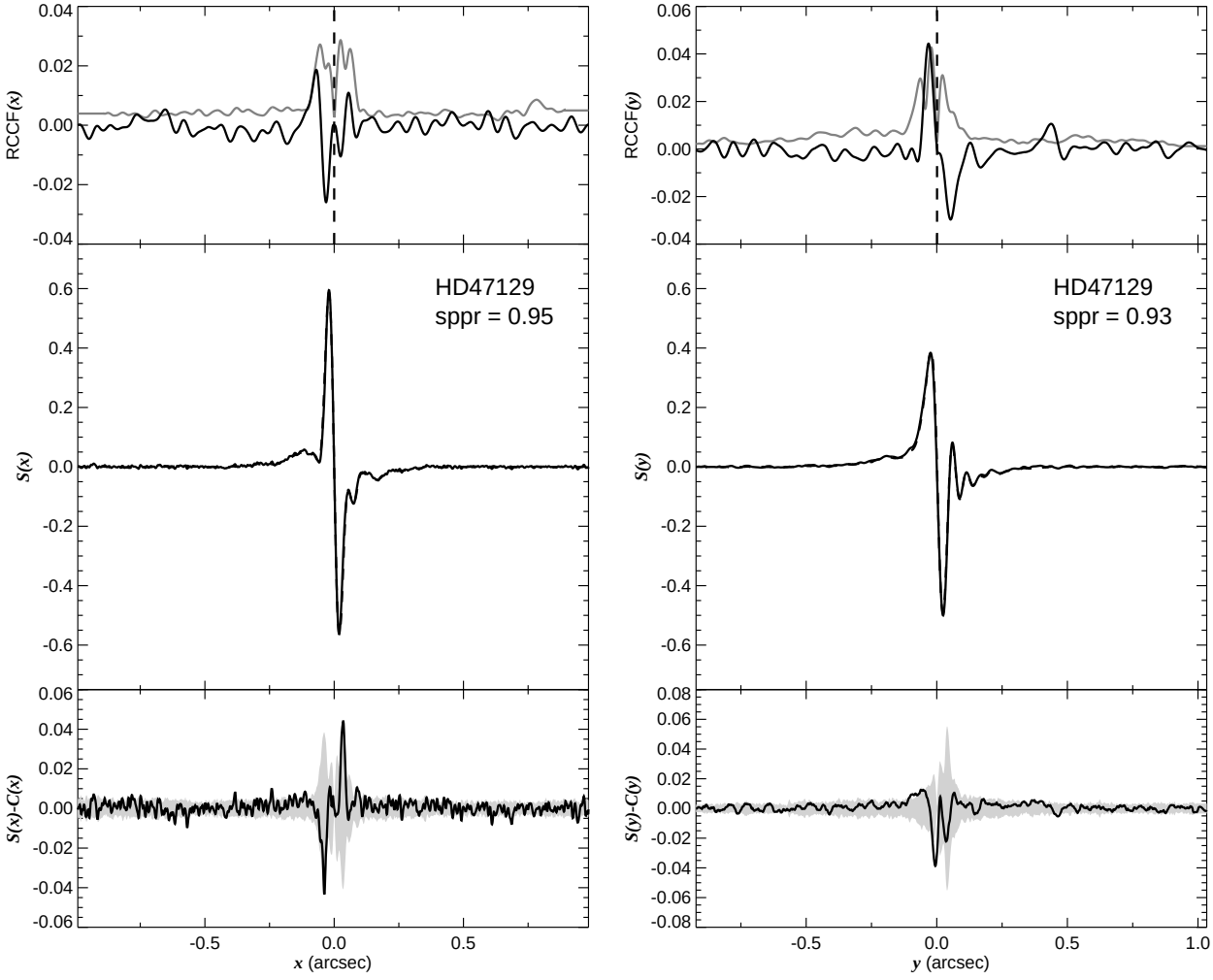

Fig. 1.63.— The FGS scans and binary detection tests for target 063724.04+060807.4 = HD47129 obtained on BY 2008.7263.

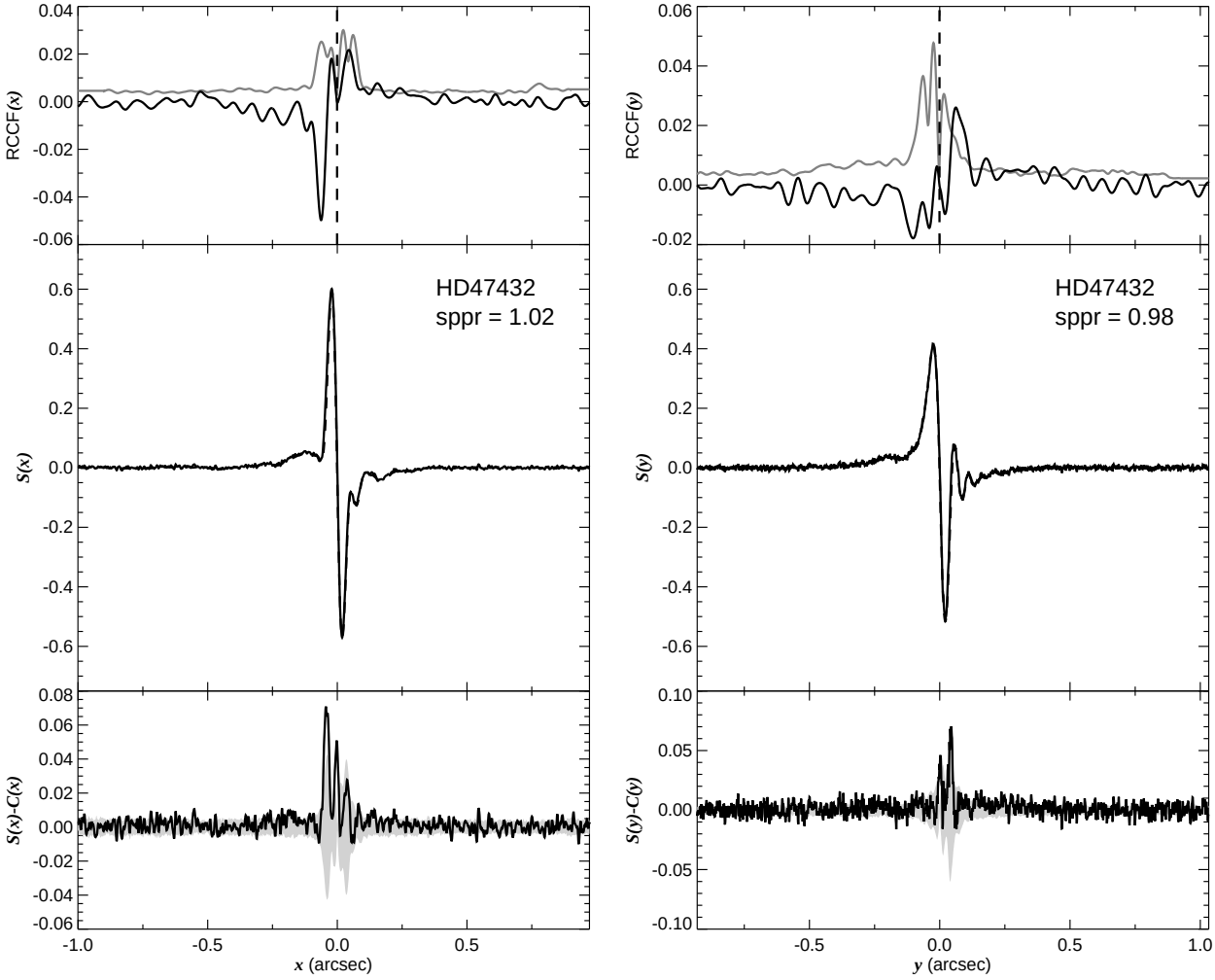

Fig. 1.64.— The FGS scans and binary detection tests for target 063838.19+013648.7 = HD47432 obtained on BY 2008.7783.

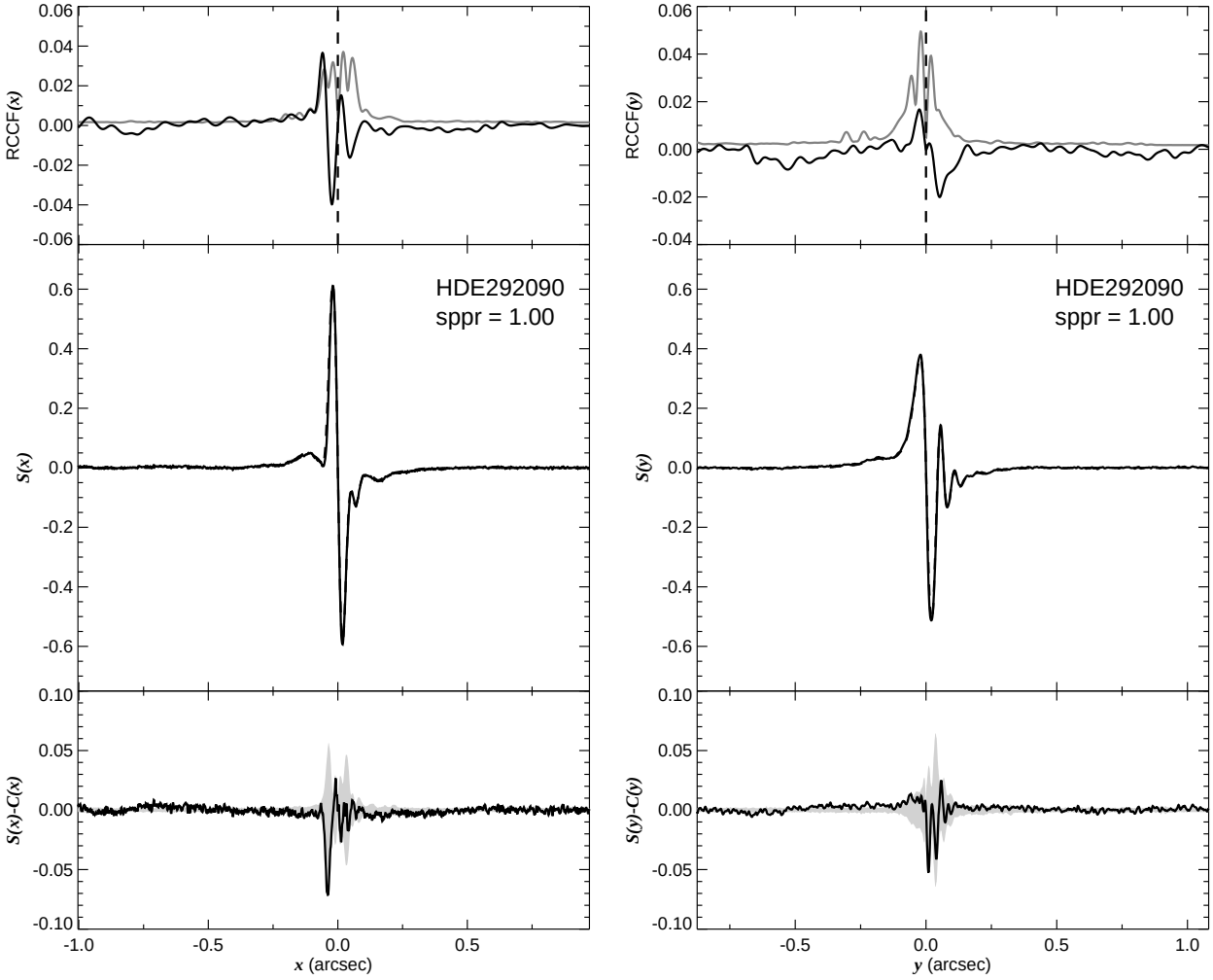

Fig. 1.65.— The FGS scans and binary detection tests for target 064021.98−002126.0 = HDE292090 obtained on BY 2008.7659.

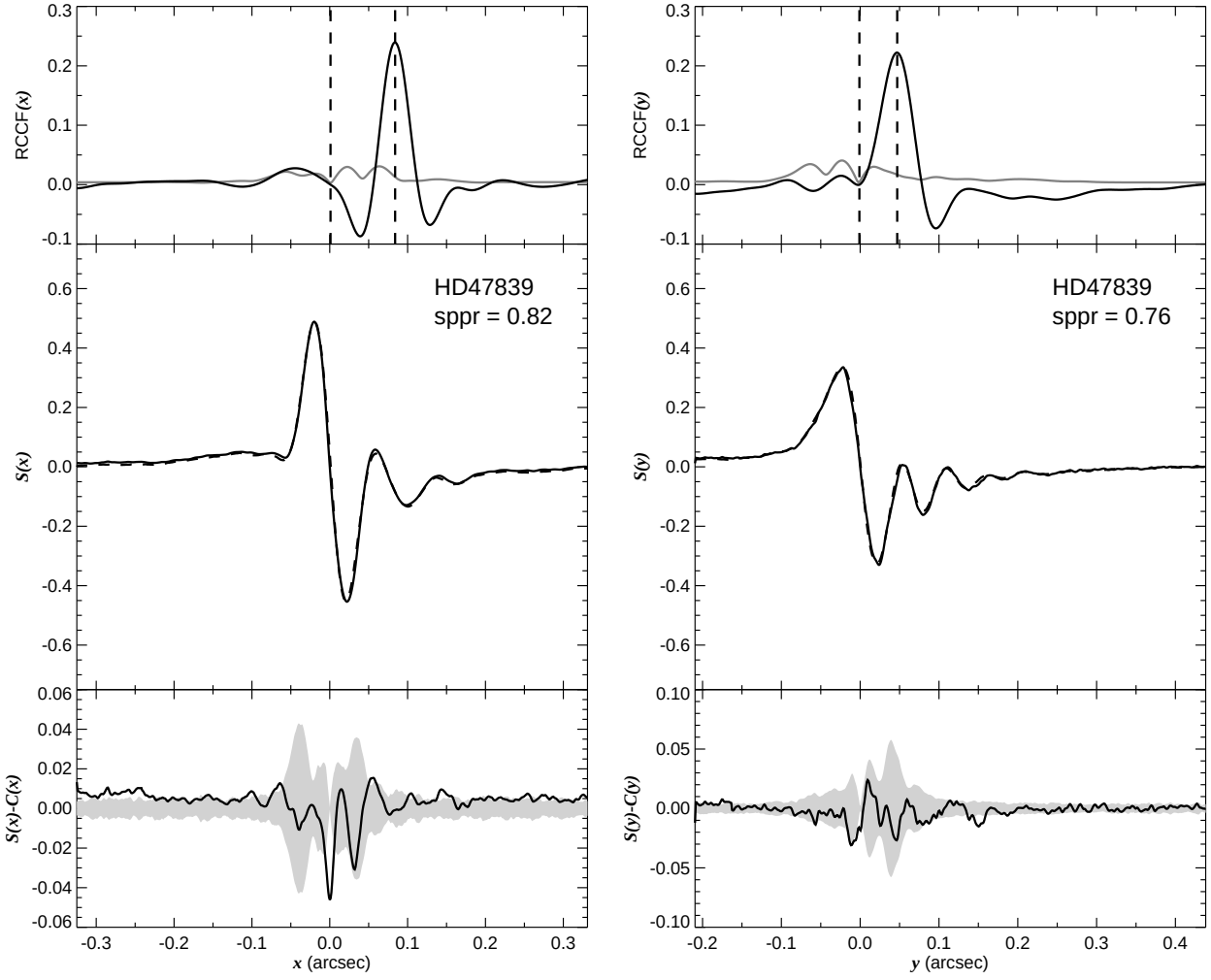

Fig. 1.66.— The FGS scans and binary detection tests for target 064058.66+095344.7 = HD47839 obtained on BY 2007.8192.

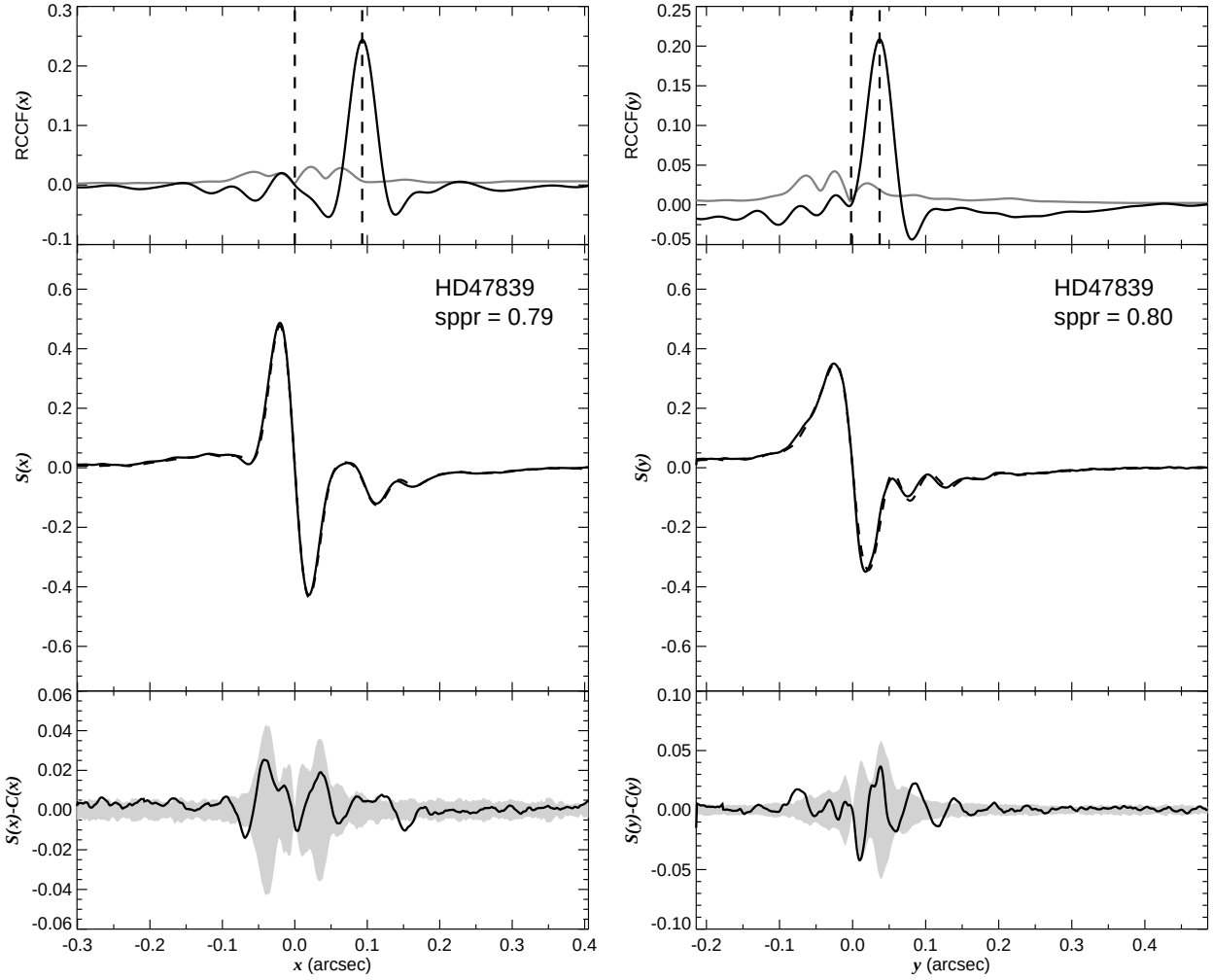

Fig. 1.67.— The FGS scans and binary detection tests for target 064058.66+095344.7 = HD47839 obtained on BY 2008.7829.

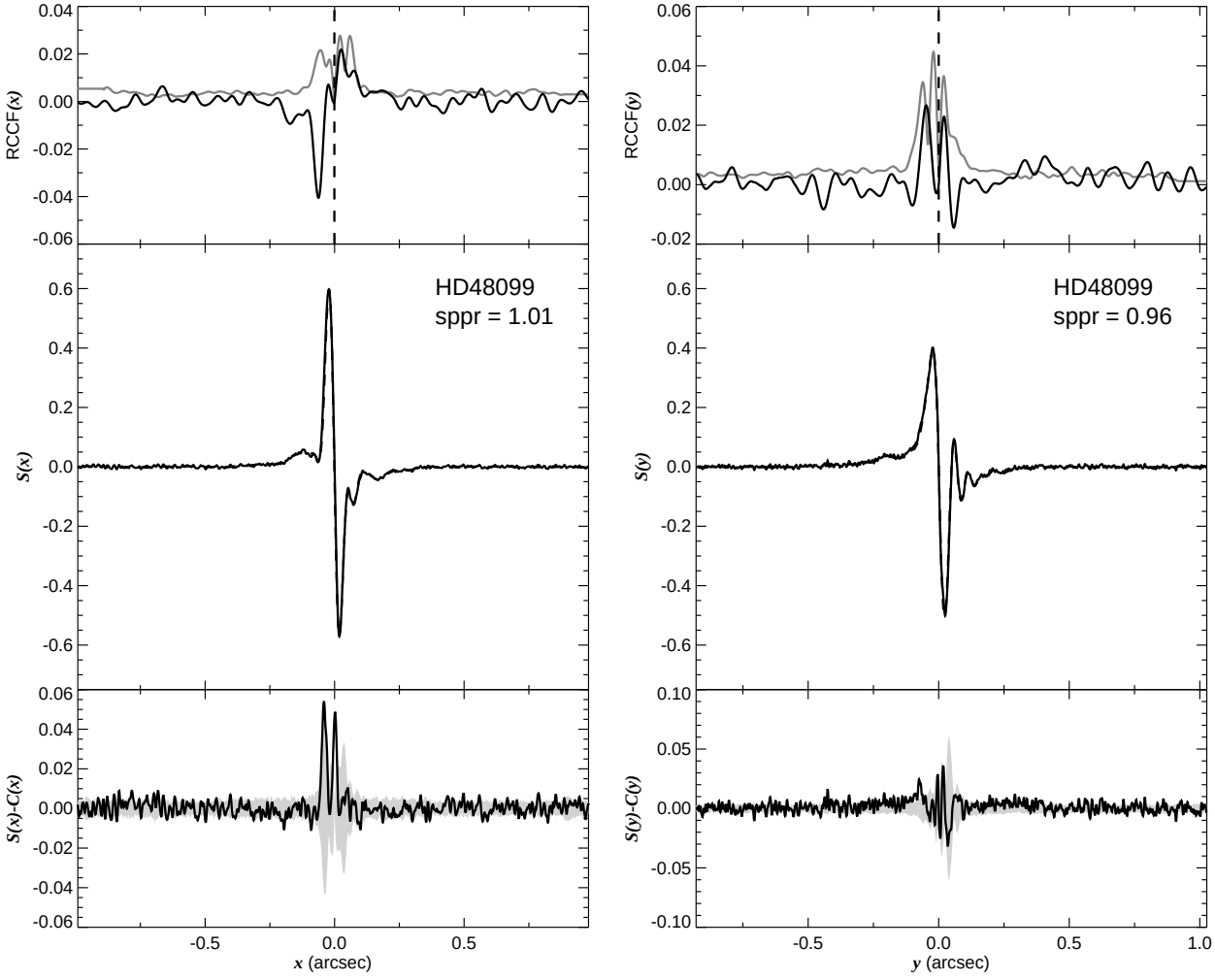

Fig. 1.68.— The FGS scans and binary detection tests for target 064159.23+062043.5 = HD48099 obtained on BY 2008.6955.

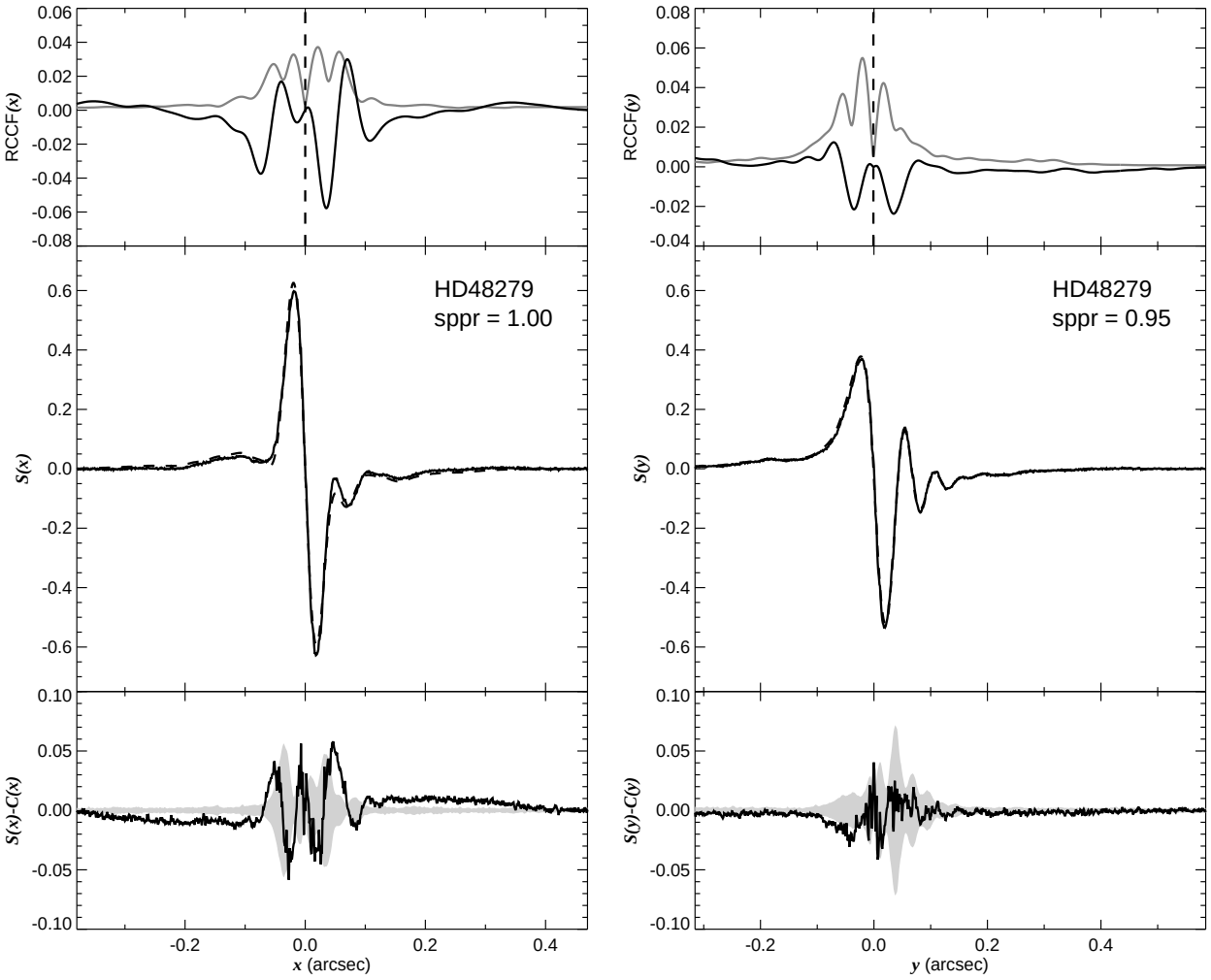

Fig. 1.69.— The FGS scans and binary detection tests for target 064240.55+014258.2 = HD48279 obtained on BY 2008.8802.

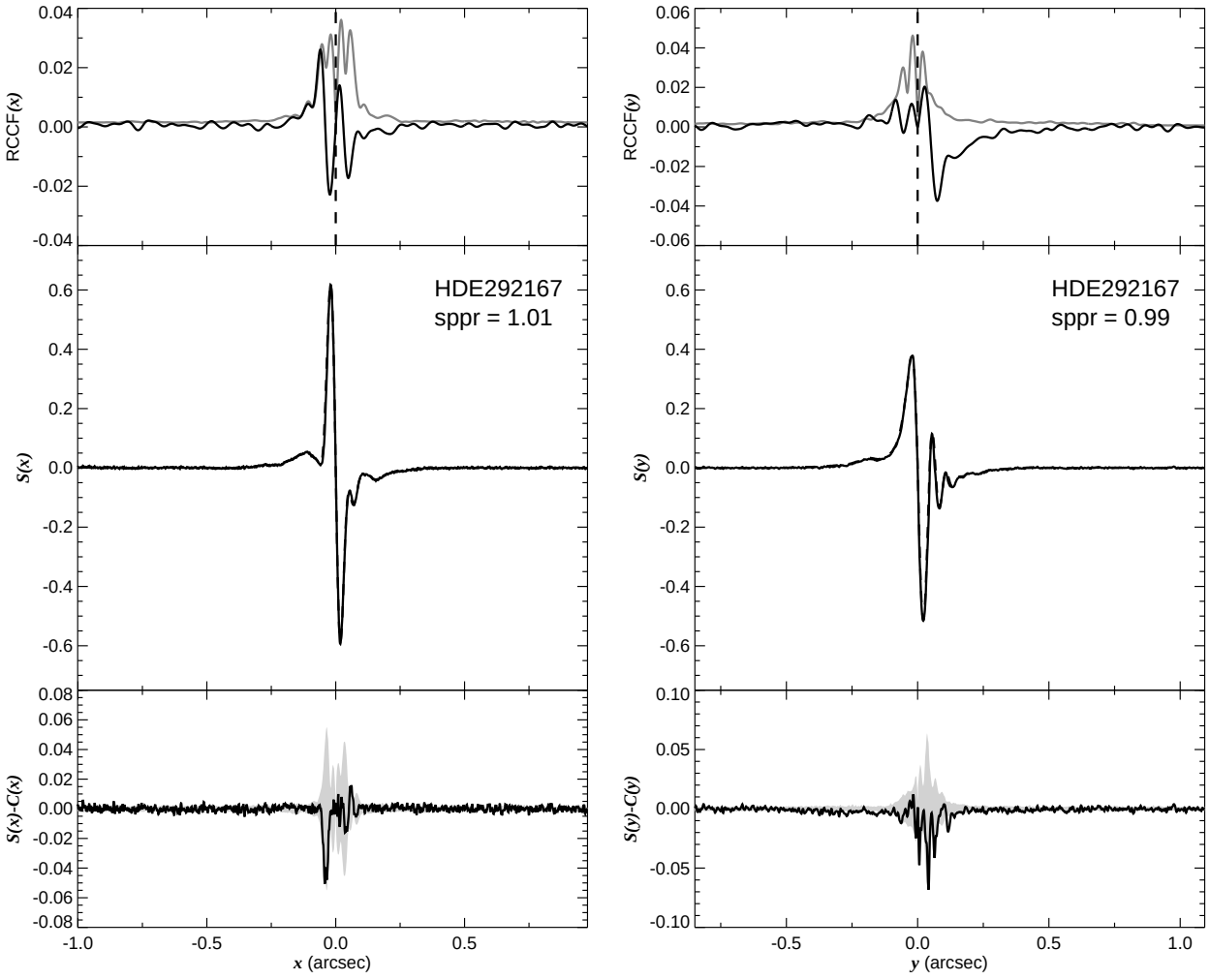

Fig. 1.70.— The FGS scans and binary detection tests for target 064453.82+003712.6 = HDE292167 obtained on BY 2008.7657.

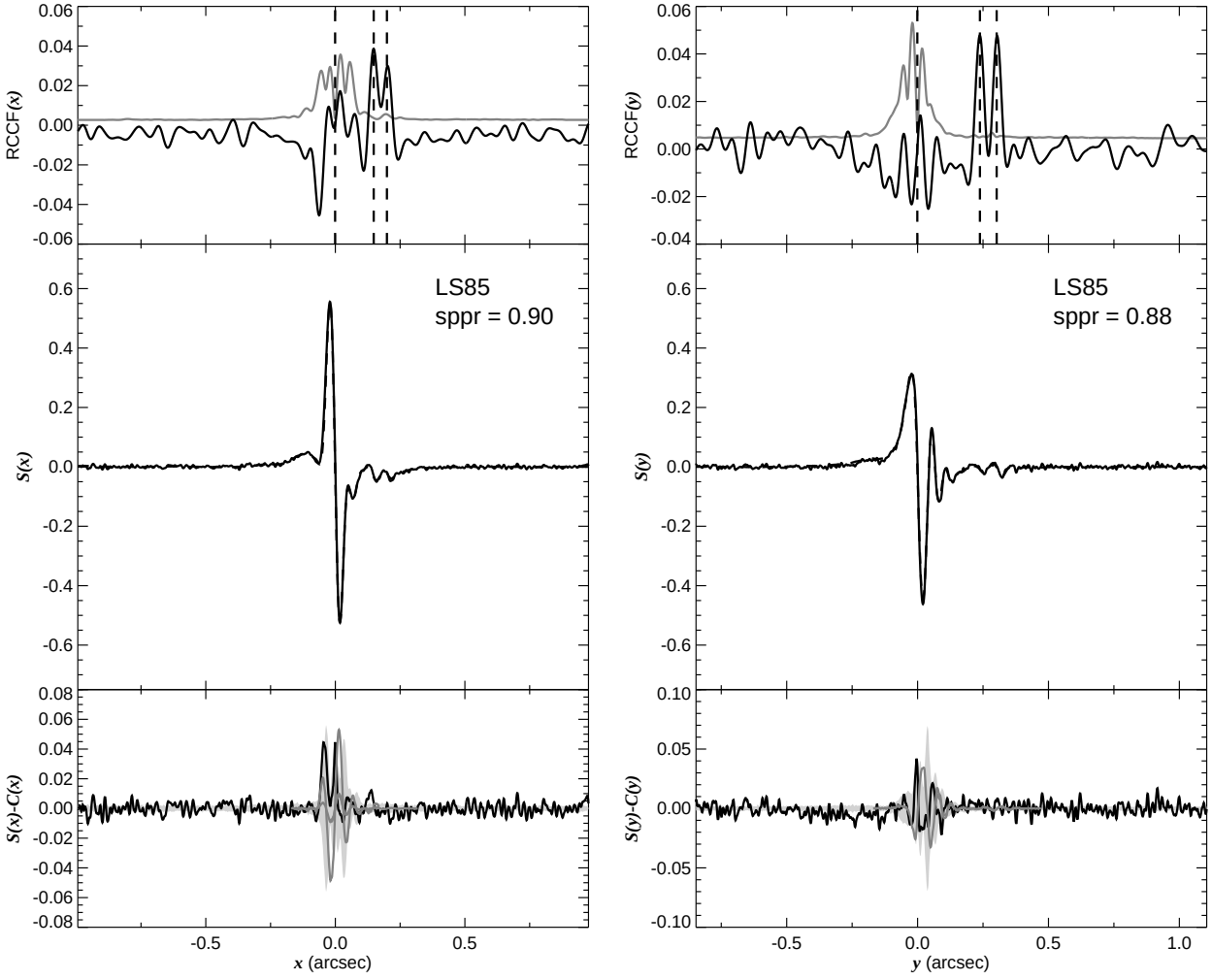

Fig. 1.71.— The FGS scans and binary detection tests for target 064548.70−071839.0 = ALS85 obtained on BY 2008.8093.

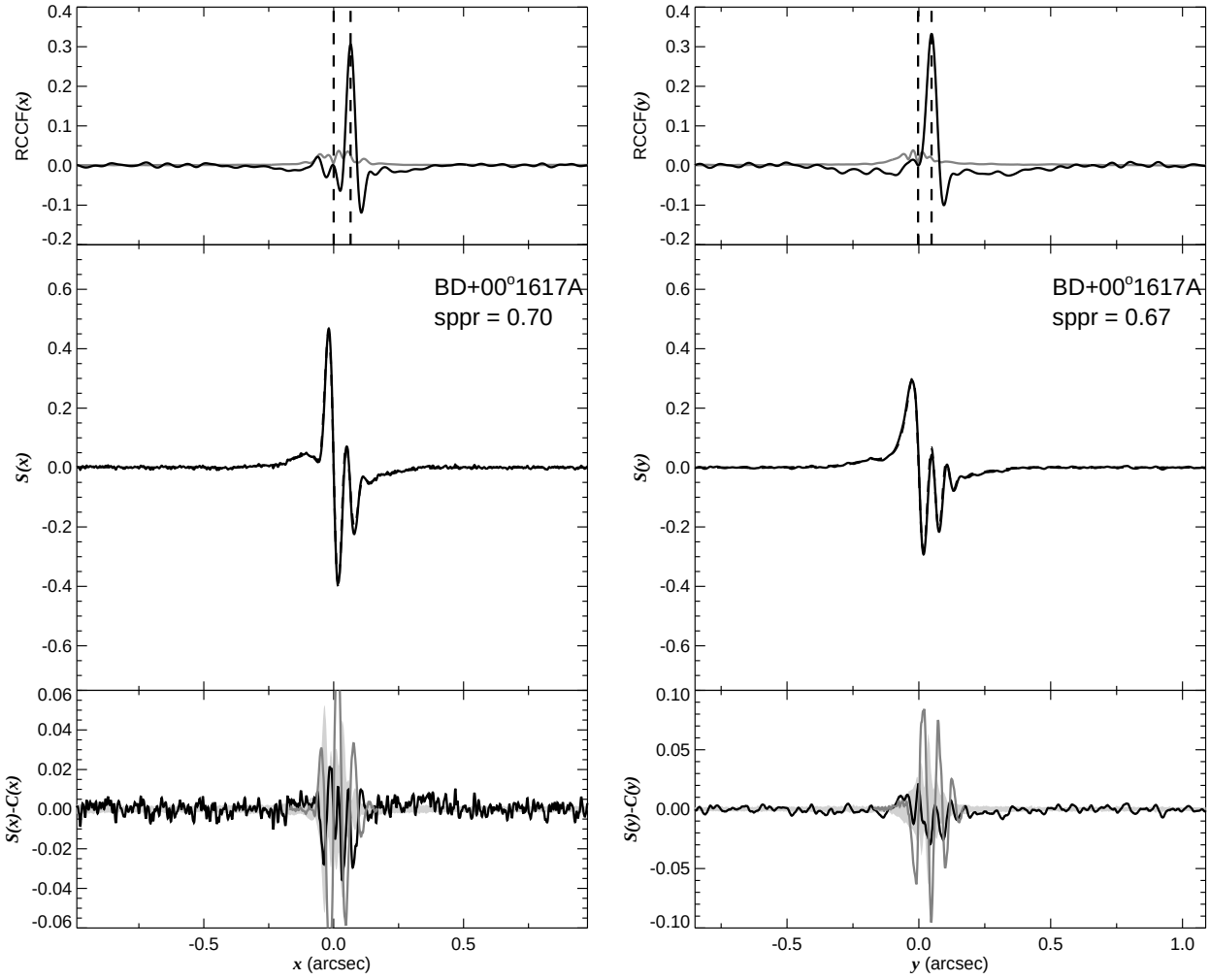

Fig. 1.72.— The FGS scans and binary detection tests for target 064849.56+002252.7 = BD+00 1617A obtained on BY 2008.8047.

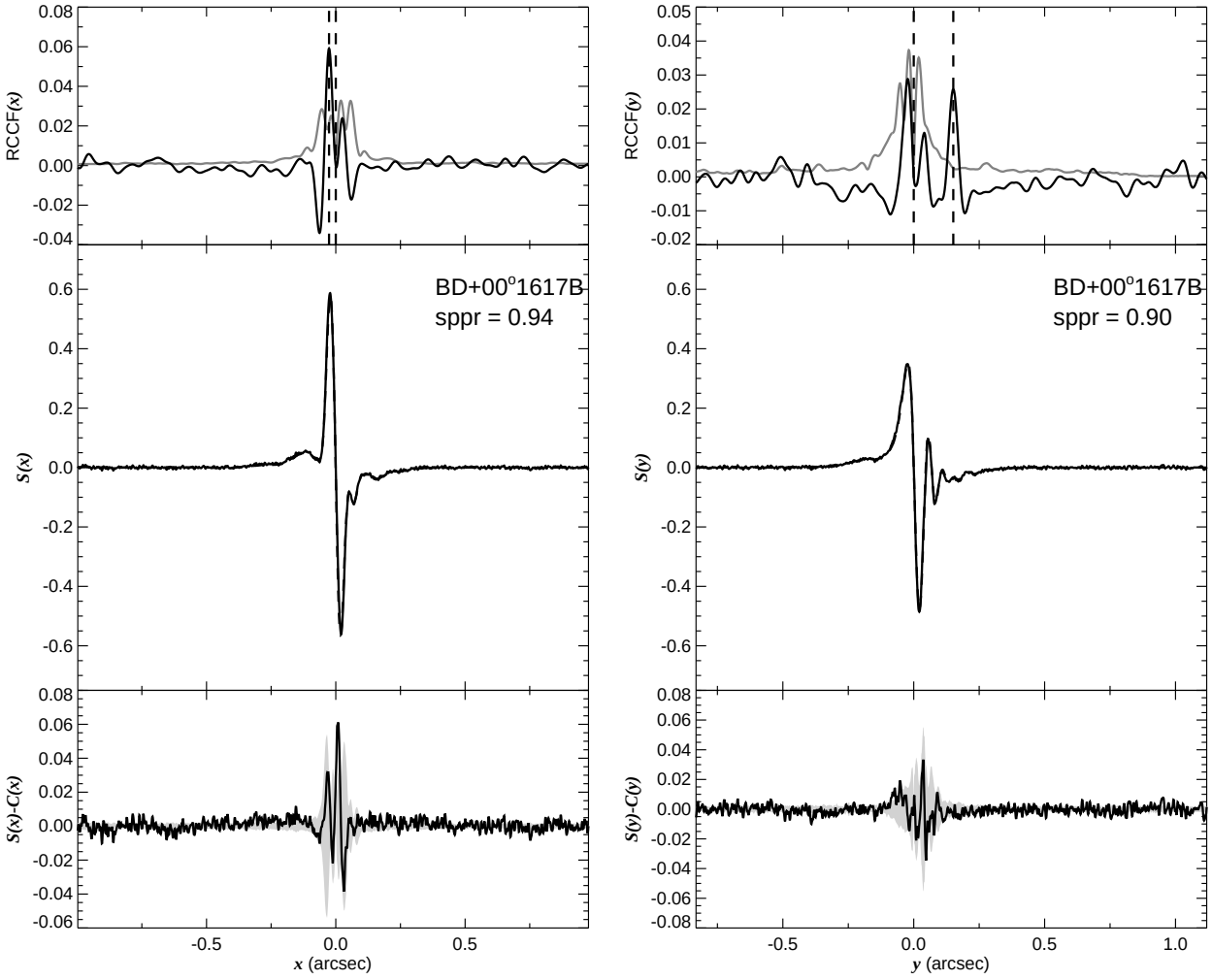

Fig. 1.73.— The FGS scans and binary detection tests for target 064850.48+002237.6 = BD+00 1617B obtained on BY 2008.8049.

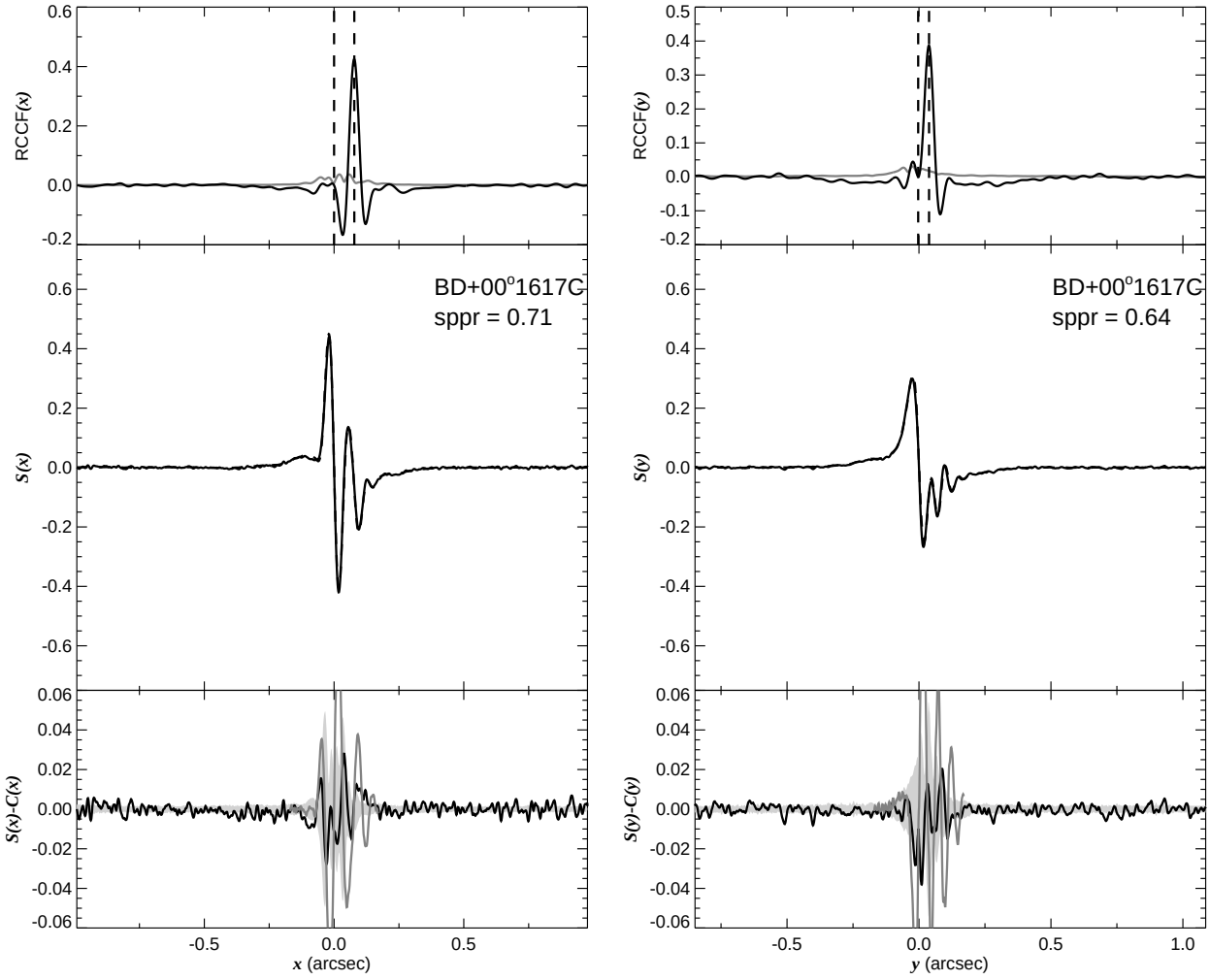

Fig. 1.74.— The FGS scans and binary detection tests for target 064851.20+002224.0 = BD+00 1617C obtained on BY 2008.8038.

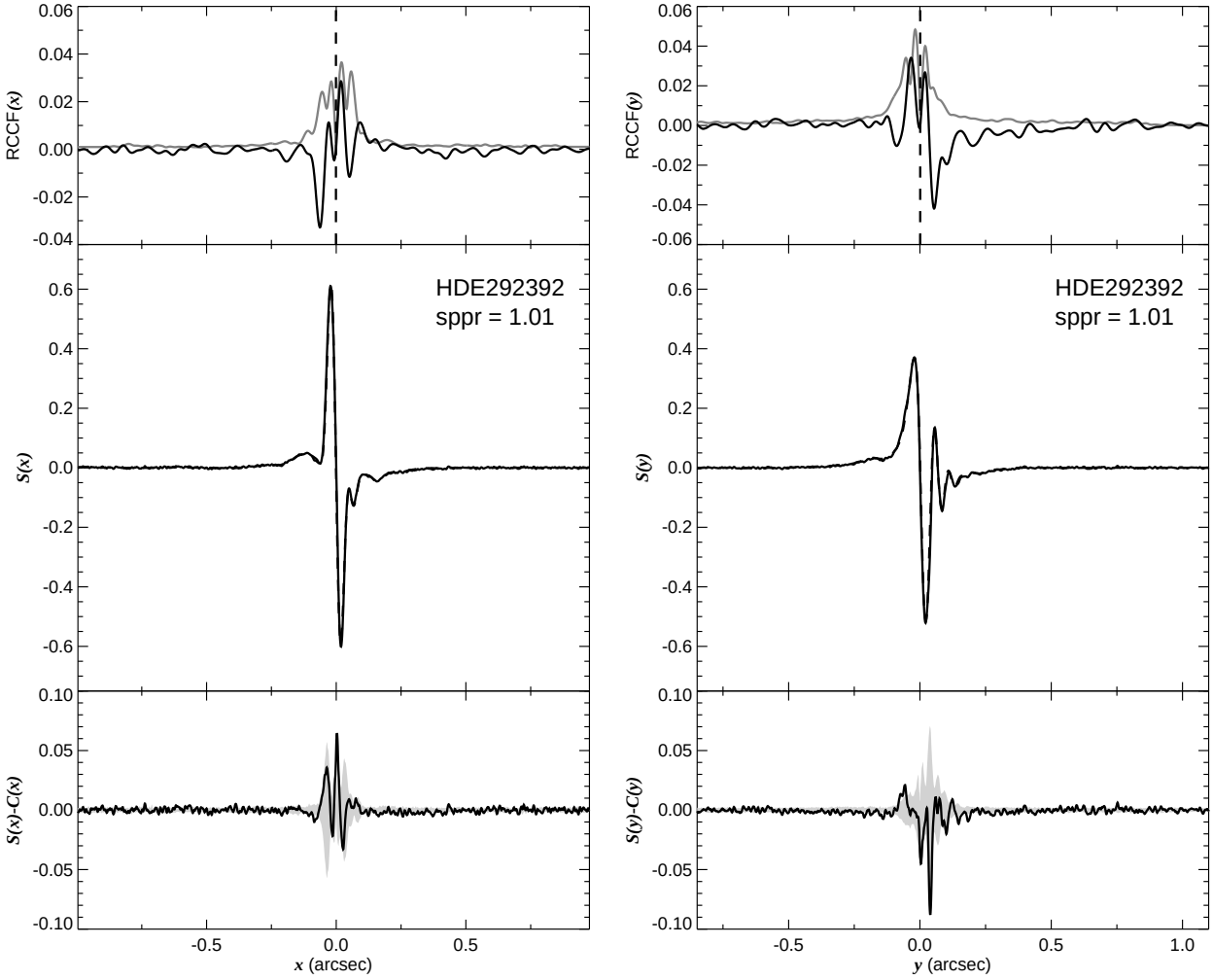

Fig. 1.75.— The FGS scans and binary detection tests for target 065017.62+002647.6 = HDE292392 obtained on BY 2008.8051.

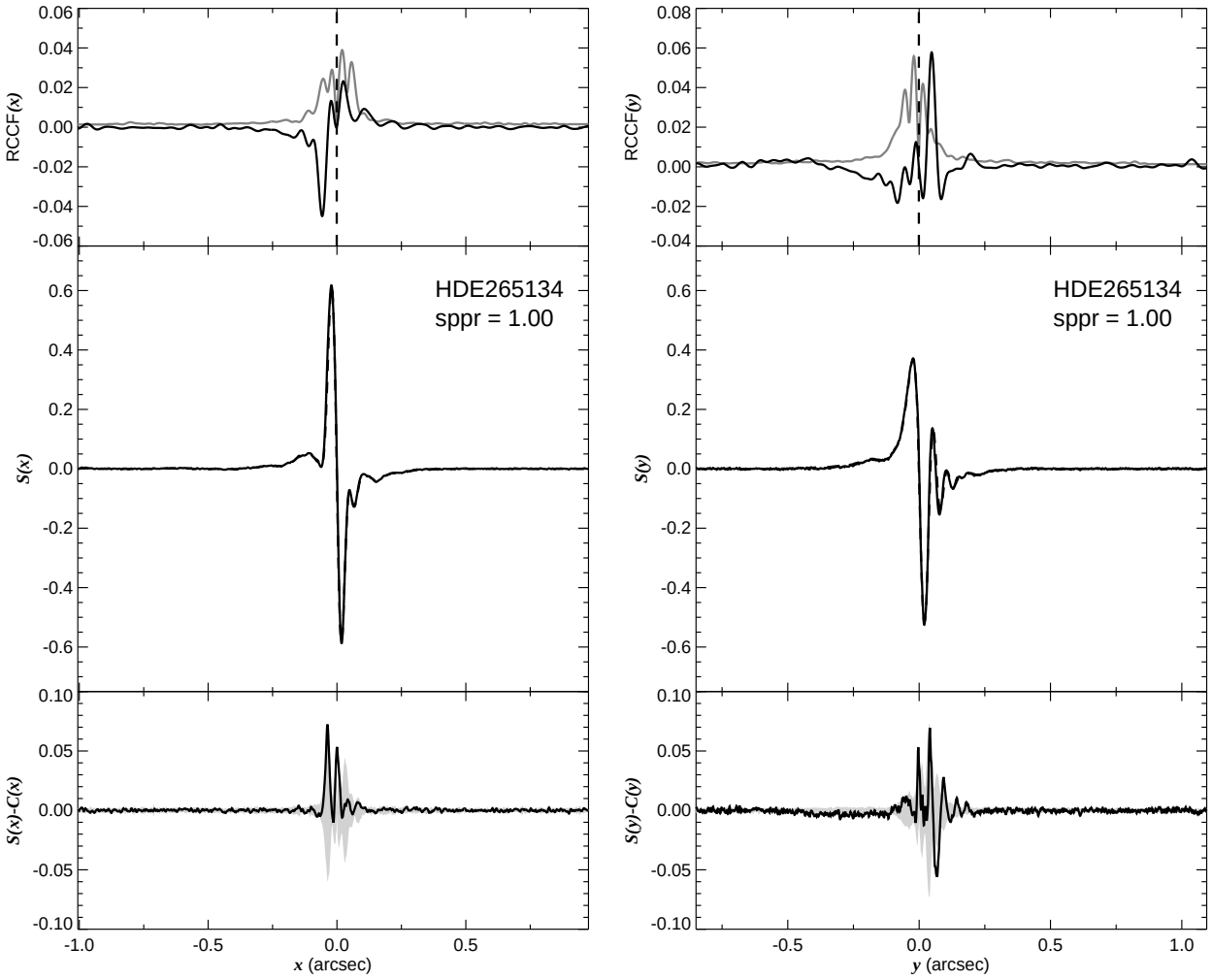

Fig. 1.76.— The FGS scans and binary detection tests for target 065133.93+133702.1 = HDE265134 obtained on BY 2008.7683.

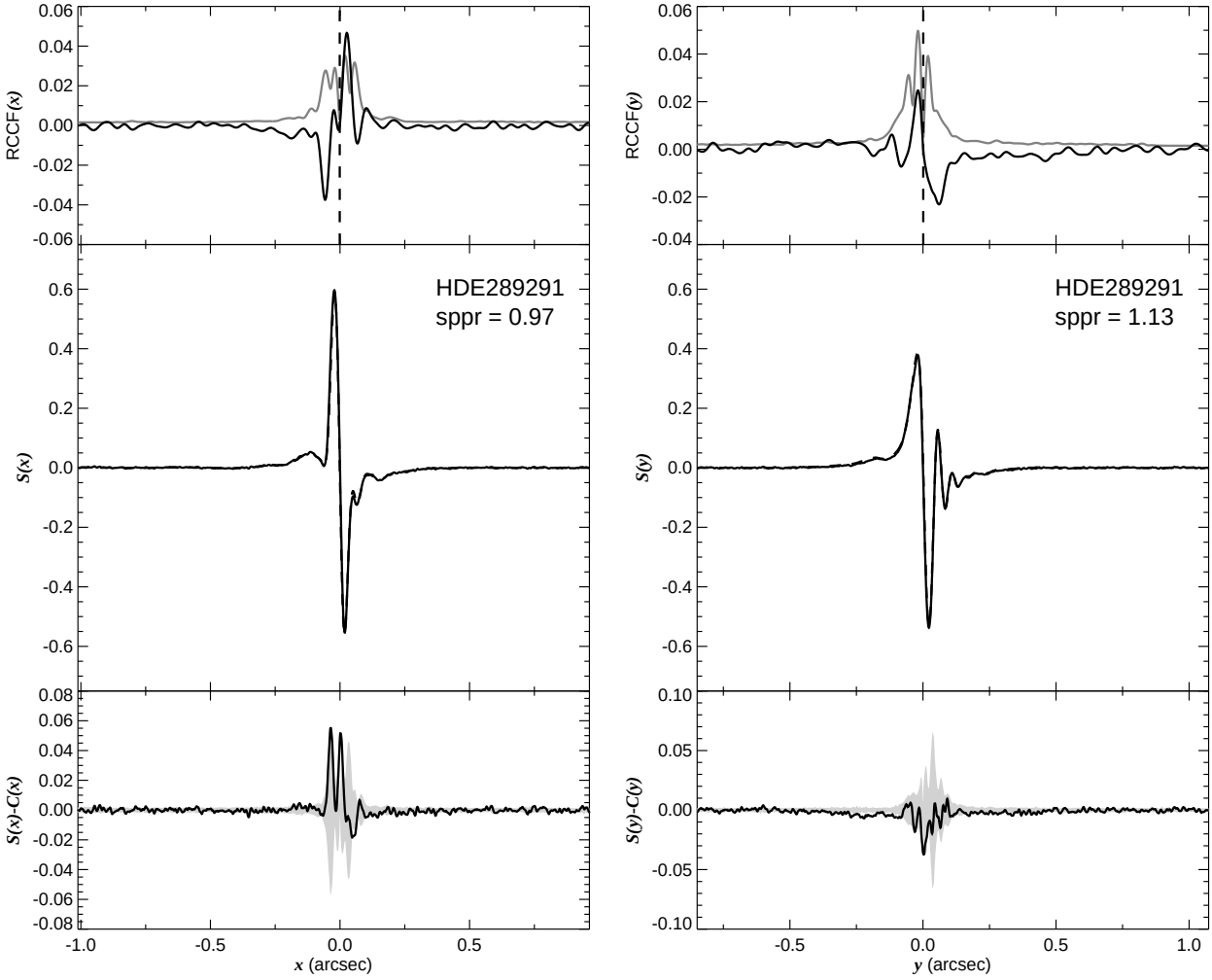

Fig. 1.77.— The FGS scans and binary detection tests for target 065158.45+012234.2 = HDE289291 obtained on BY 2008.7810.

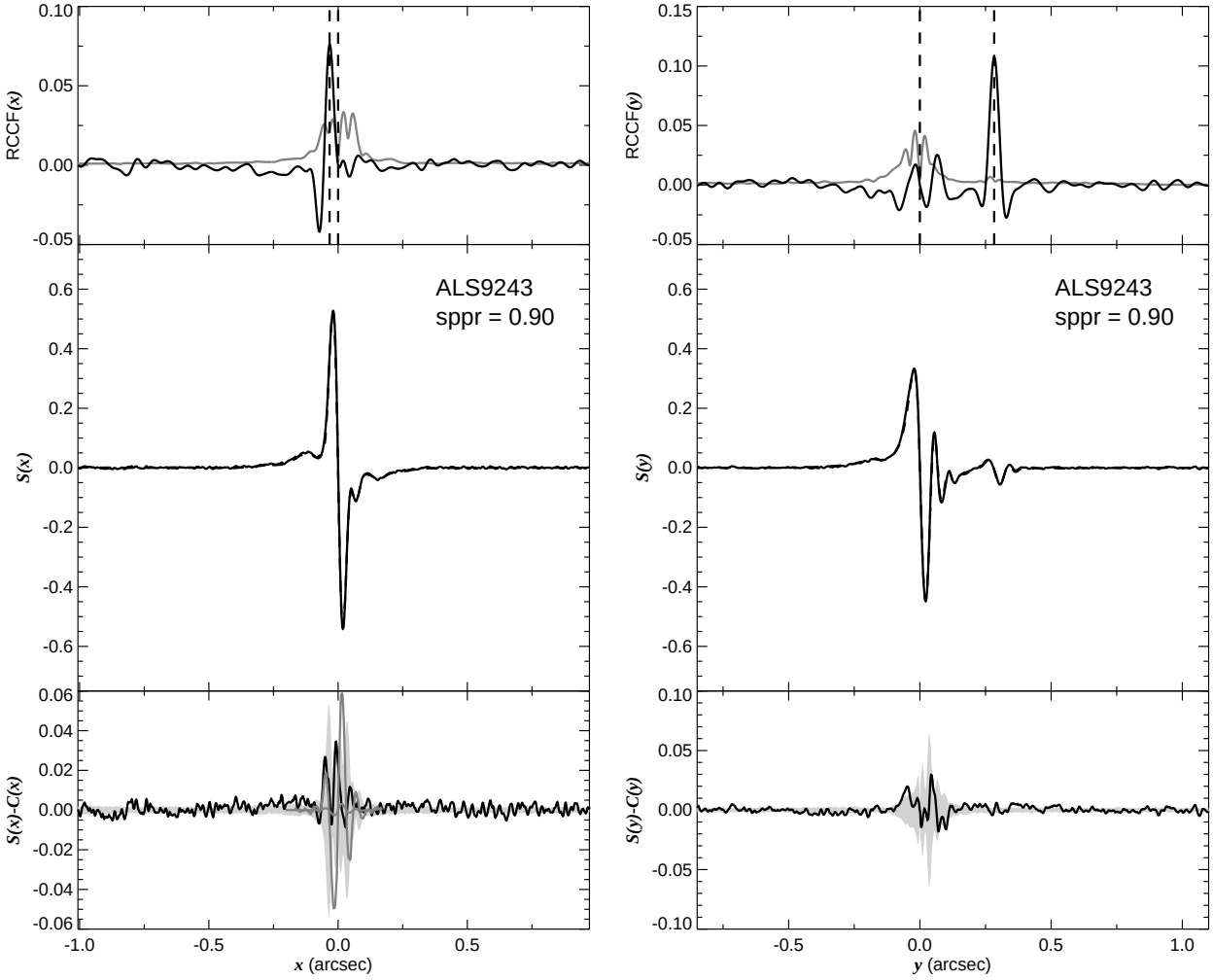

Fig. 1.78.— The FGS scans and binary detection tests for target 065930.21−044843.8 = ALS9243 obtained on BY 2008.8120.

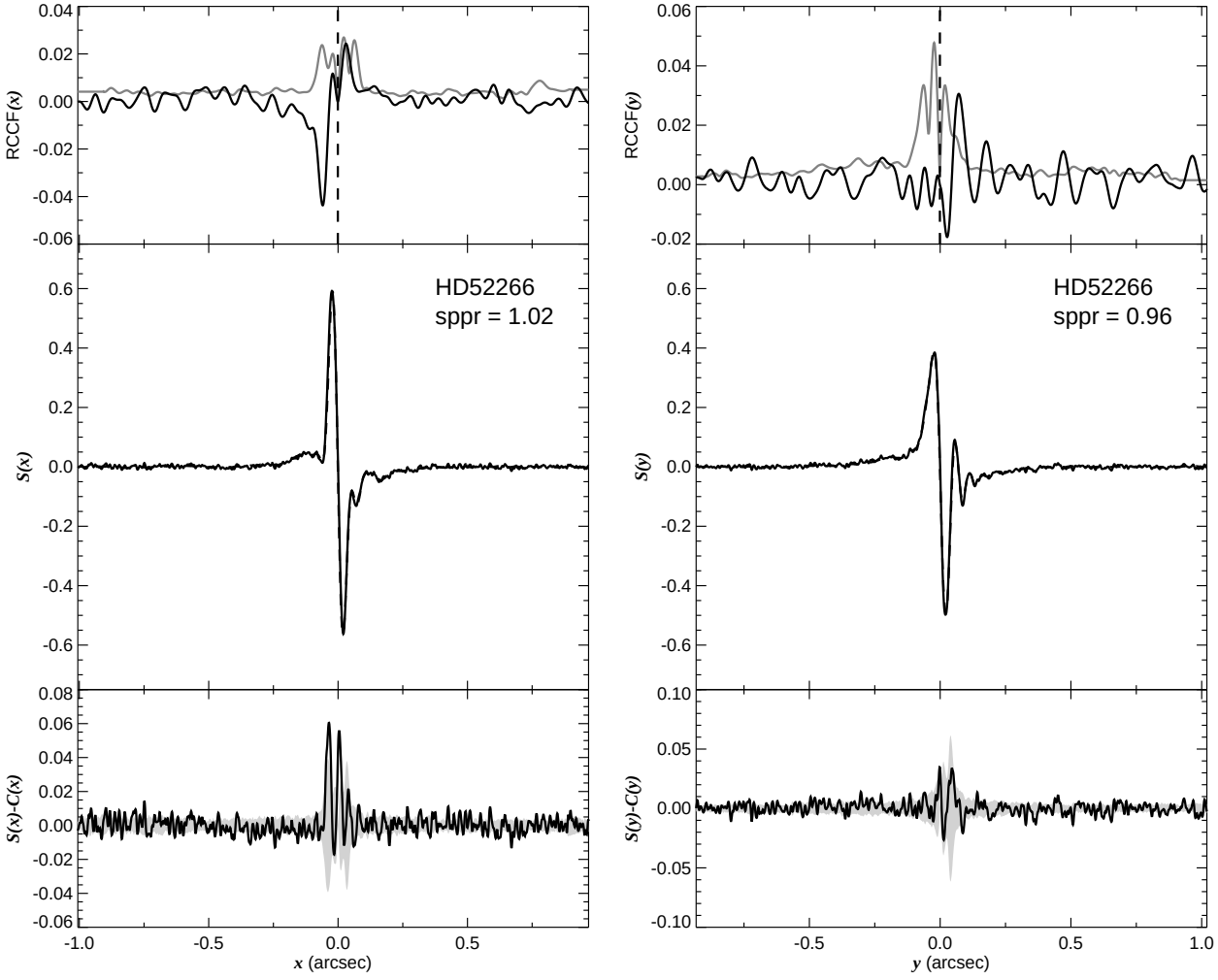

Fig. 1.79.— The FGS scans and binary detection tests for target 070021.08−054936.0 = HD52266 obtained on BY 2008.7114.

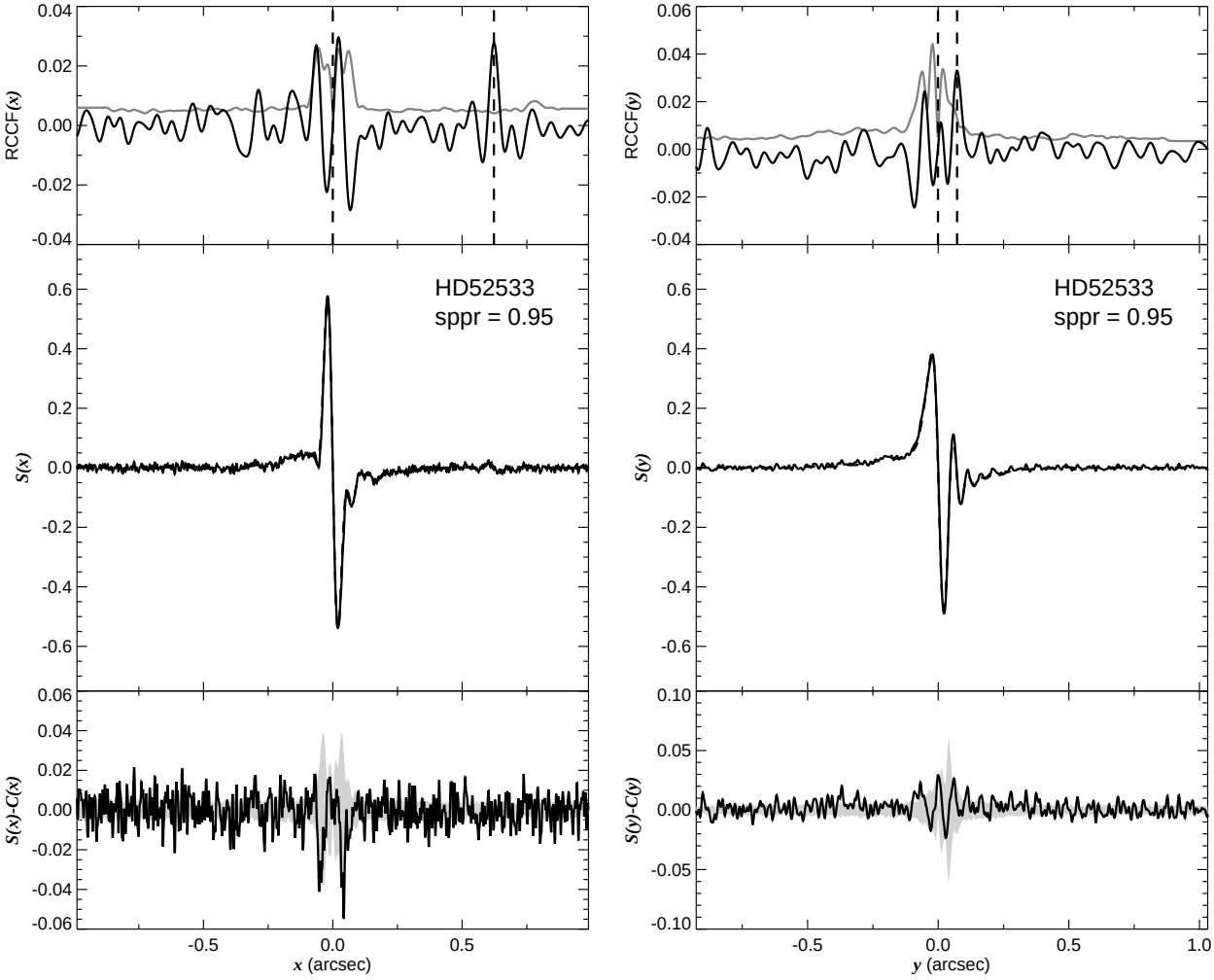

Fig. 1.80.— The FGS scans and binary detection tests for target 070127.05−030703.3 = HD52533 obtained on BY 2008.7112.

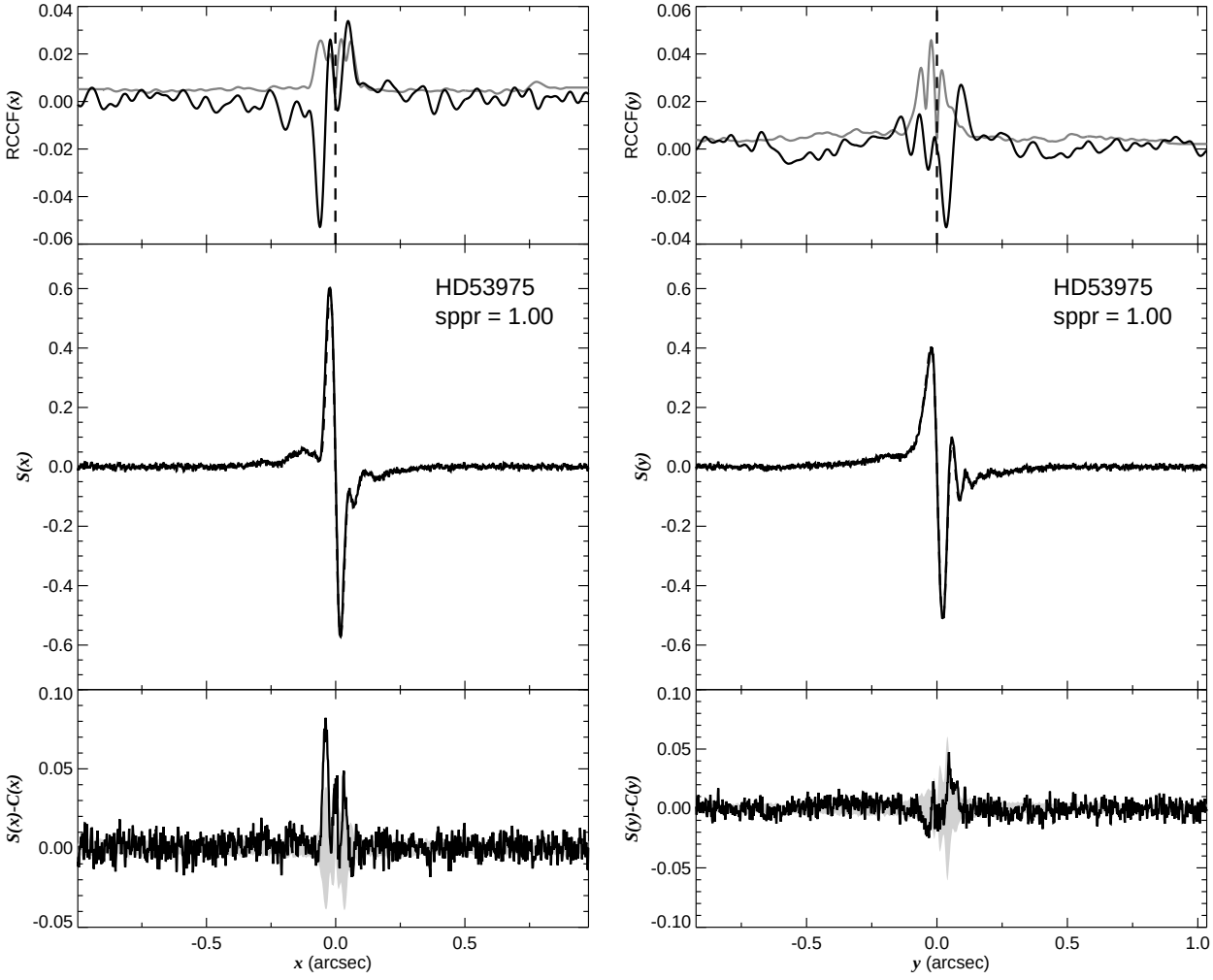

Fig. 1.81.— The FGS scans and binary detection tests for target 070635.97−122338.2 = HD53975 obtained on BY 2008.7316.

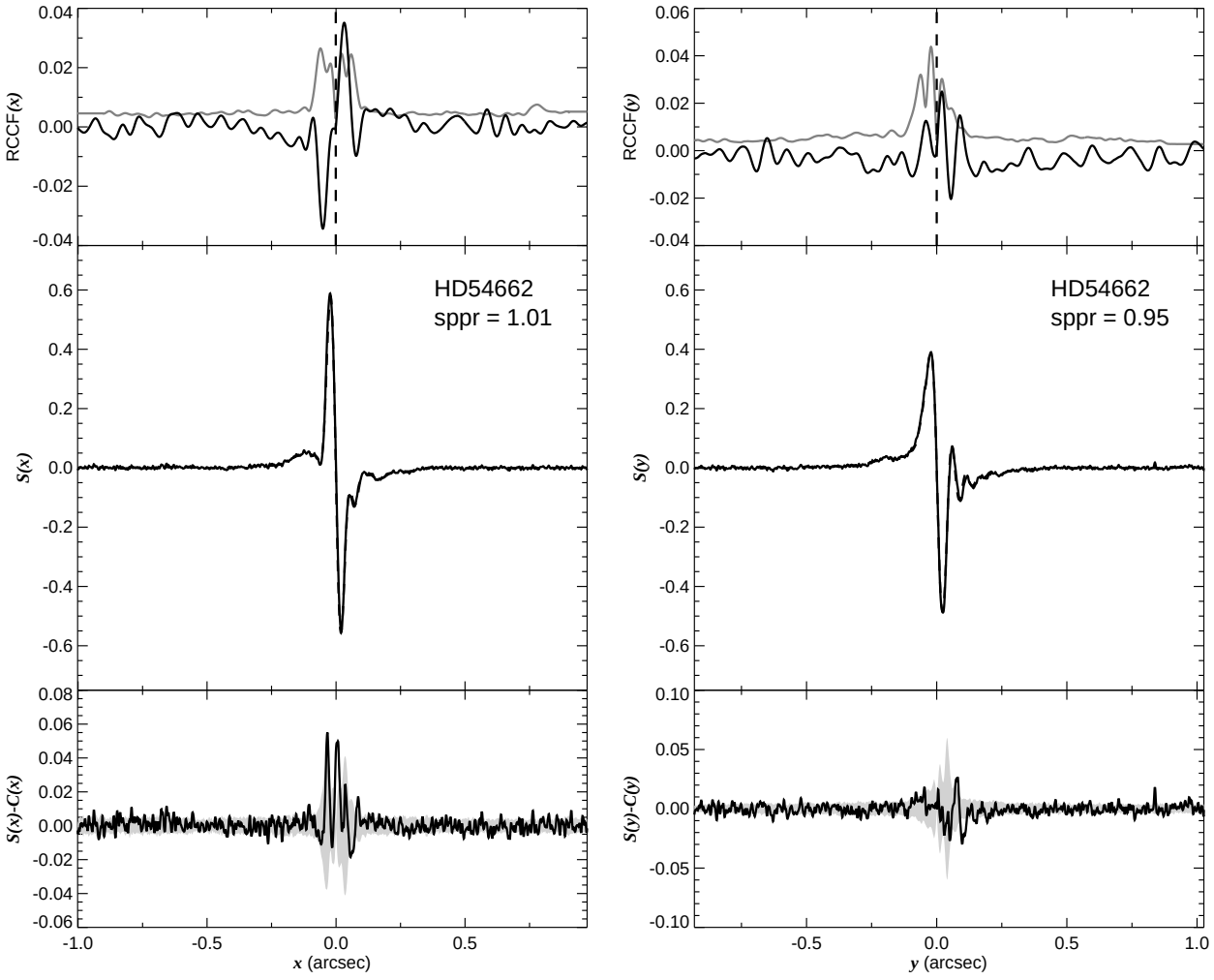

Fig. 1.82.— The FGS scans and binary detection tests for target 070920.25−102047.6 = HD54662 obtained on BY 2008.7116.

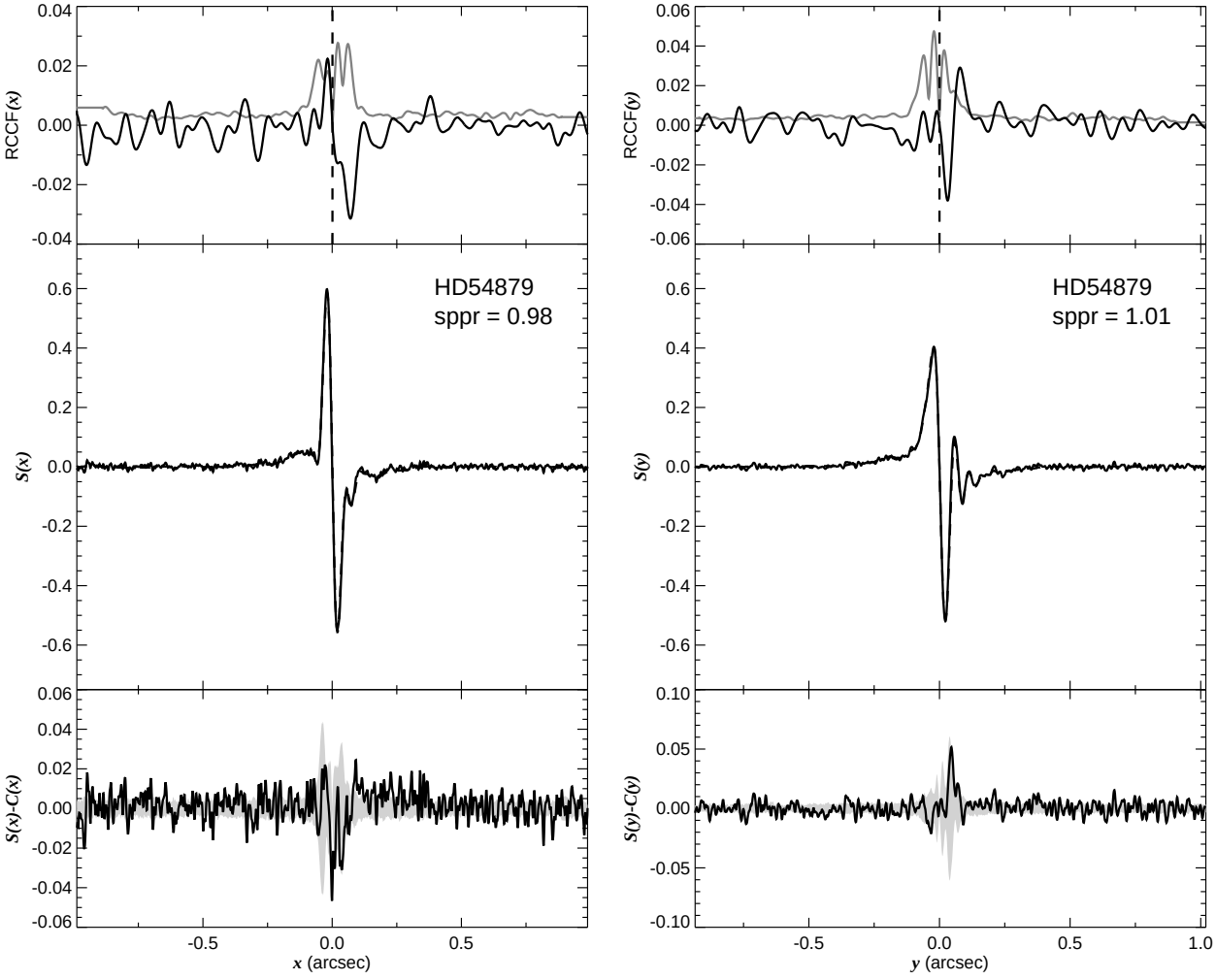

Fig. 1.83.— The FGS scans and binary detection tests for target 071008.15−114809.8 = HD54879 obtained on BY 2008.7117.

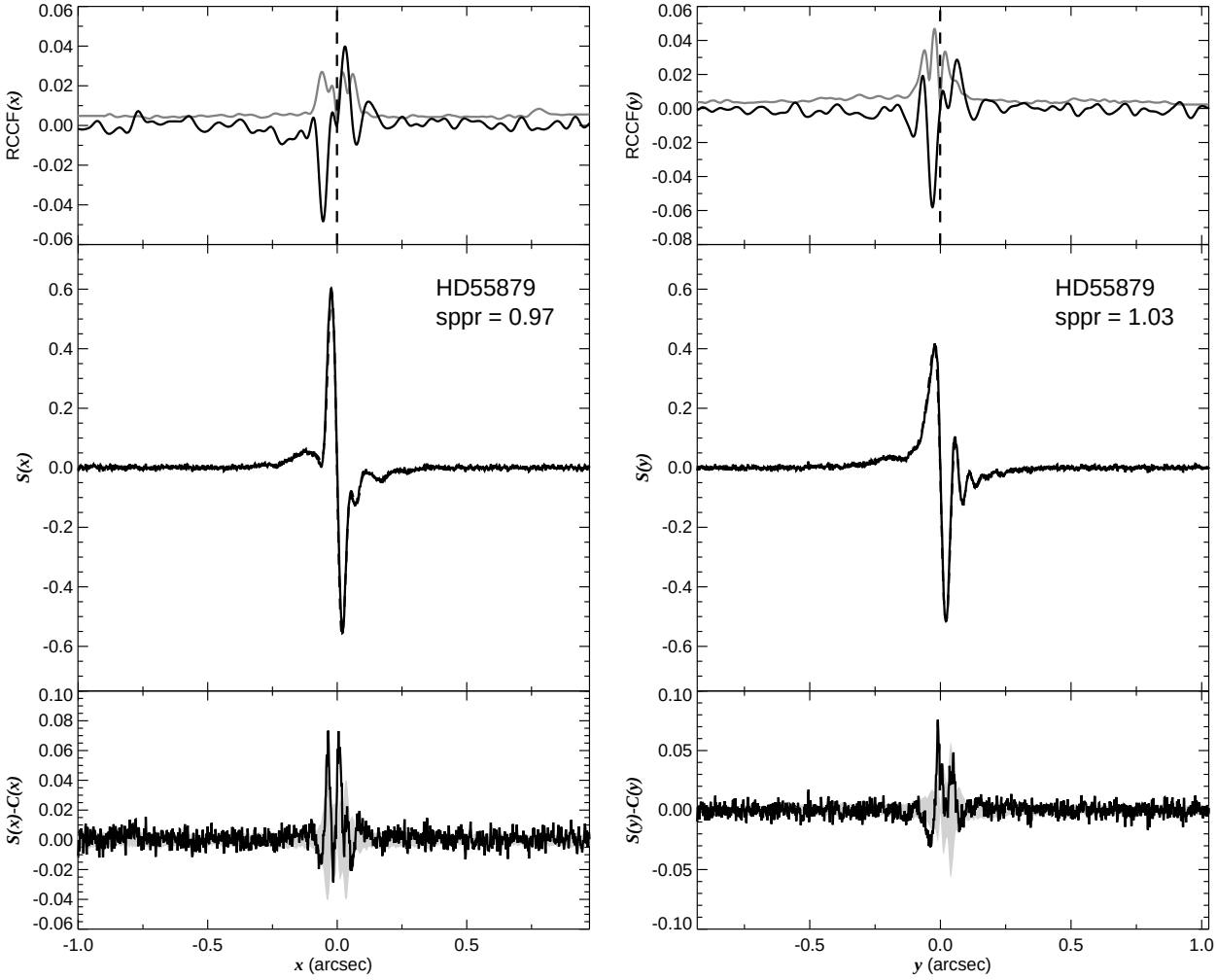

Fig. 1.84.— The FGS scans and binary detection tests for target 071428.25−101858.5 = HD55879 obtained on BY 2008.7670.

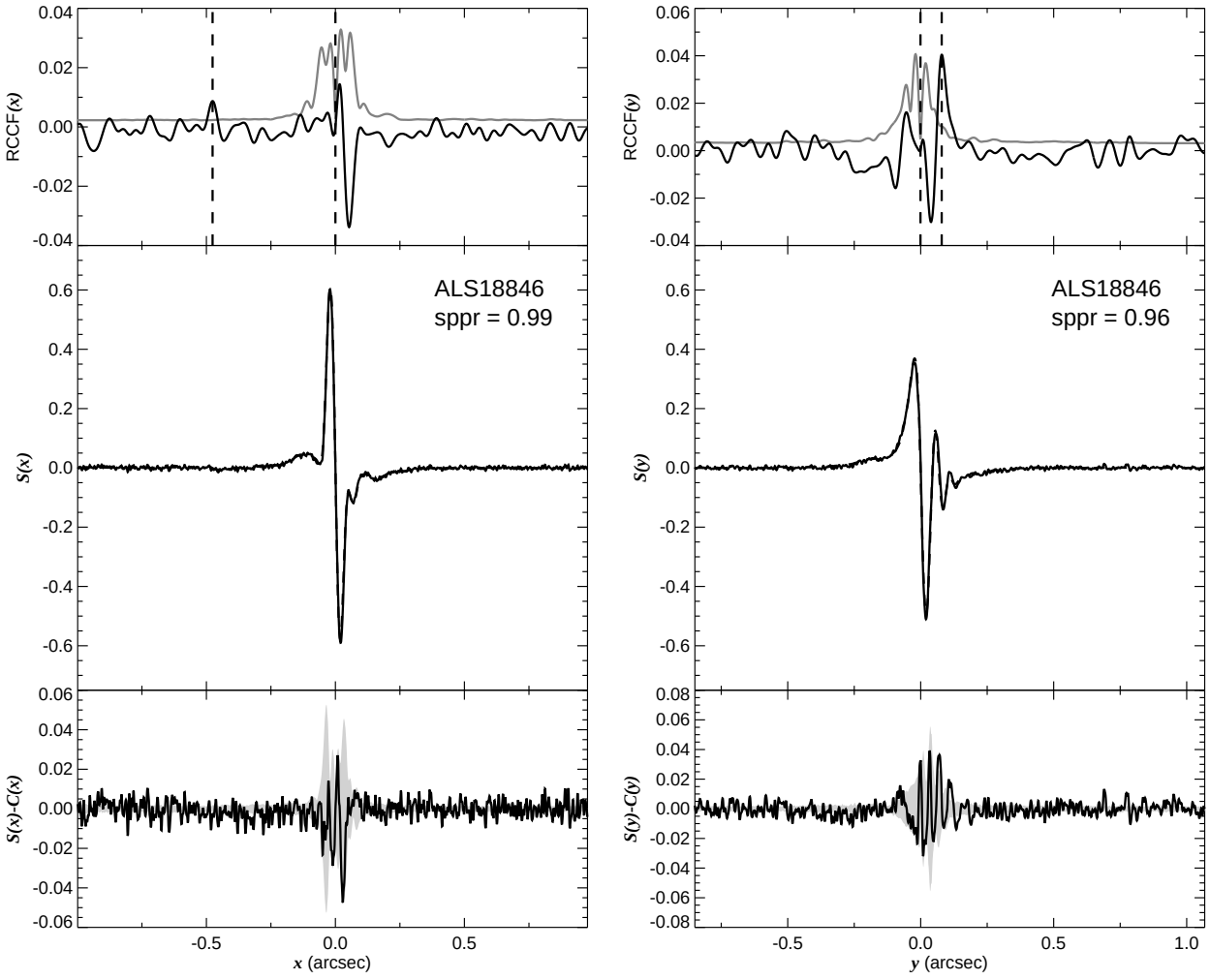

Fig. 1.85.— The FGS scans and binary detection tests for target 071821.42−245900.4 = ALS18846 obtained on BY 2008.8098.

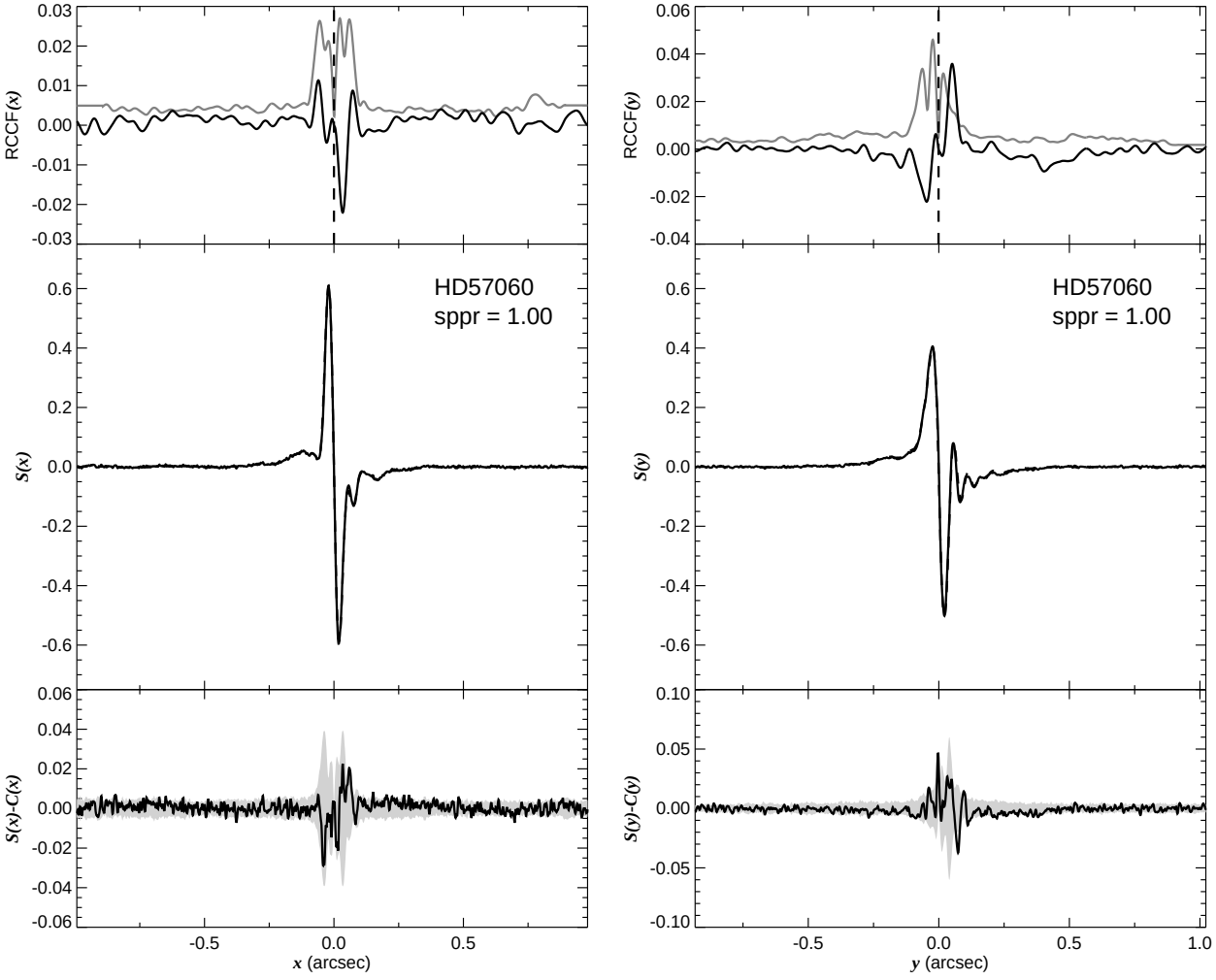

Fig. 1.86.— The FGS scans and binary detection tests for target 071840.38−243331.3 = HD57060 obtained on BY 2008.7287.

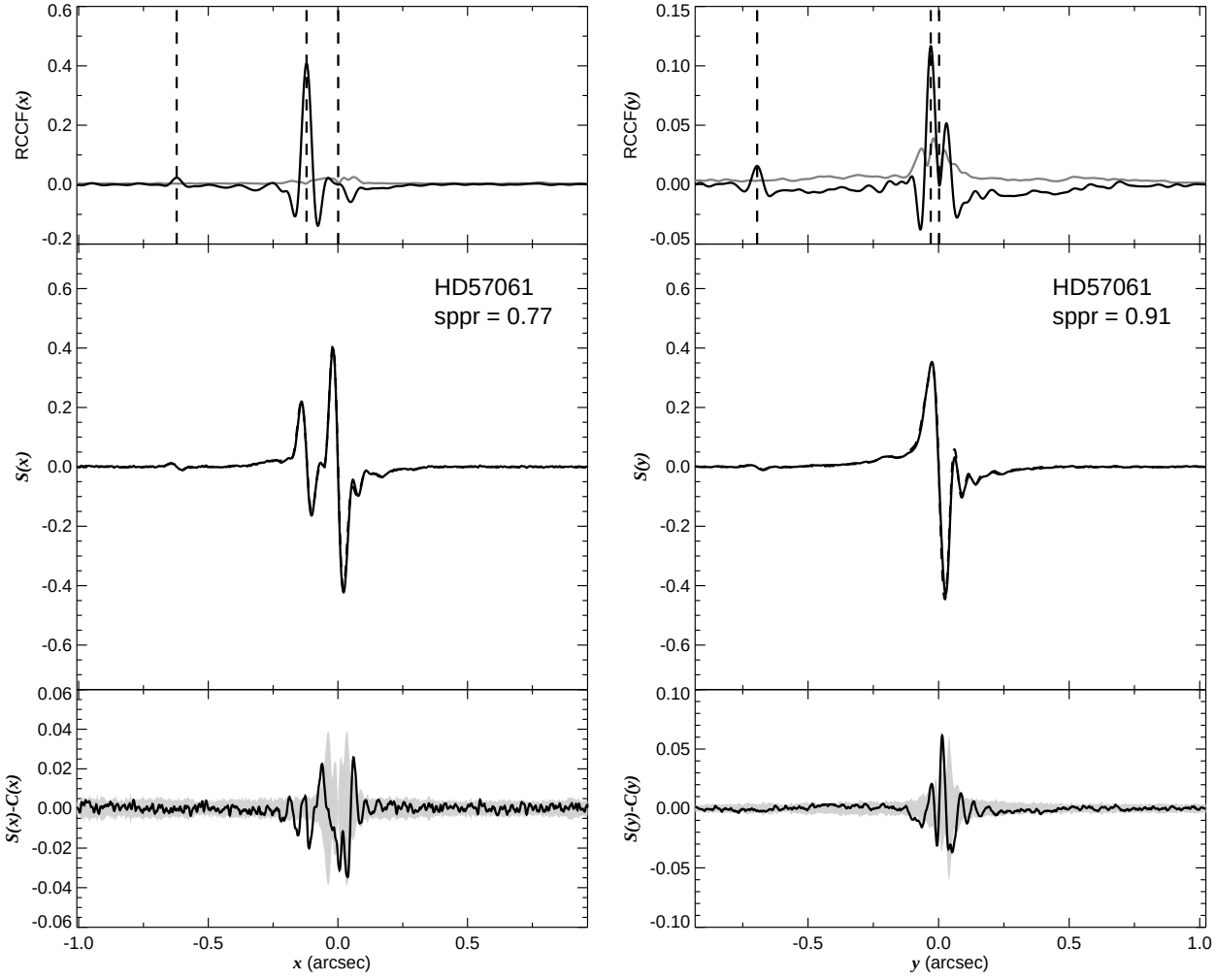

Fig. 1.87.— The FGS scans and binary detection tests for target 071842.49−245715.8 = HD57061 obtained on BY 2008.4143.

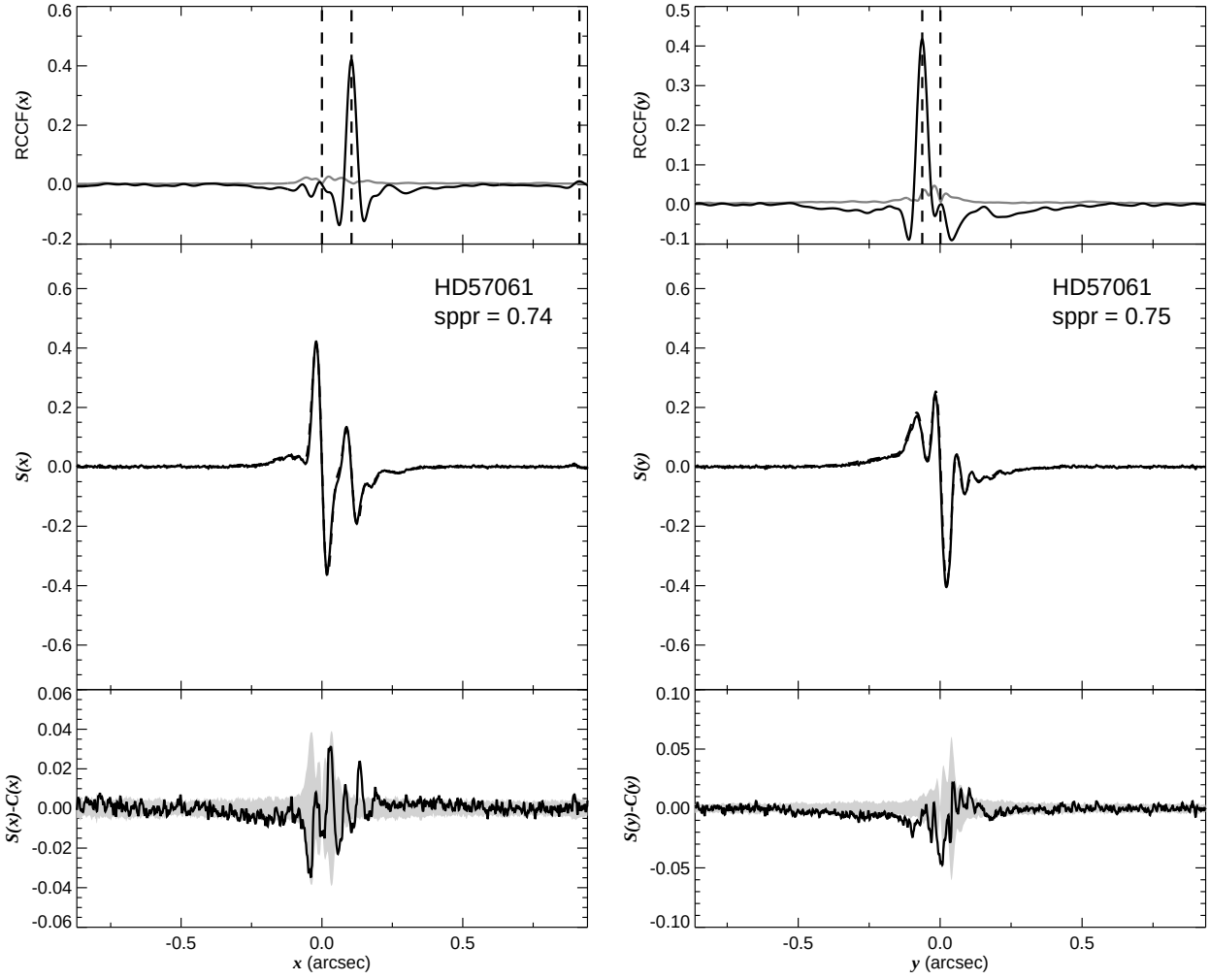

Fig. 1.88.— The FGS scans and binary detection tests for target 071842.49−245715.8 = HD57061 obtained on BY 2008.7858.

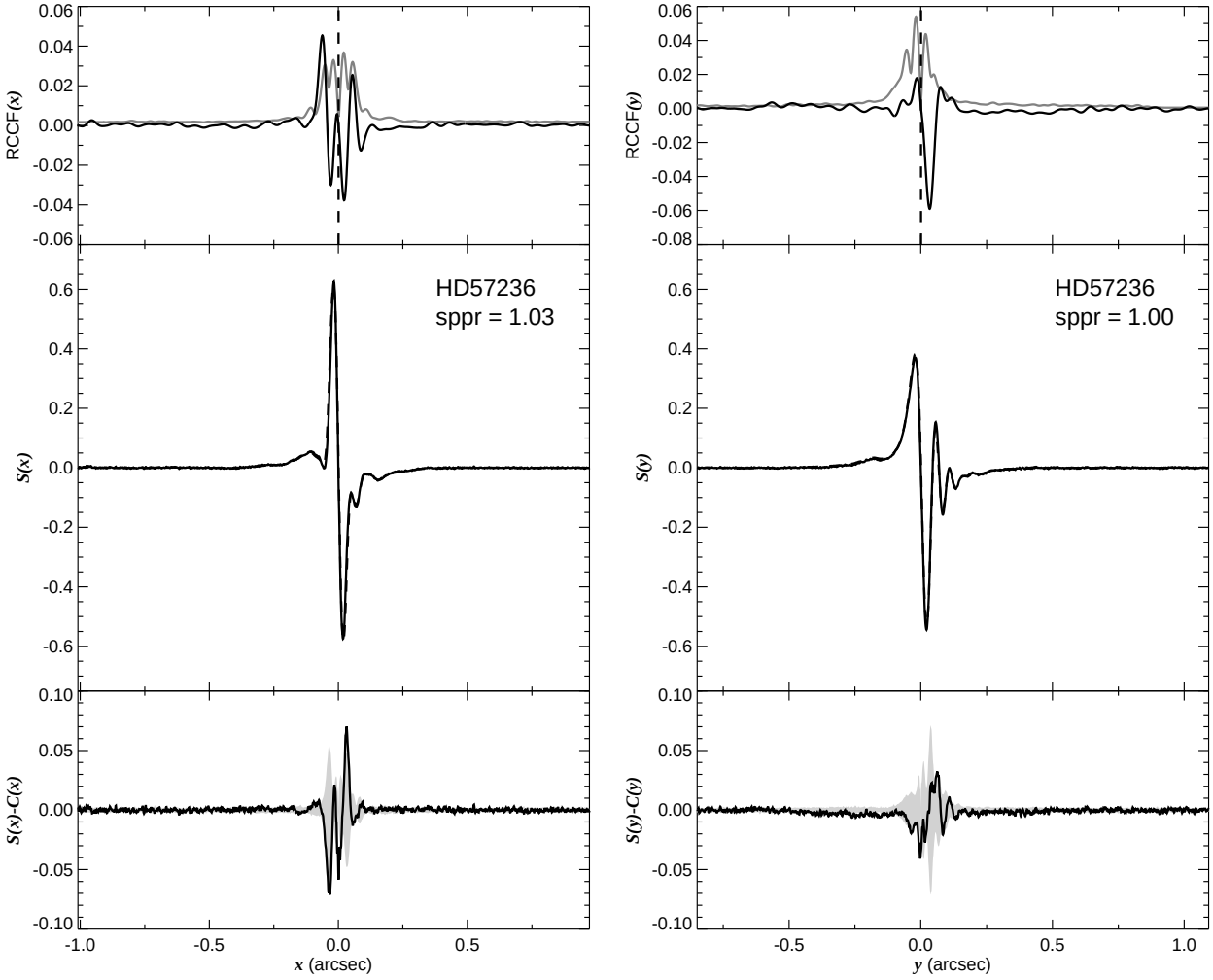

Fig. 1.89.— The FGS scans and binary detection tests for target 071930.10−220017.3 = HD57236 obtained on BY 2008.7119.

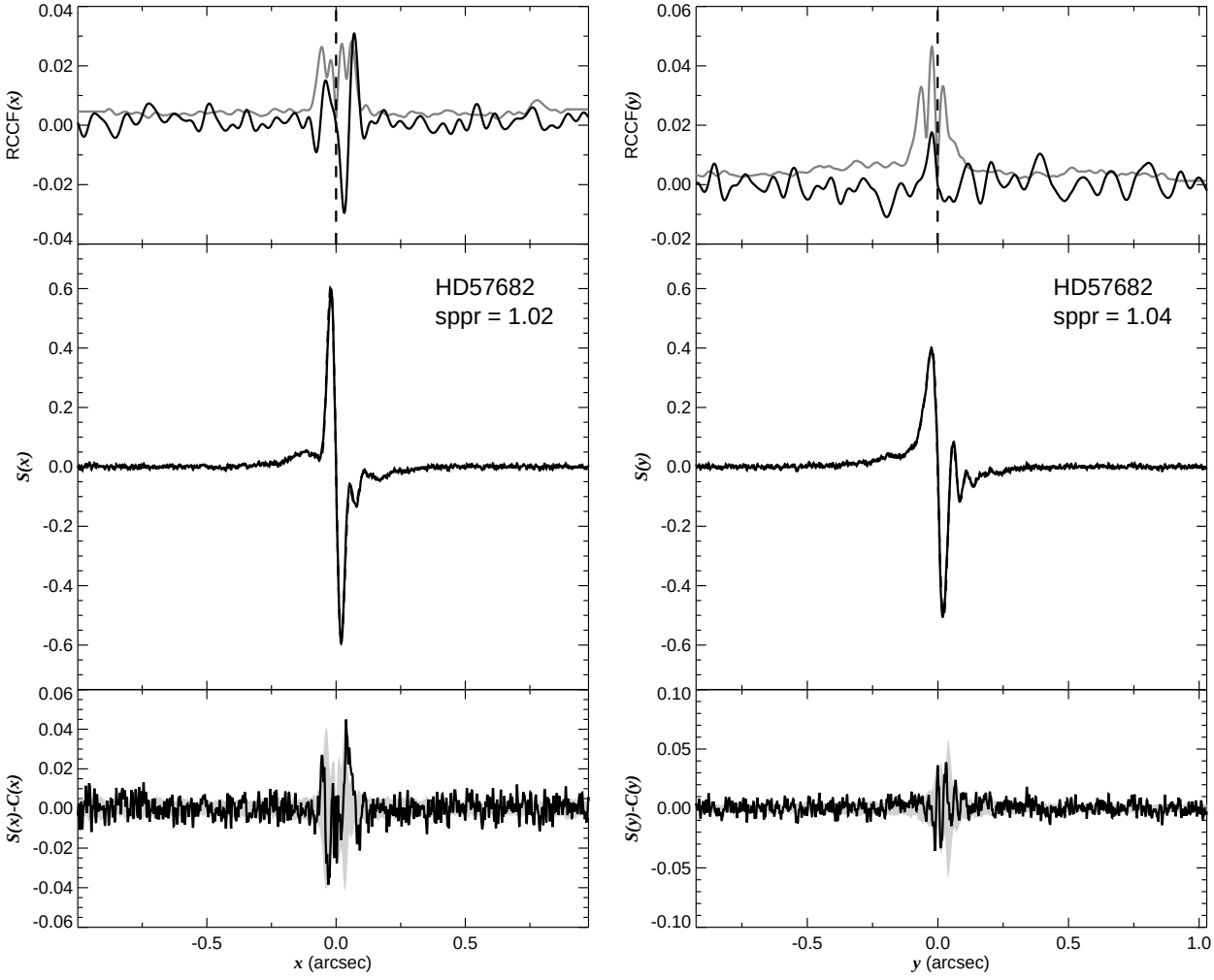

Fig. 1.90.— The FGS scans and binary detection tests for target 072202.05−085845.8 = HD57682 obtained on BY 2008.7041.

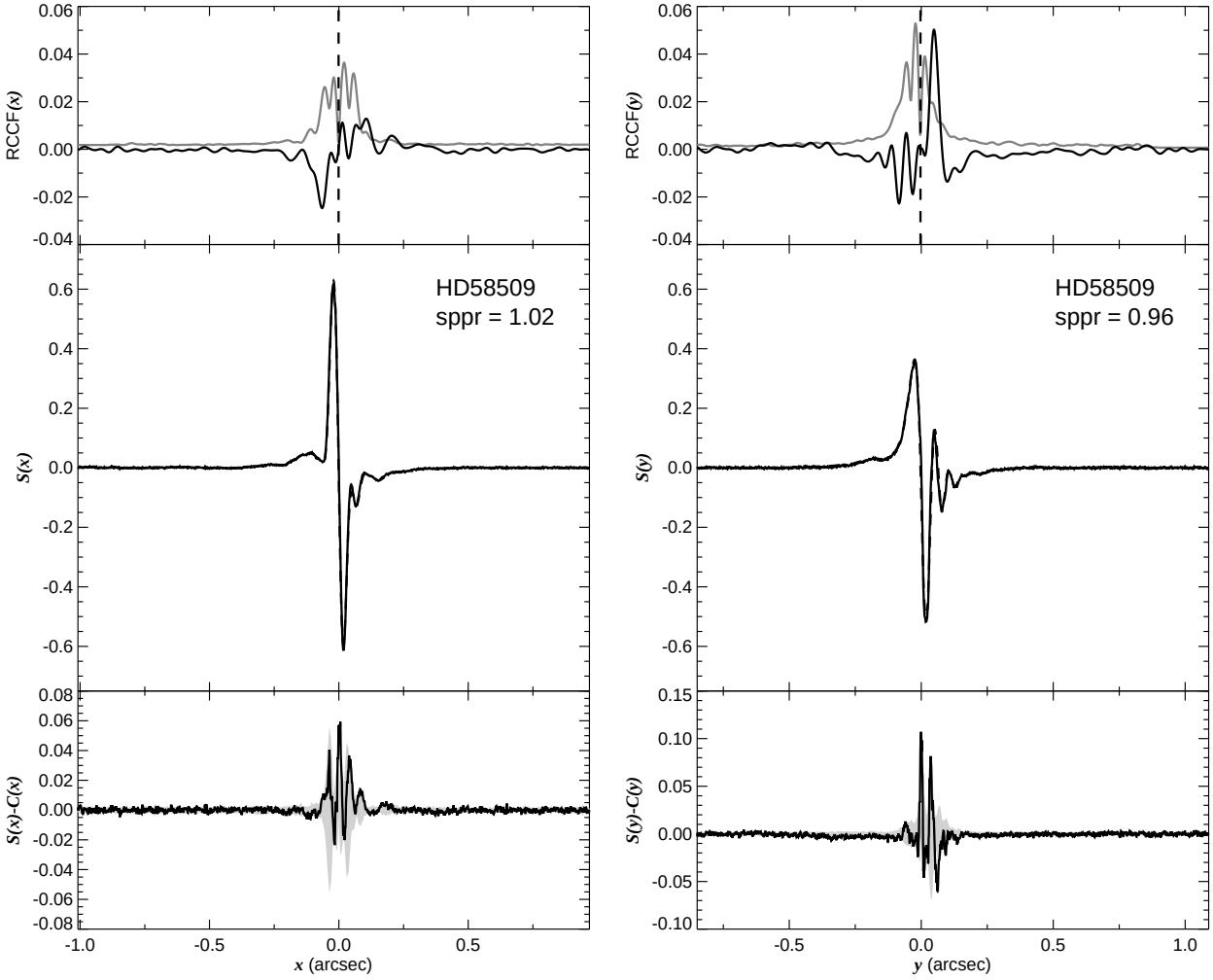

Fig. 1.91.— The FGS scans and binary detection tests for target 072512.28−210126.3 = HD58509 obtained on BY 2008.8782.

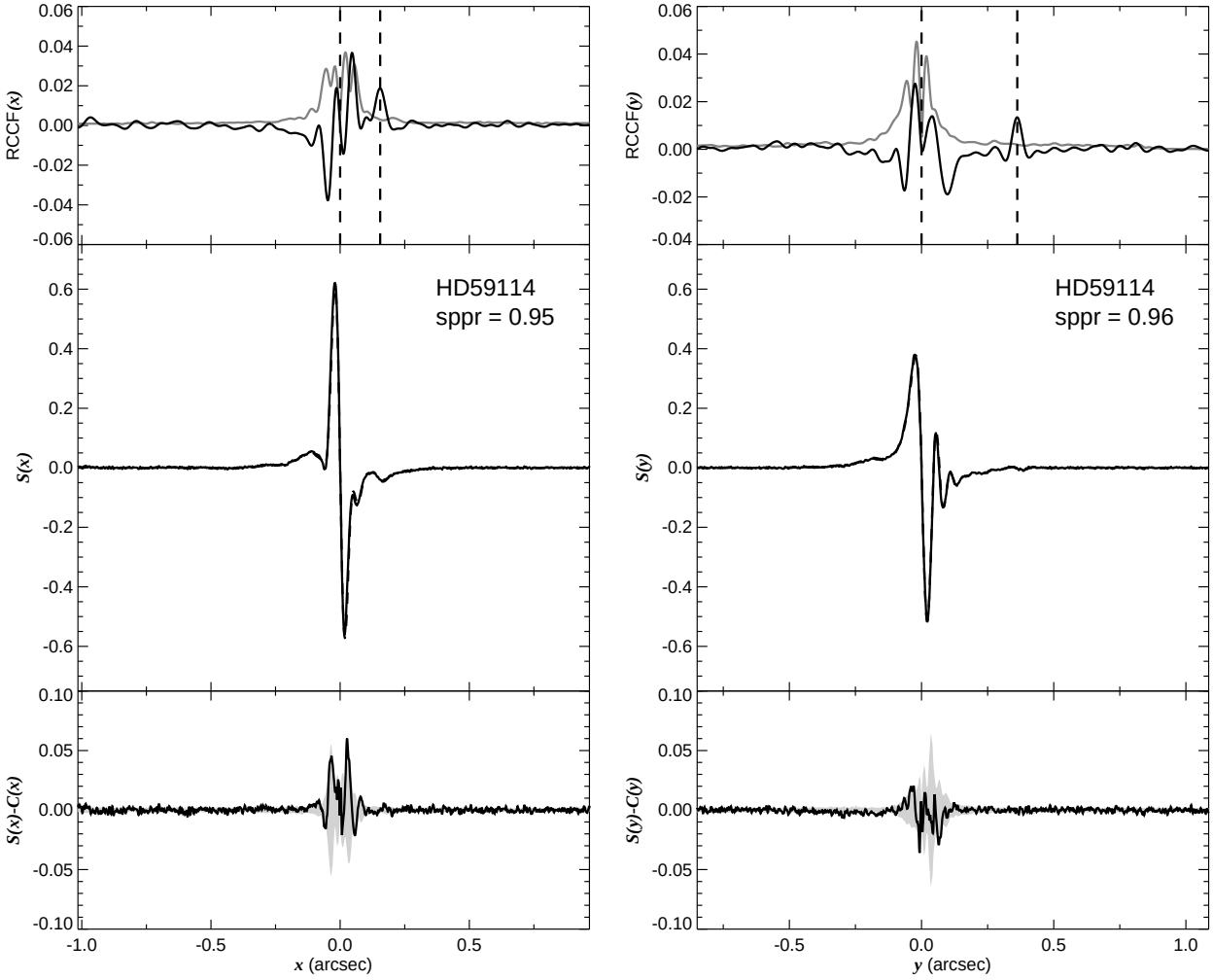

Fig. 1.92.— The FGS scans and binary detection tests for target 072755.38−152307.3 = HD59114 obtained on BY 2008.7672.

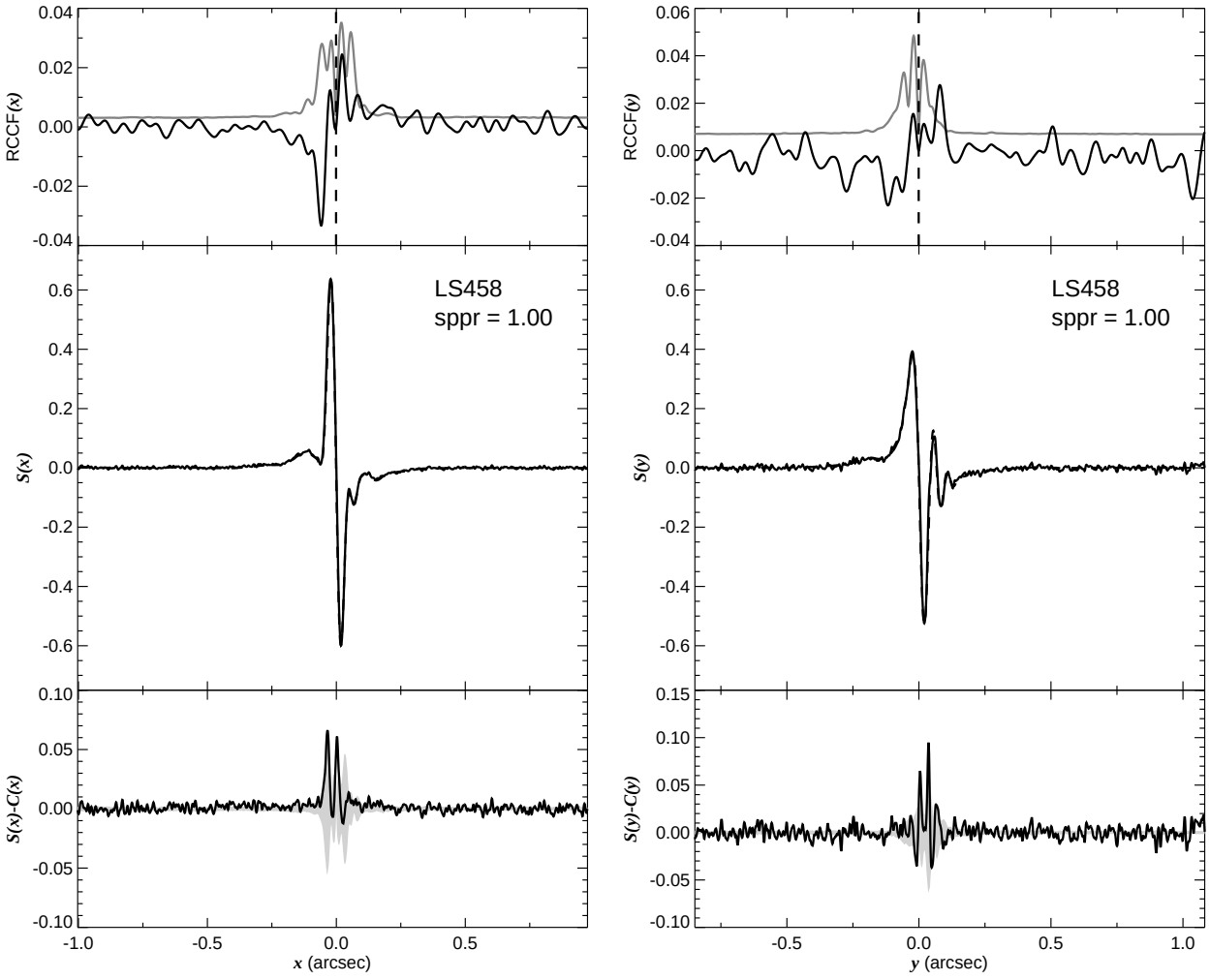

Fig. 1.93.— The FGS scans and binary detection tests for target 073001.28−190834.7 = ALS458 obtained on BY 2008.8458.

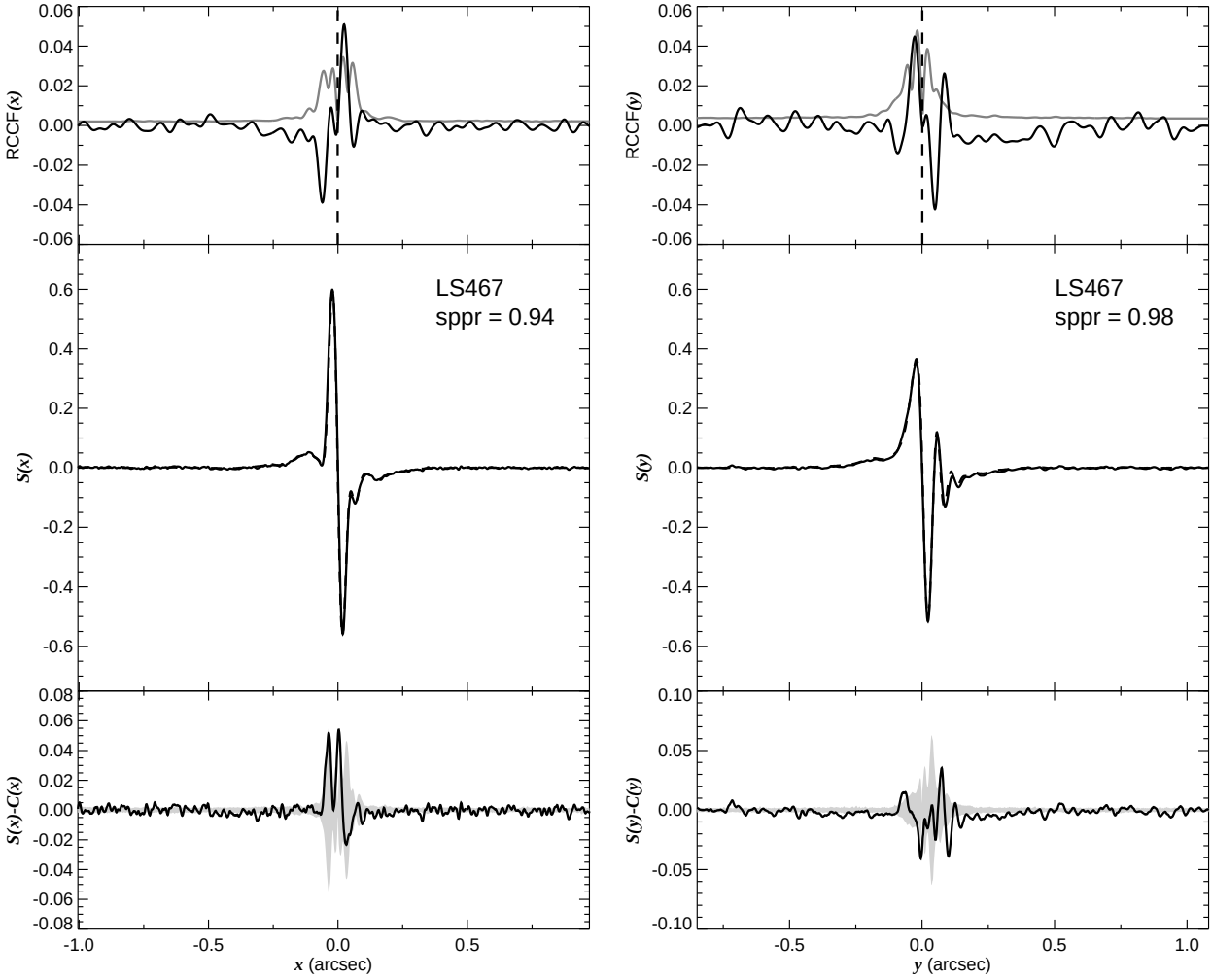

Fig. 1.94.— The FGS scans and binary detection tests for target 073035.28−190622.2 = ALS467 obtained on BY 2008.8097.

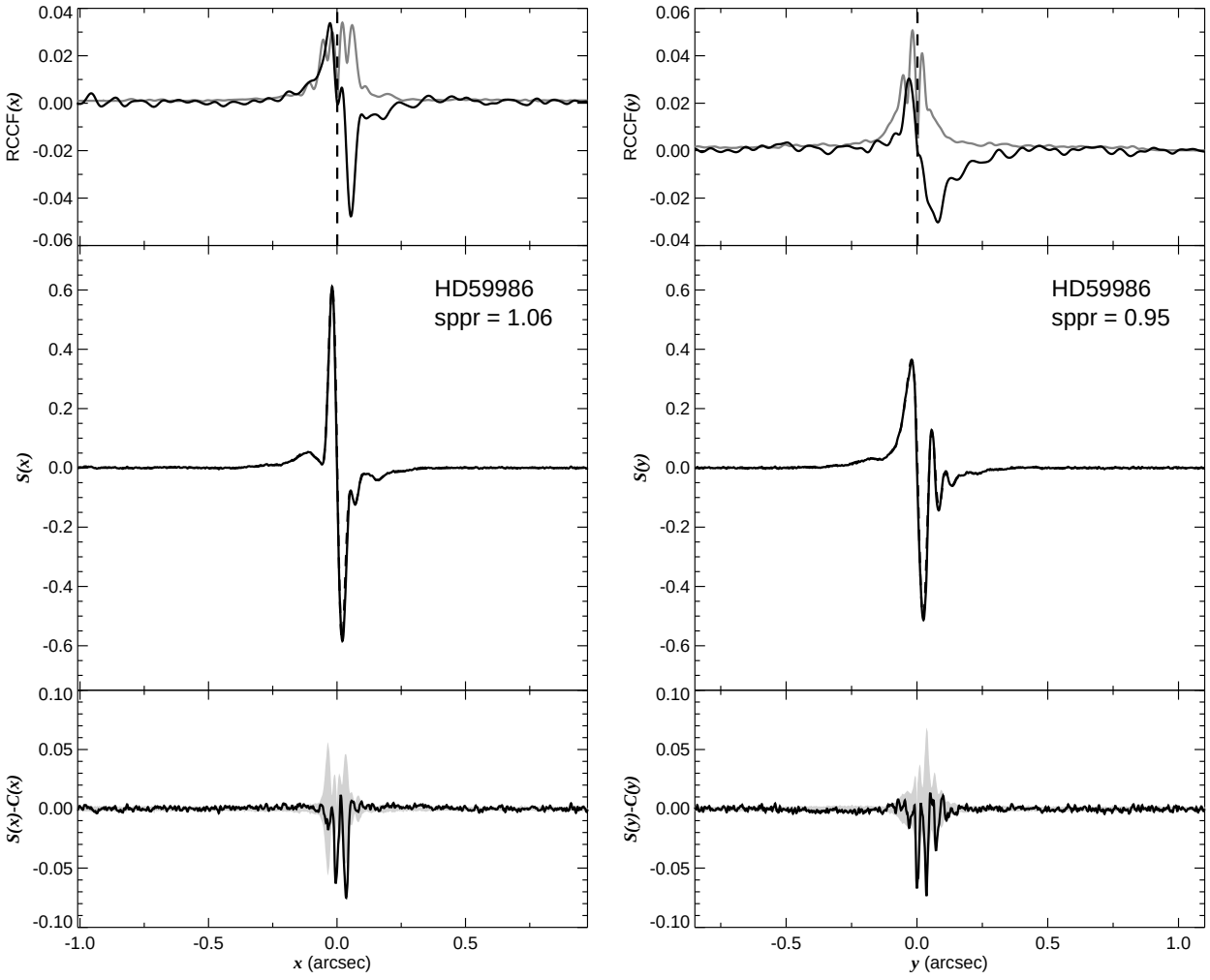

Fig. 1.95.— The FGS scans and binary detection tests for target 073146.74−165948.0 = HD59986 obtained on BY 2008.8071.

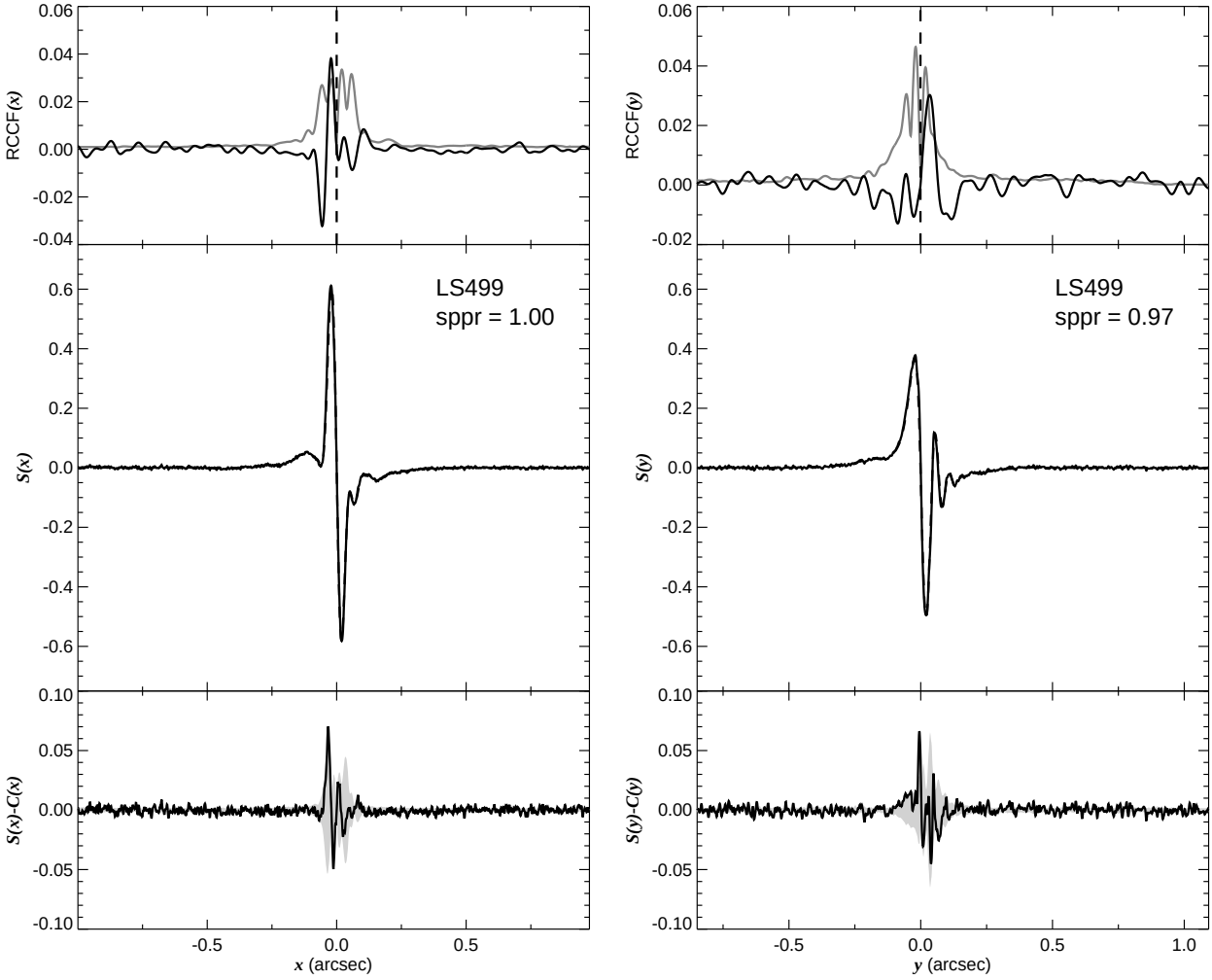

Fig. 1.96.— The FGS scans and binary detection tests for target 073202.81−192607.7 = ALS499 obtained on BY 2008.8181.

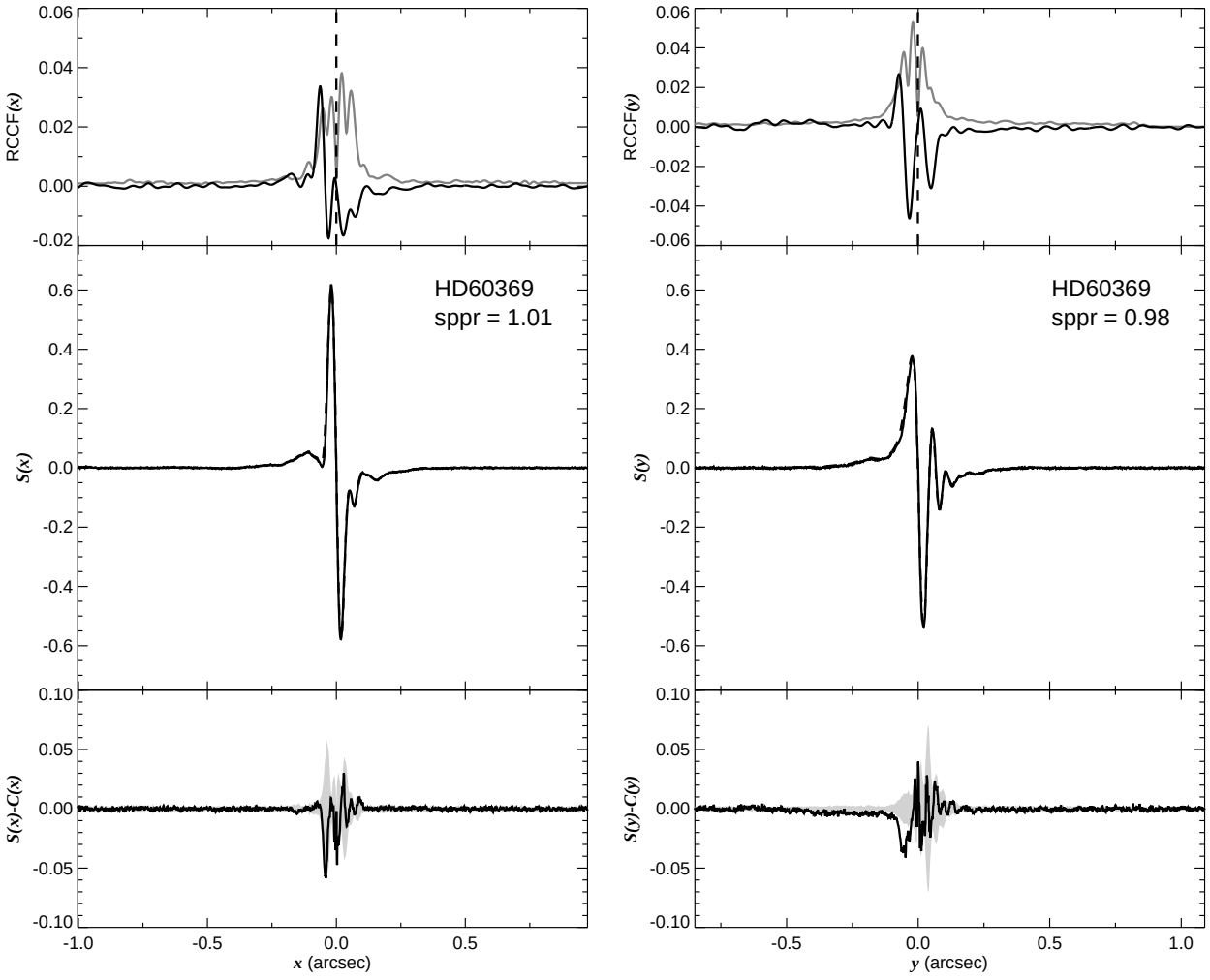

Fig. 1.97.— The FGS scans and binary detection tests for target 073301.84−281932.9 = HD60369 obtained on BY 2008.7646.

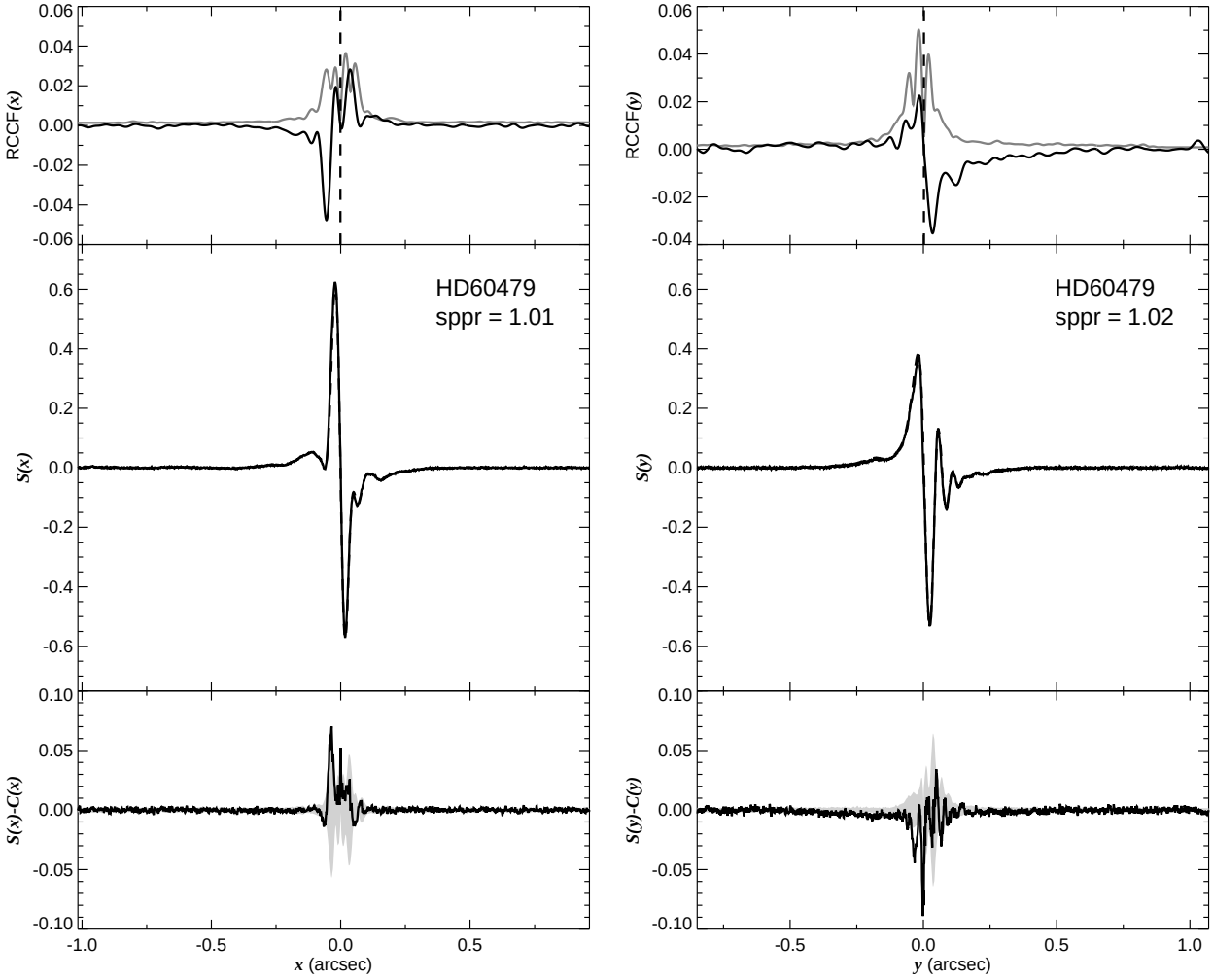

Fig. 1.98.— The FGS scans and binary detection tests for target 073334.32−275838.3 = HD60479 obtained on BY 2008.7803.

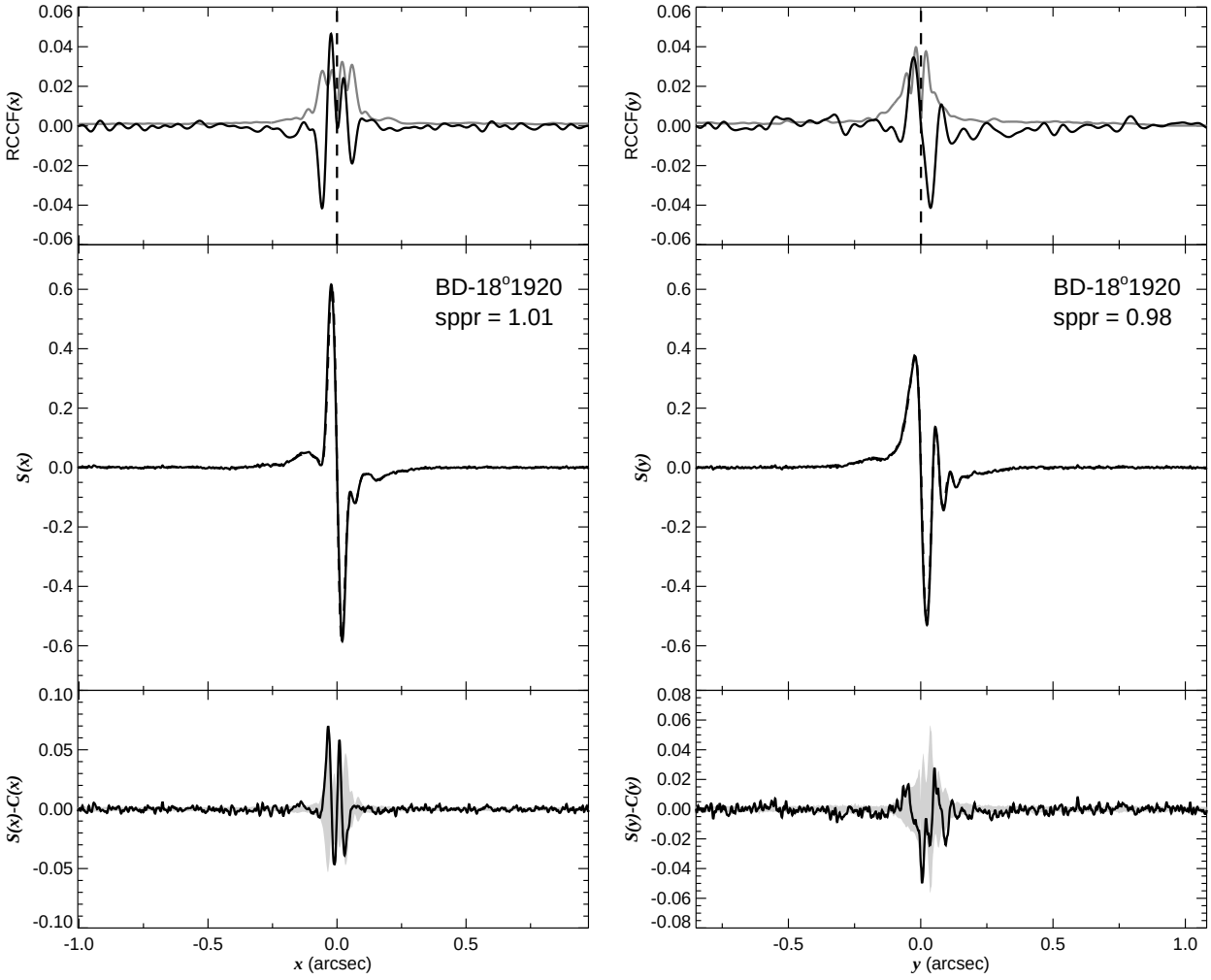

Fig. 1.99.— The FGS scans and binary detection tests for target 073513.95−184757.2 = BD−18 1920 obtained on BY 2008.8179.

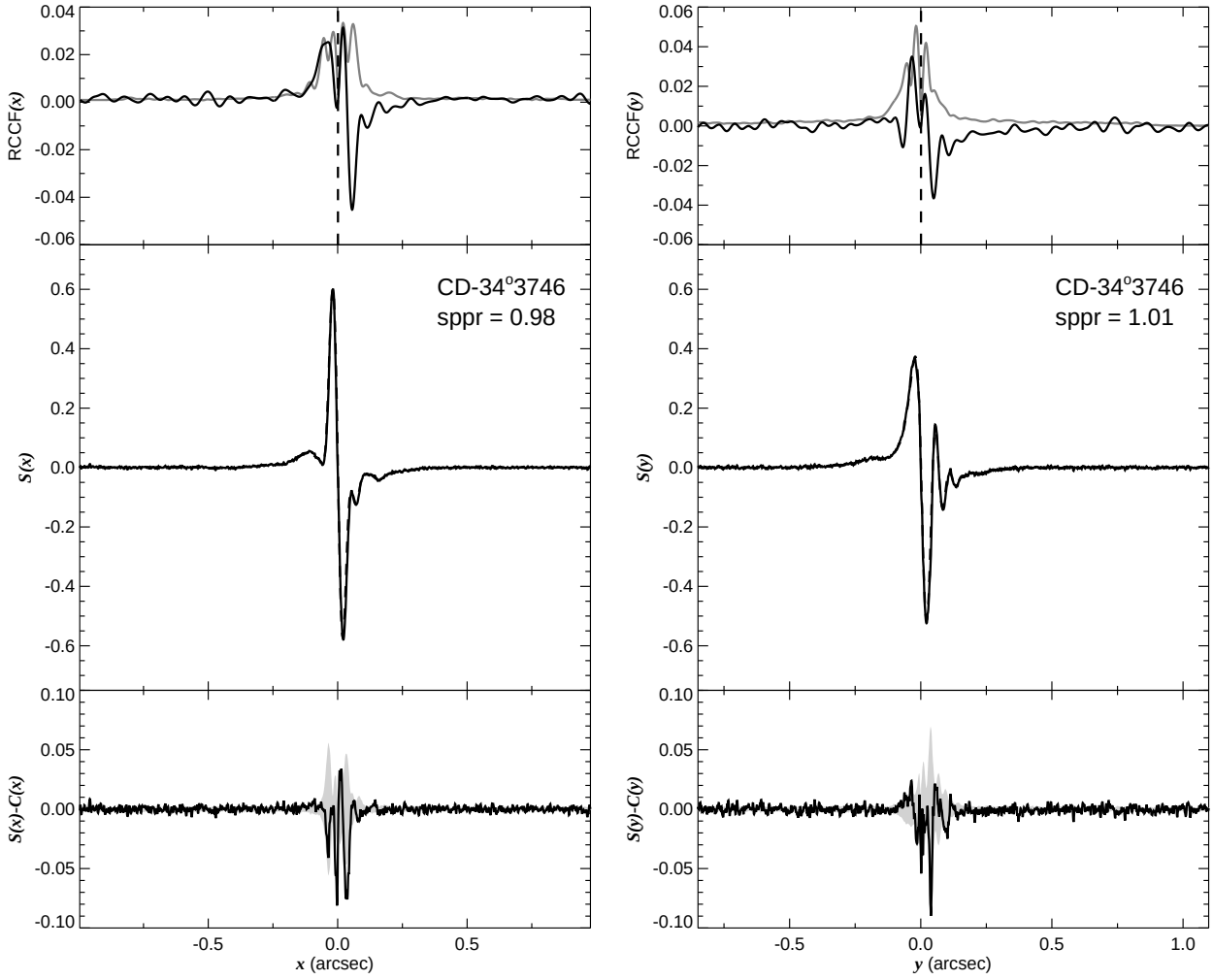

Fig. 1.100.— The FGS scans and binary detection tests for target 073642.04−342516.8 = CD−34 3746 obtained on BY 2008.8177.

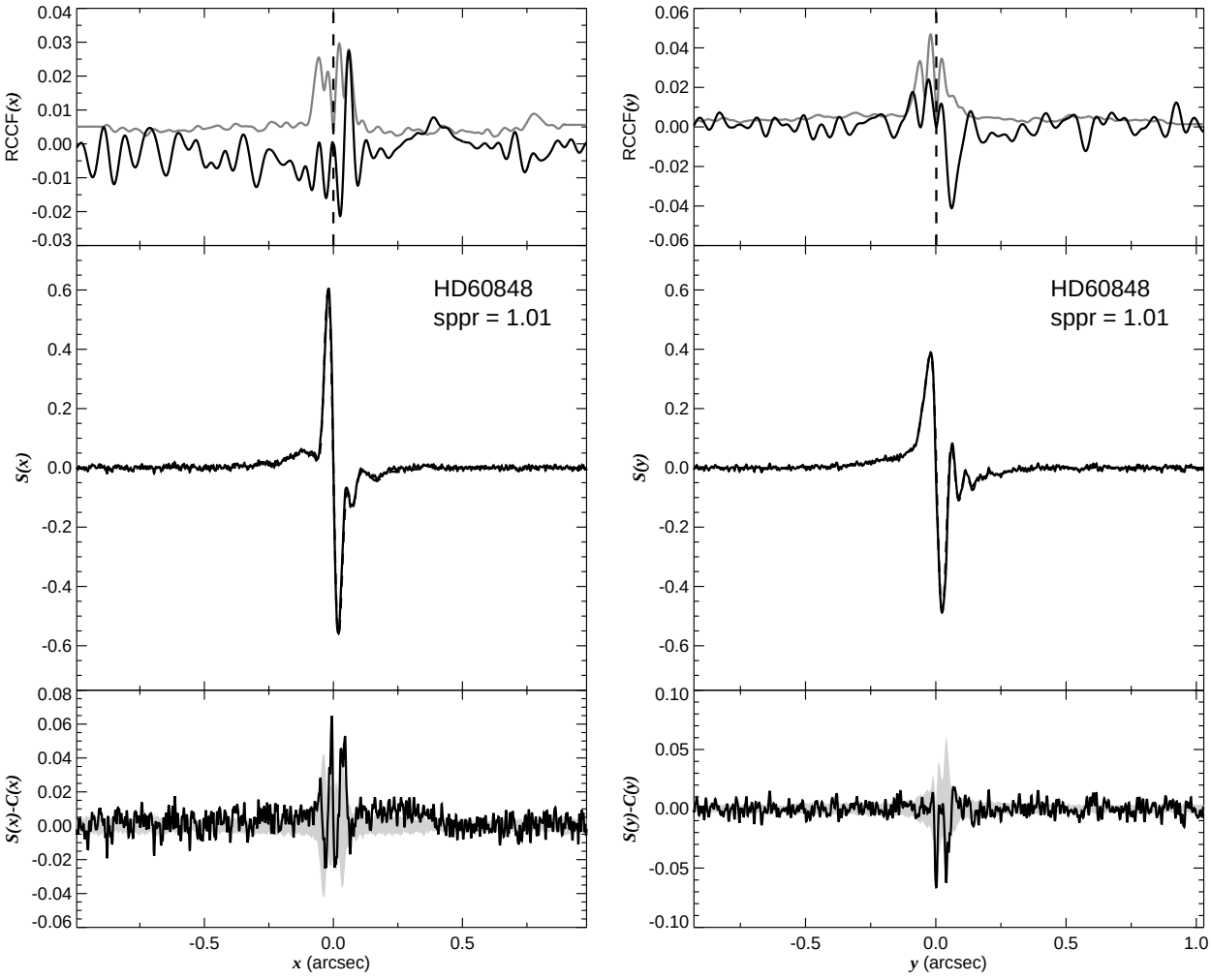

Fig. 1.101.— The FGS scans and binary detection tests for target 073705.73+165415.3 = HD60848 obtained on BY 2008.7098.

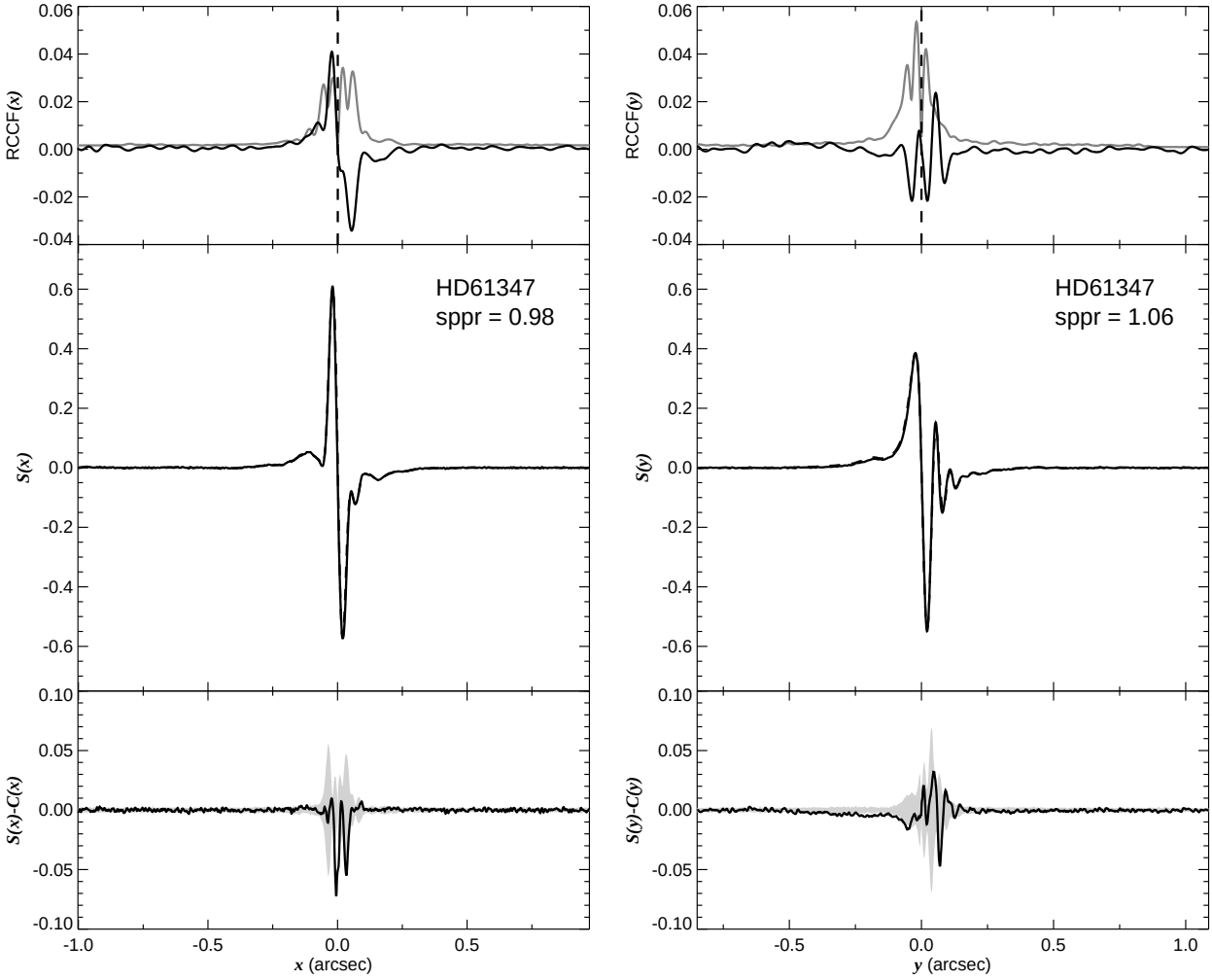

Fig. 1.102.— The FGS scans and binary detection tests for target 073816.12−135101.2 = HD61347 obtained on BY 2008.7807.

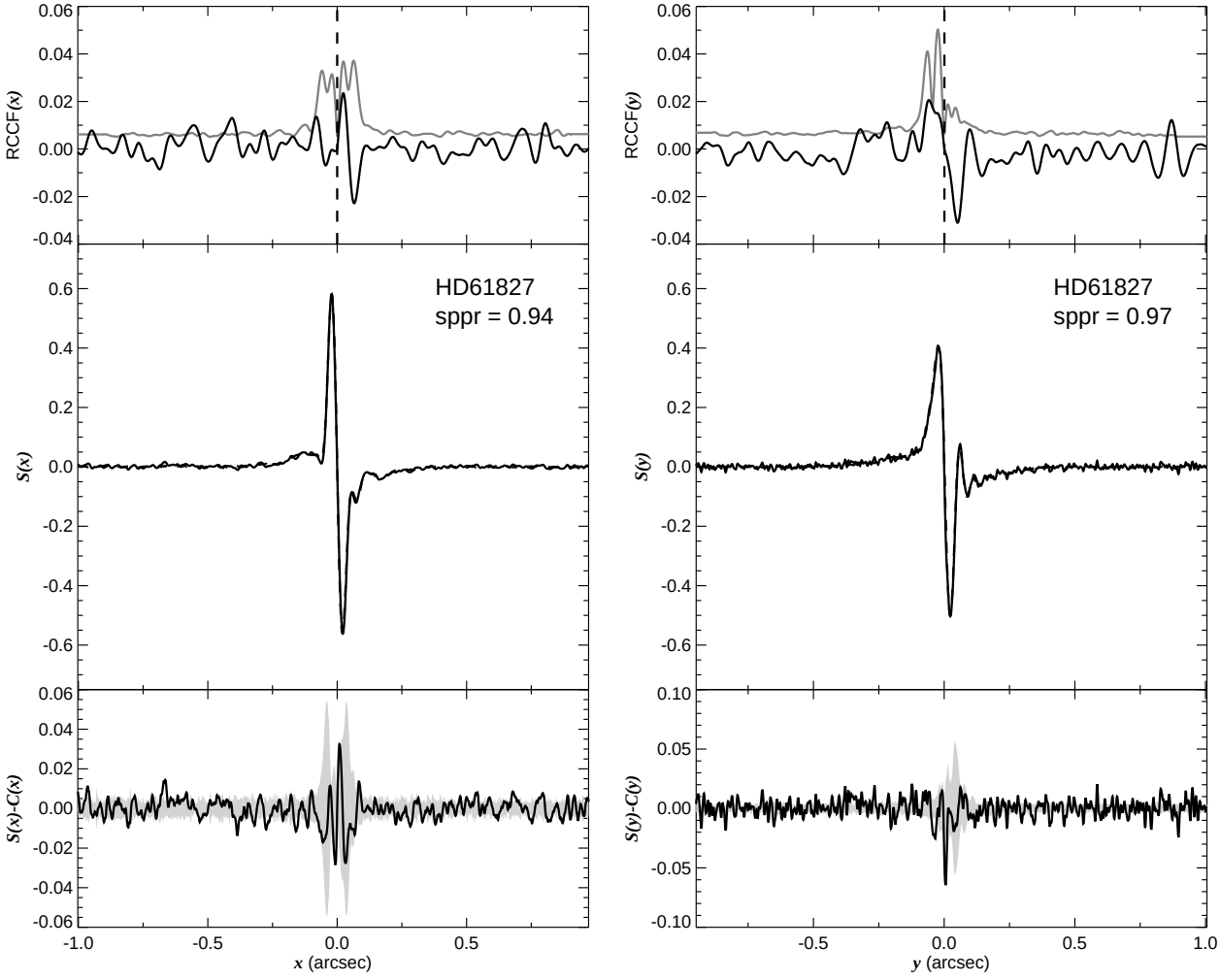

Fig. 1.103.— The FGS scans and binary detection tests for target 073949.34−323442.1 = HD61827 obtained on BY 2008.7809.

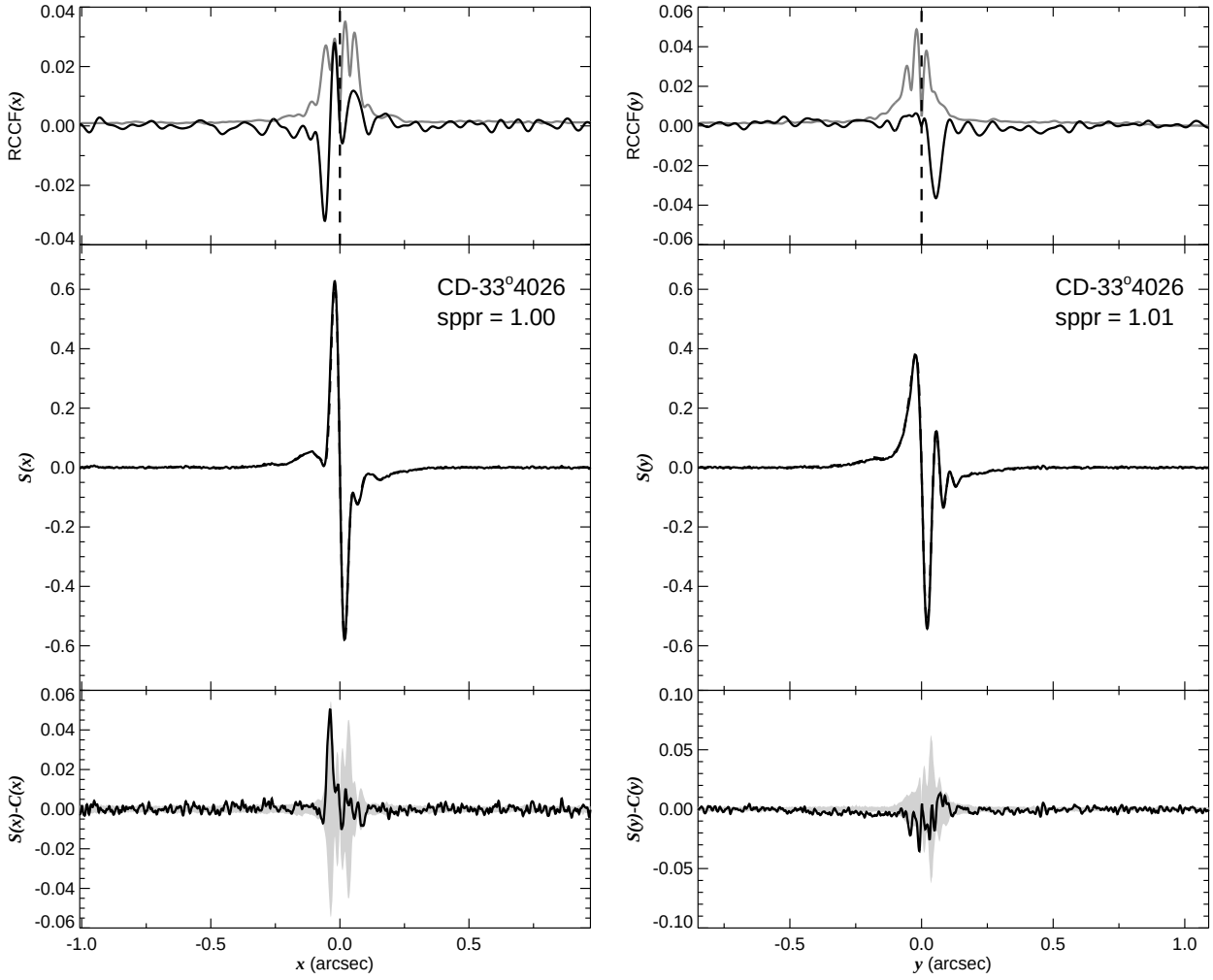

Fig. 1.104.— The FGS scans and binary detection tests for target 074030.29−333044.6 = CD−33 4026 obtained on BY 2008.8078.

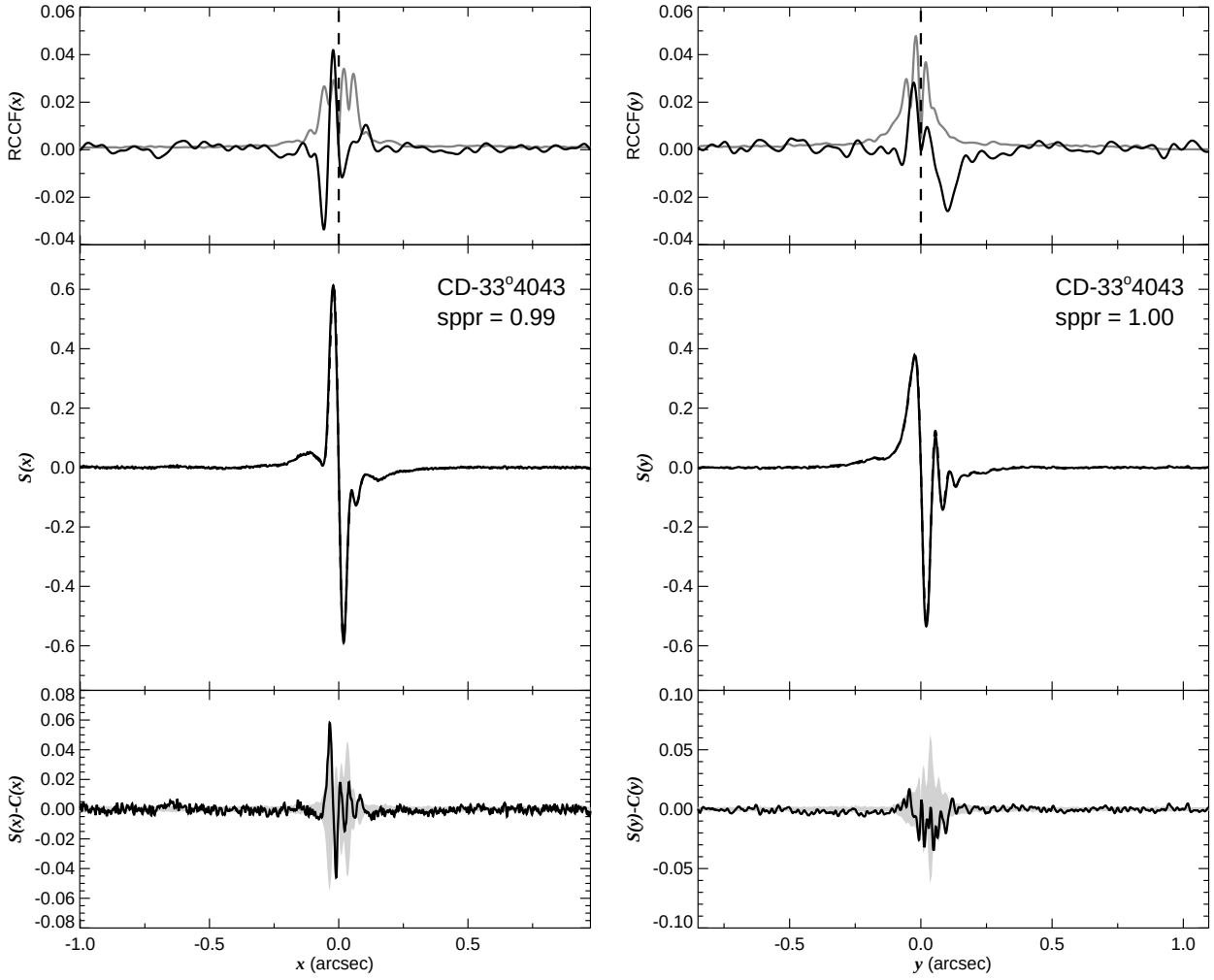

Fig. 1.105.— The FGS scans and binary detection tests for target 074139.98−334954.1 = CD−33 4043 obtained on BY 2008.8069.

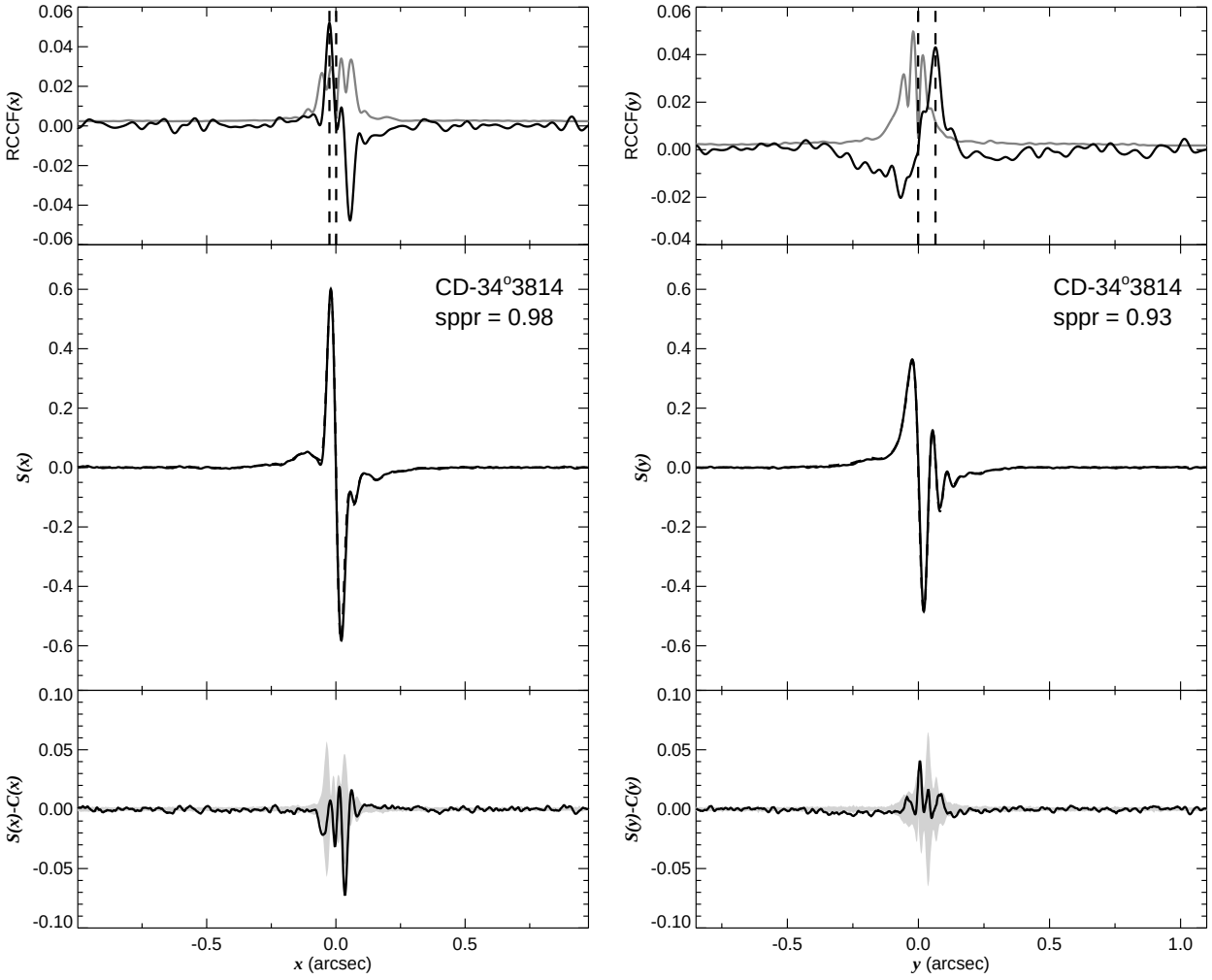

Fig. 1.106.— The FGS scans and binary detection tests for target 074143.44−344727.6 = CD−34 3814 obtained on BY 2008.8095.

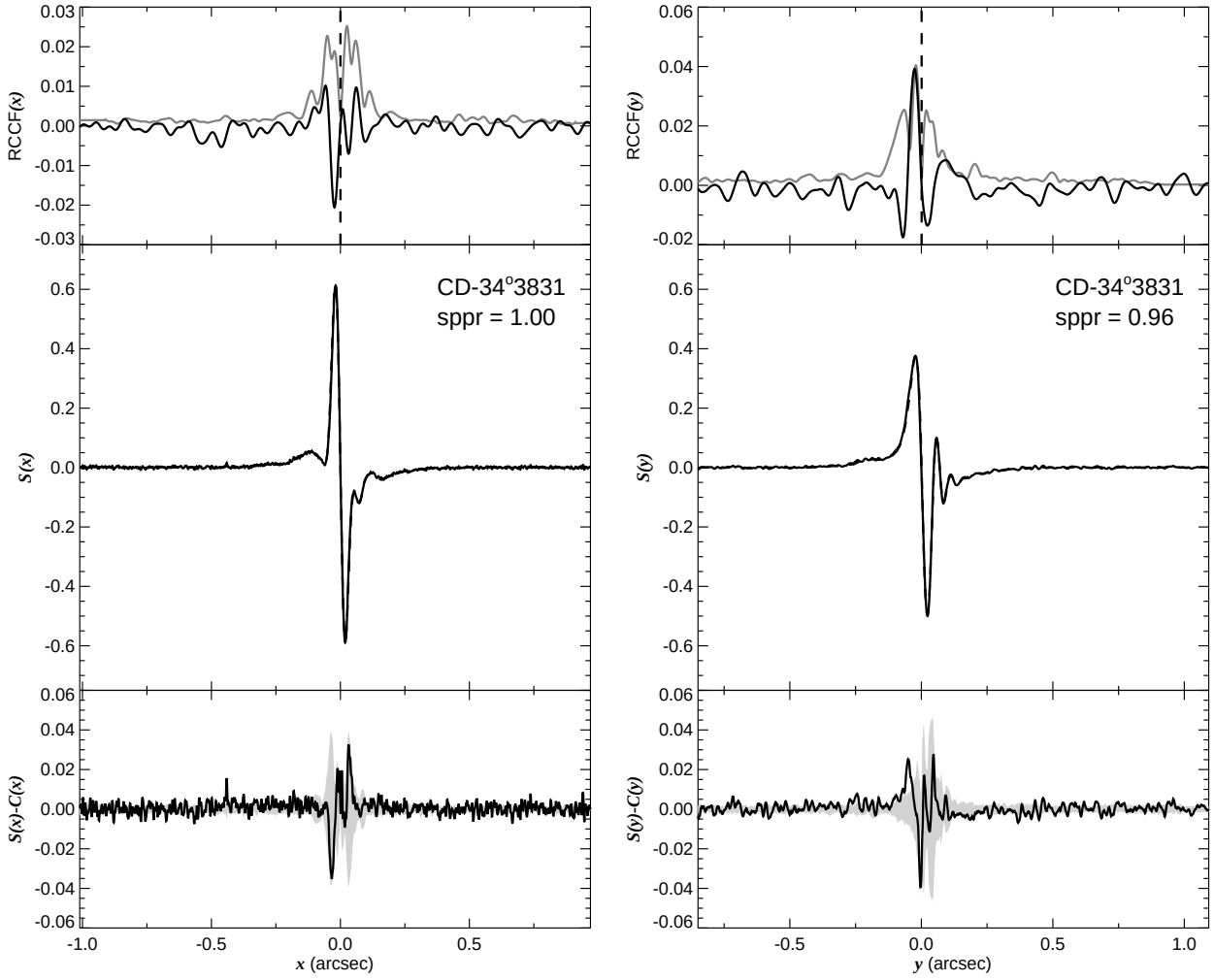

Fig. 1.107.— The FGS scans and binary detection tests for target 074254.87−341907.9 = CD−34 3831 obtained on BY 2008.8102.

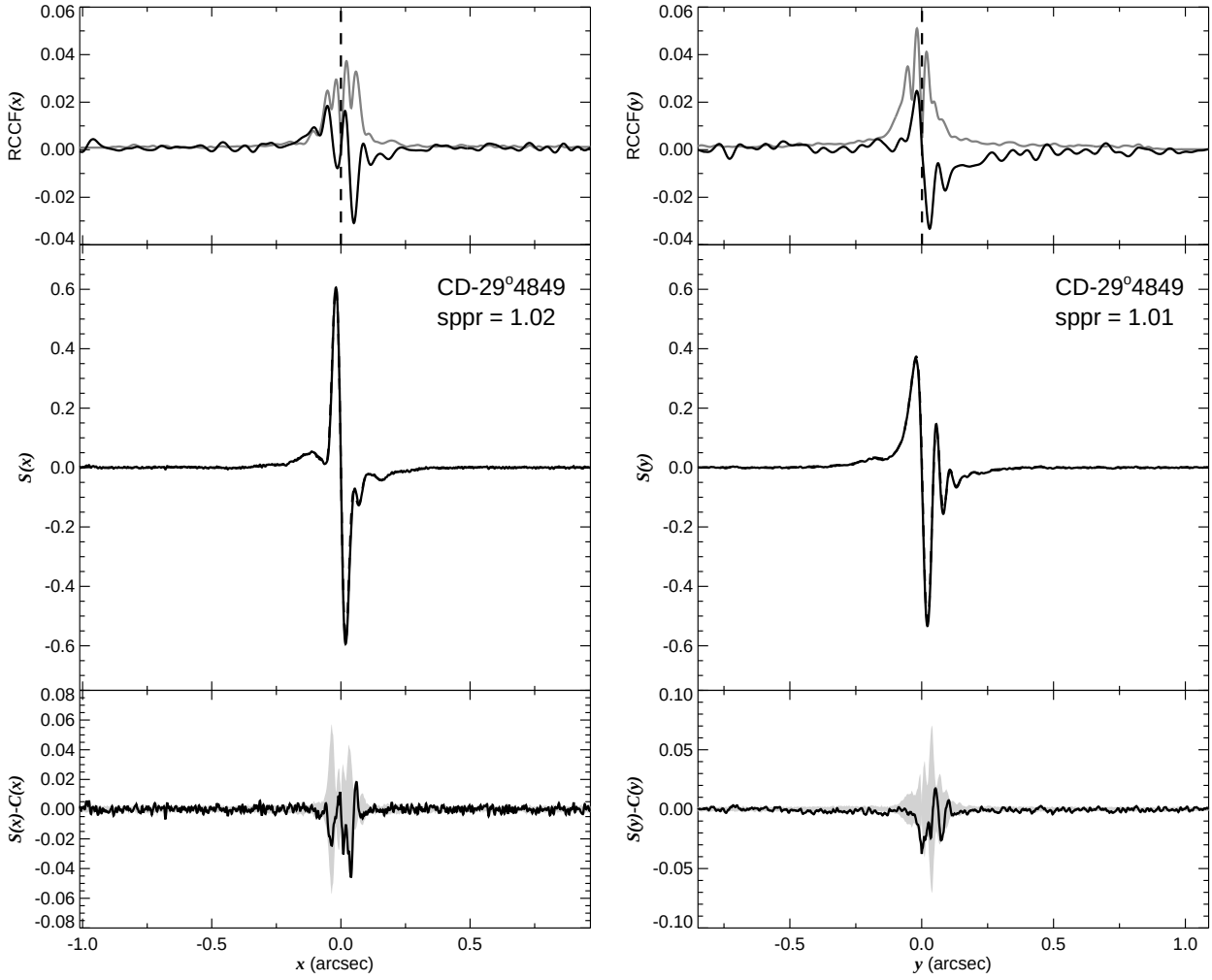

Fig. 1.108.— The FGS scans and binary detection tests for target 074328.98−291912.5 = CD−29 4849 obtained on BY 2008.8212.

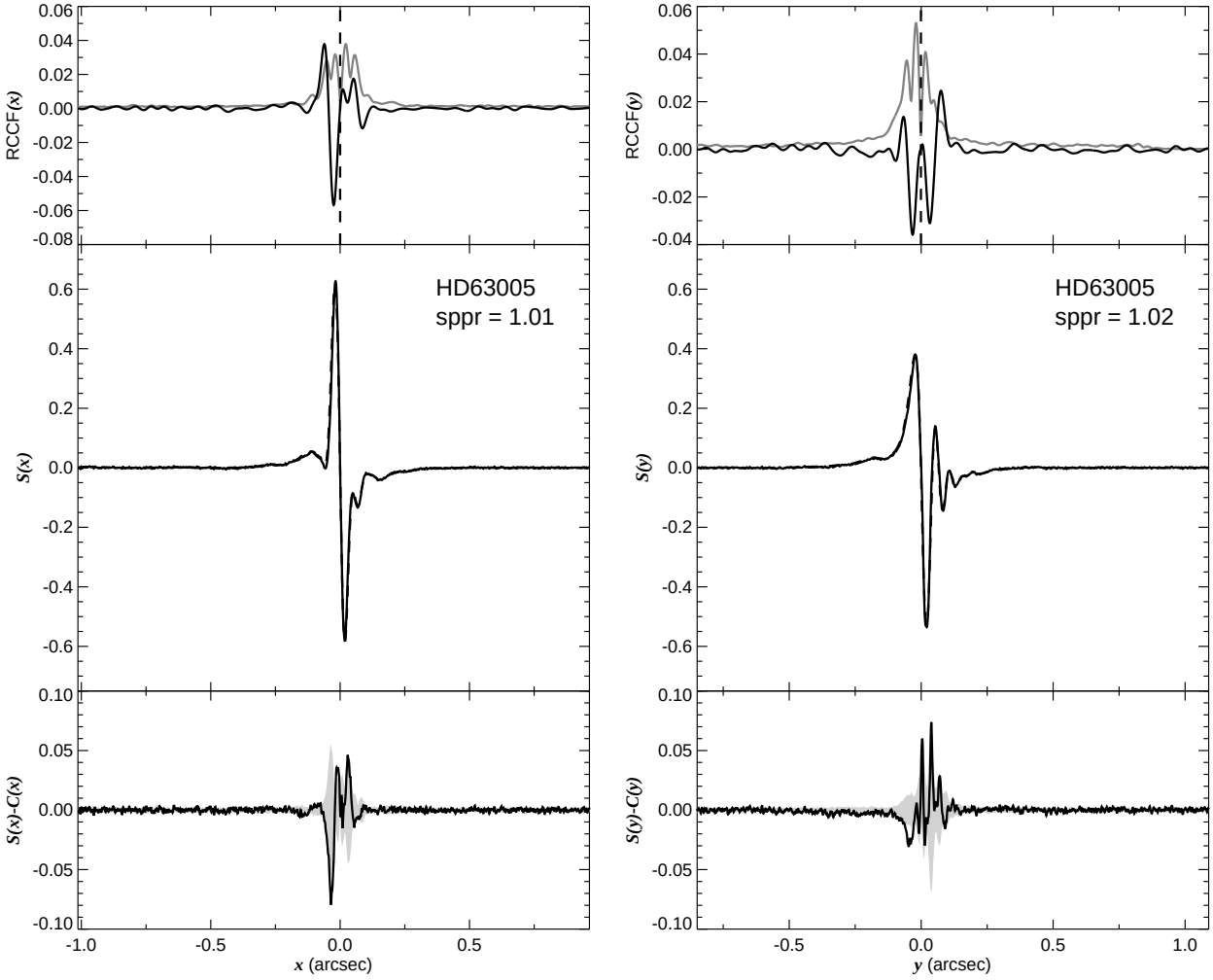

Fig. 1.109.— The FGS scans and binary detection tests for target 074549.03−262931.4 = HD63005 obtained on BY 2008.7676.

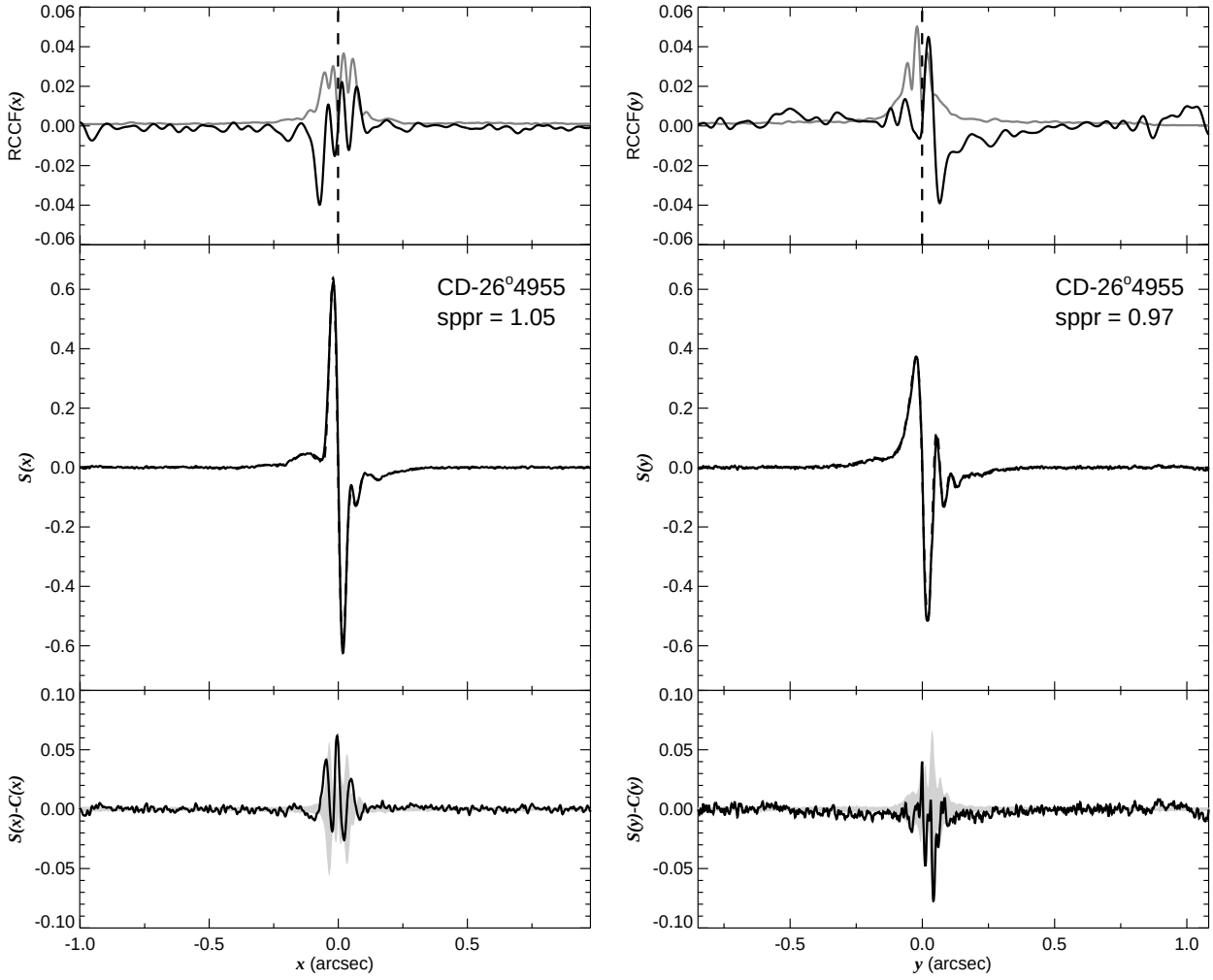

Fig. 1.110.— The FGS scans and binary detection tests for target 074636.20−264140.0 = CD−26 4955 obtained on BY 2008.8833.

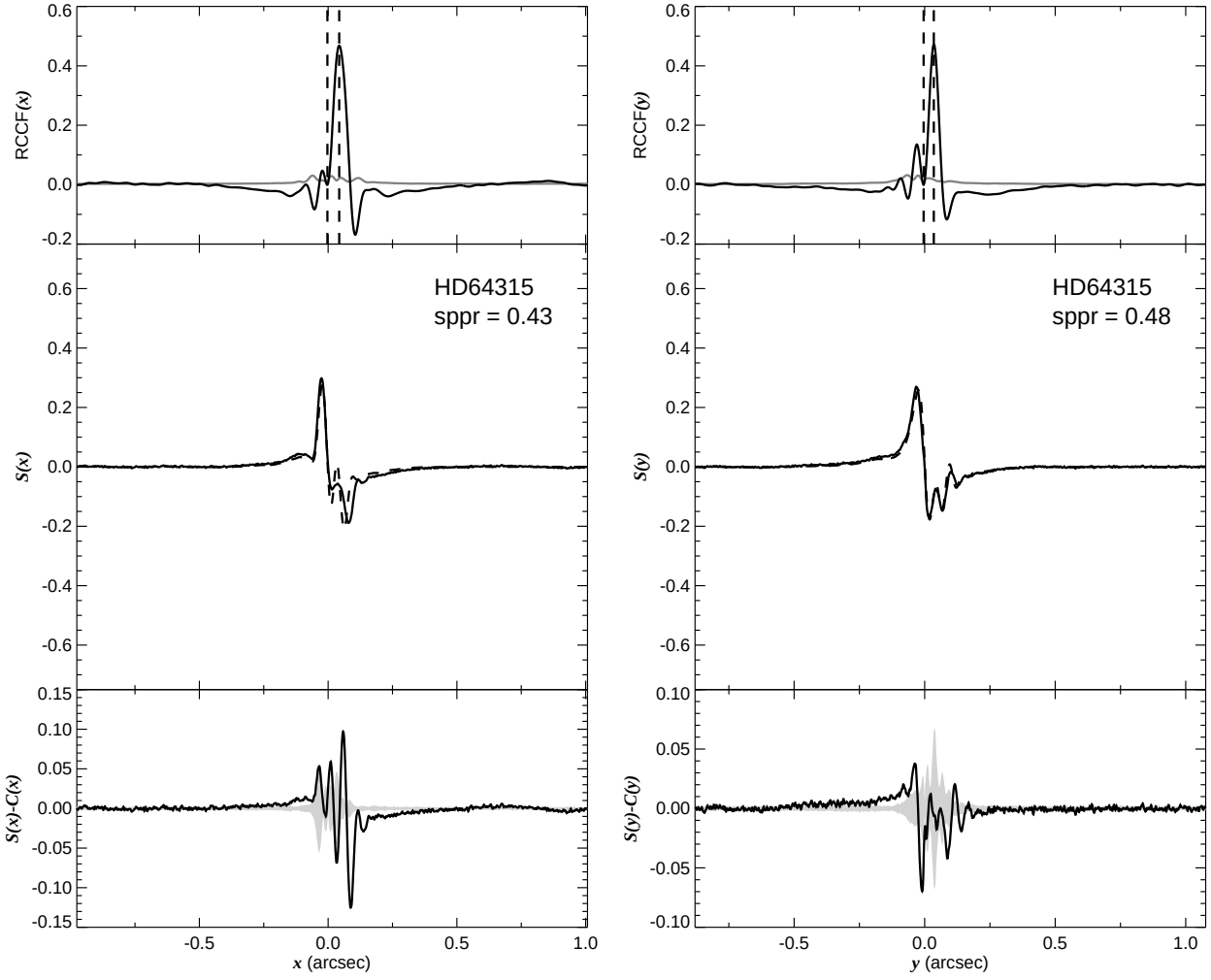

Fig. 1.111.— The FGS scans and binary detection tests for target 075220.28−262546.7 = HD64315 obtained on BY 2008.7686.

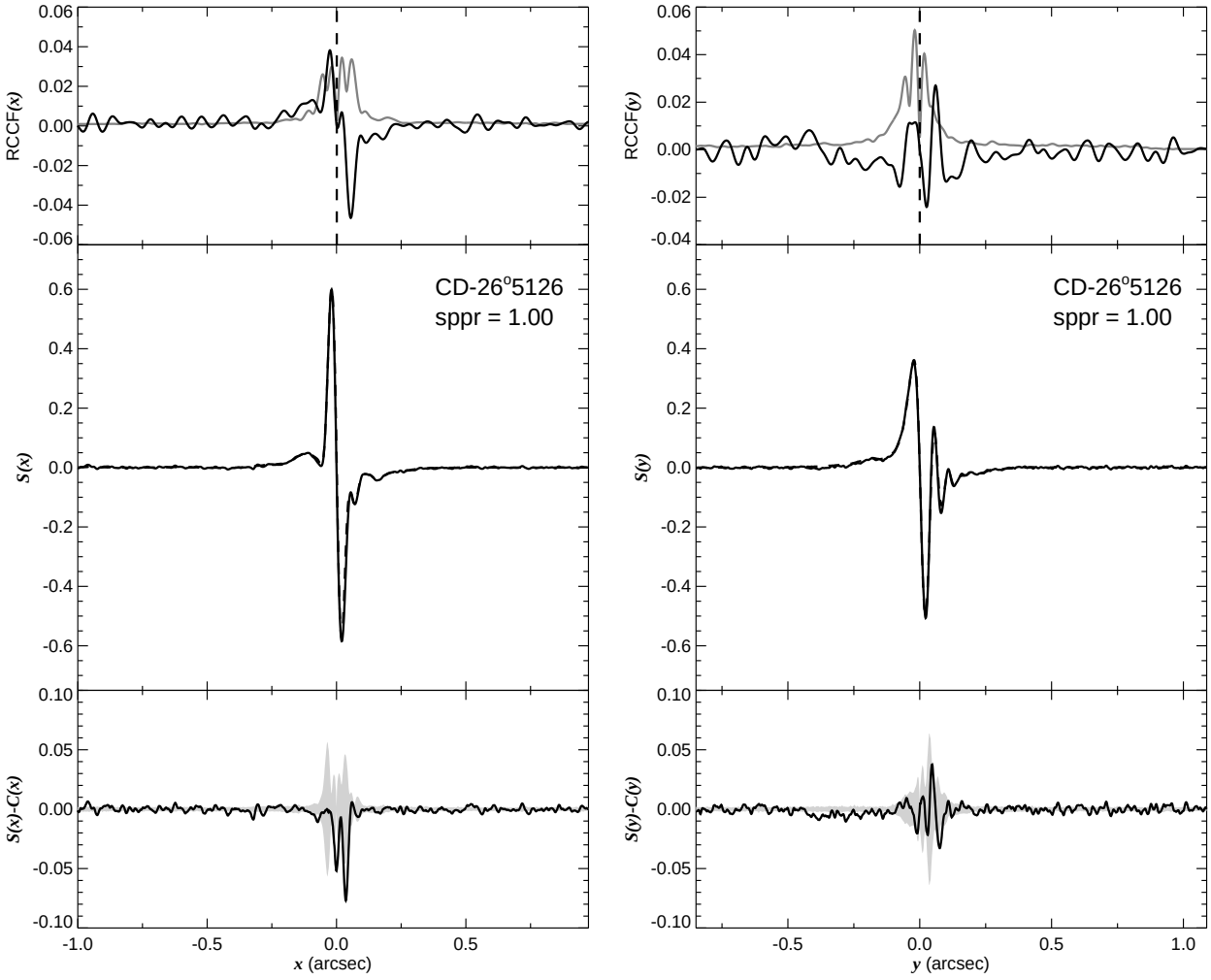

Fig. 1.112.— The FGS scans and binary detection tests for target 075250.42−262822.3 = CD−26 5126 obtained on BY 2008.8122.

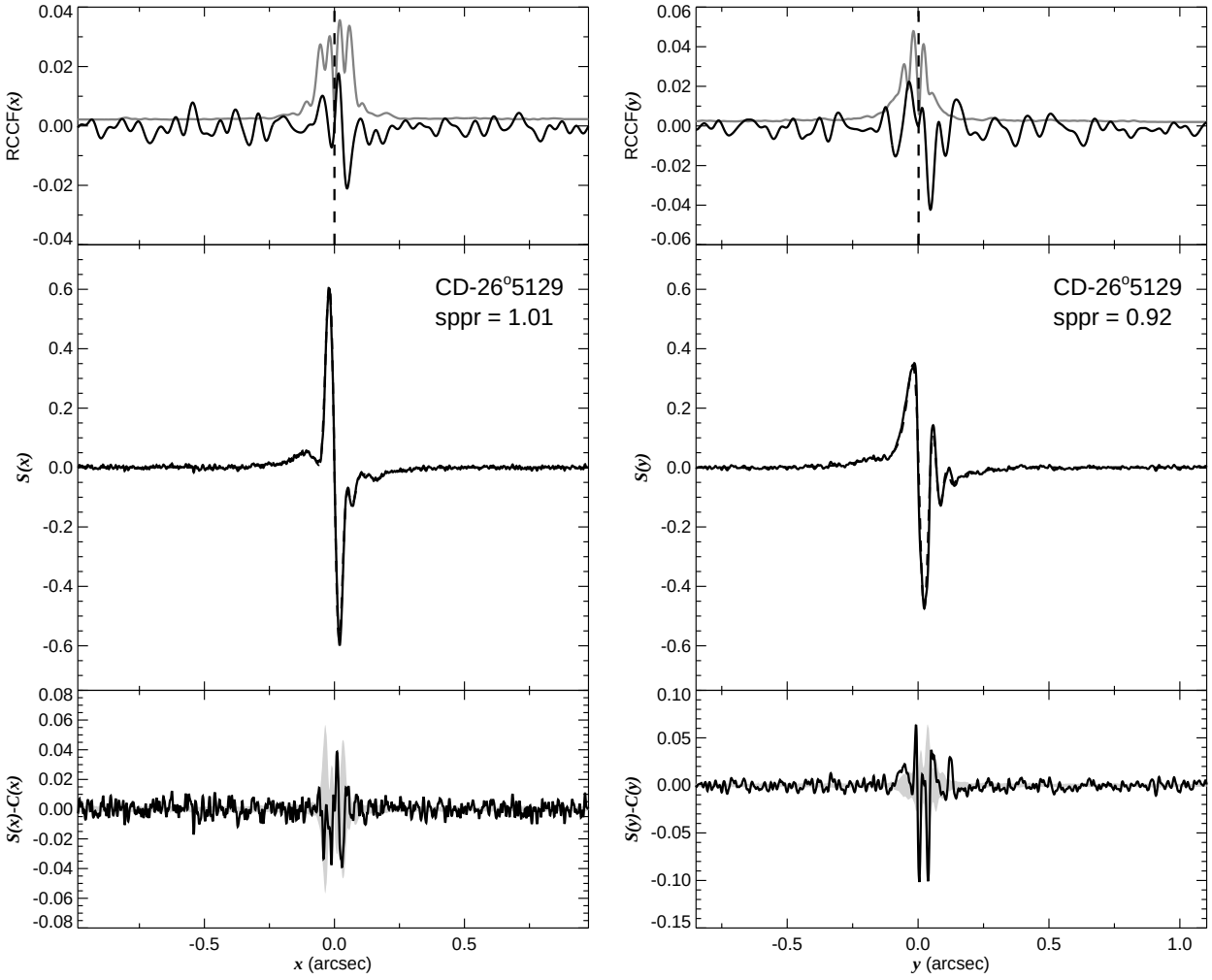

Fig. 1.113.— The FGS scans and binary detection tests for target 075255.40−262842.7 = CD−26 5129 obtained on BY 2008.8780.

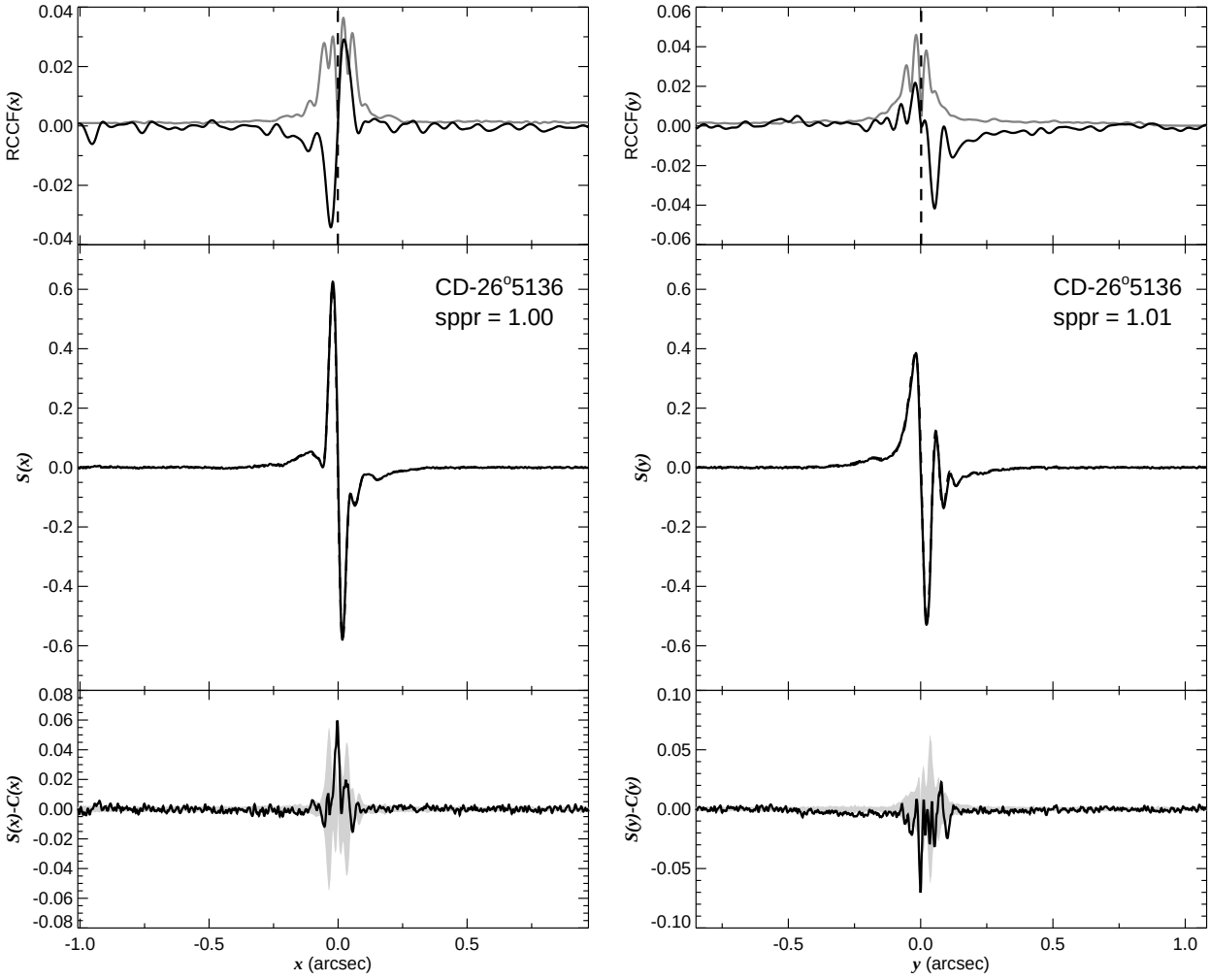

Fig. 1.114.— The FGS scans and binary detection tests for target 075301.01−270657.8 = CD−26 5136 obtained on BY 2008.7801.

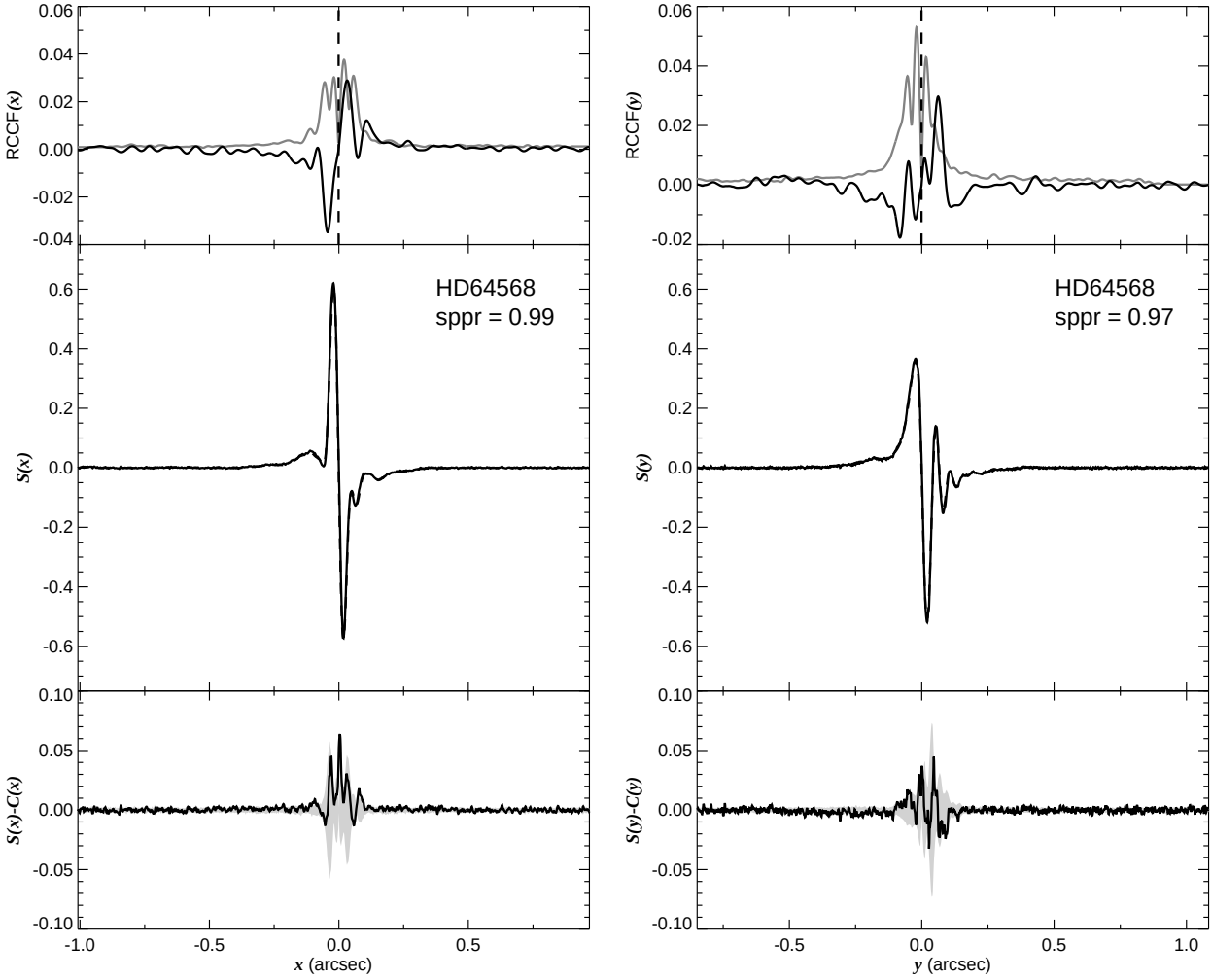

Fig. 1.115.— The FGS scans and binary detection tests for target 075338.20−261402.6 = HD64568 obtained on BY 2007.9193.

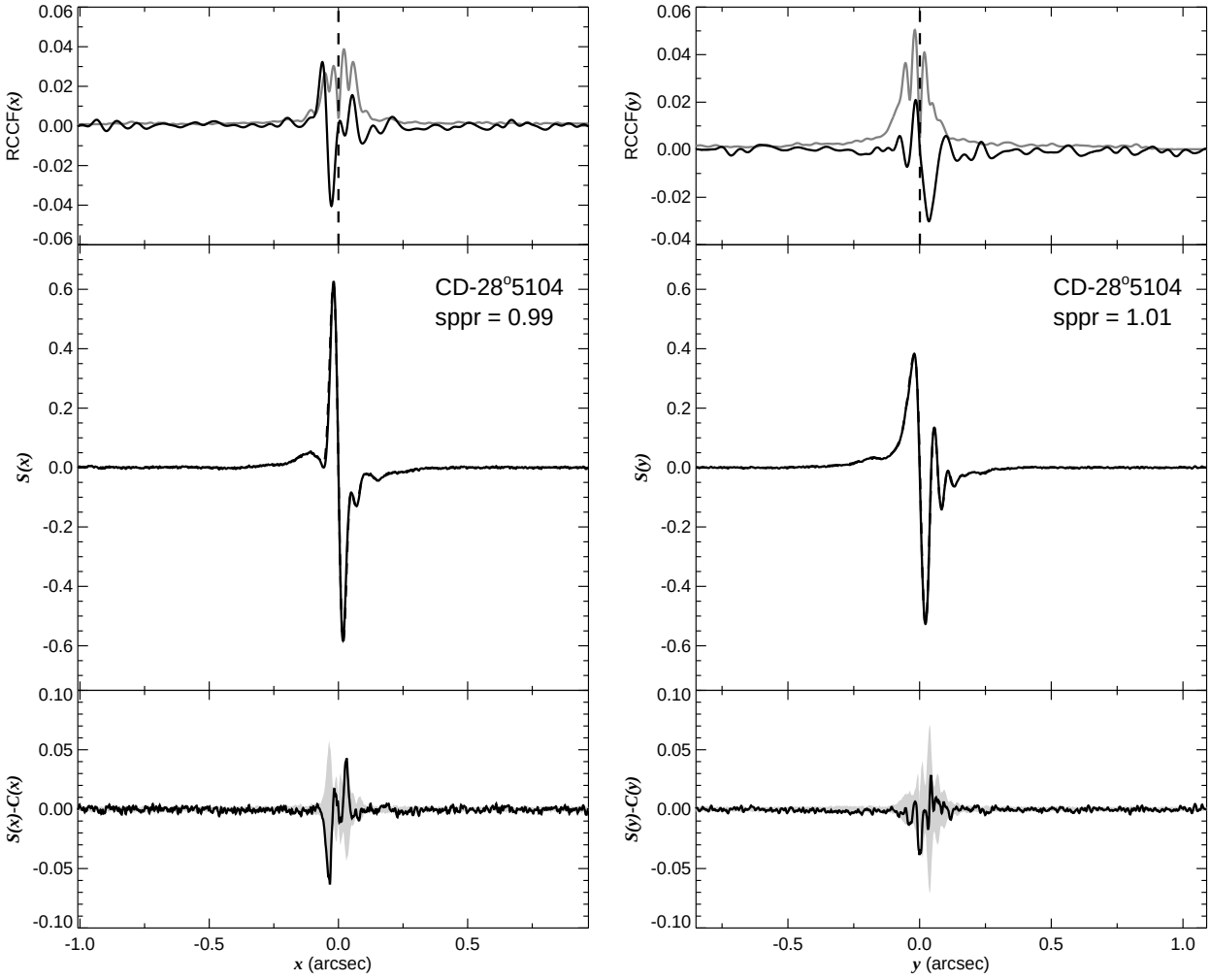

Fig. 1.116.— The FGS scans and binary detection tests for target 075552.85−283746.8 = CD−28 5104 obtained on BY 2008.7688.

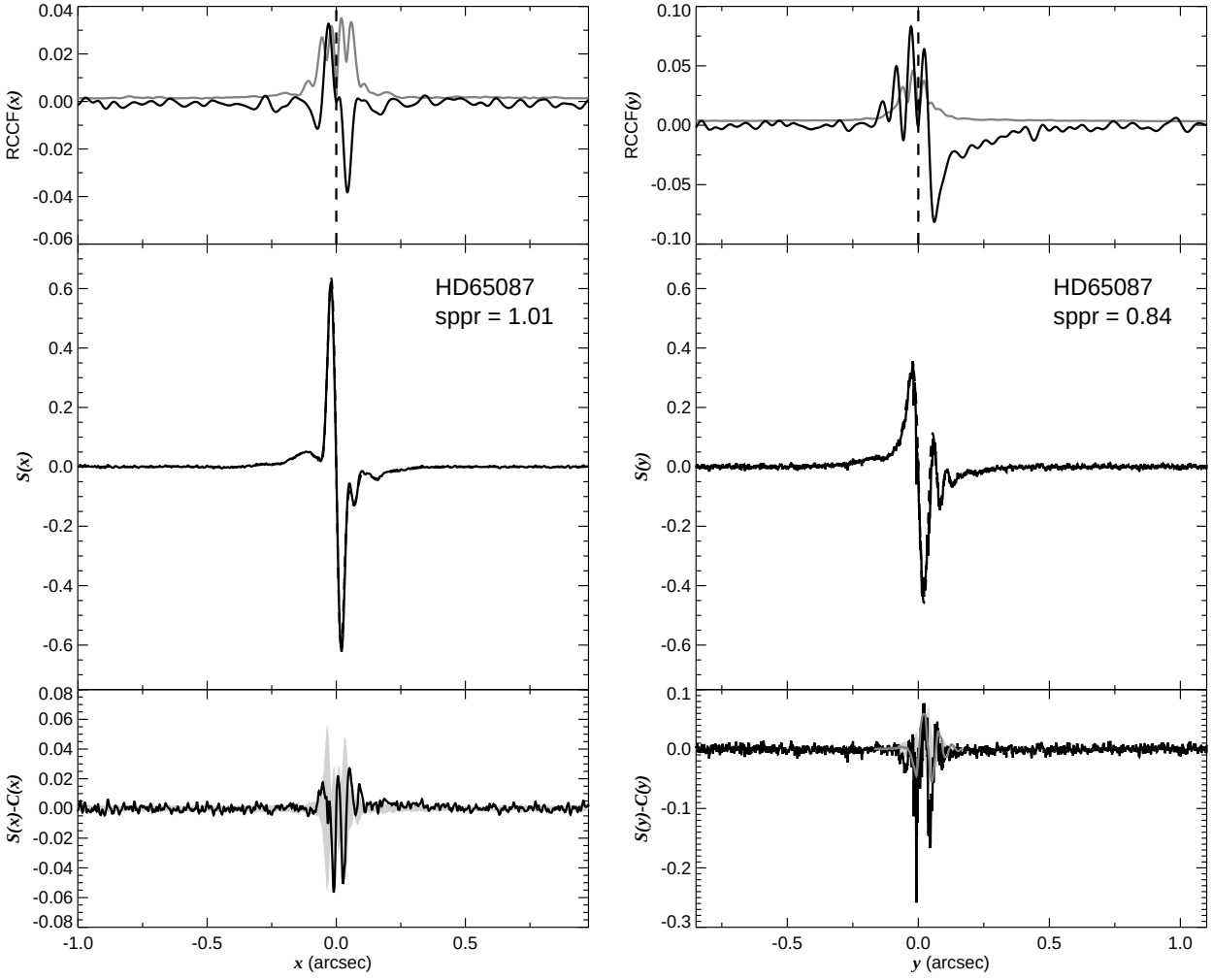

Fig. 1.117.— The FGS scans and binary detection tests for target 075557.13−283218.0 = HD65087 obtained on BY 2008.8784.

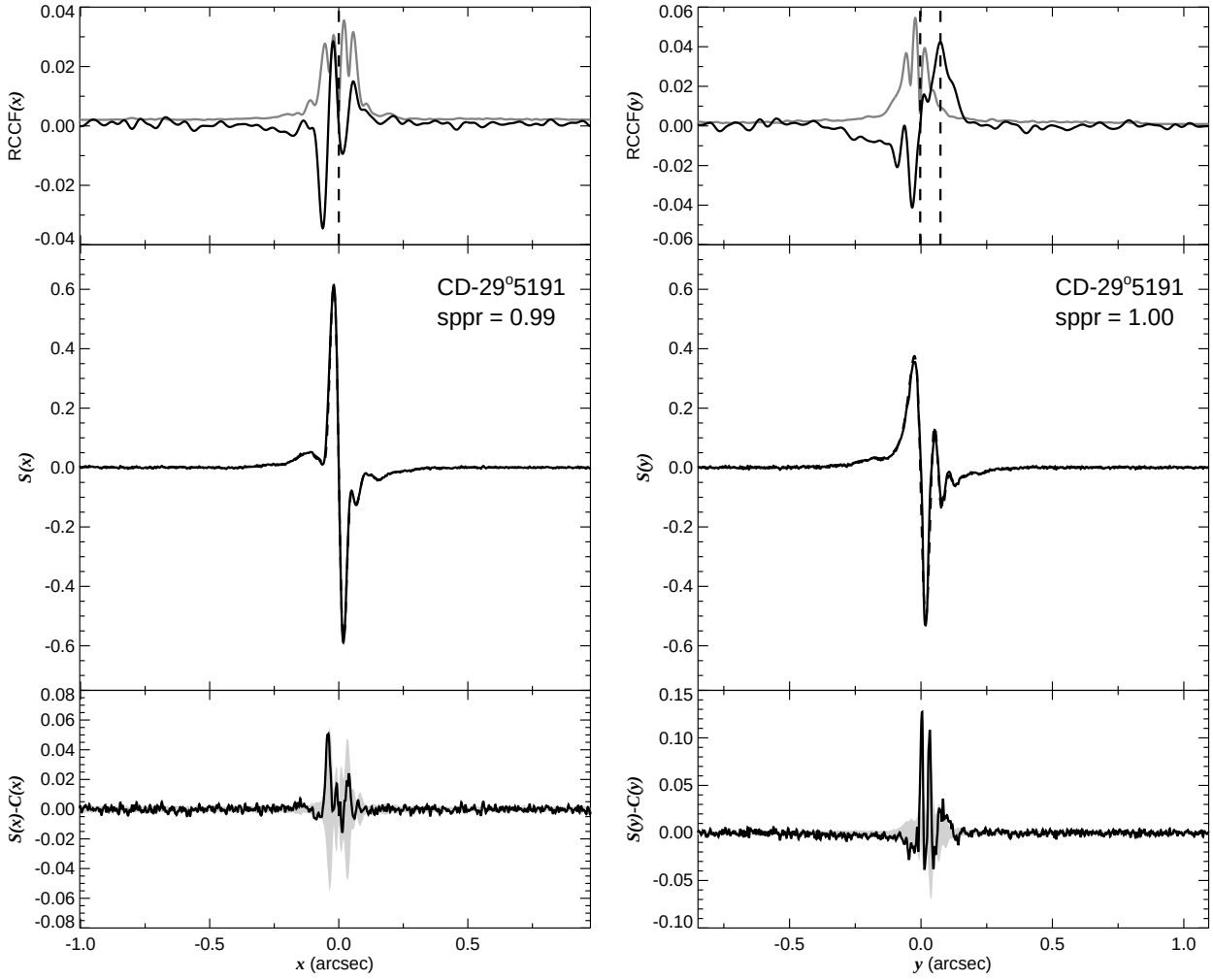

Fig. 1.118.— The FGS scans and binary detection tests for target 075626.41−292526.1 = CD−29 5191 obtained on BY 2008.8100.

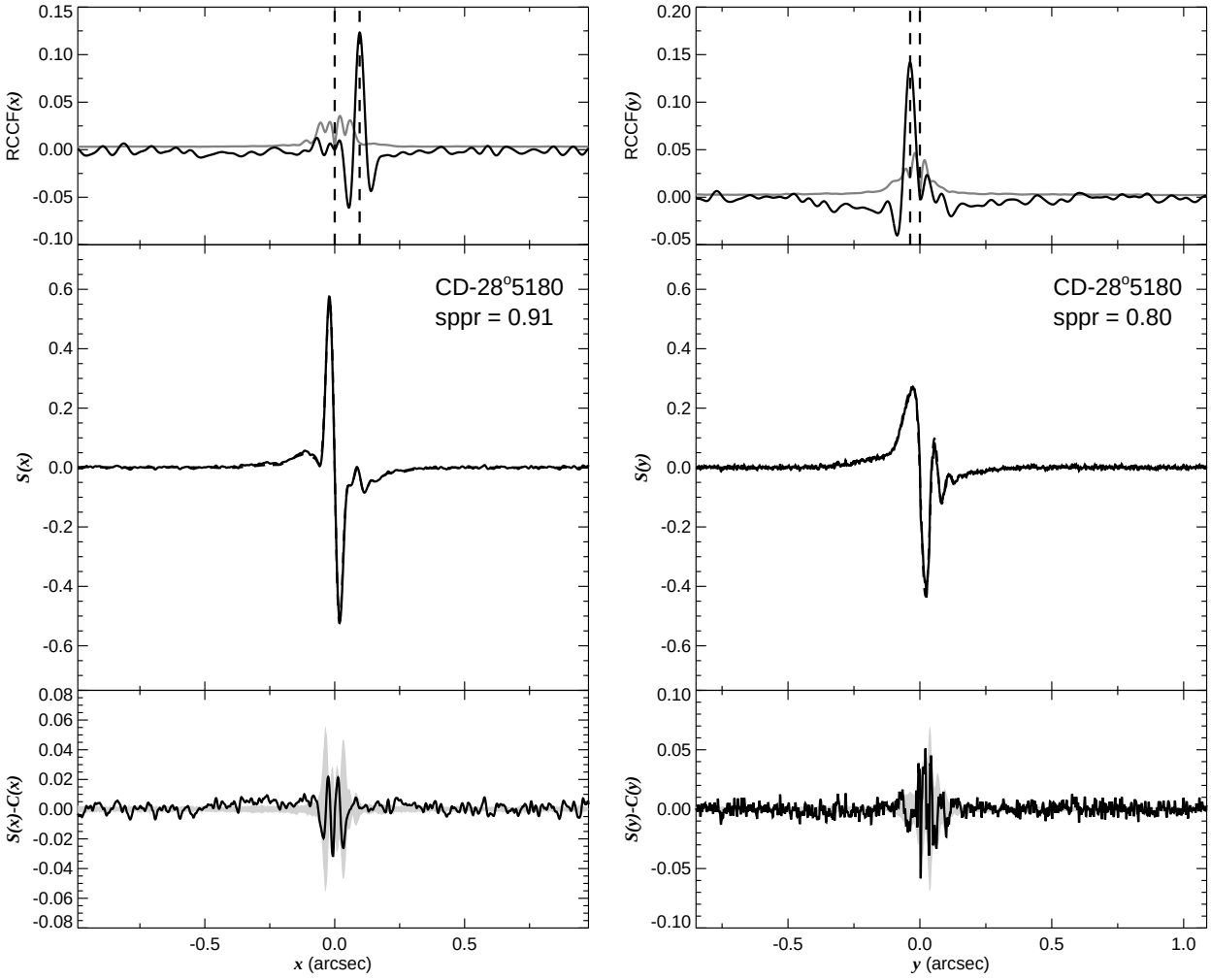

Fig. 1.119.— The FGS scans and binary detection tests for target 075758.55−283529.4 = CD−28 5180 obtained on BY 2008.8516.

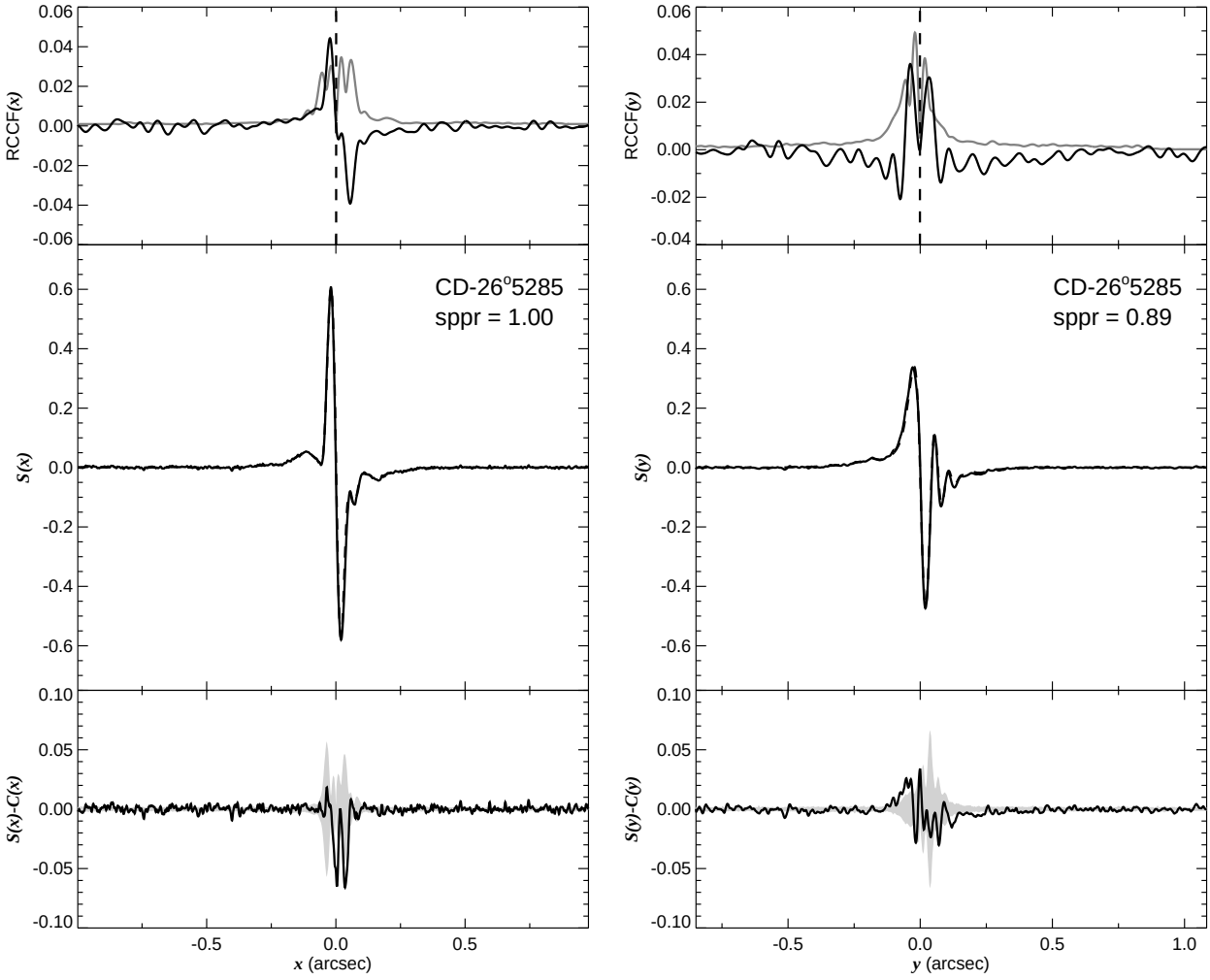

Fig. 1.120.— The FGS scans and binary detection tests for target 075830.66−263408.2 = CD−26 5285 obtained on BY 2008.8073.

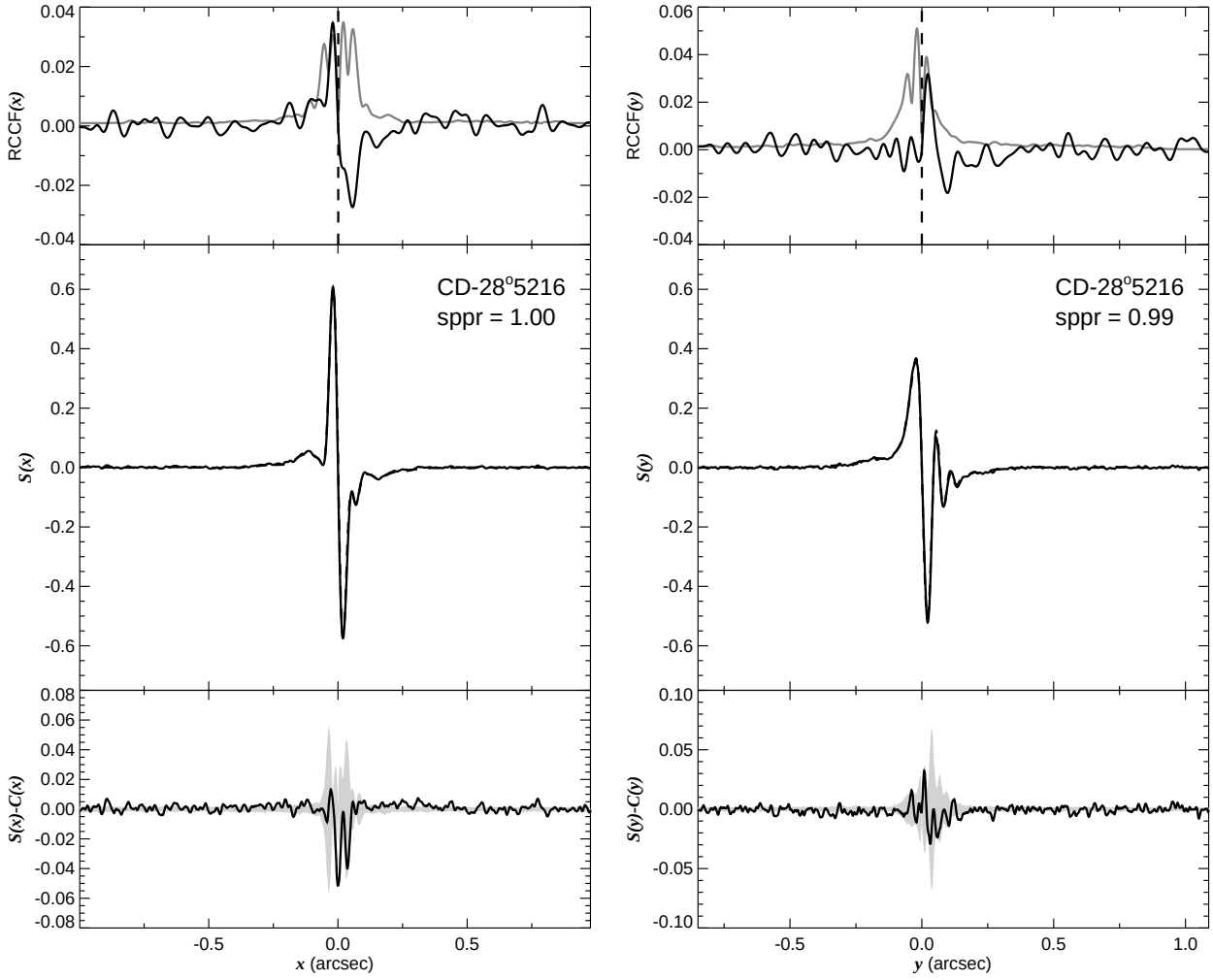

Fig. 1.121.— The FGS scans and binary detection tests for target 075851.83−284504.2 = CD−28 5216 obtained on BY 2008.8104.

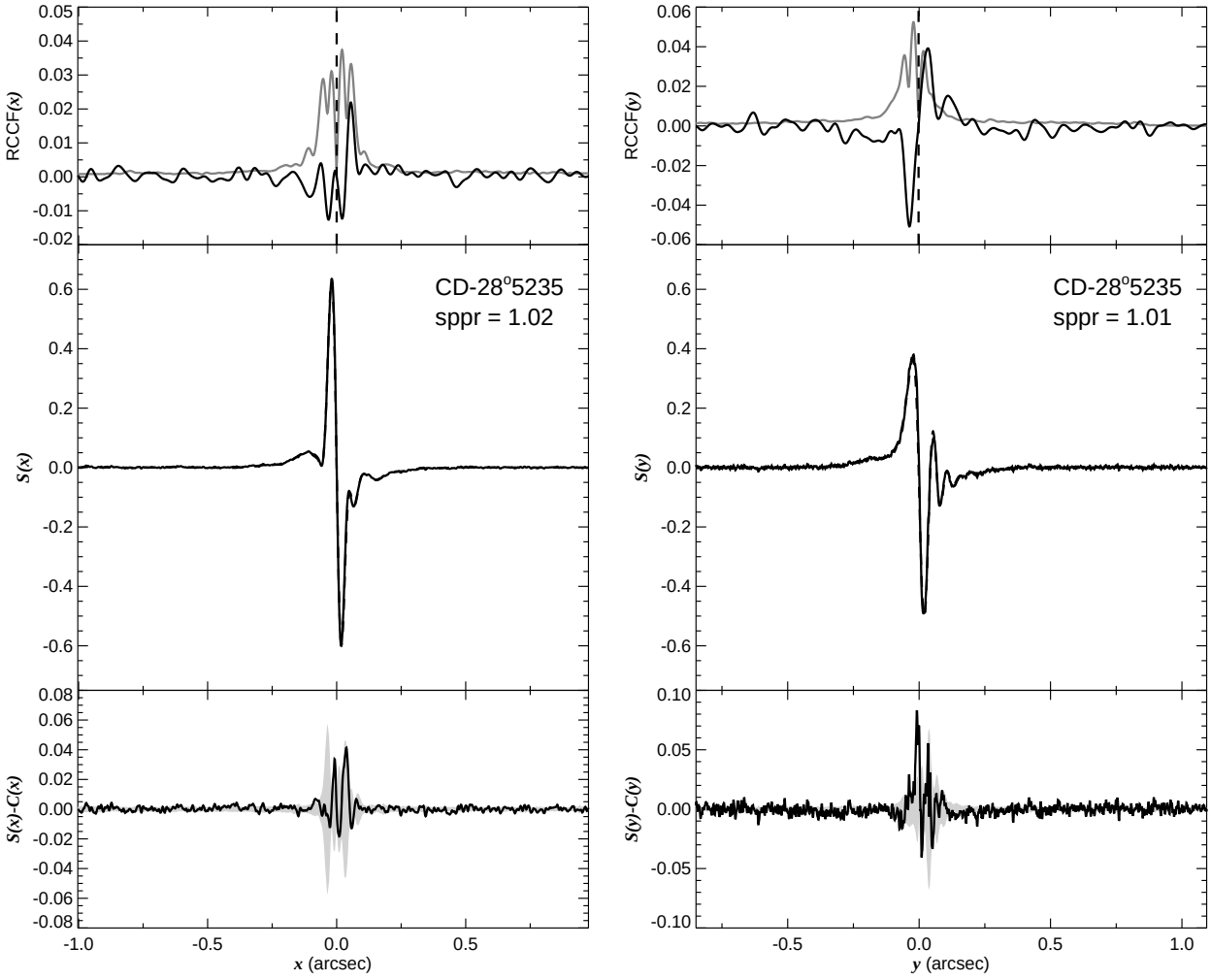

Fig. 1.122.— The FGS scans and binary detection tests for target 075922.16−285423.8 = CD−28 5235 obtained on BY 2008.8460.

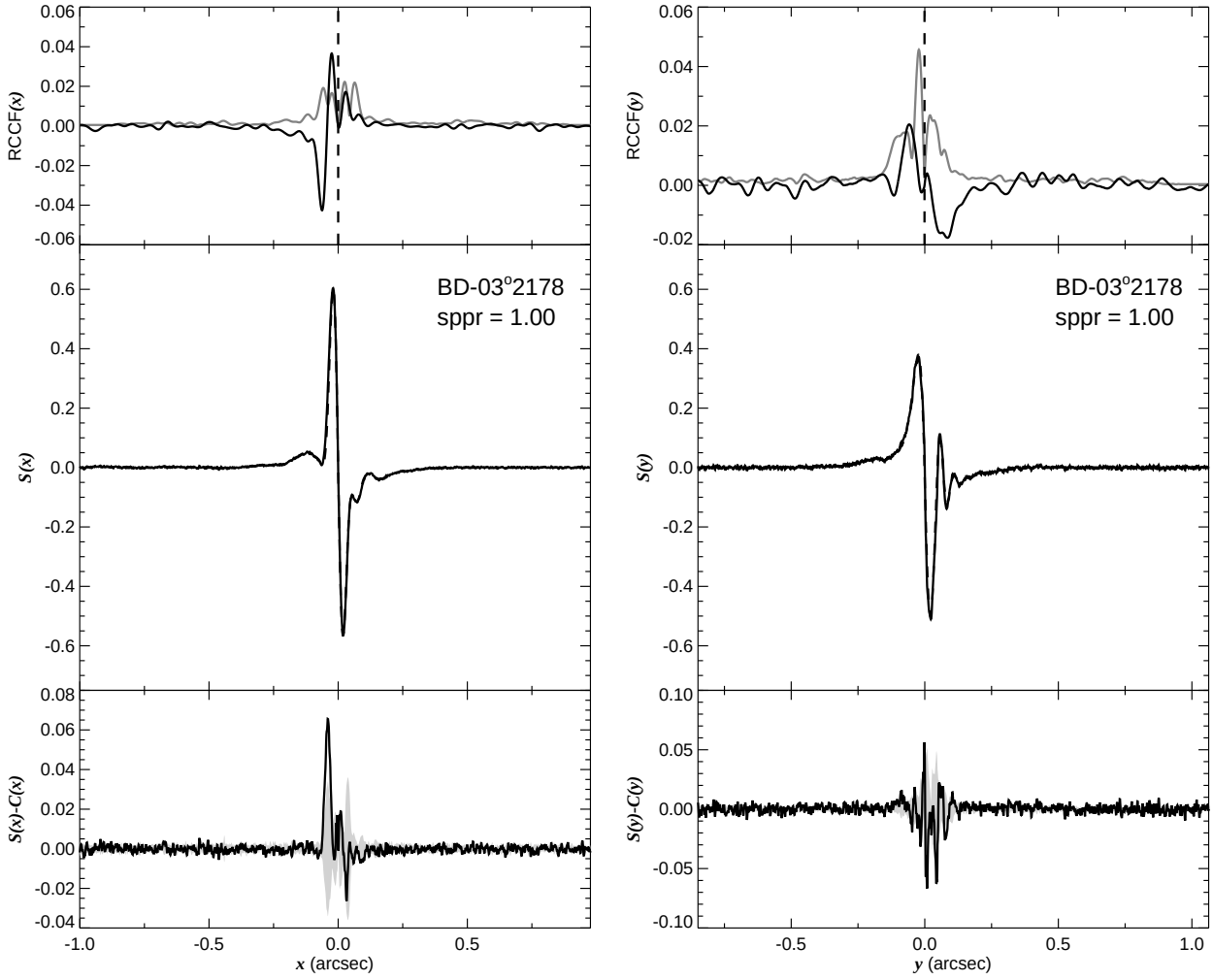

Fig. 1.123.— The FGS scans and binary detection tests for target 080210.34−040136.4 = BD−03 2178 obtained on BY 2008.8153.

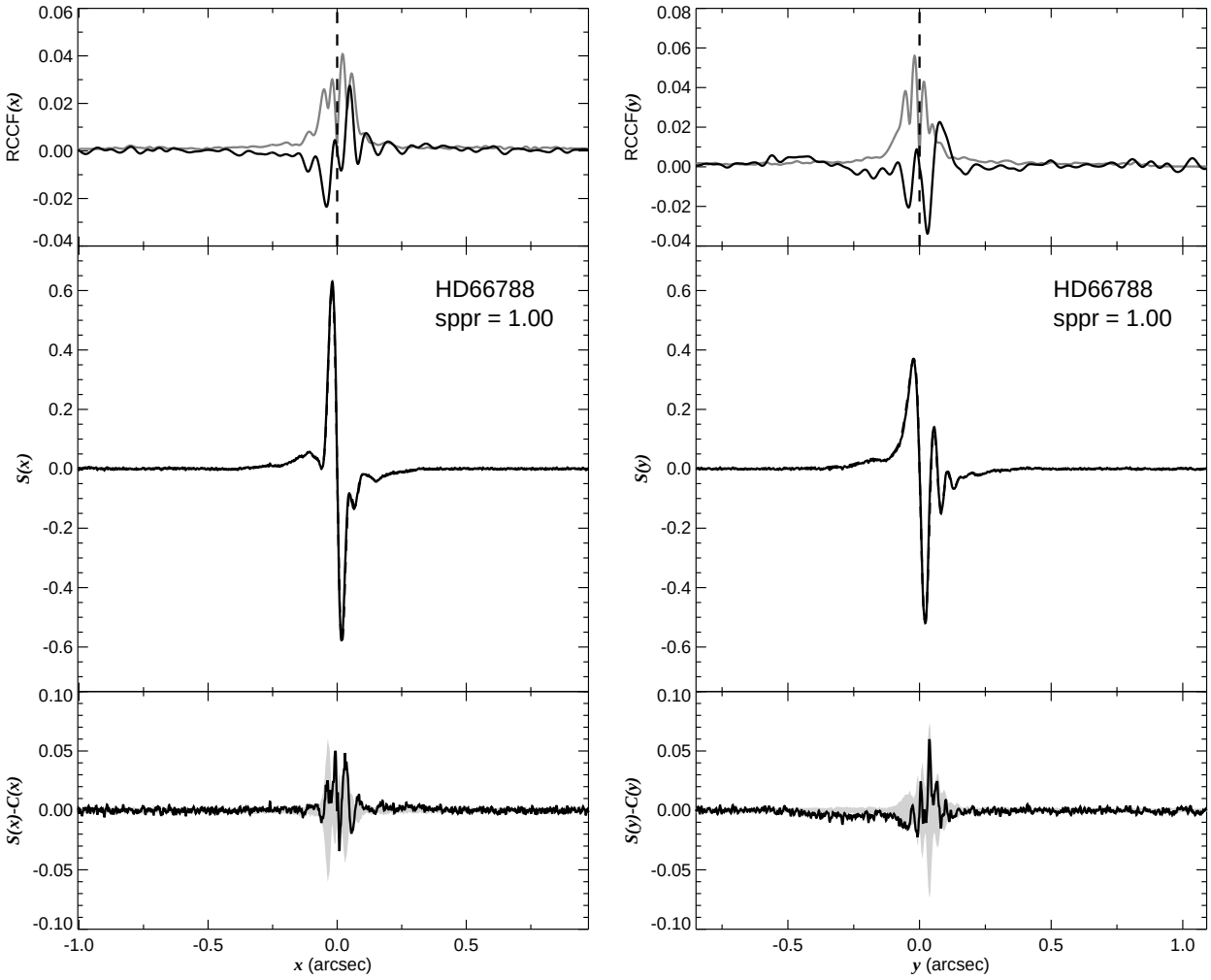

Fig. 1.124.— The FGS scans and binary detection tests for target 080408.54−272908.8 = HD66788 obtained on BY 2008.7692.

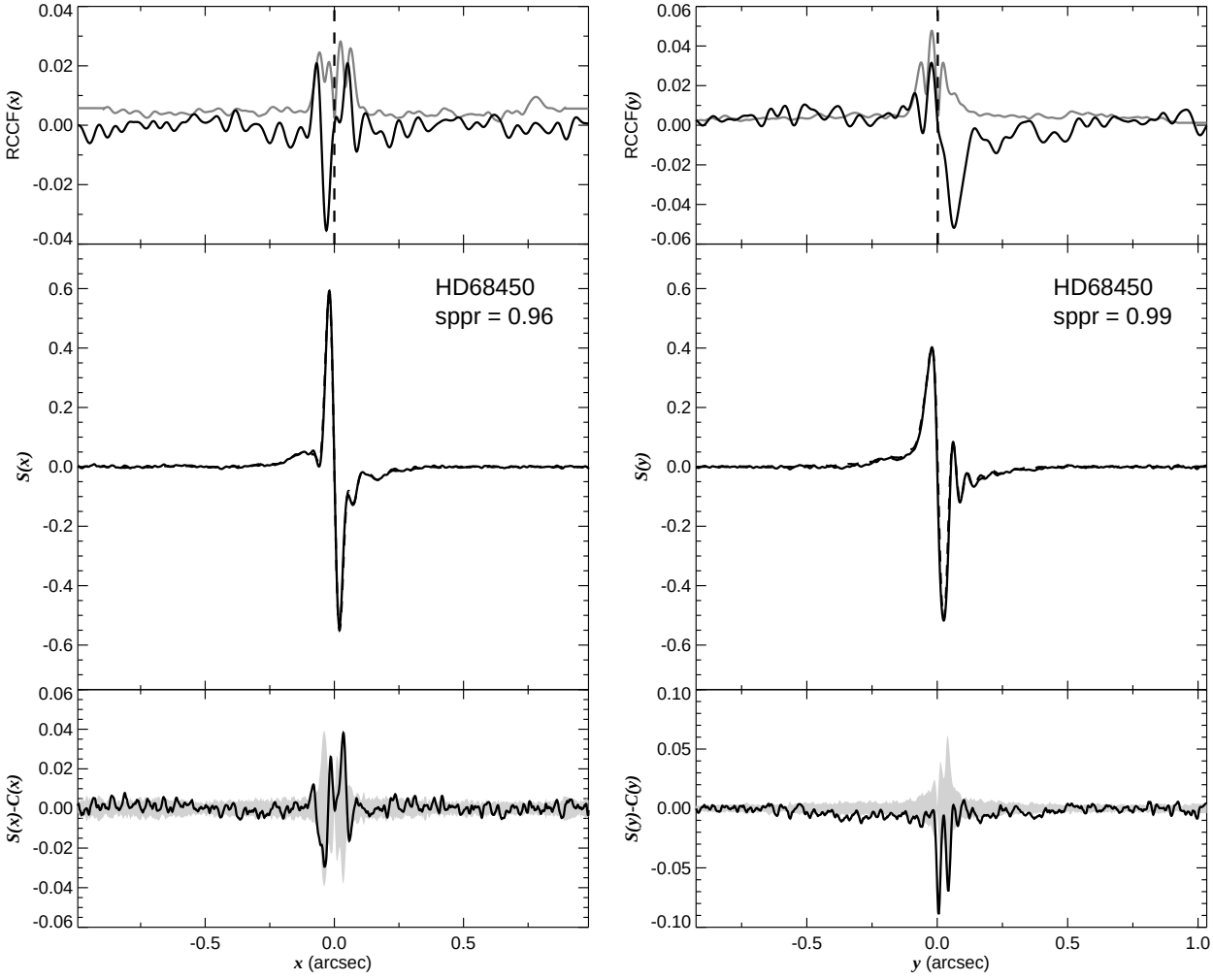

Fig. 1.125.— The FGS scans and binary detection tests for target 081101.68−371732.5 = HD68450 obtained on BY 2008.7721.

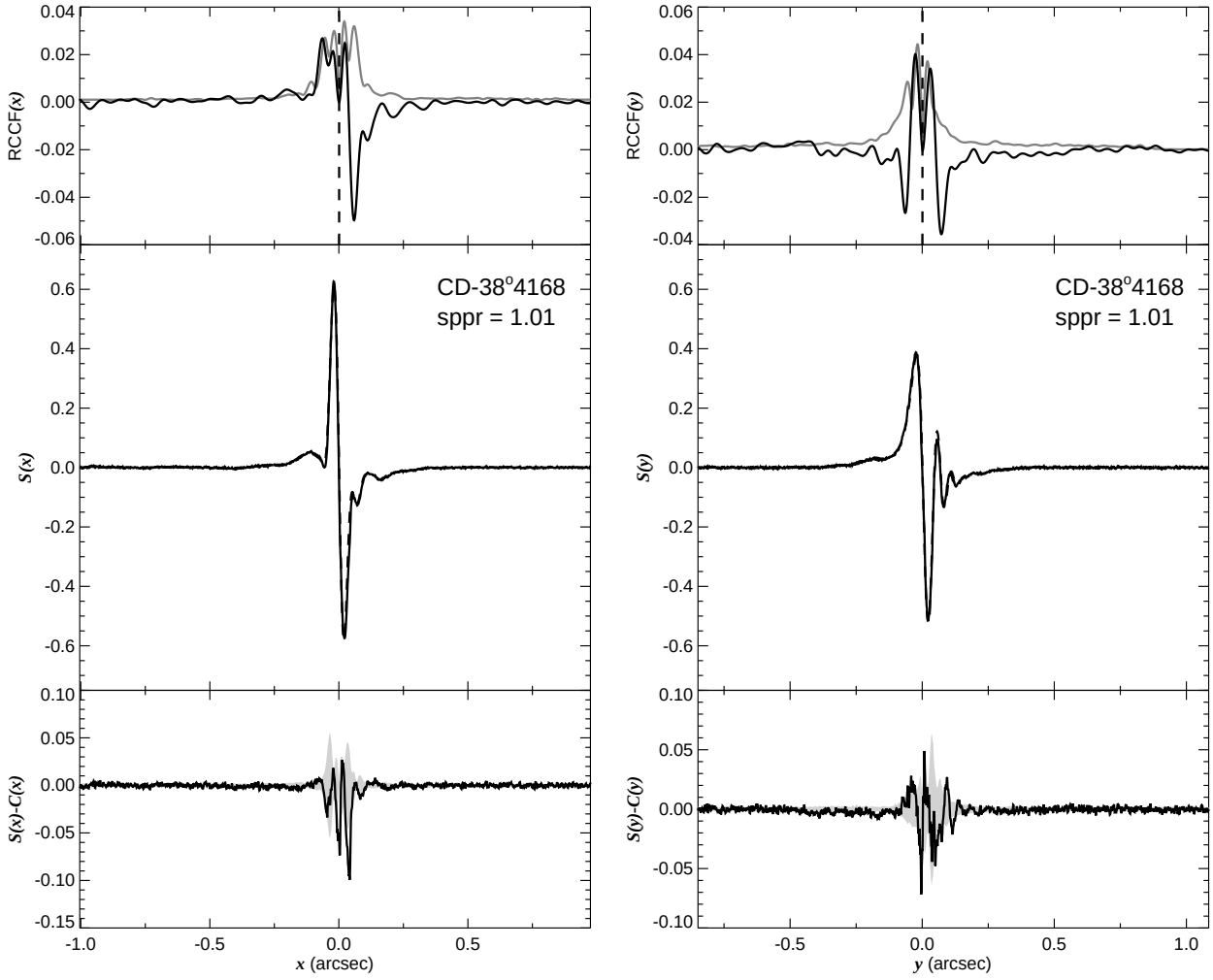

Fig. 1.126.— The FGS scans and binary detection tests for target 081200.73−390841.7 = CD−38 4168 obtained on BY 2008.7747.

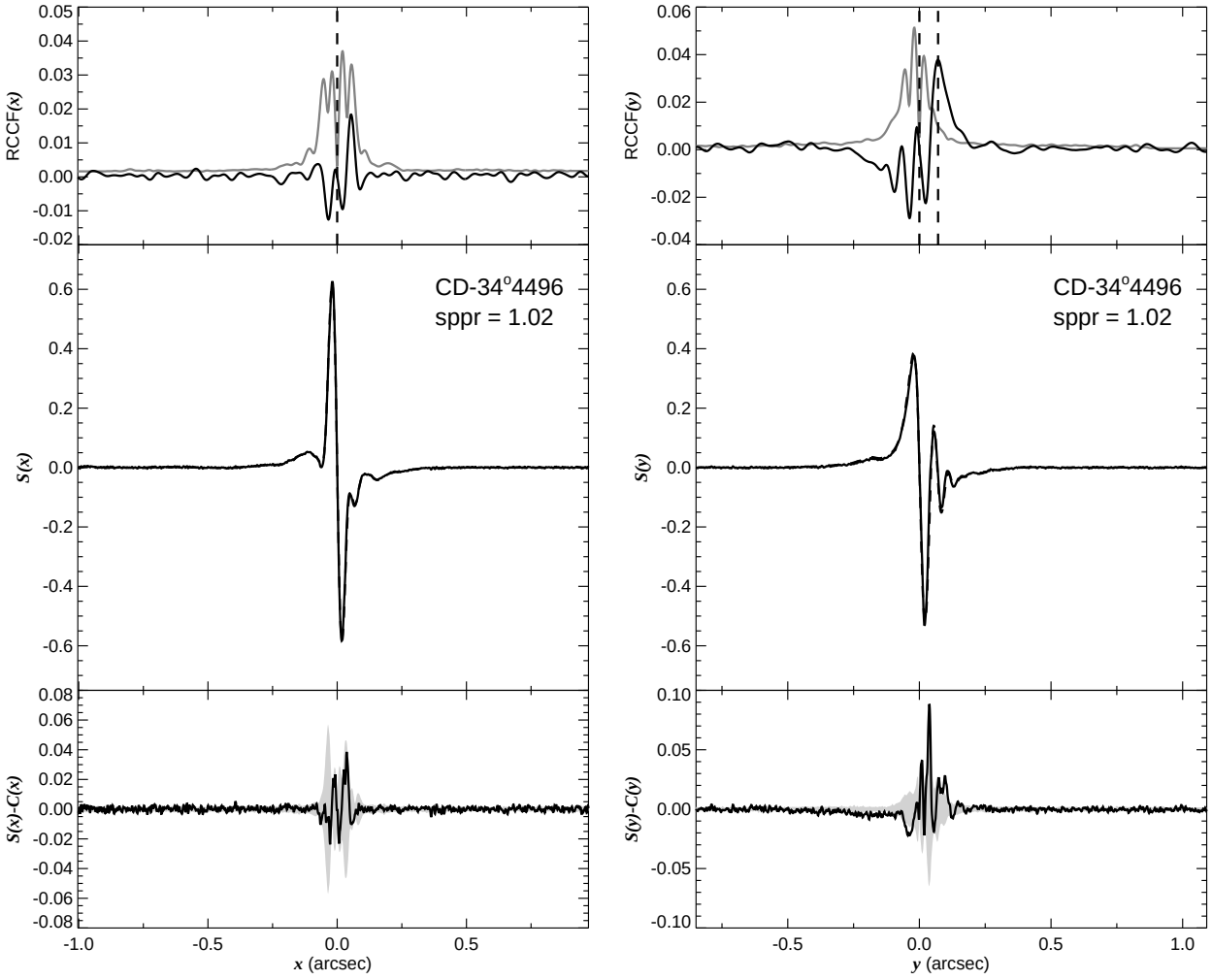

Fig. 1.127.— The FGS scans and binary detection tests for target 081335.36−342843.9 = CD−34 4496 obtained on BY 2008.7701.

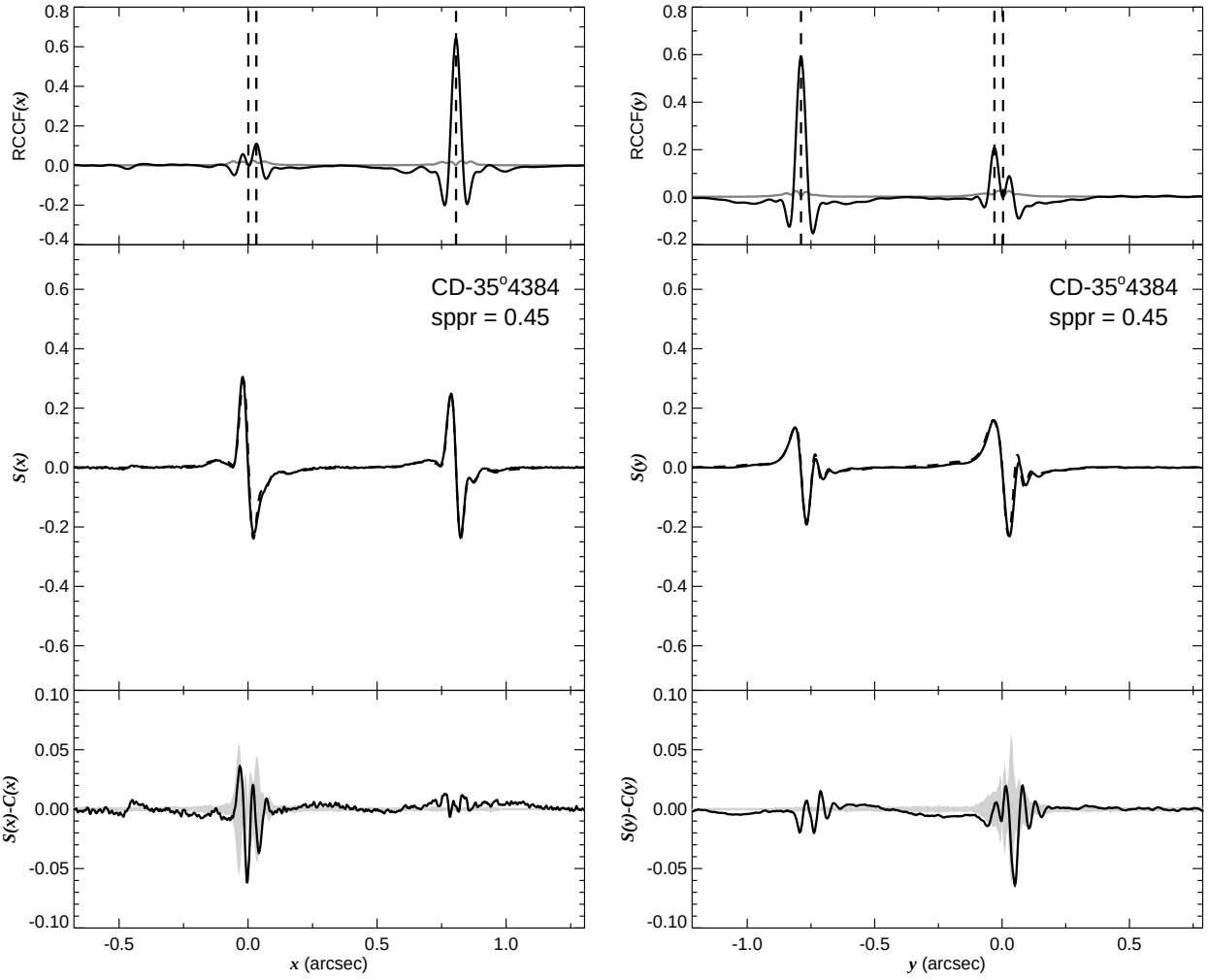

Fig. 1.128.— The FGS scans and binary detection tests for target 081517.15−354414.6 = CD−35 4384 obtained on BY 2008.7703.

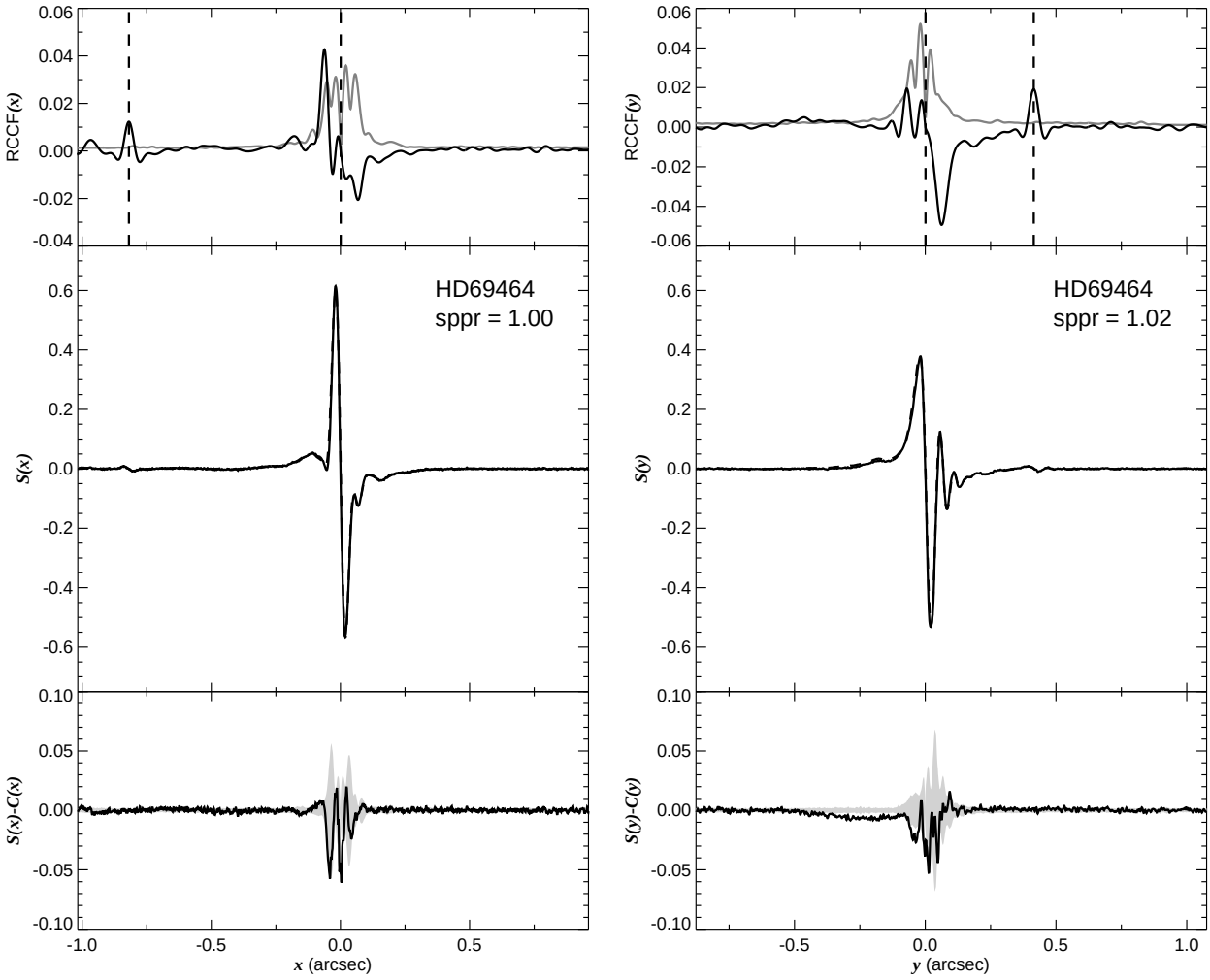

Fig. 1.129.— The FGS scans and binary detection tests for target 081548.57−353752.9 = HD69464 obtained on BY 2008.7694.

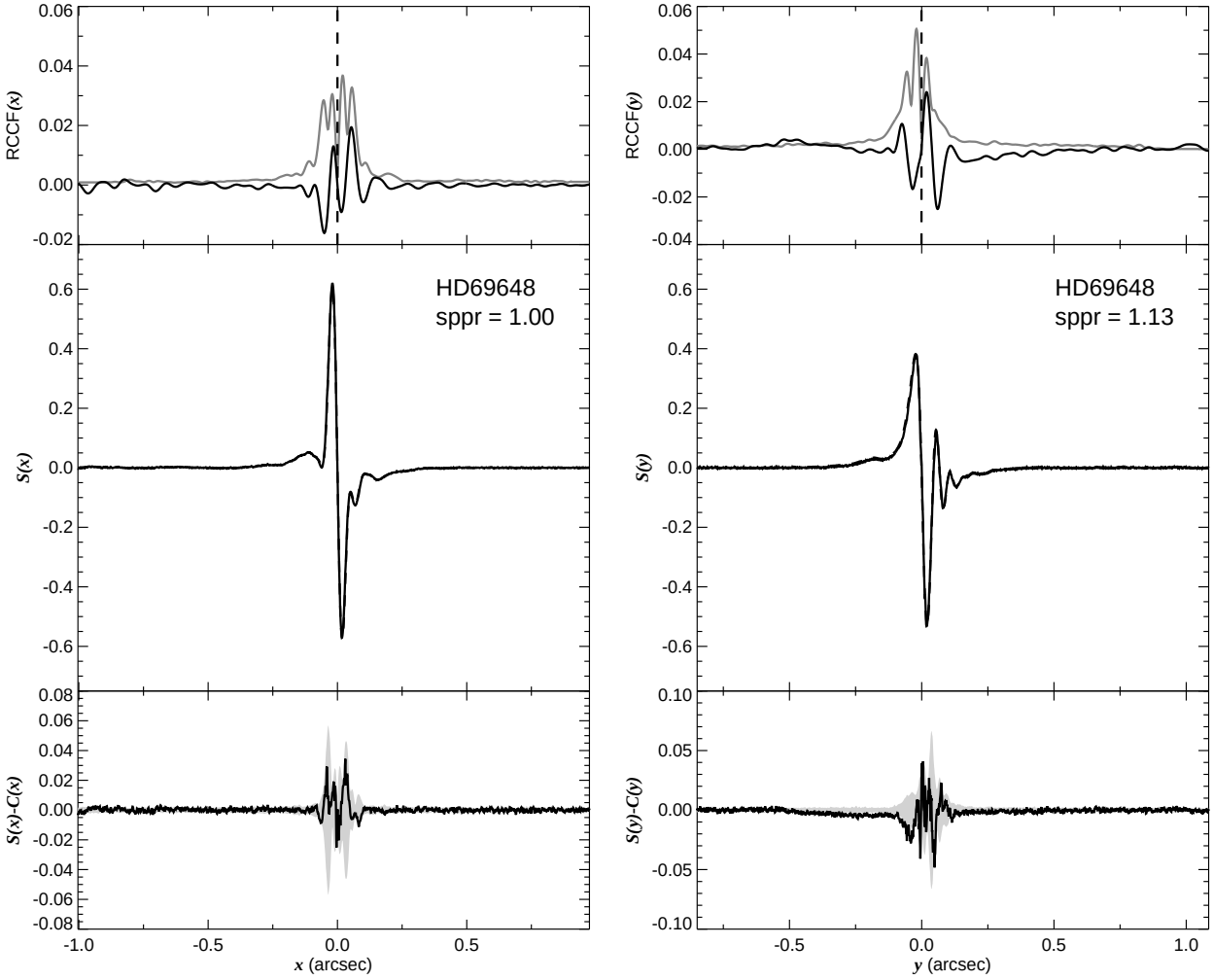

Fig. 1.130.— The FGS scans and binary detection tests for target 081602.74−441921.7 = HD69648 obtained on BY 2008.7752.

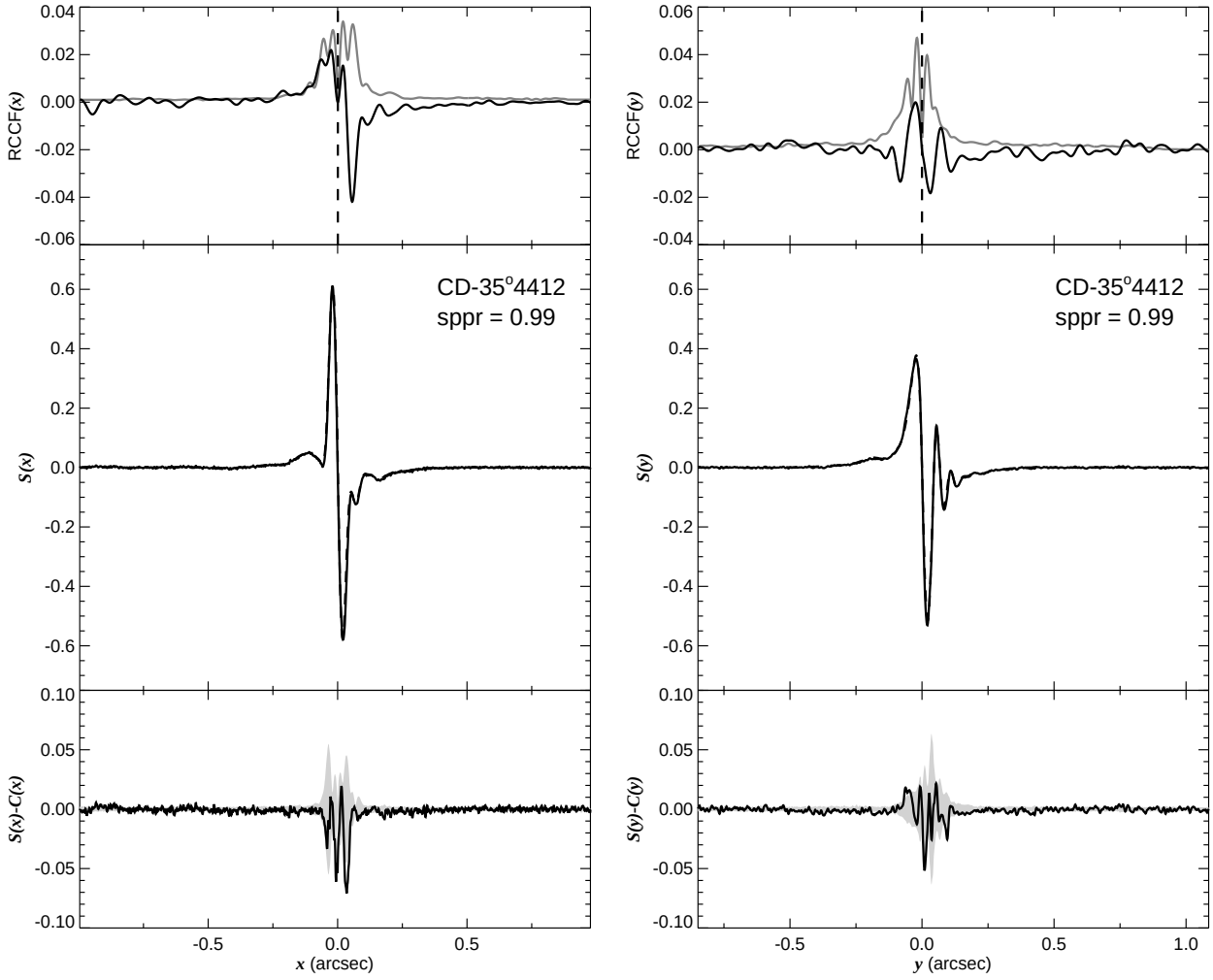

Fig. 1.131.— The FGS scans and binary detection tests for target 081624.75−354421.5 = CD−35 4412 obtained on BY 2008.8106.

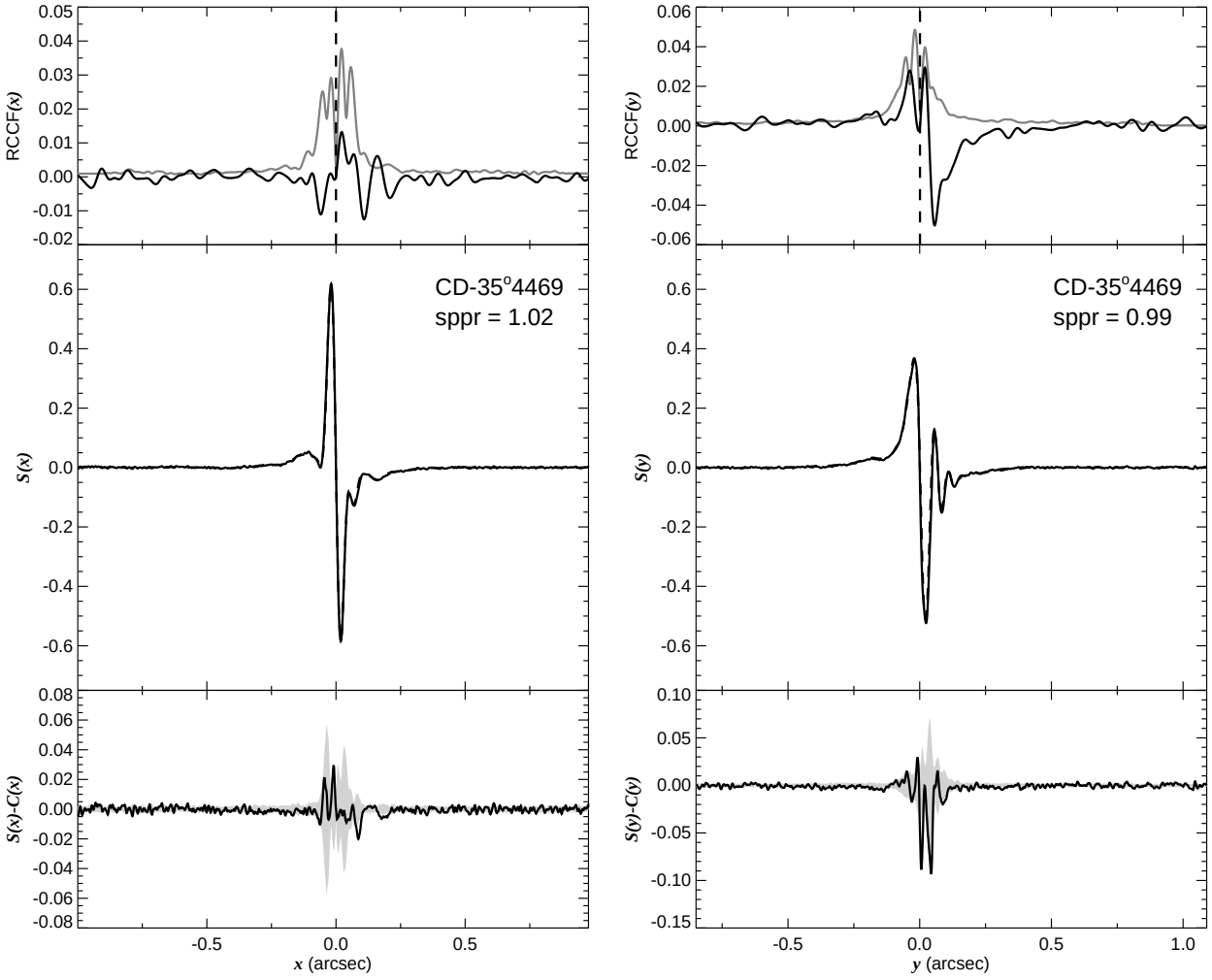

Fig. 1.132.— The FGS scans and binary detection tests for target 081854.46−360752.0 = CD−35 4469 obtained on BY 2008.8075.

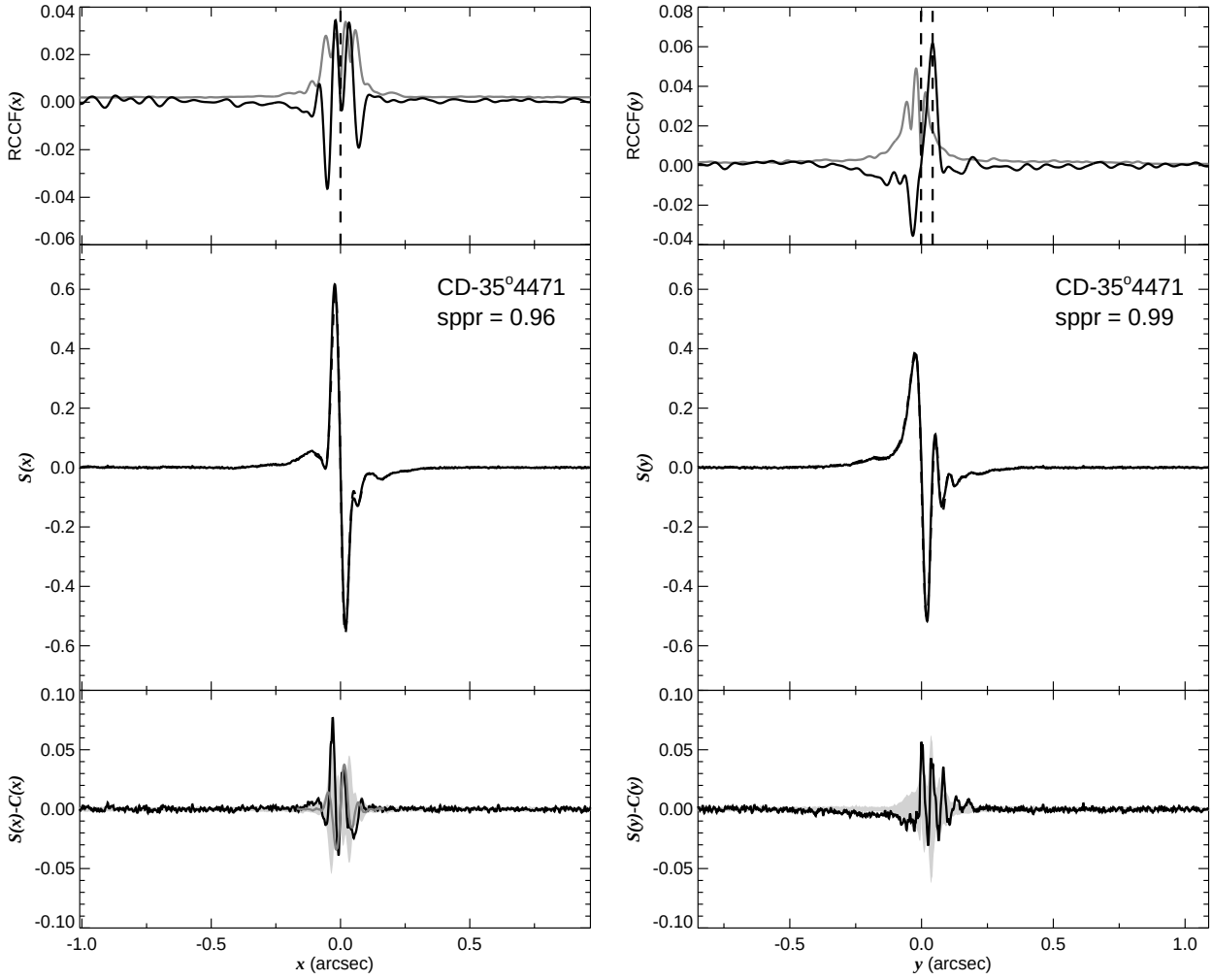

Fig. 1.133.— The FGS scans and binary detection tests for target 081903.90−360844.9 = CD−35 4471 obtained on BY 2008.7697.

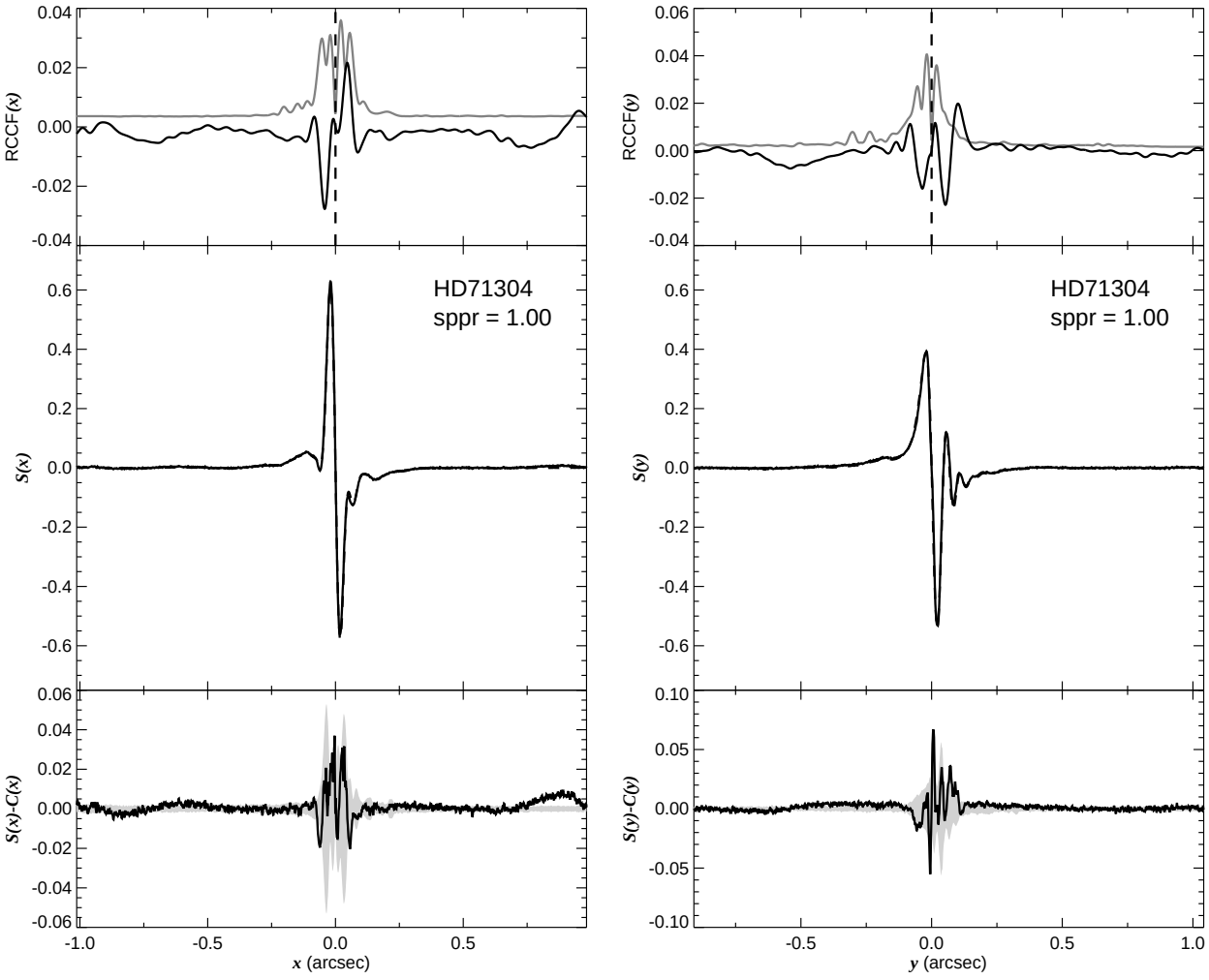

Fig. 1.134.— The FGS scans and binary detection tests for target 082455.79−441803.0 = HD71304 obtained on BY 2008.7749.

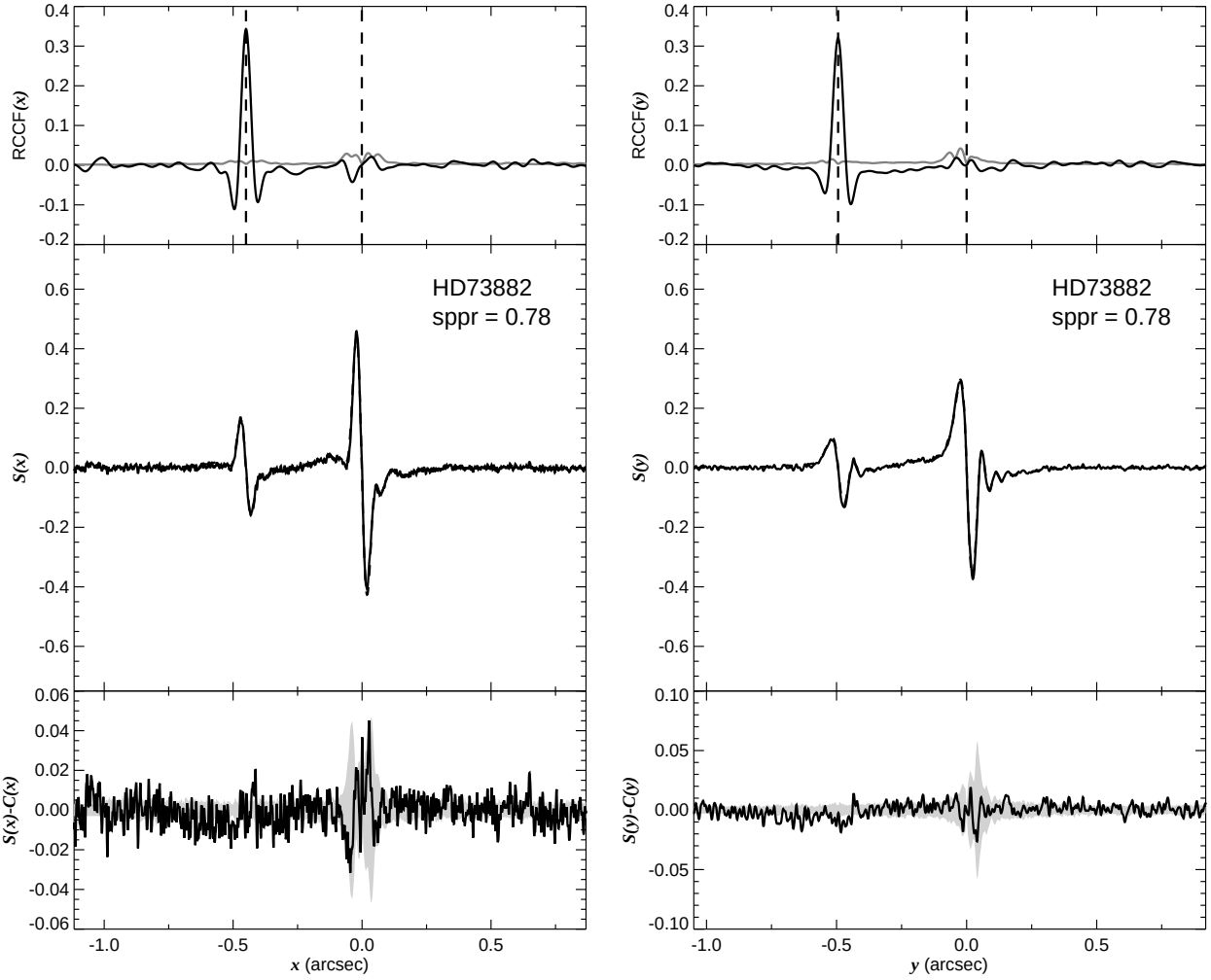

Fig. 1.135.— The FGS scans and binary detection tests for target 083909.53−402509.3 = HD73882 obtained on BY 2008.4061.

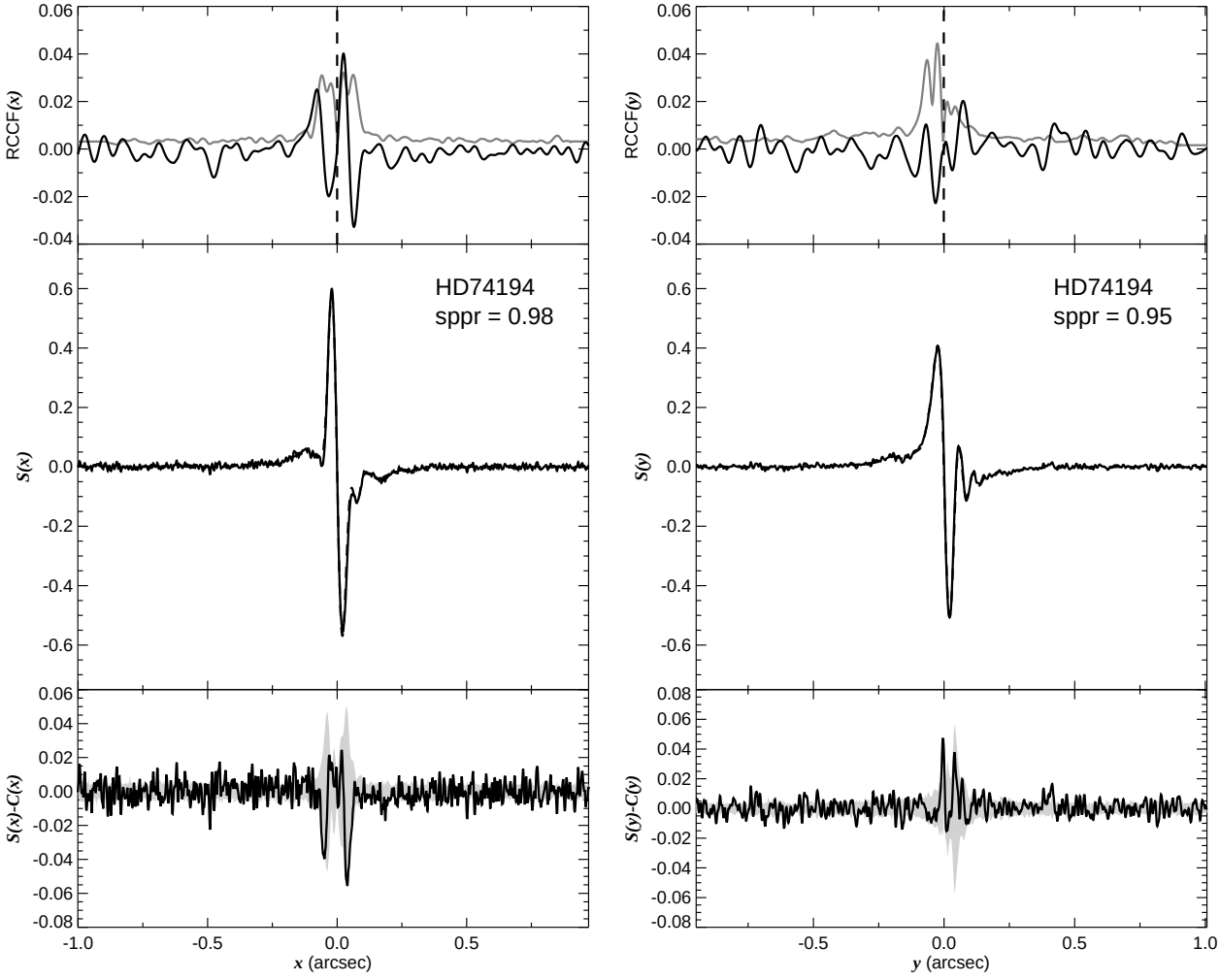

Fig. 1.136.— The FGS scans and binary detection tests for target 084047.79−450330.2 = HD74194 obtained on BY 2008.7727.

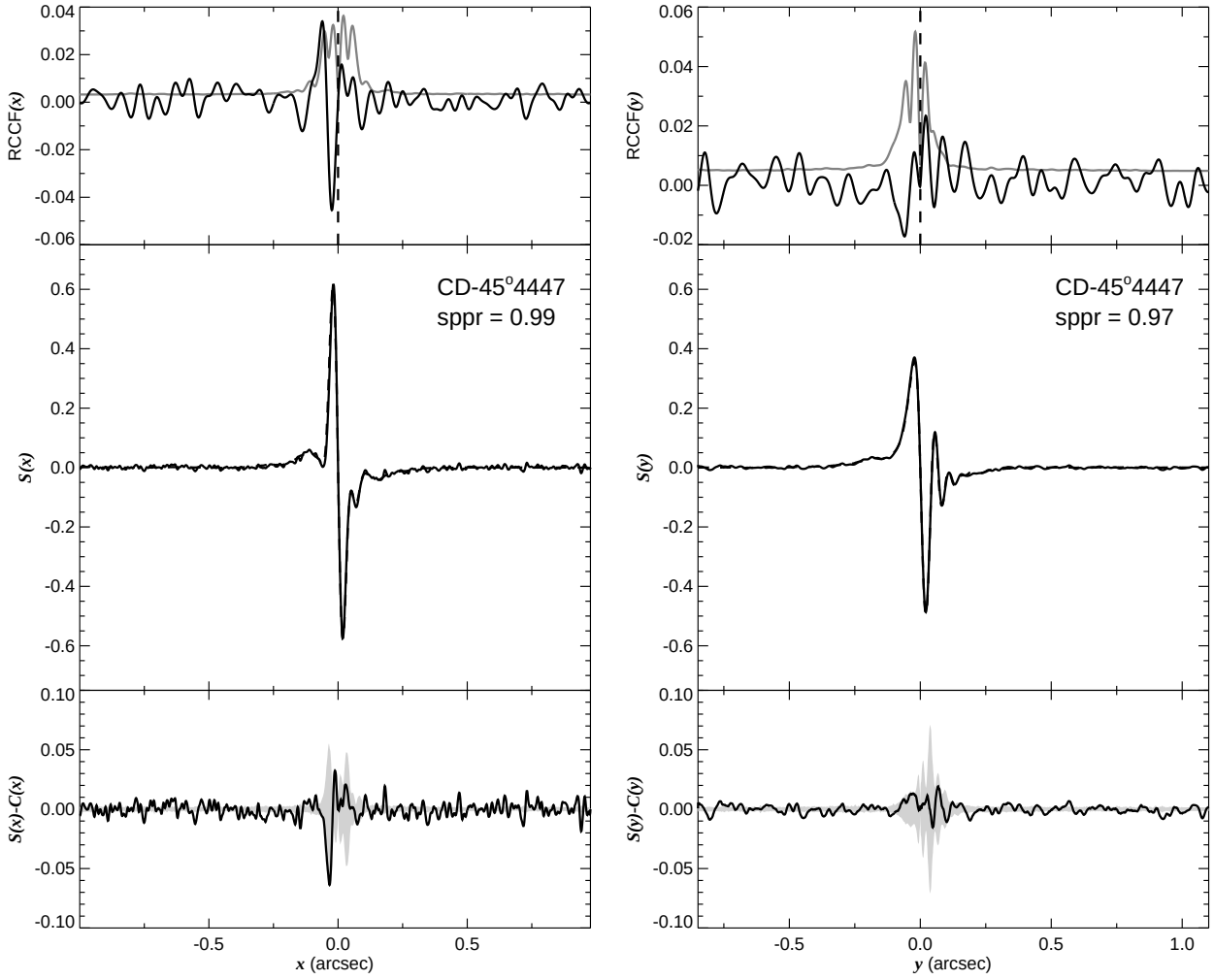

Fig. 1.137.— The FGS scans and binary detection tests for target 084324.16−460828.7 = CD−45 4447 obtained on BY 2008.8131.

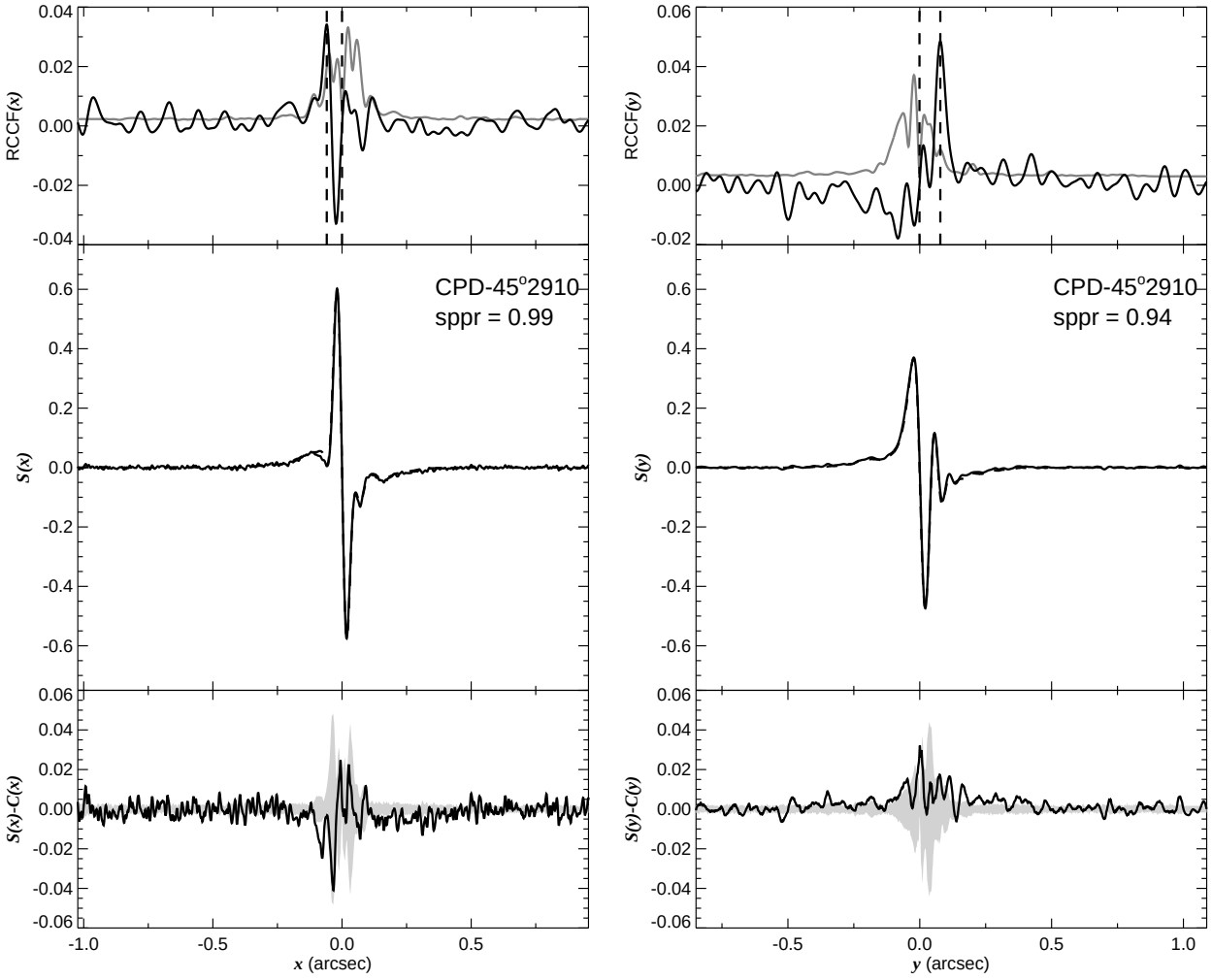

Fig. 1.138.— The FGS scans and binary detection tests for target 084338.66−460815.9 = CPD−45 2910 obtained on BY 2008.8124.

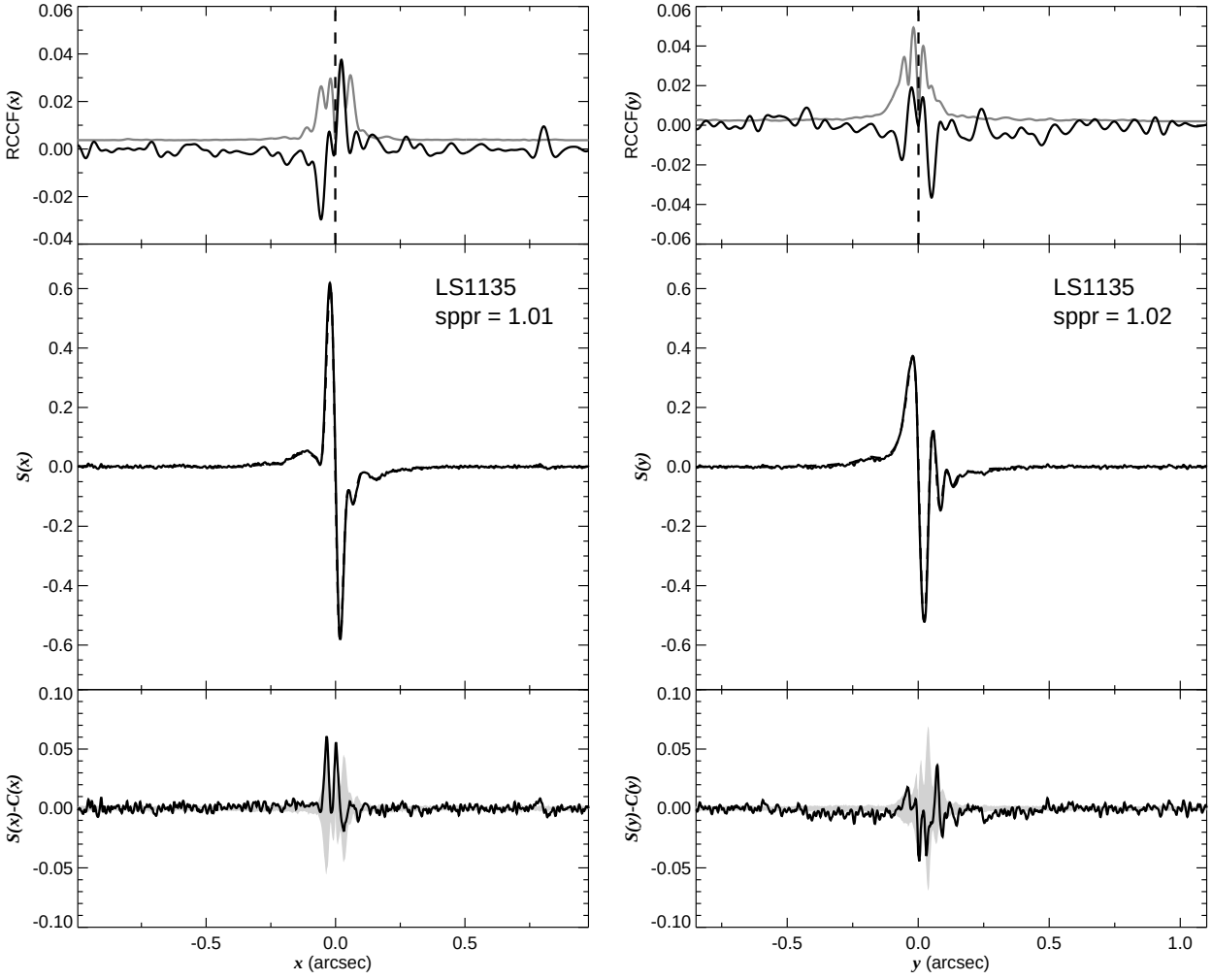

Fig. 1.139.— The FGS scans and binary detection tests for target 084349.80−460708.8 = ALS1135 obtained on BY 2008.8150.

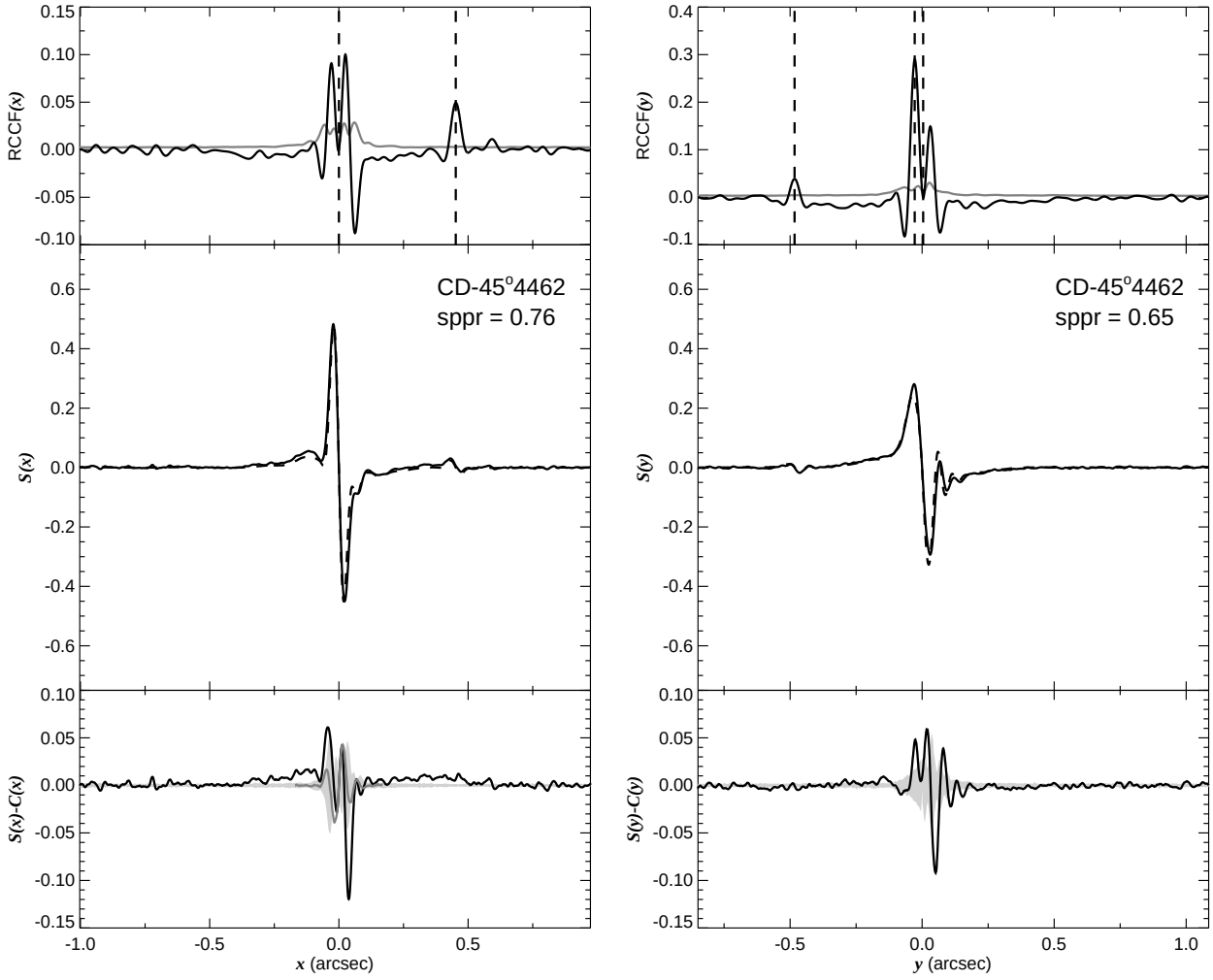

Fig. 1.140.— The FGS scans and binary detection tests for target 084351.09−460346.5 = CD−45 4462 obtained on BY 2008.8128.

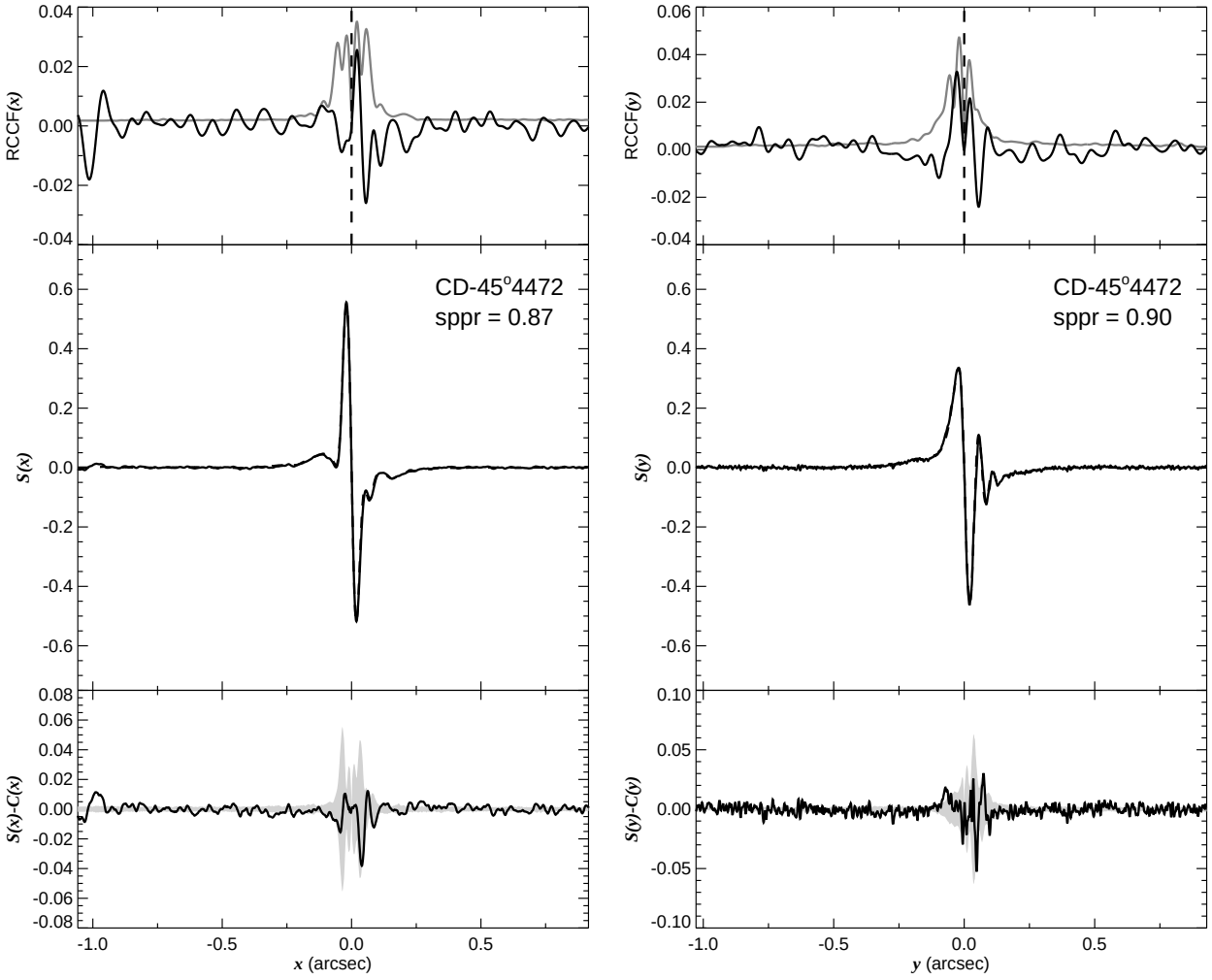

Fig. 1.141.— The FGS scans and binary detection tests for target 084425.05−455334.7 = CD−45 4472 obtained on BY 2008.8126.

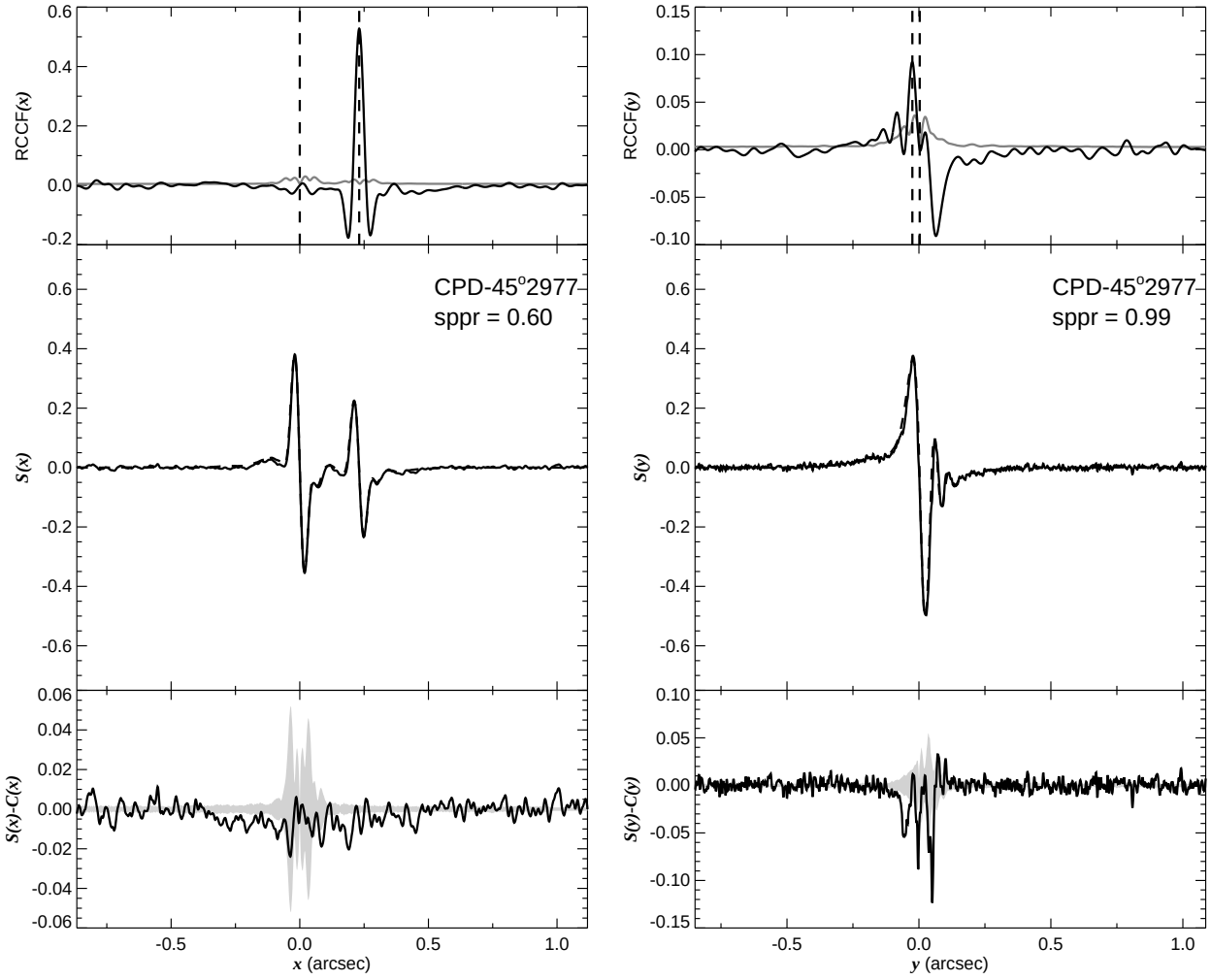

Fig. 1.142.— The FGS scans and binary detection tests for target 084510.46−455854.7 = CPD−45 2977 obtained on BY 2008.8130.

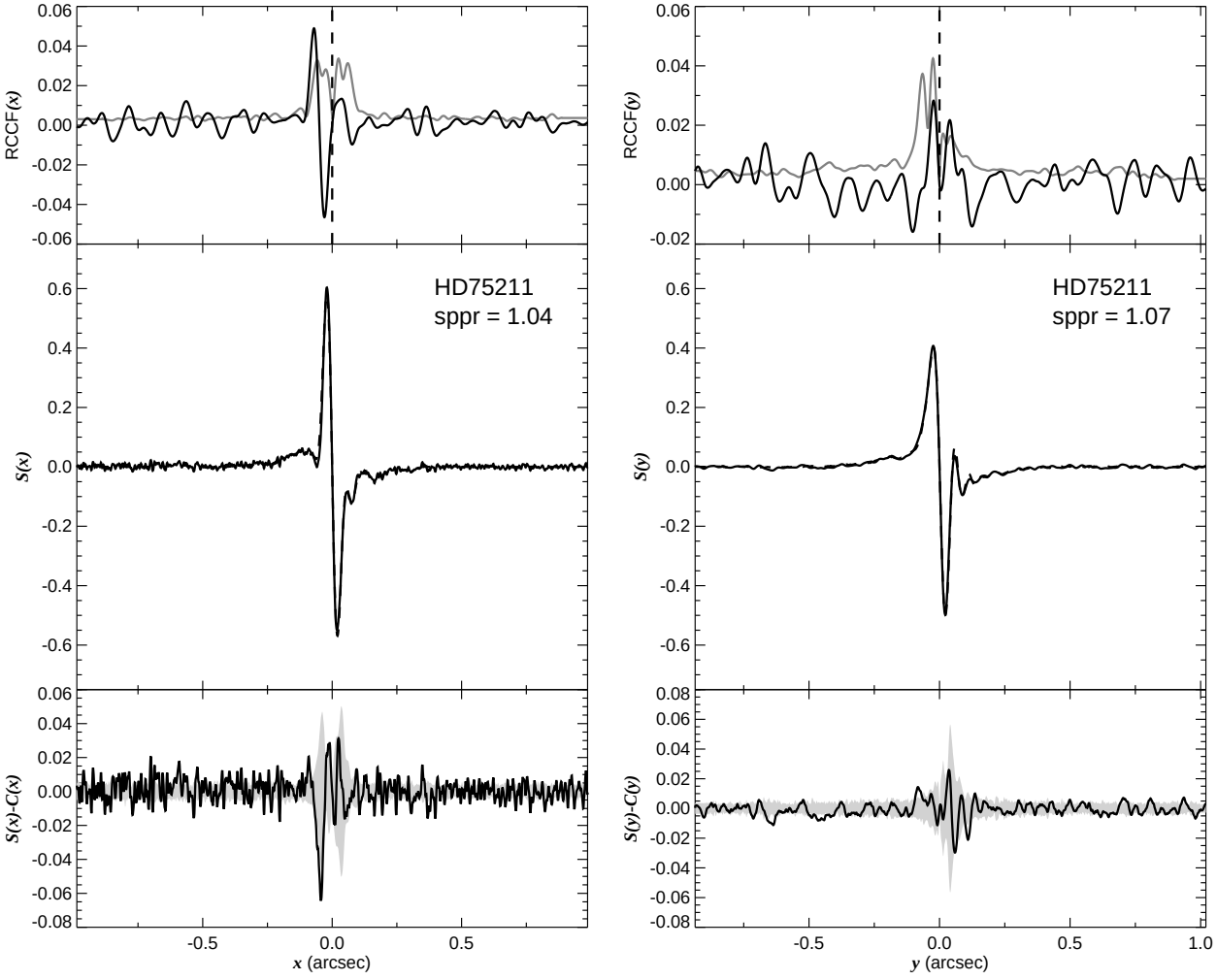

Fig. 1.143.— The FGS scans and binary detection tests for target 084701.59−440428.8 = HD75211 obtained on BY 2008.7774.

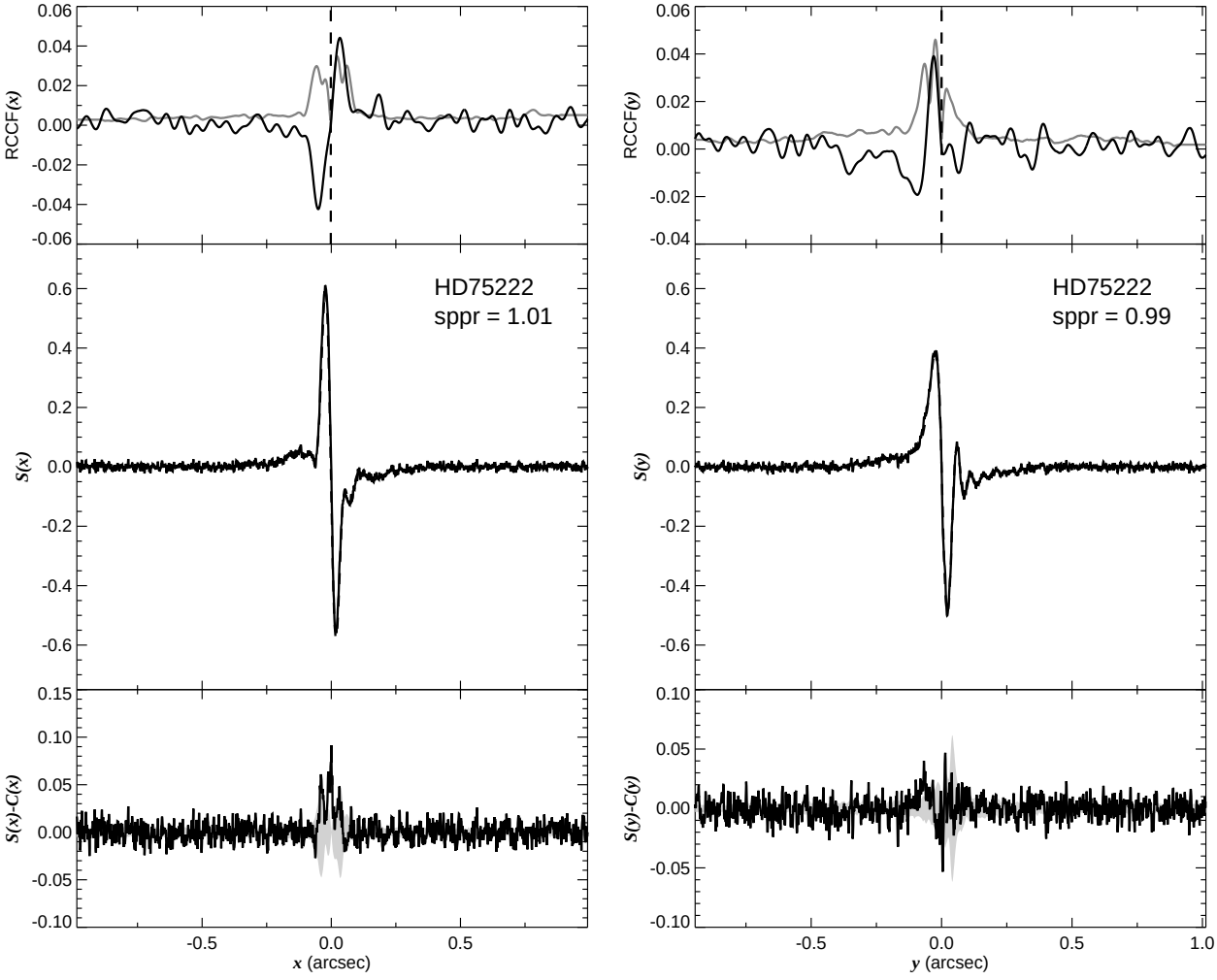

Fig. 1.144.— The FGS scans and binary detection tests for target 084725.14−364502.7 = HD75222 obtained on BY 2008.4089.

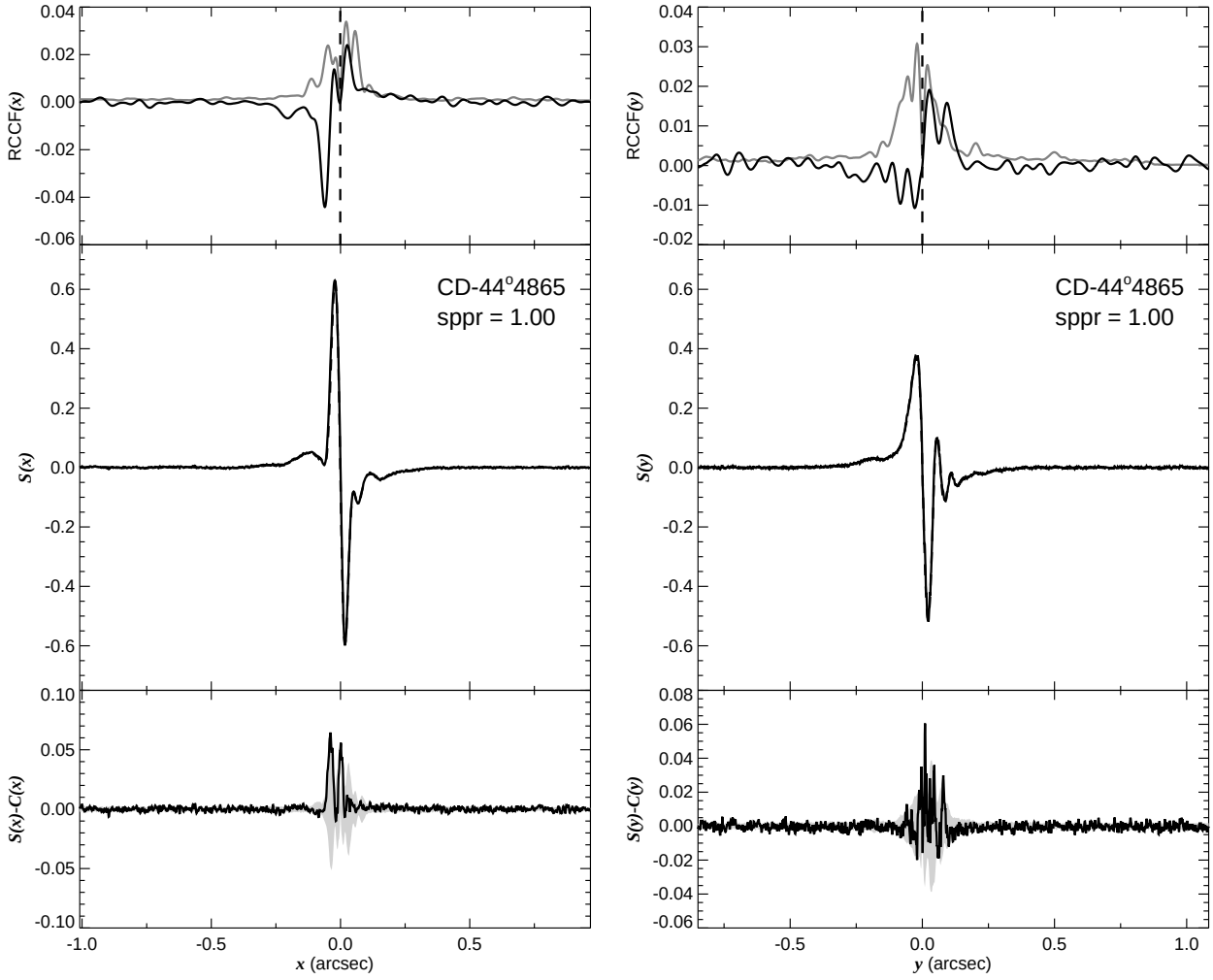

Fig. 1.145.— The FGS scans and binary detection tests for target 085002.28−443439.9 = CD−44 4865 obtained on BY 2008.7667.

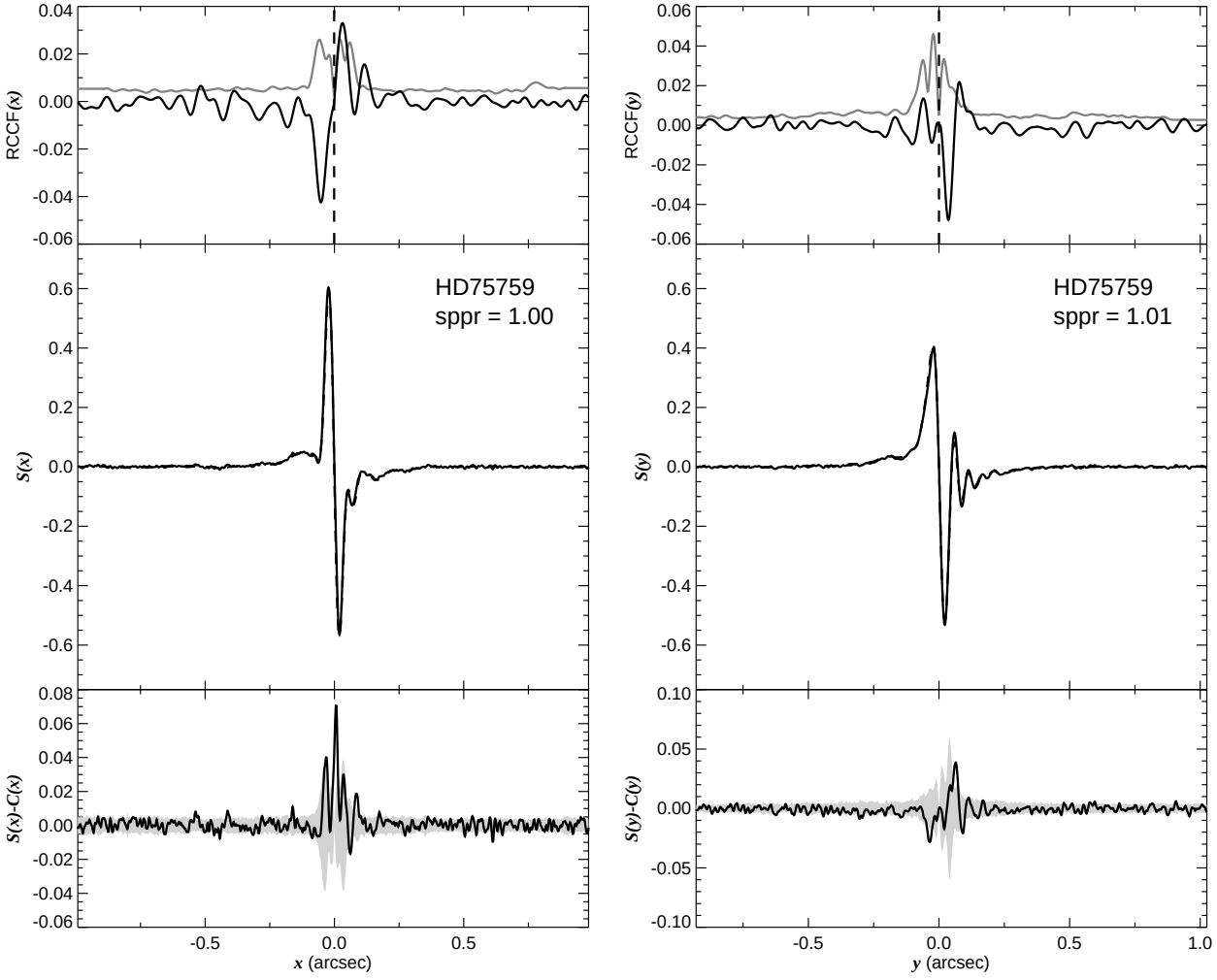

Fig. 1.146.— The FGS scans and binary detection tests for target 085021.02−420523.2 = HD75759 obtained on BY 2008.4198.

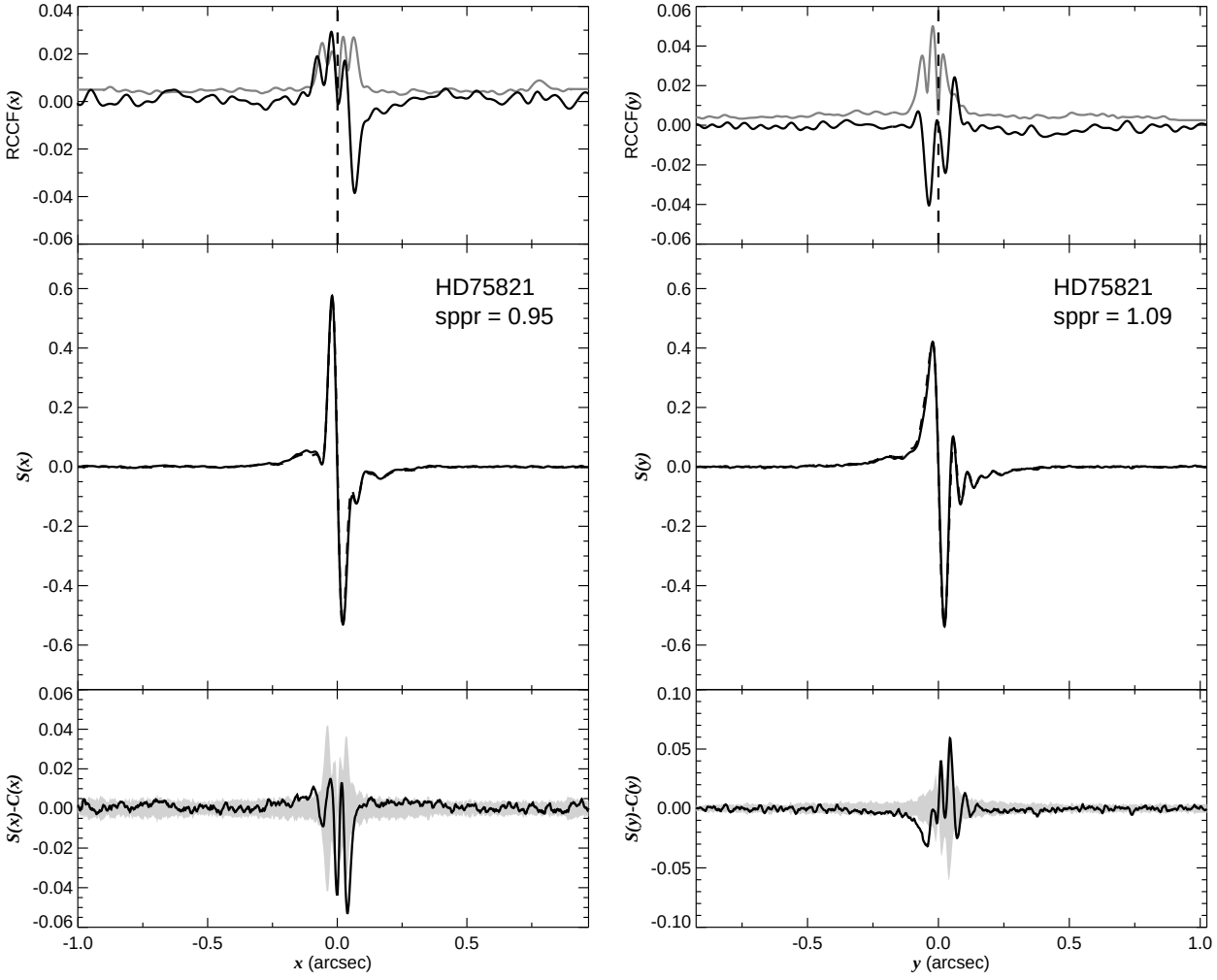

Fig. 1.147.— The FGS scans and binary detection tests for target 085033.46−463145.1 = HD75821 obtained on BY 2008.7776.

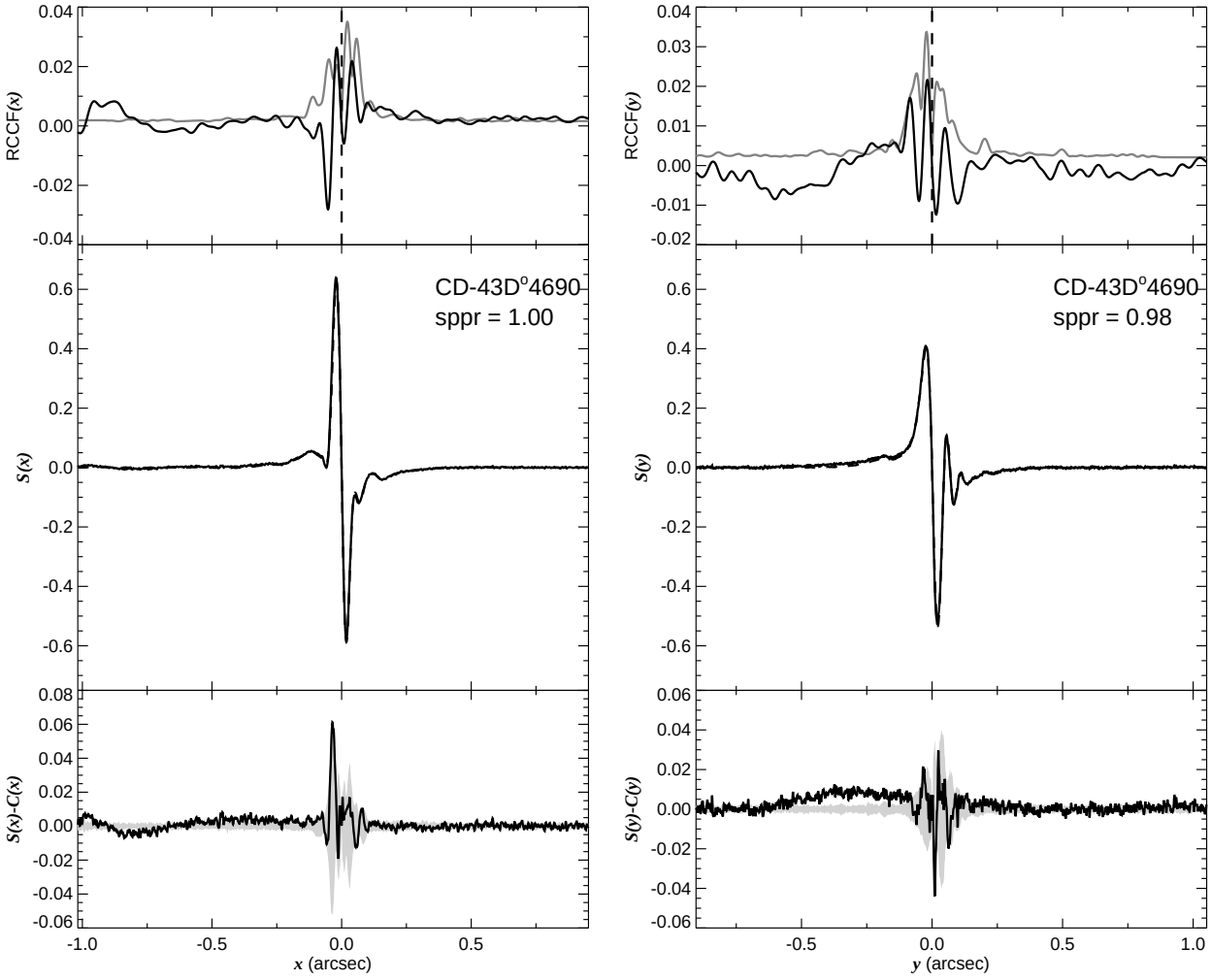

Fig. 1.148.— The FGS scans and binary detection tests for target 085052.05−435022.9 = CD−43 4690 obtained on BY 2008.7719.

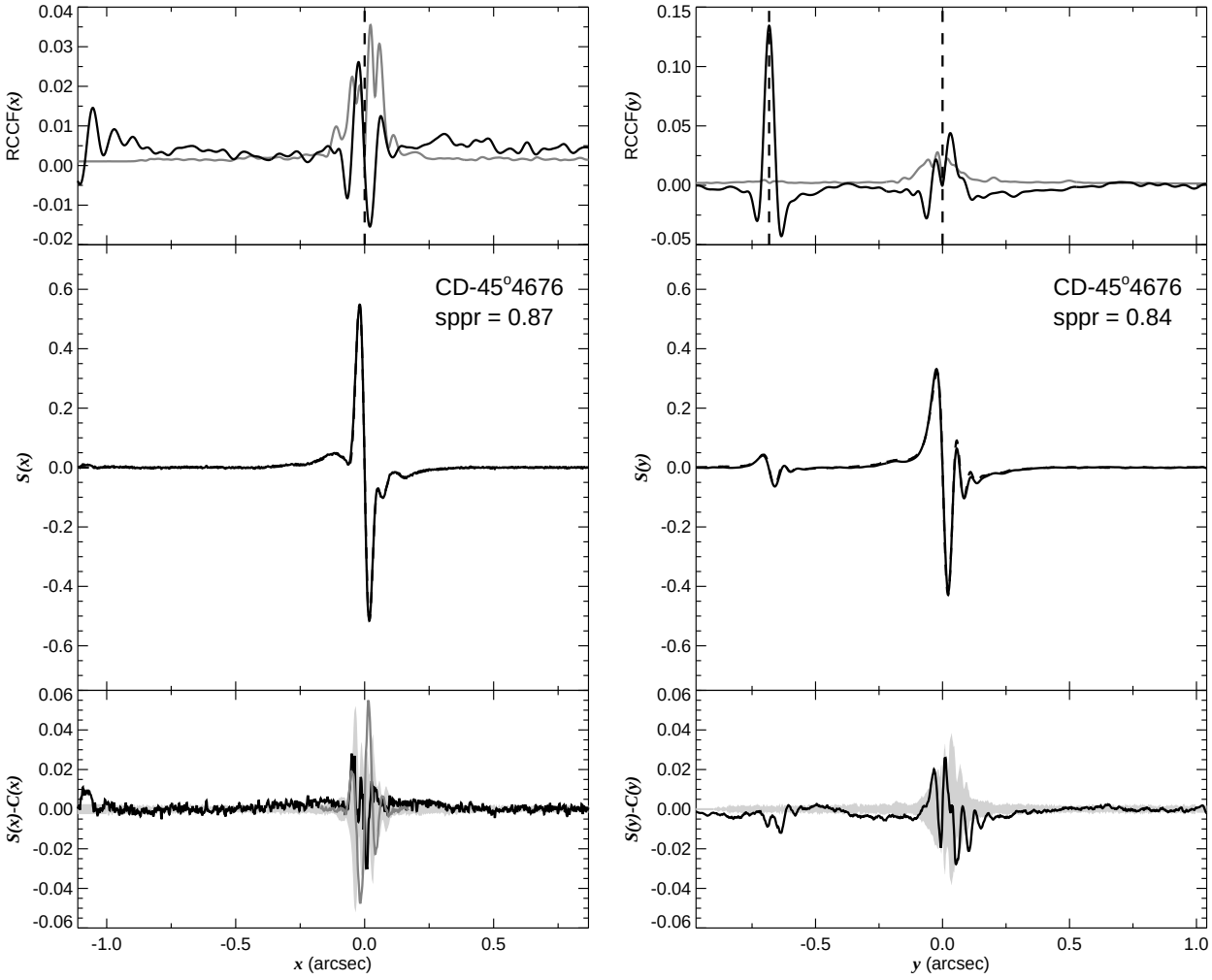

Fig. 1.149.— The FGS scans and binary detection tests for target 085322.01−460208.8 = CD−45 4676 obtained on BY 2008.7661.

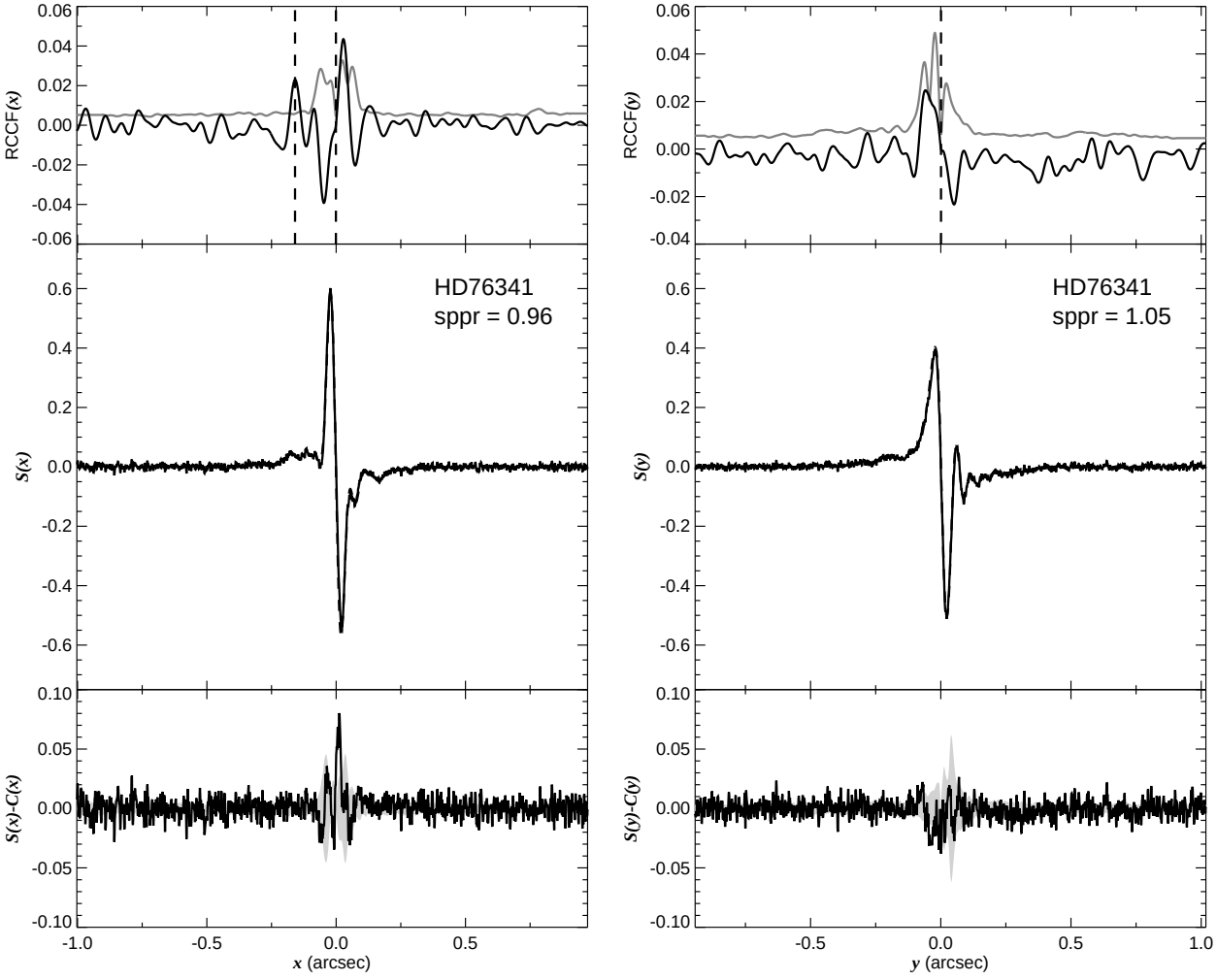

Fig. 1.150.— The FGS scans and binary detection tests for target 085400.61−422908.8 = HD76341 obtained on BY 2008.7674.

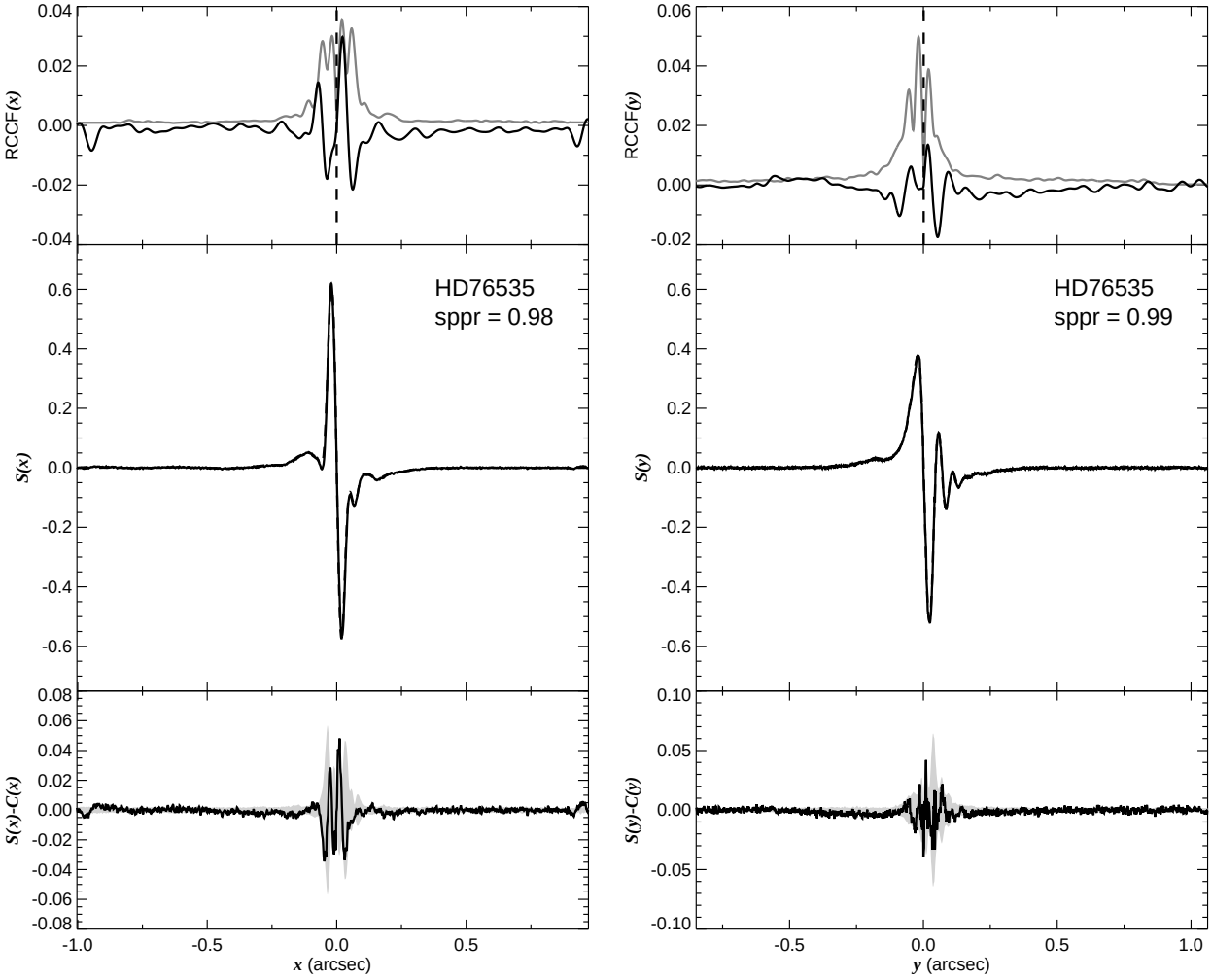

Fig. 1.151.— The FGS scans and binary detection tests for target 085500.45−472457.5 = HD76535 obtained on BY 2008.7723.

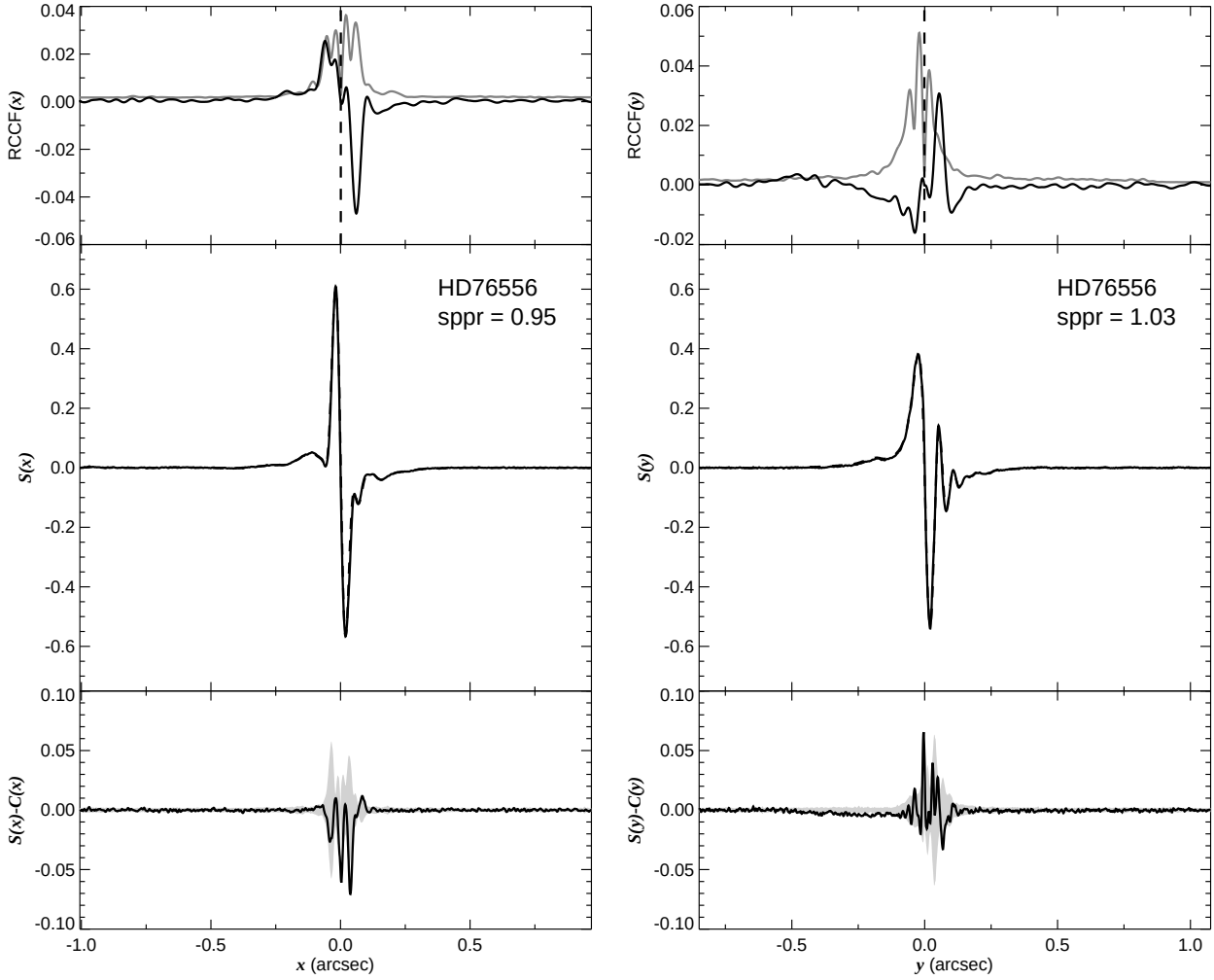

Fig. 1.152.— The FGS scans and binary detection tests for target 085507.15−473627.2 = HD76556 obtained on BY 2008.7696.

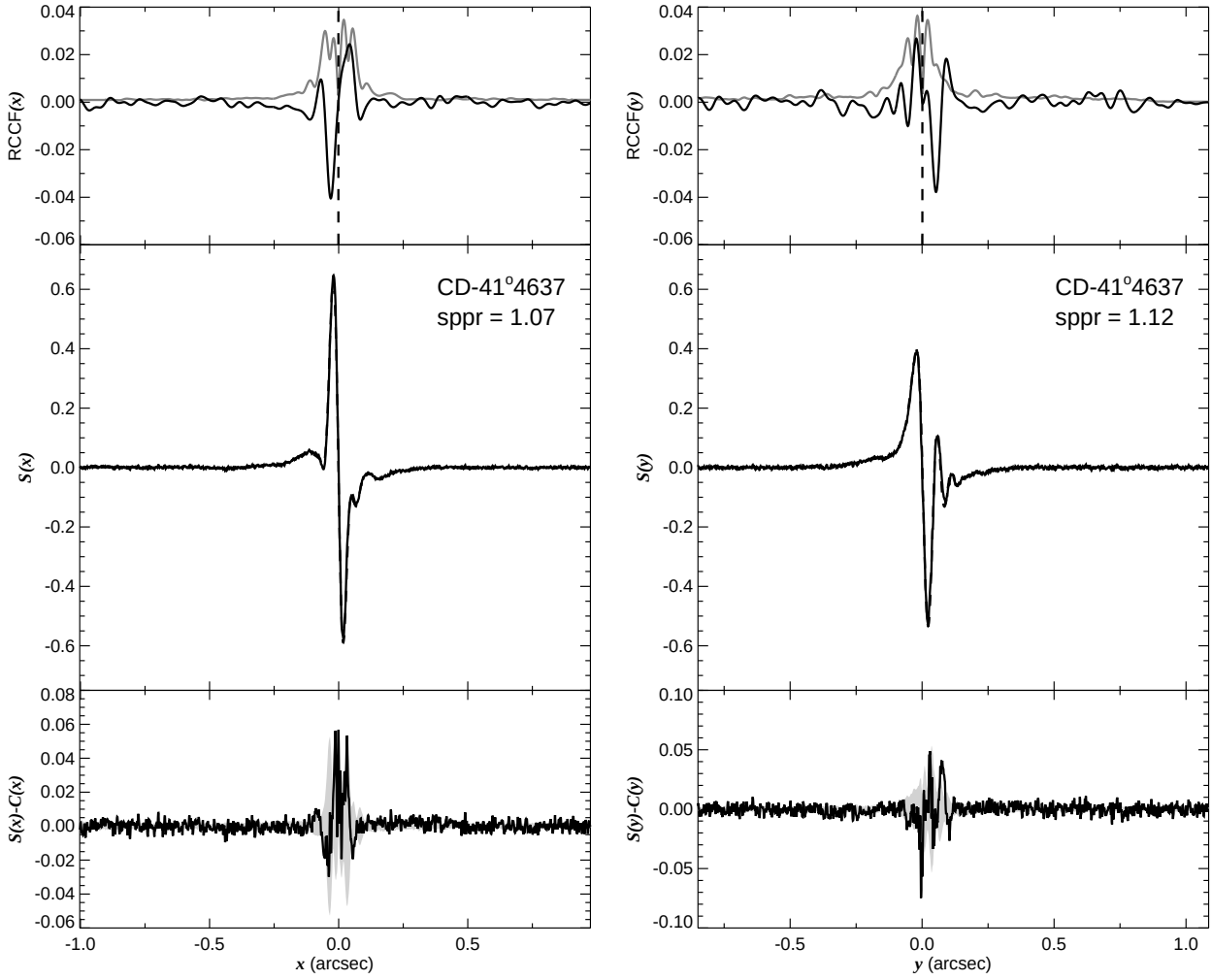

Fig. 1.153.— The FGS scans and binary detection tests for target 085527.66−413522.3 = CD−41 4637 obtained on BY 2008.8161.

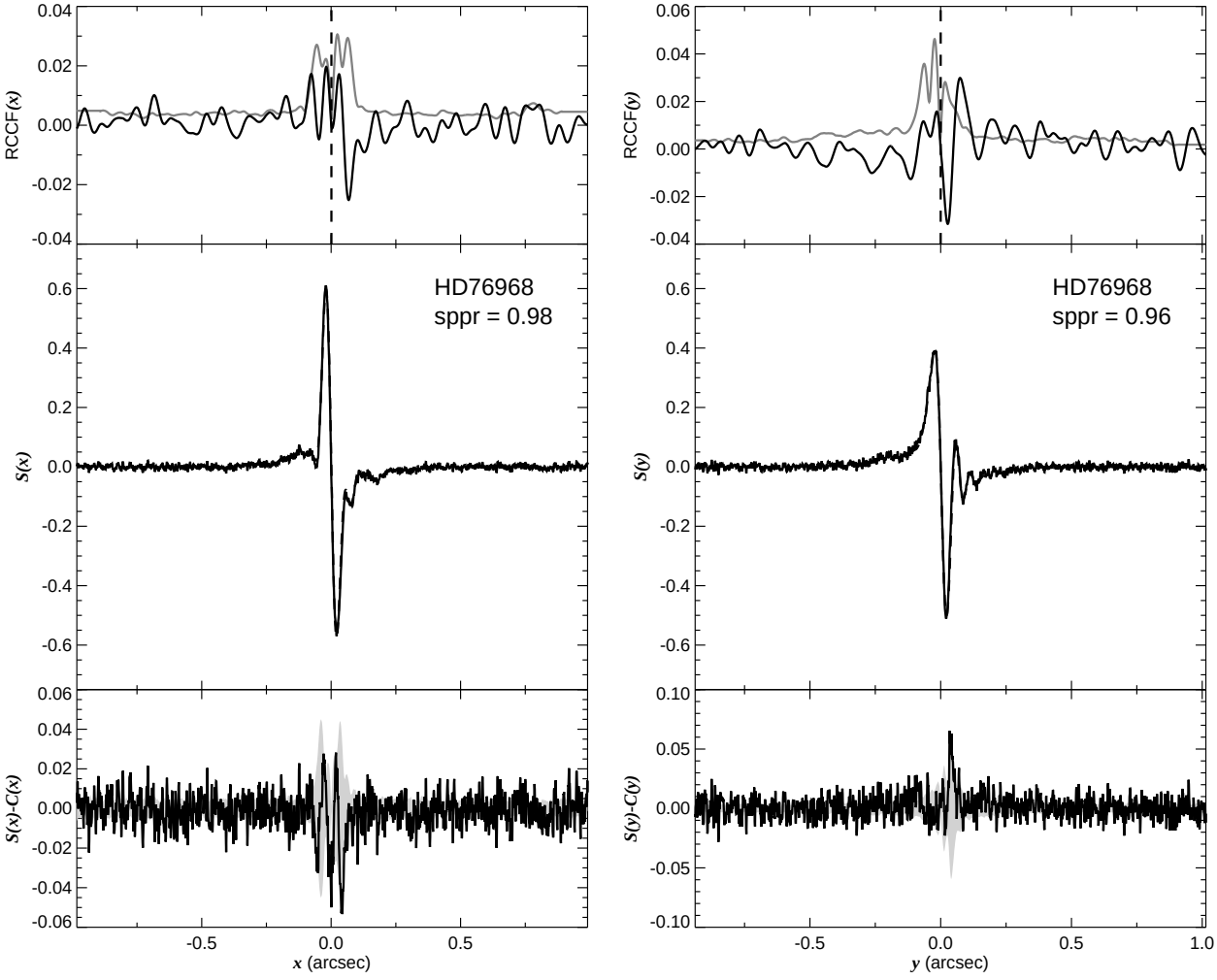

Fig. 1.154.— The FGS scans and binary detection tests for target 085728.85−504458.2 = HD76968 obtained on BY 2008.5593.

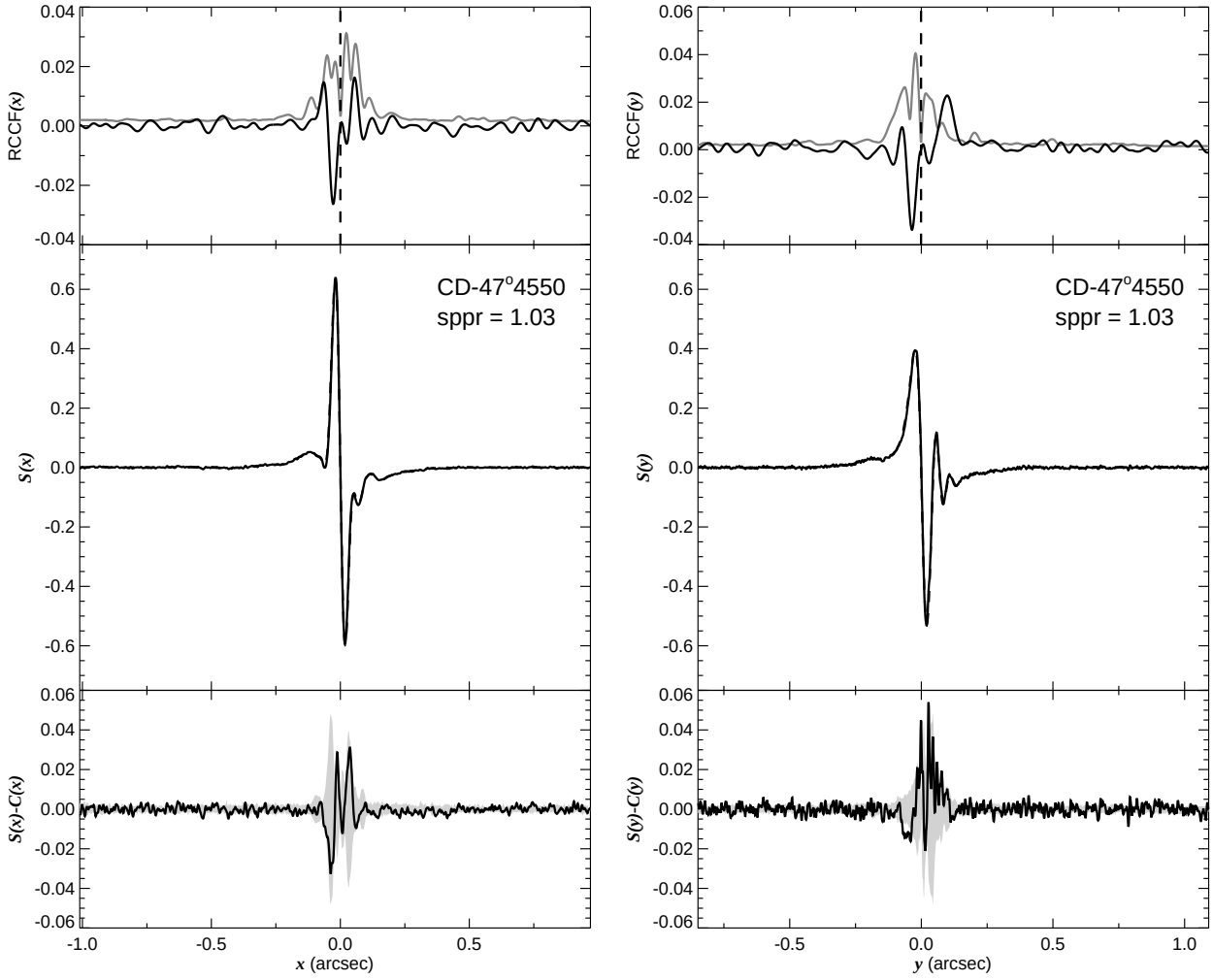

Fig. 1.155.— The FGS scans and binary detection tests for target 085751.66−474544.0 = CD−47 4550 obtained on BY 2008.8350.

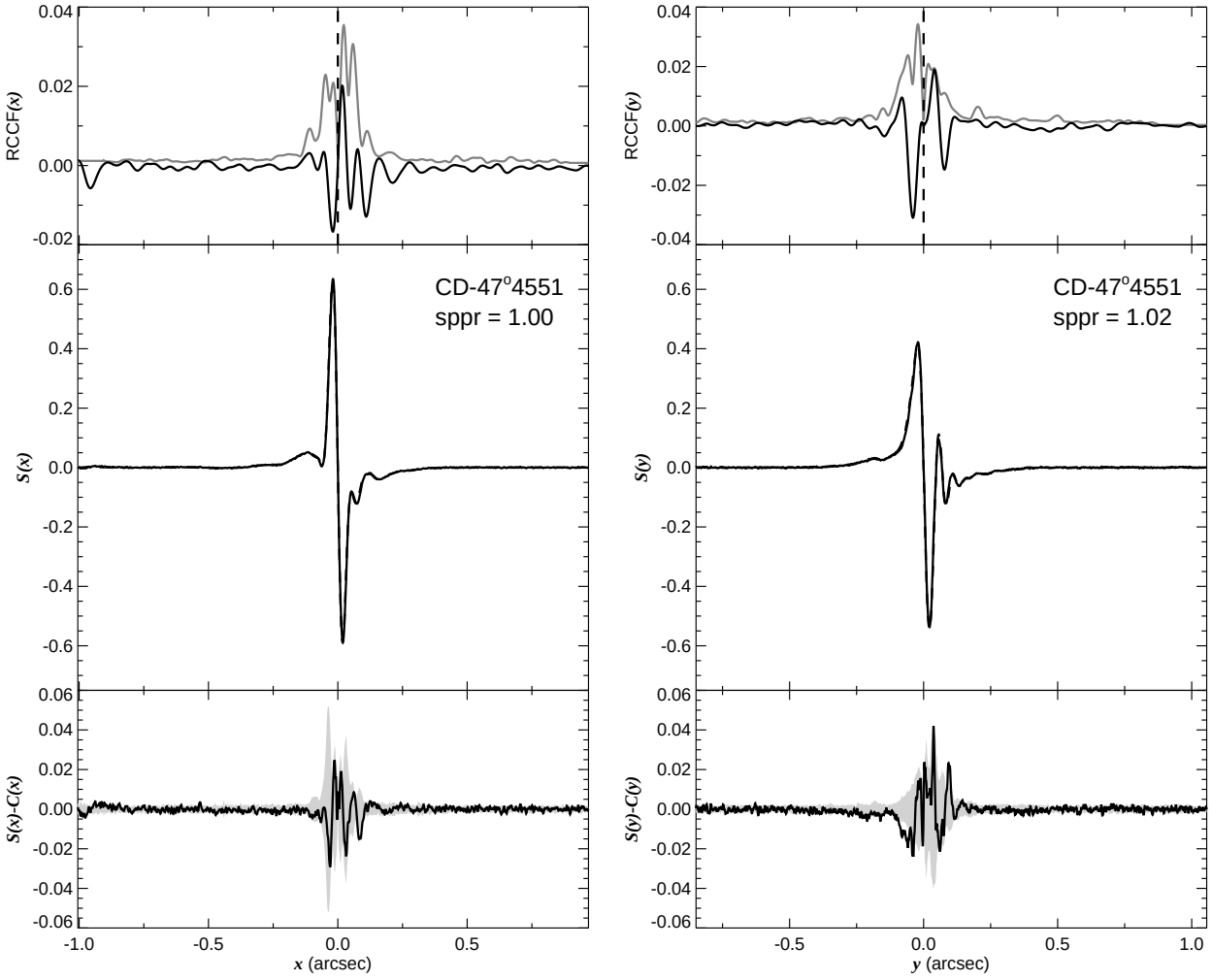

Fig. 1.156.— The FGS scans and binary detection tests for target 085754.62−474415.7 = CD−47 4551 obtained on BY 2007.4993.

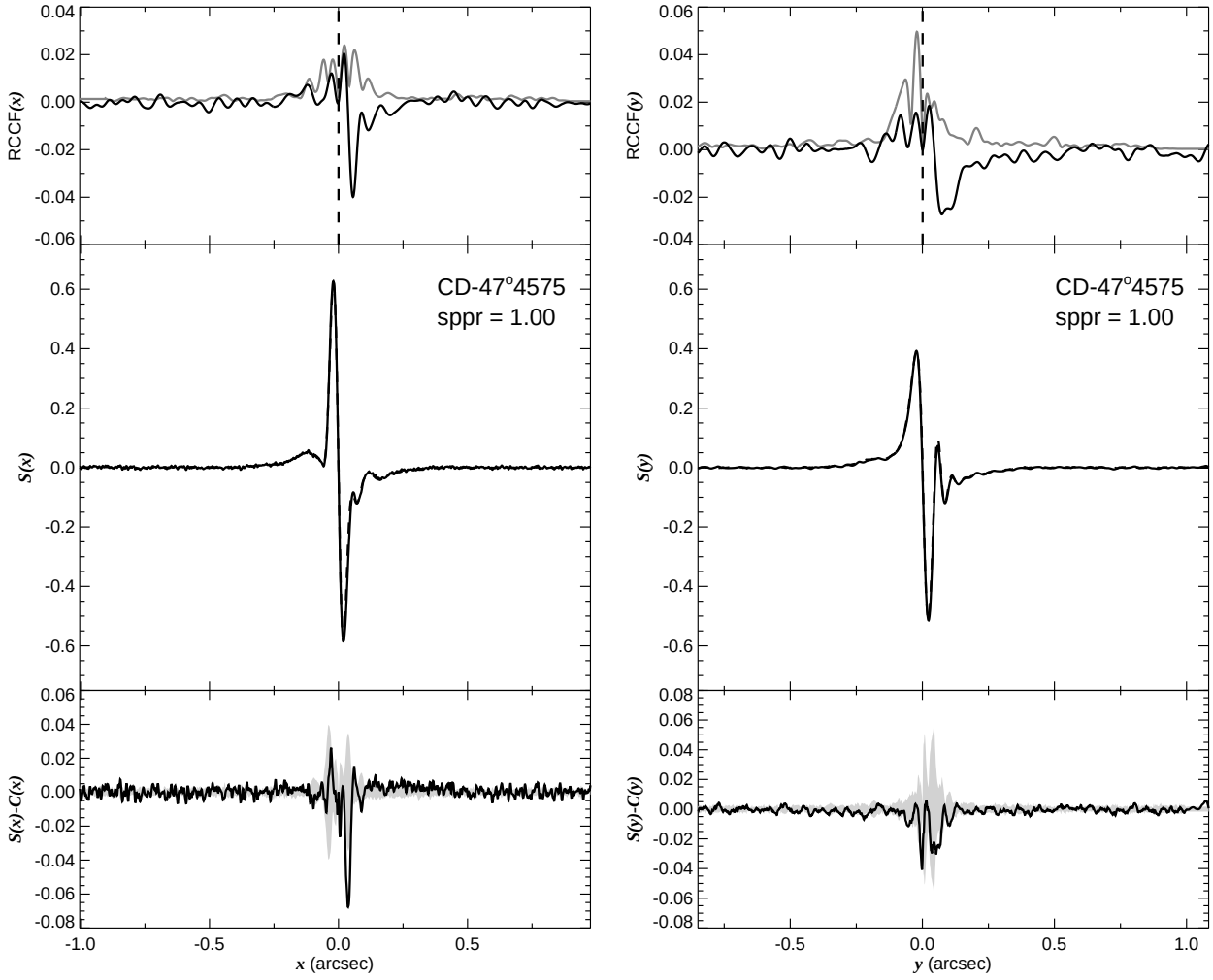

Fig. 1.157.— The FGS scans and binary detection tests for target 085956.10−473304.4 = CD−47 4575 obtained on BY 2008.8151.

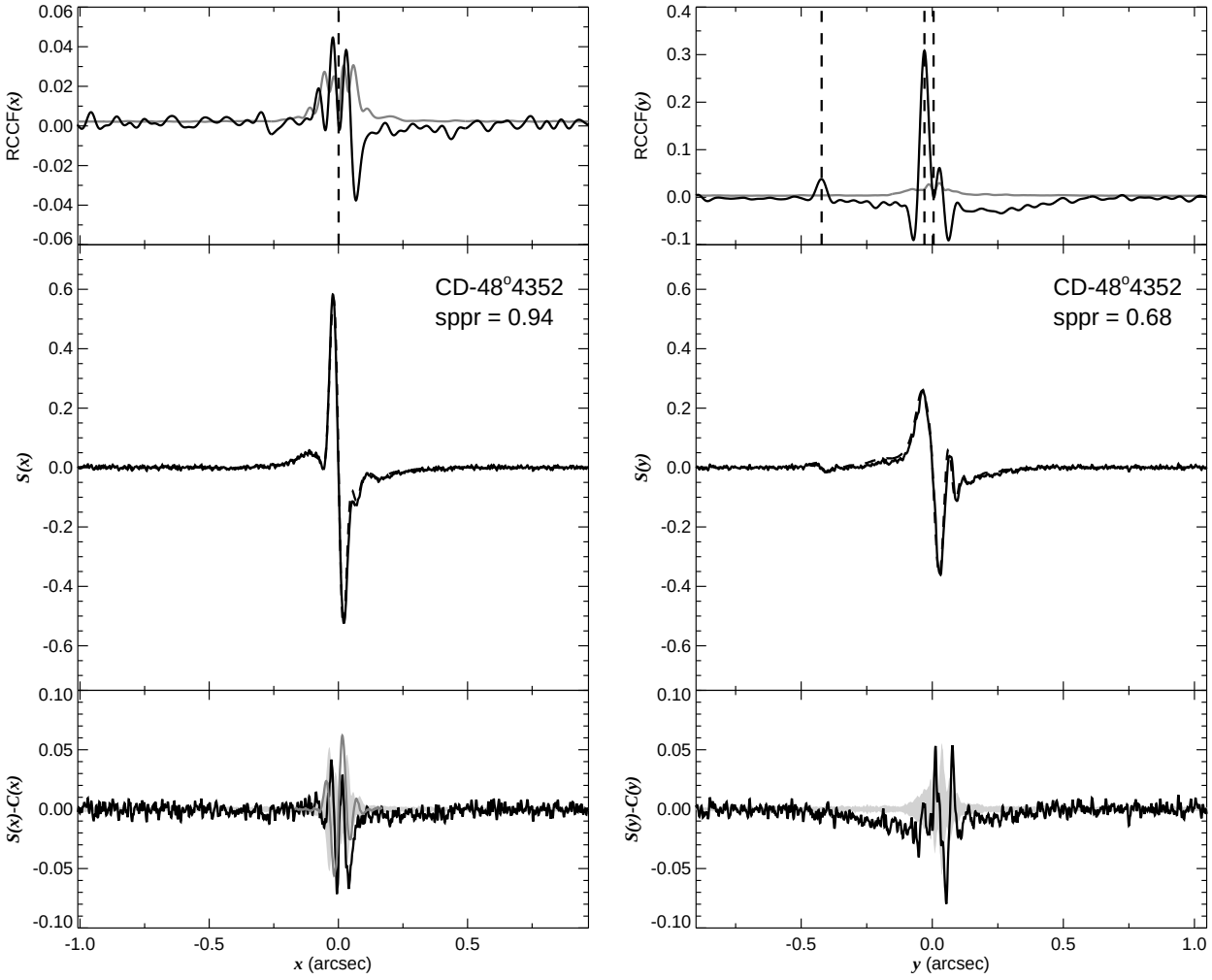

Fig. 1.158.— The FGS scans and binary detection tests for target 090221.56−484154.4 = CD−48 4352 obtained on BY 2008.8133.

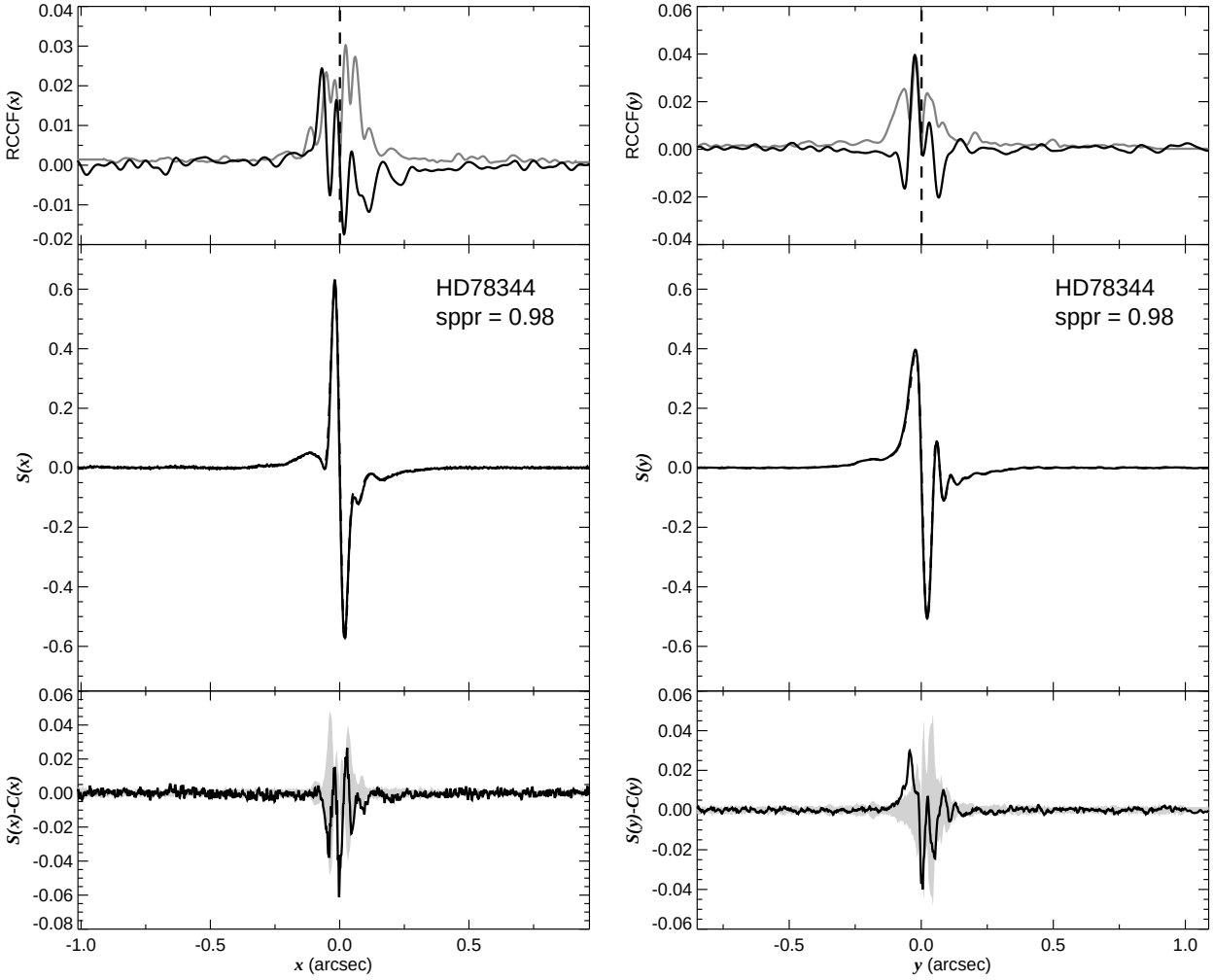

Fig. 1.159.— The FGS scans and binary detection tests for target 090551.33−474606.8 = HD78344 obtained on BY 2008.7729.

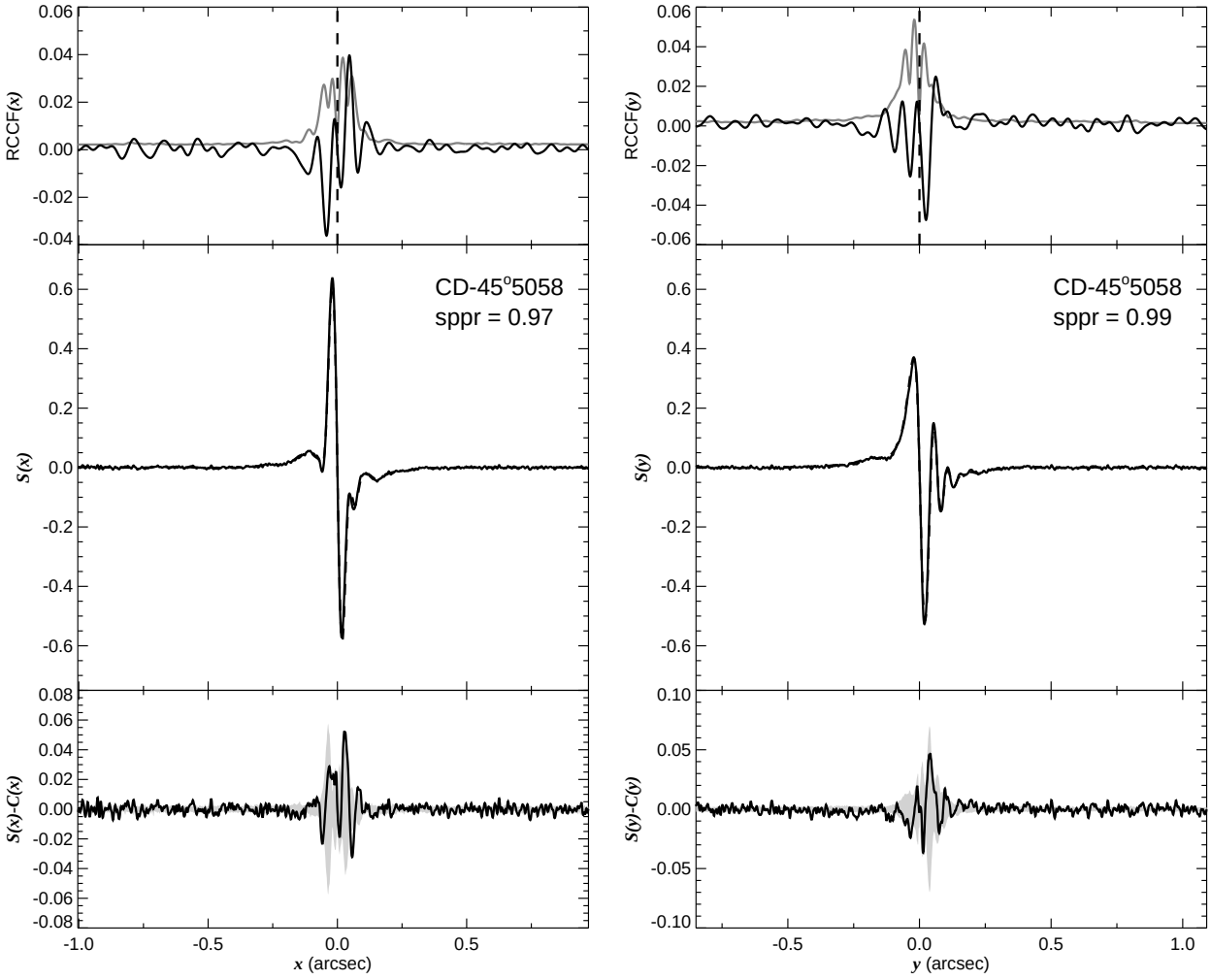

Fig. 1.160.— The FGS scans and binary detection tests for target 092010.13−453155.0 = CD−45 5058 obtained on BY 2008.8188.

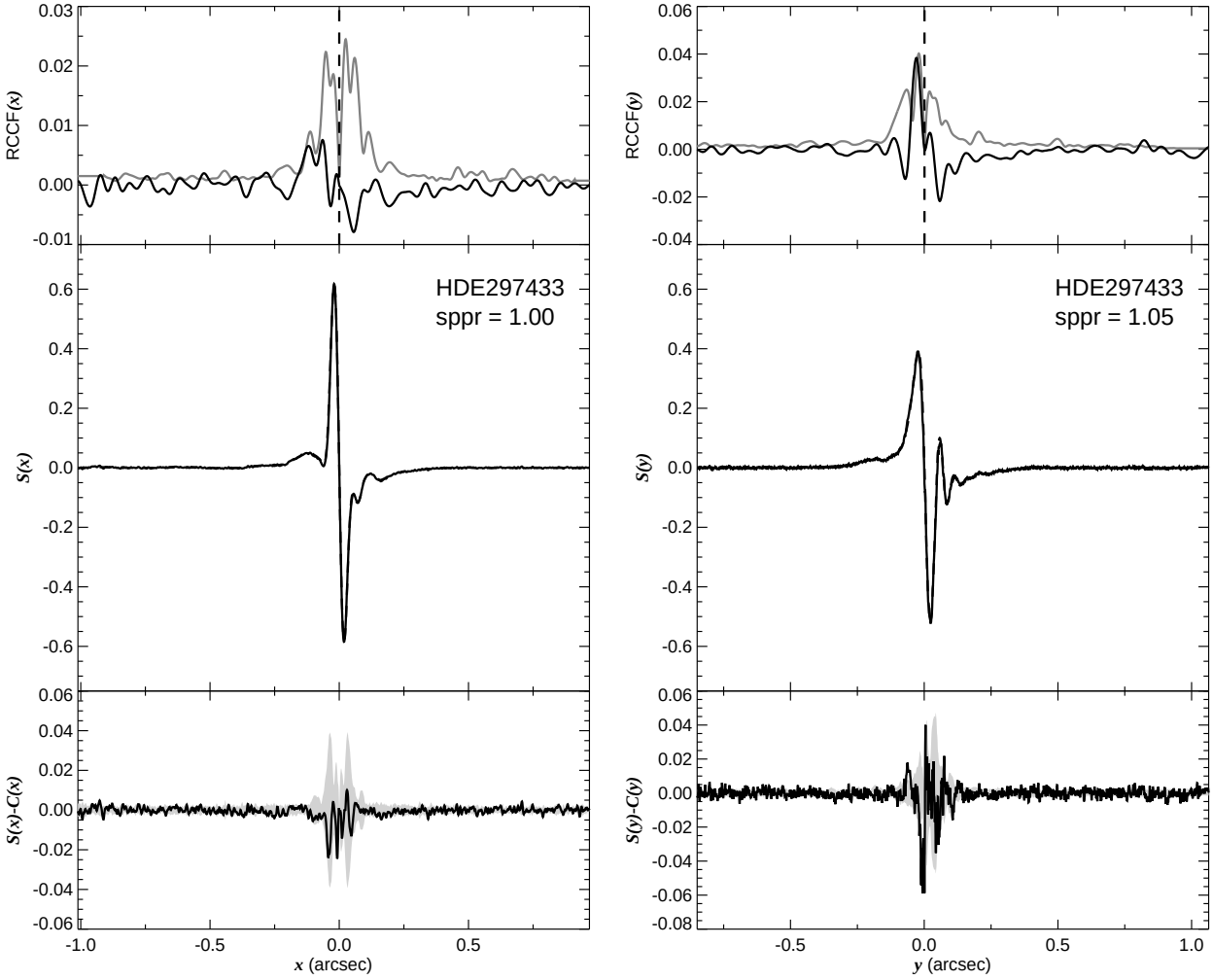

Fig. 1.161.— The FGS scans and binary detection tests for target 092244.75−493019.9 = HDE297433 obtained on BY 2008.7668.

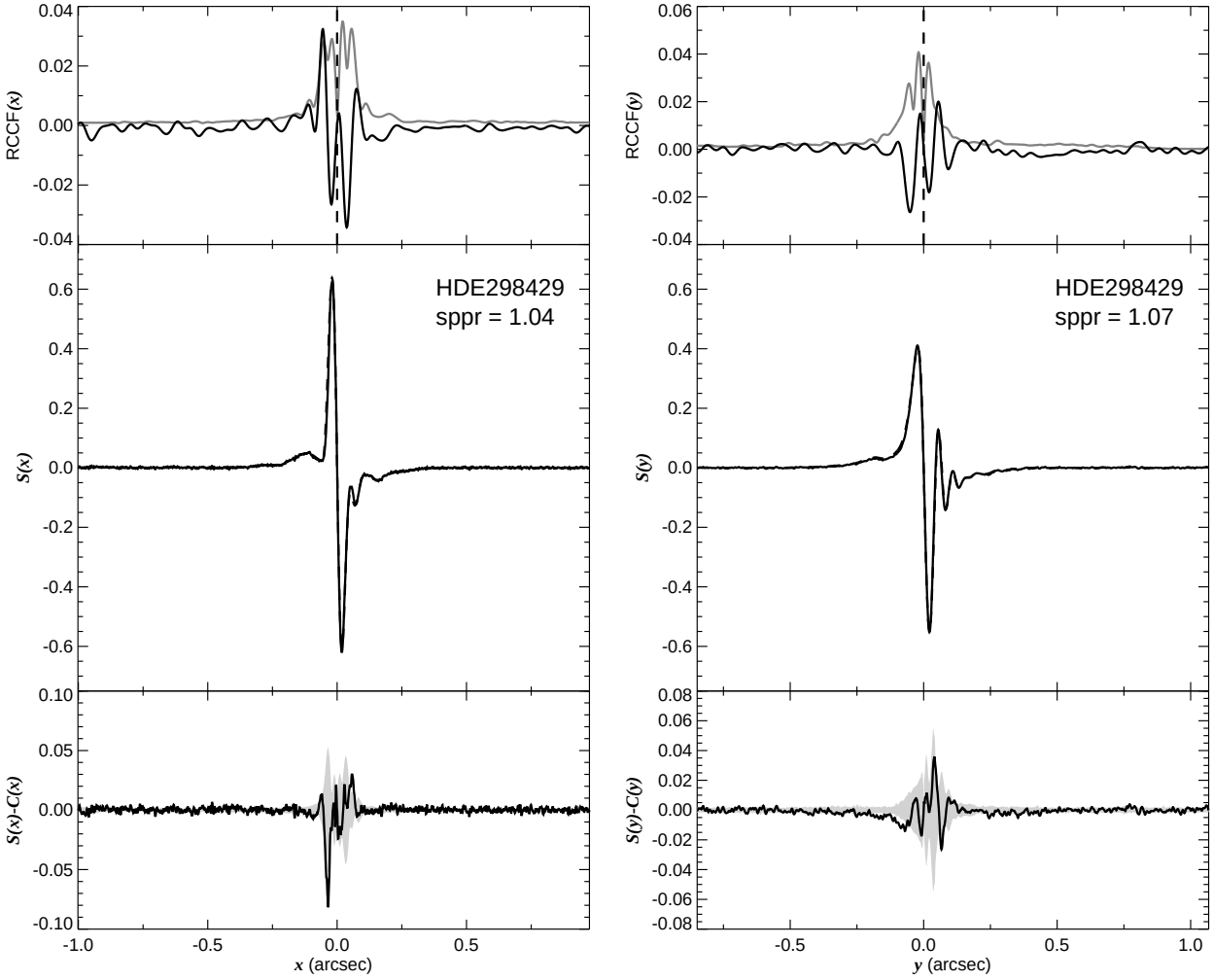

Fig. 1.162.— The FGS scans and binary detection tests for target 093037.25−513934.7 = HDE298429 obtained on BY 2008.7289.

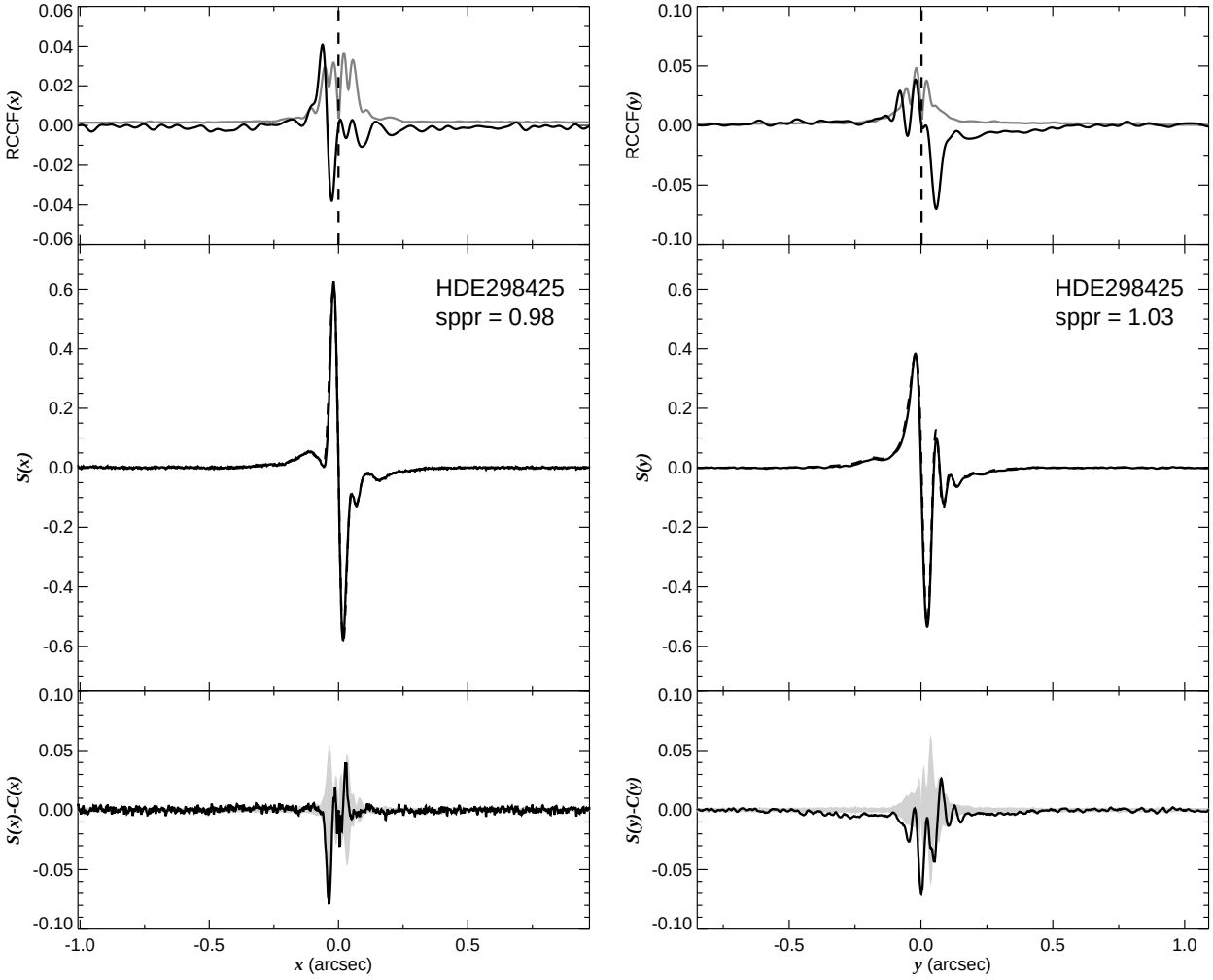

Fig. 1.163.— The FGS scans and binary detection tests for target 093054.26−512516.0 = HDE298425 obtained on BY 2008.7754.

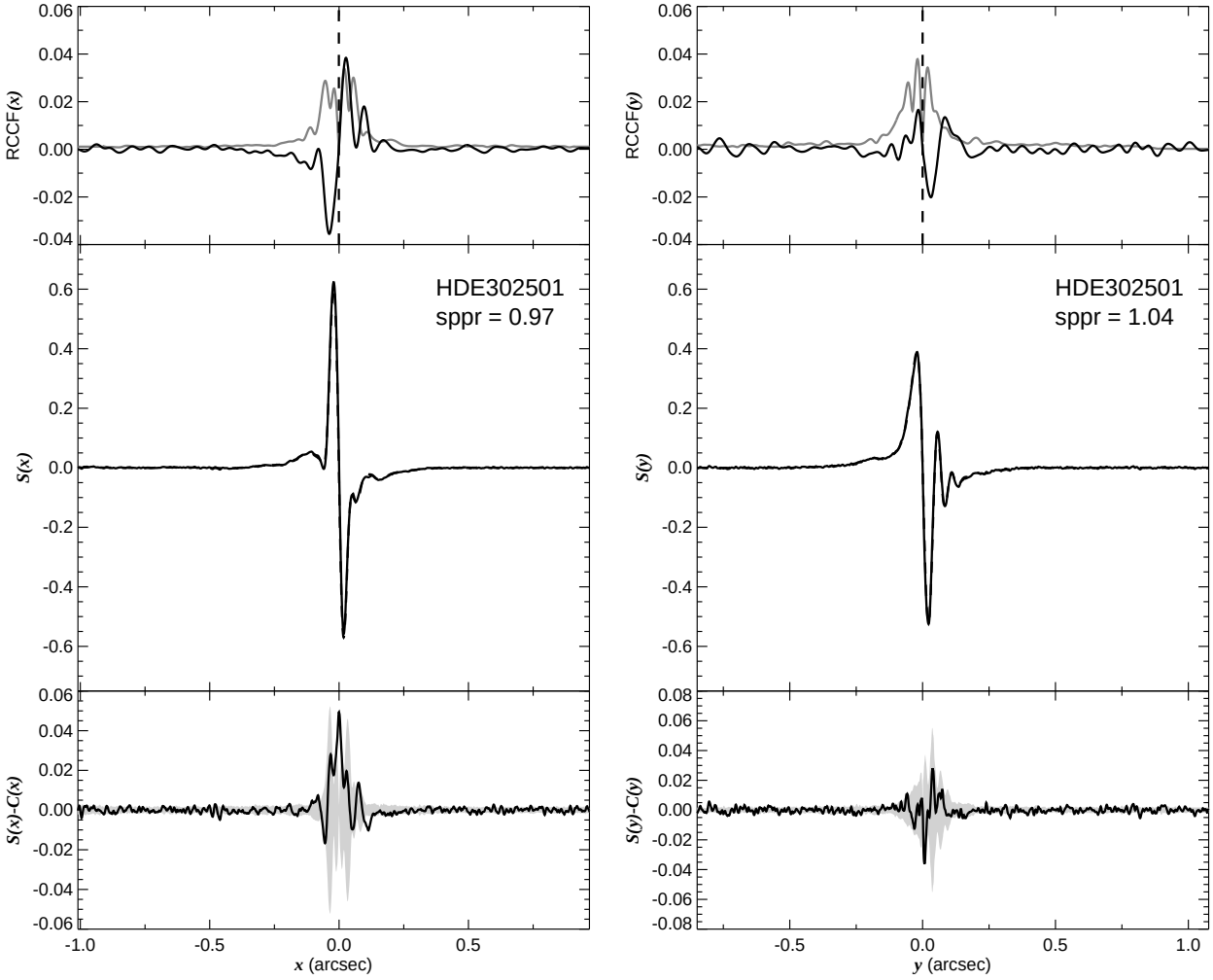

Fig. 1.164.— The FGS scans and binary detection tests for target 100440.52−583158.5 = HDE302501 obtained on BY 2008.7756.

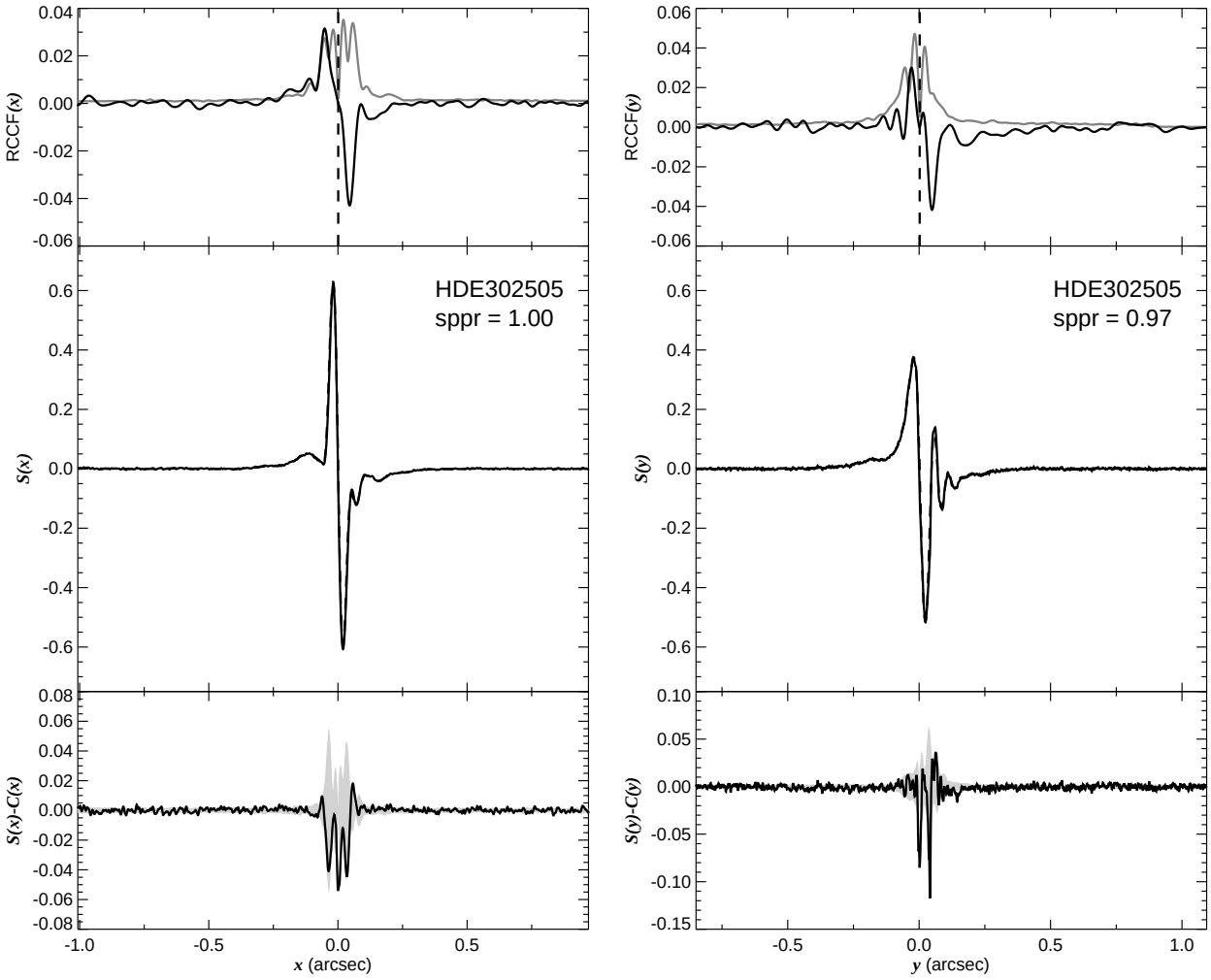

Fig. 1.165.— The FGS scans and binary detection tests for target 100520.55−584420.7 = HDE302505 obtained on BY 2008.8026.

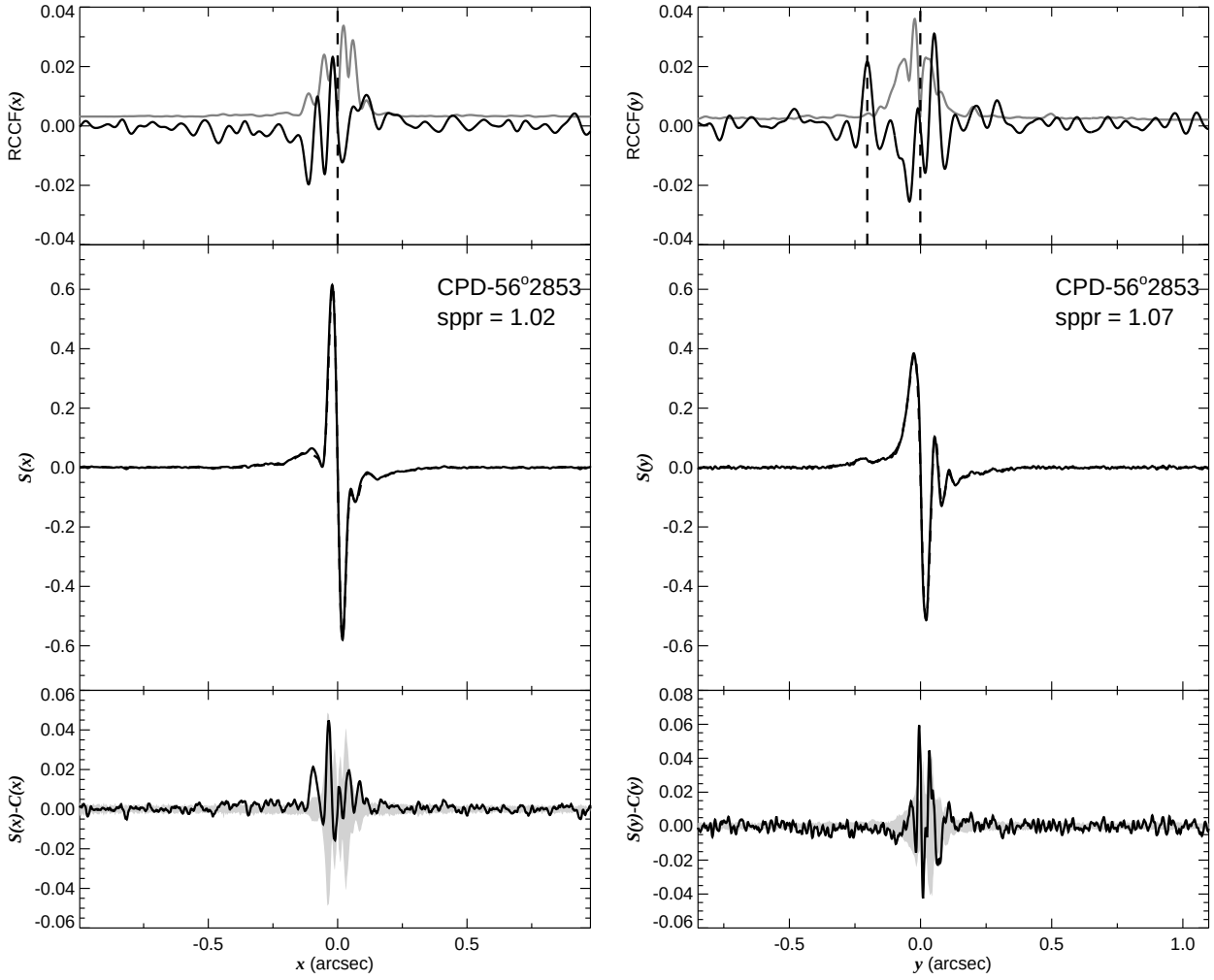

Fig. 1.166.— The FGS scans and binary detection tests for target 100639.88−572533.1 = CPD−56 2853 obtained on BY 2008.8157.

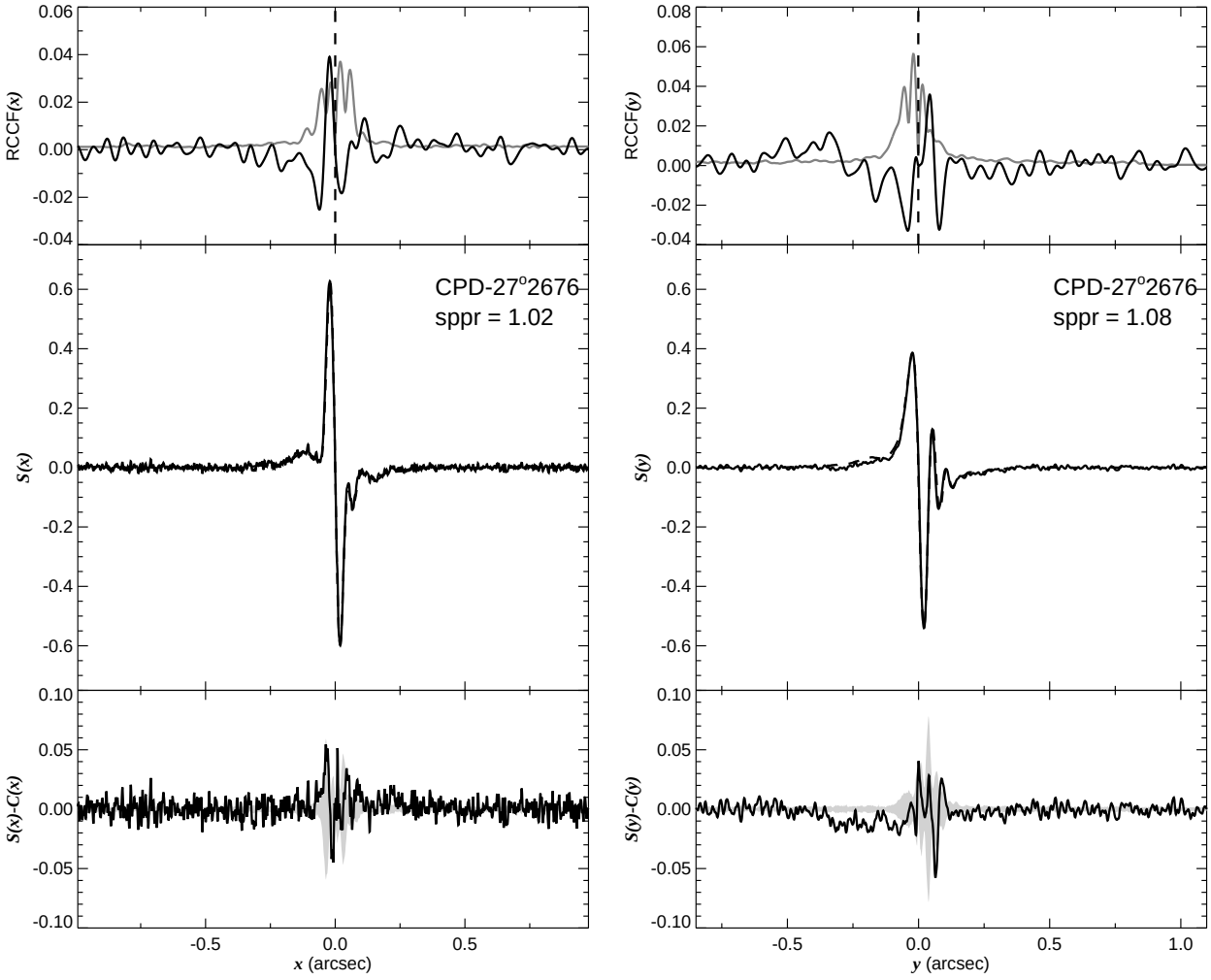

Fig. 1.167.— The FGS scans and binary detection tests for target 100712.21−580054.3 = CPD−57 2676 obtained on BY 2008.8693.

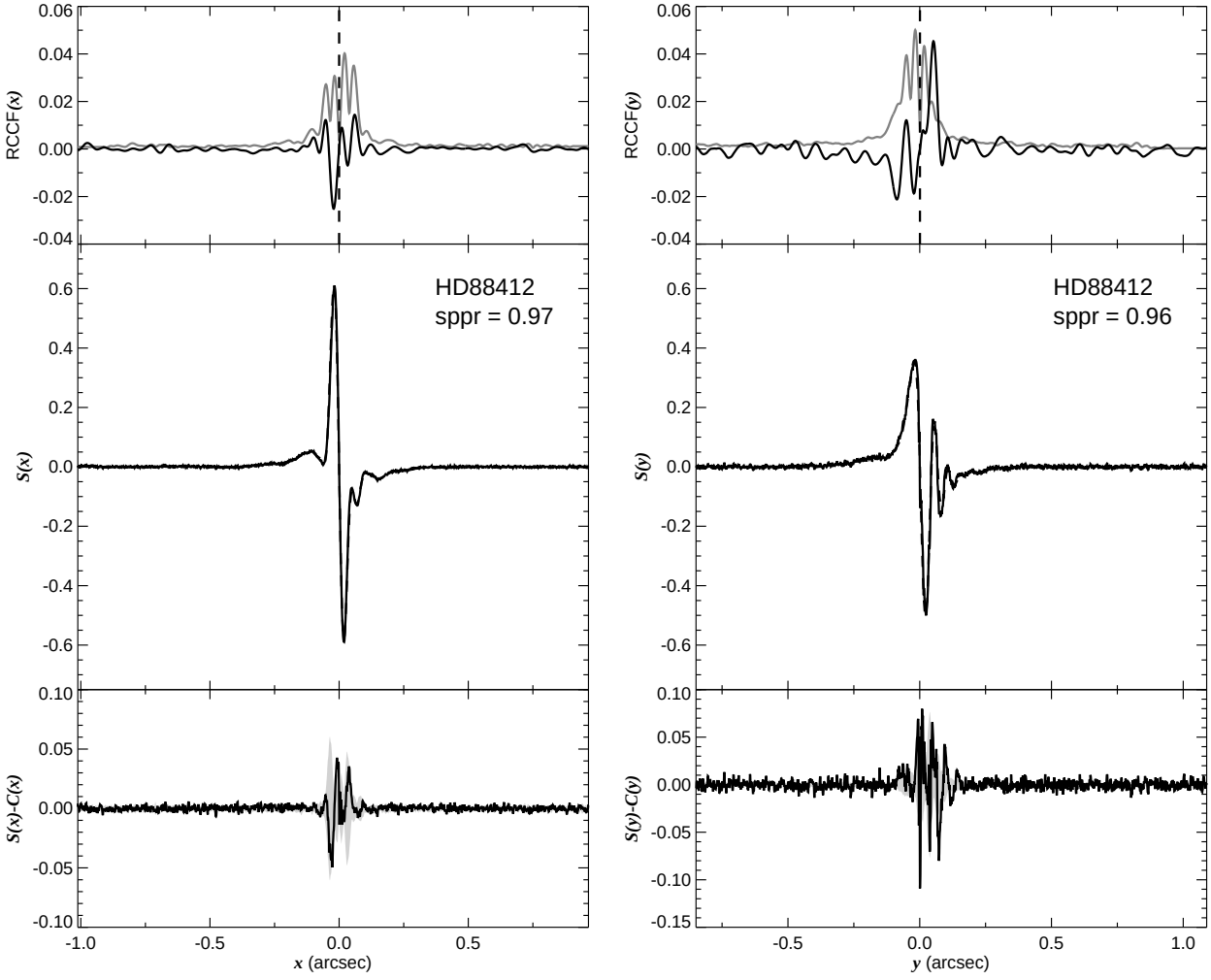

Fig. 1.168.— The FGS scans and binary detection tests for target 100947.72−605949.2 = HD88412 obtained on BY 2008.7780.

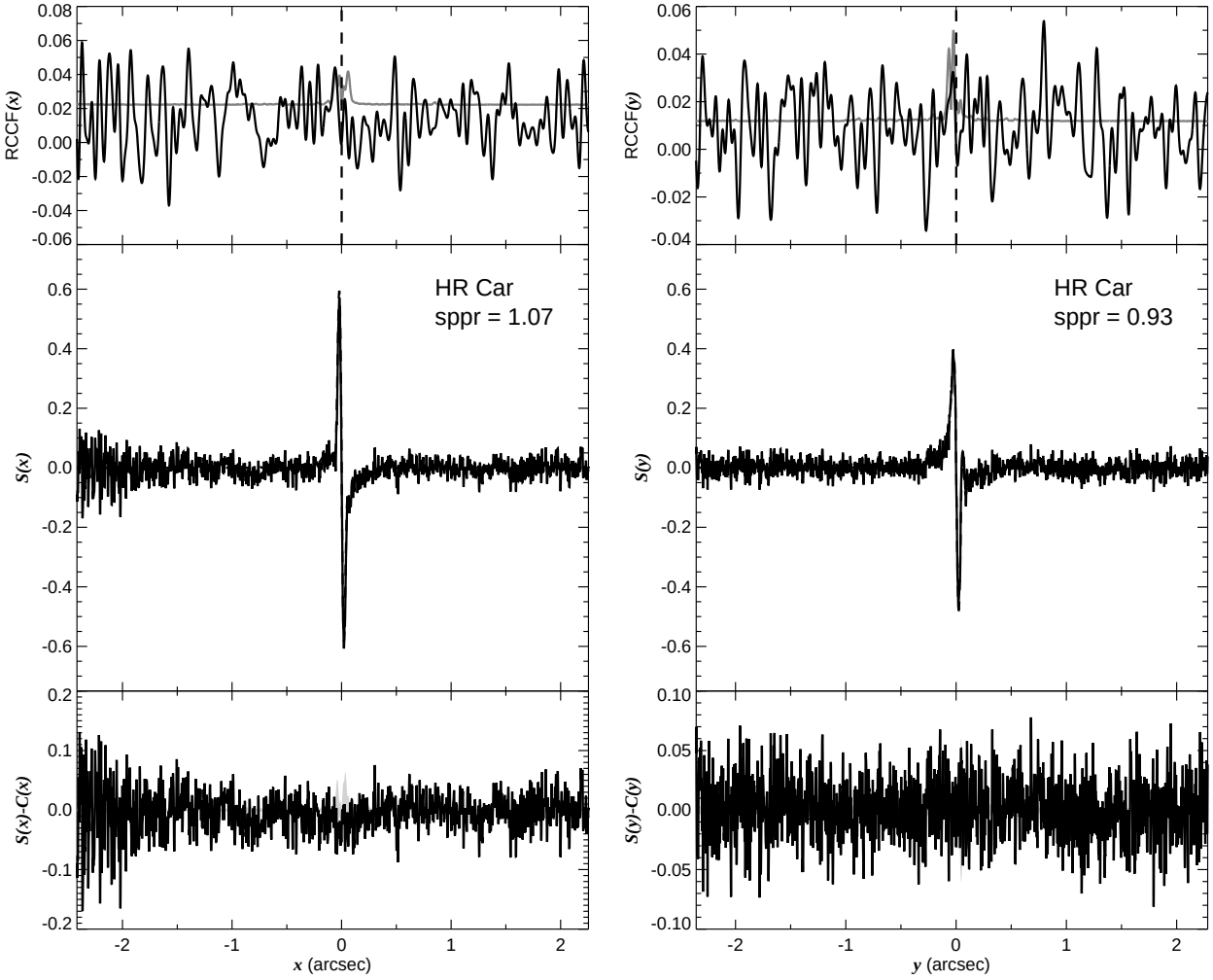

Fig. 1.169.— The FGS scans and binary detection tests for target 102253.84−593728.4 = HD90177 obtained on BY 2008.9275.

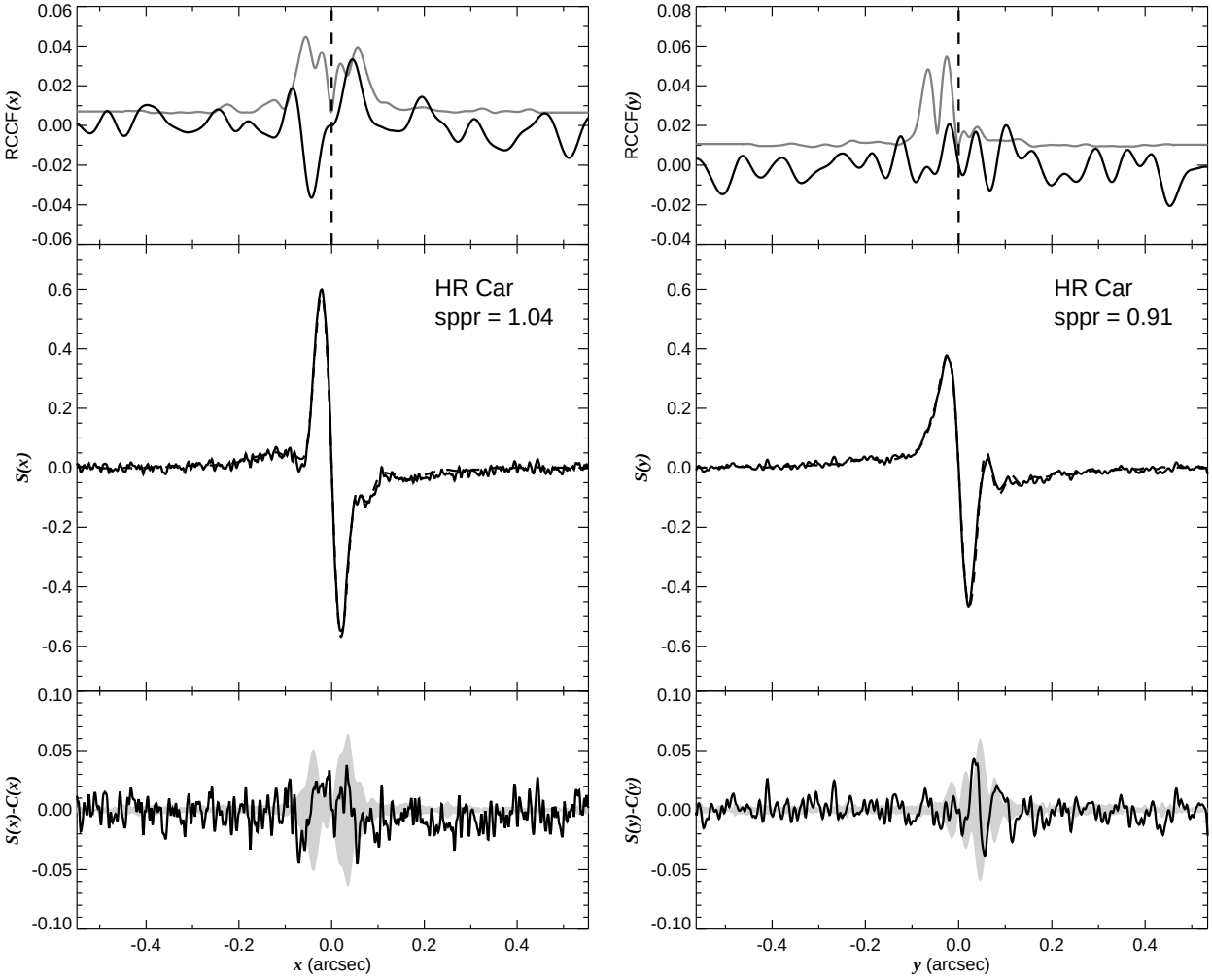

Fig. 1.170.— The FGS scans and binary detection tests for target 102253.84−593728.4 = HD90177 obtained on BY 2008.9275.

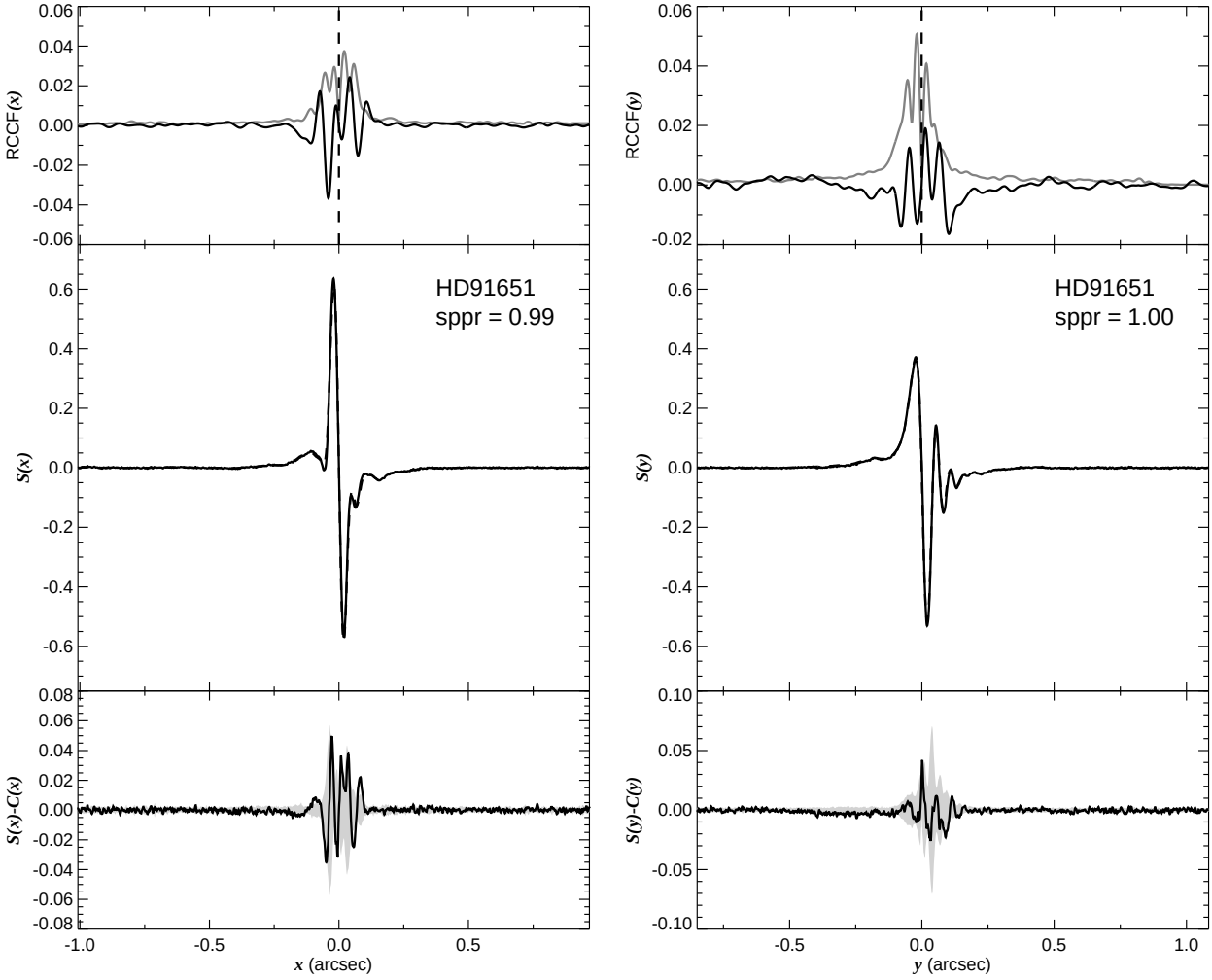

Fig. 1.171.— The FGS scans and binary detection tests for target 103330.30−600740.0 = HD91651 obtained on BY 2008.5539.

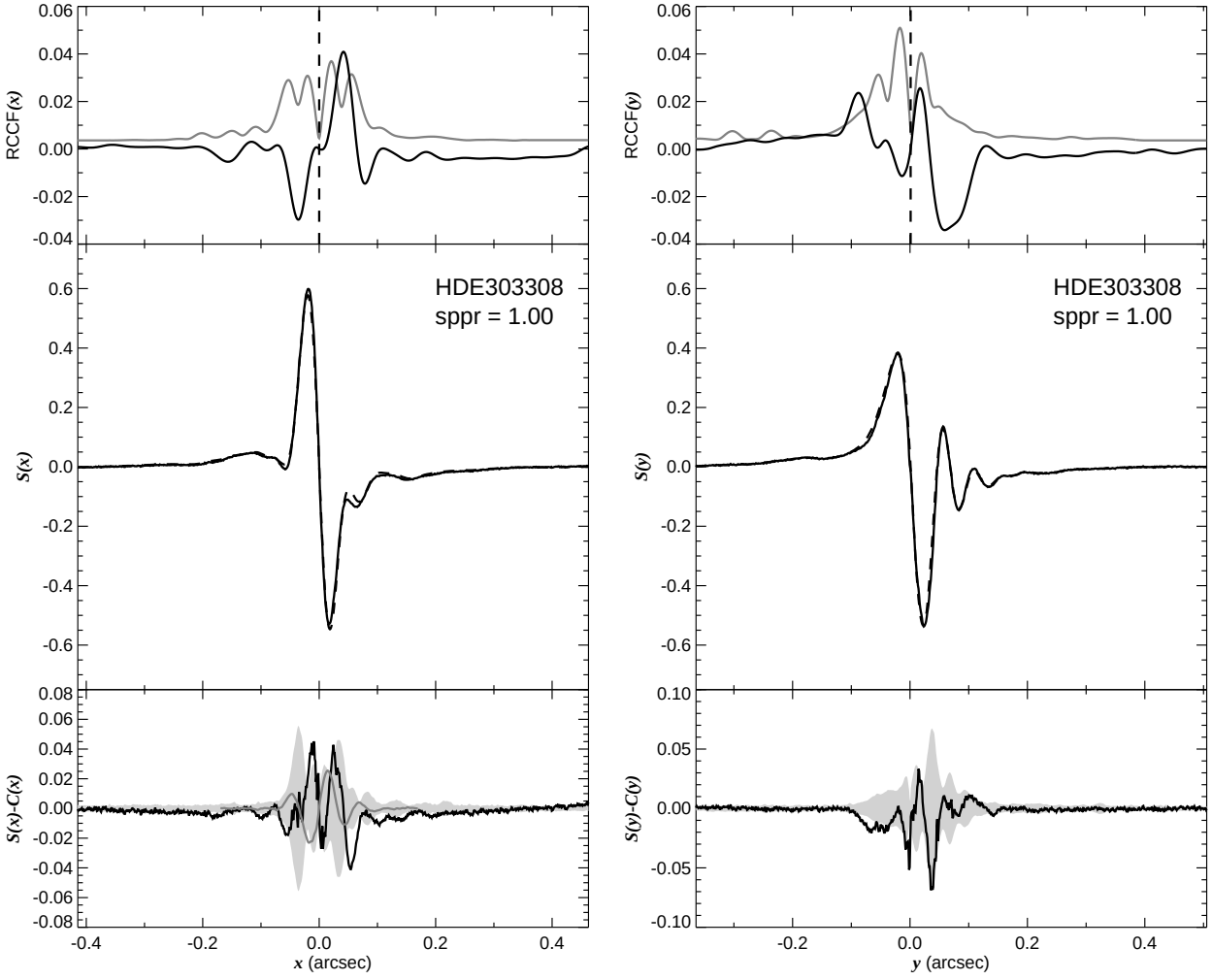

Fig. 1.172.— The FGS scans and binary detection tests for target 104505.85−594006.4 = HDE303308 obtained on BY 2008.5511.

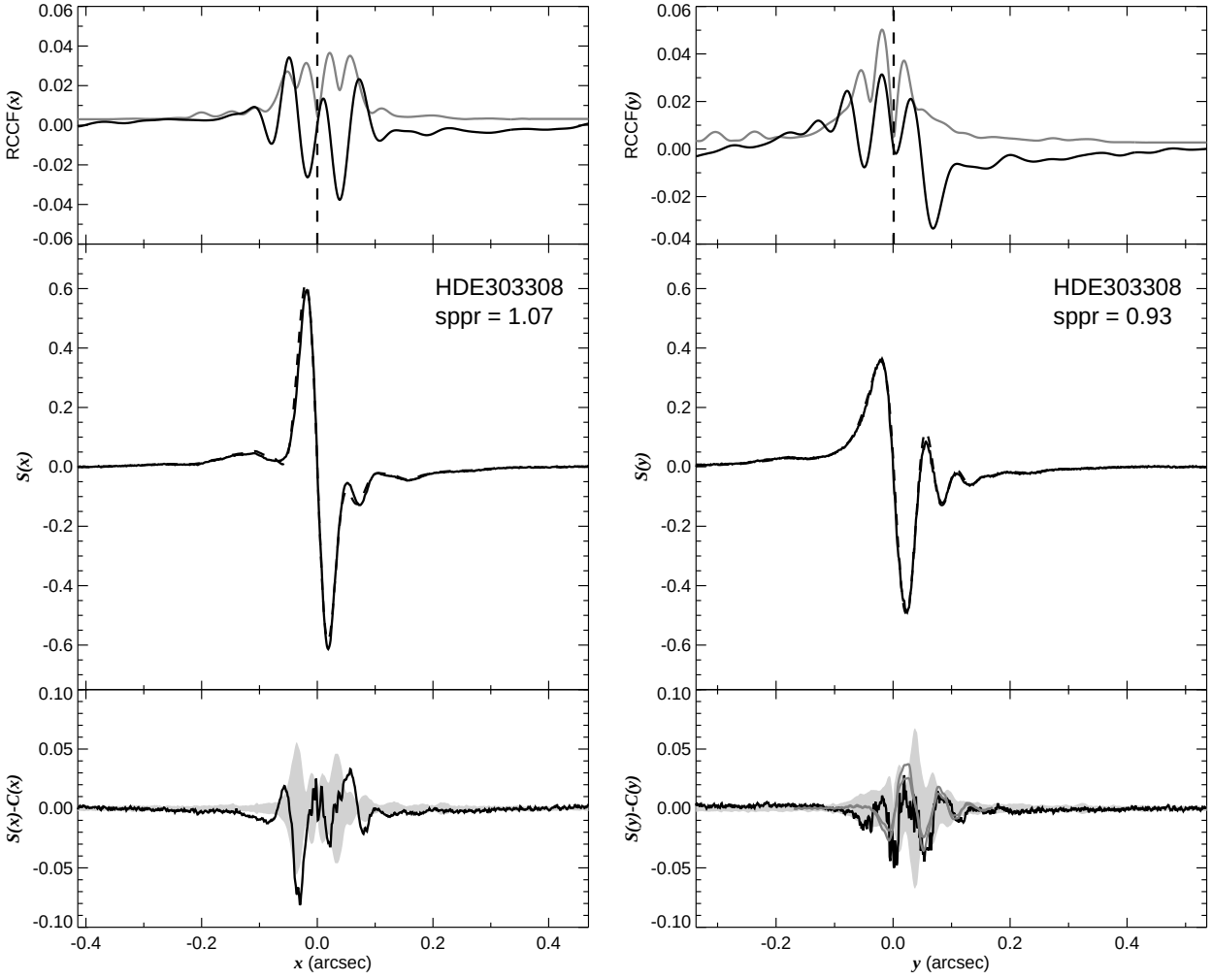

Fig. 1.173.— The FGS scans and binary detection tests for target 104505.85−594006.4 = HDE303308 obtained on BY 2008.8819.

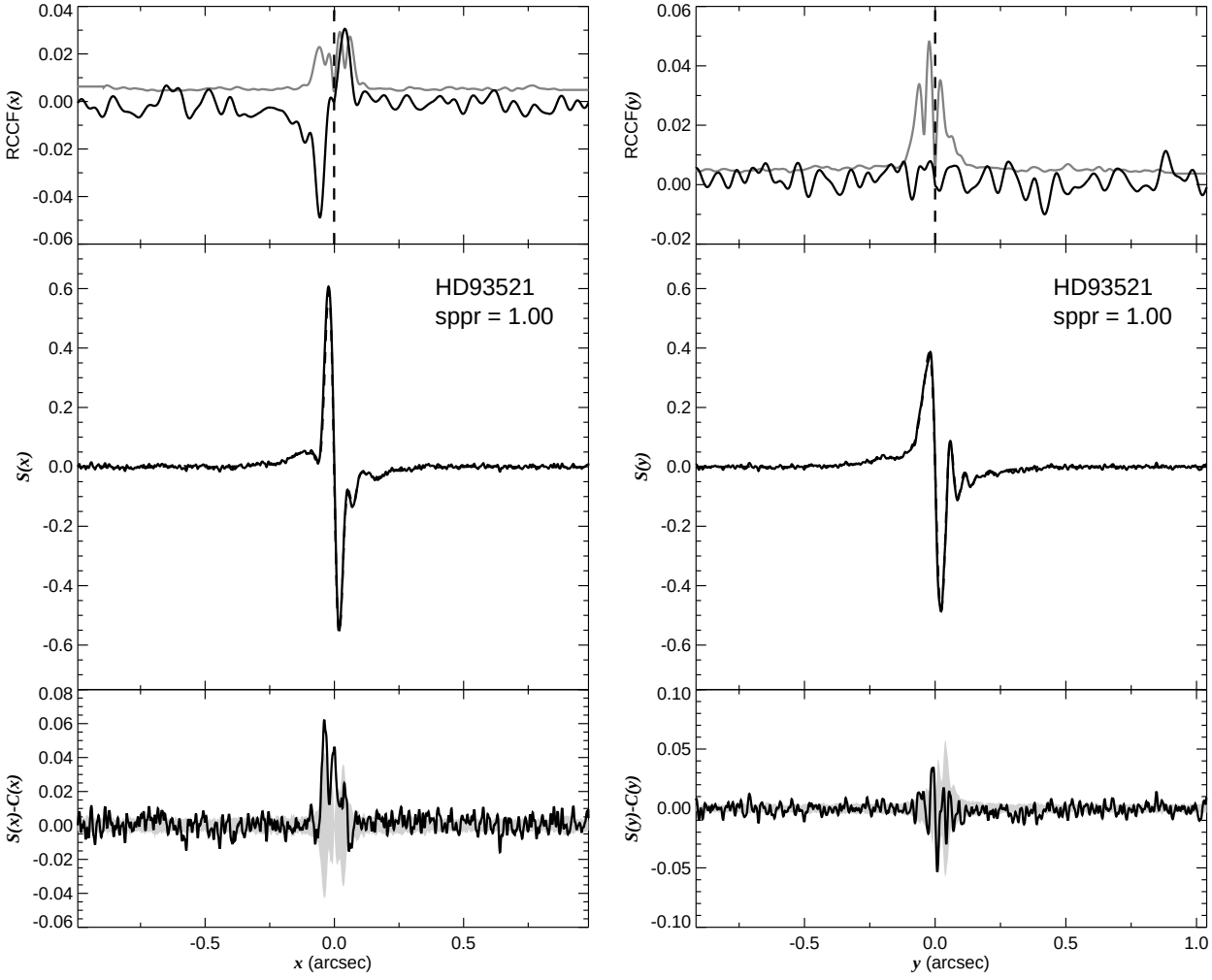

Fig. 1.174.— The FGS scans and binary detection tests for target 104823.51+373413.1 = HD93521 obtained on BY 2008.8409.

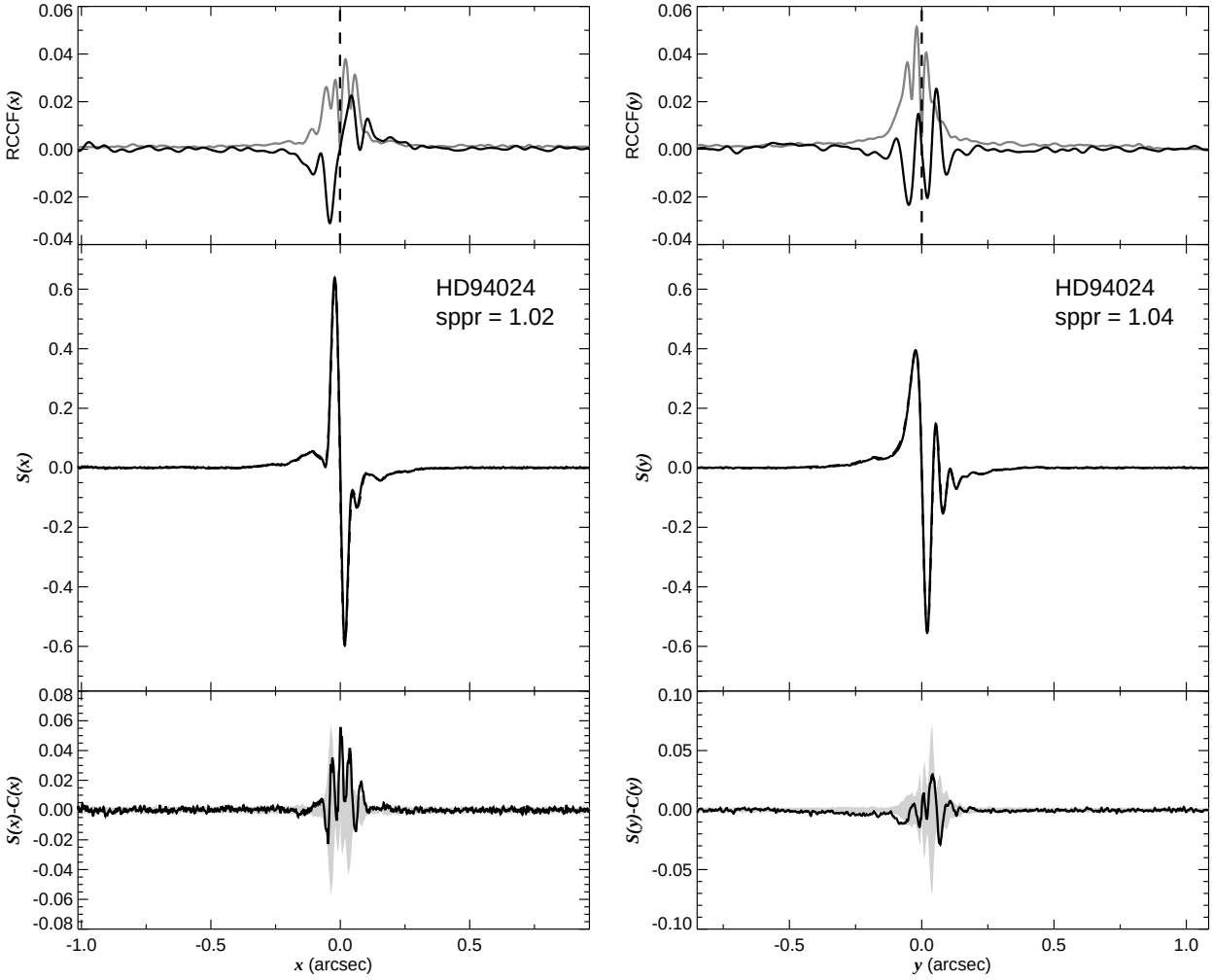

Fig. 1.175.— The FGS scans and binary detection tests for target 105001.50−575226.3 = HD94024 obtained on BY 2008.6688.

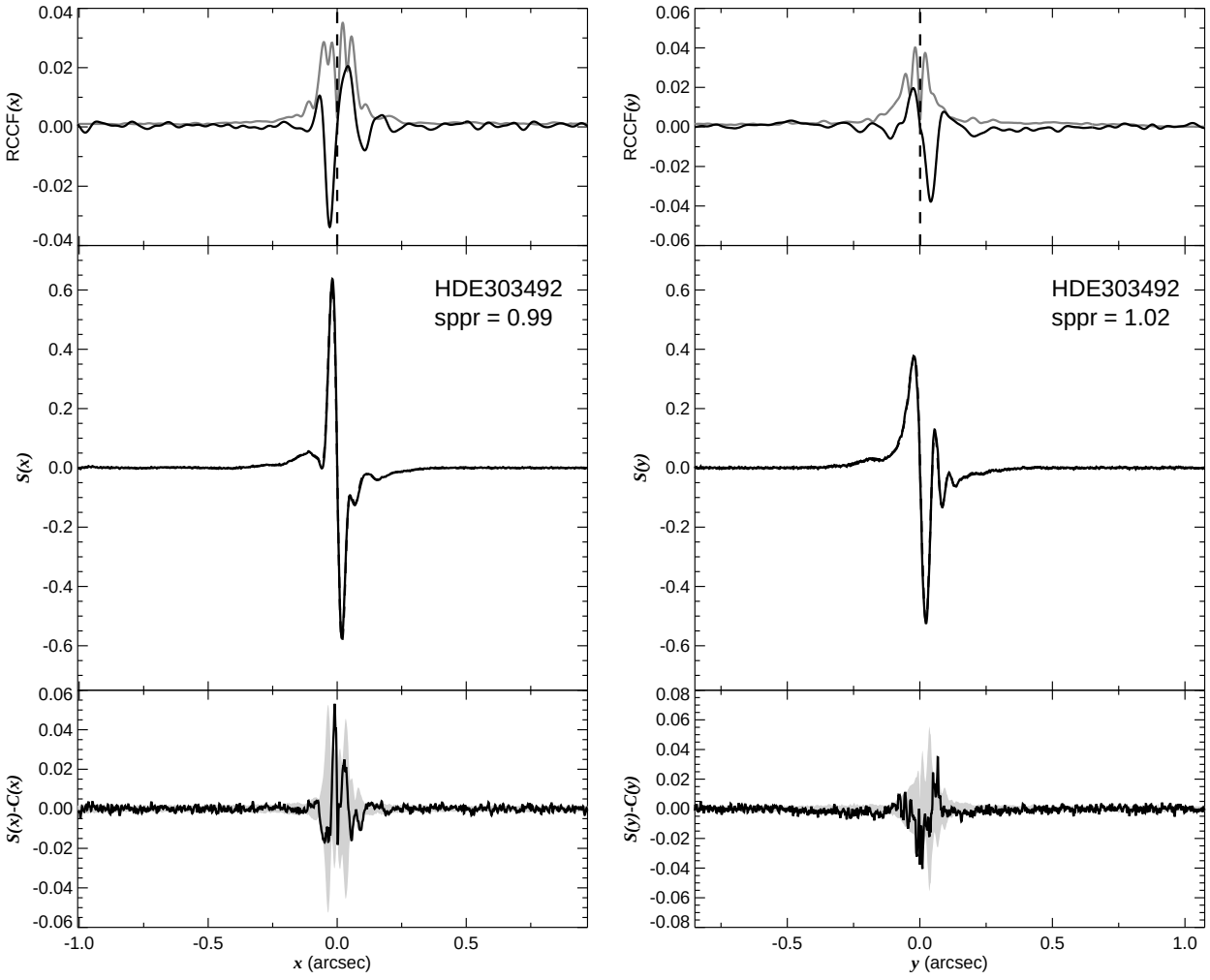

Fig. 1.176.— The FGS scans and binary detection tests for target 105152.75−585835.3 = HDE303492 obtained on BY 2008.7072.

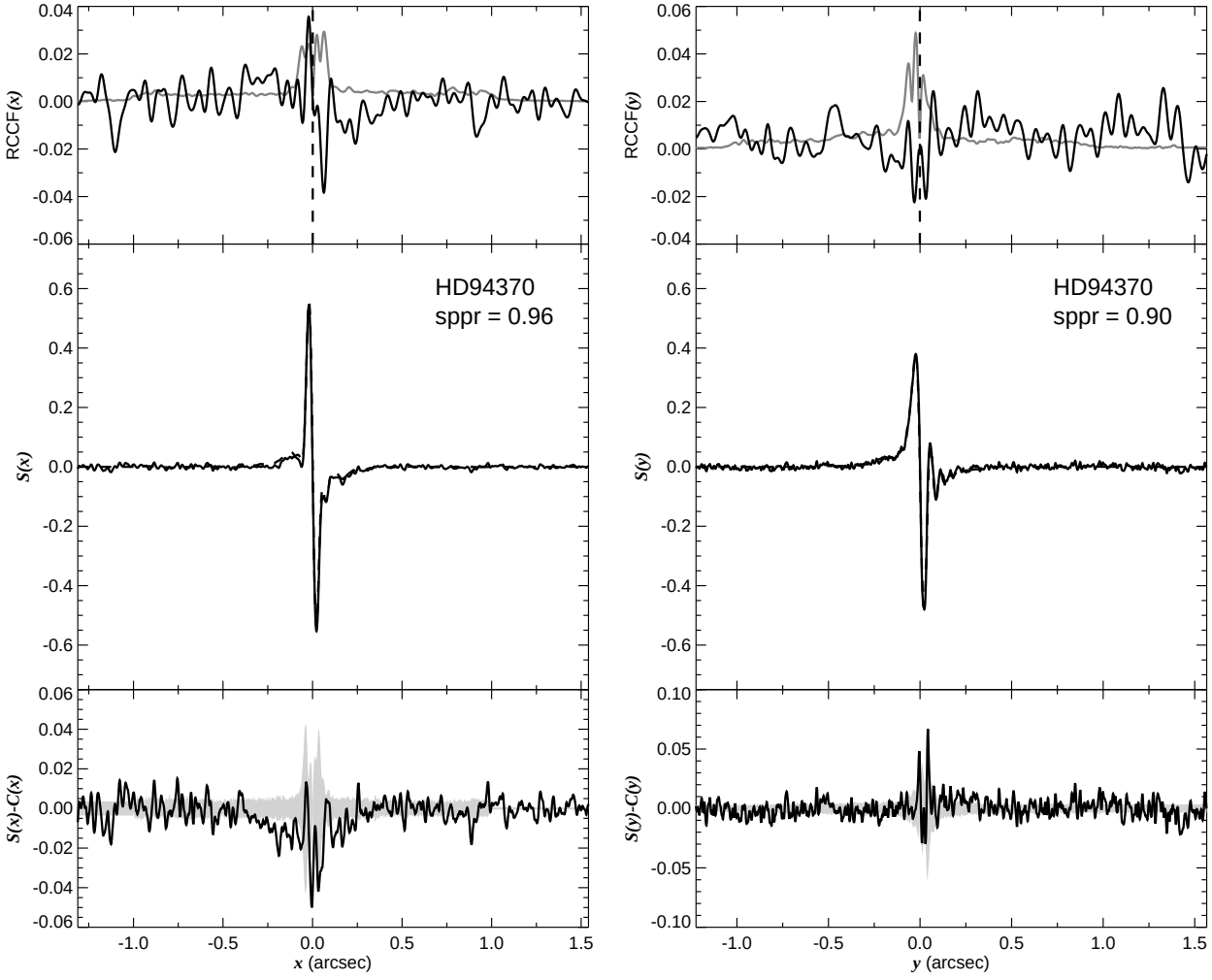

Fig. 1.177.— The FGS scans and binary detection tests for target 105223.20−584448.4 = HD94370 obtained on BY 2008.8565.

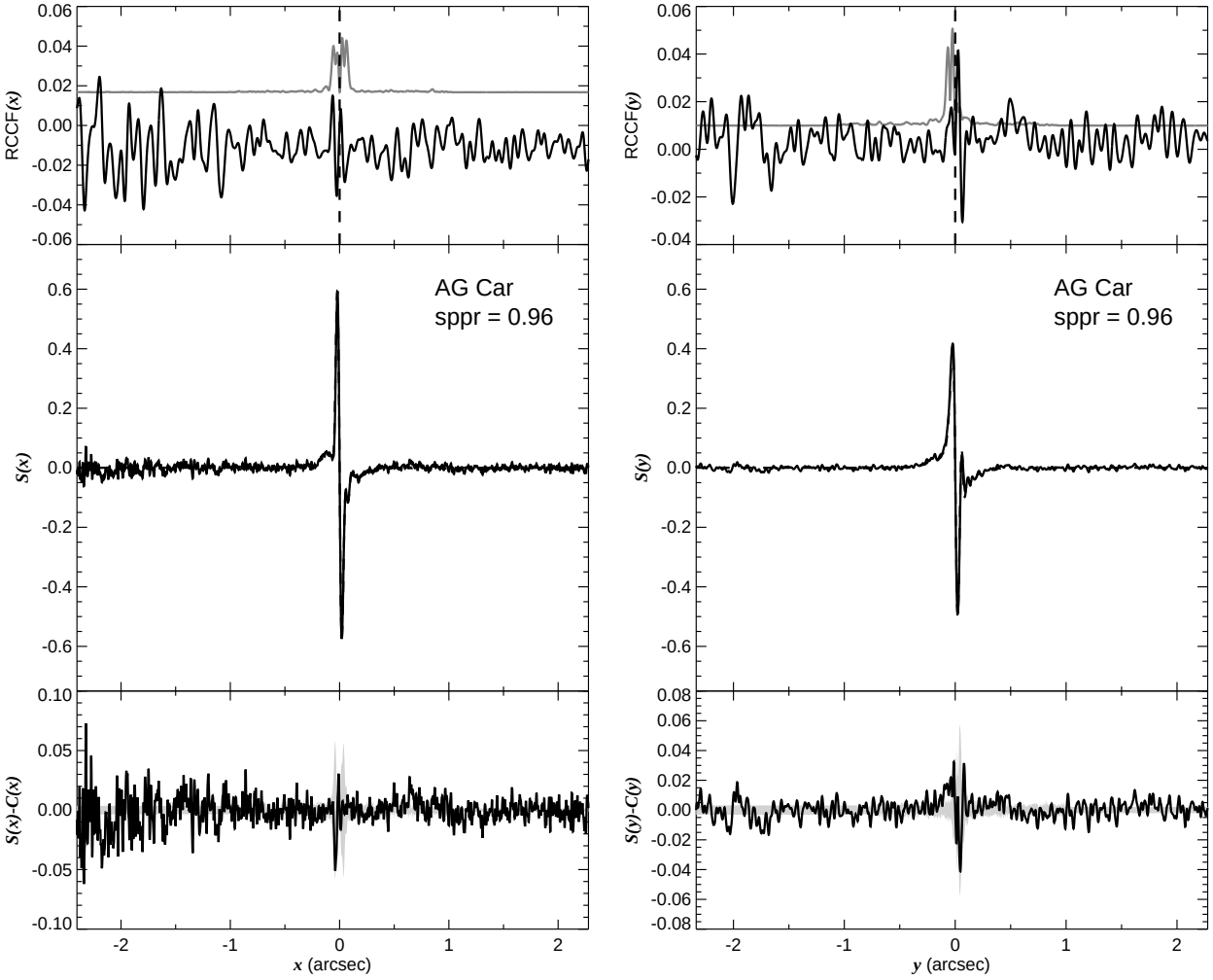

Fig. 1.178.— The FGS scans and binary detection tests for target 105611.58−602712.8 = HD94910 obtained on BY 2008.9277.

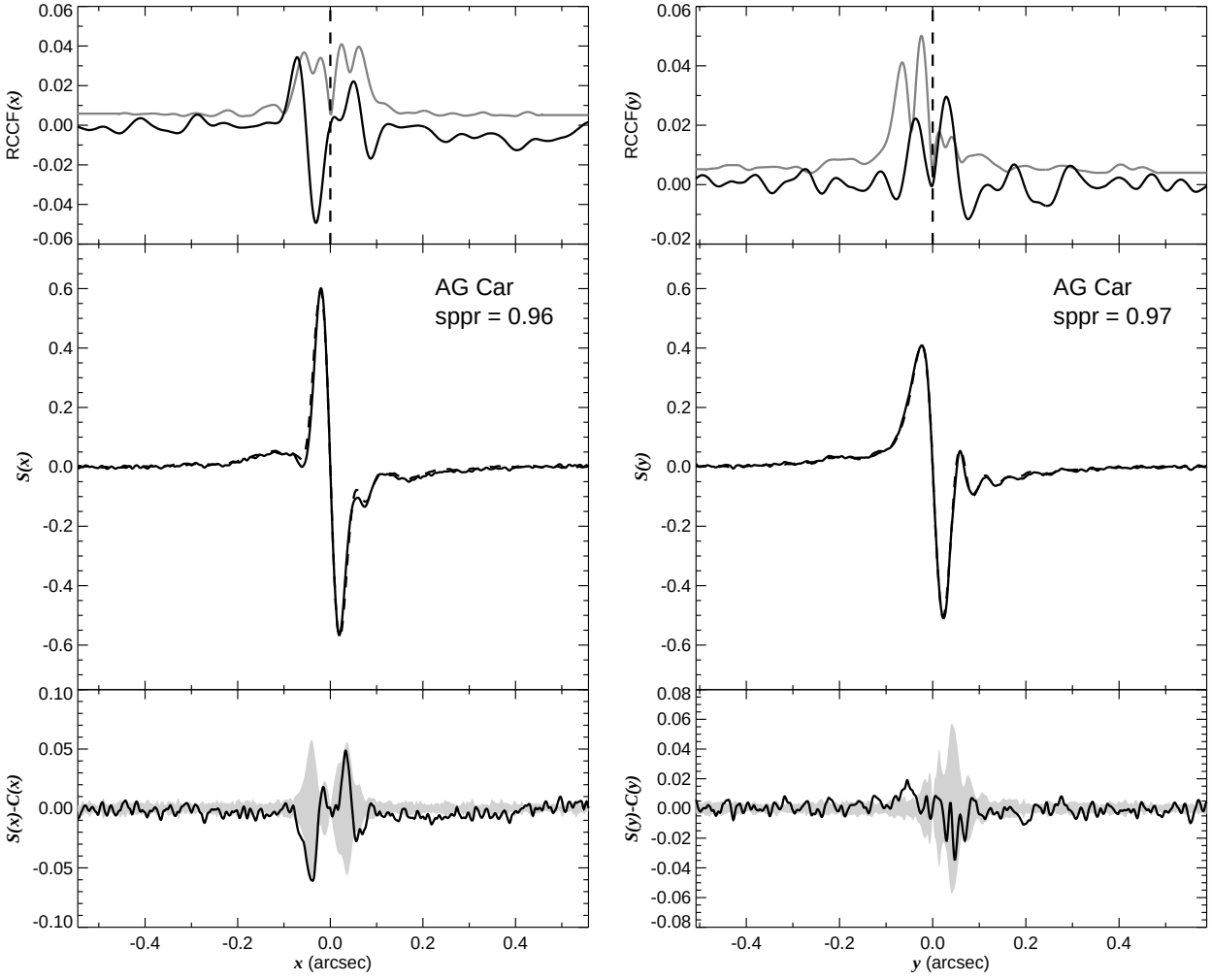

Fig. 1.179.— The FGS scans and binary detection tests for target 105611.58−602712.8 = HD94910 obtained on BY 2008.9277.

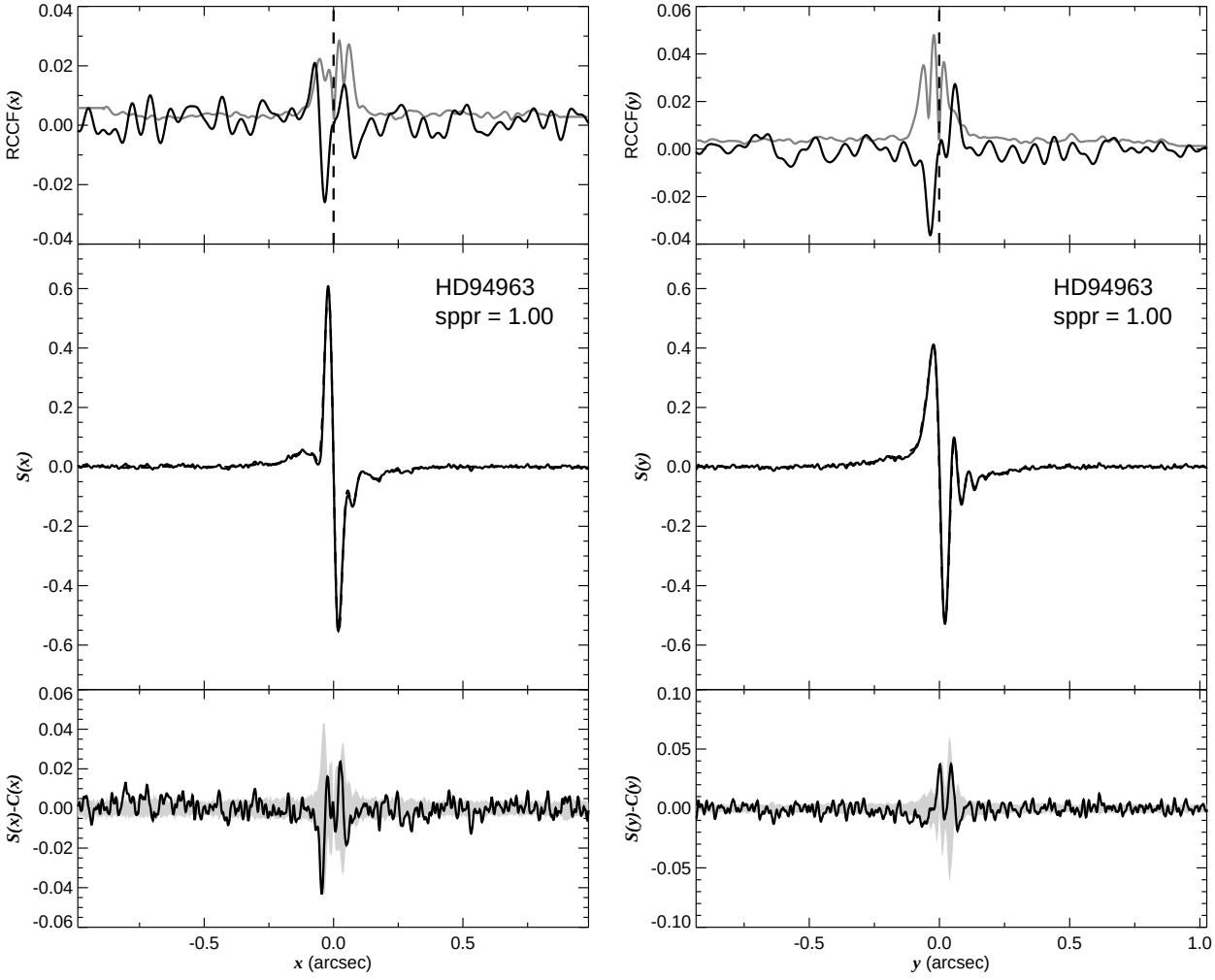

Fig. 1.180.— The FGS scans and binary detection tests for target 105635.79−614232.2 = HD94963 obtained on BY 2008.7067.

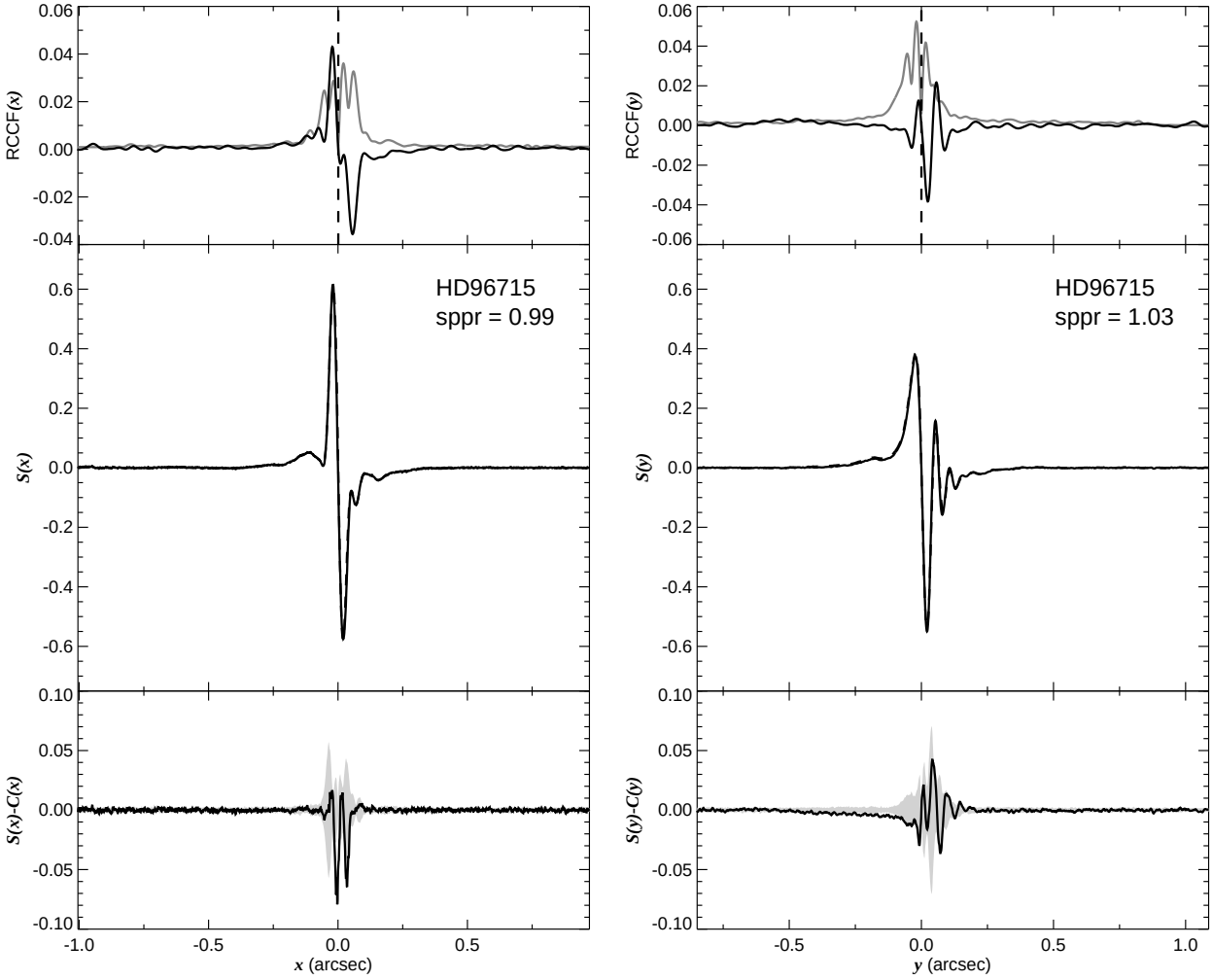

Fig. 1.181.— The FGS scans and binary detection tests for target 110732.81−595748.7 = HD96715 obtained on BY 2007.5081.

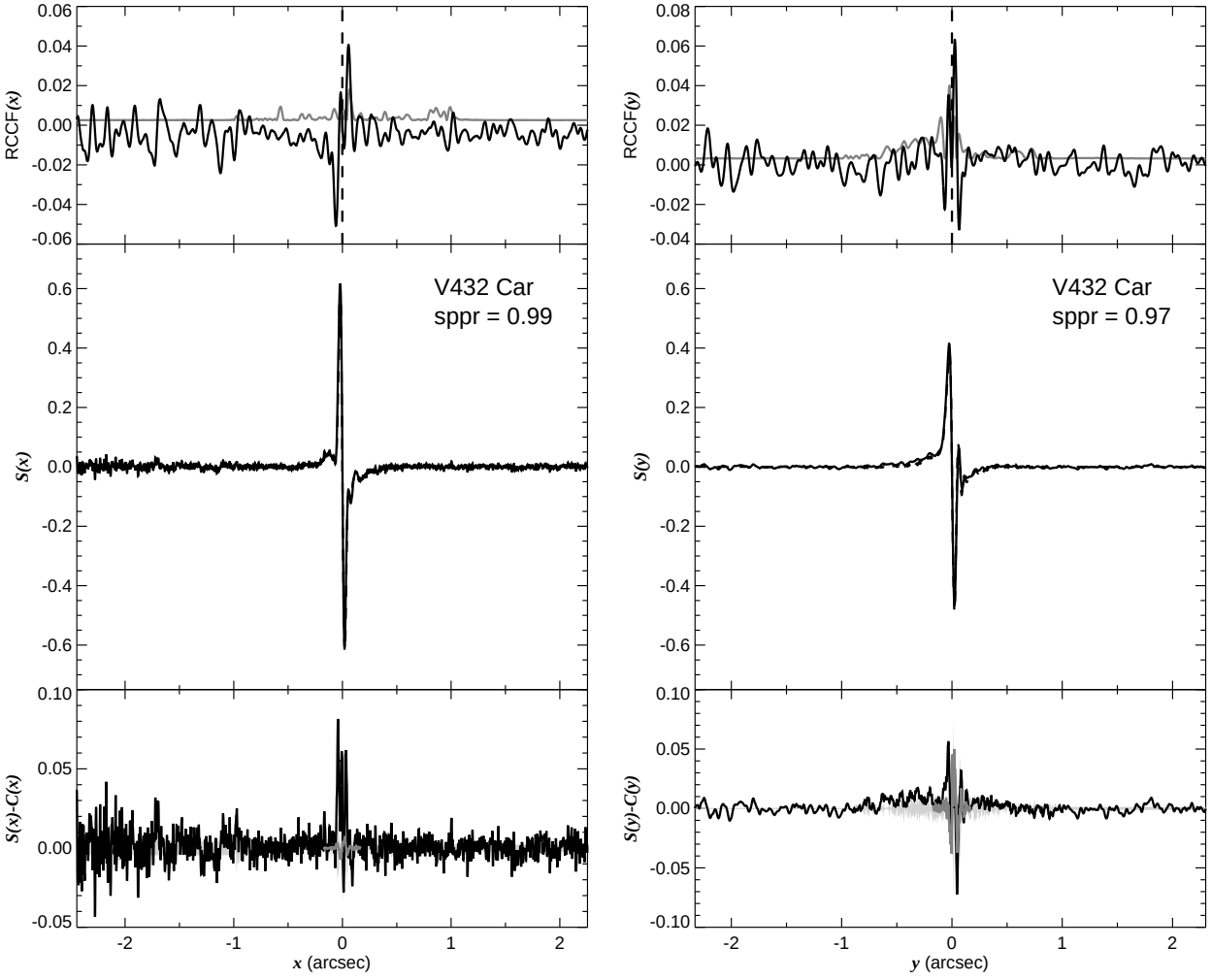

Fig. 1.182.— The FGS scans and binary detection tests for target 110840.06−604251.7 = V432 Car = Wra 751 obtained on BY 2008.9337.

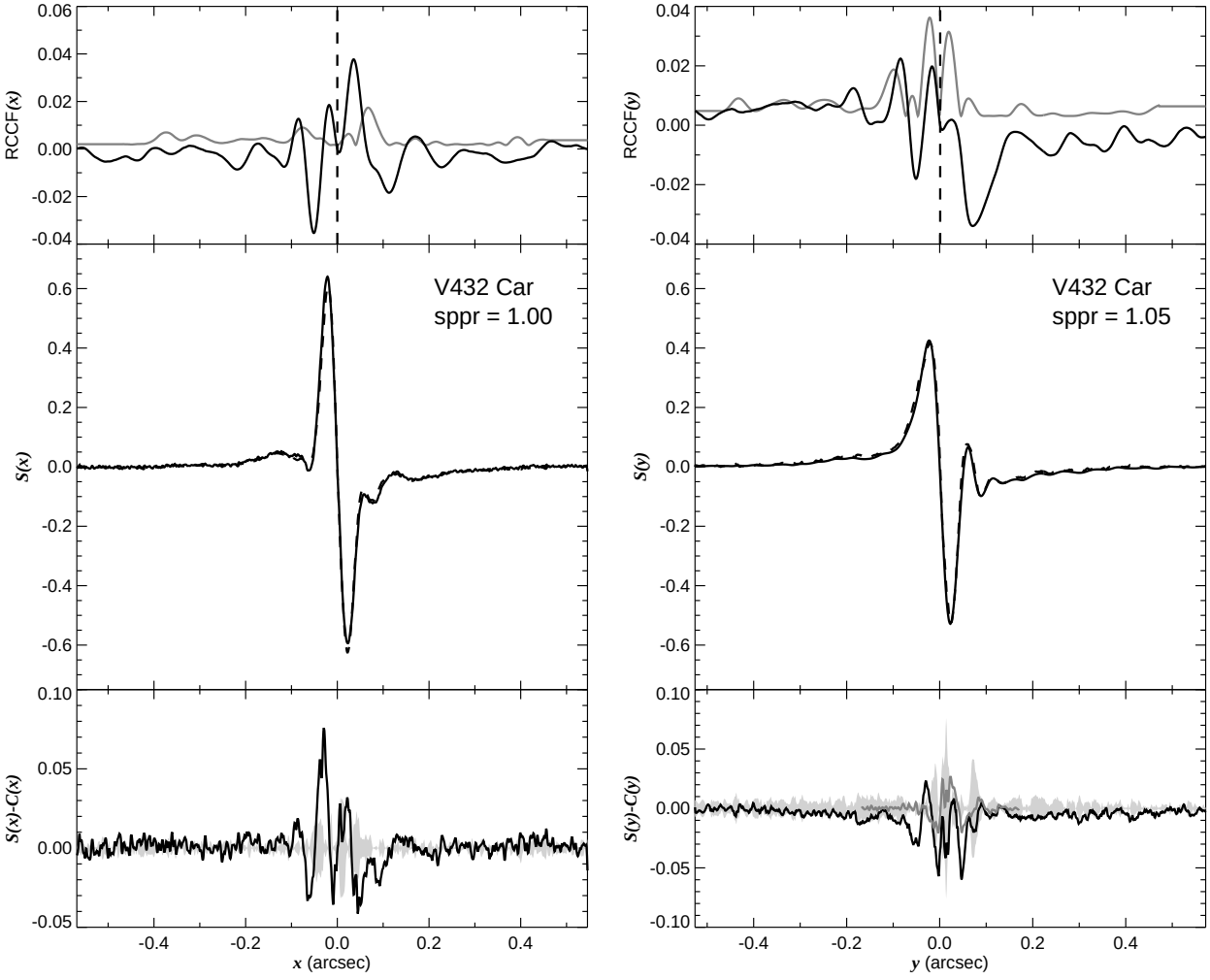

Fig. 1.183.— The FGS scans and binary detection tests for target 110840.06−604251.7 = V432 Car = Wra 751 obtained on BY 2008.9337.

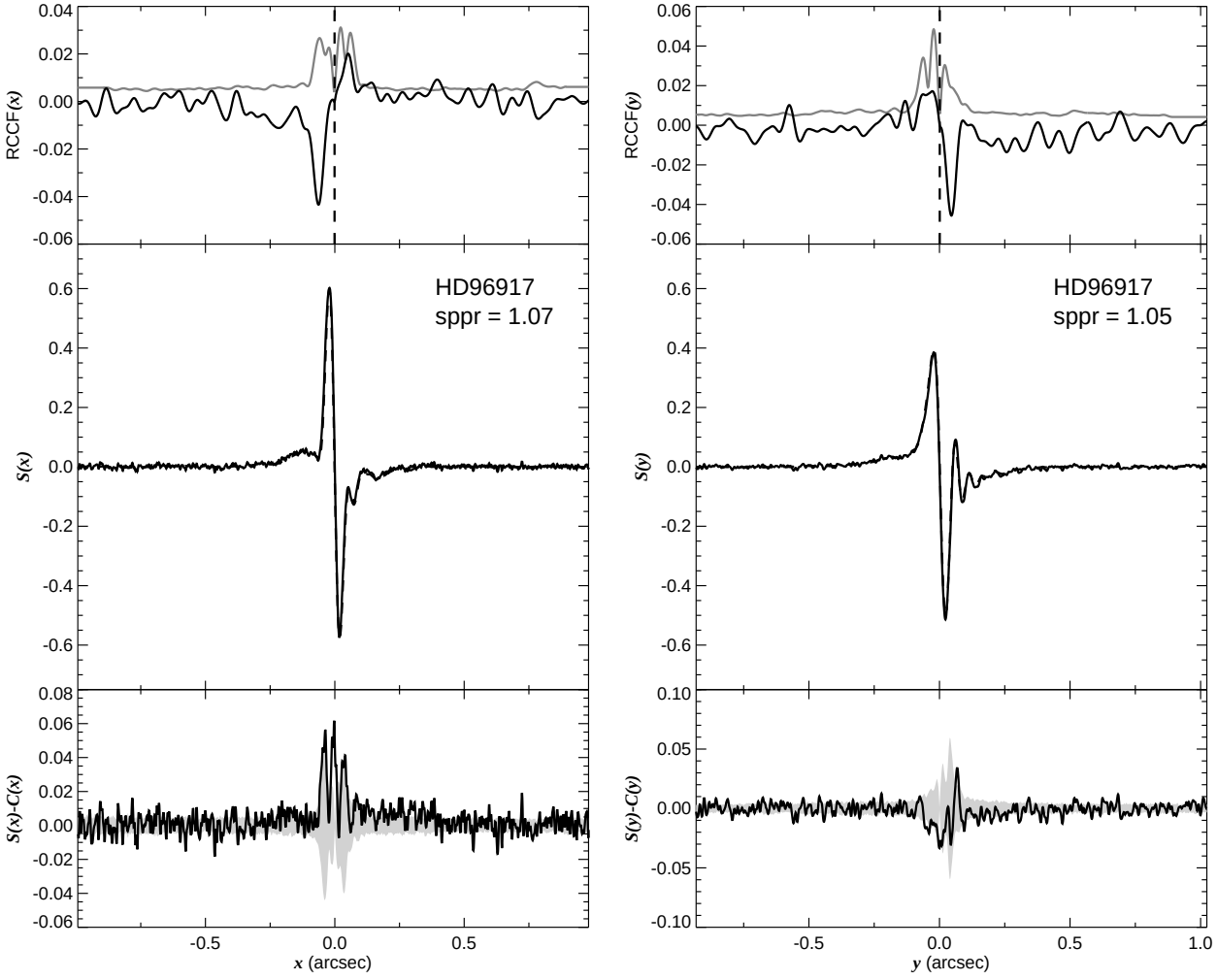

Fig. 1.184.— The FGS scans and binary detection tests for target 110842.62−570356.9 = HD96917 obtained on BY 2008.6850.

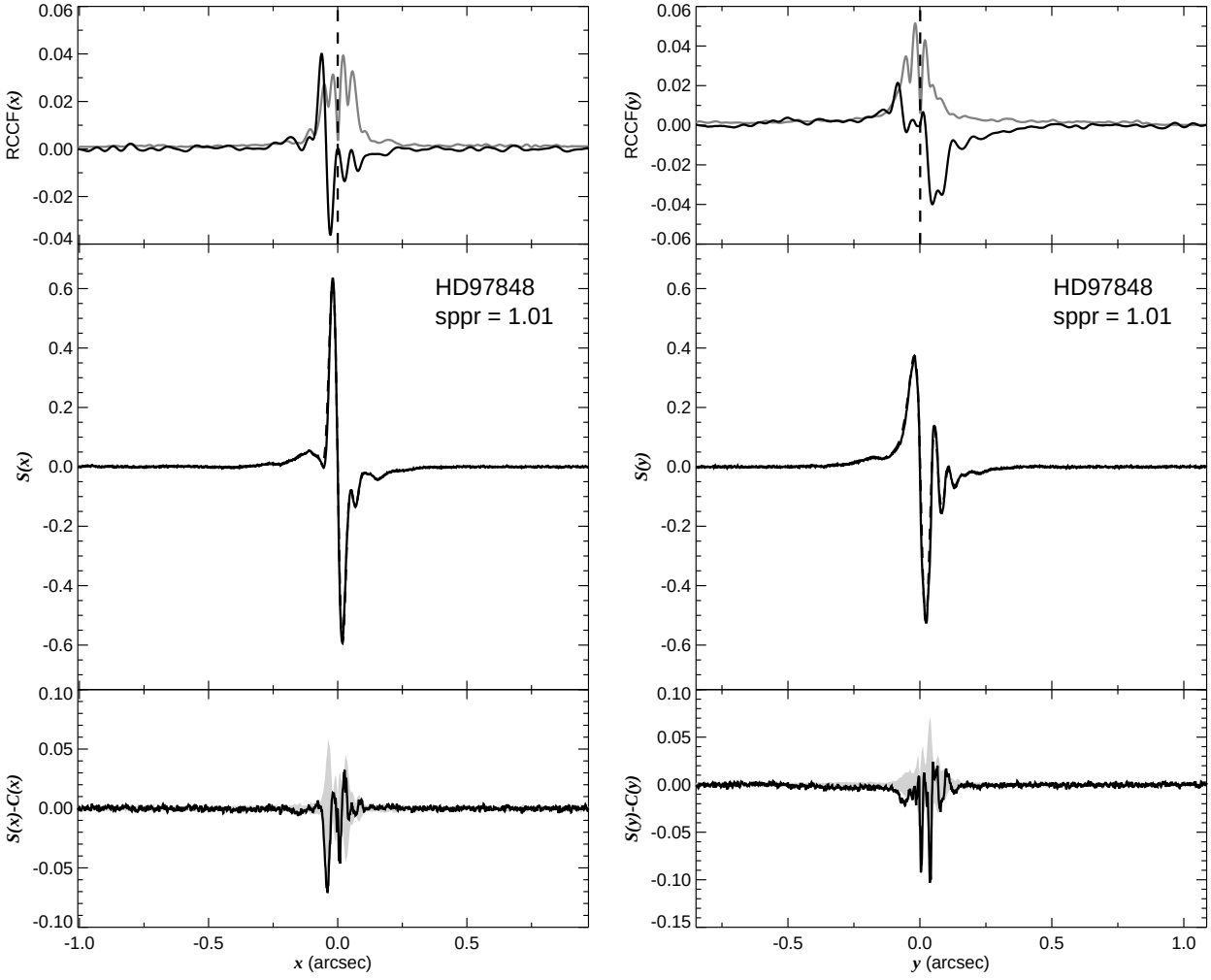

Fig. 1.185.— The FGS scans and binary detection tests for target 111431.90−590128.8 = HD97848 obtained on BY 2008.6715.

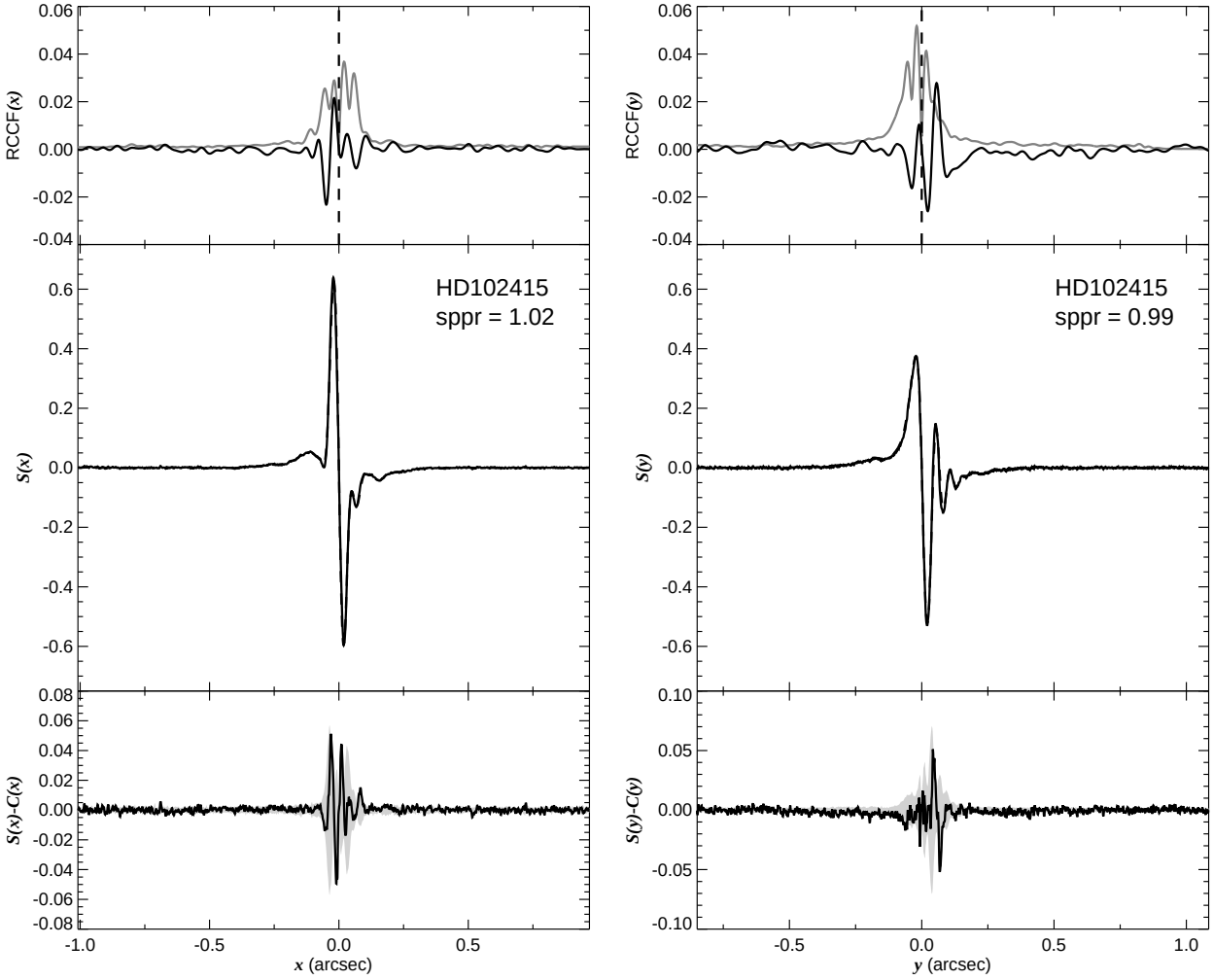

Fig. 1.186.— The FGS scans and binary detection tests for target 114654.41−612747.0 = HD102415 obtained on BY 2008.6852.

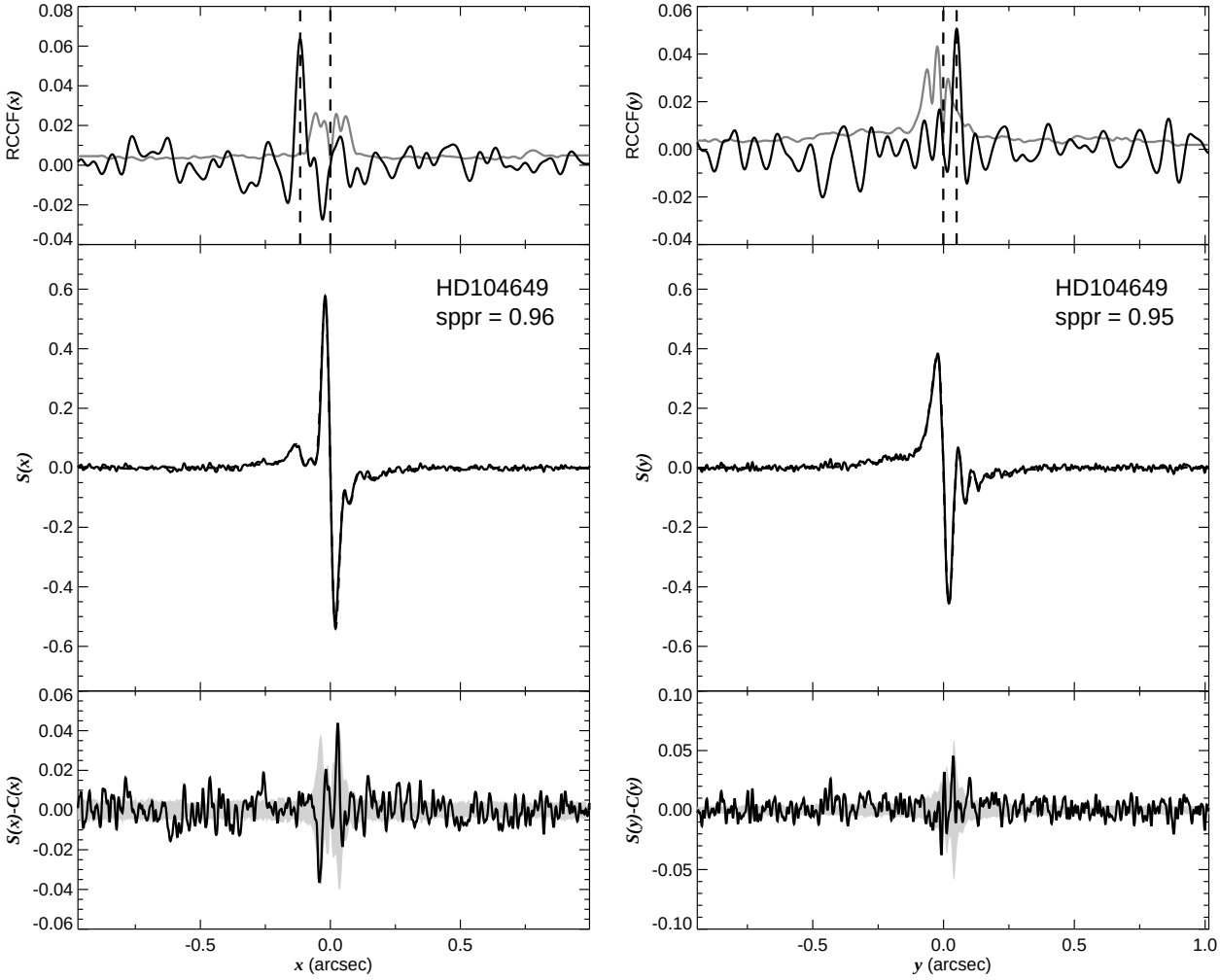

Fig. 1.187.— The FGS scans and binary detection tests for target 120258.46−624019.2 = HD104649 obtained on BY 2008.6770.

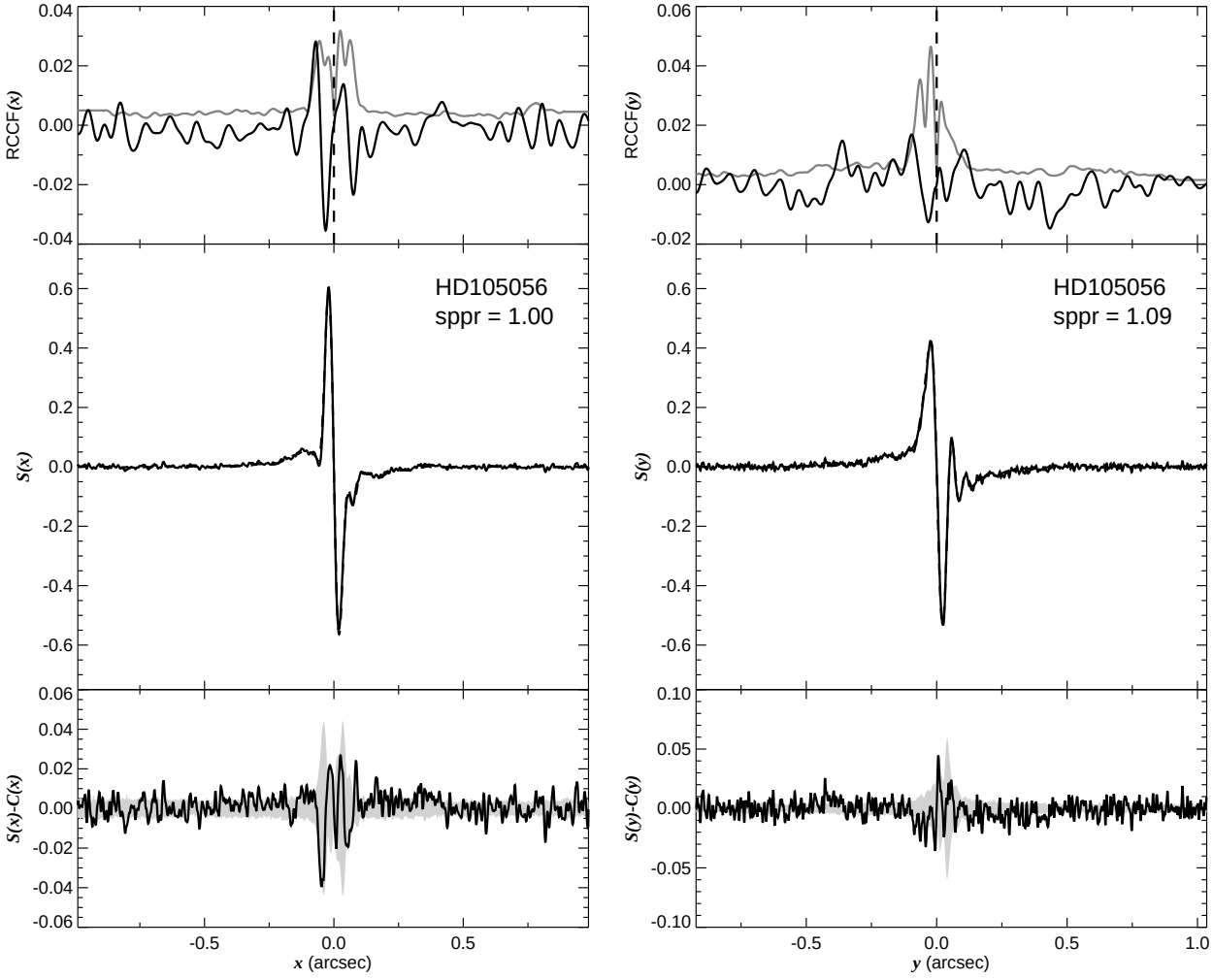

Fig. 1.188.— The FGS scans and binary detection tests for target 120549.88−693423.0 = HD105056 obtained on BY 2008.3935.

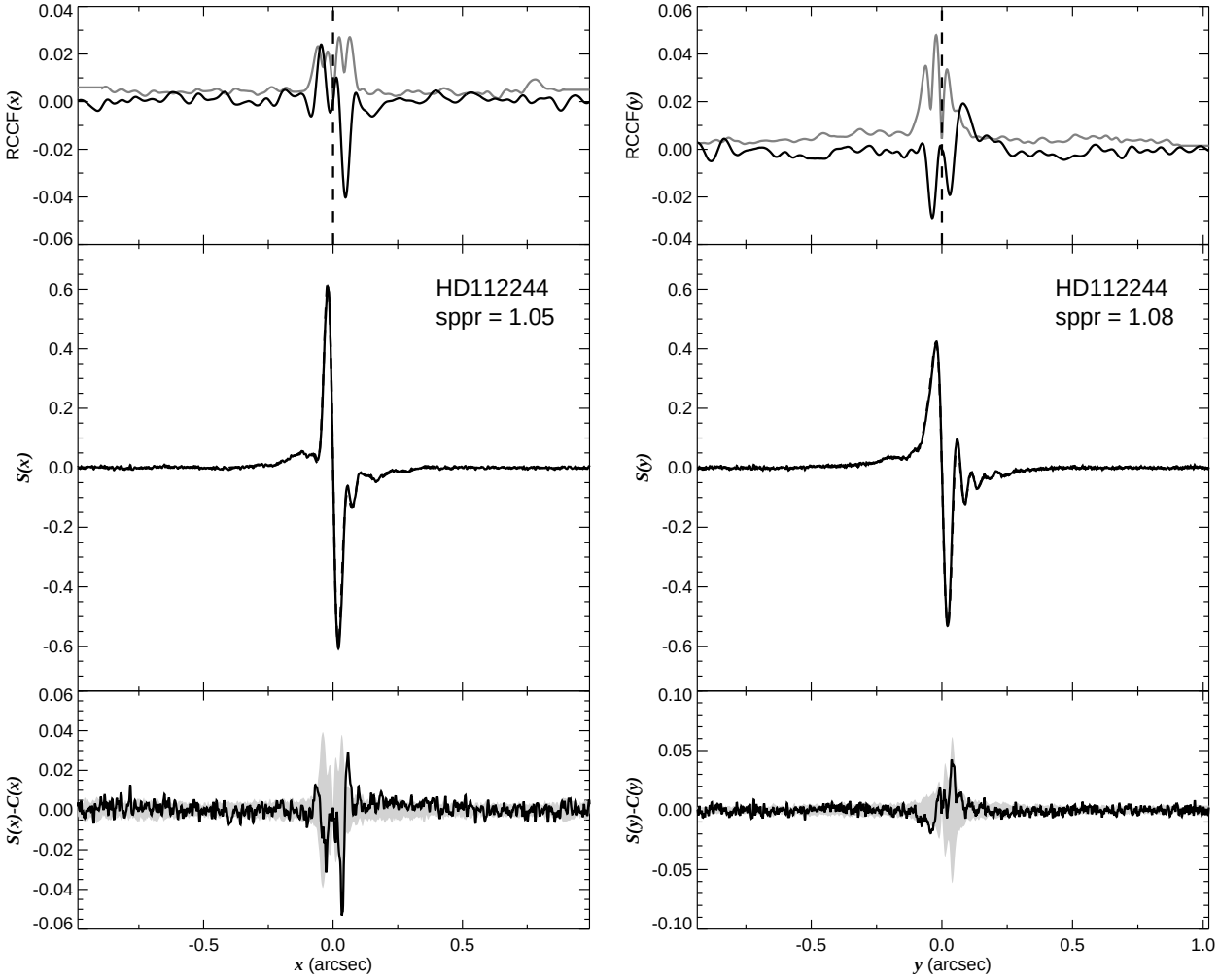

Fig. 1.189.— The FGS scans and binary detection tests for target 125557.13−565008.9 = HD112244 obtained on BY 2008.6953.

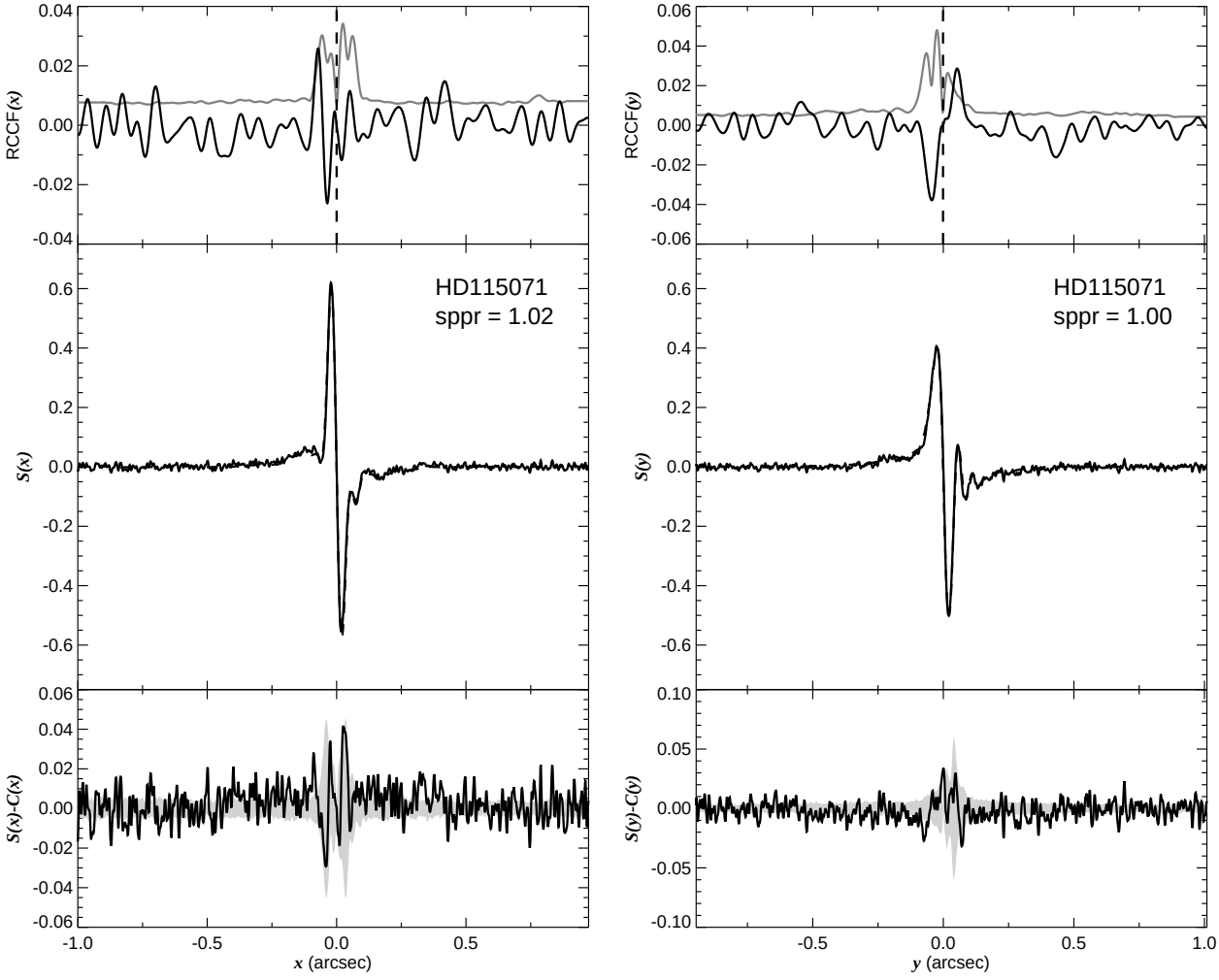

Fig. 1.190.— The FGS scans and binary detection tests for target 131604.80−623501.5 = HD115071 obtained on BY 2008.7021.

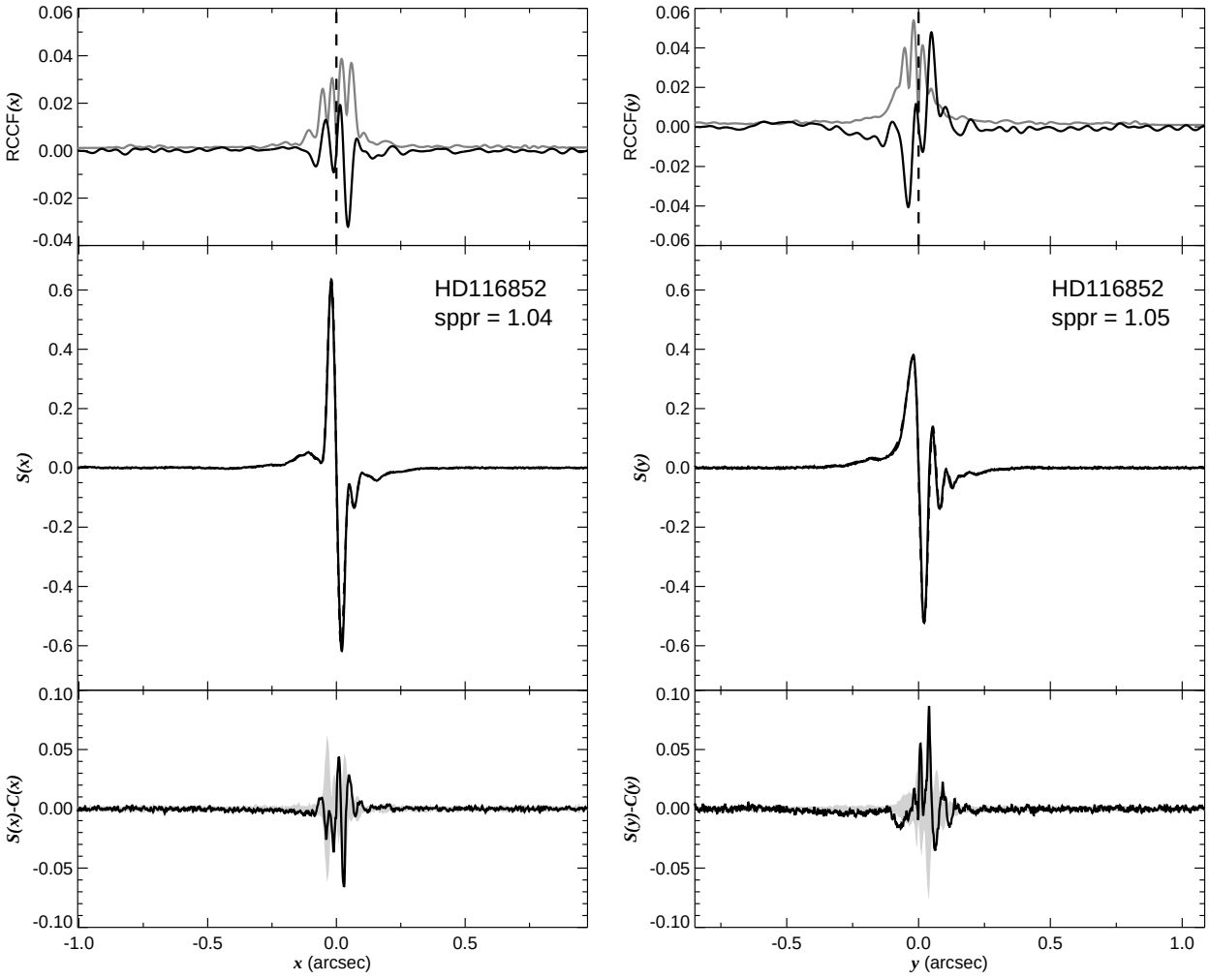

Fig. 1.191.— The FGS scans and binary detection tests for target 133023.52−785120.5 = HD116852 obtained on BY 2008.6951.

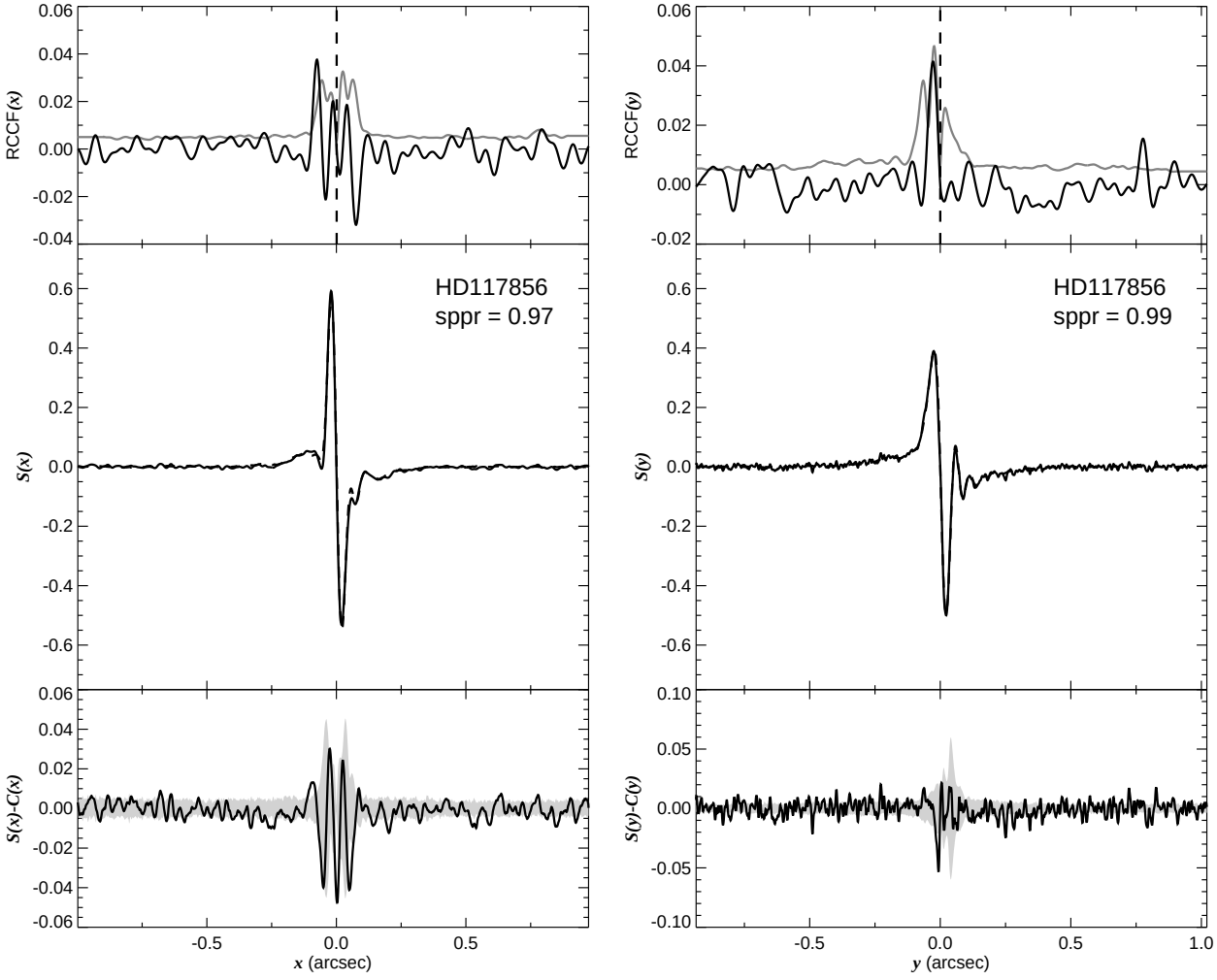

Fig. 1.192.— The FGS scans and binary detection tests for target 133443.41−632007.6 = HD117856 obtained on BY 2008.7071.

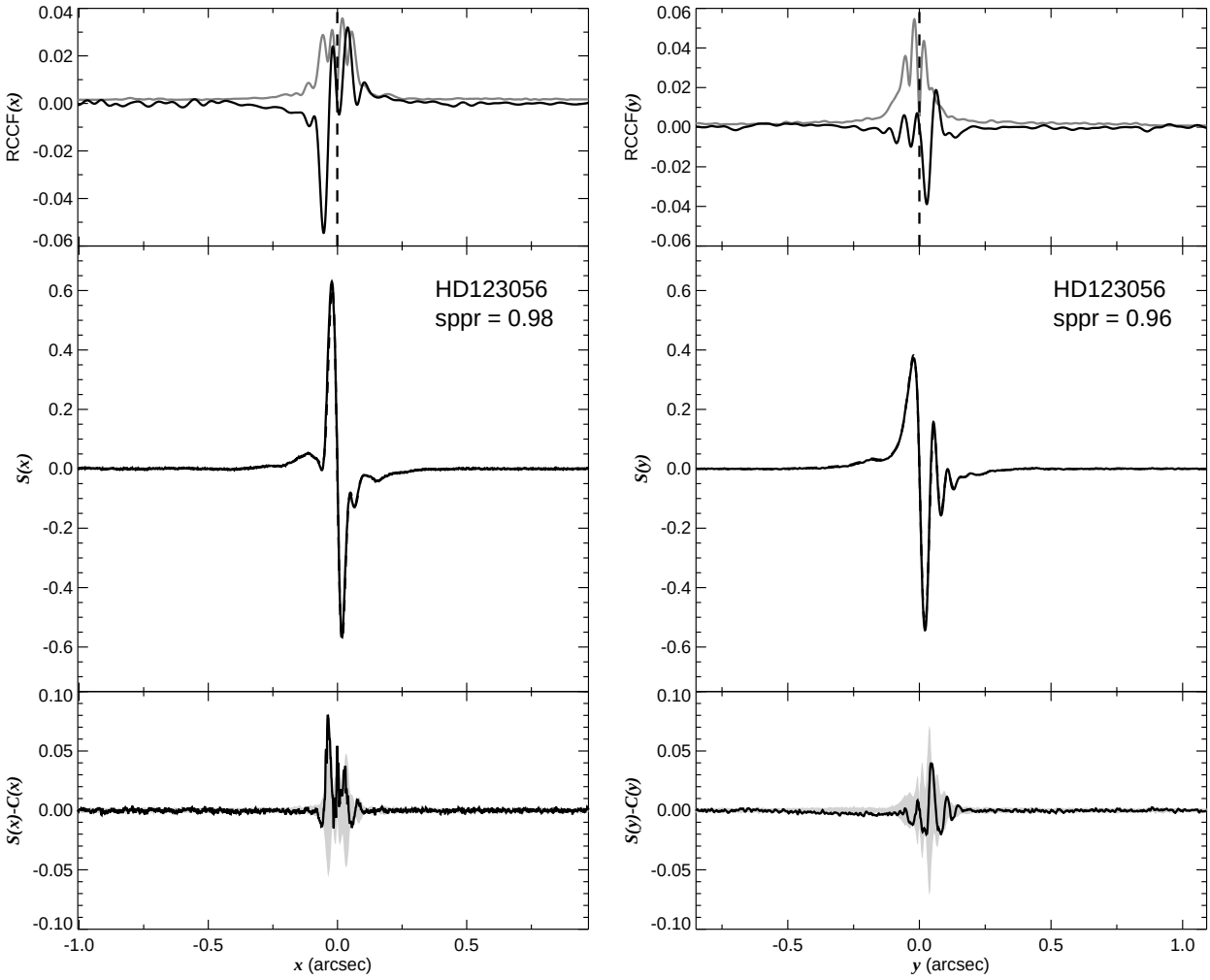

Fig. 1.193.— The FGS scans and binary detection tests for target 140725.64−602814.1 = HD123056 obtained on BY 2008.6824.

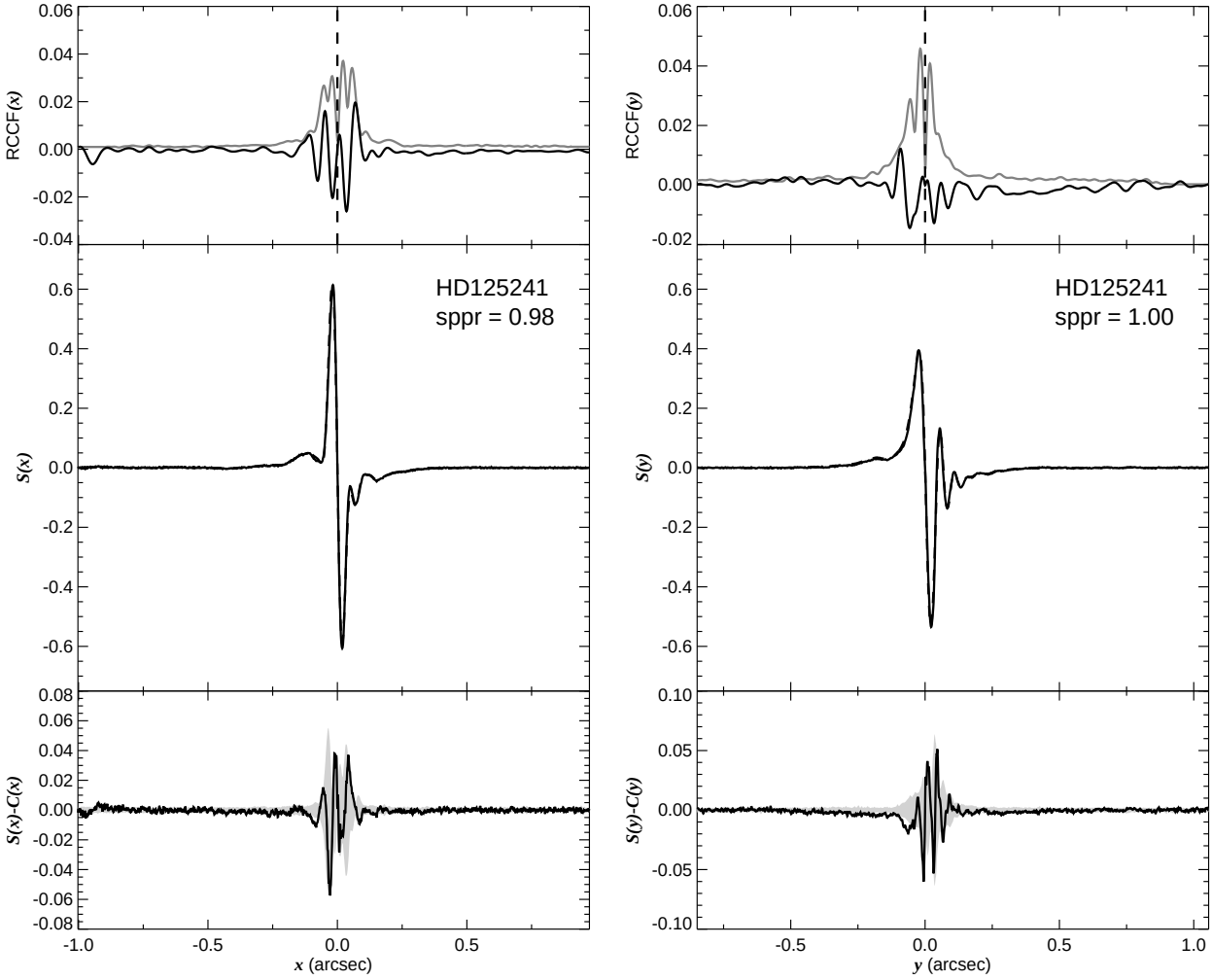

Fig. 1.194.— The FGS scans and binary detection tests for target 142022.78−605322.2 = HD125241 obtained on BY 2007.6281.

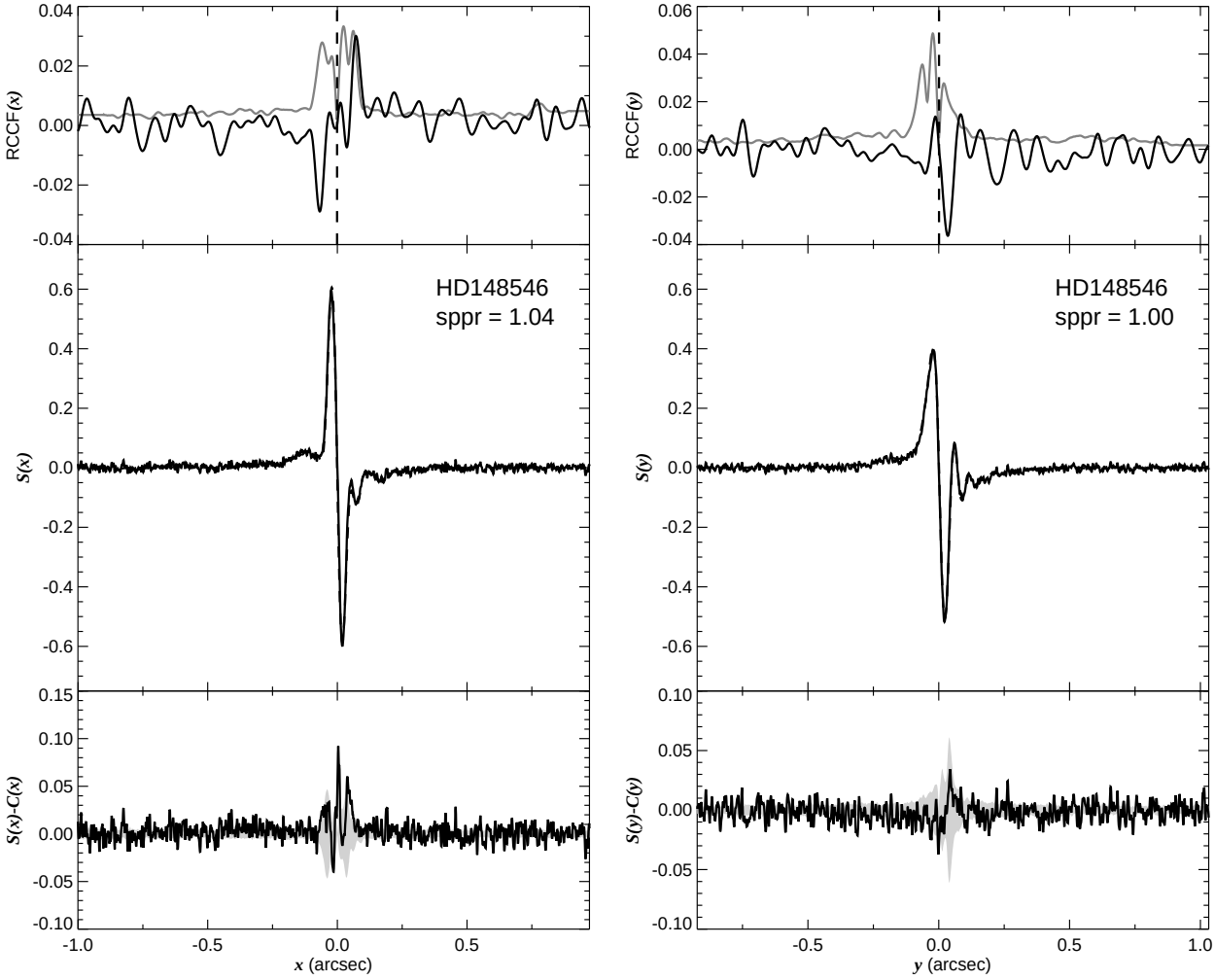

Fig. 1.195.— The FGS scans and binary detection tests for target 163023.31−375821.2 = HD148546 obtained on BY 2008.4228.

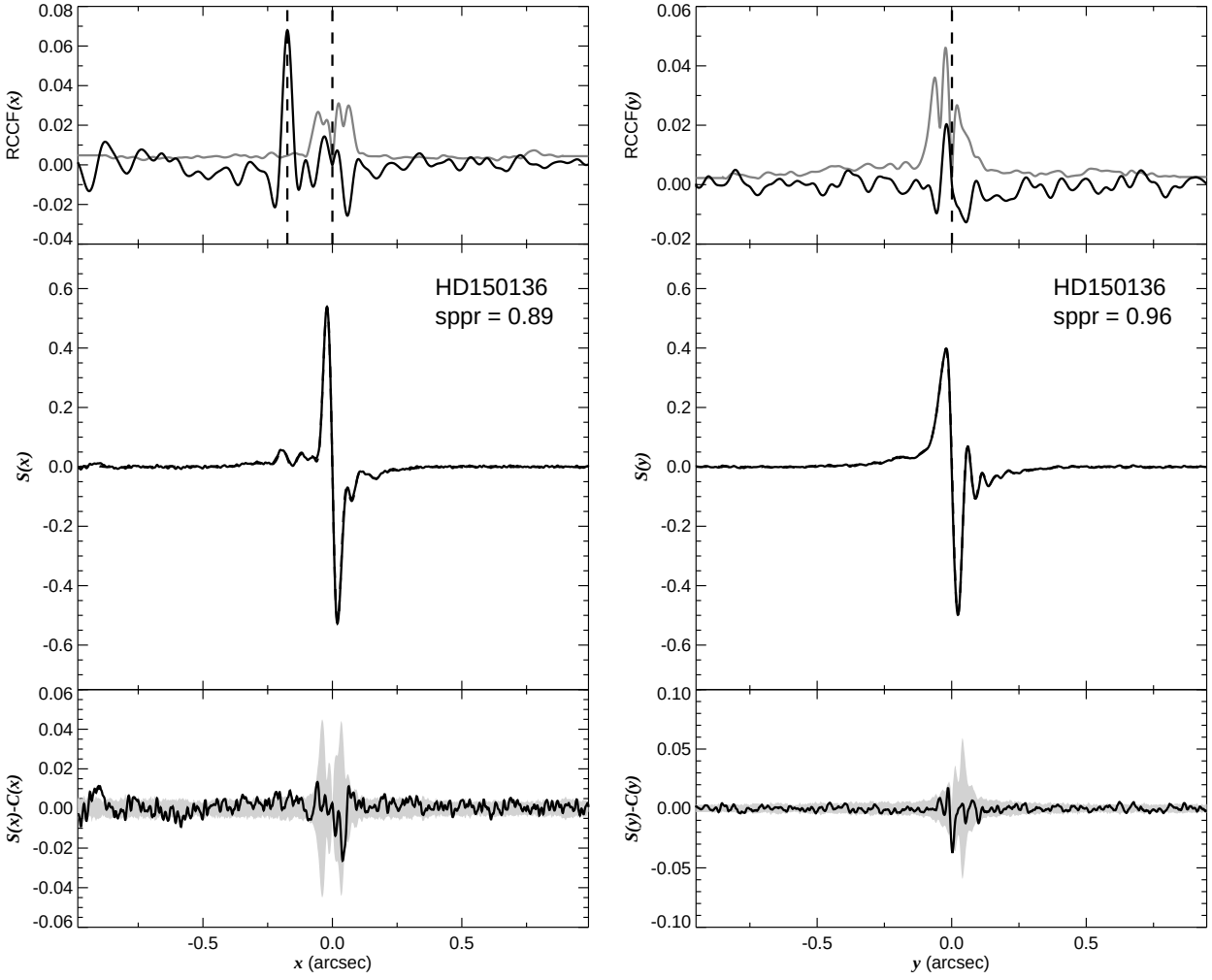

Fig. 1.196.— The FGS scans and binary detection tests for target 164120.41−484546.6 = HD150136 obtained on BY 2008.1316.

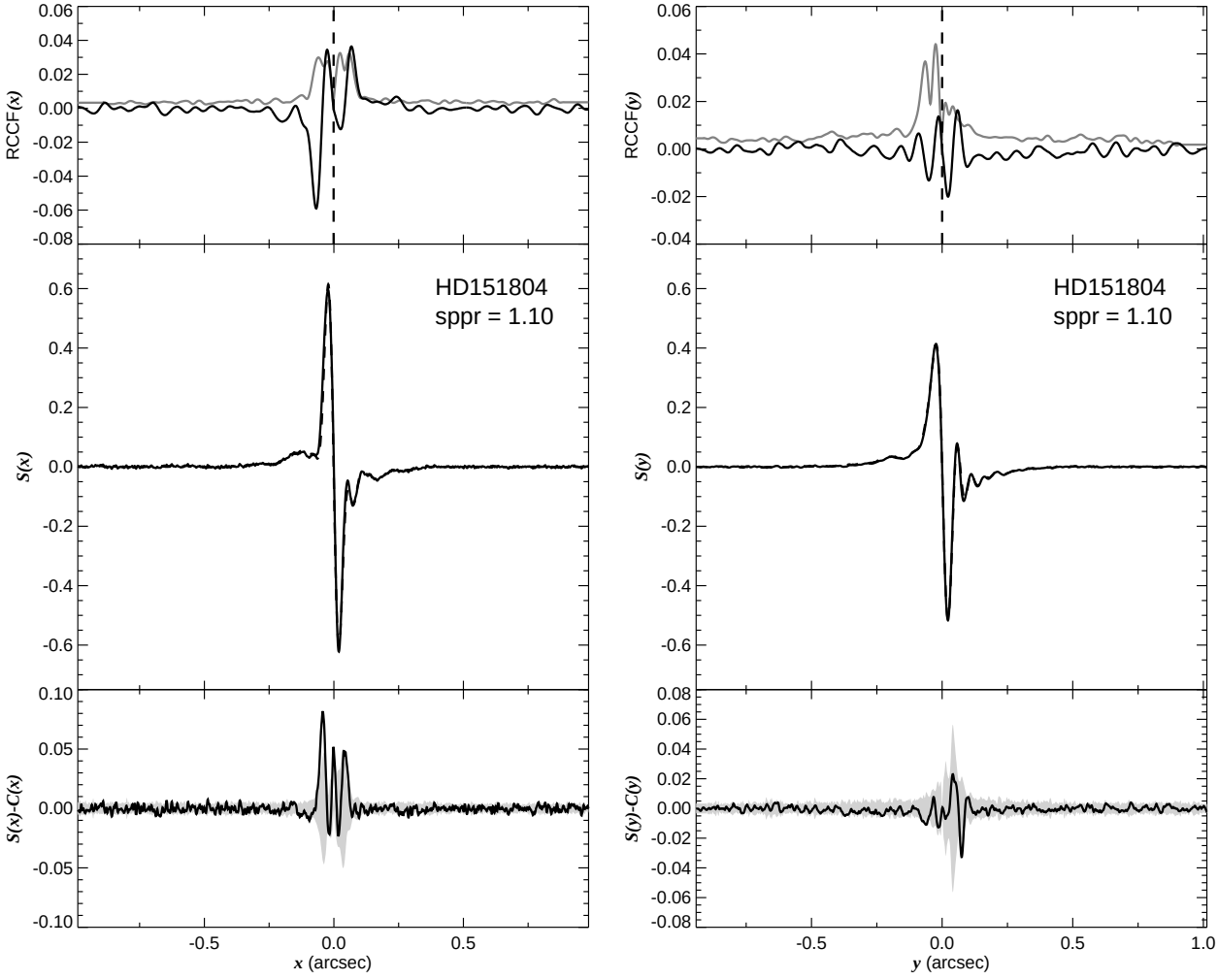

Fig. 1.197.— The FGS scans and binary detection tests for target 165133.72−411349.9 = HD151804 obtained on BY 2008.1996.

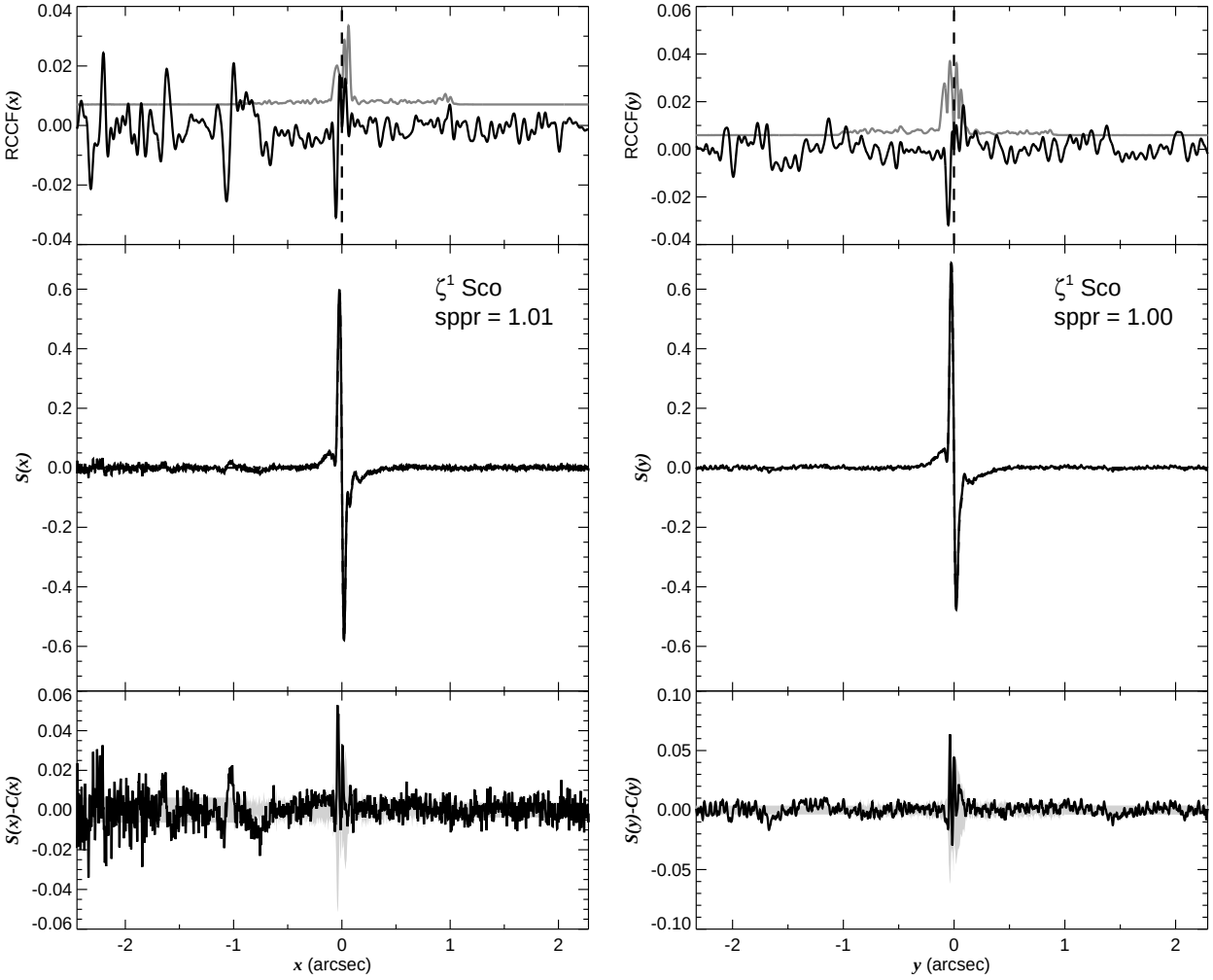

Fig. 1.198.— The FGS scans and binary detection tests for target 165359.73−422143.3 = HD152236 obtained on BY 2009.2751.

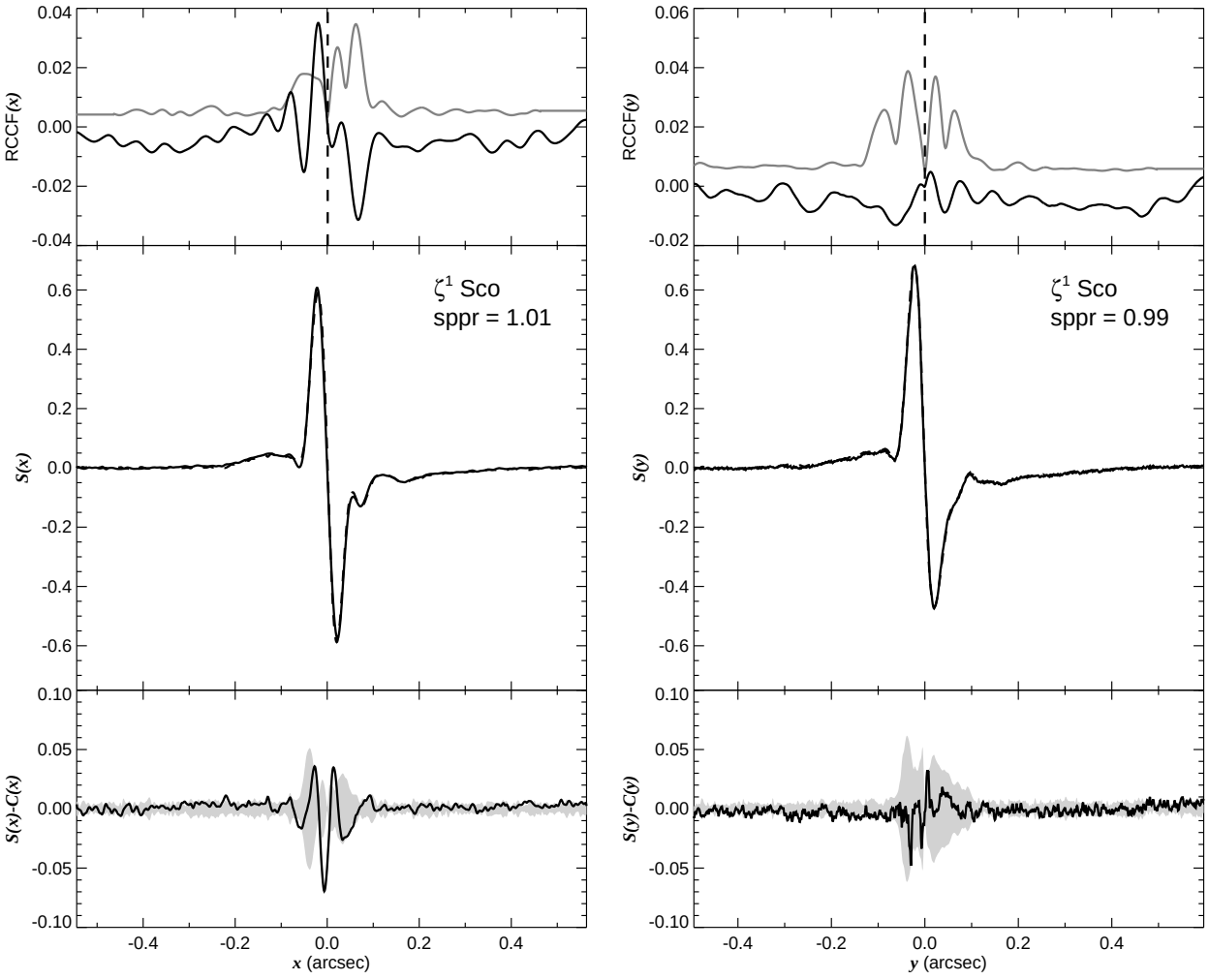

Fig. 1.199.— The FGS scans and binary detection tests for target 165359.73−422143.3 = HD152236 obtained on BY 2009.2751.

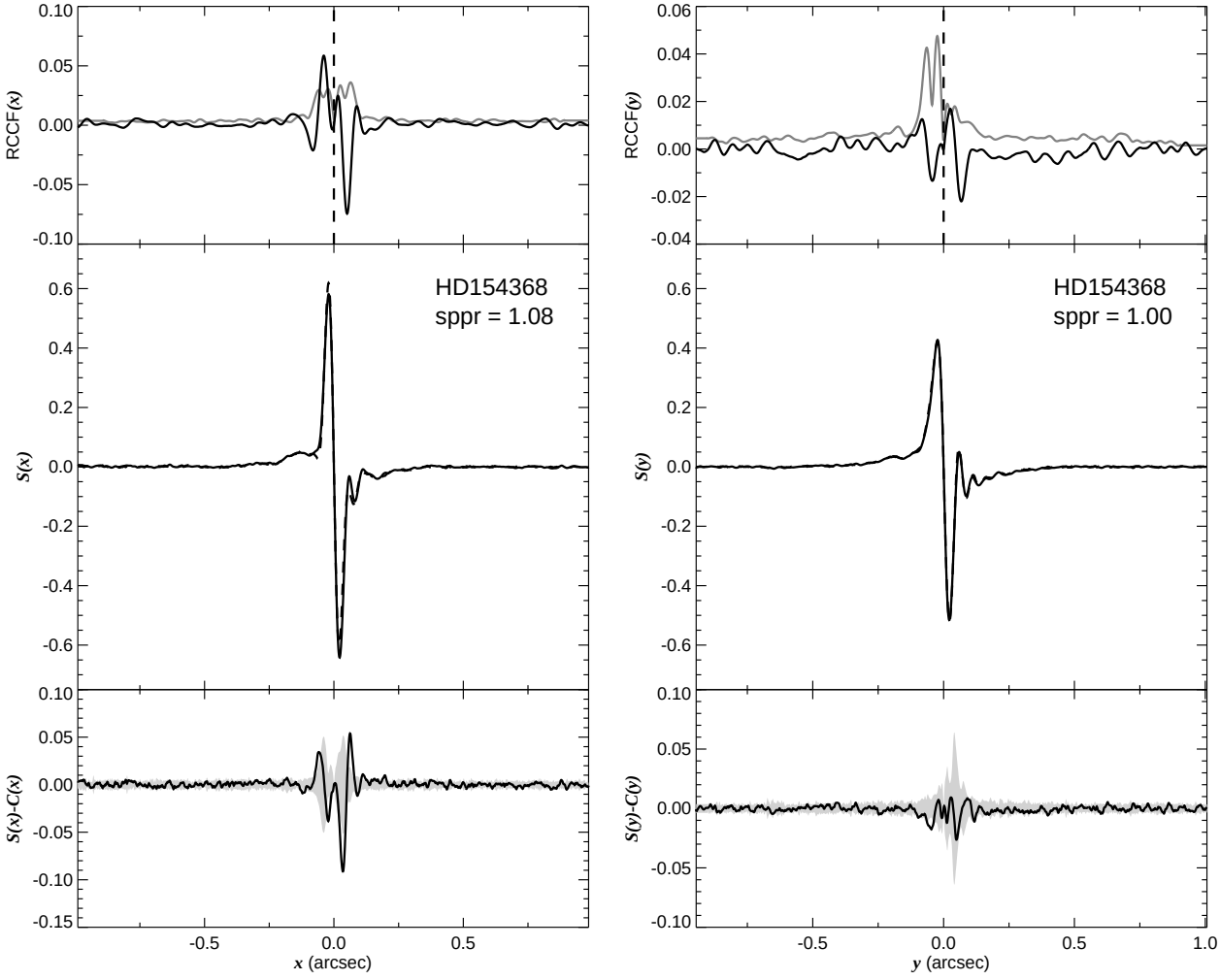

Fig. 1.200.— The FGS scans and binary detection tests for target 170628.37−352703.8 = HD154368 obtained on BY 2008.4367.

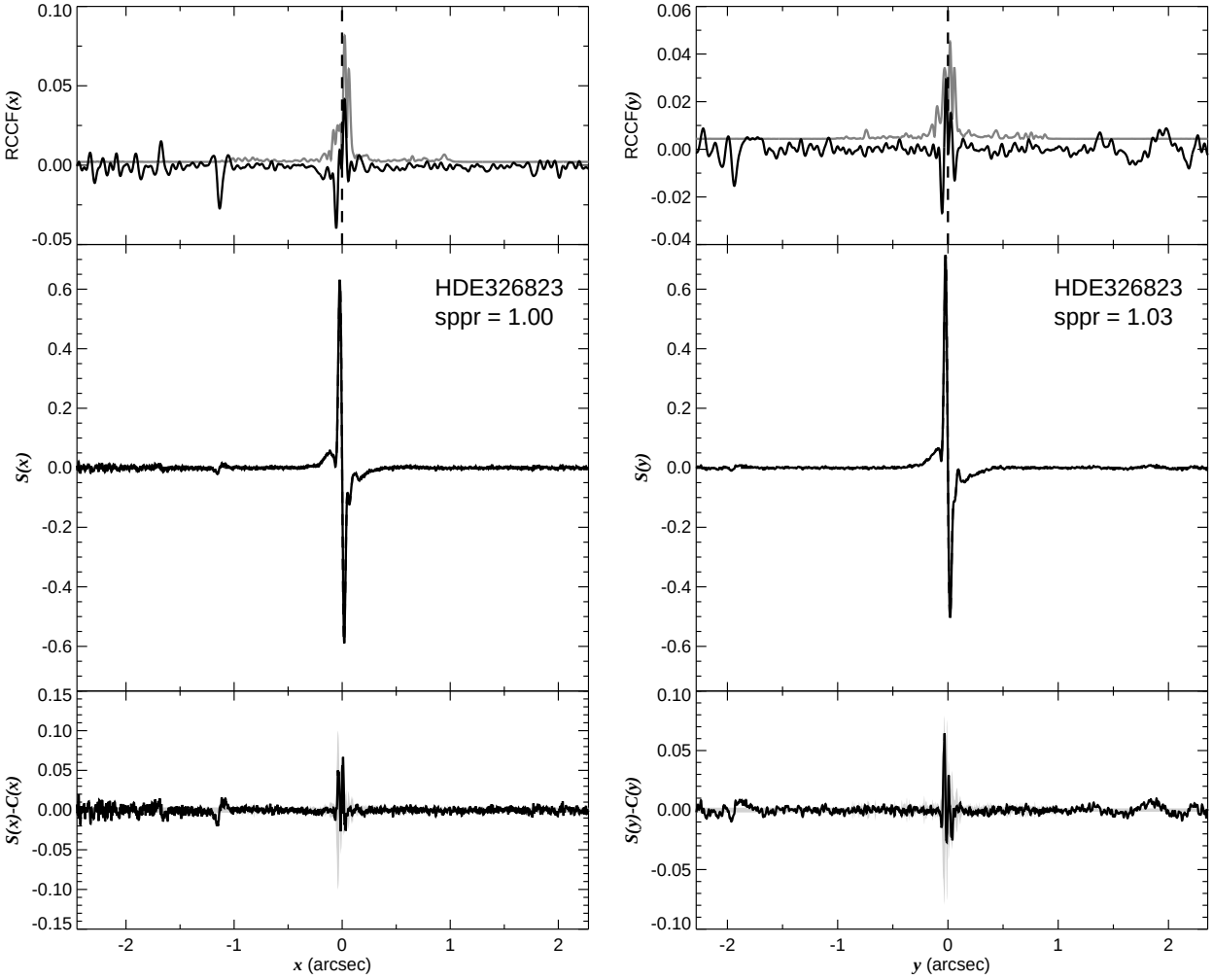

Fig. 1.201.— The FGS scans and binary detection tests for target 170653.91−423639.7 = HDE326823 obtained on BY 2009.2895.

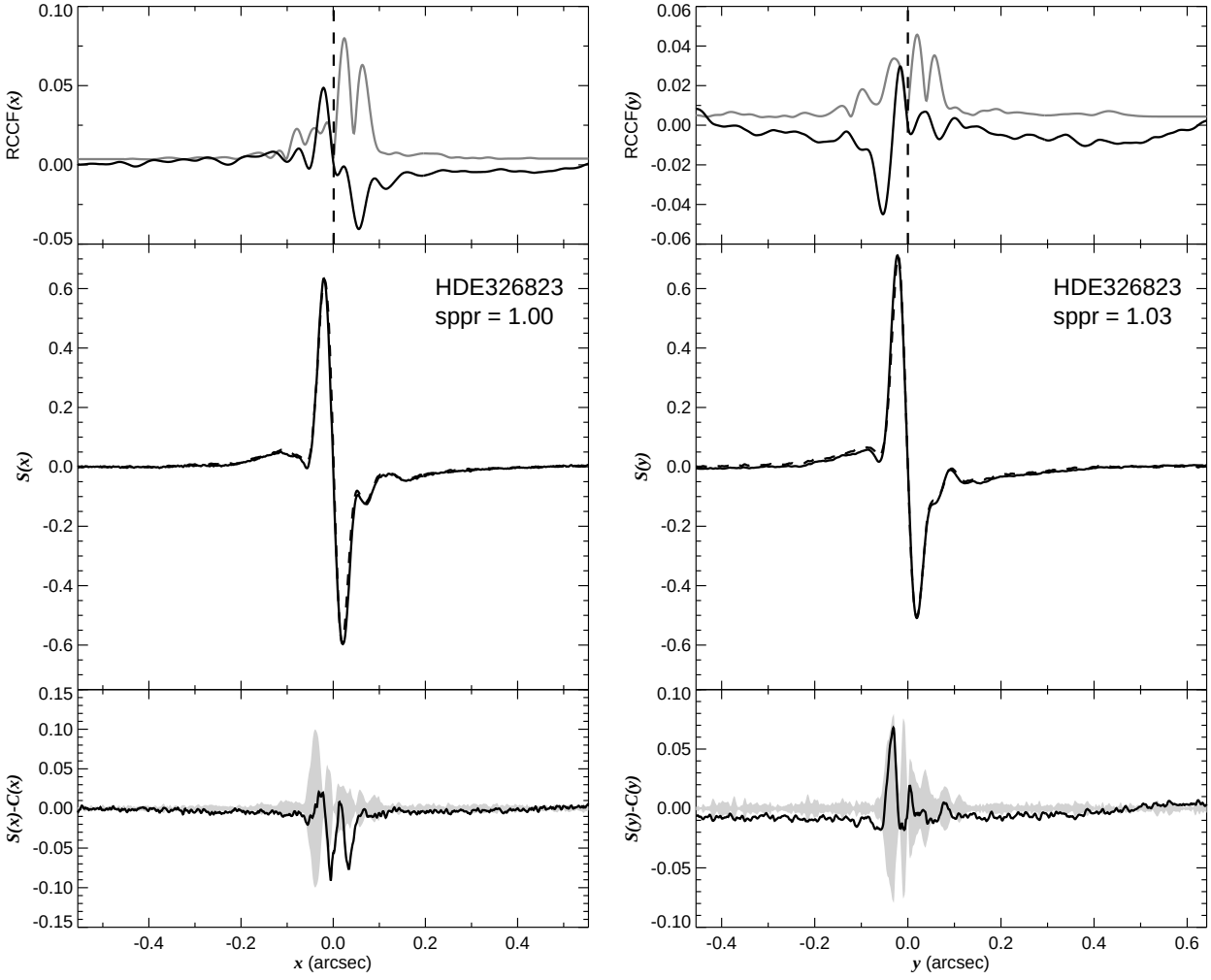

Fig. 1.202.— The FGS scans and binary detection tests for target 170653.91−423639.7 = HDE326823 obtained on BY 2009.2895.

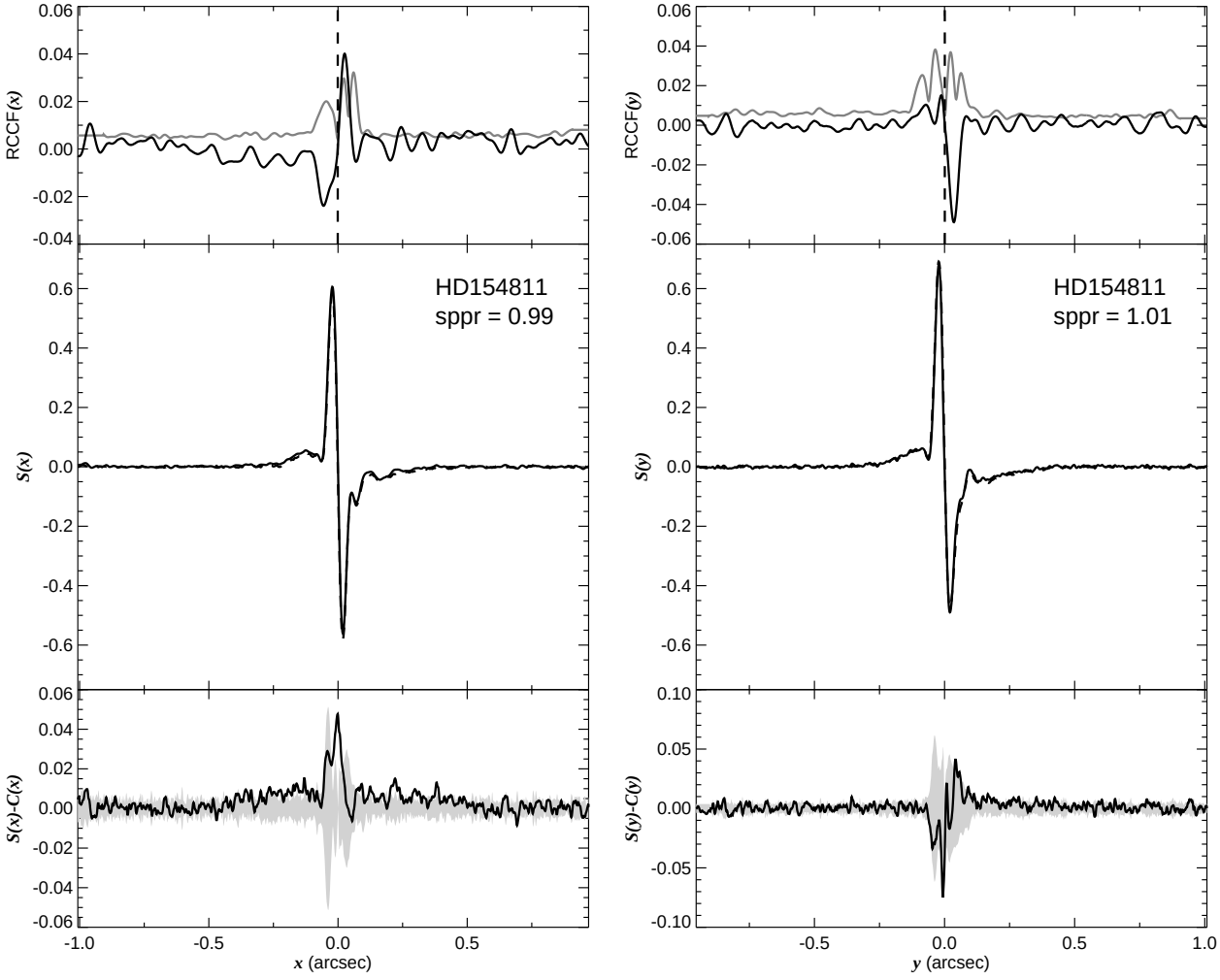

Fig. 1.203.— The FGS scans and binary detection tests for target 170953.09−470153.2 = HD154811 obtained on BY 2009.5396.

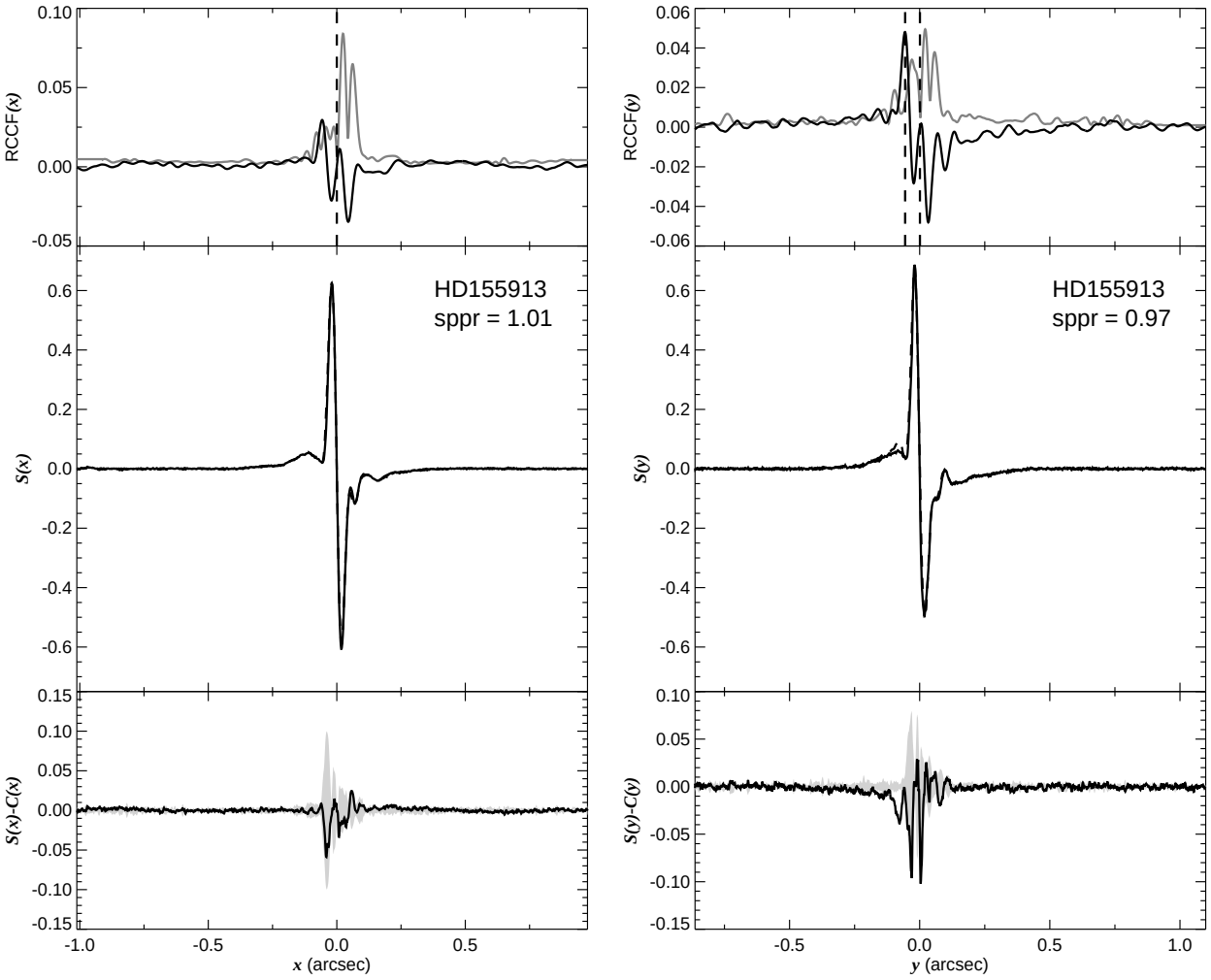

Fig. 1.204.— The FGS scans and binary detection tests for target 171626.34−424004.1 = HD155913 obtained on BY 2009.3593.

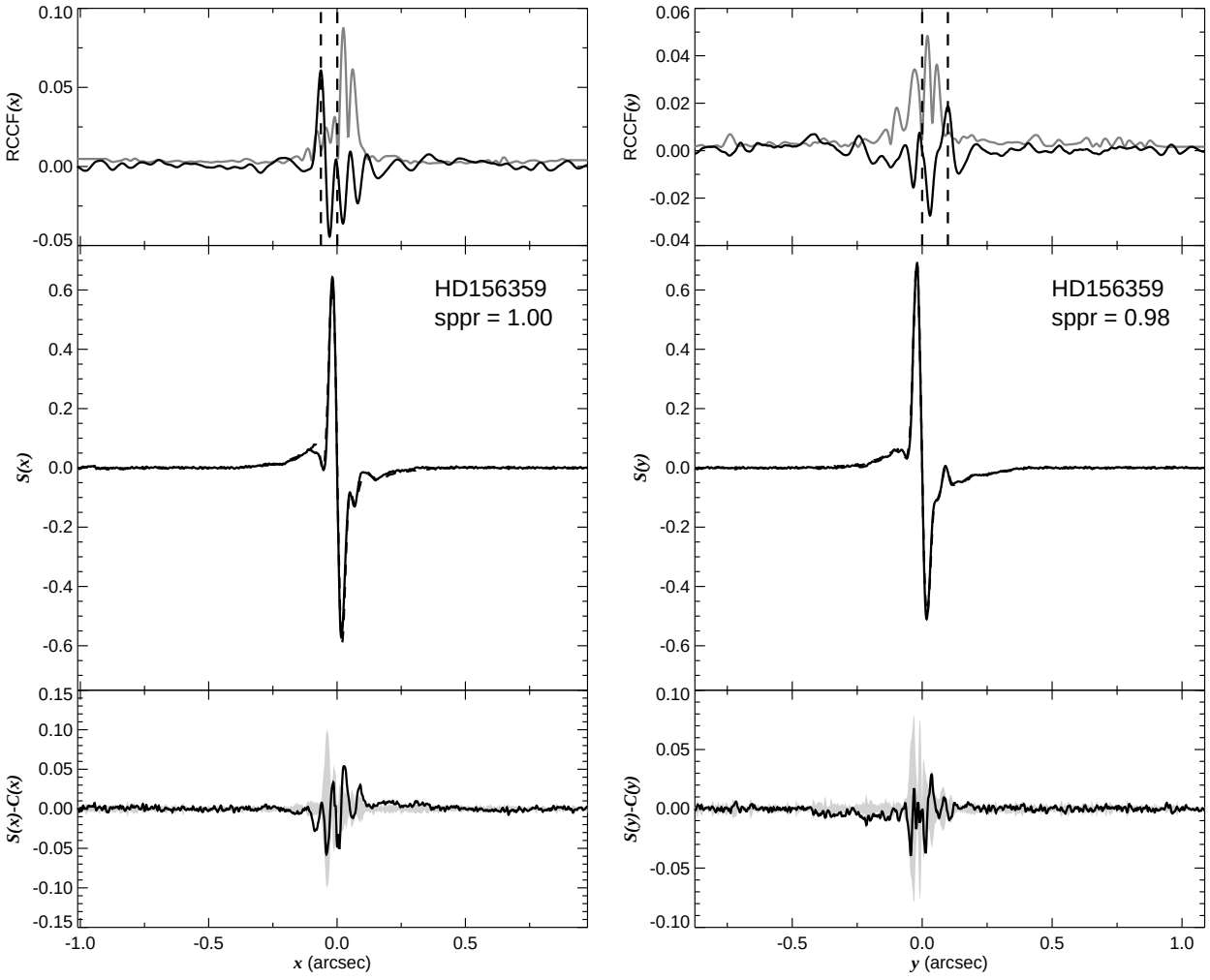

Fig. 1.205.— The FGS scans and binary detection tests for target 172118.73−625505.4 = HD156359 obtained on BY 2009.5421.

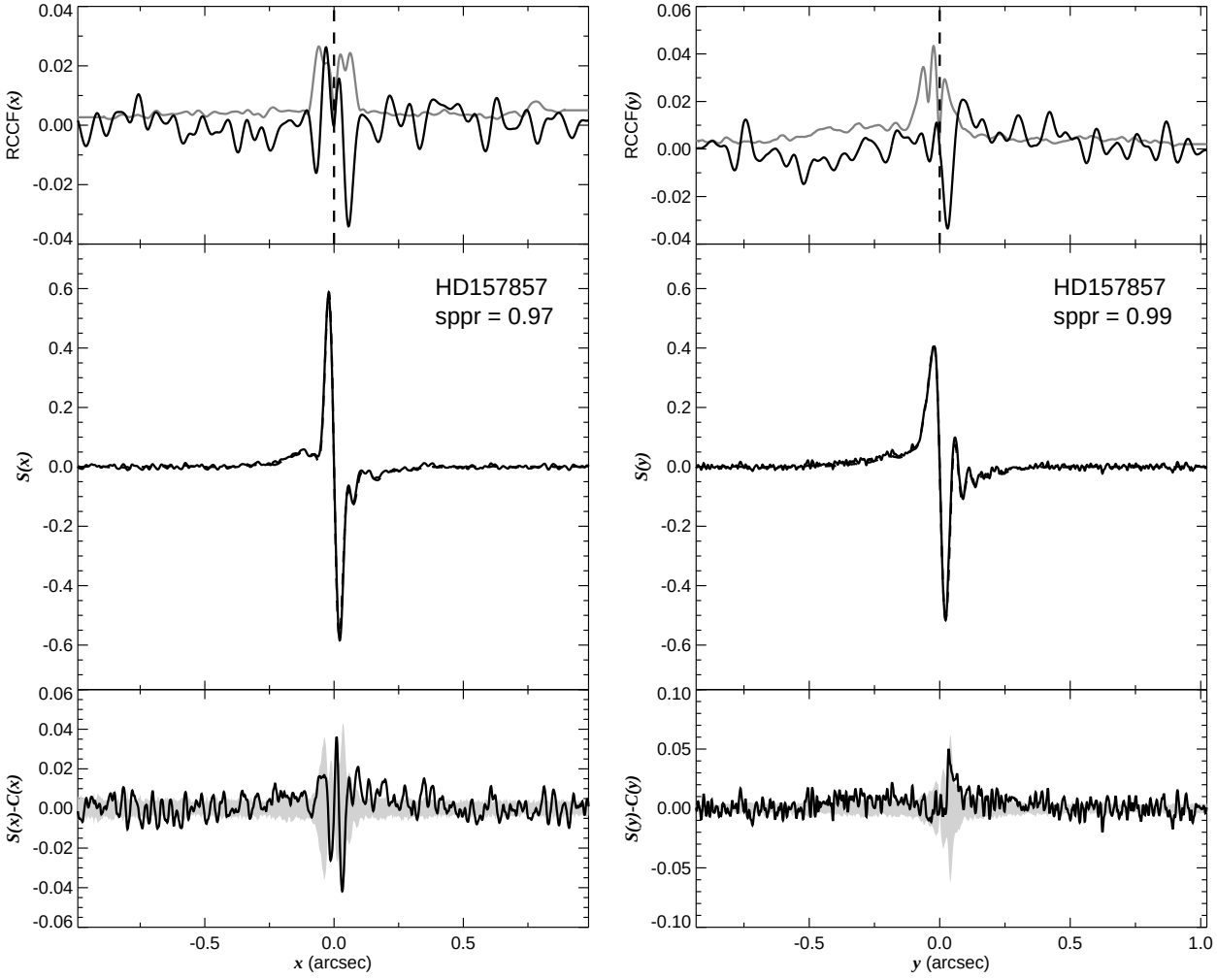

Fig. 1.206.— The FGS scans and binary detection tests for target 172617.33−105934.8 = HD157857 obtained on BY 2008.1918.

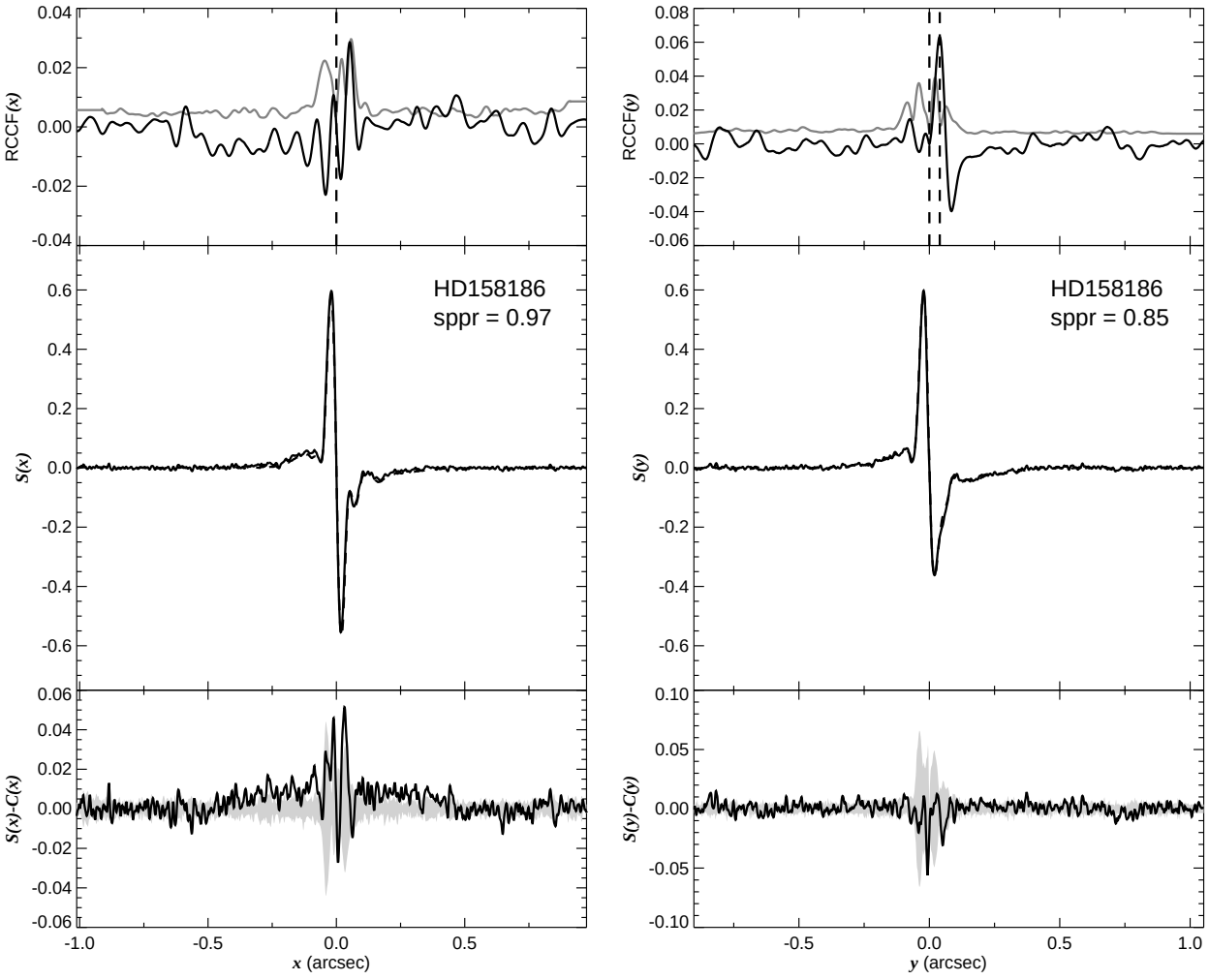

Fig. 1.207.— The FGS scans and binary detection tests for target 172912.93−313203.4 = HD158186 obtained on BY 2009.2949.

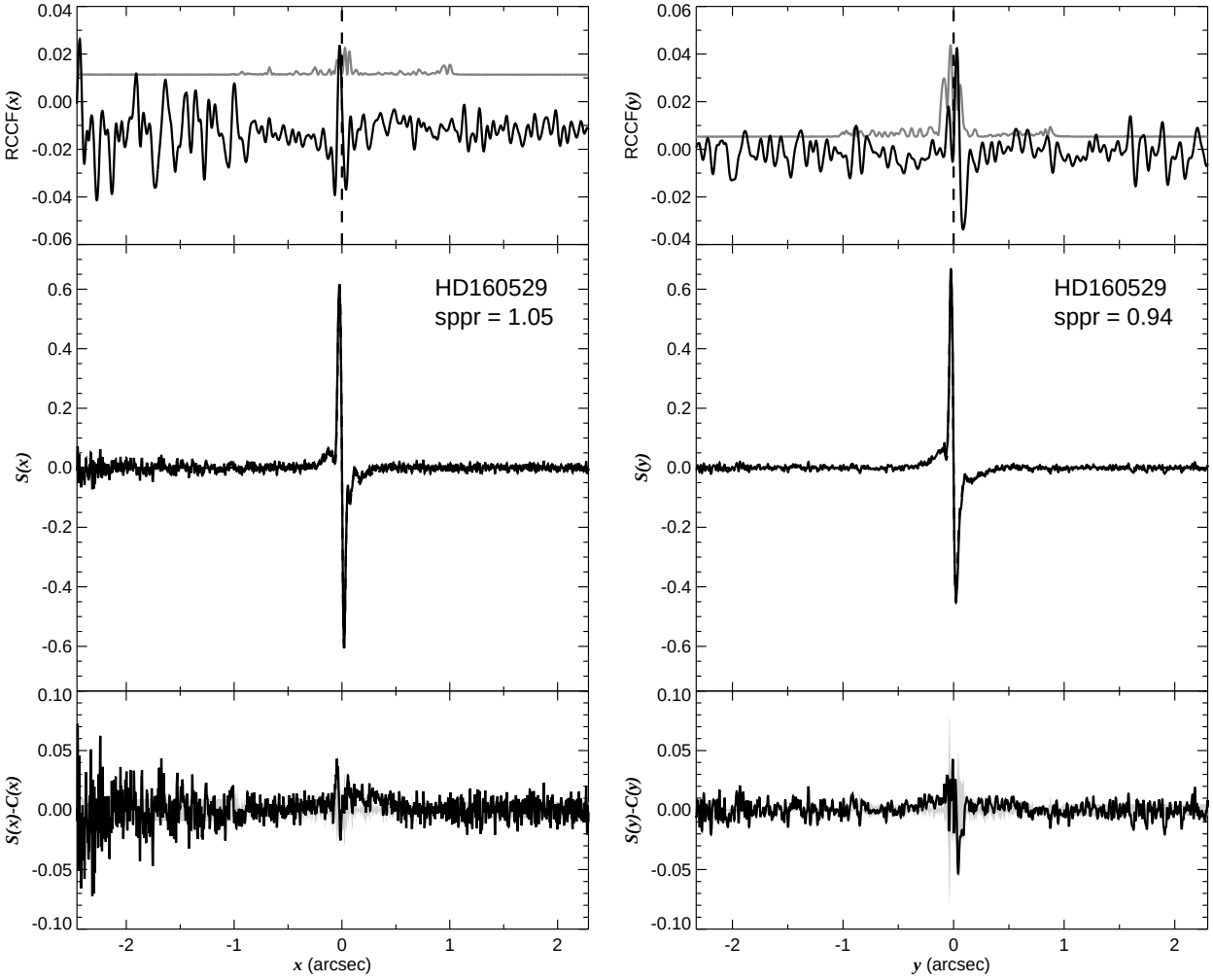

Fig. 1.208.— The FGS scans and binary detection tests for target 174159.03−333013.7 = HD160529 obtained on BY 2009.2643.

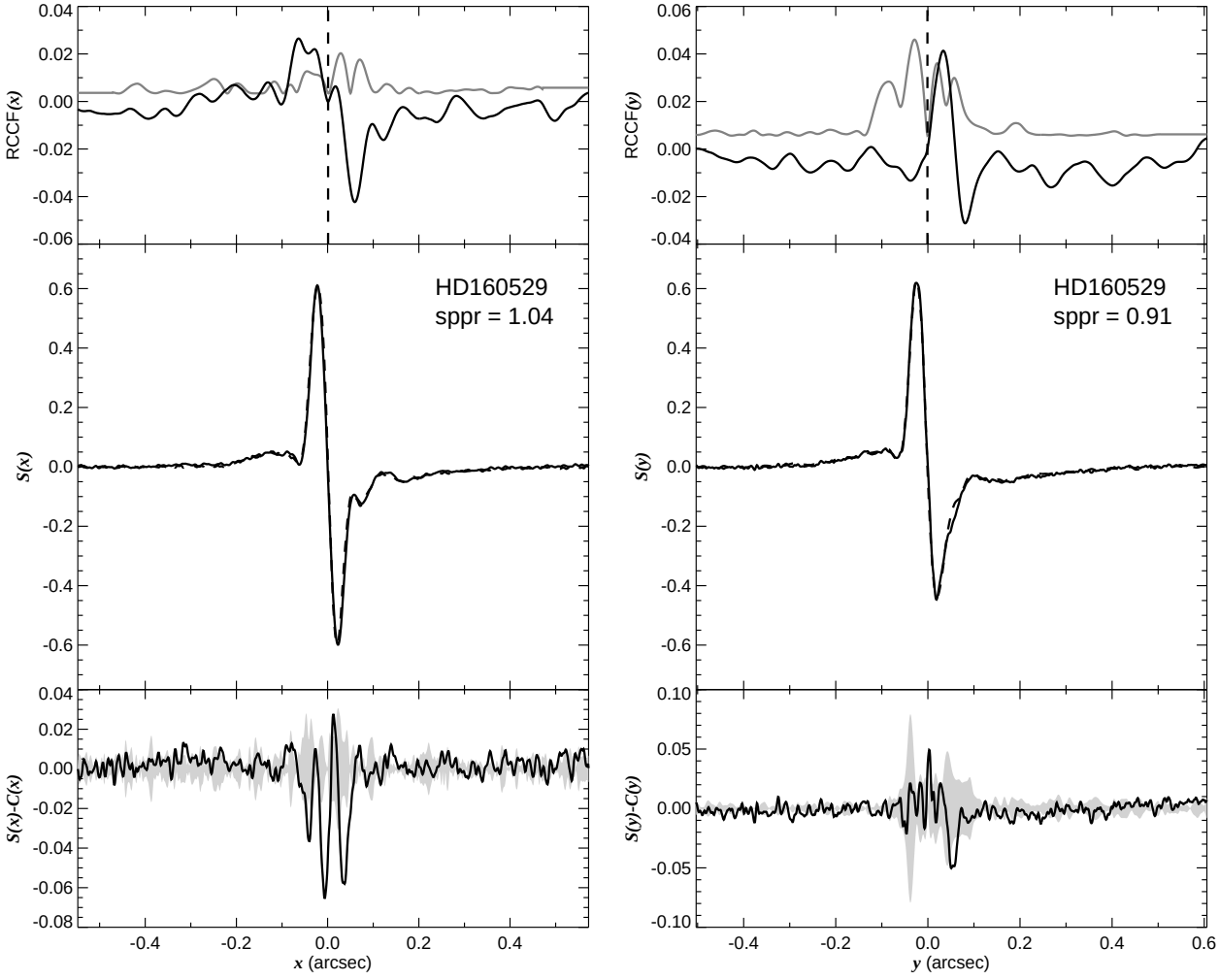

Fig. 1.209.— The FGS scans and binary detection tests for target 174159.03−333013.7 = HD160529 obtained on BY 2009.2643.

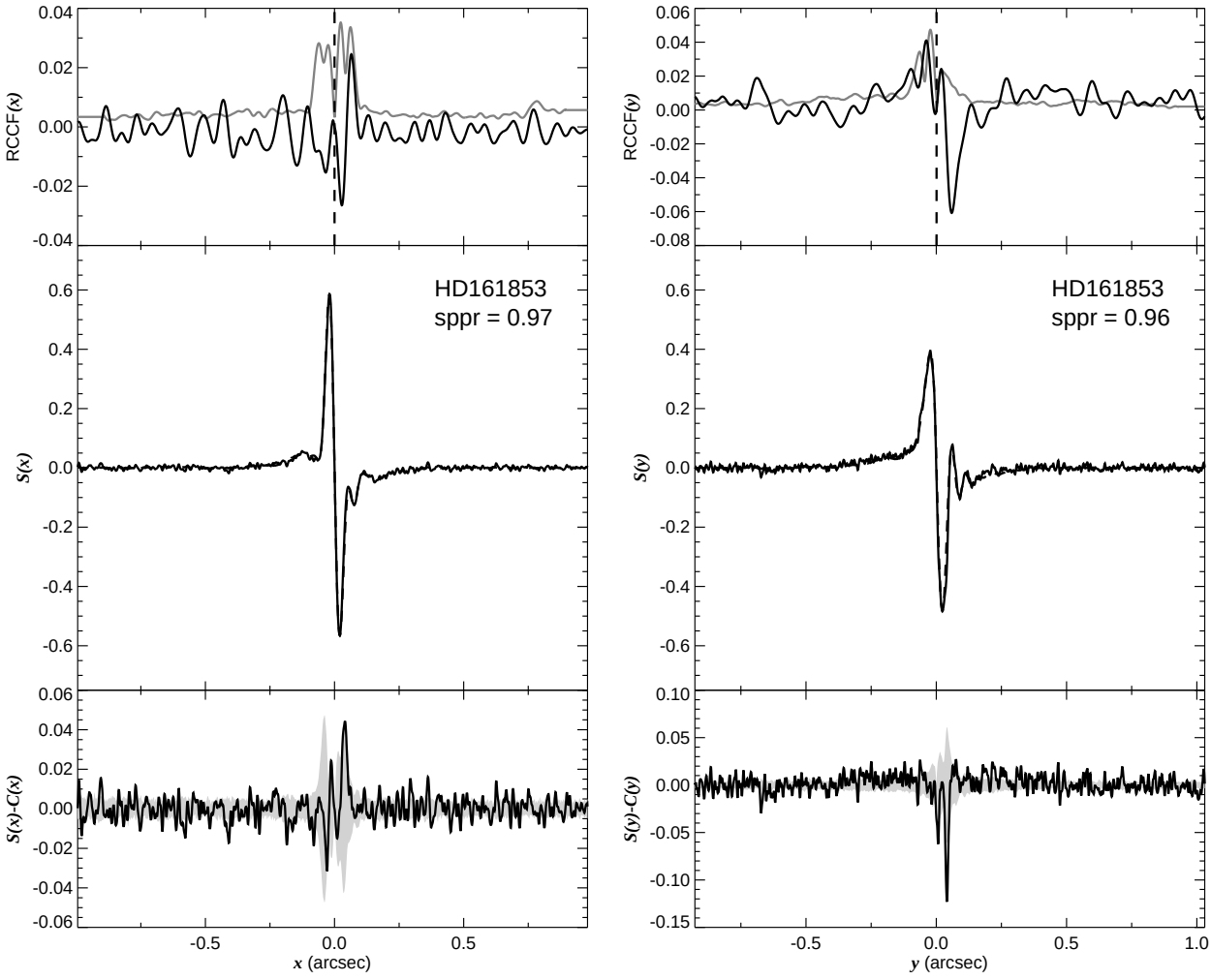

Fig. 1.210.— The FGS scans and binary detection tests for target 174916.55−311518.1 = HD161853 obtained on BY 2008.2432.

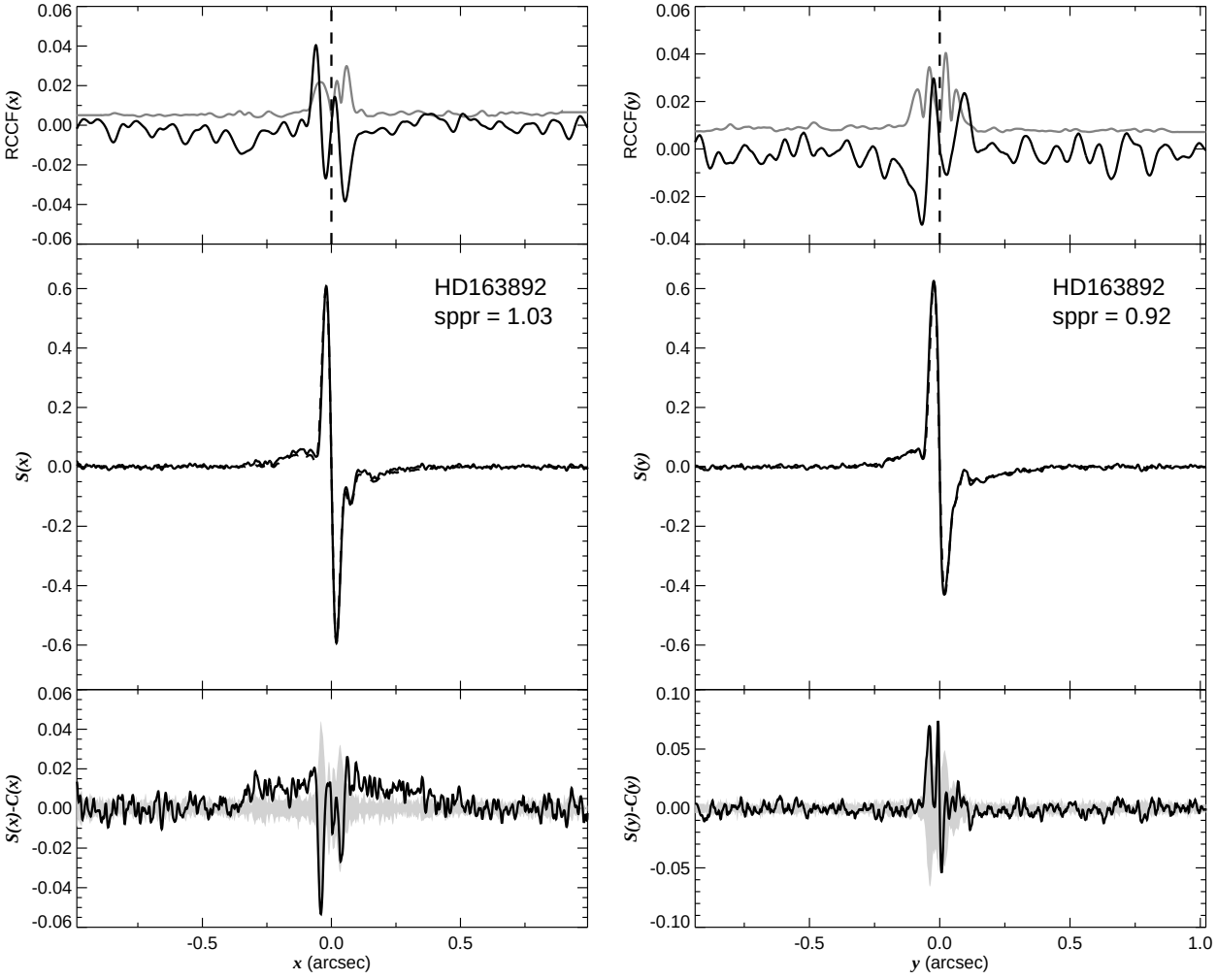

Fig. 1.211.— The FGS scans and binary detection tests for target 175926.31−222800.9 = HD163892 obtained on BY 2009.5460.

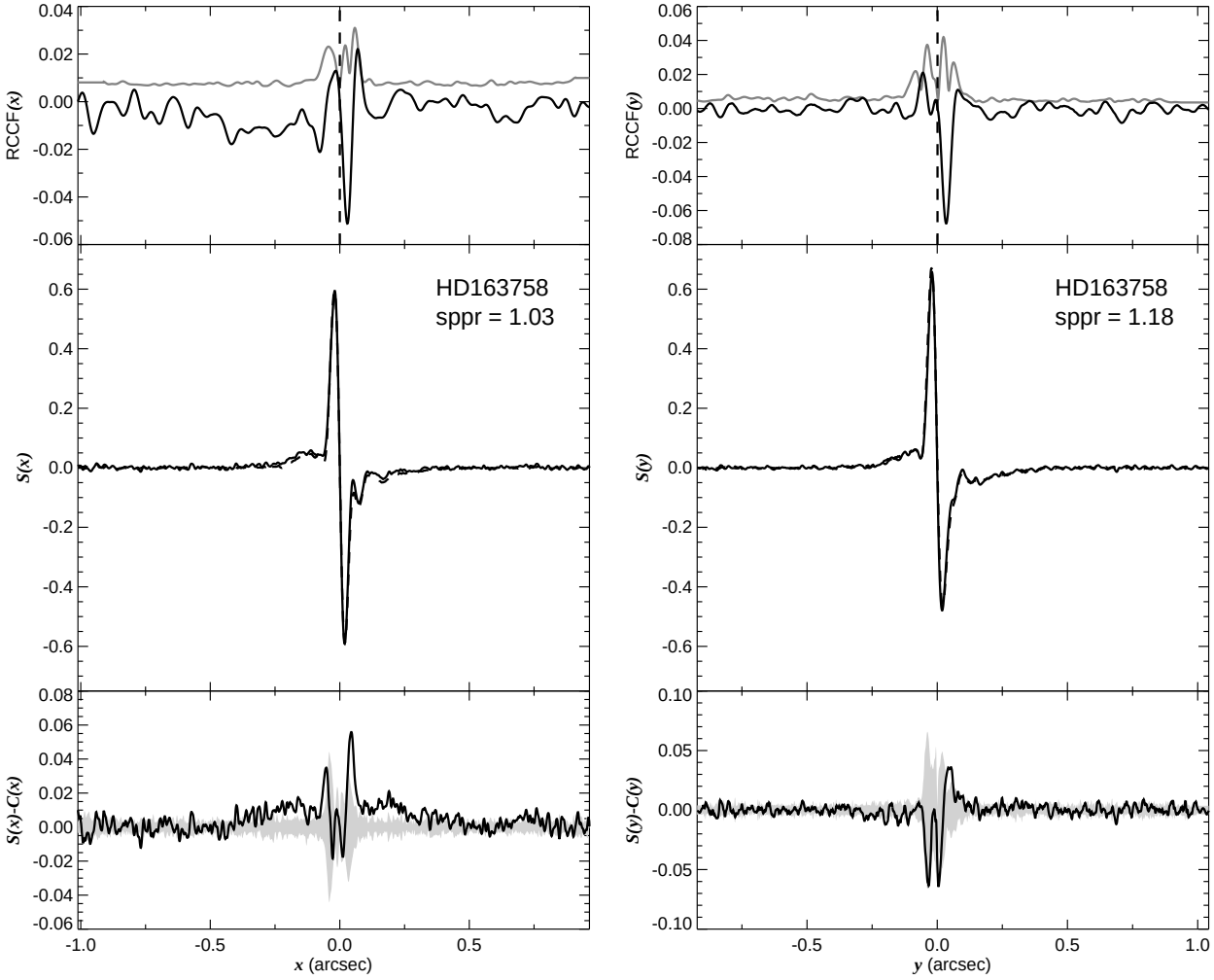

Fig. 1.212.— The FGS scans and binary detection tests for target 175928.37−360115.6 = HD163758 obtained on BY 2009.5489.

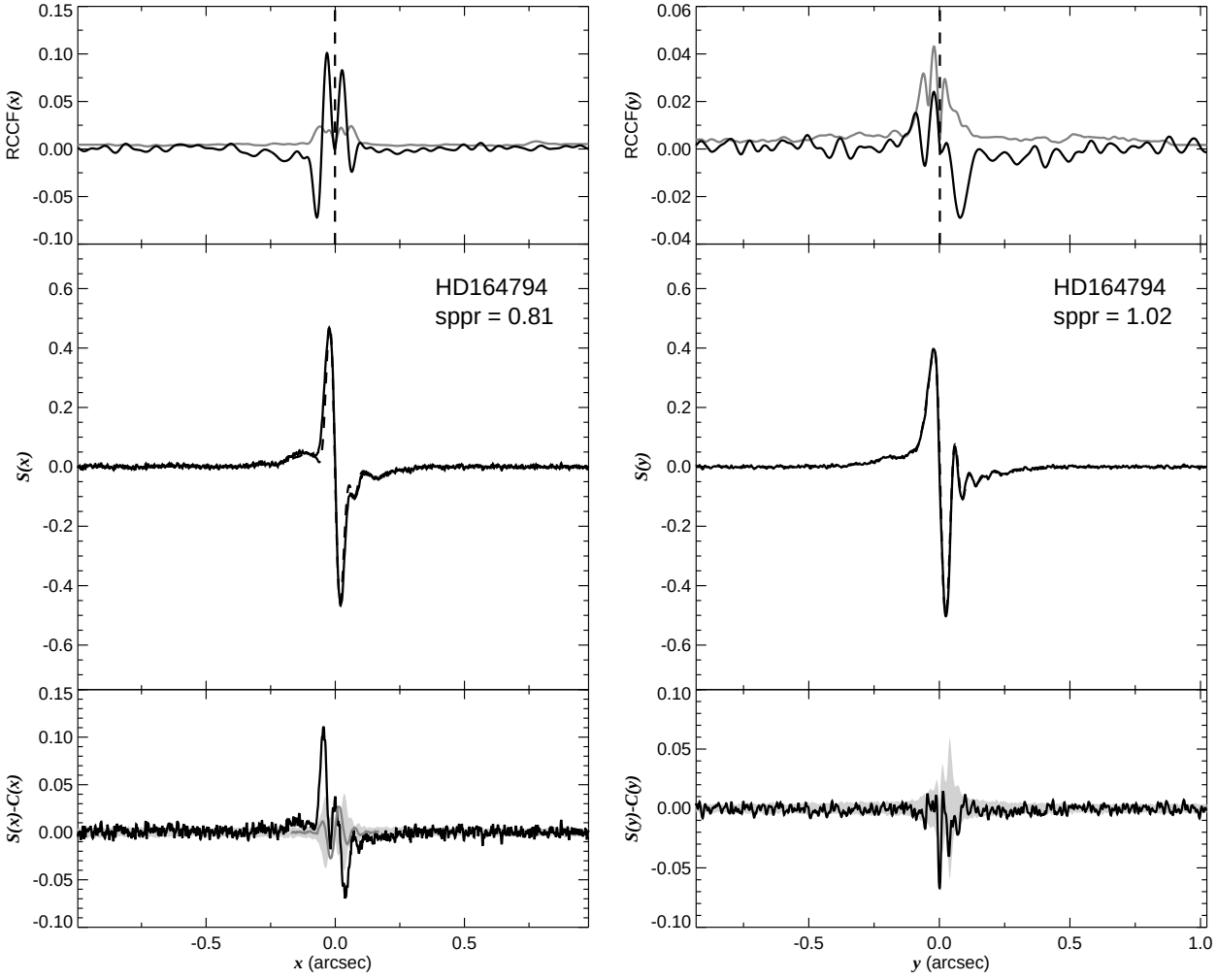

Fig. 1.213.— The FGS scans and binary detection tests for target 180352.44−242138.6 = HD164794 obtained on BY 2008.1920.

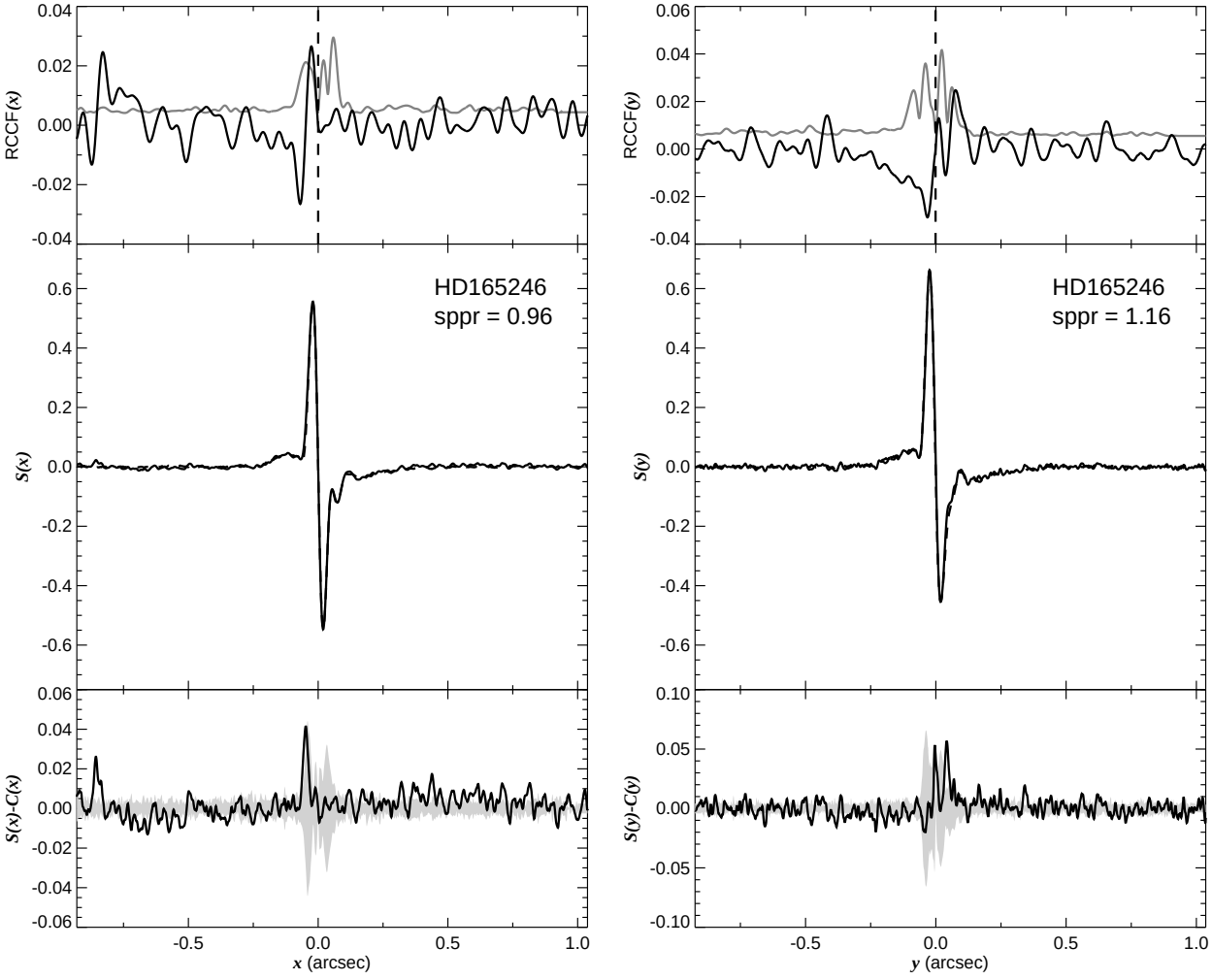

Fig. 1.214.— The FGS scans and binary detection tests for target 180604.68−241143.9 = HD165246 obtained on BY 2009.5338.

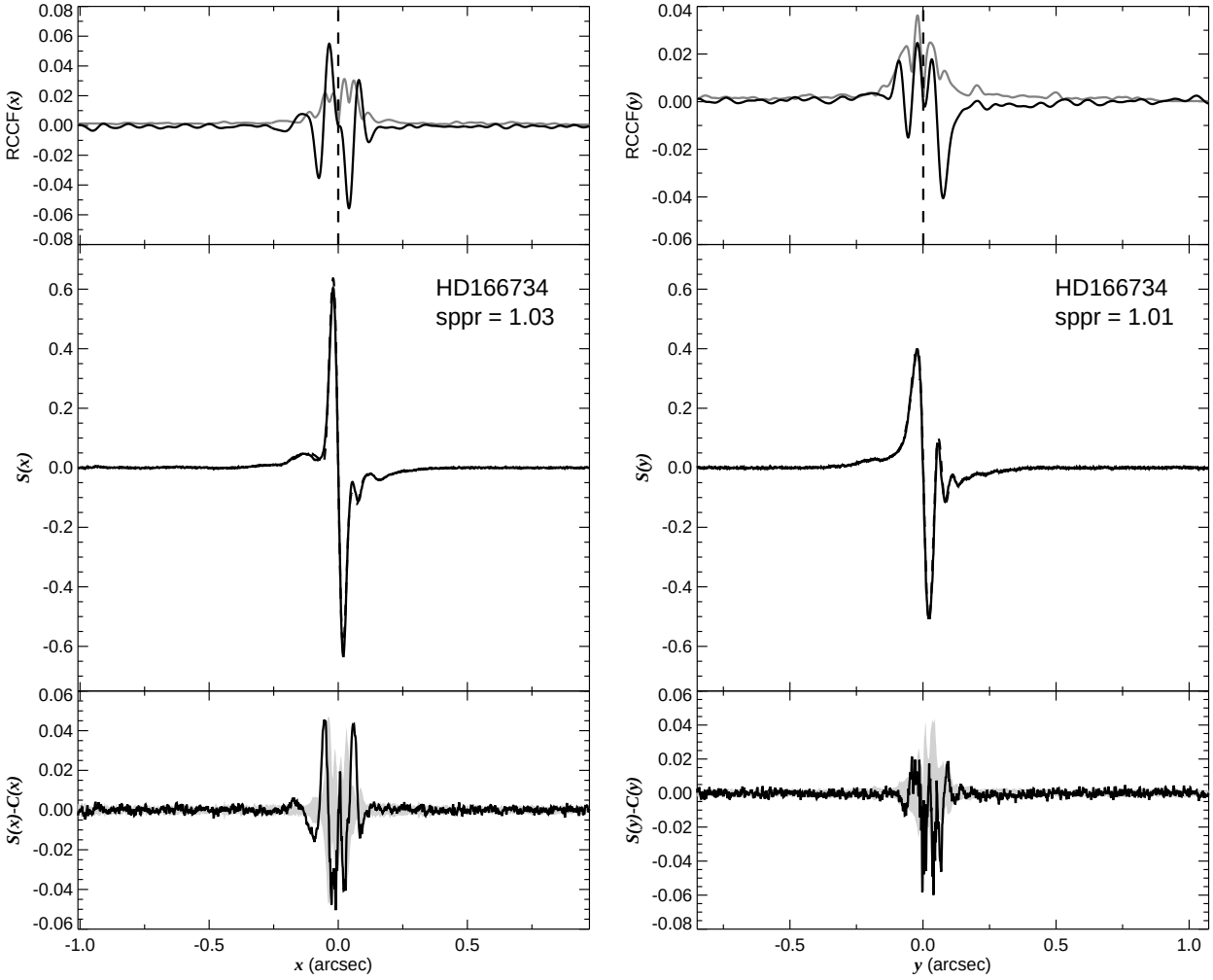

Fig. 1.215.— The FGS scans and binary detection tests for target 181224.66−104353.1 = HD166734 obtained on BY 2008.4985.

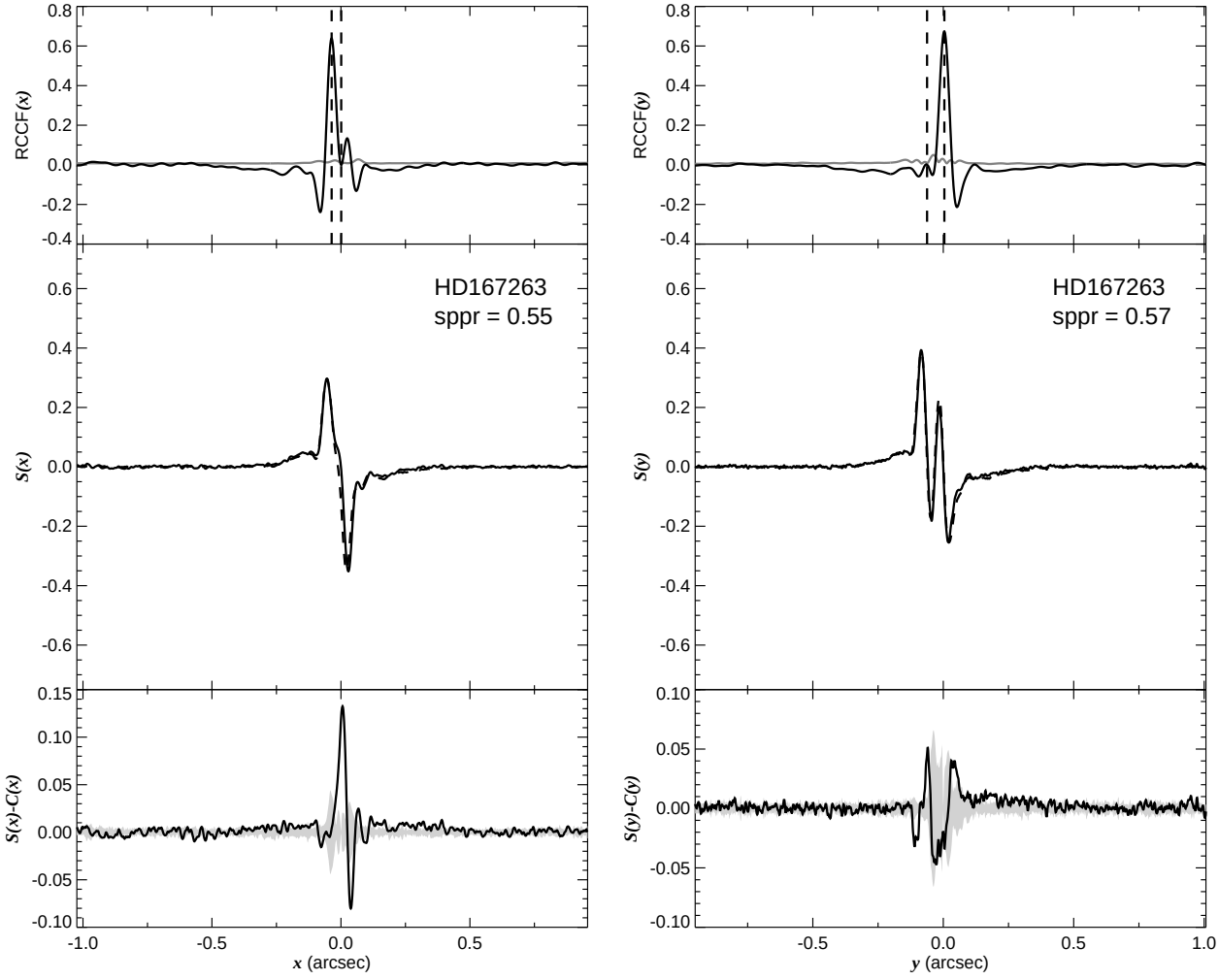

Fig. 1.216.— The FGS scans and binary detection tests for target 181512.97−202316.7 = HD167263 obtained on BY 2009.5462.

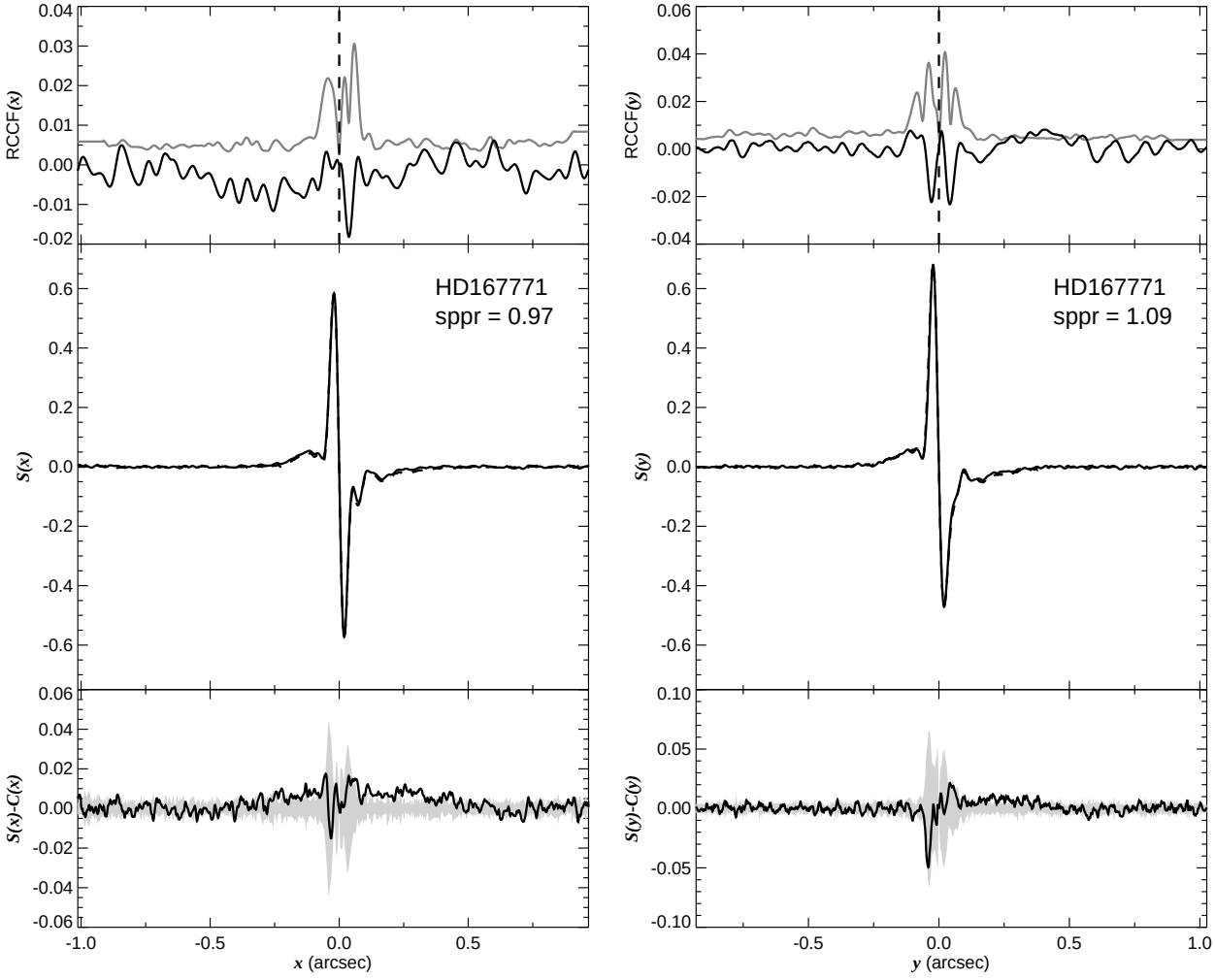

Fig. 1.217.— The FGS scans and binary detection tests for target 181728.56−182748.4 = HD167771 obtained on BY 2009.5463.

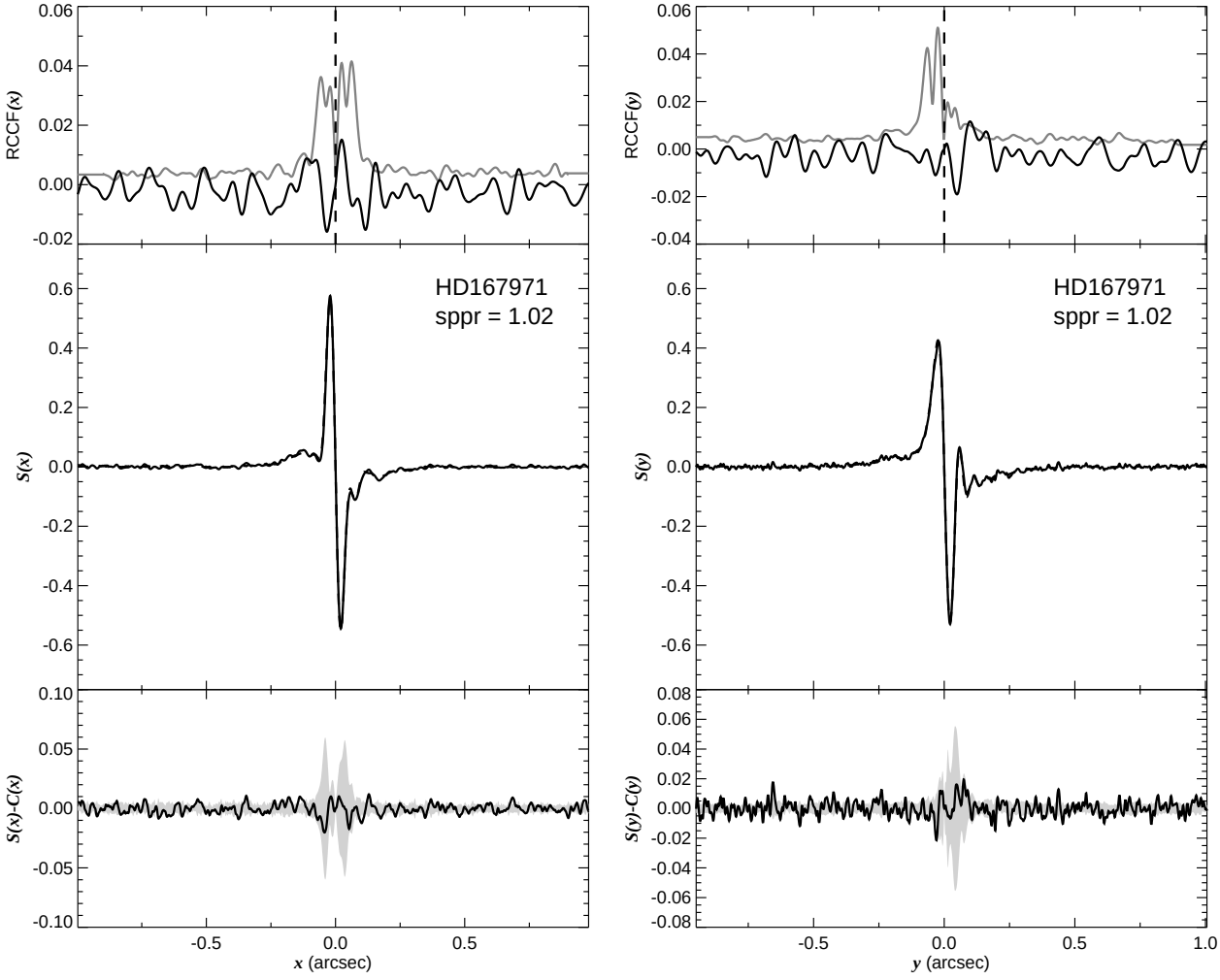

Fig. 1.218.— The FGS scans and binary detection tests for target 181805.90−121433.3 = HD167971 obtained on BY 2008.2059.

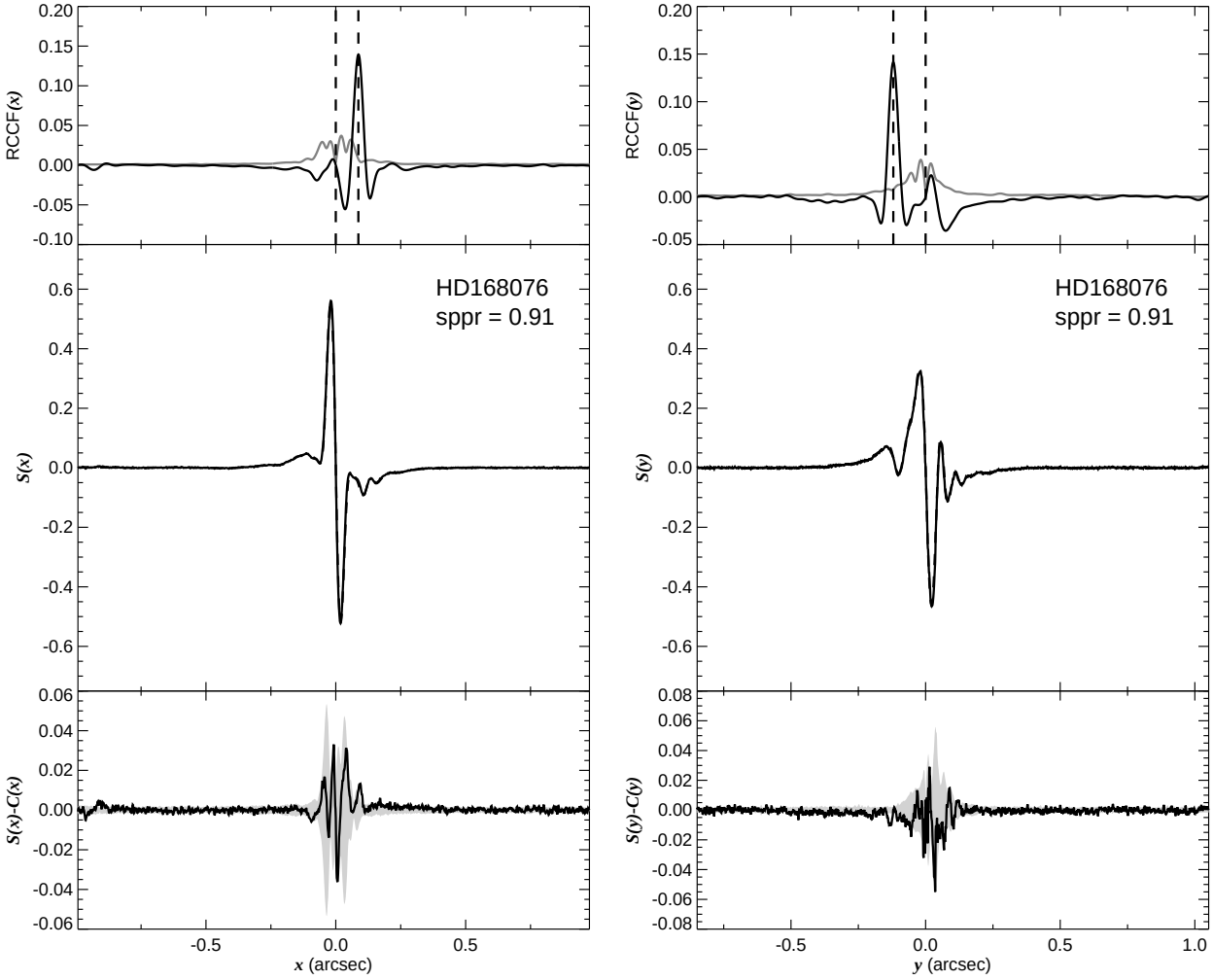

Fig. 1.219.— The FGS scans and binary detection tests for target 181836.43−134802.0 = HD168076 obtained on BY 2008.2514.

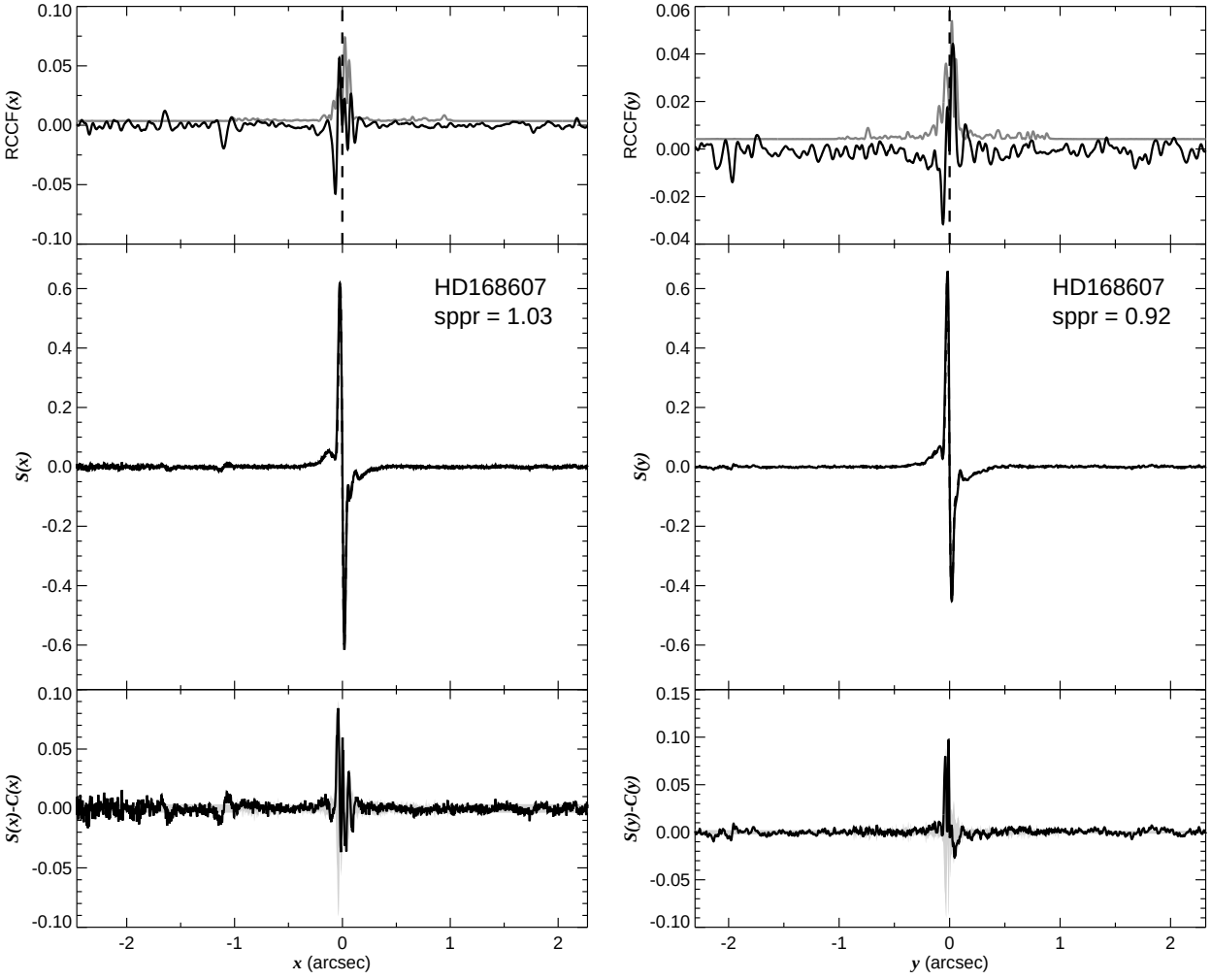

Fig. 1.220.— The FGS scans and binary detection tests for target 182114.89−162231.8 = HD168607 obtained on BY 2009.1525.

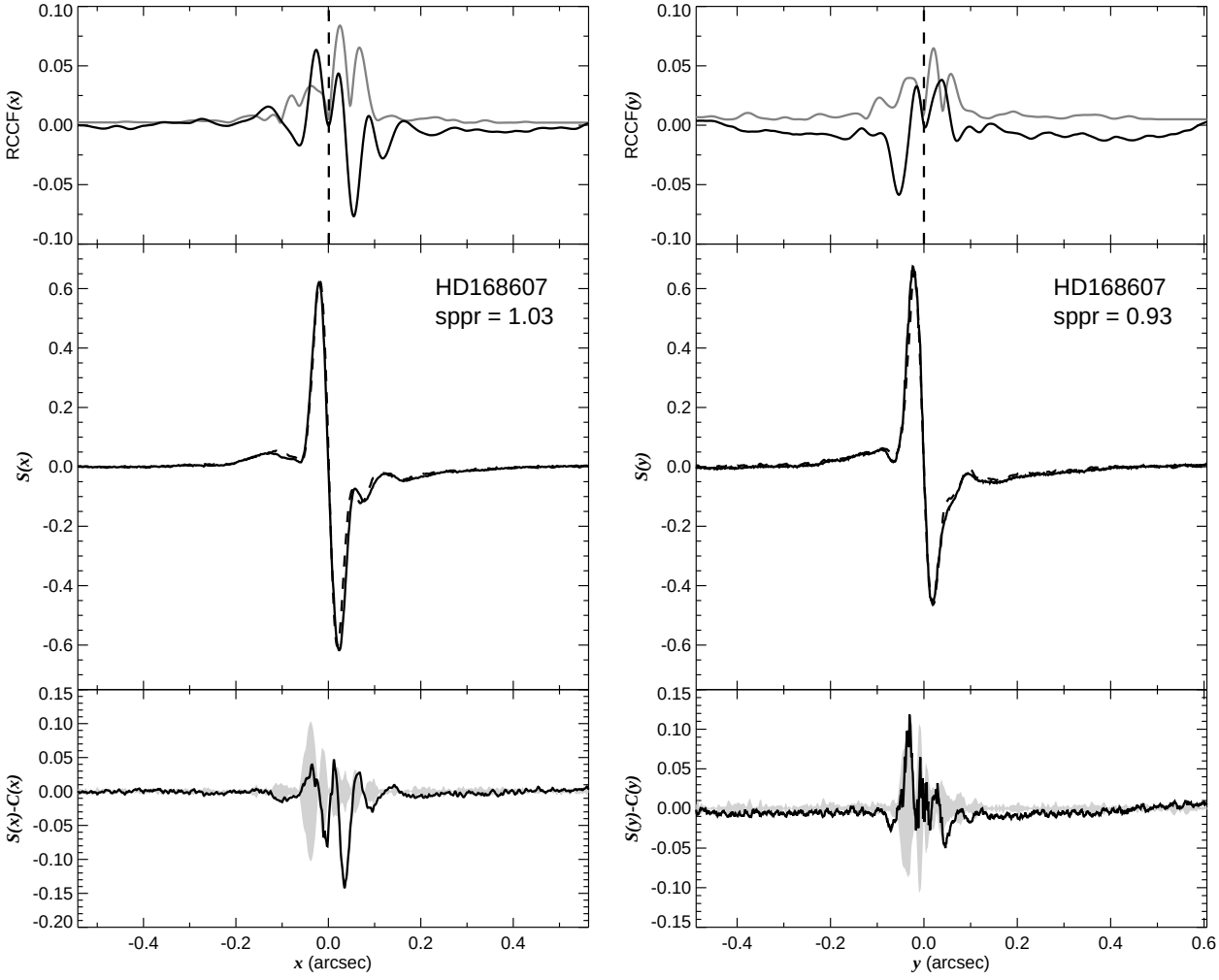

Fig. 1.221.— The FGS scans and binary detection tests for target 182114.89−162231.8 = HD168607 obtained on BY 2009.1526.

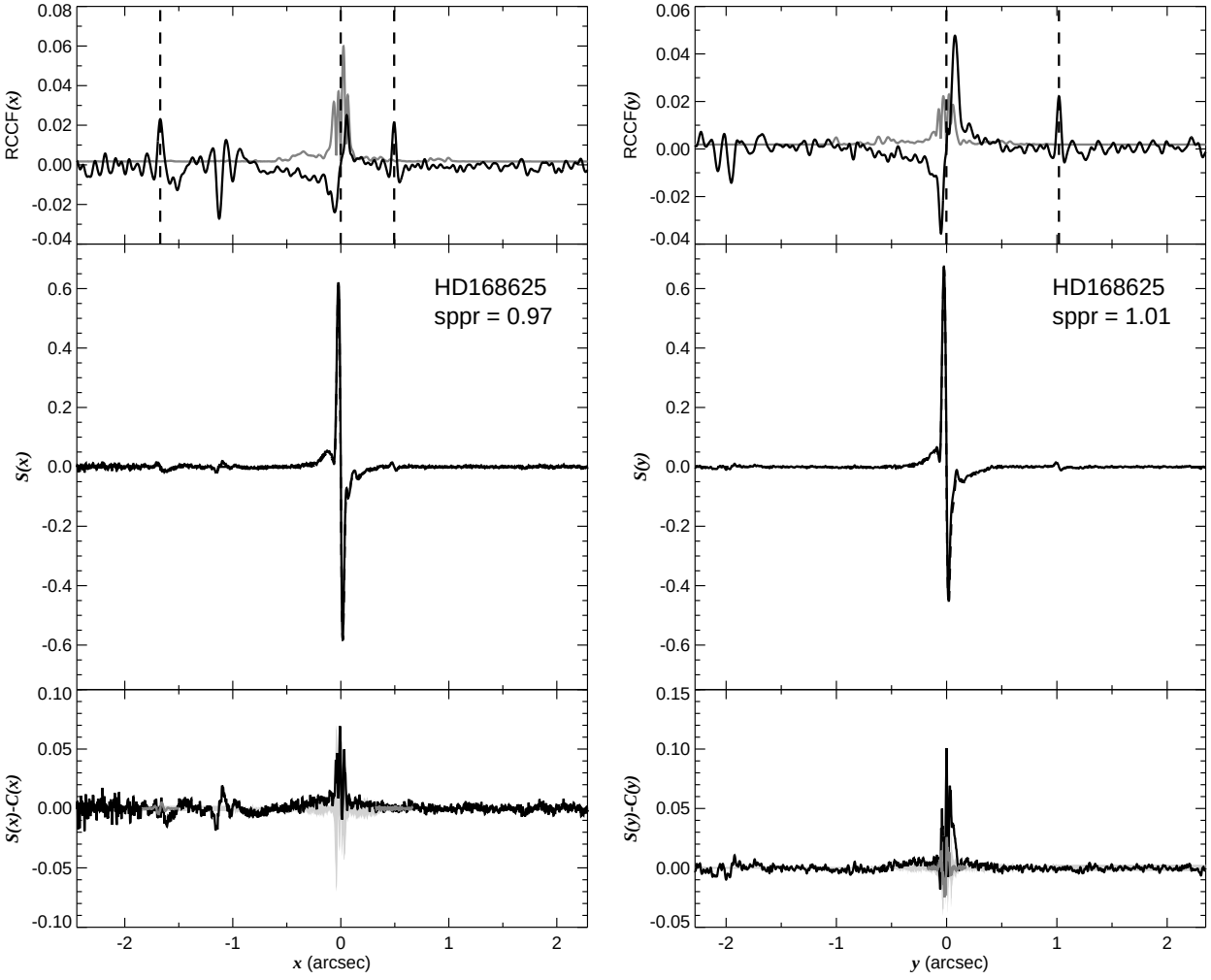

Fig. 1.222.— The FGS scans and binary detection tests for target 182119.55−162226.1 = HD168625 obtained on BY 2009.2707.

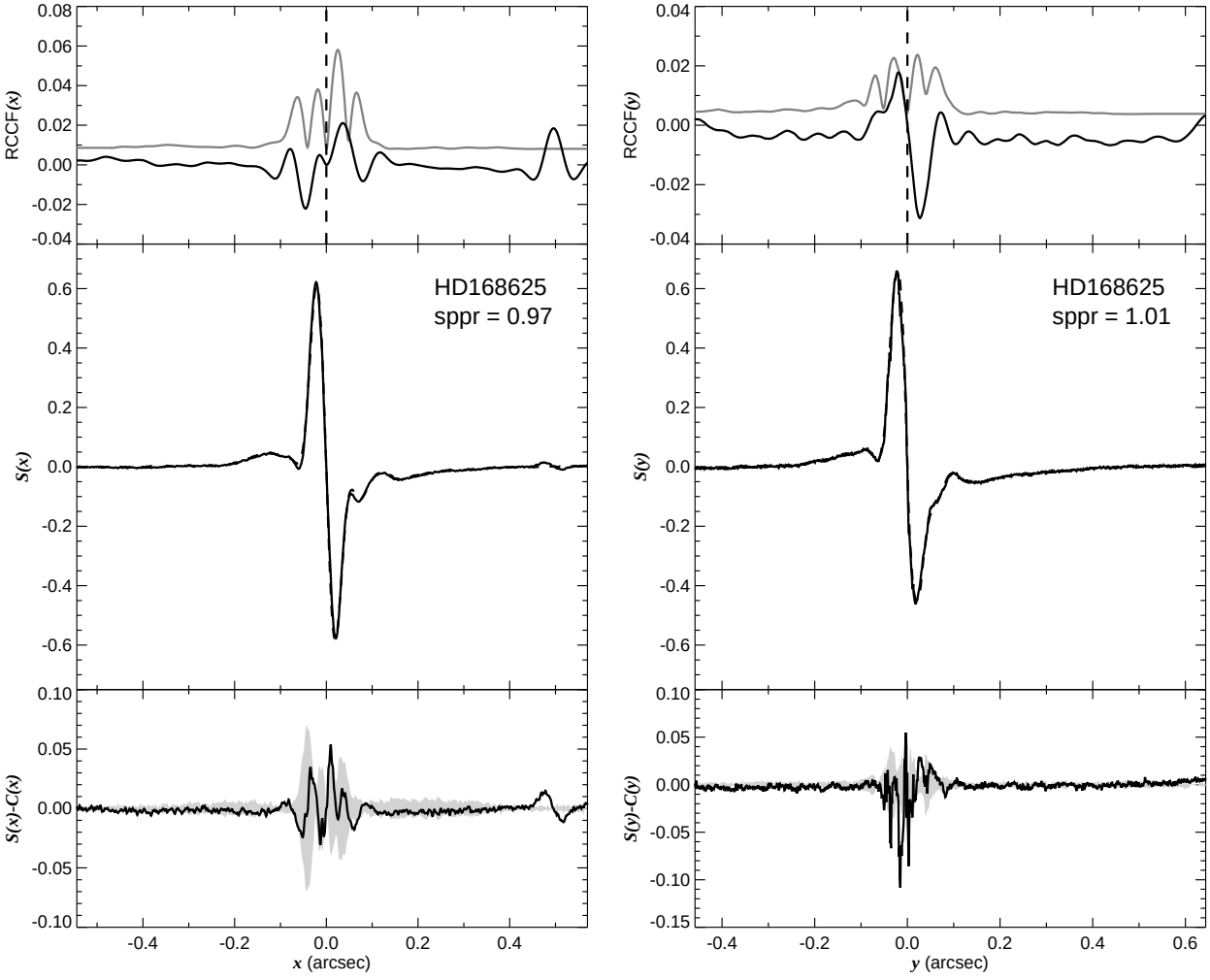

Fig. 1.223.— The FGS scans and binary detection tests for target 182119.55−162226.1 = HD168625 obtained on BY 2009.2707.

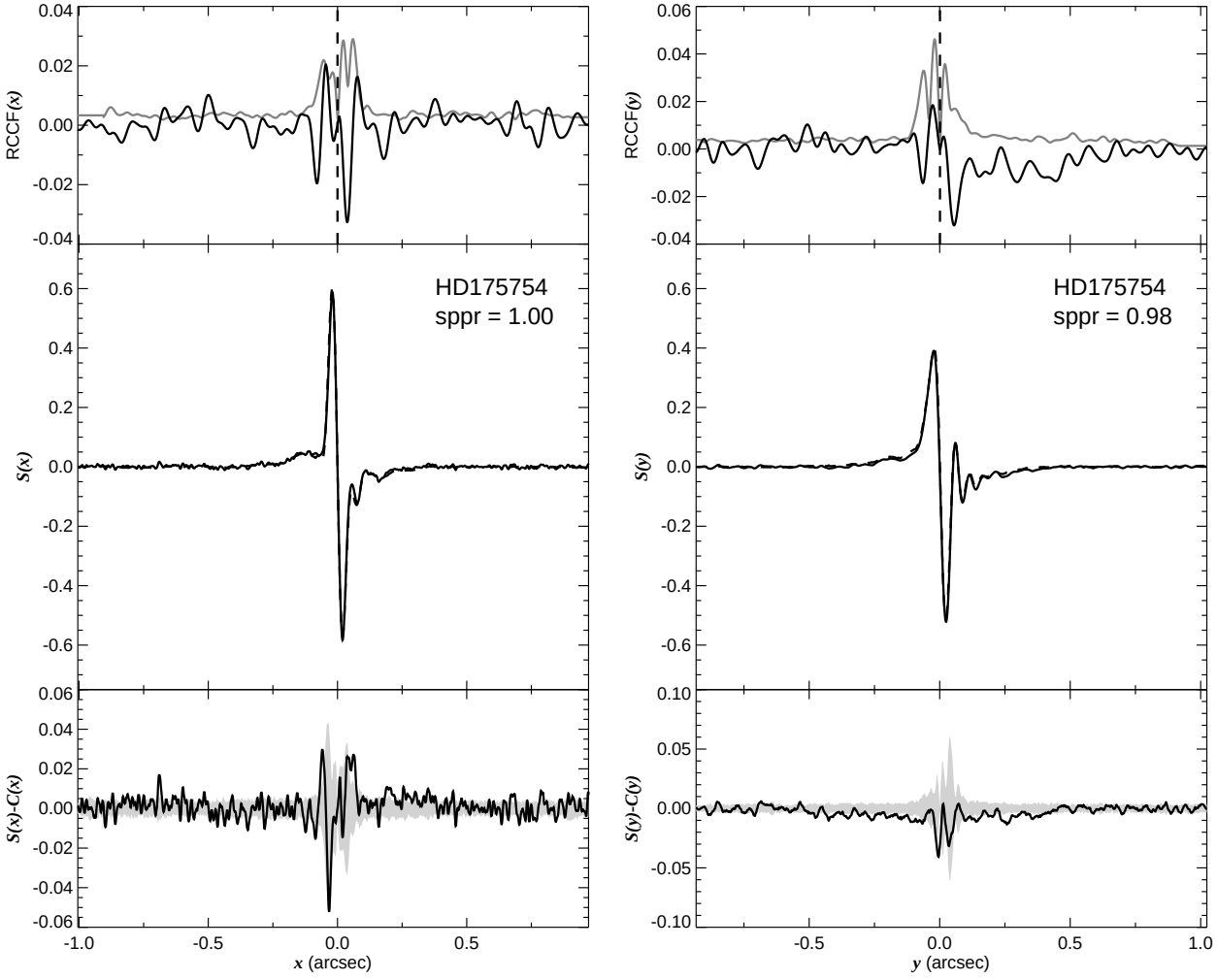

Fig. 1.224.— The FGS scans and binary detection tests for target 185735.71−190911.3 = HD175754 obtained on BY 2008.1998.

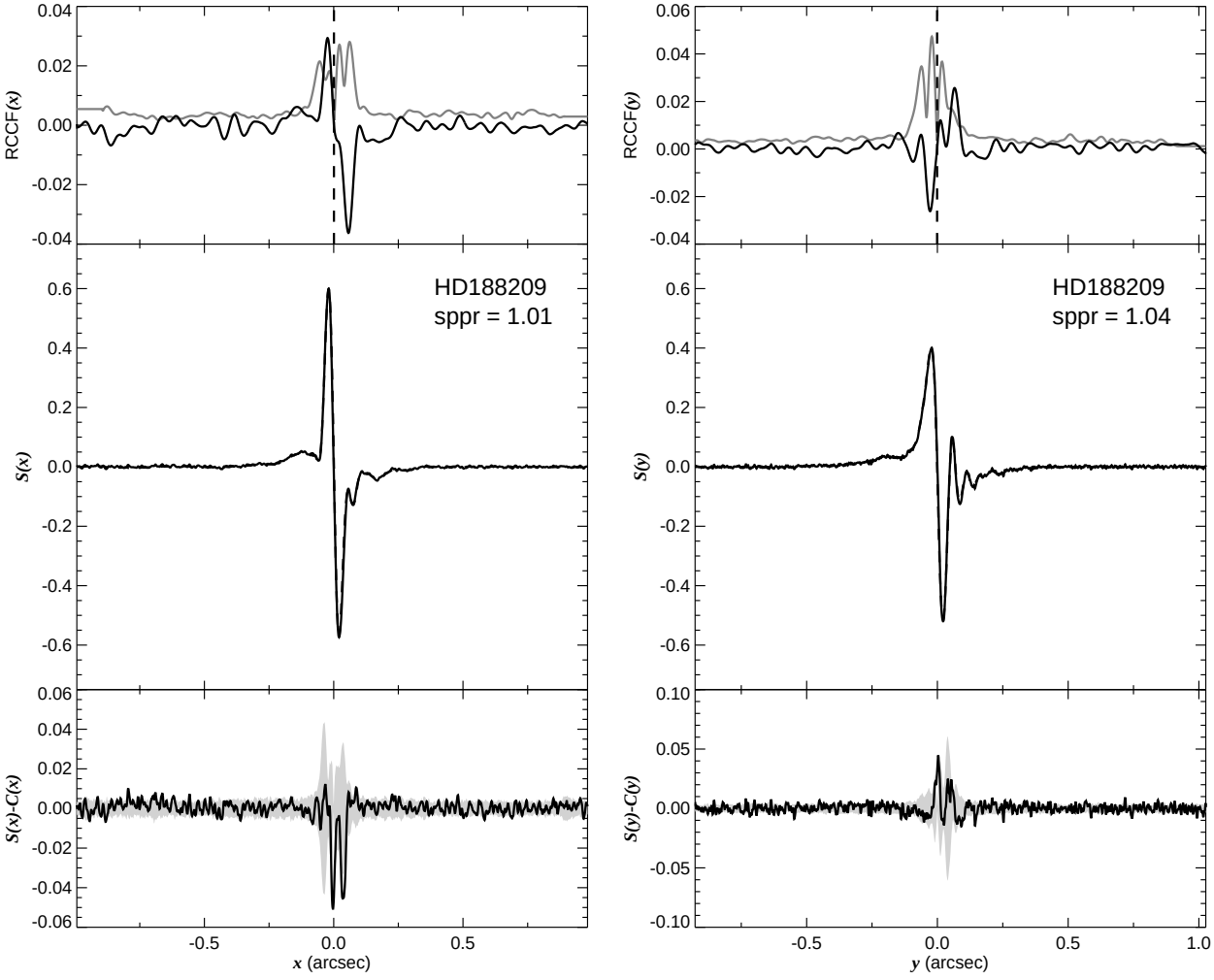

Fig. 1.225.— The FGS scans and binary detection tests for target 195159.07+470138.4 = HD188209 obtained on BY 2008.2007.

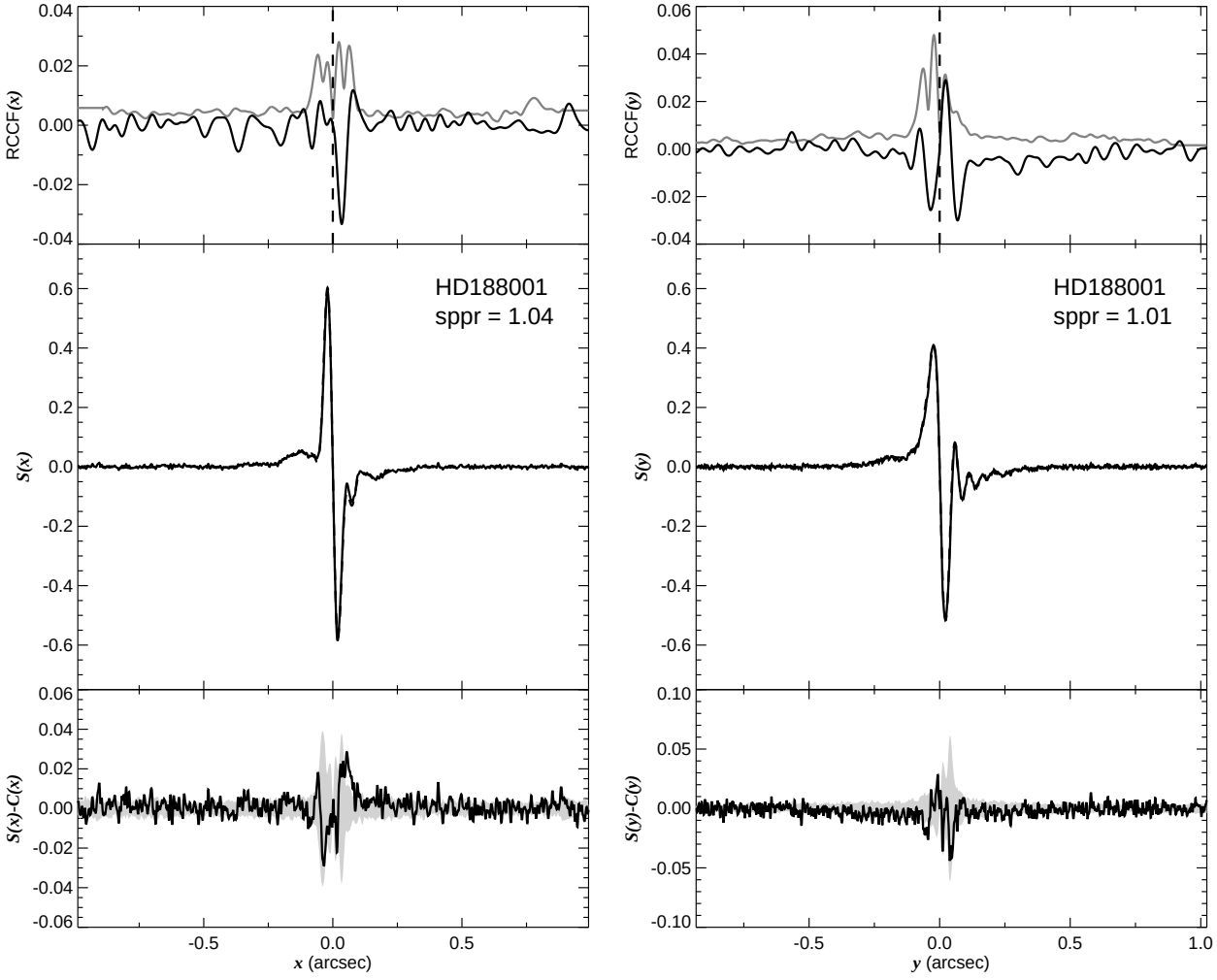

Fig. 1.226.— The FGS scans and binary detection tests for target 195221.76+184018.7 = HD188001 obtained on BY 2008.3535.

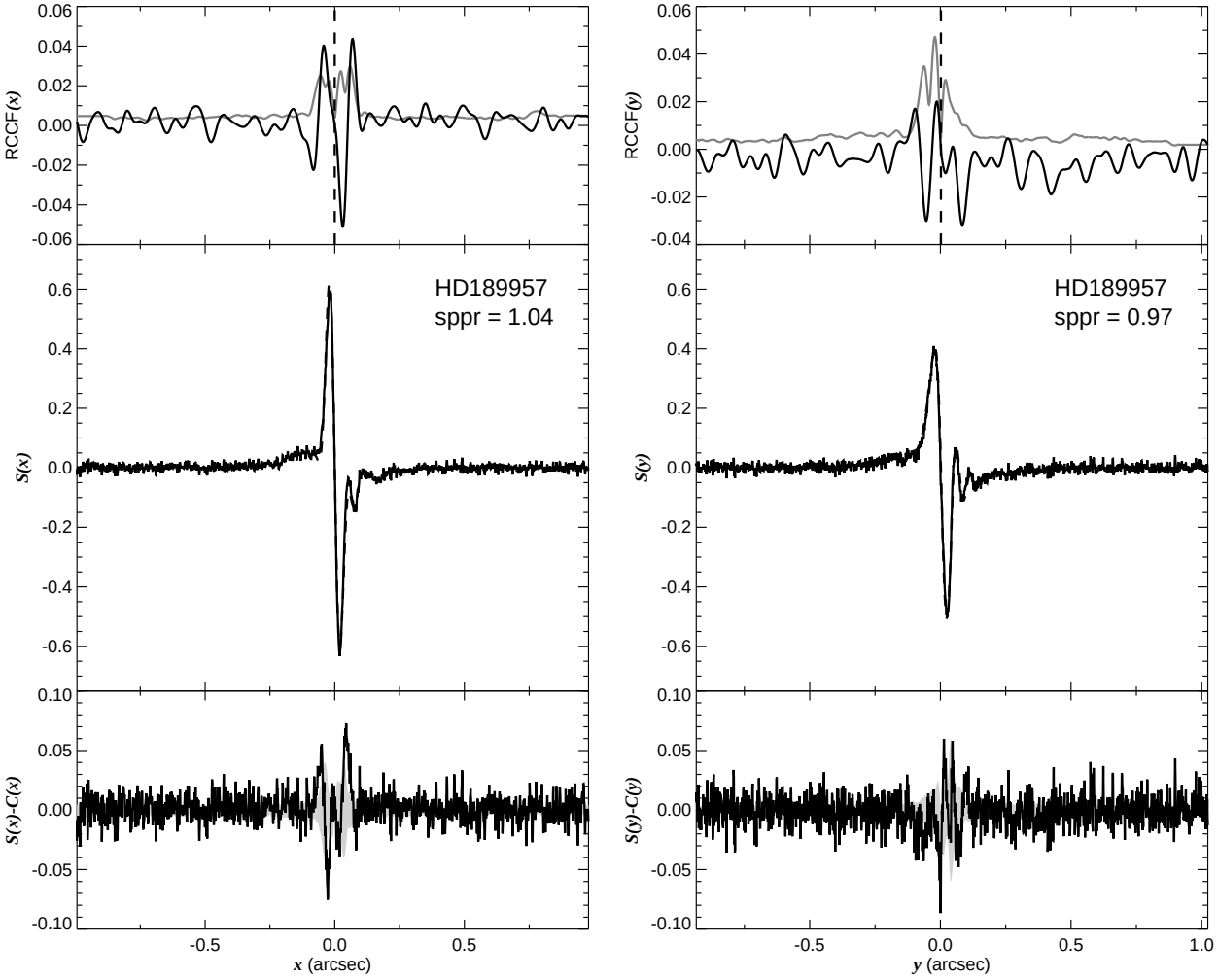

Fig. 1.227.— The FGS scans and binary detection tests for target 200100.00+420030.8 = HD189957 obtained on BY 2008.1596.

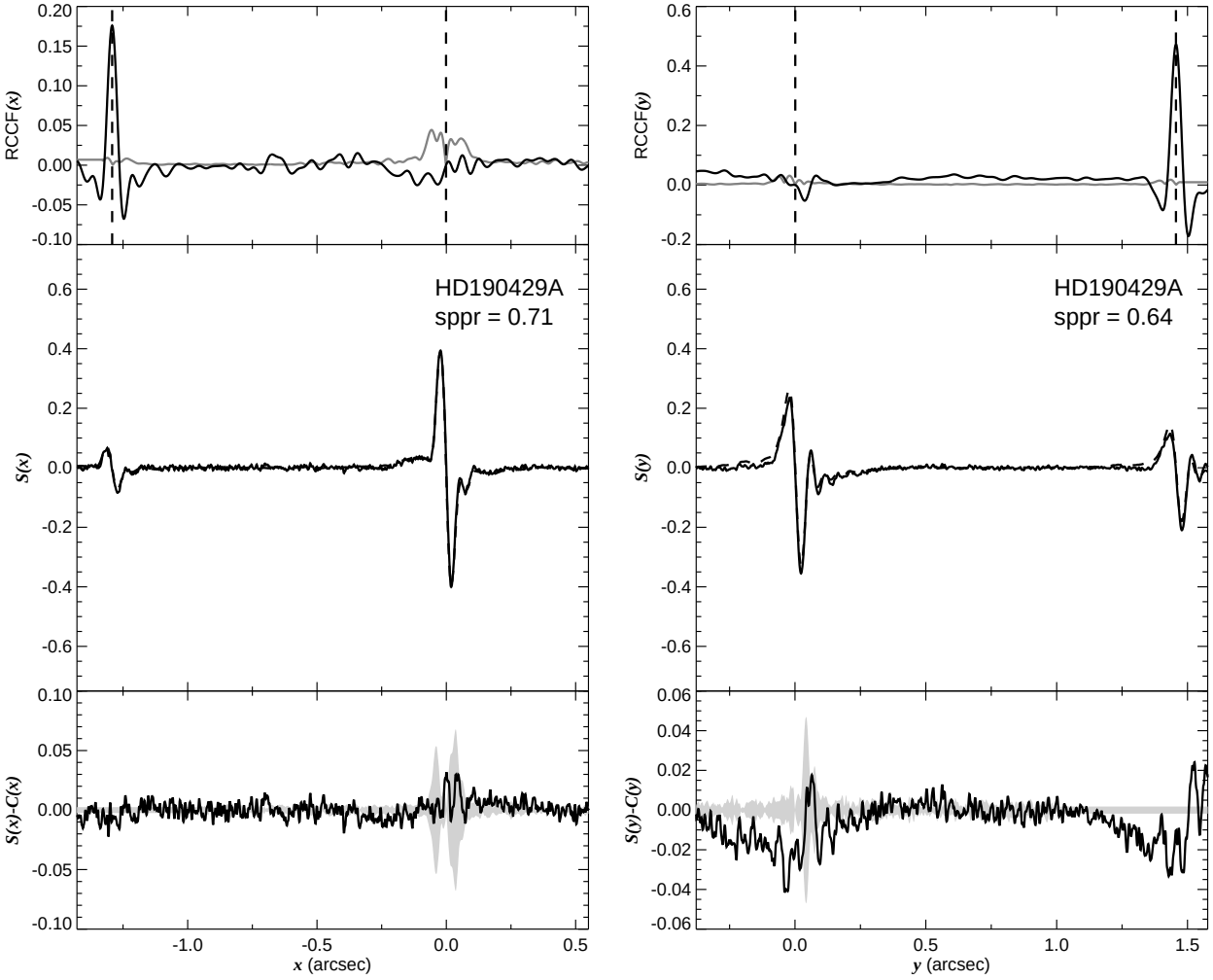

Fig. 1.228.— The FGS scans and binary detection tests for target 200329.40+360130.5 = HD190429 obtained on BY 2008.1844.

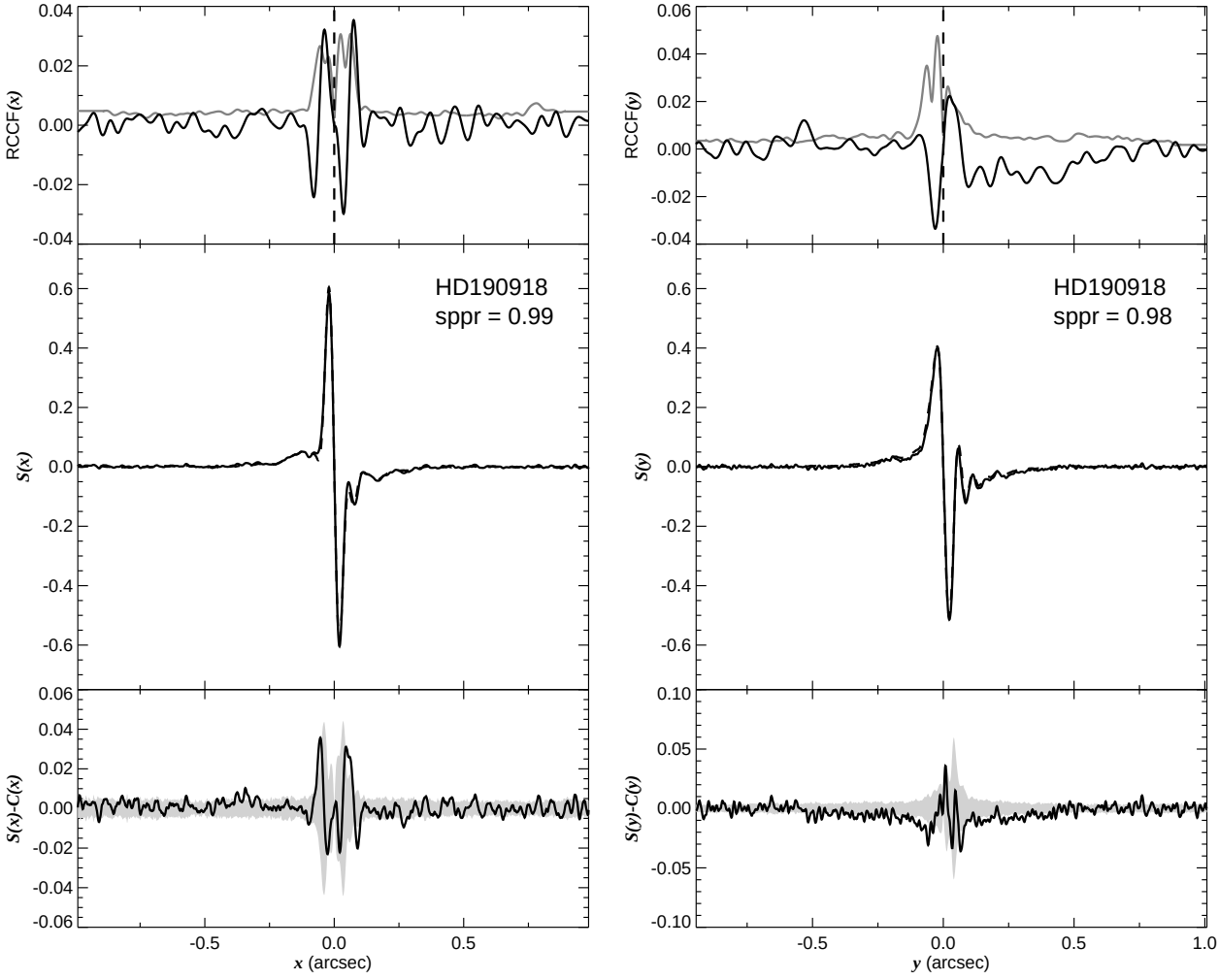

Fig. 1.229.— The FGS scans and binary detection tests for target 200557.32+354718.1 = HD190918 obtained on BY 2008.1925.

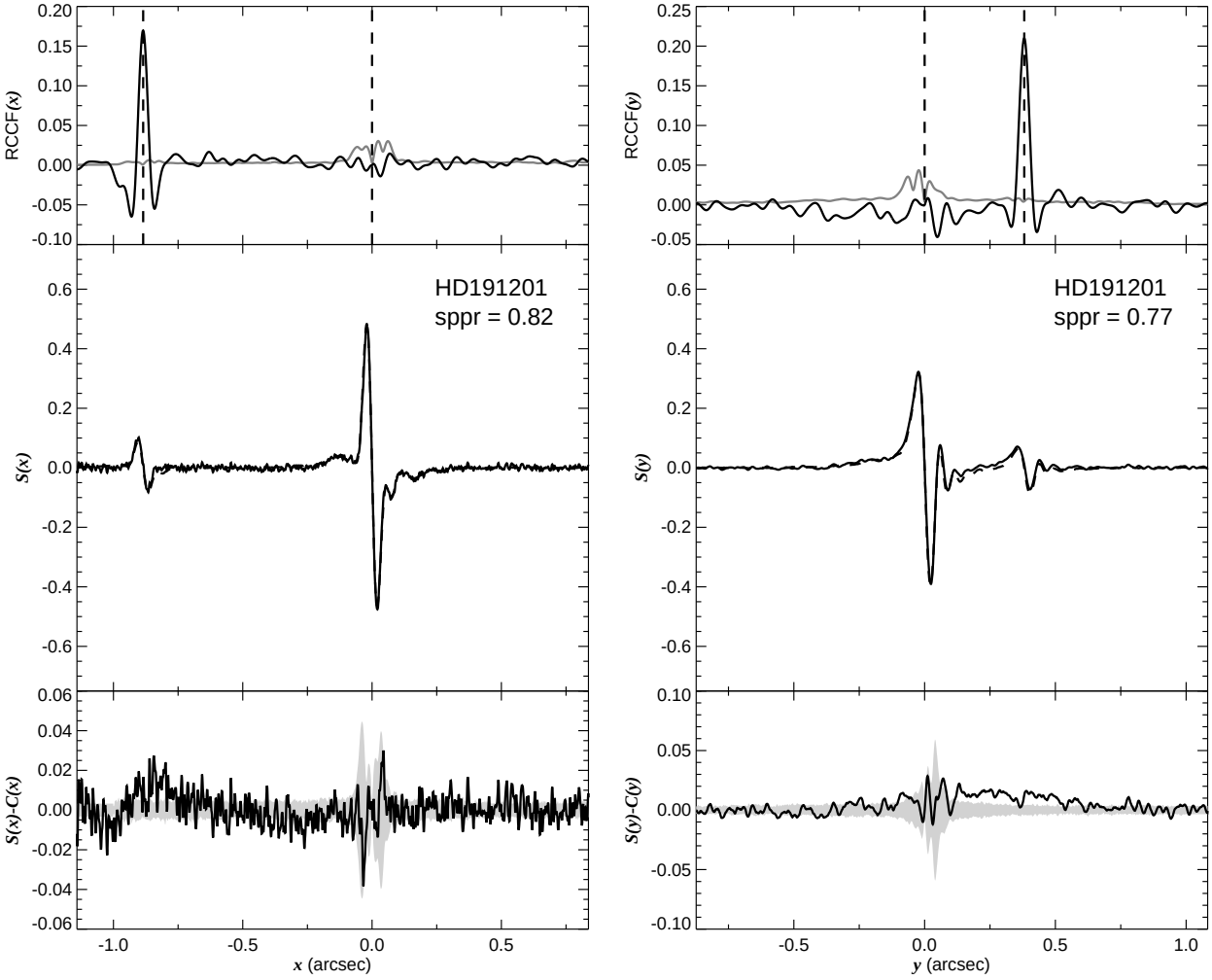

Fig. 1.230.— The FGS scans and binary detection tests for target 200723.69+354305.9 = HD191201 obtained on BY 2008.4072.

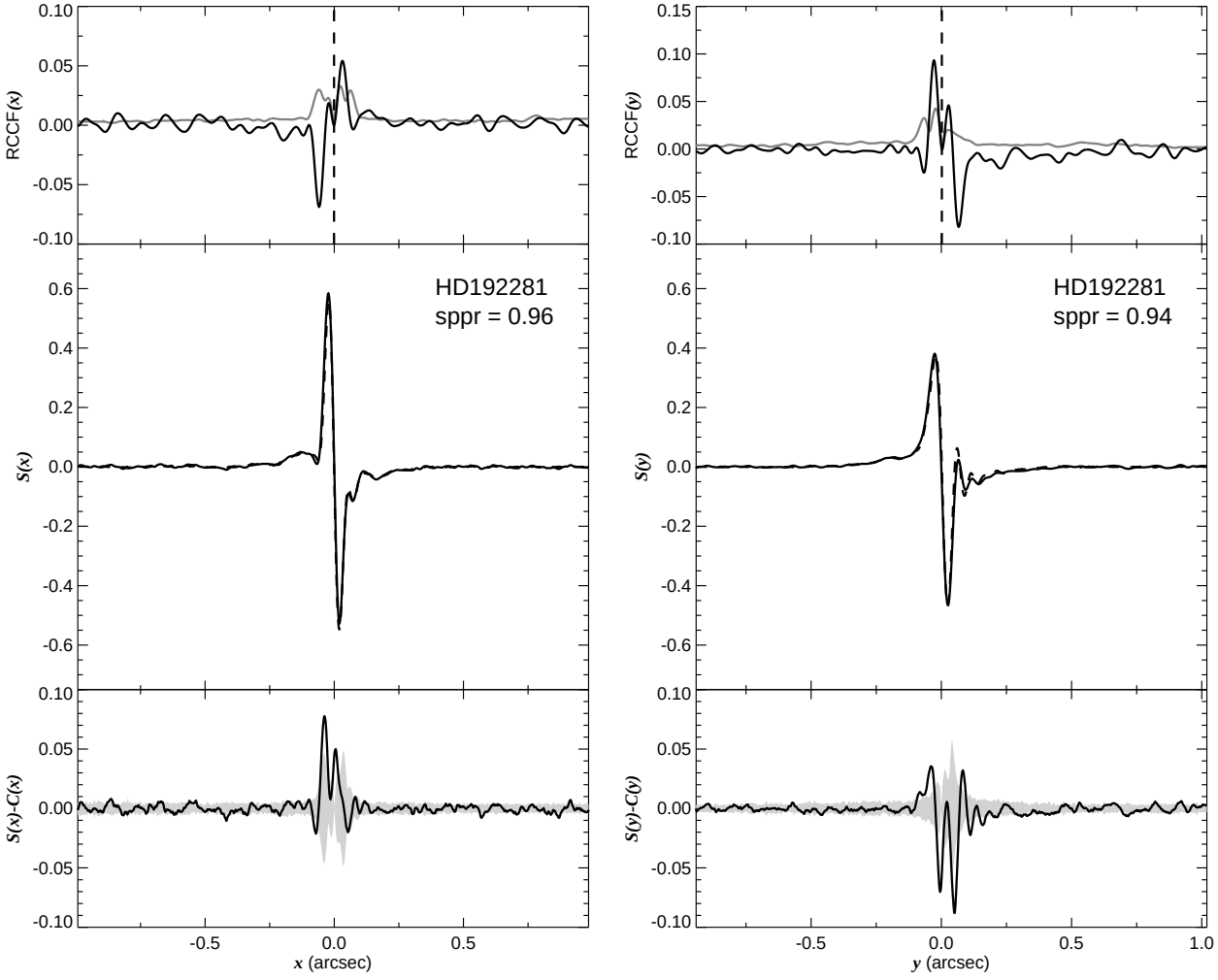

Fig. 1.231.— The FGS scans and binary detection tests for target 201233.12+401605.4 = HD192281 obtained on BY 2008.5239.

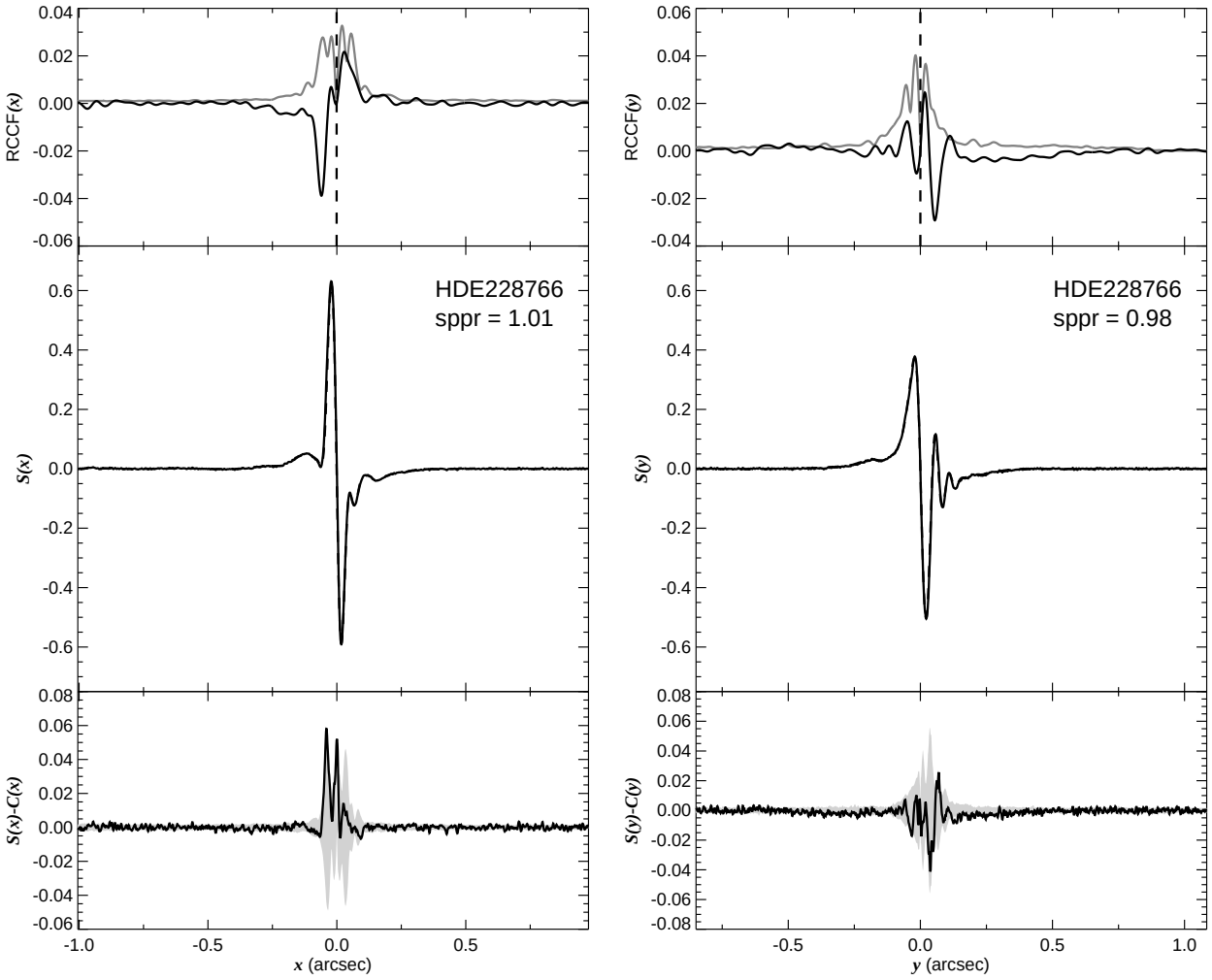

Fig. 1.232.— The FGS scans and binary detection tests for target 201729.70+371831.1 = HDE228766 obtained on BY 2008.3151.

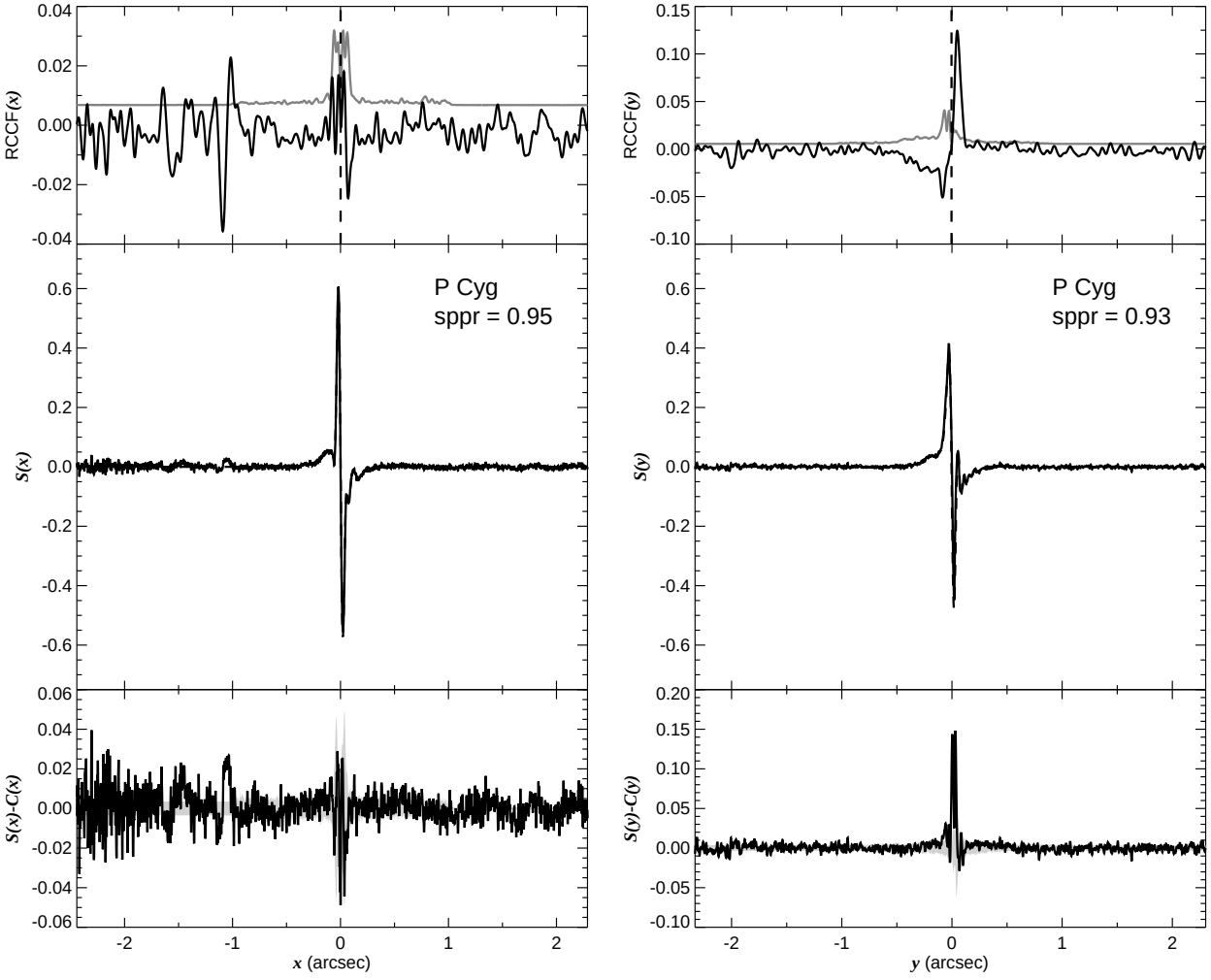

Fig. 1.233.— The FGS scans and binary detection tests for target 201747.20+380158.5 = HD193237 obtained on BY 2009.0054.

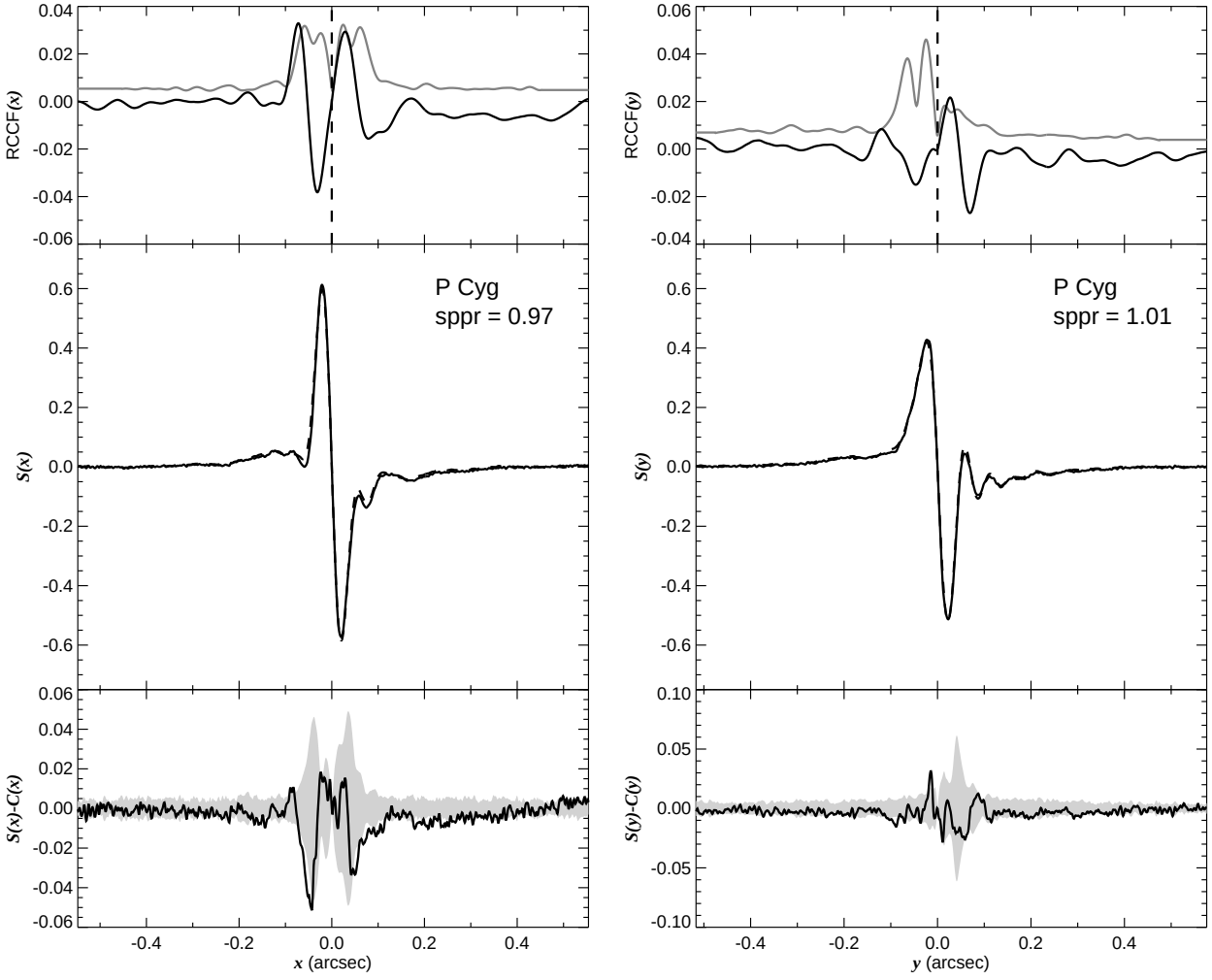

Fig. 1.234.— The FGS scans and binary detection tests for target 201747.20+380158.5 = HD193237 obtained on BY 2009.0054.

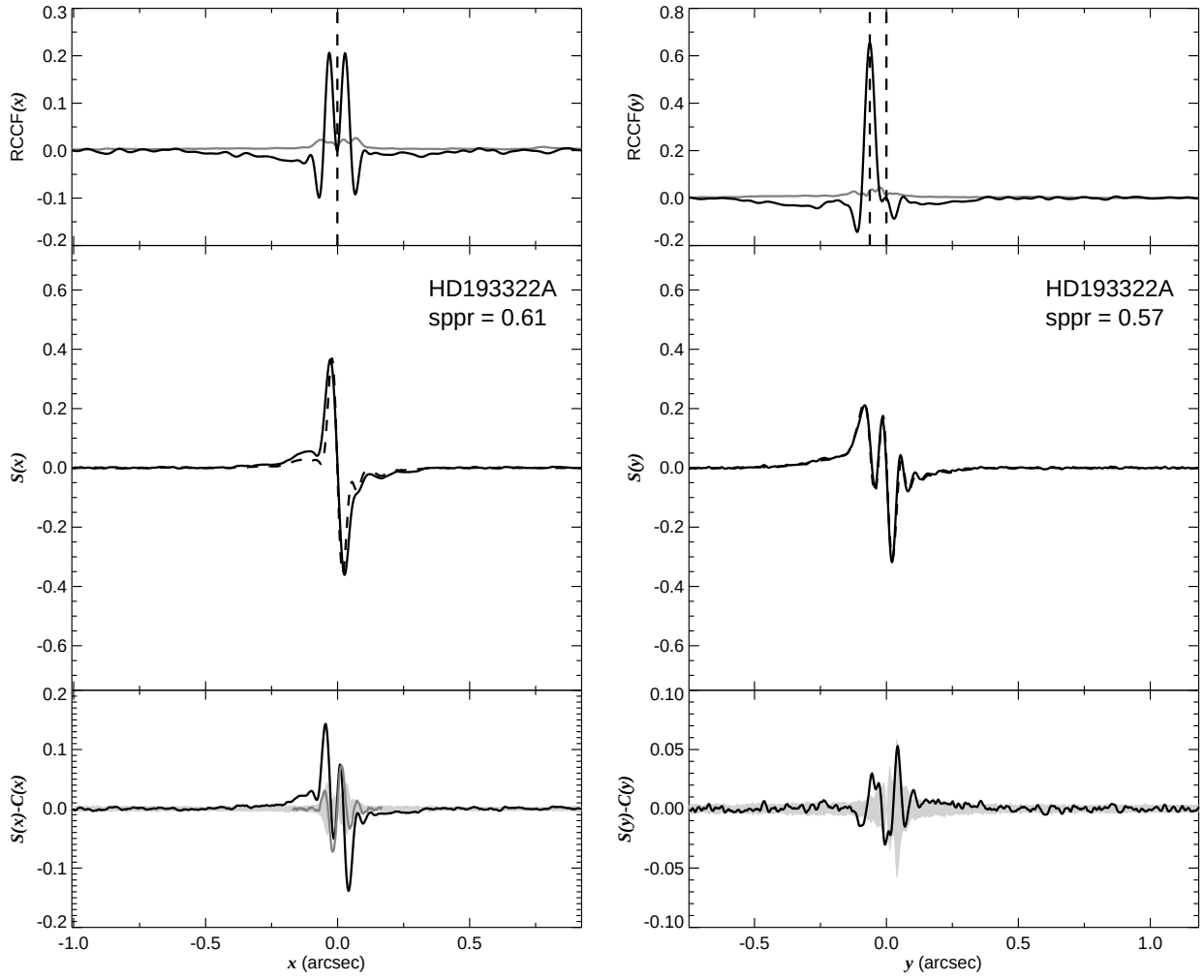

Fig. 1.235.— The FGS scans and binary detection tests for target 201806.99+404355.5 = HD193322 obtained on BY 2008.0503.

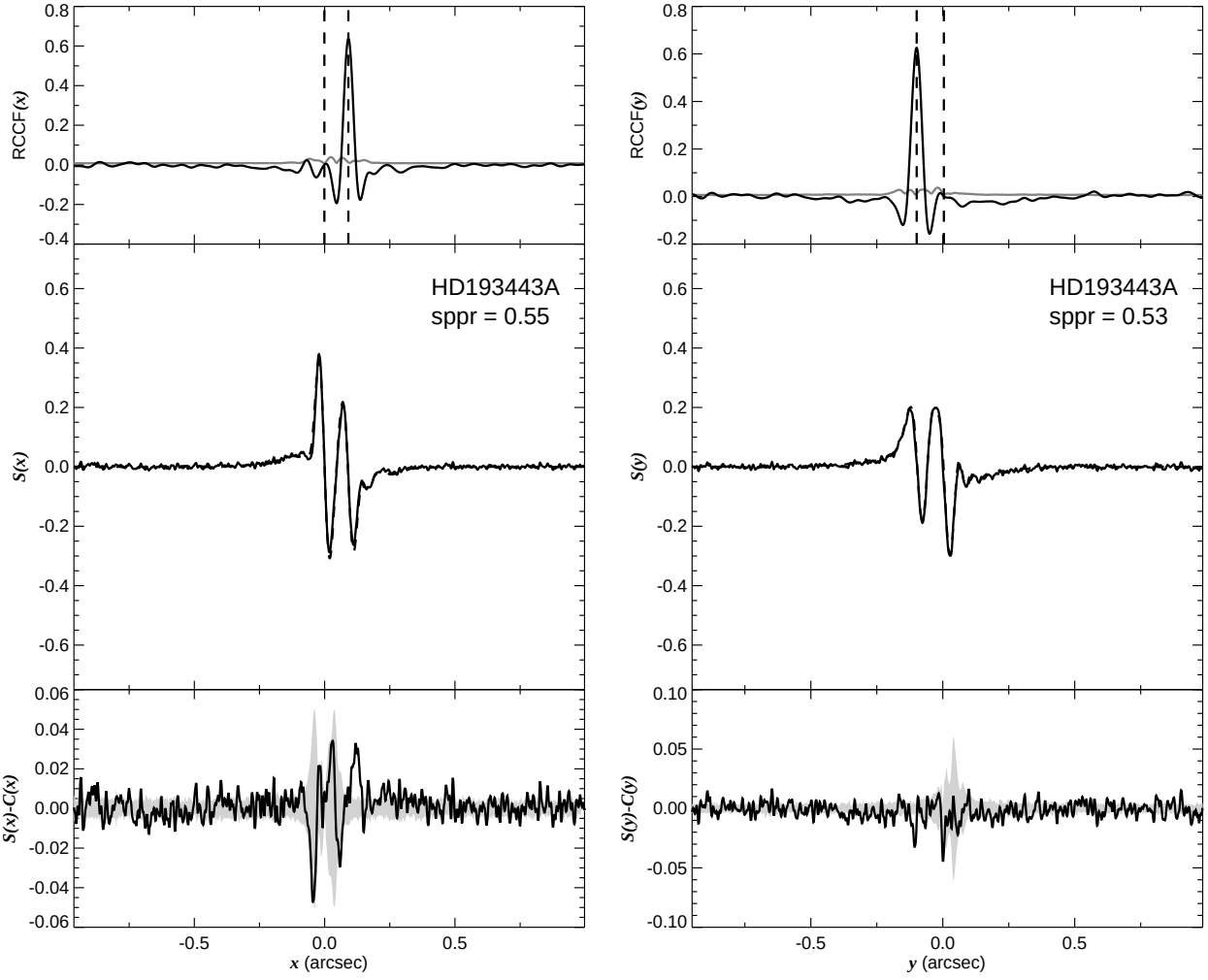

Fig. 1.236.— The FGS scans and binary detection tests for target 201851.71+381646.5 = HD193443 obtained on BY 2008.9728.

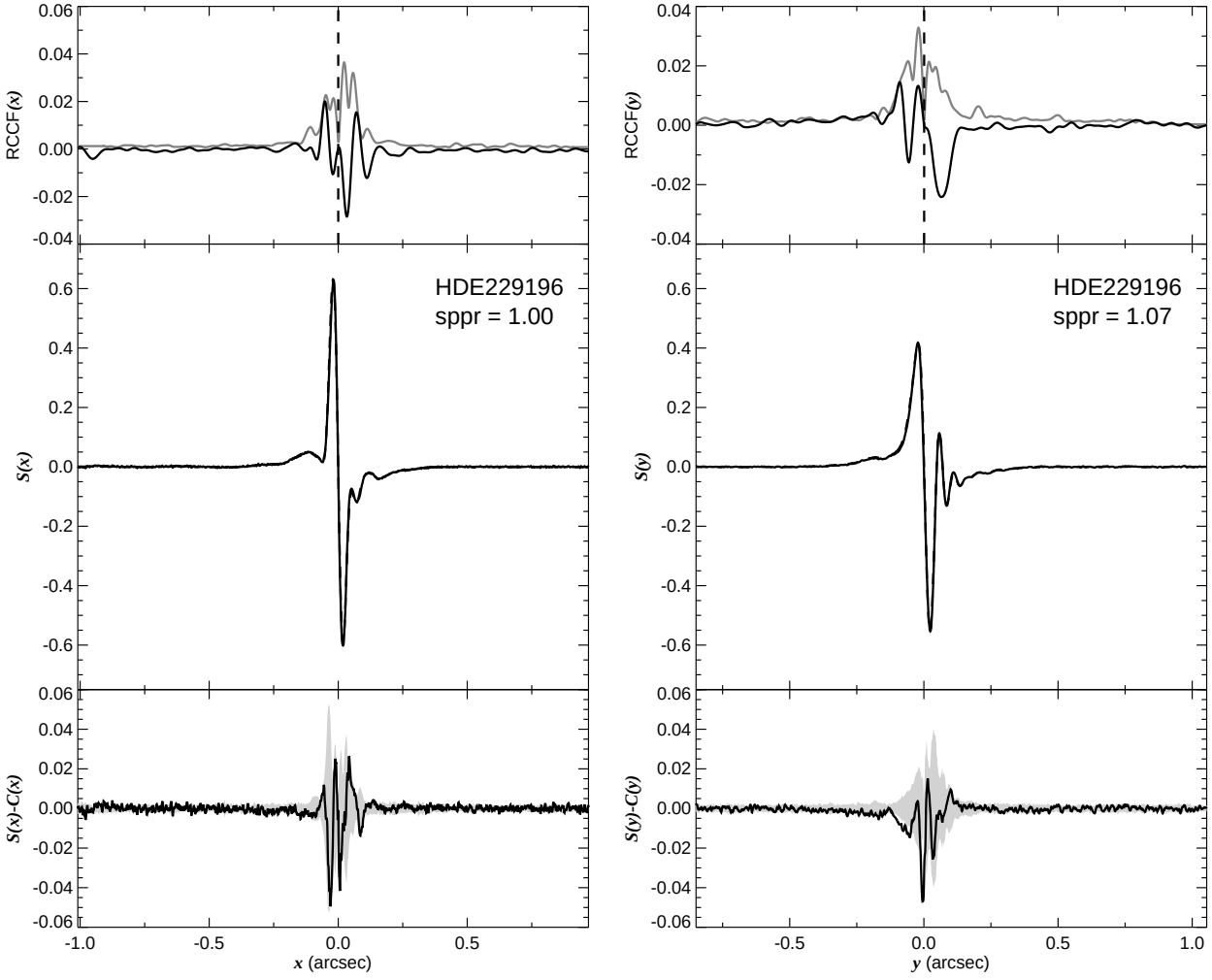

Fig. 1.237.— The FGS scans and binary detection tests for target 202310.79+405229.9 = HDE229196 obtained on BY 2008.0554.

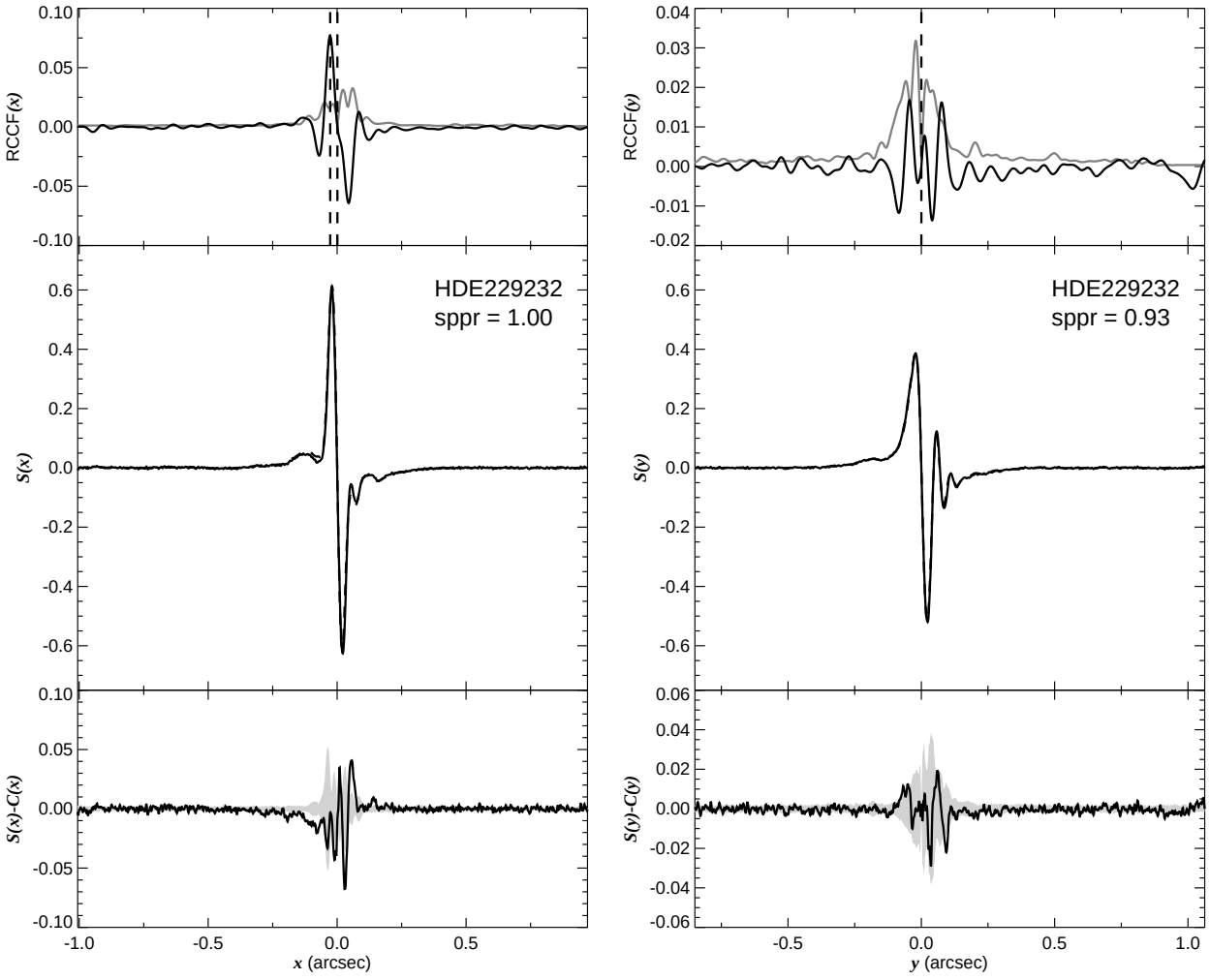

Fig. 1.238.— The FGS scans and binary detection tests for target 202359.18+390615.3 = HDE229232 obtained on BY 2008.1987.

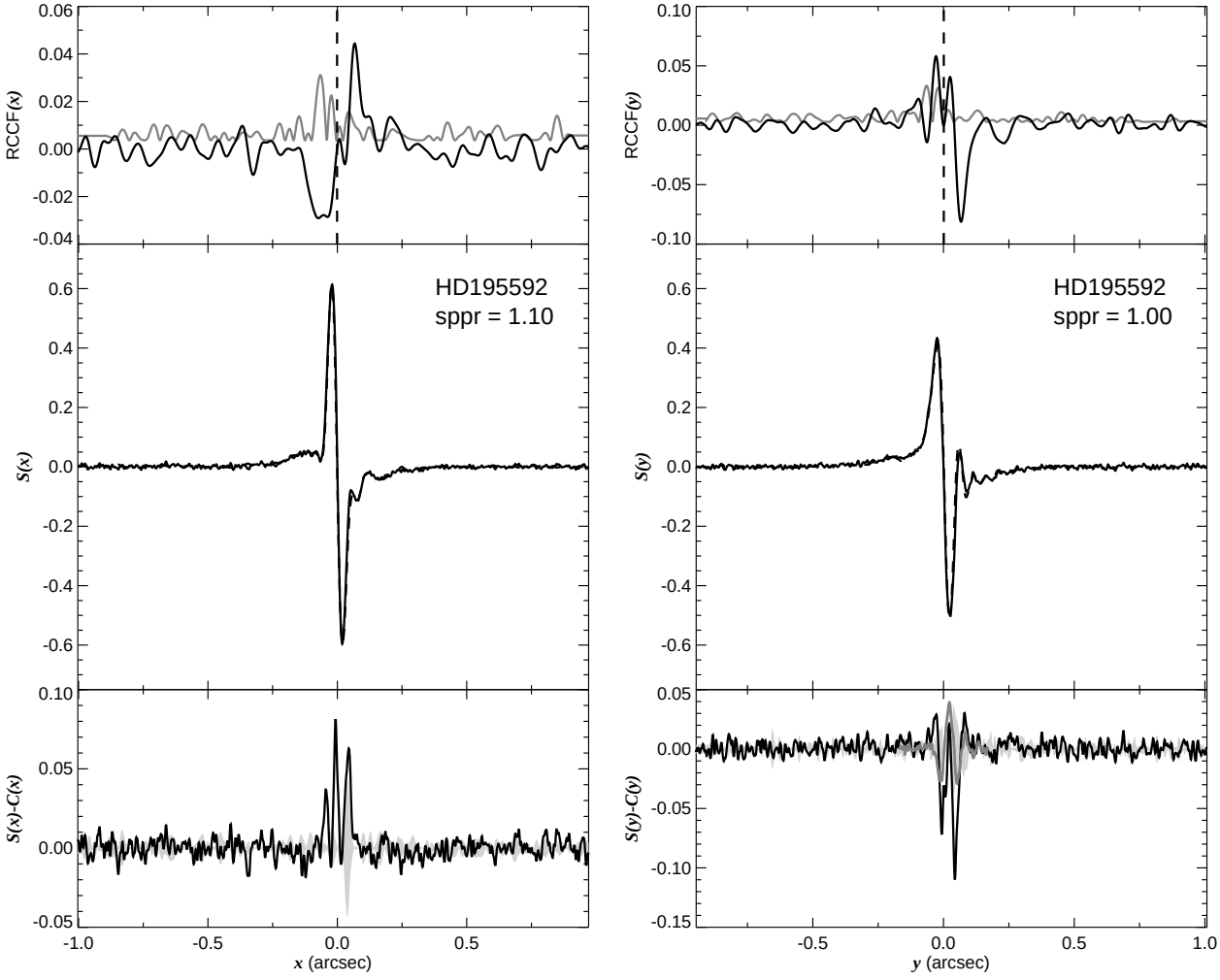

Fig. 1.239.— The FGS scans and binary detection tests for target 203034.97+441854.9 = HD195592 obtained on BY 2008.5326.

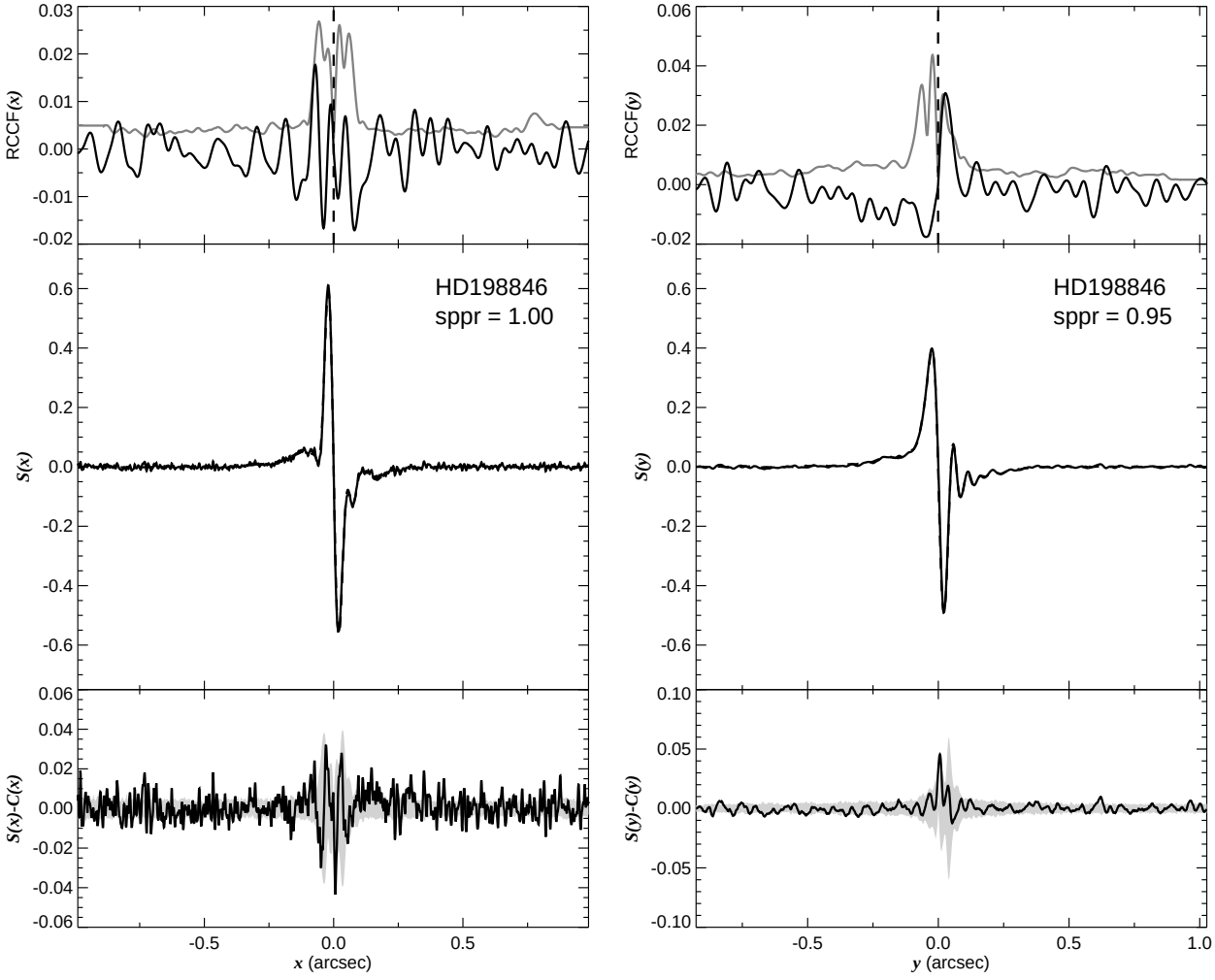

Fig. 1.240.— The FGS scans and binary detection tests for target 205203.58+343927.5 = HD198846 obtained on BY 2008.3239.

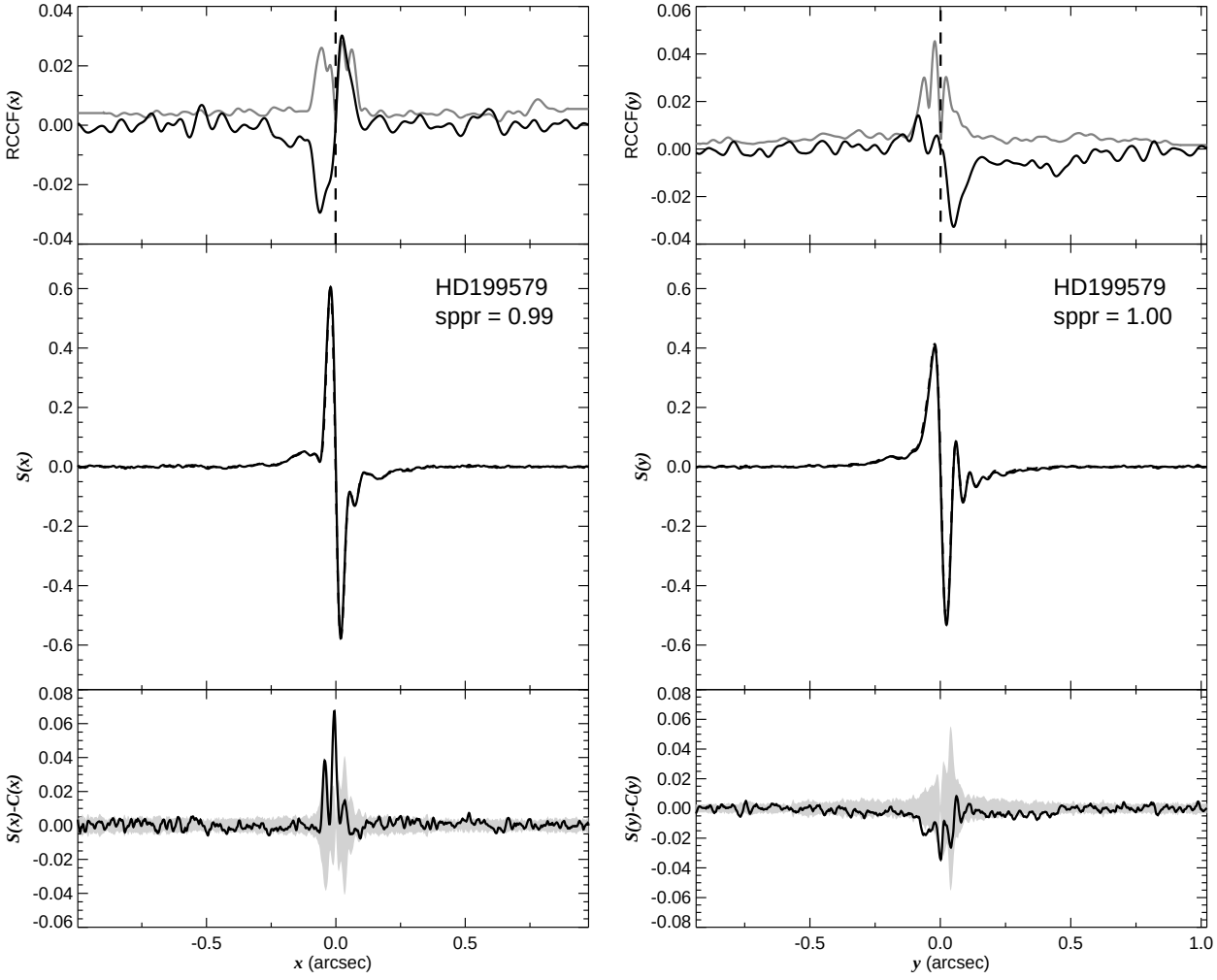

Fig. 1.241.— The FGS scans and binary detection tests for target 205634.78+445529.0 = HD199579 obtained on BY 2008.3266.

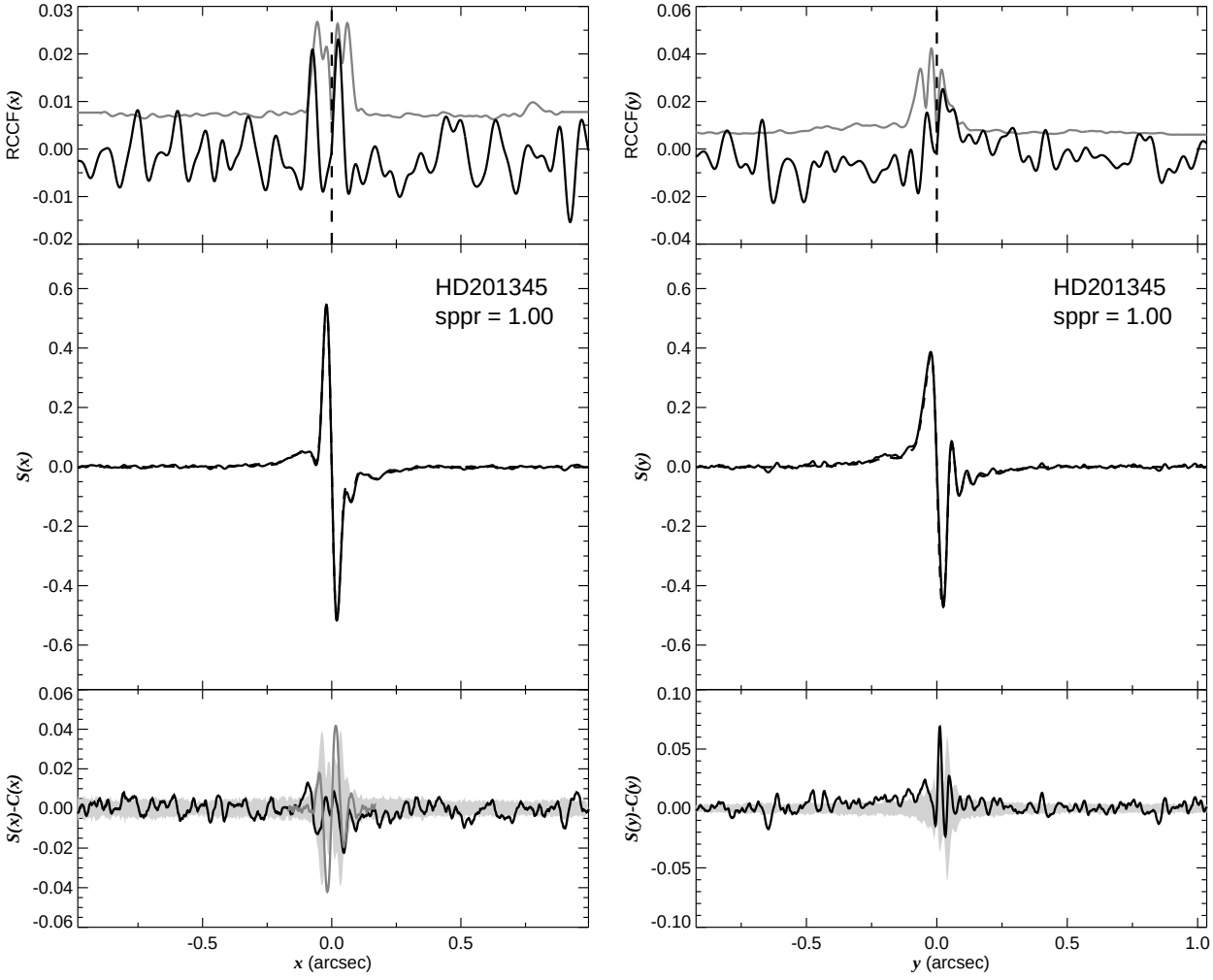

Fig. 1.242.— The FGS scans and binary detection tests for target 210755.42+332349.2 = HD201345 obtained on BY 2008.3155.

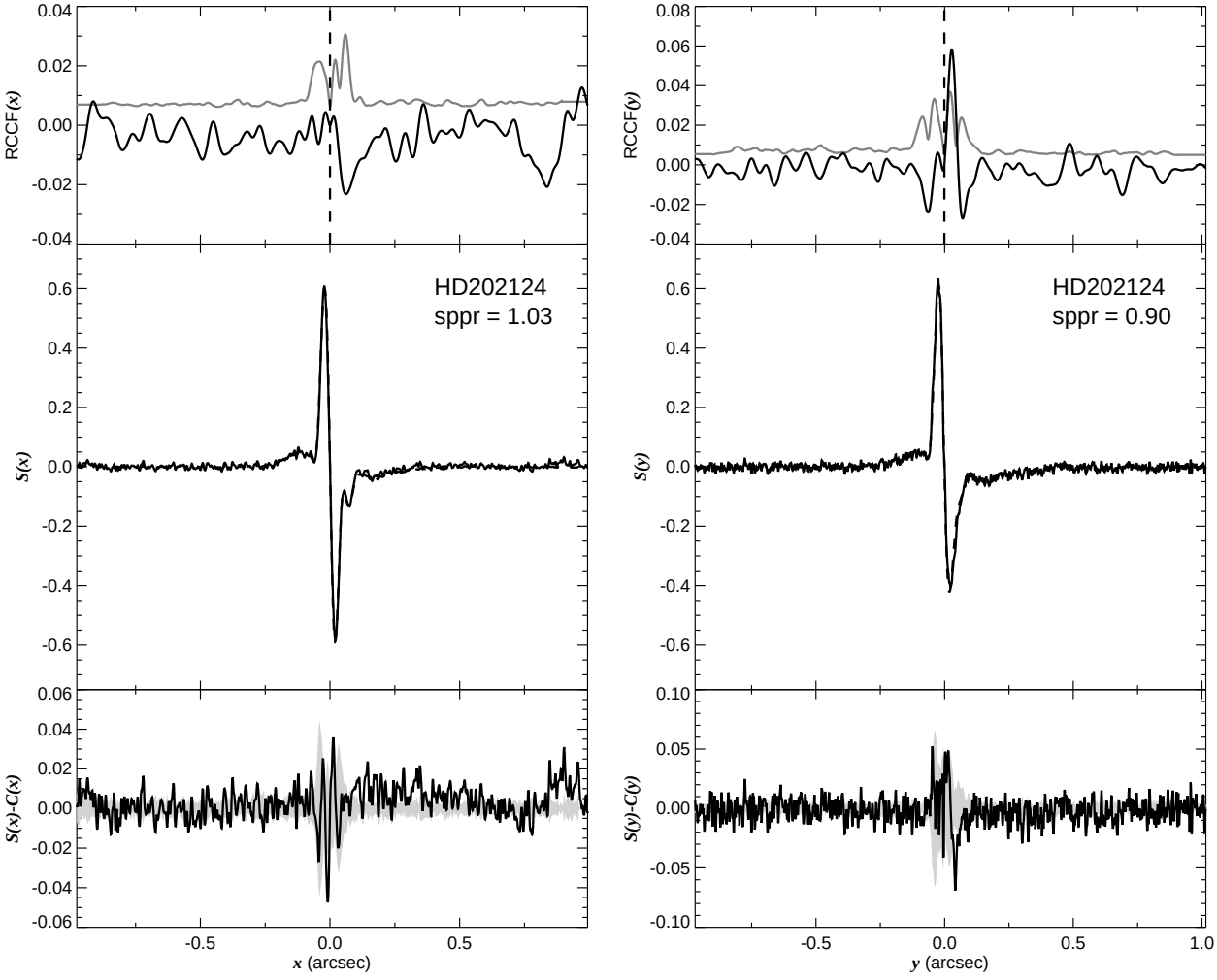

Fig. 1.243.— The FGS scans and binary detection tests for target 211228.39+443154.1 = HD202124 obtained on BY 2009.0957.

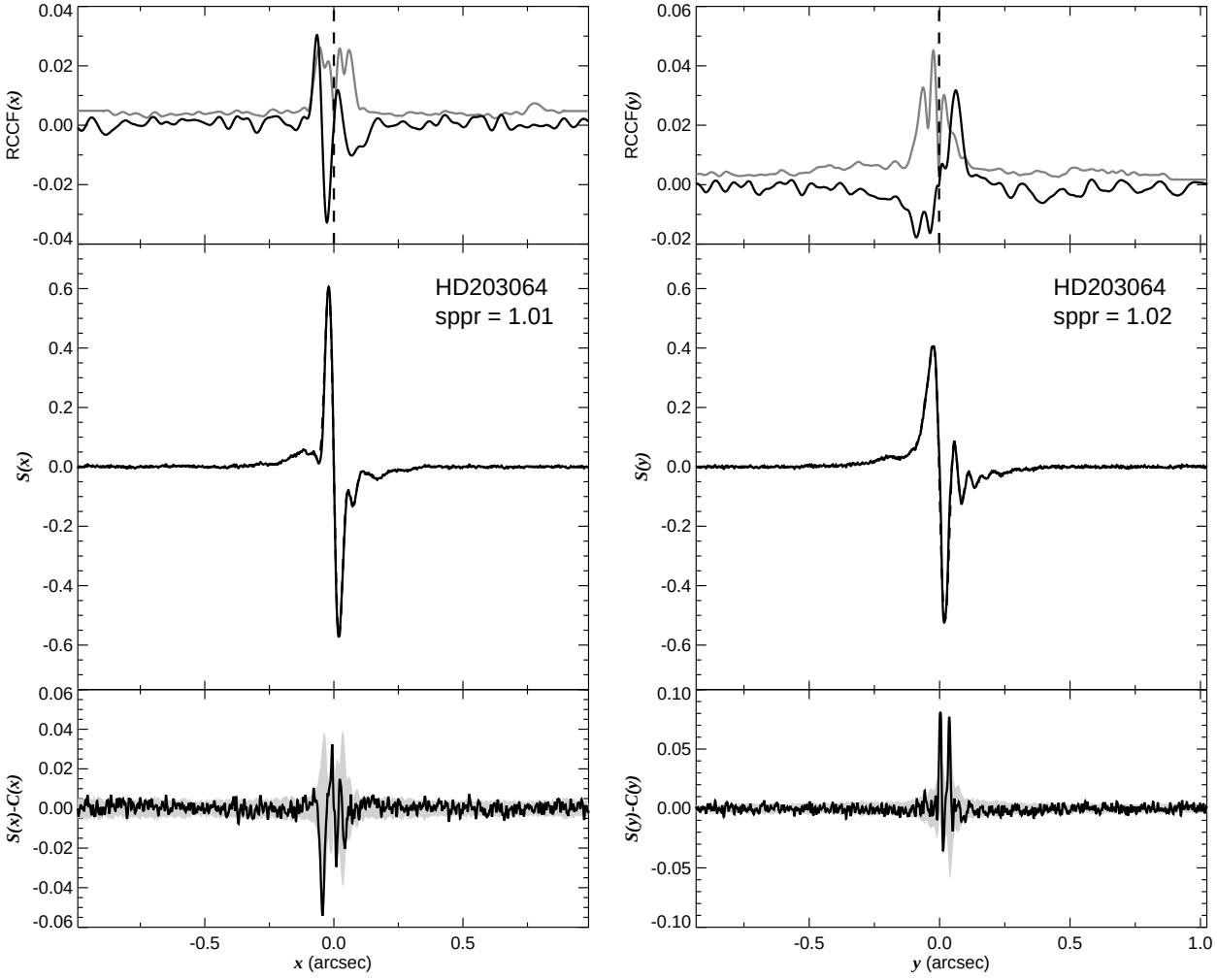

Fig. 1.244.— The FGS scans and binary detection tests for target 211827.19+435645.4 = HD203064 obtained on BY 2008.3264.

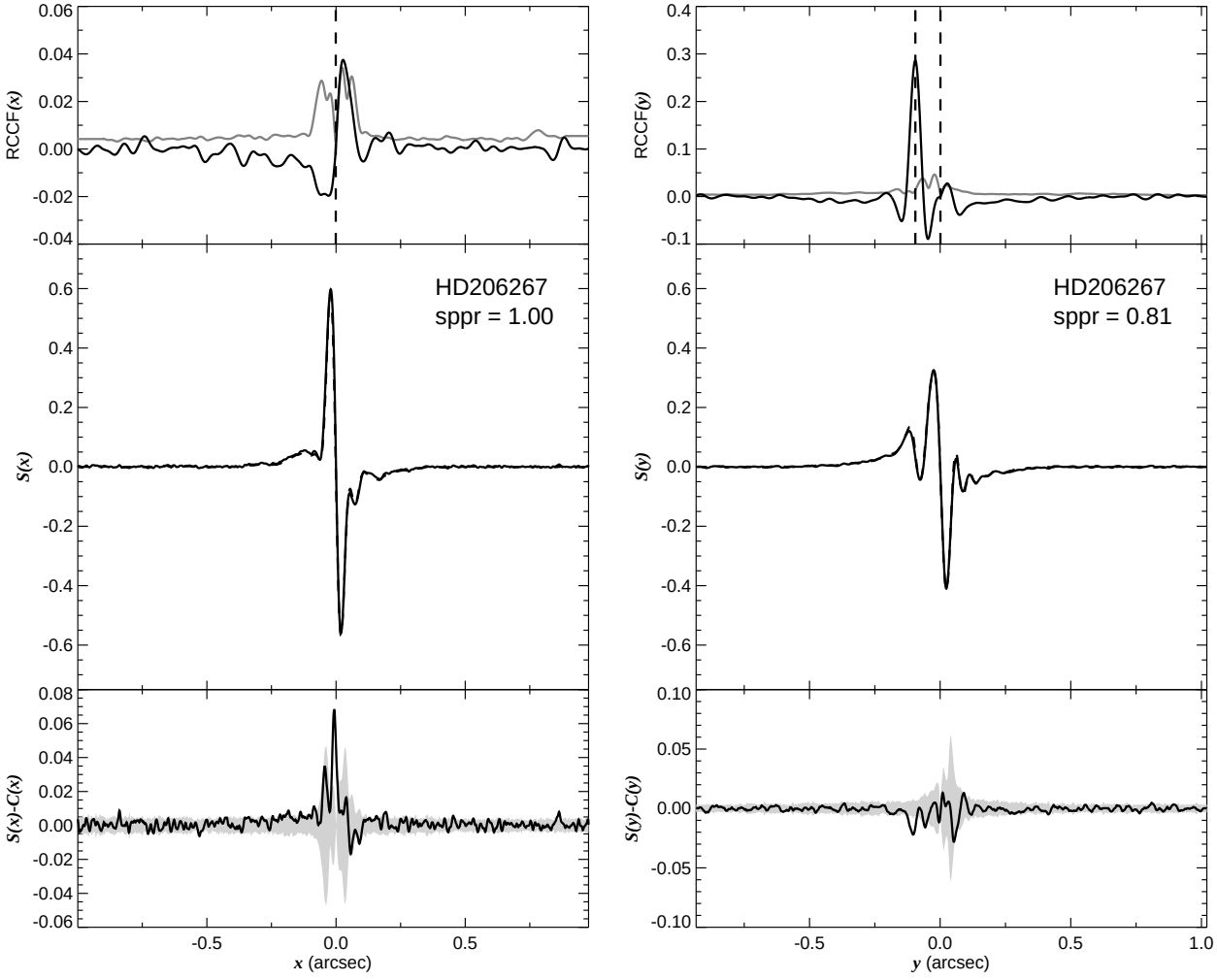

Fig. 1.245.— The FGS scans and binary detection tests for target 213857.62+572920.5 = HD206267 obtained on BY 2008.7182.

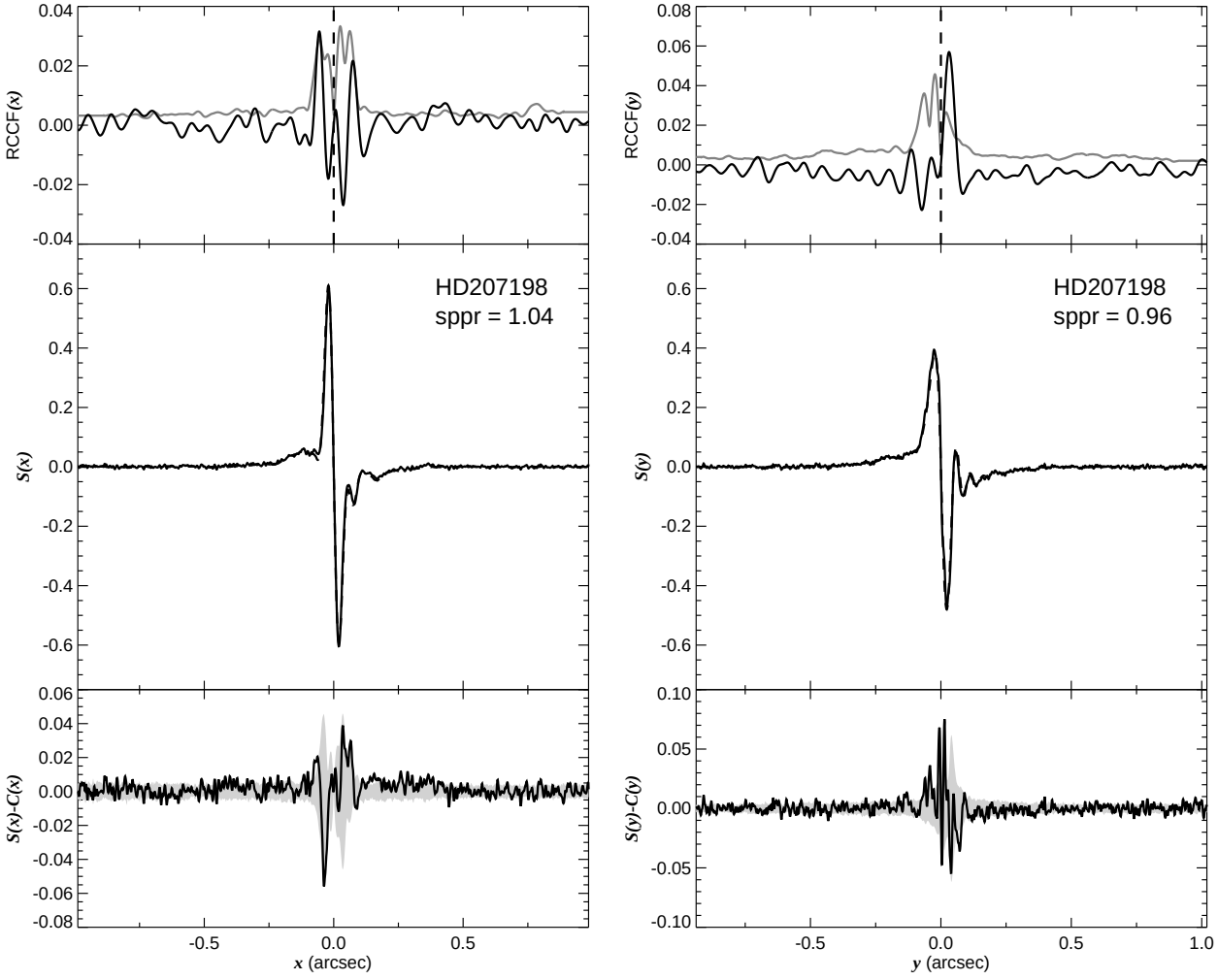

Fig. 1.246.— The FGS scans and binary detection tests for target 214453.28+622738.0 = HD207198 obtained on BY 2008.4390.

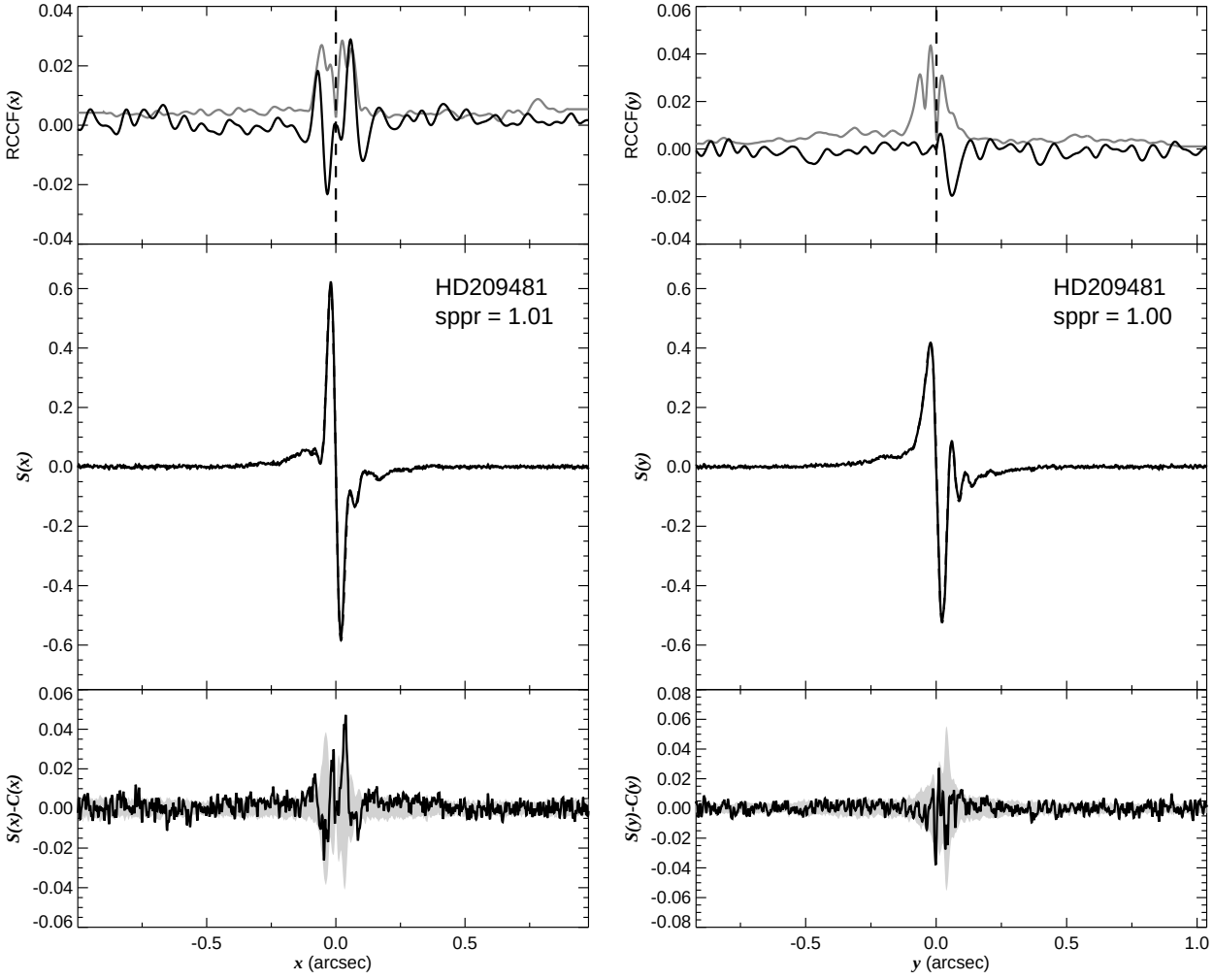

Fig. 1.247.— The FGS scans and binary detection tests for target 220204.57+580001.3 = HD209481 obtained on BY 2008.5675.

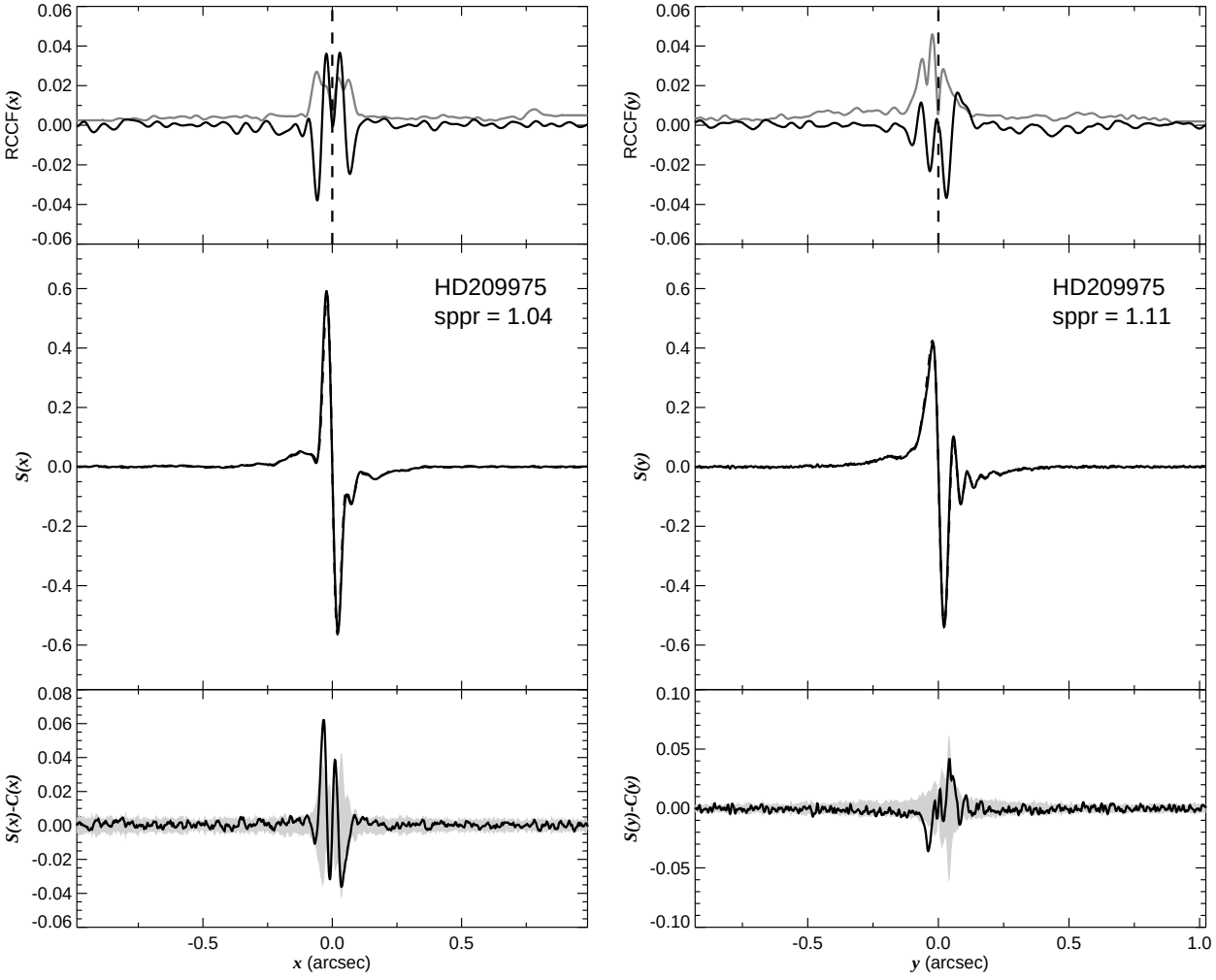

Fig. 1.248.— The FGS scans and binary detection tests for target 220508.79+621647.3 = HD209975 obtained on BY 2008.6007.

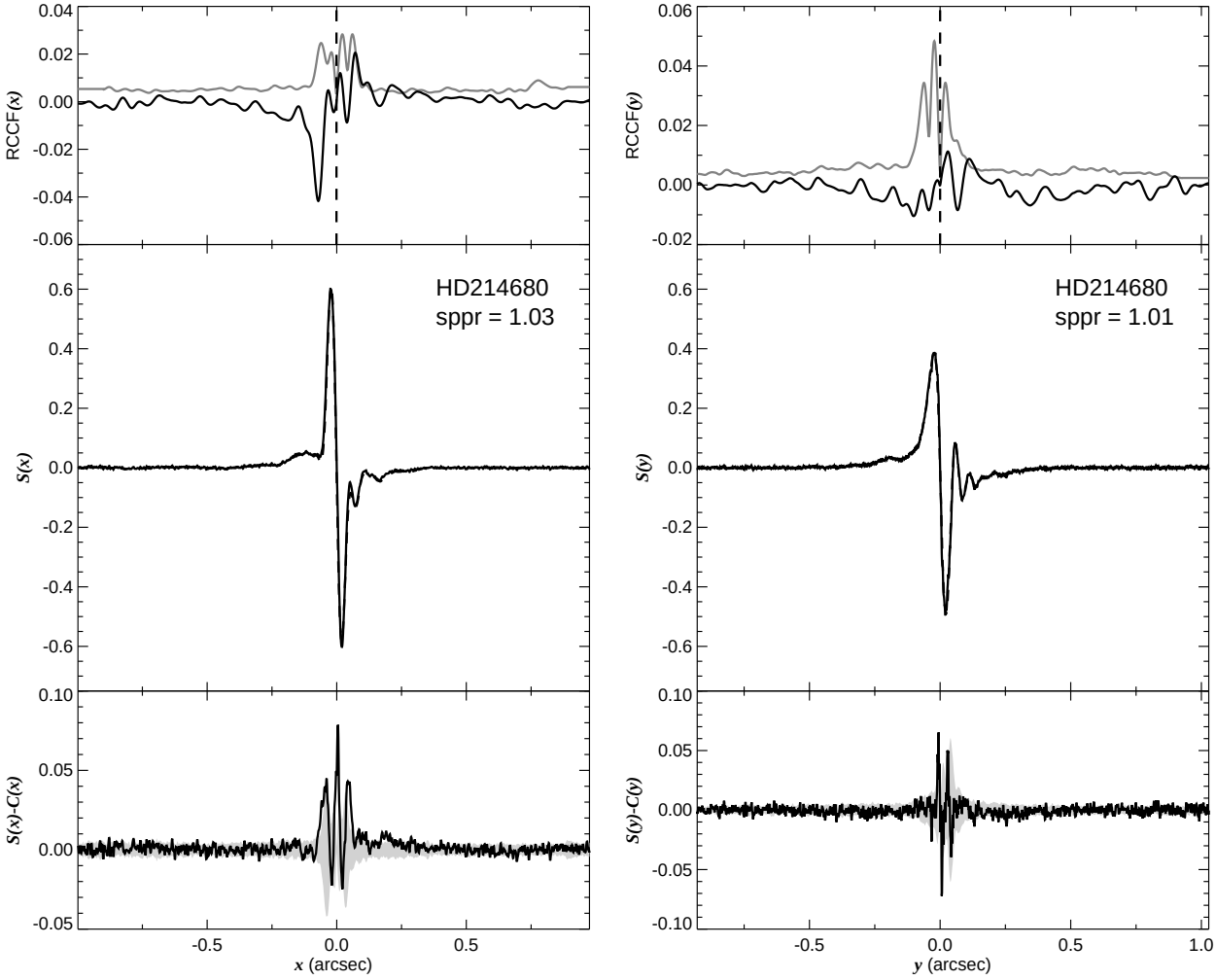

Fig. 1.249.— The FGS scans and binary detection tests for target 223915.68+390301.0 = HD214680 obtained on BY 2008.7587.

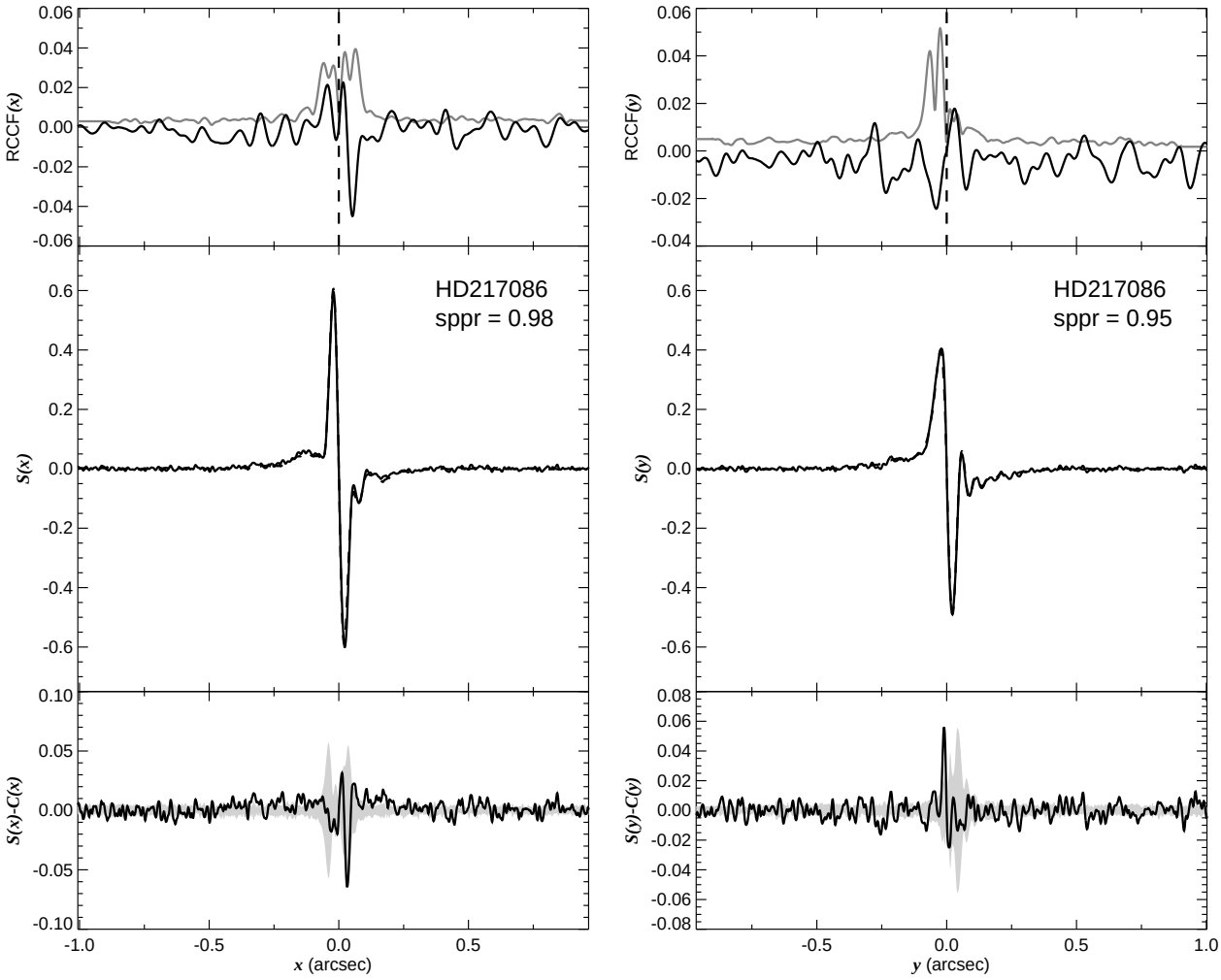

Fig. 1.250.— The FGS scans and binary detection tests for target 225647.19+624337.6 = HD217086 obtained on BY 2007.6749.

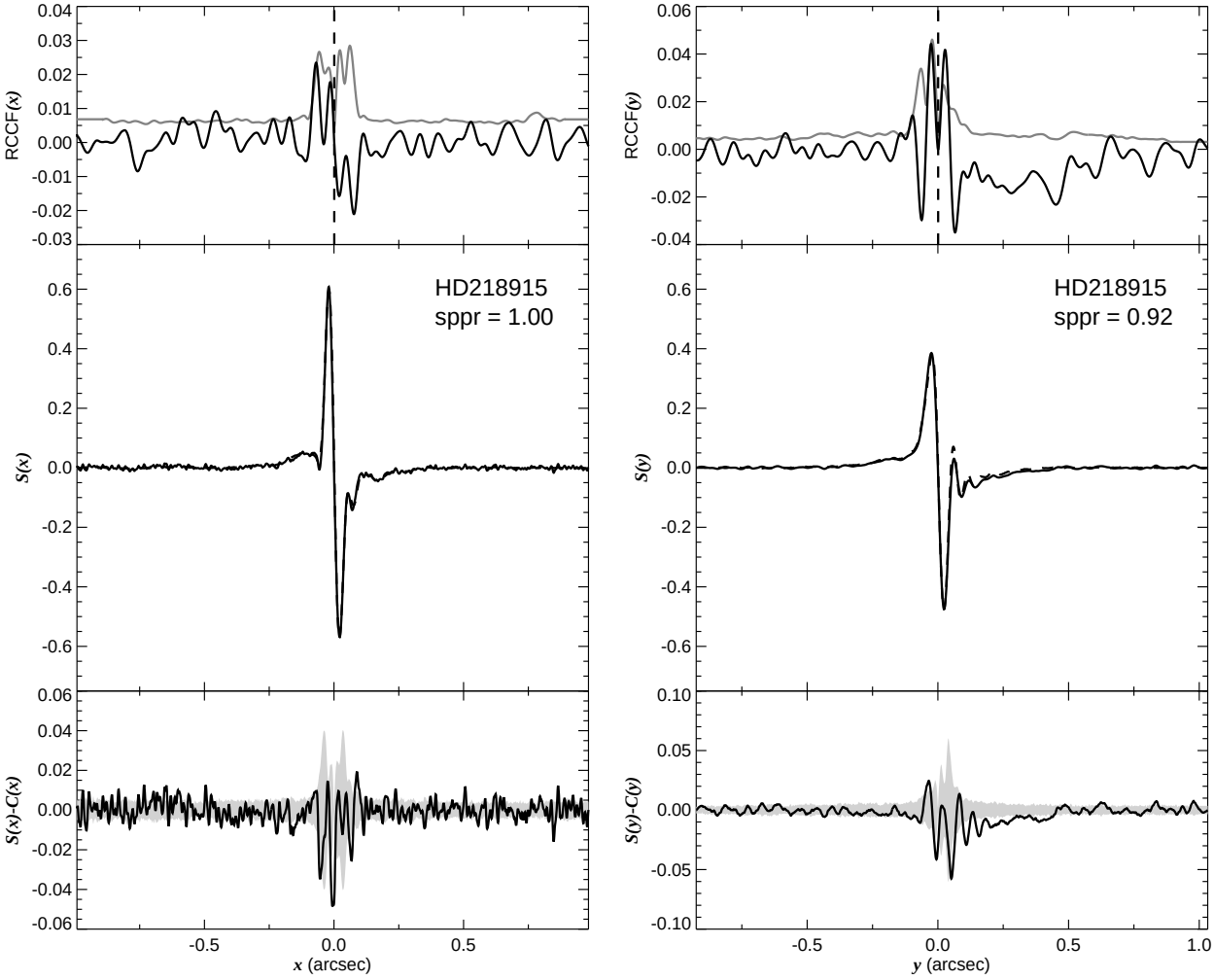

Fig. 1.251.— The FGS scans and binary detection tests for target 231106.95+530329.6 = HD218915 obtained on BY 2008.7122.

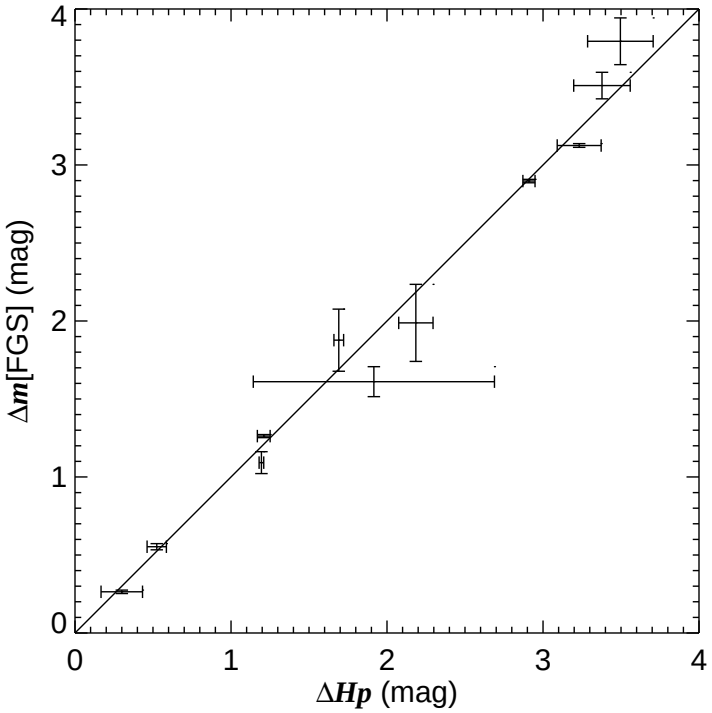

Fig. 2.— A comparison of magnitude differences from *Hipparcos* and and FGS for pairs in common. The estimates agree within uncertainties with the expected one-to-one relationship (shown as a solid line of slope unity).

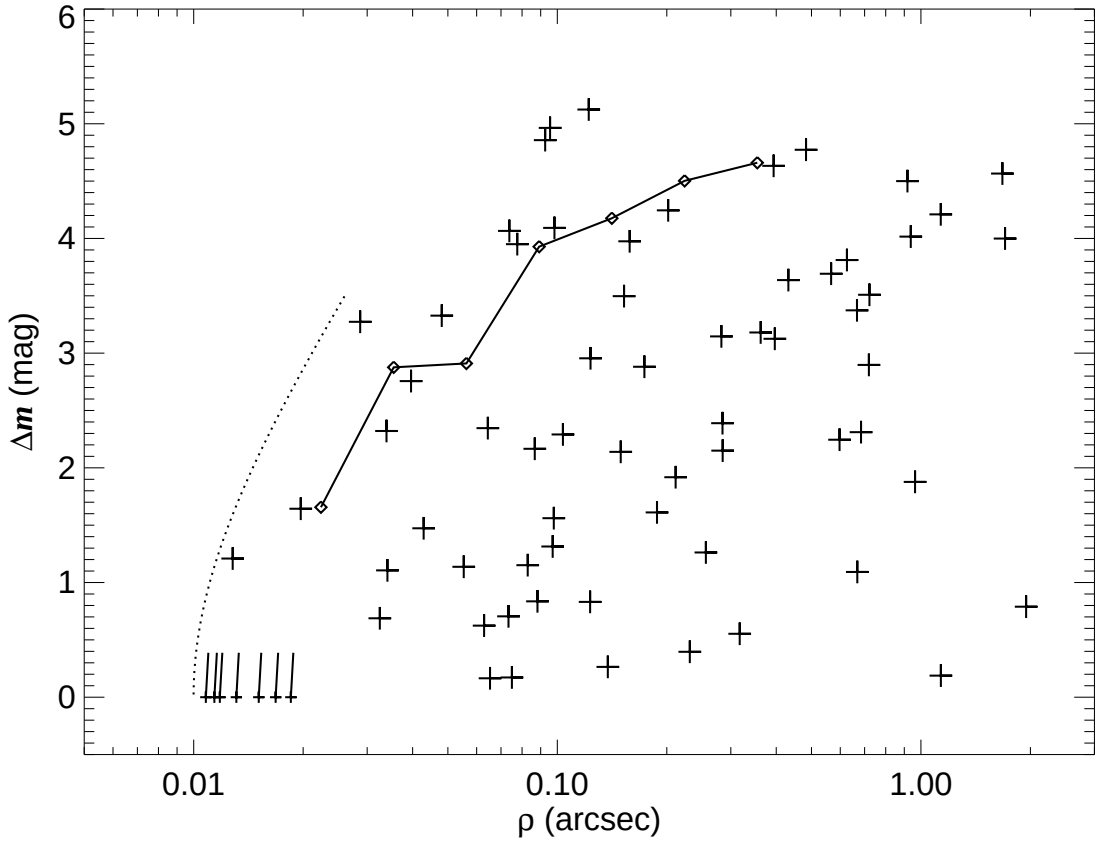

Fig. 3.— The fitted projected separation ρ and magnitude difference $\triangle m$ for the resolved pairs (large plus signs) and the partially resolved pairs (small plus signs with line segments showing the displacement from $\triangle m = 0.0$ to 0.4, i.e., for $F_2/F_1 = 1.0$ to 0.7). The diamonds connected by a solid line represent the expected faint limits for detection by the cross correlation method and the dotted line shows the corresponding faint limit for detection by the second derivative test (Caballero-Nieves et al. 2014).

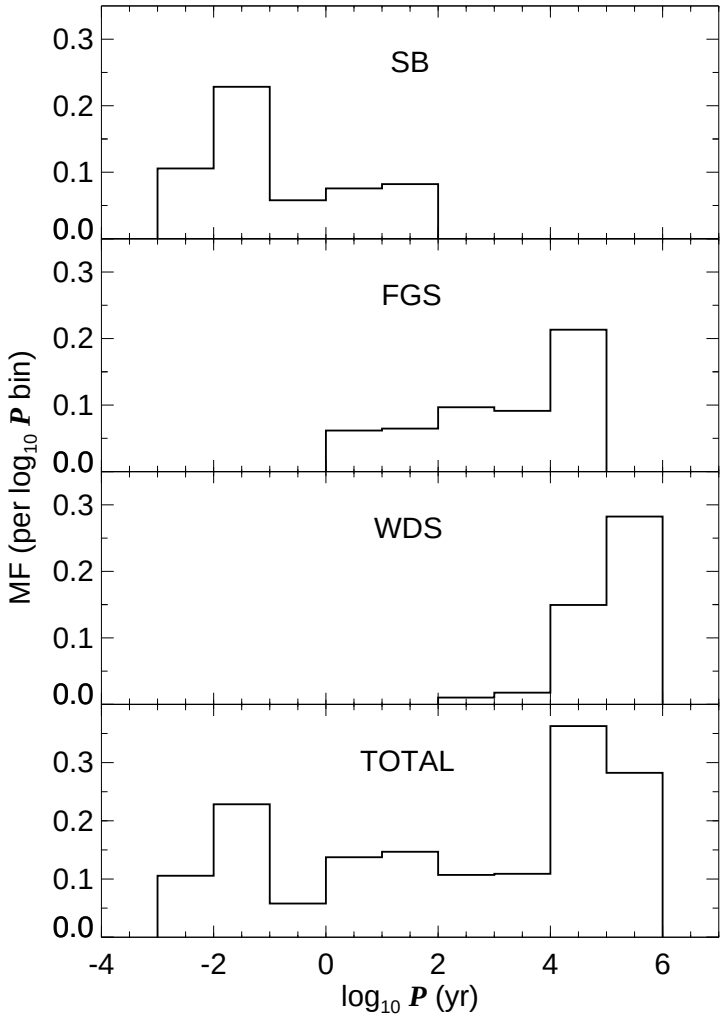

Fig. 4.— Histograms of the multiplicity fraction (MF) plotted as a function of orbital period. From top to bottom successive panels show the distributions for the spectroscopic binary (SB), Fine Guidance Sensor (FGS), Washington Double Star (WDS), and total samples, respectively.

Table 1. Stellar Parameters

(α, δ) (J2000) (1)	Star Name (2)	V (mag) (3)	$B-V$ (mag) (4)	Spectral Class. (5)	C/A/F Category (6)	Runaway Status (7)	d (kpc) (8)	Spec. Status (9)	Spectroscopic Reference (10)	N (SB) (11)	N (FGS) (12)	N (WDS) (13)	Notes (14)
000603.39+634046.8	HD108	7.39	0.17	O8 fpvar	Cas OB5	no	2.0	C	Nazé et al. (2001)	0	0	2	
001743.06+512559.1	HD1337	6.02	−0.05	O9.2 II	Field	yes	3.9	SB2OE	Stickland (1997)	1	0	3	AO Cas
014052.76+641023.1	HD10125	8.22	0.31	O9.7 II	Field	no	2.7	SB1?	Williams et al. (2011)	1	1	1	
022254.29+412847.7	HD14633	7.46	−0.20	ON8.5 V	Field	yes	2.2	SB1O	McSwain et al. (2007)	1	1	1	
022759.81+523257.6	HD15137	7.87	0.03	O9.5 II-IIIn	Field	yes	2.7	SB1O	McSwain et al. (2007)	1	0	0	
023249.42+612242.1	HD15570	8.11	0.69	O4 If	IC 1805	no	1.9	C	Hillwig et al. (2006)	0	0	0	
024044.94+611656.1	HD16429	7.67	0.62	O9 II-III(n)Nwk	Cas OB6	no	1.8	SB3O	McSwain (2003)	1	1	3	
024252.03+565416.5	HD16691	8.70	0.48	O4 If	Per OB1	no	1.8	C	De Becker et al. (2009)	1	0	0	
025107.97+602503.9	HD17505	7.07	0.40	O6.5 IIIn(f)	IC 1848	no	1.8	SB3O	Hillwig et al. (2006)	2	1	9	
025114.46+602309.8	HD17520A	8.26	0.32	O8 Vz	IC 1848	no	1.8	SB2?	Hillwig et al. (2006)	1	1	13	
031405.34+593348.5	HD19820	7.11	0.51	O8.5 III(n)((f))	Cam OB1	no	0.8	SB2OE	Hill et al. (1994)	1	0	1	CC Cas
035523.08+310245.0	HD24534	6.18	0.28	O9.5: npe	Per OB2	yes	0.3	SB1O	Grundstrom et al. (2007)	1	0	1	X Per
035538.42+523828.8	HD24431	6.74	0.37	O9 III	Cam OB1	no	0.8	C	Garmany et al. (1980)	0	1	0	
035857.90+354727.7	HD24912	4.04	0.01	O7.5 III(n)((f))	Per OB2	yes	0.3	C	Gies & Bolton (1986)	0	0	1	ξ Per
040751.39+621948.4	HD25639	6.95	0.47	B0 Ib(n)	NGC 1502	no	0.8	SB3OE	Gorda et al. (2007)	2	1	12	SZ Cam
045403.01+662033.6	HD30614	4.29	0.03	O9 Ia	Field	yes	1.1	C	McSwain et al. (2007)	0	0	0	α Cam
051022.79−684623.8	HDE269128	10.49	0.00	B3 Iaeq	LMC	···	50.0	SB1O	Tubbesing et al. (2002)	1	0	0	1, R81
051618.15+341844.3	HD34078	5.96	0.22	O9.5 V	Trapezium	yes	0.4	C	Gies & Bolton (1986)	0	0	3	AE Aur
051756.06−691603.9	HDE269321	10.79	0.09	B5 Iae	LMC	···	50.0	U	···	0	1	2	1, R85
051814.36−691501.1	HD35343	9.49	0.12	B5-9 Iae	LMC	···	50.0	U	Massey (2000)	0	1	2	1, S Dor
052229.30+333050.5	HDE242908	9.07	0.30	O4.5 V(n)((fc))z	NGC 1893	no	3.3	SB2?	Penny (1996)	1	0	0	
052942.65+352230.1	HD35921	6.78	0.19	O9.5 II	Aur OB1	no	1.1	SB2OE	Stickland et al. (1994)	1	1	0	LY Aur
053051.48−690258.6	HDE269662	10.35	0.24	B8-A2Iae	LMC	···	50.0	U	···	0	1	0	1, R110
053341.15+362735.0	HD36483	8.18	0.43	O9.5 IV(n)	Aur OB1	no	1.1	U	Petrie & Pearce (1961)	0	0	1	
053433.72−002311.5	HD36841	8.59	0.02	B7 V	Ori OB1	no	0.4	U		0	1	0	
053508.28+095603.0	HD36861A	3.39	−0.19	O8 III((f))	Cr 69	no	0.4	C	Fullerton et al. (1996)	0	0	4	λ^1 Ori A
053516.47−052322.9	HD37022C	5.07	−0.02	O7 Vp	Trapezium	no	0.4	C	Stahl et al. (2008)	0	1	6	θ^1 Ori C
053522.90−052457.8	HD37041A	5.02	−0.04	O9.5 IVp	Ori OB1	no	0.4	SB1O	Stickland & Lloyd (2001)	1	1	3	θ^2 Ori A
053540.53+212411.7	HD36879	7.57	0.20	O7 V(n)((f))z	Field	yes	1.9	C	Christy (1977)	0	0	1	
053844.77−023600.2	HD37468A	3.80	−0.24	O9.7 III	Ori OB1	no	0.4	SB2O	Simón-Díaz et al. (2011)	1	1	7	σ Ori A
053924.80+305326.8	HD37366	7.62	0.10	O9.5 IV	Aur OB1	no	1.1	SB2O	Boyajian et al. (2007b)	1	1	1	
055358.21+205234.7	HDE248894	9.29	0.24	O8.5 II-IIIn((f))	Field	no	2.6	U	···	0	0	0	
055444.73+135117.1	HD39680	7.92	0.04	O6 V:[n]pevar	Field	no	2.6	C	Gies & Bolton (1986)	0	0	1	

Table 1—Continued

(α, δ) (J2000) (1)	Star Name (2)	V (mag) (3)	$B-V$ (mag) (4)	Spectral Class. (5)	C/A/F Category (6)	Runaway Status (7)	d (kpc) (8)	Spec. Status (9)	Spectroscopic Reference (10)	N (SB) (11)	N (FGS) (12)	N (WDS) (13)	Notes (14)
060552.46+481457.4	HD41161	6.76	−0.09	O8 Vn	Field	yes	1.4	C	Fullerton et al. (1996)	0	0	2	
060855.82+154218.2	HD41997	8.41	0.38	O7.5 Vn((f))	Field	yes	1.5	C	Chini et al. (2012)	0	0	0	
060939.57+202915.5	HD42088	7.56	0.06	O6 V((f))z	NGC 2175	no	1.6	C	Conti et al. (1977)	0	0	0	
061831.77+224045.1	HDE254755	8.85	0.60	O8.5 II-III((f))	Gem OB1	no	1.2	U	Popper (1950)	0	1	0	
061941.65+231720.2	HDE255055	9.39	0.25	O9.5 IV	Field	no	2.2	U	···	0	0	0	
062258.24+225146.2	HDE256035	9.16	0.54	O9.5 Vn	Gem OB1	no	1.2	U	···	0	0	0	
062328.54+202331.7	HD44597	9.03	0.26	O9.2 V	Field	no	2.0	U	···	0	0	0	
062438.36+194215.8	HD44811	8.42	0.13	O7 V(n)z	Field	no	2.3	C	Chini et al. (2012)	0	0	1	
062715.78+145321.2	HD45314	6.63	0.15	O9: npe	Mon OB1	no	0.6	C	Boyajian et al. (2007a)	0	0	1	
063120.87+045003.3	HD46056	8.18	0.22	O8 Vn	NGC 2244	no	1.4	C	Chini et al. (2012)	1	0	3	
063152.53+050159.2	HD46149	7.60	0.17	O8.5 V	NGC 2244	no	1.4	SB2?	Chini et al. (2012)	1	0	0	
063155.52+045634.3	HD46150	6.72	0.13	O5 V((f))z	NGC 2244	no	1.4	C	Boyajian et al. (2007a)	0	0	11	
063210.47+045759.8	HD46202	8.19	0.18	O9.2 V	NGC 2244	no	1.4	C	Chini et al. (2012)	0	1	1	
063350.96+043131.6	HD46485	8.24	0.32	O7 V((f))nz var?	NGC 2244	no	1.4	C	Chini et al. (2012)	0	0	0	
063423.57+023202.9	HD46573	7.93	0.34	O7 V((f))z	Mon OB2	no	1.4	SB2?	Chini et al. (2012)	1	0	0	
063625.89+060459.5	HD46966	6.88	−0.05	O8.5 IV	Cr 106	no	1.6	C	Garmany et al. (1980)	0	1	1	
063724.04+060807.4	HD47129	6.06	0.05	O8 fpvar	Cr 106	no	1.6	SB2O	Bagnuolo & Barry (1996)	1	0	2	Plaskett's
063838.19+013648.7	HD47432	6.22	0.14	O9.7 Ib	Mon OB2	no	1.4	C	Fullerton et al. (1996)	0	0	1	
064021.98−002126.0	HDE292090	9.87	0.31	B3 Ib	Field	no	3.1	U	···	0	0	0	
064058.66+095344.7	HD47839	4.64	−0.25	O7 V((f))zvar	NGC 2264	no	0.7	SB1?	Gies et al. (1993)	1	1	13	15 Mon
064159.23+062043.5	HD48099	6.36	−0.04	O5 V((f))z	Mon OB2	no	1.4	SB2O	Stickland (1996)	1	0	0	
064240.55+014258.2	HD48279	7.89	0.15	O8.5 VzNstrvar?	Field	no	1.7	C	Levato et al. (1988)	0	0	3	
064453.82+003712.6	HDE292167	9.24	0.44	O9 Iab	Field	no	3.1	U	Crampton (1972)	0	0	0	
064548.70−071839.0	ALS85	12.17	0.14	O7.5 V z	SH 2-289	no	10.1	U	···	0	2	0	
064849.56+002252.7	BD+00 1617A	11.12	0.52	O9.7 V	Bochum 2	no	6.0	C	Munari & Tomasella (1999)	0	1	1	
064850.48+002237.6	BD+00 1617B	11.11	0.31	O9.5 III(n)	Bochum 2	no	6.0	SB1O	Munari & Tomasella (1999)	1	1	2	
064851.20+002224.0	BD+00 1617C	11.21	0.49	O9.5 IV	Bochum 2	no	6.0	SB1O	Munari & Tomasella (1999)	1	1	0	
065017.62+002647.6	HDE292392	10.01	0.33	O8 I	Field	no	7.4	U	Popper (1950)	0	0	0	
065133.93+133702.1	HDE265134	9.16	−0.07	O9.5 III	Field	no	5.8	U	Popper (1950)	0	0	0	
065158.45+012234.2	HDE289291	9.65	0.27	O9 II-III(n)	Field	no	3.0	U	Popper (1950)	0	0	0	
065930.21−044843.8	ALS9243	10.58	0.48	O9.7 IV	SH 2-287	no	3.2	U	Crampton & Fisher (1974)	0	1	0	
070021.08−054936.0	HD52266	7.20	−0.04	O9.5 IIIn	Field	no	1.3	SB1?	McSwain et al. (2007)	1	0	0	
070127.05−030703.3	HD52533	7.70	−0.09	O8.5 IVn	HD52533	no	1.9	SB1O	McSwain et al. (2007)	1	1	5	

Table 1—Continued

(α, δ) (J2000) (1)	Star Name (2)	V (mag) (3)	$B-V$ (mag) (4)	Spectral Class. (5)	C/A/F Category (6)	Runaway Status (7)	d (kpc) (8)	Spec. Status (9)	Spectroscopic Reference (10)	N (SB) (11)	N (FGS) (12)	N (WDS) (13)	Notes (14)
070635.97−122338.2	HD53975	6.47	−0.10	O7.5 Vz	CMa OB1	no	1.1	SB2O	Gies et al. (1994)	1	0	0	
070920.25−102047.6	HD54662	6.21	0.03	O7 Vzvar?	CMa OB1	no	1.1	SB2O	Boyajian et al. (2007b)	1	0	0	
071008.15−114809.8	HD54879	7.64	−0.01	O9.7 V	CMa OB1	no	1.1	C	Boyajian et al. (2007a)	0	0	0	
071428.25−101858.5	HD55879	6.01	−0.17	O9.7 III	NGC 2353	no	1.1	C	Neubauer (1943)	0	0	0	
071821.42−245900.4	ALS18846	11.80	0.48	O9 III	Field	no	9.0	U	···	0	1	0	
071840.38−243331.3	HD57060	4.96	−0.15	O7 Iafpvar	Cr 121	no	0.6	SB2OE	Bagnuolo et al. (1999)	1	0	0	UW CMa
071842.49−245715.8	HD57061	4.39	−0.15	O9 II	NGC 2362	no	1.4	SB1OE	Stickland et al. (1998)	2	2	4	τ CMa
071930.10−220017.3	HD57236	8.74	0.19	O8.5 V	Field	no	2.2	C	Neubauer (1943)	0	0	1	
072202.05−085845.8	HD57682	6.42	−0.19	O9.2 IV	Field	yes	1.2	C	Garmany et al. (1980)	0	0	0	
072512.28−210126.3	HD58509	8.58	0.02	B1 IIIn	NGC 2384	no	2.1	C	Huang & Gies (2006)	0	0	0	
072755.38−152307.3	HD59114	9.51	0.48	O7 Iaf	Field	no	5.0	U	Popper (1944)	0	1	0	
073001.28−190834.7	ALS458	11.30	0.64	O6.5 V ((f))z	SH 2-306	no	4.2	U	···	0	0	0	
073035.28−190622.2	ALS467	11.15	0.61	O9.5 III	SH 2-306	no	4.2	C	Williams et al. (2011)	0	0	0	
073146.74−165948.0	HD59986	9.44	0.23	O9.5 IV	Bochum 4	no	2.3	C	Cruz-González et al. (1974)	0	0	0	
073202.81−192607.7	ALS499	10.67	0.49	O9.7 V	Bochum 6	no	2.5	U	···	0	0	0	
073301.84−281932.9	HD60369	8.14	0.01	O9 III	Field	no	3.3	SB1?	Thackeray et al. (1973)	1	0	1	
073334.32−275838.3	HD60479	8.41	0.33	O9.2 Ib	Pup Group B	no	4.0	U	···	0	0	0	
073513.95−184757.2	BD-18 1920	10.41	0.63	O9 V	SH 2-307	no	2.2	U	···	0	0	0	
073642.04−342516.8	CD-34 3746	10.16	0.26	O9 V	Bochum 15	no	2.8	U	···	0	0	0	
073705.73+165415.3	HD60848	6.85	−0.21	O8: V:pe	Field	yes	1.6	C	Boyajian et al. (2007a)	0	0	0	
073816.12−135101.2	HD61347	8.43	0.17	O9 Iab	Field	no	5.6	U	Neubauer (1943)	0	0	0	
073949.34−323442.1	HD61827	7.65	0.55	B3 Iab	Bochum 15	no	2.8	U	···	0	0	0	
074030.29−333044.6	CD-33 4026	10.08	0.46	O7 e	Bochum 15	no	2.8	U	···	0	0	0	
074139.98−334954.1	CD-33 4043	9.85	0.43	O9 IV	Bochum 15	no	2.8	U	···	0	0	0	
074143.44−344727.6	CD-34 3814	10.35	0.30	O9 III	Bochum 15	no	2.8	U	···	0	1	0	
074254.87−341907.9	CD-34 3831	10.96	0.98	O9 V	Bochum 15	no	2.8	U	···	0	0	0	
074328.98−291912.5	CD-29 4849	10.01	0.21	B0.5 Ib	Field	no	7.4	U	···	0	0	0	
074549.03−262931.4	HD63005	9.13	−0.02	O6.5 IV((f))	Pup OB1	no	2.0	C	Markova et al. (2011)	0	0	0	
074636.20−264140.0	CD-26 4955	10.47	0.38	O5	Field	no	5.2	U	···	0	0	0	
075220.28−262546.7	HD64315	9.23	0.22	O5.5 Vz	NGC 2467	no	6.3	SB4OE	Lorenzo et al. (2010)	2	1	1	V402 Pup
075250.42−262822.3	CD-26 5126	11.37	0.40	B0.5 V	Field	no	3.9	U	Huang & Gies (2006)	0	0	0	
075255.40−262842.7	CD-26 5129	10.72	0.24	B0	Field	no	3.9	U	···	0	0	0	
075301.01−270657.8	CD-26 5136	9.67	0.32	O6.5 Iabf	Field	no	6.0	C	Williams et al. (2011)	0	0	0	

Table 1—Continued

(α, δ) (J2000) (1)	Star Name (2)	V (mag) (3)	$B-V$ (mag) (4)	Spectral Class. (5)	C/A/F Category (6)	Runaway Status (7)	d (kpc) (8)	Spec. Status (9)	Spectroscopic Reference (10)	N (SB) (11)	N (FGS) (12)	N (WDS) (13)	Notes (14)
075338.20−261402.6	HD64568	9.40	0.07	O3 V((f*))z	NGC 2467	no	6.3	C	Williams et al. (2011)	0	0	0	
075552.85−283746.8	CD-28 5104	9.97	0.16	O6.5 f?p	Field	no	4.6	SB1?	Levato et al. (1988)	1	0	0	
075557.13−283218.0	HD65087	9.52	0.09	B2.5 IV	Pup OB2	no	2.9	U	···	0	1	0	
075626.41−292526.1	CD-29 5191	9.77	0.20	B0.5 IIIn(e)	Turner 14	no	3.2	U	Duflot et al. (1995)	0	1	0	
075758.55−283529.4	CD-28 5180	10.92	0.29	O8 III(f)	Ruprecht 44	no	4.7	U	···	0	1	0	
075830.66−263408.2	CD-26 5285	10.69	0.32	O6.5 IIIf	Field	no	7.6	U	···	0	0	0	
075851.83−284504.2	CD-28 5216	11.27	0.27	O9 III	Ruprecht 44	no	4.7	U	Peton-Jonas (1981)	0	0	0	
075922.16−285423.8	CD-28 5235	10.07	0.31	B1 V	Field	no	3.1	U	Peton-Jonas (1981)	0	0	0	
080210.34−040136.4	BD-03 2178	9.46	1.14	rK1 III	Field	no	1.1	U	···	0	0	0	K-star
080408.54−272908.8	HD66788	9.45	−0.08	O9 V	Pup OB2	no	2.9	U	···	0	0	0	
081101.68−371732.5	HD68450	6.44	−0.01	O9.7 II	Field	no	1.9	C	Garmany et al. (1980)	0	0	2	
081200.73−390841.7	CD-38 4168	9.28	0.46	O8.5 III	Vel OB1	no	1.5	U	···	0	0	0	
081335.36−342843.9	CD-34 4496	9.27	0.36	O7 III	Pup OB3	no	1.7	U	···	0	1	0	
081517.15−354414.6	CD-35 4384	9.19	0.43	O9.2 III	Pup OB3	no	1.7	U	···	0	2	0	
081548.57−353752.9	HD69464	8.80	0.31	O7 Ib(f)	ASCC 45	no	3.0	SB2?	Markova et al. (2011)	1	1	0	
081602.74−441921.7	HD69648	8.05	0.29	O8.5 II	Field	no	3.7	U	···	0	0	0	
081624.75−354421.5	CD-35 4412	9.48	0.42	B0 Iab	Pup OB3	no	1.7	U	···	0	0	0	
081854.46−360752.0	CD-35 4469	10.19	0.29	O9.2 V(n)	Pup OB3	no	1.7	SB2O	Williams (2011)	1	0	0	
081903.90−360844.9	CD-35 4471	9.17	0.28	O9.5 IV	Pup OB3	no	1.7	SB1?	Crampton (1972)	1	1	0	
082455.79−441803.0	HD71304	8.26	0.53	O9 II	Vel OB1	no	1.5	C	Chini et al. (2012)	0	0	2	
083909.53−402509.3	HD73882	7.22	0.40	O8.5 IV	Ruprecht 64	no	0.8	SB1?E	Chini et al. (2012)	1	1	0	NX Vel
084047.79−450330.2	HD74194	7.55	0.23	O8.5 Ib-II(f)p	Vel OB1	no	1.5	SB1?	Götz et al. (2007)	1	0	0	LM Vel
084324.16−460828.7	CD-45 4447	11.29	0.17	O7.5 V	Bochum 7	no	5.0	SB1?	Corti et al. (2003)	1	0	0	
084338.66−460815.9	CPD-45 2910	11.97	0.80	O9.5 V	Bochum 7	no	5.0	U	···	0	1	0	
084349.80−460708.8	ALS1135	10.88	0.39	O6.5 V((f))	Bochum 7	no	5.0	SB2OE	Michalska et al. (2013)	1	0	0	V467 Vel
084351.09−460346.5	CD-45 4462	11.50	0.38	O9/9.5 V	Bochum 7	no	5.0	C	Corti et al. (2003)	0	2	0	
084425.05−455334.7	CD-45 4472	11.28	0.64	O7.5 V	Bochum 7	no	5.0	C	Corti et al. (2003)	0	0	0	
084510.46−455854.7	CPD-45 2977	10.95	0.48	O9.5 II	Bochum 7	no	5.0	U	···	0	1	0	
084701.59−440428.8	HD75211	7.51	0.40	O8.5 II((f))	Vel OB1	no	1.5	SB1?	Chini et al. (2012)	0	0	0	
084725.14−364502.7	HD75222	7.42	0.38	O9.7 Iab	Field	yes	2.7	C	Chini et al. (2012)	0	0	0	
085002.28−443439.9	CD-44 4865	9.43	0.72	B0 III	Vel OB1	no	1.5	C	Markova et al. (2011)	0	0	0	
085021.02−420523.2	HD75759	5.99	−0.10	O9 V	ASCC 50	no	0.9	SB2O	Thackeray (1966)	1	0	0	
085033.46−463145.1	HD75821	5.10	−0.21	B0 II	Vel OB1	no	1.5	SB2OE	Mayer et al. (1997)	1	0	1	KX Vel

Table 1—Continued

(α, δ) (J2000) (1)	Star Name (2)	V (mag) (3)	$B-V$ (mag) (4)	Spectral Class. (5)	C/A/F Category (6)	Runaway Status (7)	d (kpc) (8)	Spec. Status (9)	Spectroscopic Reference (10)	N (SB) (11)	N (FGS) (12)	N (WDS) (13)	Notes (14)
085052.05−435022.9	CD-43 4690	9.54	0.86	O7 III(f)	Vel OB1	no	1.5	C	Markova et al. (2011)	0	0	0	
085322.01−460208.8	CD-45 4676	8.92	0.78	B0.2 III	Vel OB1	no	1.5	C	Denoyelle (1987)	0	1	0	
085400.61−422908.8	HD76341	7.16	0.30	O9.2 IV	Vel OB1	no	1.5	C	Thackeray et al. (1973)	0	1	0	
085500.45−472457.5	HD76535	8.62	0.39	O9.7 III	Vel OB1	no	1.5	SB1?	Crampton (1972)	1	0	1	
085507.15−473627.2	HD76556	8.19	0.41	O6 IV(n)((f))p	Vel OB1	no	1.5	SB1?	Williams et al. (2011)	1	0	0	
085527.66−413522.3	CD-41 4637	9.85	0.74	O6 Ib(f)(n)	Field	no	3.7	U	···	0	0	0	
085728.85−504458.2	HD76968	7.09	0.13	O9.2 Ib	Field	no	3.3	SB1?	Feast et al. (1955)	1	0	0	
085751.66−474544.0	CD-47 4550	10.27	0.86	O7 V((f))z	Vel OB1	no	1.5	C	Denoyelle (1987)	0	0	0	
085754.62−474415.7	CD-47 4551	8.40	0.89	O5 Ifc	Vel OB1	no	1.5	C	Denoyelle (1987)	0	0	0	
085956.10−473304.4	CD-47 4575	11.12	0.90	O5 V	Field	no	3.3	U	···	0	0	0	
090221.56−484154.4	CD-48 4352	10.35	0.76	O9 Vn:	Field	no	1.9	U	Denoyelle (1987)	0	2	0	
090551.33−474606.8	HD78344	8.98	1.11	O9.5 Iab	Vel OB1	no	1.5	U	Bassino (1985)	0	0	0	
092010.13−453155.0	CD-45 5058	11.33	−0.32	sdO	Field	no	1.0	C	Rauch et al. (1991)	0	0	0	sdO, KS 292
092244.75−493019.9	HDE297433	9.35	1.12	O9 Ia	Vel OB1	no	1.5	U	Bassino (1985)	0	0	0	
093037.25−513934.7	HDE298429	9.67	0.56	O8.5 V	Field	no	1.9	C	Denoyelle (1987)	0	0	0	
093054.26−512516.0	HDE298425	9.71	0.54	O9 V	Vel OB1	no	1.5	U	Denoyelle (1987)	0	0	0	
100440.52−583158.5	HDE302501	9.69	0.64	O9 I:	Field	no	3.0	U	···	0	0	0	
100520.55−584420.7	HDE302505	9.55	0.42	O9 III	Field	no	3.6	C	Markova et al. (2011)	0	0	0	
100639.88−572533.1	CPD-56 2853	10.54	0.70	O8	Field	no	1.9	U	···	0	1	0	
100712.21−580054.3	CPD-57 2676	11.11	0.18	O9 V	Field	no	4.6	U	···	0	0	0	
100947.72−605949.2	HD88412	9.40	−0.12	O9.5 III	HD 88500	no	5.2	U	Cappa de Nicolau et al. (1986)	0	0	0	
102253.84−593728.4	HD90177	8.38	0.89	B0: Iaep	HR Car	no	5.0	U	Machado et al. (2002)	0	0	0	1, HR Car
103330.30−600740.0	HD91651	8.85	−0.01	ON9.5 IIIn	Car OB1	no	2.0	SB2?	Levato et al. (1988)	1	0	0	
104505.85−594006.4	HDE303308	8.16	0.13	O4.5 V((fc))	Tr 16	no	2.7	SB1?	Levato et al. (1991)	1	1	0	
104823.51+373413.1	HD93521	7.04	−0.28	O9.5 IInn	Field	yes	1.8	C	Rzaev & Panchuk (2008)	0	0	0	
105001.50−575226.3	HD94024	8.72	0.13	O8 IV	Field	no	2.3	SB1?	Chini et al. (2012)	1	0	0	
105152.75−585835.3	HDE303492	8.86	0.56	O8.5 Iaf	Field	no	3.9	SB2?	Chini et al. (2012)	1	0	0	
105223.20−584448.4	HD94370	7.94	0.08	O7 III(n)fp	Field	no	2.8	SB2?	Chini et al. (2012)	1	0	1	
105611.58−602712.8	HD94910	6.85	0.63	B2/3 Ibvar	AG Car	no	6.0	U	Groh et al. (2011)	0	0	0	1, AG Car
105635.79−614232.2	HD94963	7.16	−0.09	O7 II(f)	Field	no	2.5	C	Markova et al. (2011)	0	0	0	
110732.81−595748.7	HD96715	8.26	0.11	O4 V((f))z	Field	no	3.8	C	Williams et al. (2011)	0	0	0	
110840.06−604251.7	V432 Car	11.79	1.91	B8-A2: I	WRA 751	no	6.0	U	Garcia-Lario et al. (1998)	0	0	0	1, Wra 751
110842.62−570356.9	HD96917	7.07	0.08	O8 Ib(n)(f)	Field	no	3.2	SB1?	Chini et al. (2012)	1	0	0	

Table 1—Continued

(α, δ) (J2000) (1)	Star Name (2)	V (mag) (3)	$B-V$ (mag) (4)	Spectral Class. (5)	C/A/F Category (6)	Runaway Status (7)	d (kpc) (8)	Spec. Status (9)	Spectroscopic Reference (10)	N (SB) (11)	N (FGS) (12)	N (WDS) (13)	Notes (14)
111431.90−590128.8	HD97848	8.68	−0.01	O8 V	Field	no	3.5	C	Feast et al. (1957)	0	0	0	
114654.41−612747.0	HD102415	9.15	0.12	ON9 IV:nn	Field	no	2.9	SB2?	Chini et al. (2012)	1	0	0	
120258.46−624019.2	HD104649	7.91	0.01	B0.7 V	Field	no	1.6	SB2?E	Otero & Wils (2005)	1	1	0	EK Cru
120549.88−693423.0	HD105056	7.43	0.07	ON9.7 Iae	Field	yes	4.5	SB1?	Harmanec (1987)	1	0	0	
125557.13−565008.9	HD112244	5.38	0.02	O8.5 Iab(f)p	Field	no	1.7	SB1?	Buscombe & Kennedy (1965)	1	0	1	
131604.80−623501.5	HD115071	7.95	0.24	O9.5 III	Stock 16	no	1.6	SB2OE	Penny et al. (2002)	1	0	0	V961 Cen
133023.52−785120.5	HD116852	8.47	−0.09	O8.5 II-III((f))	Field	yes	4.5	C	Feast et al. (1957)	0	0	0	
133443.41−632007.6	HD117856	7.38	0.22	O9.7 II-III	Field	no	1.9	SB2O	Sota et al. (2014)	1	0	1	
140725.64−602814.1	HD123056	8.14	0.14	O9.5 IV(n)	Field	no	1.5	SB2?	Sota et al. (2014)	0	0	0	
142022.78−605322.2	HD125241	8.28	0.49	O8.5 Ib(f)	Field	no	3.2	C	Crampton (1972)	0	0	0	
163023.31−375821.2	HD148546	7.71	0.29	O9 Iab	Field	yes	3.5	C	Raboud (1996)	0	0	0	
164120.41−484546.6	HD150136	5.55	0.16	O3.5-4 III(f*)	NGC 6193	no	1.2	SB3O	Sana et al. (2013a)	2	1	4	
165133.72−411349.9	HD151804	5.22	0.07	O8 Iaf	Sco OB1	no	1.5	SB2?	Sota et al. (2014)	0	0	0	
165359.73−422143.3	HD152236	4.73	0.48	B1.5 Ia+	NGC 6231	no	1.6	SB2?	Chini et al. (2012)	1	0	0	1, ζ^1 Sco
170628.37−352703.8	HD154368	6.12	0.51	O9.2 Iab	ASCC 88	no	1.9	SBE	Perryman & ESA (1997)	1	0	1	V1074 Sco
170653.91−423639.7	HDE326823	9.03	0.86	B2 Ipec	Field	no	2.0	SB1O	Richardson et al. (2011a)	1	0	0	1, V1104 Sco
170953.09−470153.2	HD154811	6.92	0.40	OC9.7 Ib	Field	no	2.1	C	Levato et al. (1988)	0	0	0	
171626.34−424004.1	HD155913	8.26	0.48	O4.5 Vn((f))	Field	no	2.3	SB2?	Sota et al. (2014)	0	1	0	
172118.73−625505.4	HD156359	9.67	−0.14	O9.7 Ib-II	Field	yes	8.5	C	Hill (1971)	0	1	0	
172617.33−105934.8	HD157857	7.78	0.17	O6.5 II(f)	Field	yes	2.2	C	Conti et al. (1977)	0	0	0	
172912.93−313203.4	HD158186	7.00	0.03	O9.5 V(n)	Field	no	1.1	SB3?E	Otero (2005)	1	1	0	V1081 Sco
174159.03−333013.7	HD160529	6.57	1.22	A2 Iavar	Field	no	2.5	U	Clark et al. (2012)	0	1	0	1, V905 Sco
174916.55−311518.1	HD161853	7.93	0.23	O8 V(n)z	Field	no	1.5	SB2?	Sota et al. (2014)	1	0	0	
175926.31−222800.9	HD163892	7.44	0.16	O9.5 IV(n)	Sgr OB1	no	1.3	SB1?	Chini et al. (2012)	1	0	0	
175928.37−360115.6	HD163758	7.32	0.03	O6.5 Iafp	Field	yes	3.2	SB2?	Sota et al. (2014)	0	0	1	
180352.44−242138.6	HD164794	5.97	0.03	O4 V((f))z	NGC 6530	no	1.3	SB2O	Rauw et al. (2012)	1	1	0	9 Sgr
180604.68−241143.9	HD165246	7.72	0.09	O8 V(n)	Sgr OB1	no	1.3	SB2OE	Williams (2011)	1	0	1	
181224.66−104353.1	HD166734	8.42	1.08	O7.5 Iabf	Field	no	1.3	SB2OE	Conti et al. (1980)	1	0	0	V411 Ser
181512.97−202316.7	HD167263	5.96	0.02	O9.5 III	Sgr OB7	no	1.4	SB1O	Stickland & Lloyd (2001)	1	1	1	16 Sgr
181728.56−182748.4	HD167771	6.54	0.09	O7 III((f))	Sgr OB4	no	1.9	SB2O	Stickland et al. (1997)	1	0	1	
181805.90−121433.3	HD167971	7.47	0.76	O8 Iaf(n)	NGC 6604	no	1.7	SB3OE	Blomme et al. (2007)	2	0	2	MY Ser
181836.43−134802.0	HD168076	8.20	0.47	O4 III(f)	NGC 6611	no	1.7	C	Sana et al. (2009)	0	1	0	
182114.89−162231.8	HD168607	8.28	1.56	B9 Iaep	Ser OB1	no	1.5	U	Chentsov & Gorda (2004)	0	0	0	1, V4029 Sgr

Table 1—Continued

(α, δ) (J2000) (1)	Star Name (2)	V (mag) (3)	$B-V$ (mag) (4)	Spectral Class. (5)	C/A/F Category (6)	Runaway Status (7)	d (kpc) (8)	Spec. Status (9)	Spectroscopic Reference (10)	N (SB) (11)	N (FGS) (12)	N (WDS) (13)	Notes (14)
182119.55−162226.1	HD168625	8.38	1.42	B6 Iap	Ser OB1	no	1.5	U	Chentsov & Gorda (2004)	0	2	0	1, V4030 Sgr
185735.71−190911.3	HD175754	7.01	−0.08	O8 II(n)((f))p	Field	yes	2.3	C	Fullerton et al. (1996)	0	0	0	
195159.07+470138.4	HD188209	5.63	−0.07	O9.5 Iab	Field	yes	2.3	C	Israelian et al. (2000)	0	0	0	
195221.76+184018.7	HD188001	6.24	0.01	O7.5 Iabf	Field	yes	2.4	C	McSwain et al. (2007)	0	0	0	
200100.00+420030.8	HD189957	7.81	0.01	O9.5 III	Field	yes	2.5	C	Gies & Bolton (1986)	0	0	0	
200329.40+360130.5	HD190429A	6.62	0.15	O4 If	Cyg OB3	no	1.8	C	Fullerton et al. (1996)	0	1	3	
200557.32+354718.1	HD190918	6.80	0.13	O9.5 Ia	NGC 6871	no	1.6	SB2O	Underhill & Hill (1994)	1	0	7	WR 133
200723.69+354305.9	HD191201	7.26	0.13	O9.5 III	NGC 6871	no	1.6	SB2O	Burkholder et al. (1997)	1	1	1	
201233.12+401605.4	HD192281	7.55	0.38	O4.5 Vn((f))	Cyg OB8	yes	1.8	C	De Becker & Rauw (2004)	0	0	0	
201729.70+371831.1	HDE228766	9.14	0.61	O4 If	Cyg OB1	no	3.5	SB2O	Rauw et al. (2002)	1	0	0	
201747.20+380158.5	HD193237	4.81	0.41	B1 Ia+	P Cyg	no	2.3	C	Richardson et al. (2011b)	0	0	1	1, P Cyg
201806.99+404355.5	HD193322A	5.83	0.11	O9 IV(n)	Cr 419	no	0.7	SB1O	ten Brummelaar et al. (2011)	1	1	3	
201851.71+381646.5	HD193443A	7.25	0.39	O9 III	Cyg OB1	no	1.5	SB2O	Mahy et al. (2013)	1	1	1	
202310.79+405229.9	HDE229196	8.52	0.91	O6 II(f)	NGC 6910	no	1.1	C	Wilson (1953)	0	0	0	
202359.18+390615.3	HDE229232	9.52	0.82	O4 Vn((f))	Cyg OB1	no	1.5	SB1O	Williams et al. (2013)	1	1	0	
203034.97+441854.9	HD195592	7.08	0.87	O9.7 Ia	HD195592	no	1.2	SB1?	De Becker et al. (2010)	1	1	0	
205203.58+343927.5	HD198846	7.30	−0.07	O9.5 IV	Field	yes	1.6	SB2OE	Hill & Holmgren (1995)	1	0	0	Y Cyg
205634.78+445529.0	HD199579	5.96	0.05	O6.5 V((f))z	Cyg OB7	no	0.6	SB2O	Williams et al. (2001)	1	0	1	
210755.42+332349.2	HD201345	7.66	−0.13	ON9.2 IV	Field	yes	1.8	C	Gies & Bolton (1986)	0	0	1	
211228.39+443154.1	HD202124	7.82	0.23	O9 Iab	Field	no	4.1	C	Conti et al. (1977)	0	0	0	
211827.19+435645.4	HD203064	5.00	−0.03	O7.5 IIIn((f))	Field	yes	0.8	SB1?	Alduseva et al. (1982)	1	0	1	68 Cyg
213857.62+572920.5	HD206267	5.64	0.21	O6.5 V((f))	Tr 37	no	0.8	SB3O	Stickland (1995)	1	1	3	
214453.28+622738.0	HD207198	5.94	0.31	O8.5 II	Cep OB2	no	0.7	C	Garmany et al. (1980)	0	0	2	
220204.57+580001.3	HD209481	5.56	0.06	O9 IV(n)var	Cep OB2	no	0.7	SB2OE	Mahy et al. (2011)	1	0	1	LZ Cep
220508.79+621647.3	HD209975	5.10	0.09	O9 Ib	ASCC 117	no	1.2	C	Garmany et al. (1980)	0	0	4	19 Cep
223915.68+390301.0	HD214680	4.88	−0.20	O9 V	Lac OB1	no	0.5	C	Chochol & Grygar (1974)	0	0	2	10 Lac
225647.19+624337.6	HD217086	7.68	0.55	O7 Vnn((f))z	Cep OB3	no	0.7	C	Conti et al. (1977)	0	0	3	
231106.95+530329.6	HD218915	7.20	0.02	O9.2 Iab	Field	yes	4.1	C	Stone (1982)	0	0	0	

Table 1—Continued

(α, δ) (J2000) (1)	Star Name (2)	V (mag) (3)	$B-V$ (mag) (4)	Spectral Class. (5)	C/A/F Category (6)	Runaway Status (7)	d (kpc) (8)	Spec. Status (9)	Spectroscopic Reference (10)	N (SB) (11)	N (FGS) (12)	N (WDS) (13)	Notes (14)
Targets With Prior FGS Observations													
104343.67−593404.1	Tr14-28	12.50	0.39	B2 V	Tr 14	no	2.3	U	···	0	0	0	2
104344.03−593346.8	Tr14-27	11.30	0.31	O9 V	Tr 14	no	2.3	U	···	0	0	0	2
104354.37−593257.4	HD93128	8.82	0.25	O3.5 V	Tr 14	no	2.3	C	García et al. (1998)	0	0	1	2, Tr14-2
104355.43−593249.8	Tr14-9	9.89	0.21	O8.5 Vz	Tr 14	no	2.3	U	···	0	0	0	2
104357.40−593252.3	HD93129B	10.74	0.29	O3.5 V((f*))	Tr 14	no	2.3	C	García et al. (1998)	0	0	1	2
104357.46−593251.3	HD93129A	7.01	0.21	O2 If*	Tr 14	no	2.3	C	García et al. (1998)	0	1	1	2
104359.98−593524.9	Tr16-126	10.97	0.41	O9 V	Tr 16	no	2.3	U	···	0	0	0	2
104401.05−593546.3	Tr16-127	10.70	0.35	B1 V	Tr 16	no	2.3	U	···	0	0	0	2, CPD-58 262
104408.90−593434.9	HD93161	7.83	0.21	O7.5 V	Tr 16	no	2.3	SB3O	Nazé et al. (2005)	2	0	3	2, Tr16-176
104422.91−595936.0	HD93206	6.30	0.14	O9.7 Ibn	Cr 228	no	2.3	SB4OE	Mayer et al. (2001)	3	0	3	2, QZ Car
104425.60−593309.8	Tr16-122	11.33	0.16	B1.5 V	Tr 16	no	2.3	U	···	0	0	0	2
104426.59−594103.4	Tr16-94	9.86	0.14	B1.5 V	Tr 16	no	2.3	SB1?	Levato et al. (1991)	1	0	0	2, CPD-59 257
104456.39−593303.8	Tr16-31	10.44	0.27	B0.5 V	Tr 16	no	2.3	U	Levato et al. (1991)	0	1	0	2
104505.86−594519.7	Tr16-23	9.96	0.38	O7.5 V	Tr 16	no	2.3	C	Levato et al. (1991)	0	1	0	2, CPD-59 262
104505.90−594308.3	Tr16-9	9.79	0.22	O9.7 V	Tr 16	no	2.3	C	Levato et al. (1991)	0	0	0	2, CPD-59 262
104506.79−594157.1	Tr16-3	10.17	0.20	O9.5 V	Tr 16	no	2.3	C	Levato et al. (1991)	0	0	0	2, CPD-59 262
104508.29−594607.7	Tr16-22	10.97	0.49	O8.5 V	Tr 16	no	2.3	SB1?	Williams et al. (2011)	1	0	0	2, CPD-59 262
104509.79−594257.7	Tr16-74	11.70	0.27	B1 V	Tr 16	no	2.3	U	···	0	0	0	2
104511.21−594111.3	Tr16-2	10.79	0.14	B1 V	Tr 16	no	2.3	U	Levato et al. (1991)	0	0	0	2, CPD-59 263
104512.22−594500.4	HD93343	9.52	0.27	O8 Vz	Tr 16	no	2.3	SB2?	Chini et al. (2012)	1	0	0	2, Tr16-182
104512.70−594249.3	Tr16-76	11.16	0.44	B2 V	Tr 16	no	2.3	U	···	0	0	0	2
104512.71−594446.2	Tr16-34	9.27	0.25	O8 V(n)	Tr 16	no	2.3	SB2O	Albacete Colombo et al. (2001)	1	0	1	2, V731 Car
104544.12−592428.1	HD93403	7.27	0.22	O5 III	Tr 16	no	2.3	SB2O	Rauw et al. (2000)	1	0	0	2, CPD-58 268
203039.71+410849.0	A23	11.25	···	B0.7 Ib	Cyg OB2	no	1.4	U	···	0	0	0	3
203039.82+413650.7	MT5	12.93	1.64	O6 V	Cyg OB2	no	1.4	C	Kiminki & Kobulnicky (2012)	0	1	0	3
203100.20+404949.7	A46	11.40	···	O7 V((f))	Cyg OB2	no	1.4	U	···	0	0	0	3
203108.38+420242.3	A41	11.70	···	O9.7 II	Cyg OB2	no	1.4	U	···	0	1	0	3
203110.55+413153.5	MT59	11.18	1.47	O8 V	Cyg OB2	no	1.4	SB1O	Kobulnicky et al. (2014)	1	1	0	3, Schulte 1
203118.33+412121.7	MT70	12.99	2.10	O9 II	Cyg OB2	no	1.4	SB1O	Kobulnicky et al. (2014)	1	0	0	3

Table 1—Continued

(α, δ) (J2000) (1)	Star Name (2)	V (mag) (3)	$B-V$ (mag) (4)	Spectral Class. (5)	C/A/F Category (6)	Runaway Status (7)	d (kpc) (8)	Spec. Status (9)	Spectroscopic Reference (10)	N (SB) (11)	N (FGS) (12)	N (WDS) (13)	Notes (14)
203122.04+413128.4	MT83	10.64	1.18	B1 I	Cyg OB2	no	1.4	SB1?	Kiminki et al. (2007)	1	0	0	3, Schulte 2
203145.40+411826.8	MT138	12.26	1.99	O8 I	Cyg OB2	no	1.4	SB1?	Kiminki et al. (2007)	1	1	0	3
203149.66+412826.5	MT145	11.52	1.11	O9 III	Cyg OB2	no	1.4	SB1O	Kobulnicky et al. (2014)	1	0	0	3
203206.29+404829.6	WR145	11.83	1.63	WN7 o/CE	Cyg OB2	no	1.4	SB2O	Muntean et al. (2009)	1	0	0	3, V1923 Cyg
203213.13+412724.6	MT213	11.95	1.13	B0 V	Cyg OB2	no	1.4	C	Kiminki et al. (2007)	0	0	0	3
203213.83+412712.0	MT217	10.23	1.19	O7 IIIf	Cyg OB2	no	1.4	C	Kiminki et al. (2007)	0	0	2	3, Schulte 4
203216.56+412535.7	MT227	11.47	1.24	O9 V	Cyg OB2	no	1.4	C	Kiminki et al. (2007)	0	0	0	3, Schulte 14
203222.43+411819.1	Schulte 5	9.12	1.67	O7 Ianfp	Cyg OB2	no	1.4	SB2OE	Kobulnicky et al. (2014)	1	1	2	3, V729 Cyg
203226.08+412939.4	MT250	12.88	1.06	B2 III	Cyg OB2	no	1.4	C	Kiminki et al. (2007)	0	0	0	3
203227.66+412622.1	MT258	11.10	1.20	O8 V	Cyg OB2	no	1.4	SB1O	Kobulnicky et al. (2014)	1	0	0	3, Schulte 15
203227.74+412852.3	MT259	11.42	1.00	B0 Ib	Cyg OB2	no	1.4	SB1?	Kiminki et al. (2007)	1	0	0	3, Schulte 21
203238.58+412513.8	MT299	10.84	1.19	O7 V	Cyg OB2	no	1.4	C	Kiminki et al. (2007)	0	0	0	3, Schulte 16
203240.96+411429.2	MT304	11.10	3.35	B3-4 Ia+	Cyg OB2	no	1.4	U	Chentsov et al. (2013)	0	1	0	3, Schulte 12
203245.46+412537.4	MT317	10.68	1.25	O8 V	Cyg OB2	no	1.4	C	Kiminki et al. (2007)	0	0	0	3, Schulte 6
203250.02+412344.7	MT339	11.60	1.35	O8 V	Cyg OB2	no	1.4	SB1O	Kobulnicky et al. (2014)	1	0	0	3, Schulte 17
203259.19+412425.5	MT376	11.91	1.35	O8 V	Cyg OB2	no	1.4	C	Kiminki et al. (2007)	0	0	0	3
203302.92+411743.1	MT390	12.95	1.98	O8 V	Cyg OB2	no	1.4	SB1O	Kobulnicky et al. (2014)	1	0	0	3
203305.27+414336.8	MT403	12.94	1.49	B1 V	Cyg OB2	no	1.4	SB1O	Kobulnicky et al. (2014)	1	0	0	3
203308.80+411318.2	MT417	11.55	2.04	O3 If*	Cyg OB2	no	1.4	U	Chentsov et al. (2013)	0	2	1	3, Schulte 22
203310.51+412222.5	MT429	12.98	1.56	B0 V	Cyg OB2	no	1.4	SB1OE	Kobulnicky et al. (2014)	1	1	0	3, V2186 Cyg
203310.75+411508.2	MT431	10.96	1.81	O5:	Cyg OB2	no	1.4	SB2O	Nazé et al. (2012)	1	0	1	3, Schulte 9
203313.26+411328.7	MT448	13.61	2.15	O6 V	Cyg OB2	no	1.4	SB1O	Kobulnicky et al. (2014)	1	0	0	3
203313.69+411305.8	MT455	12.92	1.81	O8 V	Cyg OB2	no	1.4	C	Kiminki & Kobulnicky (2012)	0	0	0	3
203314.11+412021.8	MT457	10.55	1.45	O3 If*	Cyg OB2	no	1.4	C	Kiminki et al. (2007)	0	0	4	3, Schulte 7
203314.76+411841.6	MT462	10.33	1.44	O7 III-II	Cyg OB2	no	1.4	C	Kiminki et al. (2007)	0	0	1	3, Schulte 8B
203315.08+411850.5	MT465	9.06	1.30	O5.5 I	Cyg OB2	no	1.4	SB2O	De Becker et al. (2004)	1	0	3	3, Schulte 8A
203315.71+412017.2	MT470	12.50	1.46	O9 V	Cyg OB2	no	1.4	C	Kiminki et al. (2007)	0	0	0	3, Schulte 23
203316.34+411901.8	MT473	12.02	1.45	O8.5 V	Cyg OB2	no	1.4	SB1O	Kobulnicky et al. (2014)	1	0	0	3, Schulte 8D
203317.48+411709.3	MT480	11.88	1.59	O7 V	Cyg OB2	no	1.4	C	Kiminki et al. (2007)	0	0	0	3, Schulte 24
203317.99+411831.1	MT483	10.19	1.24	O5 III	Cyg OB2	no	1.4	SB1?	Kiminki et al. (2007)	1	0	1	3, Schulte 8C
203318.03+412136.6	MT485	12.06	1.51	O8 V	Cyg OB2	no	1.4	SB1O	Kobulnicky et al. (2014)	1	0	0	3
203321.02+411740.1	MT507	12.70	1.54	O9 V	Cyg OB2	no	1.4	C	Kiminki et al. (2007)	0	0	0	3
203323.46+410913.0	MT516	11.84	2.20	O5.5 V	Cyg OB2	no	1.4	C	Kiminki et al. (2007)	0	1	0	3

Table 1—Continued

(α, δ) (J2000) (1)	Star Name (2)	V (mag) (3)	$B-V$ (mag) (4)	Spectral Class. (5)	C/A/F Category (6)	Runaway Status (7)	d (kpc) (8)	Spec. Status (9)	Spectroscopic Reference (10)	N (SB) (11)	N (FGS) (12)	N (WDS) (13)	Notes (14)
203325.56+413327.0	MT531	11.58	1.57	O8.5 V	Cyg OB2	no	1.4	C	Kiminki et al. (2007)	0	1	0	3, Schulte 25
203326.75+411059.5	MT534	13.00	1.87	O8.5 V	Cyg OB2	no	1.4	C	Kiminki et al. (2007)	0	0	0	3
203330.31+413557.9	MT555	12.51	1.90	O8 V	Cyg OB2	no	1.4	SB1O	Kobulnicky et al. (2014)	1	0	0	3, Schulte 74
203330.79+411522.7	MT556	11.01	1.77	B1 I	Cyg OB2	no	1.4	SB1?	Kiminki et al. (2007)	1	0	0	3, Schulte 18
203337.00+411611.3	MT588	12.40	1.66	B0 V	Cyg OB2	no	1.4	SB1O	Kobulnicky et al. (2014)	1	0	0	3, Schulte 70
203339.11+411925.9	MT601	11.07	1.47	B0 Iab	Cyg OB2	no	1.4	SB1O	Kobulnicky et al. (2014)	1	0	0	3, V1393 Cyg
203339.80+412252.4	MT605	11.78	1.19	B1 V	Cyg OB2	no	1.4	SB2O	Kobulnicky et al. (2014)	1	1	0	3
203340.87+413019.0	MT611	12.77	1.55	O7 V	Cyg OB2	no	1.4	C	Kiminki et al. (2007)	0	0	0	3
203346.10+413301.1	MT632	9.88	1.59	O9 I	Cyg OB2	no	1.4	C	Kiminki et al. (2007)	0	1	0	3, Schulte 10
203347.84+412041.5	MT642	11.78	1.55	B1 III	Cyg OB2	no	1.4	SB1?	Kiminki et al. (2007)	1	0	0	3, Schulte 26
203359.25+410538.1	MT692	13.61	1.69	B0 V	Cyg OB2	no	1.4	SB2?	Kiminki et al. (2007)	1	0	0	3
203359.53+411735.5	MT696	12.32	1.65	O9.5 V	Cyg OB2	no	1.4	SB2OE	Kobulnicky et al. (2014)	1	1	0	3, Schulte 27
203408.50+413659.2	MT734	10.03	1.49	O5 I	Cyg OB2	no	1.4	SB1O	Kobulnicky et al. (2014)	1	0	0	3, Schulte 11
203409.52+413413.7	MT736	12.79	1.46	O9 V	Cyg OB2	no	1.4	C	Kiminki et al. (2007)	0	0	0	3, Schulte 75
203413.51+413502.7	MT745	11.91	1.50	O7 V	Cyg OB2	no	1.4	SB1O	Kobulnicky et al. (2014)	1	0	0	3, Schulte 29
203421.93+411701.6	Schulte 73	12.40	1.73	O8 III	Cyg OB2	no	1.4	SB2O	Kobulnicky et al. (2014)	1	0	0	3
203429.60+413145.5	MT771	12.06	2.05	O7 V	Cyg OB2	no	1.4	SB2O	Kobulnicky et al. (2014)	1	0	0	3
203443.58+412904.6	MT793	12.29	1.54	B2 IIIe	Cyg OB2	no	1.4	U	Kiminki et al. (2007)	0	0	0	3, Schulte 30
203444.72+405146.6	A27	11.26	···	B0 Ia	Cyg OB2	no	1.4	U	···	0	0	0	3

Note. — 1 = LBV or LBV candidate; 2 = FGS data from Nelan et al. (2004, 2010); 3 = FGS data from Caballero-Nieves et al. (2014)

Table 2. Resolved Companions

(α, δ) (J2000) (1)	Star Name (2)	Discovery Designation (3)	Date (BY) (4)	FGS Filter (5)	θ (deg) (6)	ρ (arcsec) (7)	$\triangle m$ (mag) (8)	Fig. 1.n (9)	Notes (10)
014052.76+641023.1	HD10125	HDS 221 AB	2008.0775	F583W	231.14±0.10	0.7216±0.0007	3.509±0.085	3	
022254.29+412847.7	HD14633	FGS 1 Aa,Ab	2007.8425	F5ND	352.31±32.32	>0.0197±0.0111	1.643±1.083	4	2
024044.94+611656.1	HD16429	CHR 208 Aa,Ab	2007.6831	F5ND	91.16±0.16	0.2849±0.0008	2.150±0.040	7	
025107.97+602503.9	HD17505	STF 306 AB	2008.5621	F5ND	···	>0.2115±0.0007	1.918±0.054	9	1,5
025114.46+602309.8	HD17520A	BU 1316 AB	2008.2139	F583W	298.83±0.08	0.3174±0.0008	0.553±0.020	10	
035538.42+523828.8	HD24431	HDS 494 AB	2007.8465	F5ND	176.72±0.09	0.7192±0.0010	2.897±0.011	13	
040751.39+621948.4	HD25639	CHR 209 Ea,Eb	2007.7682	F5ND	115.31±2.77	0.0734±0.0021	0.705±0.046	15	1
040751.39+621948.4	HD25639	CHR 209 Ea,Eb	2008.8682	F5ND	113.46±8.63	0.0727±0.0019	0.907±0.053	16	1
051756.06−691603.9	HDE269321	FGS 2 Aa,Ab	2008.9247	F583W	257.01±13.11	>0.0481±0.0125	3.327±2.471	21	1,3
051756.06−691603.9	HDE269321	FGS 2 Aa,Ab	2008.9248	F583W	257.01±10.68	>0.0590±0.0126	3.632±0.546	22	1,3
051814.36−691501.1	HD35343	FGS 3 Aa,Ab	2008.9246	F583W	173.15±0.68	1.7032±0.0009	3.999±0.033	23	
051814.36−691501.1	HD35343	FGS 3 Aa,Ab	2008.9246	F583W	···	>0.0549±0.0078	3.493±0.462	24	1,5
052942.65+352230.1	HD35921	HU 217 AB	2008.7278	F5ND	253.77±0.13	0.5973±0.0007	2.245±0.097	26	
052942.65+352230.1	HD35921	HU 217 AB	2008.7847	F5ND	253.62±0.20	0.5988±0.0005	1.731±0.069	27	
053051.48−690258.6	HDE269662	FGS 4 AB	2009.3530	F583W	50.27±6.60	>0.0955±0.0037	4.964±0.191	28	1,3
053051.48−690258.6	HDE269662	FGS 4 AB	2009.3530	F583W	50.27±7.04	>0.0895±0.0011	3.384±0.081	29	1,3
053433.72−002311.5	HD36841	FGS 5 AB	2008.8472	F583W	171.59±10.31	0.0982±0.0134	4.092±0.398	31	
053522.90−052457.8	HD37041A	CHR 249 Aa,Ab	2008.7283	F5ND	276.62±2.15	0.3964±0.0021	3.125±0.012	35	
053522.90−052457.8	HD37041A	CHR 249 Aa,Ab	2008.8452	F5ND	···	···	···	36	1
053844.77−023600.2	HD37468A	BU 1032 AB	2008.0092	F5ND	94.24±0.12	0.2562±0.0007	1.262±0.010	38	
053924.80+305326.8	HD37366	HDS 754 Aa,Ab	2008.7449	F5ND	292.98±0.23	0.5663±0.0020	3.692±0.573	39	
053924.80+305326.8	HD37366	HDS 754 Aa,Ab	2008.8647	F5ND	292.56±0.16	0.5631±0.0016	3.793±0.150	40	
061831.77+224045.1	HDE254755	HDS 863 AB	2008.7781	F583W	51.82±0.20	0.1880±0.0006	1.611±0.096	48	
063210.47+045759.8	HD46202	FGS 6 Da,Db	2008.7417	F583W	75.49±3.55	0.0867±0.0022	2.166±0.008	58	
063625.89+060459.5	HD46966	FGS 7 Aa,Ab	2008.7282	F5ND	244.82±17.38	0.0553±0.0083	1.137±0.010	61	
063625.89+060459.5	HD46966	FGS 7 Aa,Ab	2008.8651	F5ND	258.28±3.94	0.0501±0.0022	1.076±0.059	62	
064058.66+095344.7	HD47839	CHR 168 Aa,Ab	2007.8192	F5ND	252.14±0.97	0.0978±0.0011	1.561±0.005	66	
064058.66+095344.7	HD47839	CHR 168 Aa,Ab	2008.7829	F5ND	255.63±0.94	0.1000±0.0008	1.549±0.059	67	
064548.70−071839.0	ALS85	FGS 8 AB	2008.8093	F583W	225.55±0.20	0.2826±0.0010	3.146±0.021	71	1
064548.70−071839.0	ALS85	FGS 8 AC	2008.8093	F583W	226.90±0.18	0.3625±0.0013	3.180±0.081	71	1
064849.56+002252.7	BD+00 1617A	FGS 9 Aa,Ab	2008.8047	F583W	241.52±0.91	0.0829±0.0012	1.151±0.142	72	
064850.48+002237.6	BD+00 1617B	FGS 9 Ba,Bb	2008.8049	F583W	182.65±2.30	0.1526±0.0018	3.497±0.359	73	
064851.20+002224.0	BD+00 1617C	FGS 9 Ca,Cb	2008.8038	F583W	253.08±0.73	0.0882±0.0008	0.836±0.039	74	

Table 2—Continued

(α, δ) (J2000) (1)	Star Name (2)	Discovery Designation (3)	Date (BY) (4)	FGS Filter (5)	θ (deg) (6)	ρ (arcsec) (7)	$\triangle m$ (mag) (8)	Fig. 1.n (9)	Notes (10)
065930.21−044843.8	ALS9243	FGS 10 AB	2008.8120	F583W	186.69±0.77	0.2846±0.0011	2.389±0.049	78	
070127.05−030703.3	HD52533	FGS 11 Aa,Ab	2008.7112	F5ND	260.83±1.19	0.6259±0.0022	3.812±0.042	80	
071821.42−245900.4	ALS18846	FGS 12 AB	2008.8098	F583W	111.80±0.91	0.4831±0.0027	4.773±0.923	85	
071842.49−245715.8	HD57061	FIN 313 Aa,Ab	2008.4143	F5ND	126.56±2.49	0.1231±0.0010	−0.831±0.014	87	6
071842.49−245715.8	HD57061	FIN 313 Aa,Ab	2008.7858	F5ND	128.29±0.35	0.1221±0.0005	−0.834±0.022	88	6
071842.49−245715.8	HD57061	TOK 42 Ab,E	2008.4143	F5ND	267.70±0.18	0.9377±0.0031	4.016±0.159	87	1
071842.49−245715.8	HD57061	TOK 42 Ab,E	2008.7858	F5ND	···	>0.9172±0.0050	4.317±0.316	88	1,2
072755.38−152307.3	HD59114	FGS 13 AB	2008.7672	F583W	206.32±0.34	0.3934±0.0019	4.633±0.090	92	
074143.44−344727.6	CD-34 3814	FGS 14 AB	2008.8095	F583W	183.47±6.00	0.0644±0.0059	2.346±1.649	106	
075220.28−262546.7	HD64315	WSI 54 AB	2008.7686	F583W	228.55±1.73	0.0629±0.0021	0.624±0.034	111	1
075626.41−292526.1	CD-29 5191	FGS 15 AB	2008.8100	F583W	189.21±0.81	>0.0776±0.0156	3.950±0.724	118	3
075758.55−283529.4	CD-28 5180	FGS 16 AB	2008.8516	F583W	312.43±1.49	0.1036±0.0013	2.291±0.273	119	
081335.36−342843.9	CD-34 4496	FGS 17 AB	2008.7701	F583W	173.92±0.85	>0.0738±0.0167	4.066±0.930	127	3
081517.15−354414.6	CD-35 4384	JSP 248 AB	2008.7703	F583W	307.99±0.09	1.1345±0.0017	0.188±0.214	128	1
081517.15−354414.6	CD-35 4384	FGS 18 Aa,Ab	2008.7703	F583W	302.21±5.01	0.0429±0.0036	1.473±0.697	128	1
081548.57−353752.9	HD69464	FGS 19 AB	2008.7694	F583W	109.76±0.10	0.9181±0.0015	4.500±0.455	129	
081903.90−360844.9	CD-35 4471	FGS 20 AB	2008.7697	F583W	198.32±6.12	0.0396±0.0085	2.756±0.929	133	1
083909.53−402509.3	HD73882	B 1623 AB	2008.4061	F5ND	255.11±0.03	0.6683±0.0004	1.092±0.070	135	
084338.66−460815.9	CPD-45 2910	FGS 21 AB	2008.8124	F583W	145.98±11.01	0.0926±0.0128	4.857±2.403	138	
084351.09−460346.5	CD-45 4462	FGS 22 AB	2008.8128	F583W	338.77±3.33	0.0325±0.0042	0.688±0.151	140	1
084351.09−460346.5	CD-45 4462	FGS 22 AC	2008.8128	F583W	316.73±0.16	0.6671±0.0020	3.373±0.105	140	1
084510.46−455854.7	CPD-45 2977	FGS 23 AB	2008.8130	F583W	273.70±1.92	0.2314±0.0007	0.396±0.050	142	
085322.01−460208.8	CD-45 4676	DON 293 AB	2008.7661	F583W	339.26±0.68	0.6842±0.0006	2.311±0.032	149	1
085400.61−422908.8	HD76341	FGS 24 AB	2008.7674	F5ND	72.74±0.40	>0.1581±0.0030	3.975±0.155	150	2
090221.56−484154.4	CD-48 4352	FGS 25 AB	2008.8133	F583W	331.96±2.91	0.0341±0.0033	1.106±0.171	158	1,2
090221.56−484154.4	CD-48 4352	FGS 25 AC	2008.8133	F583W	···	>0.4319±0.0024	3.637±0.091	158	1,5
100639.88−572533.1	CPD-56 2853	FGS 26 AB	2008.8157	F583W	···	>0.2018±0.0024	4.245±0.320	166	1,5
120258.46−624019.2	HD104649	FGS 27 AB	2008.6770	F5ND	2.64±2.24	0.1234±0.0022	2.955±0.063	187	
164120.41−484546.6	HD150136	MLO 8 AB	2008.1316	F5ND	···	>0.1736±0.0012	2.881±0.079	196	1,4
171626.34−424004.1	HD155913	FGS 28 AB	2009.3593	F583W	33.62±2.20	>0.0287±0.0159	3.273±1.277	204	3
172118.73−625505.4	HD156359	FGS 29 AB	2009.5421	F583W	283.80±2.53	0.1220±0.0074	5.124±0.021	205	
172912.93−313203.4	HD158186	FGS 30 AB	2009.2949	F5ND	188.60±1.86	>0.0339±0.0067	2.321±0.692	207	3
181512.97−202316.7	HD167263	CHR 255 Aa,Ab	2009.5462	F5ND	333.19±1.23	0.0750±0.0012	0.172±0.020	216	1

Table 2—Continued

(α, δ) (J2000) (1)	Star Name (2)	Discovery Designation (3)	Date (BY) (4)	FGS Filter (5)	θ (deg) (6)	ρ (arcsec) (7)	$\triangle m$ (mag) (8)	Fig. 1.n (9)	Notes (10)
181836.43−134802.0	HD168076	DCH 26 AB	2008.2514	F583W	312.80±0.33	0.1494±0.0009	2.139±0.035	219	
182119.55−162226.1	HD168625	FGS 31 AB	2009.2707	F583W	201.86±0.07	1.1337±0.0013	4.210±0.058	222	1
182119.55−162226.1	HD168625	FGS 31 AB	2009.2707	F583W	···	···	···	223	1
182119.55−162226.1	HD168625	FGS 31 AC	2009.2707	F583W	···	>1.6751±0.0008	4.566±0.072	222	1,4
200329.40+360130.5	HD190429A	STF2624 AB	2008.1844	F5ND	174.98±0.01	1.9466±0.0003	0.789±0.641	228	1
200723.69+354305.9	HD191201	STT 398 AB	2008.4072	F5ND	84.32±0.04	0.9633±0.0006	1.877±0.199	230	
201806.99+404355.5	HD193322A	CHR 96 Aa,Ab	2008.0503	F5ND	116.71±0.97	0.0653±0.0011	0.165±0.053	235	1
201851.71+381646.5	HD193443A	A 1425 AB	2008.9728	F5ND	258.49±0.16	0.1377±0.0004	−0.264±0.011	236	6
202359.18+390615.3	HDE229232	FGS 32 AB	2008.1987	F583W	121.97±4.92	>0.0128±0.0082	1.209±0.752	238	2
213857.62+572920.5	HD206267	MIU 2 Aa,Ab	2008.7182	F5ND	233.73±0.65	>0.0971±0.0008	1.314±0.090	245	1,3

Note. — 1 = see Appendix; 2 = resolved on the x-axis, unresolved on the y-axis, so the position angle and separation are estimated assuming $\triangle y = 0$; 3 = resolved on the y-axis, unresolved on the x-axis, so the position angle and separation are estimated assuming $\triangle x = 0$; 4 = resolved on the x-axis, off scan on the y-axis, so no position angle is listed and only a lower limit on the separation is given; 5 = resolved on the y-axis, off scan on the x-axis, so no position angle is listed and only a lower limit on the separation is given; 6 = reassignment of bright star designation for consistency with WDS.

Table 3. Partially Resolved Companions

(α, δ) (J2000) (1)	Star Name (2)	Discovery Designation (3)	Date (BY) (4)	FGS Filter (5)	${}^{a}\theta_1$ (deg) (6)	${}^{a}\theta_2$ (deg) (7)	$\rho_{\rm min}$ (arcsec) (8)	Fig. 1.n (9)	Notes (10)
053516.47−052322.9	HD37022C	WGT 1 Ca,Cb	2007.9029	F5ND	247±19	35±19	0.0151±0.0025	34	
075557.13−283218.0	HD65087	FGS 33 AB	2008.8784	F583W	221±14	16±14	0.0168±0.0019	117	
104505.85−594006.4	HDE303308	NEL 5 Ha,Hb	2008.5511	F583W	100±19	174±19	0.0096±0.0025	172	1
104505.85−594006.4	HDE303308	NEL 5 Ha,Hb	2008.8819	F583W	195±15	155±15	0.0114±0.0019	173	1
110840.06−604251.7	V432 Car	FGS 34 AB	2008.9337	F583W	209±8	349±8	0.0118±0.0006	182	
110840.06−604251.7	V432 Car	FGS 34 AB	2008.9337	F583W	240±10	318±10	0.0075±0.0014	183	
174159.03−333013.7	HD160529	FGS 35 AB	2009.2643	F5ND	191±17	11±17	0.0084±0.0037	208	
174159.03−333013.7	HD160529	FGS 35 AB	2009.2643	F5ND	219±5	342±5	0.0131±0.0009	209	
180352.44−242138.6	HD164794	FGS 36 AB	2008.1920	F5ND	246±13	292±13	0.0185±0.0019	213	
203034.97+441854.9	HD195592	FGS 37 AB	2008.5326	F5ND	105±59	285±59	0.0108±0.0011	239	

Note. — 1 = see Appendix.

Table 4. Unresolved Targets

(α, δ) (J2000) (1)	Star Name (2)	Date (BY) (3)	FGS Filter (4)	Fig. 1.n (5)	Notes (6)
000603.39+634046.8	HD108	2008.5566	F5ND	1	
001743.06+512559.1	HD1337	2008.7090	F5ND	2	
022759.81+523257.6	HD15137	2007.6777	F5ND	5	
023249.42+612242.1	HD15570	2007.6478	F583W	6	
024252.03+565416.5	HD16691	2007.5274	F583W	8	
031405.34+593348.5	HD19820	2008.5757	F5ND	11	
035523.08+310245.0	HD24534	2007.8372	F5ND	12	
035857.90+354727.7	HD24912	2008.7092	F5ND	14	
045403.01+662033.6	HD30614	2007.6615	F5ND	17	
051022.79−684623.8	HDE269128	2008.9280	F583W	18	
051022.79−684623.8	HDE269128	2008.9280	F583W	19	
051618.15+341844.3	HD34078	2008.7276	F5ND	20	1
052229.30+333050.5	HDE242908	2007.6279	F583W	25	
053341.15+362735.0	HD36483	2007.6529	F583W	30	
053508.28+095603.0	HD36861A	2008.7110	F5ND	32	
053508.28+095603.0	HD36861A	2008.8065	F5ND	33	
053540.53+212411.7	HD36879	2008.7587	F5ND	37	
055358.21+205234.7	HDE248894	2008.7642	F583W	41	
055444.73+135117.1	HD39680	2008.7094	F5ND	42	
055444.73+135117.1	HD39680	2008.8514	F583W	43	
060552.46+481457.4	HD41161	2007.8598	F5ND	44	
060855.82+154218.2	HD41997	2008.7096	F583W	45	
060855.82+154218.2	HD41997	2008.8678	F583W	46	
060939.57+202915.5	HD42088	2008.7644	F5ND	47	
061941.65+231720.2	HDE255055	2008.7655	F583W	49	
062258.24+225146.2	HDE256035	2008.7648	F583W	50	
062328.54+202331.7	HD44597	2008.7650	F583W	51	
062438.36+194215.8	HD44811	2008.7085	F583W	52	
062715.78+145321.2	HD45314	2008.0037	F5ND	53	1
063120.87+045003.3	HD46056	2008.7653	F583W	54	
063152.53+050159.2	HD46149	2007.6908	F5ND	55	
063152.53+050159.2	HD46149	2008.8454	F5ND	56	
063155.52+045634.3	HD46150	2008.0311	F5ND	57	
063350.96+043131.6	HD46485	2008.7730	F583W	59	
063423.57+023202.9	HD46573	2008.7684	F5ND	60	
063724.04+060807.4	HD47129	2008.7263	F5ND	63	
063838.19+013648.7	HD47432	2008.7783	F5ND	64	
064021.98−002126.0	HDE292090	2008.7659	F583W	65	
064159.23+062043.5	HD48099	2008.6955	F5ND	68	
064240.55+014258.2	HD48279	2008.8802	F583W	69	
064453.82+003712.6	HDE292167	2008.7657	F583W	70	
065017.62+002647.6	HDE292392	2008.8051	F583W	75	
065133.93+133702.1	HDE265134	2008.7683	F583W	76	
065158.45+012234.2	HDE289291	2008.7810	F583W	77	

Table 4—Continued

(α, δ) (J2000) (1)	Star Name (2)	Date (BY) (3)	FGS Filter (4)	Fig. 1.n (5)	Notes (6)
070021.08−054936.0	HD52266	2008.7114	F5ND	79	
070635.97−122338.2	HD53975	2008.7316	F5ND	81	
070920.25−102047.6	HD54662	2008.7116	F5ND	82	
071008.15−114809.8	HD54879	2008.7117	F5ND	83	
071428.25−101858.5	HD55879	2008.7670	F5ND	84	
071840.38−243331.3	HD57060	2008.7287	F5ND	86	
071930.10−220017.3	HD57236	2008.7119	F583W	89	
072202.05−085845.8	HD57682	2008.7041	F5ND	90	
072512.28−210126.3	HD58509	2008.8782	F583W	91	
073001.28−190834.7	ALS458	2008.8458	F583W	93	
073035.28−190622.2	ALS467	2008.8097	F583W	94	
073146.74−165948.0	HD59986	2008.8071	F583W	95	
073202.81−192607.7	ALS499	2008.8181	F583W	96	
073301.84−281932.9	HD60369	2008.7646	F583W	97	
073334.32−275838.3	HD60479	2008.7803	F583W	98	
073513.95−184757.2	BD-18 1920	2008.8179	F583W	99	
073642.04−342516.8	CD-34 3746	2008.8177	F583W	100	
073705.73+165415.3	HD60848	2008.7098	F5ND	101	
073816.12−135101.2	HD61347	2008.7807	F583W	102	
073949.34−323442.1	HD61827	2008.7809	F5ND	103	
074030.29−333044.6	CD-33 4026	2008.8078	F583W	104	
074139.98−334954.1	CD-33 4043	2008.8069	F583W	105	
074254.87−341907.9	CD-34 3831	2008.8102	F583W	107	
074328.98−291912.5	CD-29 4849	2008.8212	F583W	108	
074549.03−262931.4	HD63005	2008.7676	F583W	109	
074636.20−264140.0	CD-26 4955	2008.8833	F583W	110	
075250.42−262822.3	CD-26 5126	2008.8122	F583W	112	
075255.40−262842.7	CD-26 5129	2008.8780	F583W	113	
075301.01−270657.8	CD-26 5136	2008.7801	F583W	114	
075338.20−261402.6	HD64568	2007.9193	F583W	115	
075552.85−283746.8	CD-28 5104	2008.7688	F583W	116	
075830.66−263408.2	CD-26 5285	2008.8073	F583W	120	
075851.83−284504.2	CD-28 5216	2008.8104	F583W	121	
075922.16−285423.8	CD-28 5235	2008.8460	F583W	122	
080210.34−040136.4	BD-03 2178	2008.8153	F583W	123	
080408.54−272908.8	HD66788	2008.7692	F583W	124	
081101.68−371732.5	HD68450	2008.7721	F5ND	125	
081200.73−390841.7	CD-38 4168	2008.7747	F583W	126	
081602.74−441921.7	HD69648	2008.7752	F583W	130	
081624.75−354421.5	CD-35 4412	2008.8106	F583W	131	
081854.46−360752.0	CD-35 4469	2008.8075	F583W	132	
082455.79−441803.0	HD71304	2008.7749	F583W	134	
084047.79−450330.2	HD74194	2008.7727	F5ND	136	
084324.16−460828.7	CD-45 4447	2008.8131	F583W	137	

Table 4—Continued

(α, δ) (J2000) (1)	Star Name (2)	Date (BY) (3)	FGS Filter (4)	Fig. 1.n (5)	Notes (6)
084349.80−460708.8	ALS1135	2008.8150	F583W	139	
084425.05−455334.7	CD-45 4472	2008.8126	F583W	141	
084701.59−440428.8	HD75211	2008.7774	F5ND	143	
084725.14−364502.7	HD75222	2008.4089	F5ND	144	
085002.28−443439.9	CD-44 4865	2008.7667	F583W	145	
085021.02−420523.2	HD75759	2008.4198	F5ND	146	
085033.46−463145.1	HD75821	2008.7776	F5ND	147	
085052.05−435022.9	CD-43 4690	2008.7719	F583W	148	
085500.45−472457.5	HD76535	2008.7723	F583W	151	
085507.15−473627.2	HD76556	2008.7696	F583W	152	
085527.66−413522.3	CD-41 4637	2008.8161	F583W	153	
085728.85−504458.2	HD76968	2008.5593	F5ND	154	
085751.66−474544.0	CD-47 4550	2008.8350	F583W	155	
085754.62−474415.7	CD-47 4551	2007.4993	F583W	156	
085956.10−473304.4	CD-47 4575	2008.8151	F583W	157	
090551.33−474606.8	HD78344	2008.7729	F583W	159	
092010.13−453155.0	CD-45 5058	2008.8188	F583W	160	
092244.75−493019.9	HDE297433	2008.7668	F583W	161	
093037.25−513934.7	HDE298429	2008.7289	F583W	162	
093054.26−512516.0	HDE298425	2008.7754	F583W	163	
100440.52−583158.5	HDE302501	2008.7756	F583W	164	
100520.55−584420.7	HDE302505	2008.8026	F583W	165	
100712.21−580054.3	CPD-57 2676	2008.8693	F583W	167	
100947.72−605949.2	HD88412	2008.7780	F583W	168	
102253.84−593728.4	HD90177	2008.9275	F5ND	169	
102253.84−593728.4	HD90177	2008.9275	F5ND	170	
103330.30−600740.0	HD91651	2008.5539	F583W	171	
104823.51+373413.1	HD93521	2008.8409	F5ND	174	
105001.50−575226.3	HD94024	2008.6688	F583W	175	
105152.75−585835.3	HDE303492	2008.7072	F583W	176	
105223.20−584448.4	HD94370	2008.8565	F5ND	177	
105611.58−602712.8	HD94910	2008.9277	F5ND	178	
105611.58−602712.8	HD94910	2008.9277	F5ND	179	
105635.79−614232.2	HD94963	2008.7067	F5ND	180	
110732.81−595748.7	HD96715	2007.5081	F583W	181	
110842.62−570356.9	HD96917	2008.6850	F5ND	184	
111431.90−590128.8	HD97848	2008.6715	F583W	185	
114654.41−612747.0	HD102415	2008.6852	F583W	186	
120549.88−693423.0	HD105056	2008.3935	F5ND	188	
125557.13−565008.9	HD112244	2008.6953	F5ND	189	
131604.80−623501.5	HD115071	2008.7021	F5ND	190	
133023.52−785120.5	HD116852	2008.6951	F583W	191	
133443.41−632007.6	HD117856	2008.7071	F5ND	192	
140725.64−602814.1	HD123056	2008.6824	F583W	193	

Table 4—Continued

(α, δ) (J2000) (1)	Star Name (2)	Date (BY) (3)	FGS Filter (4)	Fig. 1.n (5)	Notes (6)
142022.78−605322.2	HD125241	2007.6281	F583W	194	
163023.31−375821.2	HD148546	2008.4228	F5ND	195	
165133.72−411349.9	HD151804	2008.1996	F5ND	197	
165359.73−422143.3	HD152236	2009.2751	F5ND	198	
165359.73−422143.3	HD152236	2009.2751	F5ND	199	
170628.37−352703.8	HD154368	2008.4367	F5ND	200	
170653.91−423639.7	HDE326823	2009.2895	F583W	201	
170653.91−423639.7	HDE326823	2009.2895	F583W	202	
170953.09−470153.2	HD154811	2009.5396	F5ND	203	
172617.33−105934.8	HD157857	2008.1918	F5ND	206	
174916.55−311518.1	HD161853	2008.2432	F5ND	210	
175926.31−222800.9	HD163892	2009.5460	F5ND	211	
175928.37−360115.6	HD163758	2009.5489	F5ND	212	
180604.68−241143.9	HD165246	2009.5338	F5ND	214	
181224.66−104353.1	HD166734	2008.4985	F583W	215	
181728.56−182748.4	HD167771	2009.5463	F5ND	217	
181805.90−121433.3	HD167971	2008.2059	F5ND	218	1
182114.89−162231.8	HD168607	2009.1525	F583W	220	
182114.89−162231.8	HD168607	2009.1526	F583W	221	
185735.71−190911.3	HD175754	2008.1998	F5ND	224	
195159.07+470138.4	HD188209	2008.2007	F5ND	225	
195221.76+184018.7	HD188001	2008.3535	F5ND	226	
200100.00+420030.8	HD189957	2008.1596	F5ND	227	
200557.32+354718.1	HD190918	2008.1925	F5ND	229	
201233.12+401605.4	HD192281	2008.5239	F5ND	231	
201729.70+371831.1	HDE228766	2008.3151	F583W	232	
201747.20+380158.5	HD193237	2009.0054	F5ND	233	
201747.20+380158.5	HD193237	2009.0054	F5ND	234	
202310.79+405229.9	HDE229196	2008.0554	F583W	237	
205203.58+343927.5	HD198846	2008.3239	F5ND	240	
205634.78+445529.0	HD199579	2008.3266	F5ND	241	
210755.42+332349.2	HD201345	2008.3155	F5ND	242	
211228.39+443154.1	HD202124	2009.0957	F5ND	243	
211827.19+435645.4	HD203064	2008.3264	F5ND	244	
214453.28+622738.0	HD207198	2008.4390	F5ND	246	
220204.57+580001.3	HD209481	2008.5675	F5ND	247	
220508.79+621647.3	HD209975	2008.6007	F5ND	248	
223915.68+390301.0	HD214680	2008.7587	F5ND	249	
225647.19+624337.6	HD217086	2007.6749	F5ND	250	
231106.95+530329.6	HD218915	2008.7122	F5ND	251	

Note. — 1 = see Appendix.

Table 5. Frequency of Multiple Systems and Companion Frequency

Group (Number)	Cluster/Association (214)	Field (58)	Runaway (29)
A. FGS Visual Binaries			
n(FGS)	67	9	2
MF(FGS)	0.31±0.03	0.16±0.05	0.07±0.05
CF(FGS)	0.34±0.04	0.17±0.05	0.07±0.05
B. WDS Visual Binaries			
n(WDS)	61	10	10
MF(WDS)	0.29±0.03	0.17±0.05	0.34±0.09
CF(WDS)	0.84±0.14	0.22±0.07	0.52±0.16
C. Spectroscopic Binaries			
n(SBO+E)	68	5	5
n(SB?)	28	14	3
n(C)	65	14	21
n(U)	53	25	0
MF(SBO+E)	0.42±0.04	0.15±0.06	0.17±0.07
MF(SBO+E+?)	0.60±0.04	0.58±0.08	0.28±0.08
CF(SBO+E)	0.51±0.05	0.15±0.06	0.17±0.07
CF(SBO+E+?)	0.68±0.05	0.58±0.09	0.28±0.08
D. Any Companion			
MF(min)	0.51±0.03	0.21±0.05	0.21±0.07
MF(max)	0.69±0.03	0.50±0.06	0.48±0.09
CF(min)	0.70±0.06	0.26±0.07	0.24±0.09
CF(max)	1.67±0.17	0.72±0.11	0.86±0.20